ICP/EXT-04-00702

Surface Geophysics and Downhole Geophysical Logging Results for the Radioactive Waste Management Complex, 2003-2004

Idaho Completion Project

Bechtel BWXT Idaho, LLC

March 2005

ICP/EXT-04-00702
Project No. 23957

Surface Geophysics and Downhole Geophysical Logging Results for the Radioactive Waste Management Complex, 2003-2004

Nick Josten

March 2005

GeoSense
Idaho Falls, Idaho 83415

Prepared under Subcontract No. 00022841
for the
U.S. Department of Energy
Assistant Secretary for Environmental Management
Under DOE Idaho Operations Office
Contract DE-AC07-99ID13727

ABSTRACT

Surface geophysics and downhole geophysical logging activities are performed as needed to support the Idaho Completion Project at the Idaho National Laboratory Radioactive Waste Management Complex. The logging efforts are performed to collect data directly from the waste zone for characterization purposes.

This report is a compilation of a large number of informal analyses of surface geophysics and downhole geophysical logging data collected between September 2003 and August 2004. Much of the material collected in this report has not been published in any form, though it has been used to support the ongoing environmental restoration decision-making process. The primary purpose of this report is to provide Subsurface Disposal Area surface geophysics and downhole geophysical logging information in a form that can be easily referenced.

CONTENTS

ABSTRACT iii

ACRONYMS xi

1. INTRODUCTION 1-1

1.1 Purpose and Scope 1-1

1.2 Description of Logging Area 1-1

2. BACKGROUND 2-1

2.1 Description of Geophysical Investigations 2-1

2.1.1 Surface Geophysics 2-1
2.1.2 Downhole Geophysical Logging 2-1
2.1.3 Notes on Quantitative Use of Type A Geophysical Logging Data 2-2

3. ANALYSIS BY FOCUS AREA 3-1

3.1 Overview of FY 2004 Focus Areas 3-1

3.2 Focus Area 1A: Building 881 Waste 3-3

3.3 Focus Area 1B: Naval Reactors Facility Reactor Core Components 3-5

3.4 Focus Area 1D: Undocumented Disposals 3-10

3.5 Focus Area 2: Naval Reactors Facility Liquid-Waste Disposals 3-12

3.6 Focus Area 3: Pit 5 Rocky Flats Plant Plutonium and Enriched Uranium Waste 3-14

3.7 Focus Area 4: Pit 10 Plutonium Waste (741-08 Probe Cluster) 3-17

3.7.1 Investigation of Plutonium in Lysimeters L1 and L2 3-20
3.7.2 Investigation of Plutonium in Probe 741-08 3-21

3.8 Focus Area 5: Pit 6 Plutonium Waste from the Rocky Flats Plant 3-22

3.9 Focus Area 6: Pit 10 Plutonium Waste 3-23

3.10 Focus Area 7: Pit 2 Concentrated Rocky Flats Plant Drums 3-25

4. OTHER ANALYSES 4-1

4.1 Evaluation of Logging Tool Calibration 4-1

4.1.1 Report Summary 4-1

4.2 Comparison of Moisture Sampling and Logging Data 4-2

4.2.1 Report Conclusions and Recommendations 4-2

4.3 Comparison of Moisture Sampling and Logging Data in Focus Area 3 4-3

4.3.1 Density Effect on Moisture Logging Data 4-3
4.3.2 Field Verification of the Moisture Tool Calibration 4-3

4.4 Results from the Long-count Gamma Ray Study 4-6

4.4.1 Three-thousand-second Long-count Results 4-6
4.4.2 Eight-hour Long-count Results 4-6

4.5 Logging Data Analysis to Support Replacement Tensiometers 4-9

4.6 Analysis of Azimuthal Logging Data 4-15

4.6.1 Subsurface Waste Heterogeneity as Observed from Azimuthal Logging Data 4-17

4.7 Geophysics Database Compilation 4-17

4.8 Beryllium Block Investigation 4-18

4.9 Volatile Organic Compound Analysis using n-Gamma Logging Data 4-18

5. REFERENCES 5-1

Appendix A—Sage Earth Science Report A-1

Appendix B—Stoller Logging Data – Stripcharts B-1

Appendix C—Anomalous Uranium and Thorium Signals in Two Passive Gamma-Ray Spectra from P2-PU-3 ..... C-1

Appendix D—Stoller Long Count Reports D-1

Appendix E—Moisture Sampling Data E-1

FIGURES

1-1. Map of the Idaho National Laboratory showing the location of the Radioactive Waste Management Complex and other major Site facilities 1-2

1-2. Map of the Radioactive Waste Management Complex showing the pits and trenches at the Subsurface Disposal Area 1-3

3-1. Location of the FY 2004 Subsurface Disposal Area logging probes, divided into focus areas 3-2

3-2. Map showing the location of Focus Area 1 probes and Rocky Flats Plant shipment RFODOWSR102/10/55800 in Trench 3 3-4

3-3. Map showing the location of targeted shipments of Naval Reactors Facility core components in Focus Area 1B 3-6

3-4. Comparison of selected logging results for probes T47-IF-1 and T47-IF-6 3-8

3-5. Comparison of selected logging results for probes T47-IF-2 and T47-IF-5 3-9

3-6a. Map showing the areas of conductive soil in Focus Area 1D-north 3-11

3-6b. Map showing the location of probes in Focus Area 1D-south 3-11

3-7. Map showing the location of probes HAL1 through HAL4 in Focus Area 2 3-13

3-8. Map showing the location of Focus Area 3 3-15

3-9. Comparison of selected logging results for probes P5-UEU-4 and P5-UEU-9 3-18

3-10. Map showing the location of lysimeters and probes in Focus Area 4 3-19

3-11. Comparison of selected logging results for probeholes 741-08, 741-08C, and 741-08D 3-21

3-12. Map showing the location of Focus Area 5 3-22

3-13. Map showing location of Focus Area 6 probes 3-24

3-14. Targeted drum concentrations, surface geophysics (magnetic field data), and the installed position of the six Pit 2 probes 3-26

4-1. Sketch map showing location of Pit 5 P5-UEU-series and P5-04-series Type A probes 4-4

4-2. Diagram showing the depth variation of neutron-neutron soil moisture readings for the Pit 5 UEU-series and P5-04-series Type A probes 4-5

4-3. Comparison of neutron-neutron moisture logs (curves) and soil moisture sampling results (square point data for three depth locations for each of three probes). Sampling data were converted from weight percent to volume percent based on an assumed dry bulk density of 1.44 g/cc 4-5

4-4a. Detail of the depth range from 12–16 ft in Probehole P6-PU-1 4-7

4-4b. Detail of the waste and soil interface in Probehole P6-PU-2 4-8

4-5. Cross-section sketches compiled from Type A logging data near Probe DU-08 4-10

4-6. Cross-section sketches compiled from Type A logging data near Probe DU-10 4-11

4-7. Cross-section sketches compiled from Type A logging data near Probe DU-14 4-12

4-8. Cross-section sketches compiled from Type A logging data near Probe 743-03 4-13

4-9. Cross-section sketches compiled from Type A logging data near Probe 743-18 4-14

4-10. Azimuthal data plots showing examples of a highly directional gamma ray flux (left) and marginally directional gamma ray flux (right) 4-16

4-11. Azimuthal plots for total gamma ray flux in Probe P5-UEU-1 4-17

TABLES

2-1. Summary of Subsurface Disposal Area surface geophysical surveys conducted in 2003–2004 2-1

2-2. Summary of Subsurface Disposal Area FY 2004 geophysical logging program 2-1

2-3. Overall summary of downhole logging results for the FY 2004 logging program 2-2

3-1. Descriptive summary of focus areas investigated during the FY 2004 logging program 3-1

3-2. Logging completion summary showing depth intervals logged for each Focus Area 1A probe 3-3

3-3. Radionuclide detection summary for Focus Area 1A 3-3

3-4. Summary of uranium detection and ratios in Focus Area 1A 3-5

3-5. Logging completion summary showing depth intervals logged for each Focus Area 1B probe 3-6

3-6. Radionuclide detection summary for Focus Area 1B 3-7

3-7. Logging completion summary showing depth intervals logged for each Focus Area 1D probe 3-10

3-8. Radionuclide detection summary for Focus Area 1D 3-10

3-9. Logging completion summary showing depth intervals logged for each Focus Area 2 probe 3-14

3-10. Radionuclide detection summary for Focus Area 2D 3-14

3-11. Logging completion summary showing depth intervals logged for each Focus Area 3 probe 3-15

3-12. Radionuclide detection summary for Focus Area 3 3-16

3-13. Summary of uranium detection in Focus Area 3 3-17

3-14. Logging completion summary showing depth intervals logged for each Focus Area 4 probe..... 3-19

3-15. Radionuclide detection summary for Focus Area 4 3-19

3-16. Summary of uranium detection in Focus Area 4 3-20

3-17. Logging completion summary showing depth intervals logged for each Focus Area 5 probe..... 3-23

3-18. Radionuclide detection summary for Focus Area 5 3-23

3-19. Logging completion summary showing depth intervals logged for each Focus Area 6 probe..... 3-24

3-20. Radionuclide detection summary for Focus Area 6 3-25

3-21. Logging completion summary for the new Pit 2 probes..... 3-26

3-22. Radionuclide detection summary for Focus Area 7 3-26

4-1. Summary of sampling and logging results. Sample volume percent values calculated assuming soil dry-bulk density of 1.44 g/cc 4-5

4-2. Comparison of theoretical detection limits for count times..... 4-6

4-3. Tensiometers requiring replacement and recommended locations for new tensiometers 4-9

4-4. Azimuthal logging data acquisition summary (November–December 2003) 4-15

4-5. Azimuthal logging data results summary 4-16

ACRONYMS

bgs	below ground surface
FY	fiscal year
INL	Idaho National Laboratory
NA	not applicable
ND	not detected
NRF	Naval Reactors Facility
OU	operable unit
PLN	plan
RFP	Rocky Flats Plant
RWMC	Radioactive Waste Management Complex
SDA	Subsurface Disposal Area
TRU	transuranic
VOC	volatile organic compound
vol%	volume percent
wt%	weight percent

Surface Geophysics and Downhole Geophysical Logging Results for the Radioactive Waste Management Complex, 2003-2004

1. INTRODUCTION

Surface geophysics and Type A downhole geophysical logging activities have been performed at the Radioactive Waste Management Complex (RWMC) Subsurface Disposal Area (SDA) as needed in support of the Idaho Completion Project at the Idaho National Laboratory (INL). The logging efforts are performed to collect data directly from the waste zone for characterization purposes.

An initial Type A probing effort was performed from 1999–2001, during which 139 Type A probes were installed in Pits 4, 5, 6, 9, and 10. Probing equipment and methods are described in *OU 7-10 Initial Probing Campaign Downhole Logging Results* (Josten and Okeson 2000) and *Type A Nuclear Logging Data Acquisition and Processing for Operable Units 7- 13/14 and 7-10* (INL 2002). Interpretation, results, and discussion may be found in various reports. General results for the entire probing effort are documented in the *Compilation of Analytical Notes and Data Analyses for the Integrated Probing Project 1999–2002* (Josten 2002). Pit 9 probing results are recorded in *OU 7-10 Stage I Subsurface Exploration and Treatability Studies Report (Draft) - Initial Probing Campaign - December 1999–June 2000* (Okeson et al. 2000). *Evaluation of OU 7-10 Stage I Soil Moisture Readings* (Beitel et al. 2000) contains a detailed discussion of soil-moisture logging tool performance and results at Pit 9. *Estimating the Mass of Pu-239 Waste Near P9-20 Probe Hole for the OU 7-10 Glovebox Excavator Method Project* (Jewell et. al. 2002) describes efforts to perform quantitative calculations of Pu-239 mass at Pit 9. *Estimating Carbon Tetrachloride and Total Volatile Organic Compound Mass Remaining in Subsurface Disposal Area Pits* (Sondrup et al. 2004) describes efforts to perform quantitative calculations of volatile organic compound (VOC) mass based on nuclear logging measurements.

1.1 Purpose and Scope

This report is a compilation of a large number of informal analyses of surface geophysics and downhole geophysical logging efforts performed between September 2003 and August 2004. For the purposes of this report, this testing period is referred to as Fiscal Year (FY) 2004. Much of the material collected in this report has not been published in any form, though it has been used to support the ongoing environmental restoration decision-making process. The primary purpose of this report is to provide the surface geophysics and downhole geophysical logging information in a form that can be easily referenced.

It should be noted that some of the analysis results contained in this report represent interim compilations and conclusions.

1.2 Description of Logging Area

The INL is a U.S. Department of Energy facility located 52 km (32 mi) west of Idaho Falls, Idaho that occupies 2,305 km^2 (890 mi^2) of the northeastern portion of the Eastern Idaho Snake River Plain. The RWMC is located in the southwestern portion of the INL as shown in Figure 1-1. The SDA is a 39-ha (97-acre) portion of the RWMC. Low-level, transuranic (TRU), mixed, and other radioactive waste was buried in shallow pits and trenches in the SDA (see Figure 1-2) from 1952 until 1970, when burial of the TRU portion of the waste ceased. Since 1985, only low-level waste has been buried at the SDA. Contaminants of concern detected in the unsaturated zone beneath the SDA include nitrates, carbon tetrachloride, C-14, Tc-99, and uranium isotopes (Holdren et al. 2002).

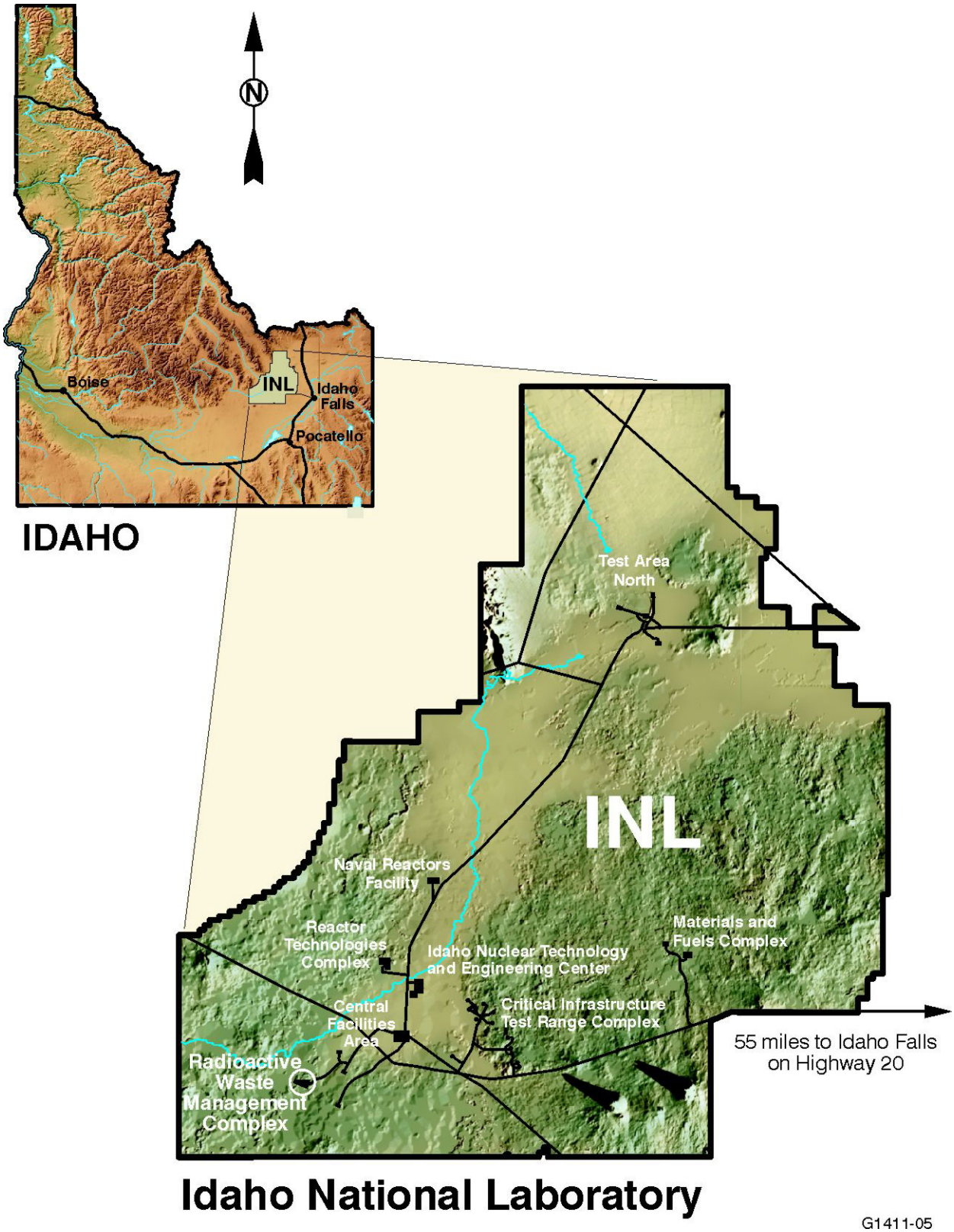

Figure 1-1. Map of the Idaho National Laboratory showing the location of the Radioactive Waste Management Complex and other major Site facilities.

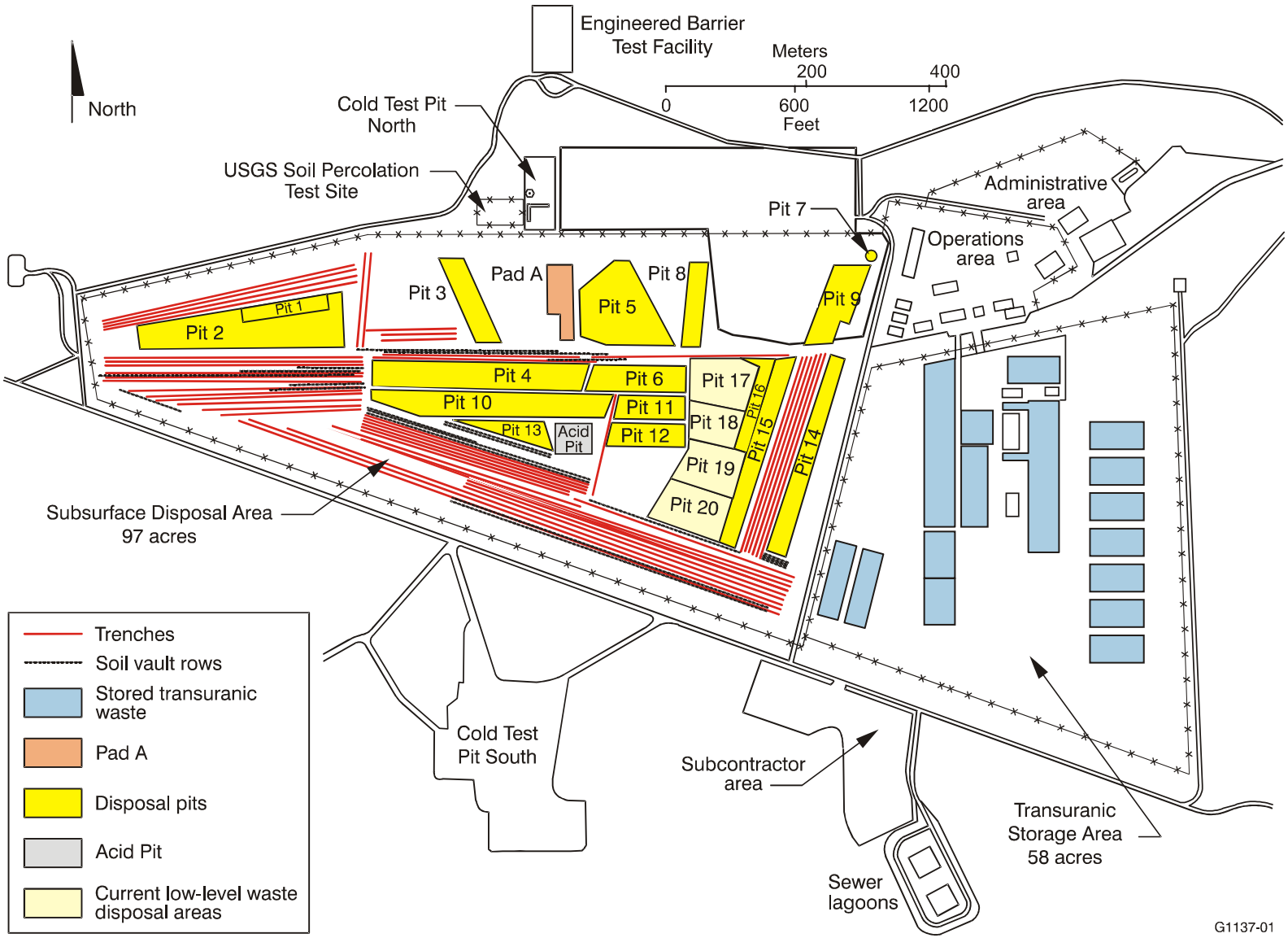

Figure 1-2. Map of the Radioactive Waste Management Complex showing the pits and trenches at the Subsurface Disposal Area.

2. BACKGROUND

2.1 Description of Geophysical Investigations

Two types of geophysical data were used for the analyses presented in this report. The first was surface geophysics data, collected over many years of SDA operations including several new surveys collected in FY 2003 and 2004. Surface geophysics data were used mainly to delineate waste versus nonwaste areas, a basic segregation that supports many of the analyses presented in this report. The second was downhole geophysical logging data, which provide information on in situ conditions within the waste zone, overburden, and underburden.

2.1.1 Surface Geophysics

Table 2-1 lists two surface geophysical studies performed by Sage Earth Science at the SDA from FY 2003 through 2004. These studies were conducted to support analysis of remedial alternatives and future environmental restoration needs for the SDA, with the exception of Pit 9 and the low-level waste pit. The FY 2004 survey produced comprehensive, high-resolution geophysical data for most of the SDA. The subcontractor report for this survey is included as Appendix A. All SDA surface geophysical data, including the surveys listed in Table 2-1, have been archived in Plan (PLN) -1709, "Software Documentation for the Nuclear Logging and Surface Geophysics Database."

Table 2-1. Summary of Subsurface Disposal Area surface geophysical surveys conducted in 2003–2004.

Performer	Year	Methods	Survey Area
Sage Earth Science	2003	Magnetics, electromagnetic induction	Pad A, SDA east, SDA southwest, Trench 3, Trench 47, Trench 57
Sage Earth Science	2004	Magnetics, electromagnetic induction	Entire SDA except Pit 9 and low-level waste pit

SDA = Subsurface Disposal Area

2.1.2 Downhole Geophysical Logging

From August 2003 through January 2004, 48 Type A steel probes were installed at various locations in the SDA. Probe locations were selected based on combined analysis of surface geophysical data and waste inventory records. A suite of geophysical logging tools was deployed in these probes to investigate subsurface characteristics of buried waste. Table 2-2 lists the geophysical tools used and gives a brief summary of the scope of the FY 2004 logging program. All SDA geophysical logging data, including the surveys listed in Table 2-2, have been archived in the Nuclear Logging and Surface Geophysics Database, housed in the Environmental Data Warehouse.

Table 2-2. Summary of Subsurface Disposal Area FY 2004 geophysical logging program.

Tool	Primary Application	Number of Probes Logged	Linear Feet Logged
Passive spectral gamma ray	Detect gamma-emitting radionuclides	48	527.90
Passive neutron	Detect neutrons associated with TRU radionuclides	48	477.55
Neutron-activated spectral gamma ray	Detect chlorine	48	477.80

Table 2-2. (continued).

Tool	Primary Application	Number of Probes Logged	Linear Feet Logged
Neutron-neutron moisture	Measure moisture content	48	649.73
Azimuthal spectral gamma ray	Delineate compact versus distributed radioactive sources	13	57[a]

a. Azimuthal surveys conducted at 57 depths.

TRU = transuranic

Geophysical logging was performed in accordance with specifications defined in the "Statement of Work for Nuclear Geophysical Logging" (SOW-561). These data have yielded qualitative and semiquantitative information about the distribution and environment of radionuclides and chlorinated solvents in the subsurface. Table 2-3 gives a summary of contaminant detections for the FY 2004 logging program.

Table 2-3. Overall summary of downhole logging results for the FY 2004 logging program.

Parameter	Pu-239 375 keV	Am-241[a] 662 keV	Np-237 312 keV	U-235 186 keV	U-238 1,001 keV	Cs-137[a] 662 keV	Co-60 1,333 keV	Chlorine 1,165 keV
Total measurements	1,145	1,145	1,145	1,145	1,145	1,145	1,145	1,039
Number of detects	199	229	116	69	172	177	85	486
Number of nondetects	946	916	1,029	1,076	973	968	1,060	553
Detect percent	17.4	20.0	10.1	6.0	15.0	15.5	7.4	46.8
Nondetect percent	82.6	80.0	89.9	94.0	85.0	84.5	92.6	53.2

a. After subcontractor correction for interference between Cs-137 and Am-241 662-keV gamma rays.

The subcontractor chart summary for all logging data acquired under this program is reproduced in Appendix B.

2.1.3 Notes on Quantitative Use of Type A Geophysical Logging Data

Responses of the Type A nuclear logging tools (and in particular the passive gamma-ray logging tool) are known to depend on many factors, but the three most important are (1) the amount of radionuclide source present, (2) geometry of the radionuclide source distribution (i.e., anywhere between a compact point source and a homogenous distribution), and (3) density of the waste and soil matrix surrounding the source. Modeling exercises show that these three factors have roughly equal influence on the logging-tool response. As a consequence, the logging data cannot provide an unequivocal estimate for one factor unless the other factors are known. The existing calibration method handles this problem by making simplifying assumptions for the source geometry and soil-matrix density such that the third factor, the amount of radionuclide, can be estimated directly.

Radionuclide estimates produced by the existing calibration methodology have very limited utility because the underlying uniformity assumptions are indefensible. Inventory records, waste drum scan records, and logging data all indicate highly heterogeneous conditions within SDA waste. Furthermore, no known methods will independently measure the waste and soil matrix density.

3. ANALYSIS BY FOCUS AREA

The FY 2004 SDA logging program was part of an overall plan to evaluate long-term health and safety risks associated with waste buried in the SDA. The logging program was subdivided into focus areas selected to address a specific data need.

3.1 Overview of FY 2004 Focus Areas

Figure 3-1 shows the location of the FY 2004 logging probes, subdivided by focus area. Table 3-1 presents the nomenclature used in this report to identify each focus area along with brief descriptions of each focus area, location information, and a list of the probes installed. Probe locations for each focus area were selected after combined analysis of inventory records and surface geophysics data. Each installed probe was first logged using the neutron-neutron moisture tool. Moisture data then were analyzed to determine thickness of the soil overburden at each probe location. The passive spectral gamma ray, neutron-activated spectral gamma ray, and passive-neutron tools were then deployed from near the base of the overburden down to the bottom of the probe. Several probes were selected for deployment of the azimuthal spectral gamma ray tool in cases where these data were considered useful for meeting focus area objectives.

Table 3-1. Descriptive summary of focus areas investigated during the FY 2004 logging program.

Focus Area	Waste Type Investigated	Pit or Trench Location	Probes Installed
1A	Enriched uranium-bearing waste from RFP Building 881	Trench 3	T3-EU-01, T3EU-02, T3-EU-03, T3-EU-04
1B	Eight NRF shipments of waste similar to spent nuclear fuel	Trench 47	T47-IF-1, T47-IF-2, T47-IF-3, T47-IF-4, T47-IF-5, T47-IF-6
1D North	Various undocumented waste disposals	North SDA	UD-01, UD-03, UD-03B
1D South	Various undocumented waste disposals	South SDA	UD-04, UD-05, UD-05B, UD-05C, UD-05-D, UD-05-E
2	Liquid radioactive waste associated with a diatomaceous absorbent material	Trench 24	HAL1, HAL2, HAL3, HAL4
3	Uranium- and plutonium-contaminated RFP sludge and graphite waste	Pit 5	P5-UEU-1, P5-UEU-2, P5-UEU-3, P5-UEU-4, P5-UEU-5, P5-UEU-6, P5-UEU-7, P5-UEU-8, P5-UEU-9
4	Follow-up investigation of suspected RFP Series 741 sludge disposal	Pit 10	741-08C, 741-08D, 741-10, 741-11
5	Suspected plutonium waste area	Pit 6	P6-PU-1, P6-PU-2, P6-PU-3
6	Suspected plutonium waste area	Pit 10	P10-PU-1, P10-PU-2, P10-PU-3
7	Suspected concentrated plutonium waste area	Pit 2	P2-PU-1, P2-PU-2, P2-PU-3, P2-PU-4, P2-PU-5, P2-PU-6

NRF = Naval Reactors Facility
RFP = Rocky Flats Plant
SDA = Subsurface Disposal Area

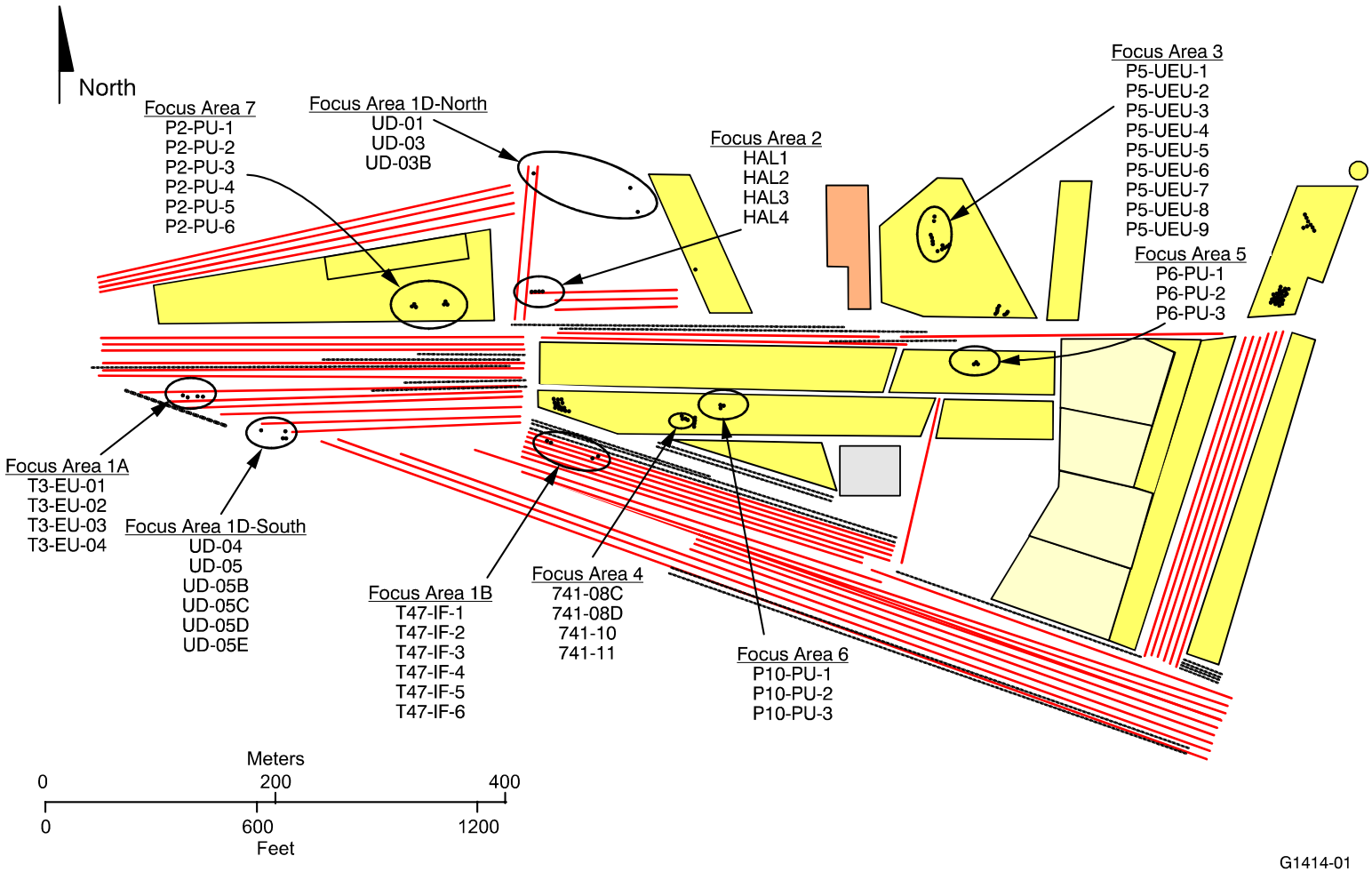

Figure 3-1. Location of the FY 2004 Subsurface Disposal Area logging probes, divided into focus areas.

3.2 Focus Area 1A: Building 881 Waste

Four probes were installed in Focus Area 1A to explore for enriched uranium waste that could be a source of contaminated vadose zone pore water. Figure 3-2 shows the interpreted location of a Rocky Flats Plant (RFP) waste shipment (RFODOWSR102/10/55800) that included 16 55-gal drums and one 30-gal drum of Building 881 solid waste. Building 881 waste is suspected of containing material contaminated with enriched uranium. The four probes installed in the vicinity of this shipment, T3-EU-01 through T3-EU-04, are also shown.

Tables 3-2 and 3-3 present summaries of the logged intervals and detected contaminants for each of the Focus Area 1A probes. A logging data summary chart for each Focus Area 1A probe is included in Appendix B. Note that radionuclide levels are presented in units of activity concentration. These values should be understood as *apparent* concentrations, because the actual concentration is highly dependent on heterogeneity in the vicinity of the probehole.

Table 3-2. Logging completion summary showing depth intervals logged for each Focus Area 1A probe.

	Passive Neutron		Passive Gamma		N-gamma		Moisture	
Well_ID	Minimum (ft bgs)	Maximum (ft bgs)	Minimum (ft bgs)	Maximum (ft bgs)	Minimum (ft bgs)	Maximum (ft bgs)	Minimum (ft bgs)	Maximum (ft bgs)
T3-EU-01	2.25	17.57	2.00	17.97	2.00	16.92	0.25	18.06
T3-EU-02	2.25	20.94	2.00	21.41	2.00	20.33	0.25	21.41
T3-EU-03	2.25	10.96	2.00	11.41	2.00	10.32	0.25	11.48
T3-EU-04	2.25	12.58	2.00	12.17	2.00	11.94	0.25	13.09

Table 3-3. Radionuclide detection summary for Focus Area 1A.[a]

Well ID	Cs-137 662 keV (pCi/g)	Co-60 1,332 keV (pCi/g)	Pu-239 375 keV (pCi/g)	Am-2416 62 keV (pCi/g)	Np-237 312 keV (pCi/g)	U-235 186 keV (pCi/g)	U-238 1,001 keV (pCi/g)	Chlorine 1,151 keV (counts/ second)
T3-EU-01	3.2	5.0	ND	ND	ND	ND	ND	2.9
T3-EU-02	5,504.8	1.0	ND	ND	ND	26.5	1,235.7	8.0
T3-EU-03	31.7	ND	ND	ND	ND	3.4	178.8	2.0
T3-EU-04	0.3	ND	ND	ND	ND	ND	22.9	1.2
MAX[b]	140.5	814.2	194,171,000	30,449,000	4,881	344.9	220,894	38
PROBE	741-04	P9-FI-05	P9-20	743-08-02	DU-08	743-08	743-08	P9-03

a. Concentration estimates obtained from geophysical logging measurements can be significantly affected by heterogeneous subsurface conditions; values presented in this table should be viewed as *apparent* concentration.
b. Maximum observed value of radionuclide or element from all previous SDA logging.

NA = not applicable
ND = not detected

Table 3-3 shows that both cesium–cobalt and U-235:U-238 radionuclide associations are present. The highest observed Cs-137 apparent concentration is 5,504.8 pCi/g, which exceeds the previous highest Cs-137 level logged anywhere at the SDA.

The uranium observed in probes T3-EU-02 and T3-EU-03 was evaluated to assess the evidence for enriched uranium waste. Table 3-4 gives the U-235:U-238 activity ratios and mass ratios at each point where both U-235 and U-238 were detected. These ratios have not been corrected for differential gamma ray attenuation, but are suggestive of depleted uranium. The chlorine collocated with uranium in these probes may reflect PERC sill bottoms.

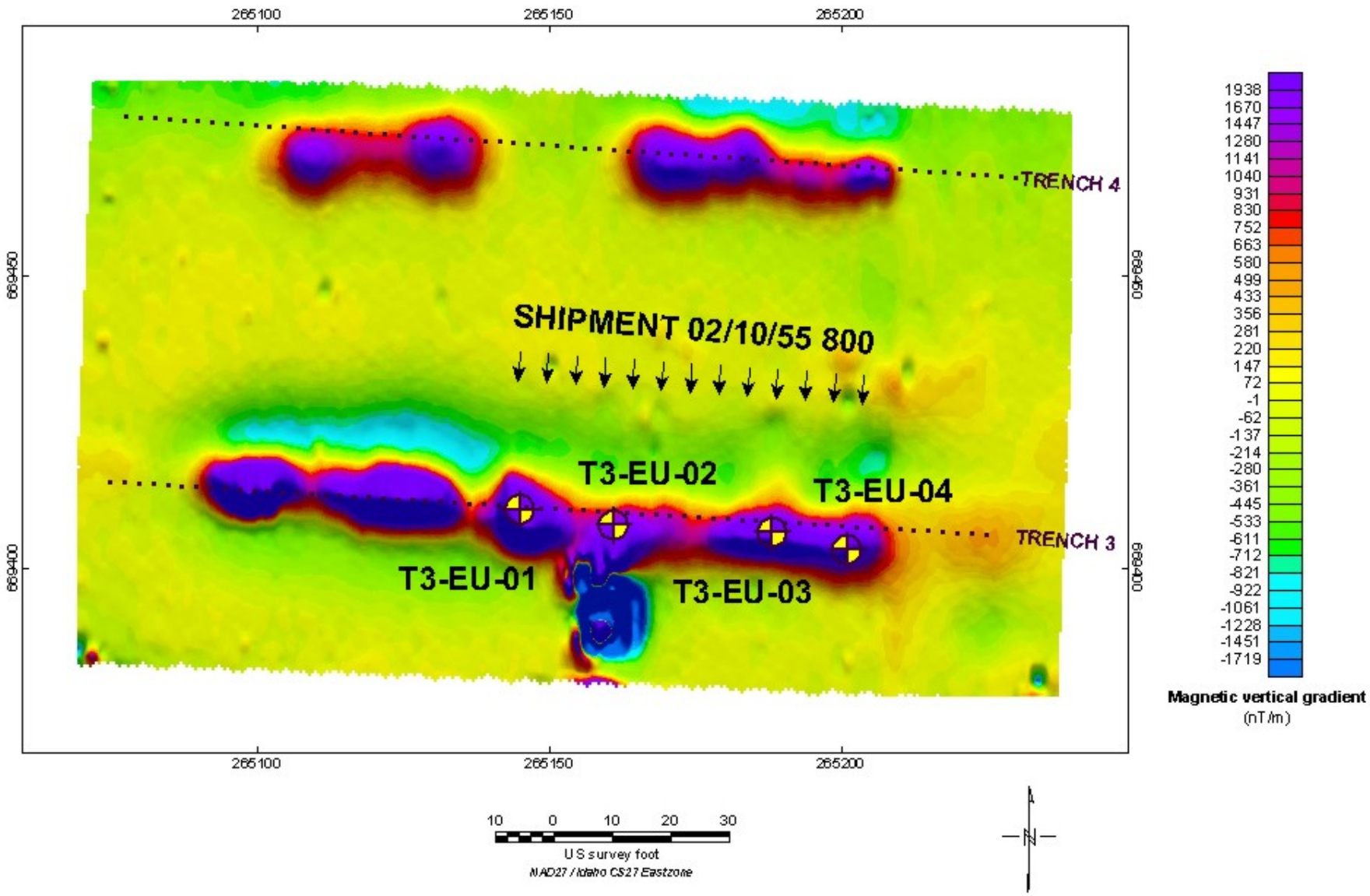

Figure 3-2. Map showing the location of Focus Area 1 probes and Rocky Flats Plant shipment RFODOWSR102/10/55800 in Trench 3.

Table 3-4. Summary of uranium detection and ratios in Focus Area 1A.[a]

Well_ID	Depth (ft)	U-235[b] 186-keV (pCi/g)	U-238 1,001-keV (pCi/g)	Activity Ratio[c] U-235:U-238	Mass Ratio[c] U-235:U-238
T3-EU-02	9.50	17.4	982.1	0.0177	0.0028
T3-EU-02	8.89	19.3	1,130.8	0.0171	0.0027
T3-EU-02	8.50	26.5	1,235.7	0.0215	0.0033
T3-EU-02	8.00	19.8	1,060.1	0.0187	0.0029
T3-EU-02	7.50	12.7	681.8	0.0187	0.0029
T3-EU-02	7.00	4.0	275.4	0.0147	0.0023
T3-EU-03	5.00	3.4	1,78.8	0.0190	0.0029

a. Concentration estimates obtained from geophysical logging measurements can be significantly affected by heterogeneous subsurface conditions; values presented in this table should be viewed as *apparent* concentration.
b. U-235 apparent concentrations not corrected for potential Ra-226 interference.
c. Activity ratios are derived from constants obtained from GE (1989): (1) typical activity ratios: <0.04507 (depleted), 0.04507 (natural), >0.04507 (enriched); (2) typical mass ratios: <0.00696 (depleted), 0.00696 (natural), >0.00696 (enriched).

Azimuthal logging was performed at 8.0 ft in probeholes T3-EU-02 and T3-EU-03. Azimuthal data are presented in Section 4.5.

3.3 Focus Area 1B: Naval Reactors Facility Reactor Core Components

Target shipments for Focus Area 1B are reactor core and loop components generated at the Naval Reactors Facility (NRF) and buried in Trench 47. Figure 3-3 shows the location of the targeted shipments. Locations of the new probes, T47-IF-1 through T47-IF-6, are also shown. Probes T47-IF-1 through T47-IF-4 were placed adjacent to geophysical anomalies that were indicative of massive metal objects. Probes T47-IF-5 and T46-IF-6 were installed directly adjacent to probes T47-IF-2 and T47-IF-1 to facilitate detailed investigation of radionuclide zones observed in logging results from the first four probes. All six probes met refusal from 9–12 ft below ground surface (bgs).

Tables 3-5 and 3-6 present summaries of the logged intervals and the detected contaminants for each of the Focus Area 1B probes. A logging-data-summary chart for each Focus Area 1B probe is included in Appendix B. Note that radionuclide levels are presented in units of activity concentration. These values should be understood as *apparent* concentrations, because the actual concentration is highly dependent on heterogeneity in the vicinity of the probehole.

Table 3-6 shows that the cesium-cobalt radionuclide group is observed in all six probeholes. The maximum measured levels are 17,184 pCi/g of Cs-137 and 24 pCi/g of Co-60. A small Am-241 peak correlates with the cesium-cobalt peak in Probehole T47-IF-1. Weak, single-point U-235 and U-238 anomalies occur in Probehole T47-IF-5. Low-level chlorine counts were observed in all probes except Probehole T47-IF-3.

In probes T47-IF-2, T47-IF-3, and T47-IF-5, the cesium-cobalt levels reach a maximum value at the deepest measurement point, suggesting that the radionuclide zone continues below the probe bottom. This may reflect contamination that has migrated into basalt or other type of hard layer beneath the waste zone, or it may mean that the probe struck impenetrable waste at the refusal depth. In either case, it is impossible to determine the peak radionuclide level for these zones.

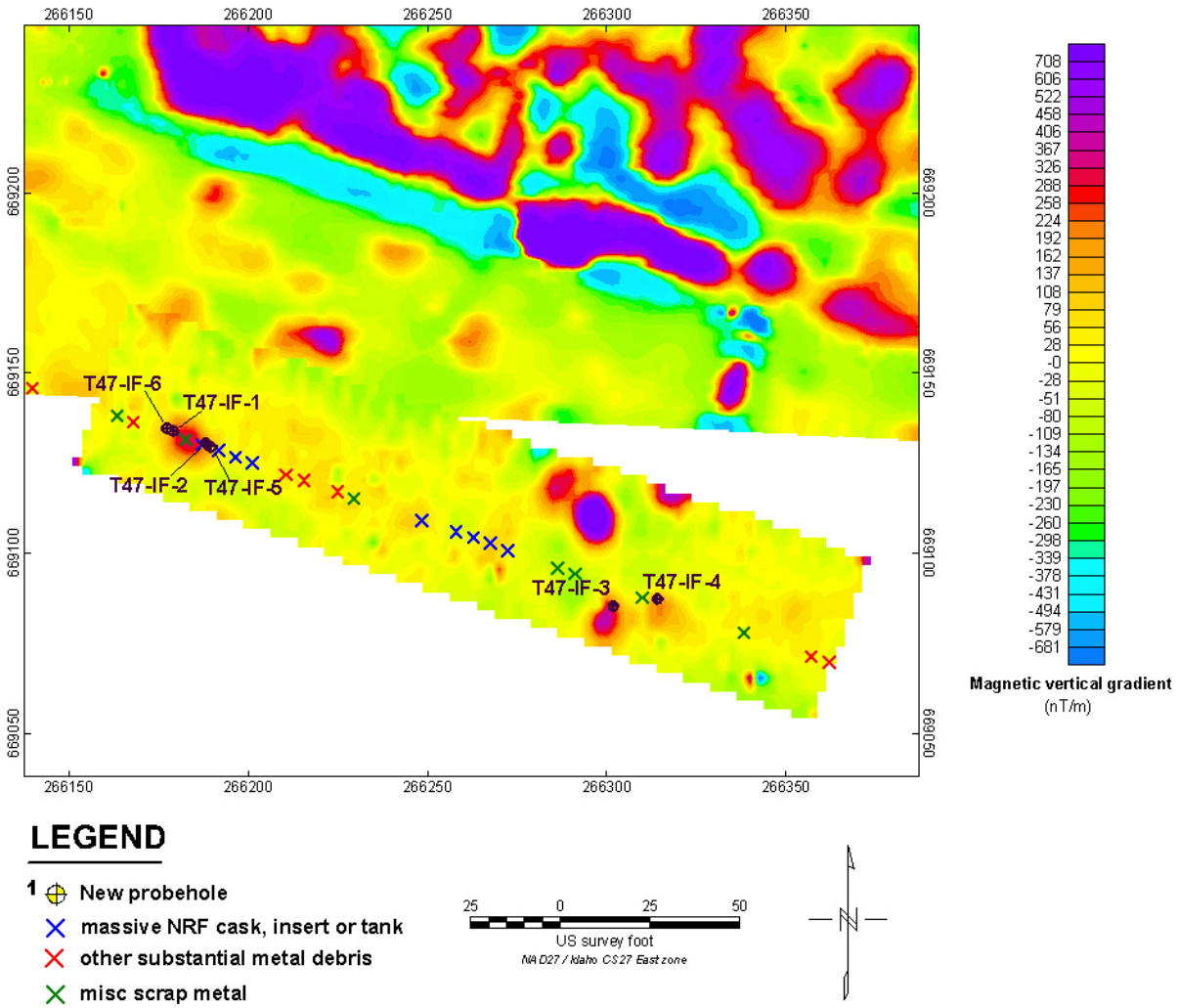

Figure 3-3. Map showing the location of targeted shipments of Naval Reactors Facility core components in Focus Area 1B.

Table 3-5. Logging completion summary showing depth intervals logged for each Focus Area 1B probe.

	Passive Neutron		Passive Gamma		N-gamma		Moisture	
Well_ID	Minimum (ft bgs)	Maximum (ft bgs)	Minimum (ft bgs)	Maximum (ft bgs)	Minimum (ft bgs)	Maximum (ft bgs)	Minimum (ft bgs)	Maximum (ft bgs)
T47-IF-1	2.25	10.67	2.00	11.05	2.00	9.97	0.25	11.13
T47-IF-2	2.25	9.92	2.00	10.29	2.00	9.26	0.24	10.37
T47-IF-3	2.25	10.66	2.00	11.03	2.00	10.00	0.24	11.10
T47-IF-4	2.25	8.78	2.00	9.19	2.00	8.15	0.24	9.26
T47-IF-5	2.25	10.14	2.00	10.61	2.00	9.53	0.25	10.64
T47-IF-6	2.25	10.71	2.00	11.12	2.00	10.04	0.25	11.17

Table 3-6. Radionuclide detection summary for Focus Area 1B.[a]

WELL_ID	Cs-137 662 keV (pCi/g)	Co-60 1,332 keV (pCi/g)	Pu-239 375 keV (pCi/g)	Am-241 662 keV (pCi/g)	Np-237 312 keV (pCi/g)	U-235 186 keV (pCi/g)	U-238 1,001 keV (pCi/g)	Chlorine 1,151 keV (counts/ second)
T47-IF-1	1,942.9	3.4	ND	ND	ND	ND	ND	1.1
T47-IF-2	2,295.5	13.2	ND	ND	ND	ND	ND	1.2
T47-IF-3	3.2	24.6	ND	ND	ND	ND	ND	0.1
T47-IF-4	8.9	0.2	ND	ND	ND	ND	ND	1.4
T47-IF-5	17,184.2	1.2	ND	ND	ND	ND	ND	2.0
T47-IF-6	2,275.4	0.8	ND	ND	ND	24.3	21.0	1.8
MAX[b]	140.5	814.2	194,171,000	30,449,000	4,881	344.9	220,894	38
PROBE	741-04	P9-FI-05	P9-20	743-08-02	DU-08	743-08	743-08	P9-03

a. Concentration estimates obtained from geophysical logging measurements can be significantly affected by heterogeneous subsurface conditions; values presented in this table should be viewed as *apparent* concentration.
b. Maximum observed value of radionuclide or element from all previous SDA logging.

NA = not applicable
ND = not detected
SDA = Subsurface Disposal Area

The cesium-cobalt peaks at 8 ft in Probehole T47-IF-1 and 7.5 ft in Probehole T47-IF-2 could correspond to a single radionuclide zone that lies between these two probes and corresponds exactly with a geophysical anomaly. The association between Cs-137 (a fission product) and Co-60 (an activation product) suggests fuel-related materials, though fuel specimens are unlikely, considering the lack of uranium peaks. It is worth noting that the cesium and cobalt peaks are well correlated (i.e., they increase and decrease in tandem). This pattern suggests that the radiation sources are cesium-contaminated metal objects rather than separate distributions of activated metals and fission products. In the latter case, cesium and cobalt peaks would not be expected to have such a high degree of correlation.

Figure 3-4 shows a comparison between probeholes T47-IF-1 and T47-IF-6. The thickness, magnitude, and depth of the cesium-cobalt radionuclide zone in Probehole T47-IF-6 are similar to counterparts observed in Probehole T47-IF-1, suggesting that both probes intersect a common radionuclide zone. Figure 3-5 shows a comparison between probeholes T47-IF-2 and T47-IF-5. Probeholes T47-IF-2 and T47-IF-5 show increasing cesium-cobalt levels at the deepest measurement point, suggesting that the radionuclide zone continues within the soil layer (or waste) beneath the probe. The apparent Cs-137 concentration of 17,184 pCi/g observed at the bottom of Probehole T47-IF-5 is the highest Cs-137 level observed anywhere during SDA Type A probehole logging.

Careful examination of Figure 3-3 shows that Probe T47-IF-5 is closer to the historic position of several NRF casks than is Probe T47-IF-2. One possible interpretation of the evidence is that the targeted geophysical anomaly is not associated with the NRF cask shipments, and that the historical records give an accurate depiction of the true shipment locations. In this case, the increased Cs-137 levels in Probe T47-IF-5 are interpreted as an indication that this probe is very close to an NRF shipment.

Azimuthal logging was performed at 8.0 and 10.0 ft in probeholes T47-IF-1 and T47-IF-2. Azimuthal data are presented in Section 4.5.

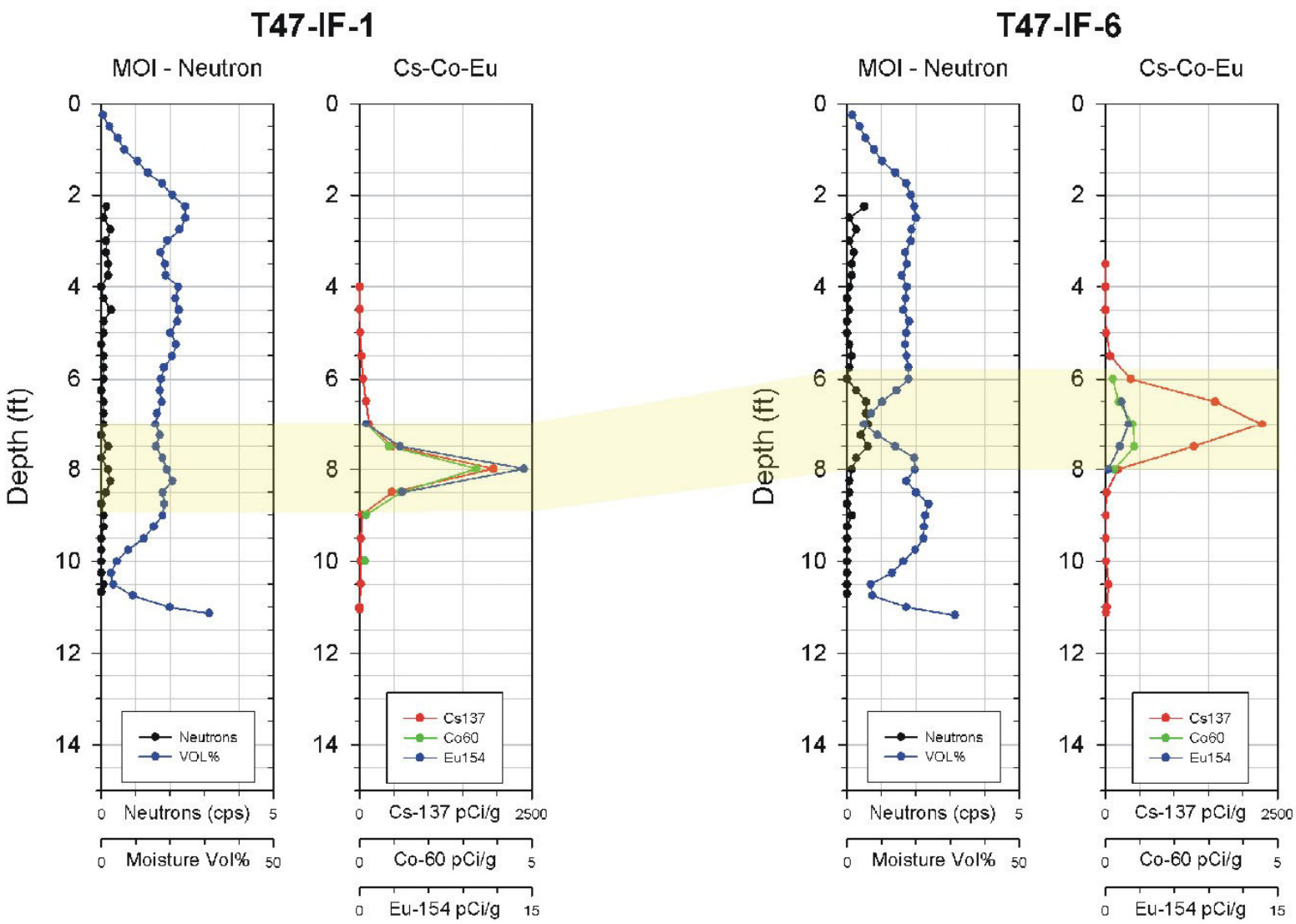

Figure 3-4. Comparison of selected logging results for probes T47-IF-1 and T47-IF-6.

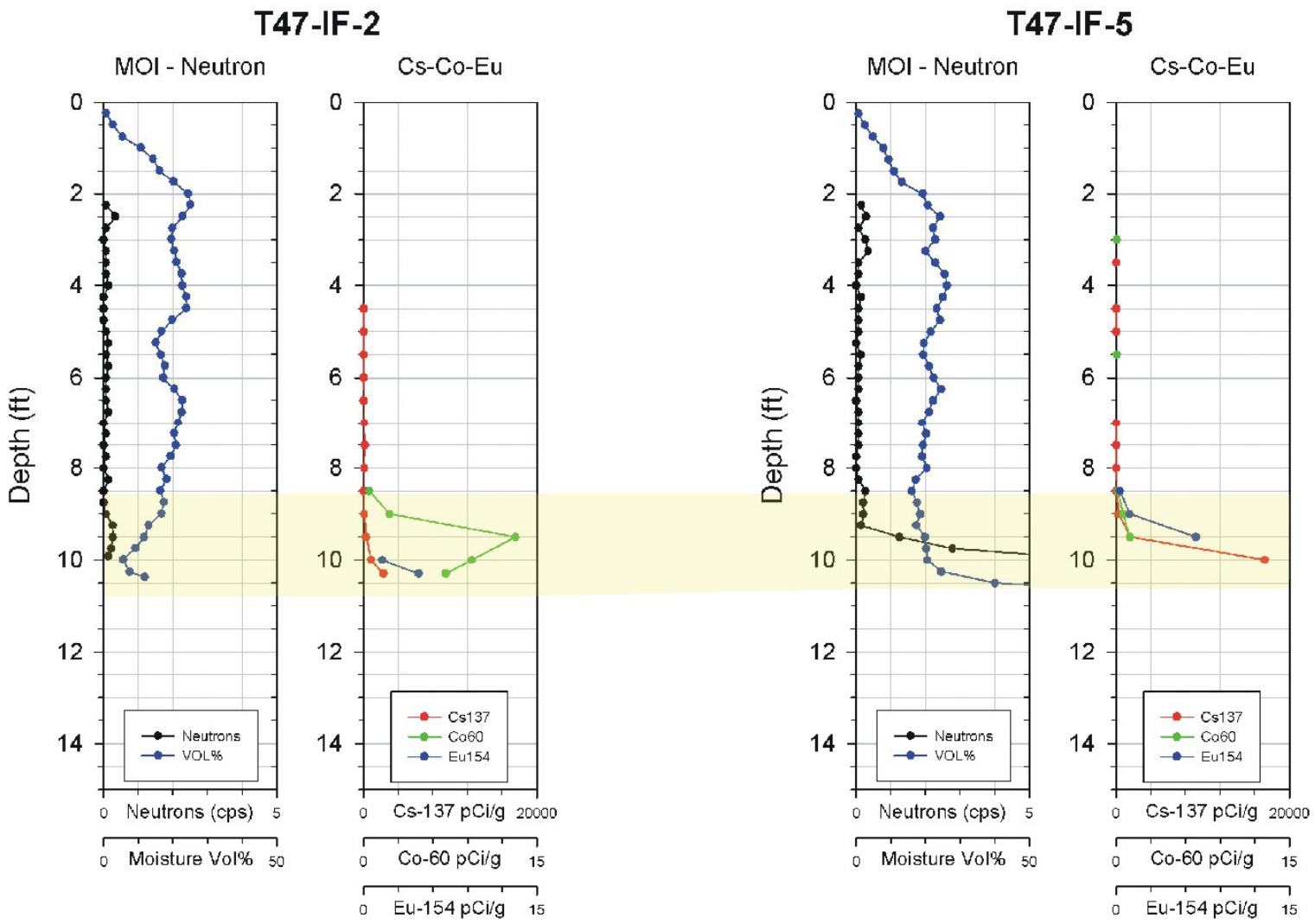

Figure 3-5. Comparison of selected logging results for probes T47-IF-2 and T47-IF-5.

3.4 Focus Area 1D: Undocumented Disposals

Nine probes were installed in Focus Area 1D to explore for undocumented waste disposals in the SDA (i.e., three in the north and six in the south part of the SDA) as shown in Figures 3-6a and 3-6b. Disposal records contain no additional information concerning possible characteristics of these disposals, if they exist. Focus Area 1D-north probes were installed into regions with elevated soil conductivity. Focus Area 1D-south probes were installed directly adjacent to areas suspected of containing buried metal. Table 3-7 provides the logging completion summary showing depth intervals logged for each Focus Area 1D probe. Table 3-8 provides the radionuclide detection summary for Focus Area 1D.

Table 3-7. Logging completion summary showing depth intervals logged for each Focus Area 1D probe.

	Passive Neutron		Passive Gamma		N-gamma		Moisture	
Well_ID	Minimum (ft bgs)	Maximum (ft bgs)	Minimum (ft bgs)	Maximum (ft bgs)	Minimum (ft bgs)	Maximum (ft bgs)	Minimum (ft bgs)	Maximum (ft bgs)
ID North								
UD-01	2.24	9.58	2.00	10.02	2.00	8.95	0.25	10.13
UD-03	2.25	3.65	2.00	4.04	2.00	3.03	0.25	4.13
UD-03B	2.25	13.84	2.00	14.22	2.00	13.22	0.25	14.33
ID South								
UD-04	2.25	13.40	2.00	13.86	2.00	12.81	0.25	13.91
UD-05	2.25	3.62	2.00	4.03	2.00	2.83	0.25	4.13
UD-05B	2.25	4.13	2.00	4.49	2.00	3.48	0.25	4.60
UD-05C	2.25	4.42	2.00	4.80	2.00	3.75	0.25	4.86
UD-05D	2.25	4.56	2.00	4.92	2.00	3.92	0.25	5.00
UD-05E	2.25	9.78	2.00	10.24	2.00	9.15	0.25	10.28

Table 3-8. Radionuclide detection summary for Focus Area 1D.[a]

Well_ID	Cs-137 662 keV (pCi/g)	Co-60 1,332 keV (pCi/g)	Pu-239 375 keV (pCi/g)	Am-241 662 keV (pCi/g)	Np-237 312 keV (pCi/g)	U-235 186 keV (pCi/g)	U-238 1,001 keV (pCi/g)	Chlorine 1,151 keV (counts/ second)
1D North								
UD-01	ND	ND	ND	ND	ND	ND	ND	2.3
UD-03	ND	ND	ND	ND	ND	ND	ND	ND
UD-03B	ND	ND	ND	ND	ND	ND	ND	1.1
1D South								
UD-04	42.1	157.7	ND	ND	ND	ND	ND	1.3
UD-05	ND	ND	ND	ND	ND	ND	ND	0.9
UD-05B	0.5	ND	ND	ND	ND	ND	ND	0.0
UD-05C	0.3	ND	ND	ND	ND	ND	ND	ND
UD-05D	0.4	ND	ND	ND	ND	ND	ND	ND
UD-05E	1.9	ND	ND	ND	ND	ND	ND	2.3
MAX[b]	140.5	814.2	194,171,000	30,449,000	4,881	344.9	220,894	38
PROBE	741-04	P9-FI-05	P9-20	743-08-02	DU-08	743-08	743-08	P9-03

a. Concentration estimates obtained from geophysical logging measurements can be significantly affected by heterogeneous subsurface conditions; values presented in this table should be viewed as *apparent* concentration.
b. Maximum observed value of radionuclide or element from all previous SDA logging.

NA = not applicable
ND = not detected
SDA = Subsurface Disposal Area

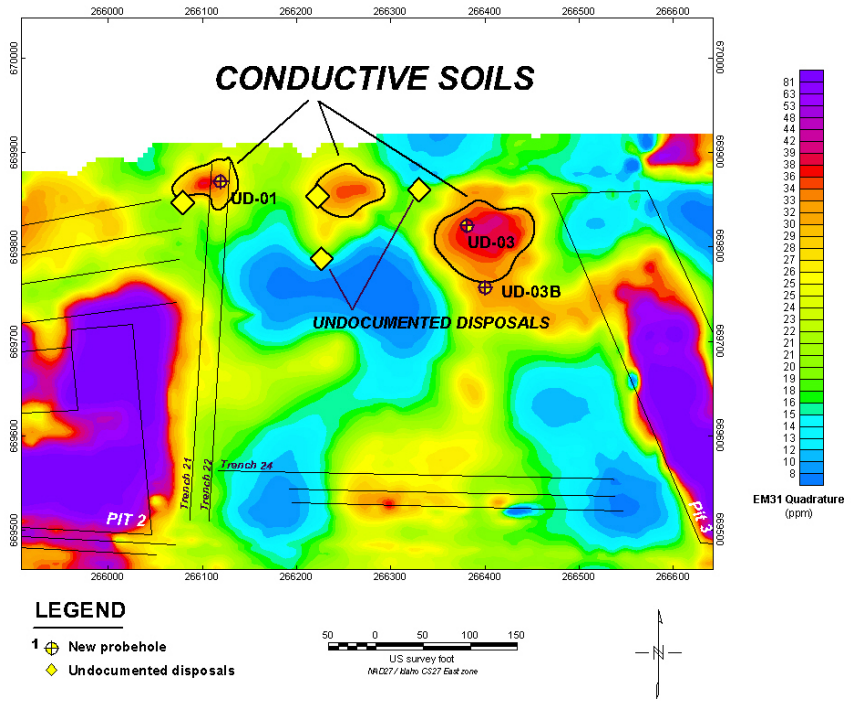

Figure 3-6a. Map showing the areas of conductive soil in Focus Area 1D-north.

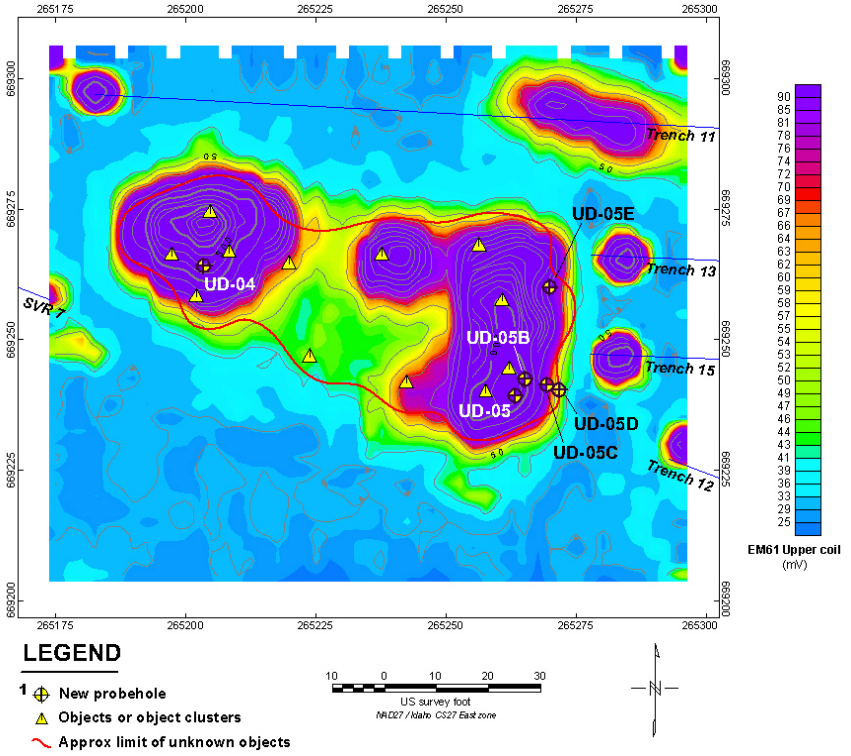

Figure 3-6b. Map showing the location of probes in Focus Area 1D-south.

Table 3-8 shows that no man-made radionuclides were detected within Focus Area 1D-north. Probe UD-03 only penetrated to 4 ft and may not be diagnostic of the subsurface conditions associated with this high soil-conductivity zone. Moisture data suggest a typical soil profile for all probes throughout the logged depths with no apparent presence of significant void space or man-made materials. Probehole UD-01 shows chlorine within the depth interval from 2.0–8.5 ft. Because chlorine has very seldom been detected by logging in clean overburden soils at the SDA, the chlorine indications in Probe UD-01 may be evidence for some type of undocumented disposal. Chlorine was also found at 12.0–12.5 ft in Probe UD-03B. If the elevated soil conductivity and chlorine are related, these data suggest the possible presence of a soluble chlorine compound.

Table 3-8 shows that Cs-137 was detected in five of the six Focus Area 1D-south probes. Low detection levels in the overburden fill soils (less than 5 ft) in probes UD-05B, UD-05C, UD-05D, and UD-05E suggest Cs-137 from nuclear testing fallout. These probes (as well as Probe UD-05) show no other evidence of man-made contaminants except for three low-level chlorine detections in Probe UD-05E and one low-level chlorine detection in Probe UD-05. Probes UD-05 through UD-05D met refusal at depths of 5 ft or less, which suggests the possibility that the probes encountered impenetrable man-made objects.

Cesium-137 and Co-60 were both detected at significant levels in Probe UD-04. The radionuclide zone occurs beneath a clean 5-ft overburden, and has sporadic associated chlorine. No increased neutron flux is observed. Overall, data suggest that Probe UD-04 penetrated a non-RFP radioactive waste disposal.

3.5 Focus Area 2: Naval Reactors Facility Liquid-Waste Disposals

Focus Area 2 targets are Trench 24 liquid-waste disposals associated with a diatomaceous absorbent material. Figure 3-7 shows the location of the targeted shipments and the four new probes, HAL1 through HAL4. Probes HAL1 and HAL2 penetrated 19–21 ft bgs. Probes HAL3 and HAL4, though located only 10–20 ft further east, penetrated only 8–12 ft bgs.

Tables 3-9 and 3-10 present summaries of the logged intervals and the detected contaminants for each of the Focus Area 2 probes. A logging-summary-data chart for each Focus Area 2 probe is included in Appendix B. Note that radionuclide levels are presented in units of activity concentration. These values should be understood as *apparent* concentrations, because the actual concentration is highly dependent on heterogeneity in the vicinity of the probehole.

No americium-neptunium-plutonium, uranium, or significant chlorine is observed in any of the Focus Area 2 probes. Cesium-137 is observed in all the probes, accompanied by Co-60 in probes HAL2 and HAL4. The total gamma activity observed in Probe HAL2 was sufficient to saturate the measurement system throughout an 8.5-ft depth interval such that no useful gamma ray data were obtained. The 8.5-ft depth interval showed elevated neutron flux, suggesting the possible presence of plutonium or americium, although these radionuclides could not be verified because of the high gamma activity.

The cesium-cobalt count rate in Probe HAL4 increases abruptly in the bottom few feet of the probe, suggesting that the radionuclide zone continues below the probe bottom. This may reflect contamination that has migrated into basalt or other hard layer beneath the waste zone, or it may mean that the probe struck impenetrable waste at the refusal depth. In either case, peak radionuclide level for these zones could not be determined.

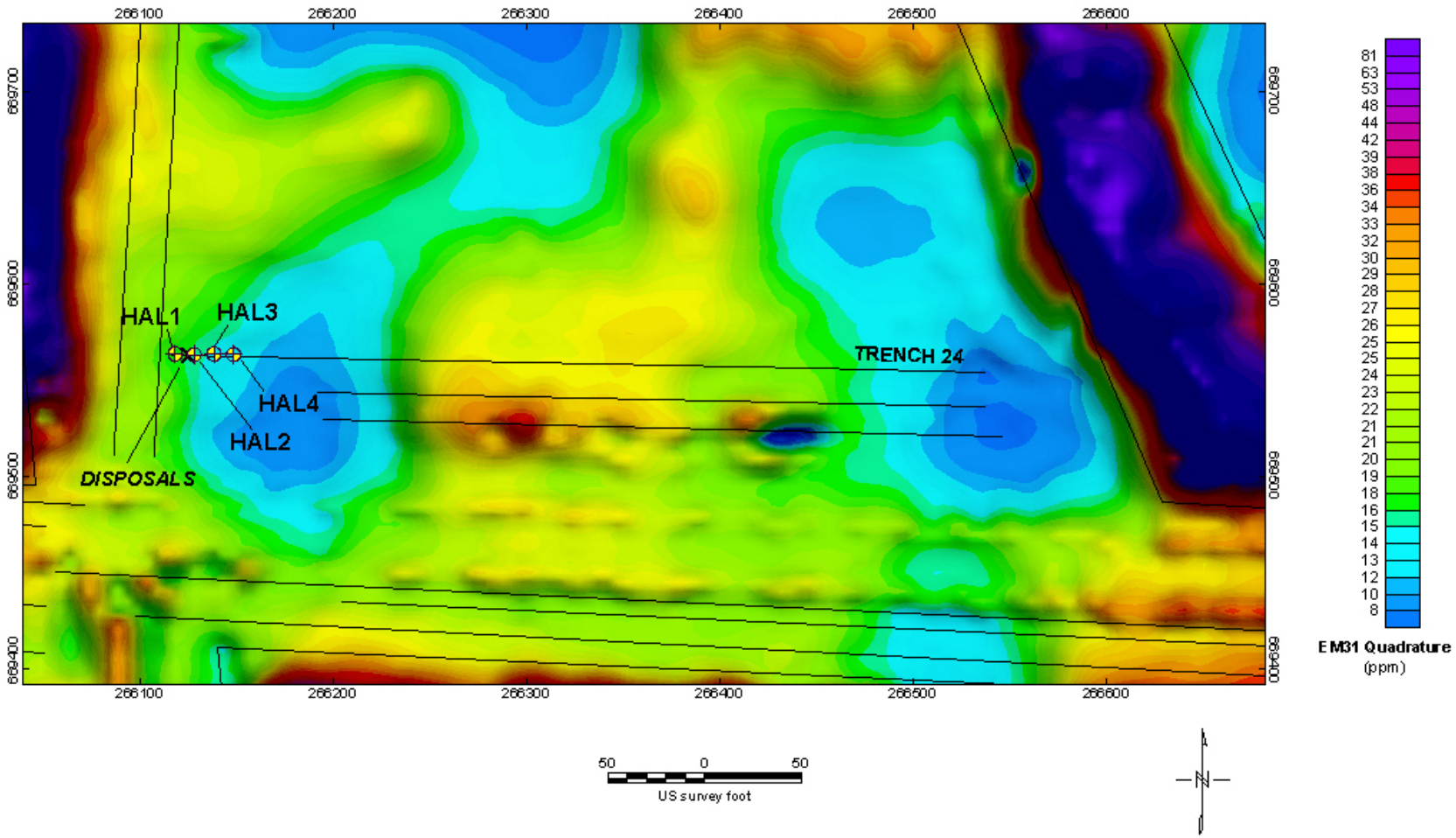

Figure 3-7. Map showing the location of probes HAL1 through HAL4 in Focus Area 2.

Table 3-9. Logging completion summary showing depth intervals logged for each Focus Area 2 probe.

	Passive Neutron		Passive Gamma		N-gamma		Moisture	
Well_ID	Minimum (ft bgs)	Maximum (ft bgs)	Minimum (ft bgs)	Maximum (ft bgs)	Minimum (ft bgs)	Maximum (ft bgs)	Minimum (ft bgs)	Maximum (ft bgs)
HAL1	2.25	19.21	2.00	19.65	2.00	18.58	0.25	19.68
HAL2	2.25	21.63	2.00	22.04	2.00	21.03	0.24	22.08
HAL3	2.25	7.76	2.00	8.16	2.00	7.06	0.25	8.18
HAL4	2.25	12.04	2.00	12.48	2.00	11.42	0.25	12.52

Table 3-10. Radionuclide detection summary for Focus Area 2D.[a]

Well_ID	Cs-137 662 keV (pCi/g)	Co-60 1,332 keV (pCi/g)	Pu-239 375 keV (pCi/g)	Am-241 662 keV (pCi/g)	Np-237 312 keV (pCi/g)	U-235 186 keV (pCi/g)	U-238 1,001 keV (pCi/g)	Chlorine 1,151 keV (counts/ second)
HAL1	0.3	ND	ND	ND	ND	ND	ND	0.6
HAL2	6,773.5	228.0	ND	ND	ND	ND	ND	1.0
HAL3	1.0	ND	ND	ND	ND	ND	ND	0.2
HAL4	240.7	45.8	ND	ND	ND	ND	ND	ND
MAX[b]	140.5	814.2	194,171,000	30,449,000	4,881	344.9	220,894	38
PROBE	741-04	P9-FI-05	P9-20	743-08-02	DU-08	743-08	743-08	P9-03

a. Concentration estimates obtained from geophysical logging measurements can be significantly affected by heterogeneous subsurface conditions; values presented in this table should be viewed as *apparent* concentration.
b. Maximum observed value of radionuclide or element from all previous SDA logging.

NA = not applicable
ND = not detected
SDA = Subsurface Disposal Area

Moisture logs for all four probes are very similar, suggesting a common soil and waste environment with depth throughout the probe area. This observation provides no explanation for the large difference in refusal depth for probes HAL3 and HAL4 compared with probes HAL1 and HAL2.

Azimuthal logging was performed at 12.0 and 21.0 ft in probes HAL2 and HAL4, respectively. Azimuthal data are presented in Section 4.5.

3.6 Focus Area 3: Pit 5 Rocky Flats Plant Plutonium and Enriched Uranium Waste

Eight probes were installed in Focus Area 3 within portions of Pit 5 believed to contain RFP waste (see Figure 3-8). Target shipments consisted of 55-gal drums containing RFP Building 776 waste, RFP Building 881 waste, and graphite waste. These shipments could potentially contain highly enriched uranium or Pu-239.

Tables 3-11 and 3-12 present summaries of the logged intervals and detected contaminants for each of the Focus Area 3 probes. A logging data summary chart for each Focus Area 3 probe is included in Appendix B. Note that radionuclide levels are presented in units of activity concentration. These values should be understood as *apparent* concentrations because the actual concentration is highly dependent on heterogeneity in the vicinity of the probehole.

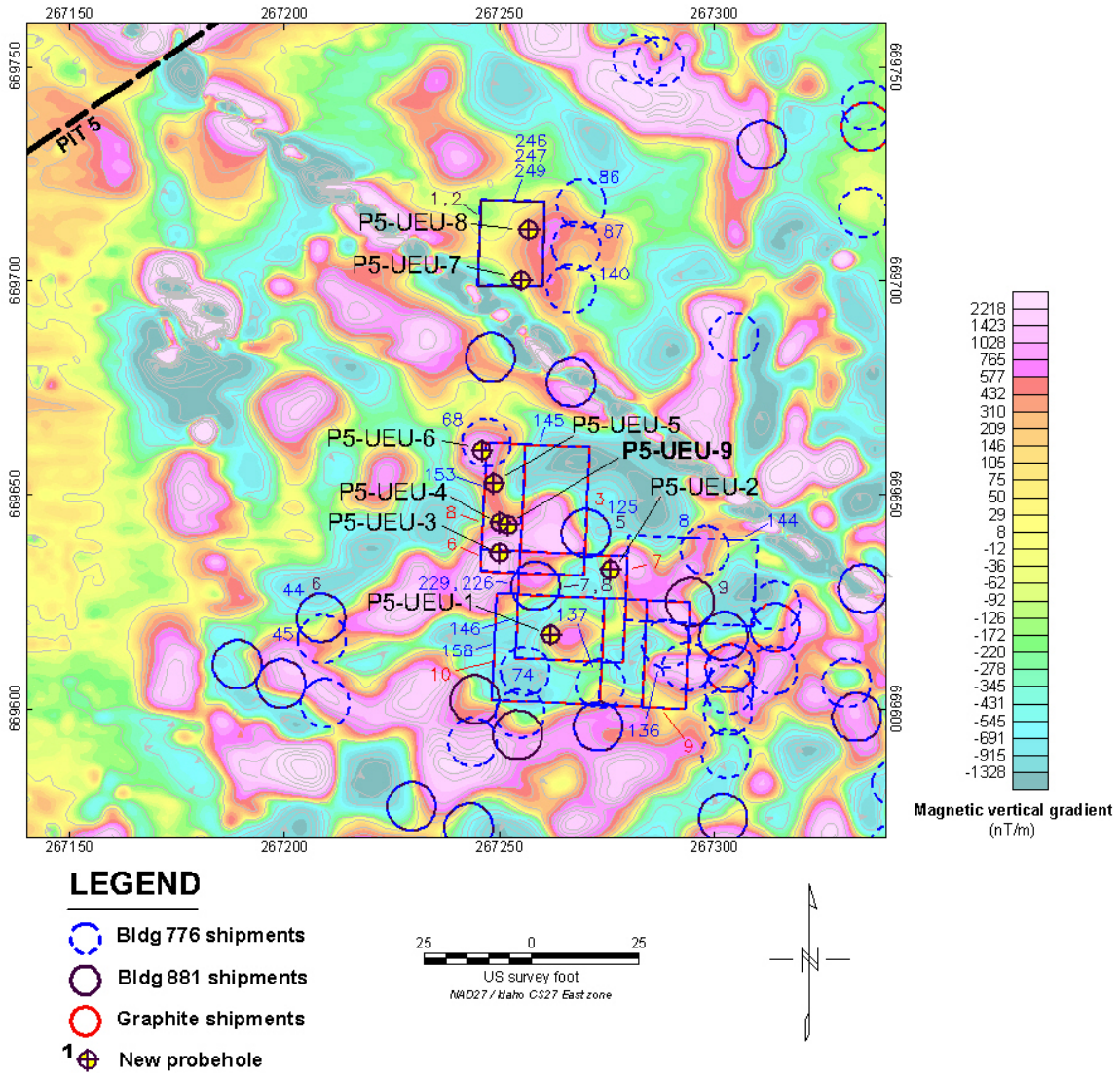

Figure 3-8. Map showing the location of Focus Area 3.

Table 3-11. Logging completion summary showing depth intervals logged for each Focus Area 3 probe.

	Passive Neutron		Passive Gamma		N-gamma		Moisture	
Well_ID	Minimum (ft bgs)	Maximum (ft bgs)	Minimum (ft bgs)	Maximum (ft bgs)	Minimum (ft bgs)	Maximum (ft bgs)	Minimum (ft bgs)	Maximum (ft bgs)
P5-UEU-1	4.24	17.60	4.00	18.11	4.00	17.12	0.25	18.16
P5-UEU-2	4.23	17.30	4.00	17.76	4.00	16.68	0.25	17.75
P5-UEU-3	4.24	15.24	4.00	15.74	4.00	14.66	0.25	15.80
P5-UEU-4	4.25	16.80	4.00	17.27	4.00	16.18	0.25	17.29
P5-UEU-5	4.25	15.26	4.00	15.70	4.00	14.66	0.25	15.79
P5-UEU-6	4.24	15.06	4.00	15.51	3.98	14.46	0.25	15.57
P5-UEU-7	4.25	16.19	4.00	16.64	4.00	15.54	0.25	16.71
P5-UEU-8	4.25	11.26	4.00	11.72	4.00	10.64	0.25	11.74
P5-UEU-9	4.25	16.78	4.00	17.13	4.00	16.10	4.25	17.27

Table 3-12. Radionuclide detection summary for Focus Area 3.[a]

WELL_ID	Cs-137 662 keV (pCi/g)	Co-60 1,332 keV (pCi/g)	Pu-239 375 keV (pCi/g)	Am-241 662 keV (pCi/g)	Np-237 312 keV (pCi/g)	U-235 186 keV (pCi/g)	U-238 1,001 keV (pCi/g)	Chlorine 1,151 keV (counts/ second)
P5-UEU-1	ND	0.3	3,074,661.0	1,370,885.8	12.2	ND	ND	38.7
P5-UEU-2	ND	ND	1,272,732.6	4,350,311.1	52.5	ND	363.8	4.9
P5-UEU-3	ND	ND	5,330,961.1	1,668,578.2	21.4	10.5	940.6	20.4
P5-UEU-4	ND	ND	31,924,850.6	8,106,524.5	96.5	26.4	2,102.5	34.6
P5-UEU-5	ND	ND	3,214,037.3	6,104,438.0	87.7	109.3	32,920.6	1.9
P5-UEU-6	ND	ND	2,399,686.7	4,285,269.1	62.3	ND	63.4	5.2
P5-UEU-7	ND	ND	11,800,803.1	2,759,951.1	26.4	2.8	ND	24.2
P5-UEU-8	ND	ND	219,000.5	387,750.5	ND	ND	29.1	6.2
P5-UEU-9	ND	ND	1,491,067.5	2,098,481.9	32.5	ND	1,274.2	10.1
MAX[a]	140.5	814.2	194,171,000	30,449,000	4,881	344.9	220,894	38
PROBE	741-04	P9-FI-05	P9-20	743-08-02	DU-08	743-08	743-08	P9-03

a. Concentration estimates obtained from geophysical logging measurements can be significantly affected by heterogeneous subsurface conditions; values presented in this table should be viewed as *apparent* concentration.
b. Maximum observed value of radionuclide or element from previous SDA logging.

NA = not applicable
ND = not detected
SDA = Subsurface Disposal Area

All nine Study Area 3 probes encountered high levels of americium, neptunium, and plutonium. Although higher levels of americium, neptunium, and plutonium have been observed in some other SDA probes, the Focus Area 3 americium-neptunium-plutonium radionuclide zone is unique because the very high radiation levels are sustained over a thick interval, with peaks at about 8–9 and 13-15 ft bgs. Very high chlorine peaks also are observed. The americium-neptunium-plutonium, uranium, and chlorine contamination zones are closely correlated and give the general impression of two vertically stacked waste zones. The similarity between logging results for these probes is somewhat surprising because the probes are scattered along nearly 100 ft of Pit 5, and are associated with several distinctly separate geophysical anomalies.

Elevated thorium is observed to coincide with some, but not all, americium-neptunium-plutonium peaks. Elevated thorium has been observed in logging data elsewhere in the SDA, but the source and significance of this phenomenon is not known (see Appendix C). The only plausible thorium series decay disequilibrium that could account for the observed discrepancy is an excess of Th-228 relative to Th-232. Separation of Th-228 from Th-232 in the subsurface by geochemical processes is too improbable to consider, so mechanisms other than decay of Th-232 that could produce thorium-series nuclides below Ac-228 were investigated. An example is alpha decay of U-232 to Th-228. None of the mechanisms produce detectable gamma rays, so the passive gamma ray spectra do not contain information that can confirm or rule out such processes.

All probes, except Probe P5-UEU-1, contain U-238, U-235, or both uranium isotopes. Table 3-13 gives the U-235:U-238 activity ratios and mass ratios at each point where both U-235 and U-238 were detected. These ratios have not been corrected for differential gamma ray attenuation, but are suggestive of depleted or natural uranium. The single exception is near the bottom of Probe P5-UEU-7, where U-235 was detected without U-238. The U-235 in this probe was just above the minimum detection level. Note that the “natural” uranium observed in Probe P5-UEU-5 (see KUT chart for Probe P5-UEU-5 in Appendix B) is also elevated, suggesting that, at least for Probe P5-UEU-5, uranium could occur in the form of uranium ore or other uranium material from early in the fuel-production cycle.

Table 3-13. Summary of uranium detection in Focus Area 3.[a]

Well_ID	Depth (ft)	U-235[b] 0186-keV (pCi/g)	U-238 1,001-keV (pCi/g)	Activity Ratio[b] U-235:U-238	Mass Ratio[b] U-235:U-238
P5-UEU-3	13.0	10.5	883.4	0.019	0.0018
P5-UEU-3	13.5	7.6	940.6	0.008	0.0013
P5-UEU-4	13.0	15.7	1,436.3	0.011	0.0017
P5-UEU-4	14.0	25.3	1,933.1	0.013	0.0020
P5-UEU-4	13.5	26.4	2,102.5	0.013	0.0020
P5-UEU-5	10.5	14.5	2,236.6	0.006	0.0010
P5-UEU-5	11.0	30.4	2,354.0	0.013	0.0020
P5-UEU-5	10.0	33.6	6,530.2	0.005	0.0008
P5-UEU-5	9.5	63.0	13,968.6	0.005	0.0007
P5-UEU-5	9.0	109.3	30,933.9	0.004	0.0005
P5-UEU-5	8.5	75.9	32,920.6	0.002	0.0004
P5-UEU-7	14.5	2.8	ND	No value	No value

a. Concentration estimates obtained from geophysical logging measurements can be significantly affected by heterogeneous subsurface conditions; values presented in this table should be viewed as *apparent* concentration.
b. U-235 apparent concentrations not corrected for potential Ra-226 interference.
c. The following are derived from constants obtained from GE (1989): (1) typical activity ratios: <0.04507 (depleted), 0.04507 (natural), >0.04507 (enriched); (2) typical mass ratios: <0.00696 (depleted), 0.00696 (natural), >0.00696 (enriched).

ND = nondetect

Figure 3-9 shows a comparison between probeholes P5-UEU-4 and P5-UEU-9. Logging data from Probehole P5-UEU-4 suggest two distinct waste streams: an upper waste stream from 8.5–11 ft characterized by high plutonium-americium-neptunium and chlorine and a lower waste stream from 11–14 ft dominated by americium-neptunium with only minor plutonium and chlorine. The interval from 9–10.5 ft in Probehole P5-UEU-9 exhibits plutonium-americium-neptunium-chlorine characteristics similar to the upper waste stream in Probehole P5-UEU-4, but at lower levels. This waste stream could be continuous between these probes. The lower waste stream in Probehole P5-UEU-4 has no clear counterpart in Probehole P5-UEU-9, and does not appear to be continuous between the two probes. These two probes are located only 2.0 ft apart. The ambiguous correlation between logging data over this short distance provides an excellent illustration of the apparent heterogeneity of the waste zone.

Azimuthal logging was conducted in probeholes P5-UEU-1 (10 depths), P5-UEU-4 (two depths), P5-UEU-5 (three depths) and P5-UEU-7 (five depths). Azimuthal data are presented in Section 4.5.

3.7 Focus Area 4: Pit 10 Plutonium Waste (741-08 Probe Cluster)

Four new probes (i.e., 741-10, 741-11, 741-08C, and 741-08D) were installed in Focus Area 4 to assist in the interpretation of results from previously installed Type A probes (i.e., 741-08, 741-08A, and 741-08B) and Type B lysimeters (i.e., 741-8-L1 and 741-8-L2) in Pit 10 (see Figure 3-10). The previously installed probes indicated at least two separate sources of plutonium, but the location and extent of these sources could not be determined. The new probes provided additional information about the distribution of plutonium sources.

Tables 3-14 and 3-15 present summaries of the logged intervals and the detected radionuclides for each of the Focus Area 4 probes. A logging data summary chart for each Focus Area 4 probe is included in Appendix B. Note that radionuclide levels are presented in units of activity concentration. These values should be understood as *apparent* concentrations, because the actual concentration is highly dependent on heterogeneity in the vicinity of the probehole.

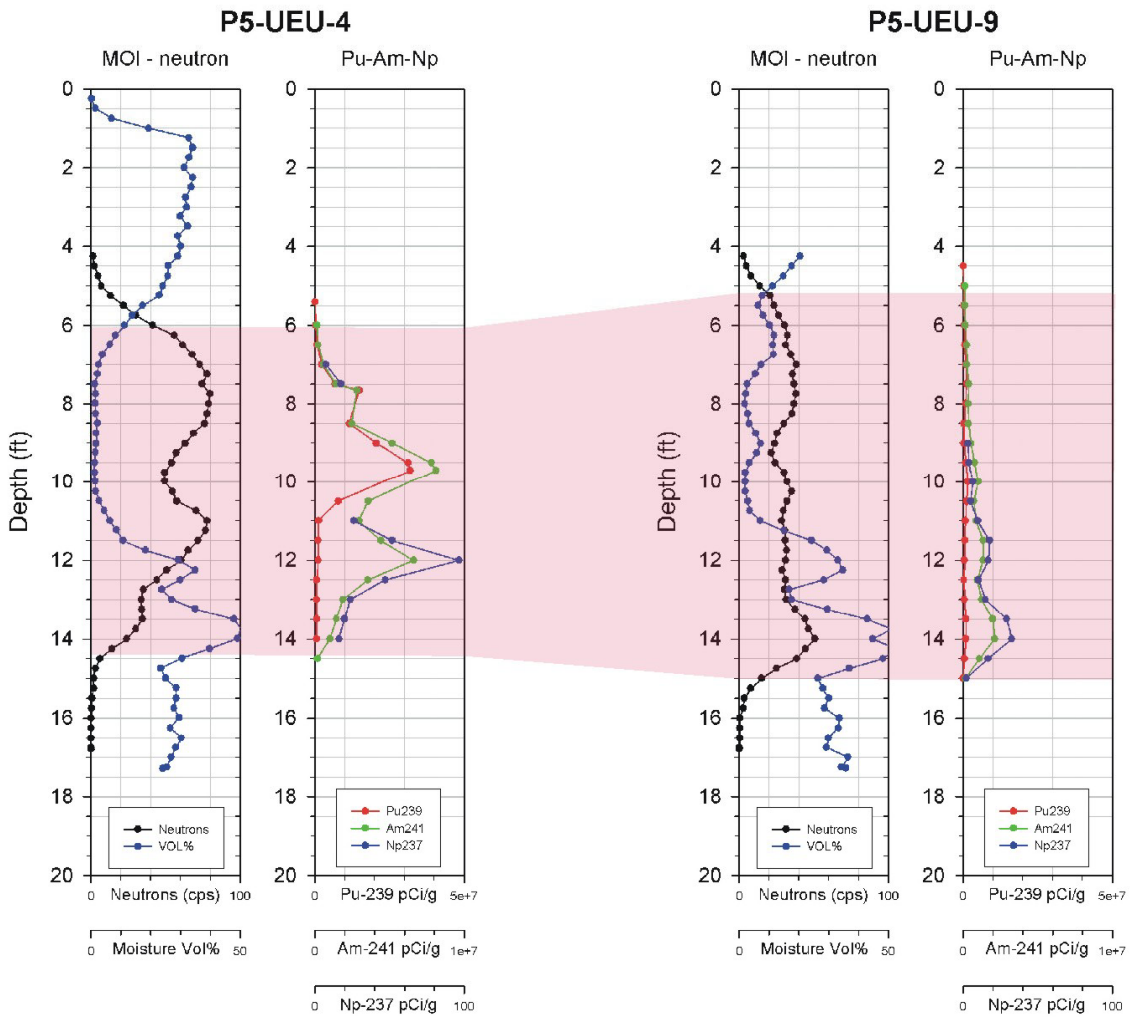

Figure 3-9. Comparison of selected logging results for probes P5-UEU-4 and P5-UEU-9.

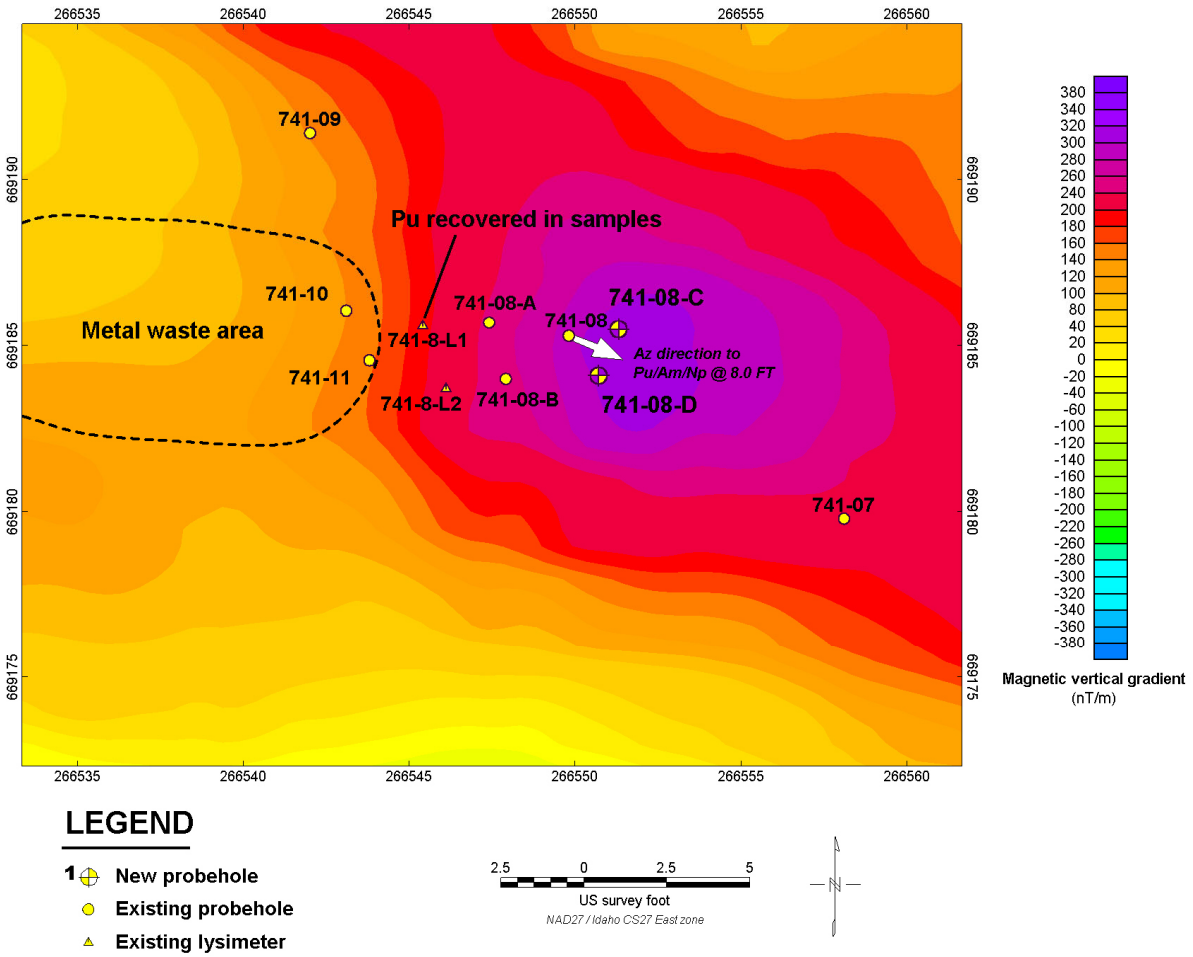

Figure 3-10. Map showing the location of lysimeters and probes in Focus Area 4.

Table 3-14. Logging completion summary showing depth intervals logged for each Focus Area 4 probe.

	Passive Neutron		Passive Gamma		N-gamma		Moisture	
Well_ID	Minimum (ft bgs)	Maximum (ft bgs)	Minimum (ft bgs)	Maximum (ft bgs)	Minimum (ft bgs)	Maximum (ft bgs)	Minimum (ft bgs)	Maximum (ft bgs)
741-08C	4.25	21.23	4.00	21.71	3.98	20.64	0.25	21.74
741-08D	4.26	18.33	4.00	18.80	3.99	17.75	0.05	18.80
741-10	4.24	19.20	4.00	19.67	4.00	18.56	0.25	19.69
741-11	4.25	19.32	4.00	19.73	4.00	18.66	0.25	19.76

Table 3-15. Radionuclide detection summary for Focus Area 4.[a]

Well_ID	Cs-137 662 keV (pCi/g)	Co-60 1,332 keV (pCi/g)	Pu-239 375 keV (pCi/g)	Am-241 662 keV (pCi/g)	Np-237 312 keV (pCi/g)	U-235 186 keV (pCi/g)	U-238 1,001 keV (pCi/g)	Chlorine 1,151 keV (counts/ second)
741-08C	ND	ND	462,187.1	6,064,204.2	56.4	ND	ND	6.4
741-08D	2.6	ND	ND	ND	134.5	ND	406.4	4.8
741-10	ND	ND	ND	ND	ND	173.1	174.6	10.5

Table 3-15. (continued).

Well_ID	Cs-137 662 keV (pCi/g)	Co-60 1,332 keV (pCi/g)	Pu-239 375 keV (pCi/g)	Am-241 662 keV (pCi/g)	Np-237 312 keV (pCi/g)	U-235 186 keV (pCi/g)	U-238 1,001 keV (pCi/g)	Chlorine 1,151 keV (counts/ second)
741-11	ND	ND	ND	ND	ND	12.0	74.8	6.1
MAX[b]	140.5	814.2	194,171,000	30,449,000	4,881	344.9	220,894	38
PROBE	741-04	P9-FI-05	P9-20	743-08-02	DU-08	743-08	743-08	P9-03

a. Concentration estimates obtained from geophysical logging measurements can be significantly affected by heterogeneous subsurface conditions; values presented in this table should be viewed as *apparent* concentration.
b. Maximum observed value of radionuclide or element from previous SDA logging.

NA = not applicable
ND = not detected
SDA = Subsurface Disposal Area

3.7.1 Investigation of Plutonium in Lysimeters L1 and L2

Lysimeters L1 and L2 and Type A Probe 741-08 showed evidence for the presence of plutonium. Probes 741-08A and 741-08B, installed between the lysimeters and Probe 741-08, showed no evidence for plutonium, suggesting that the plutonium observed in Probe 741-08 was most likely not the source of plutonium found in the lysimeter samples. Therefore, new probes (i.e., 741-10 and 741-11) were installed on the opposite side of the lysimeters, in the direction of a geophysical anomaly that could indicate the presence of buried drum-waste, to explore for an alternative plutonium source. These probes showed no evidence of plutonium.

The new probes show low-level U-235 and U-238 intervals. Table 3-16 gives the U-235:U-238 activity ratios and mass ratios at each point where both U-235 and U-238 were detected. These ratios have not been corrected for differential gamma ray attenuation, but are suggestive of enriched uranium. In addition to the measurements shown in Table 3-16, 15 additional measurements showed detection of U-235 with no corresponding detection of U-238. Note that low levels of U-235 (and no U-238) were also detected in probes 741-08A and 741-08B.

Table 3-16. Summary of uranium detection in Focus Area 4.[a]

Well_ID	Depth (ft)	U-235[a] 186-keV (pCi/g)	U-238 1,001-keV (pCi/g)	Activity Ratio[c] U-235:U-238	Mass Ratio[c] U-235:U-238
741-10	13.0	7.04	59.24	0.019	0.0185
741-11	11.5	12.01	64.44	0.186	0.0290
741-11	11.0	6.67	74.83	0.089	0.0139
741-10	11.5	107.07	118.48	0.904	0.1406
741-10	12.0	173.12	148.62	1.16	0.1812
741-10	12.5	38.22	174.60	0.219	0.0340

a. Concentration estimates obtained from geophysical logging measurements can be significantly affected by heterogeneous subsurface conditions; values presented in this table should be viewed as *apparent* concentration.
b. U-235 apparent concentrations not corrected for potential Ra-226 interference.
c. The following are derived from constants obtained from GE (1989): (1) typical activity ratios: <0.04507 (depleted), 0.04507 (natural), >0.04507 (enriched); (2) typical mass ratios: <0.00696 (depleted), 0.00696 (natural), >0.00696 (enriched)

Moderate chlorine levels and elevated Th-228 also are observed in both probes. The chlorine and thorium intervals coincide with and overlap the uranium interval.

3.7.2 Investigation of Plutonium in Probe 741-08

Azimuthal logging in Probe 741-08 indicated that the plutonium source observed in this probe was located to the east-southeast at 8 ft bgs. This radionuclide zone also contained Am-241 and Np-237. New probes (i.e., 741-08C and 741-08D) were installed in this direction to investigate the extent of plutonium.

Figure 3-11 shows a comparison between probeholes 741-08, 741-08C, and 741-08D. These plots show evidence that the americium-neptunium-plutonium zone in Probe 741-08 extends toward Probe 741-08C, but not toward Probe 741-08D. The radionuclide zone observed in Probe 741-08C has depth and thickness similar to its counterpart in Probe 741-08; however, the apparent Pu-239 and Np-237 concentrations are nearly an order of magnitude lower. The apparent Am-241 concentrations for the two probes are comparable. This circumstance suggests that the plutonium and neptunium are directly associated with each other in the waste form, but are not directly associated with the americium.

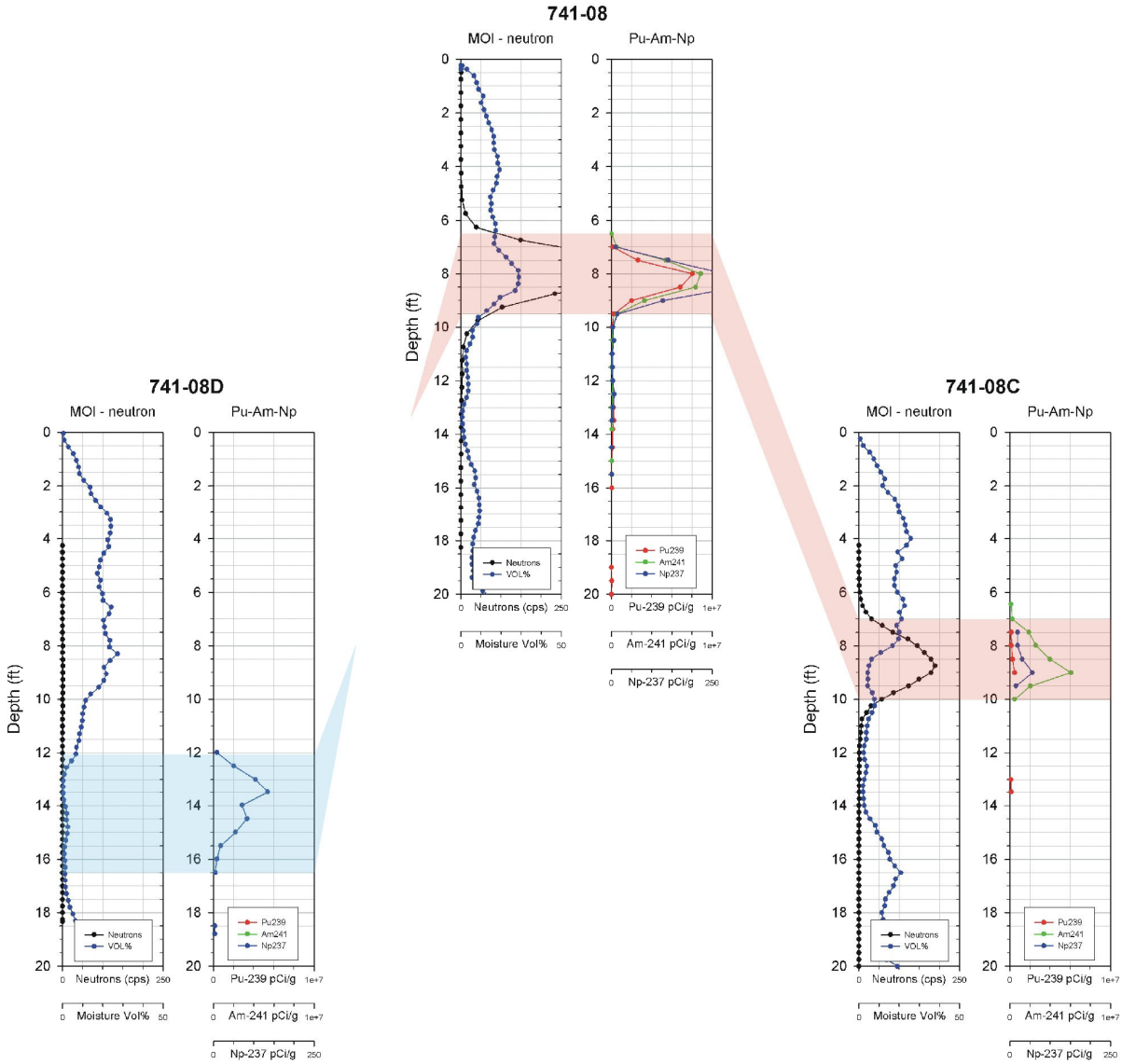

Figure 3-11. Comparison of selected logging results for probeholes 741-08, 741-08C, and 741-08D.

3.8 Focus Area 5: Pit 6 Plutonium Waste from the Rocky Flats Plant

Focus Area 5 targets are RFP drum shipments in Pit 6 suspected to contain plutonium-contaminated waste. Three probes were installed based on the combined evaluation of inventory records and surface geophysics (see Figure 3-12). Probes P6-PU-1 and P6-PU-2 were installed to a depth of 20.0 ft. Probe P6-PU-3 met refusal at 8.0 ft, where it is suspected to have struck impenetrable waste. Moisture data at the bottom of Probe P6-PU-3 suggest a waste zone beginning at 7.5-8.0 ft bgs.

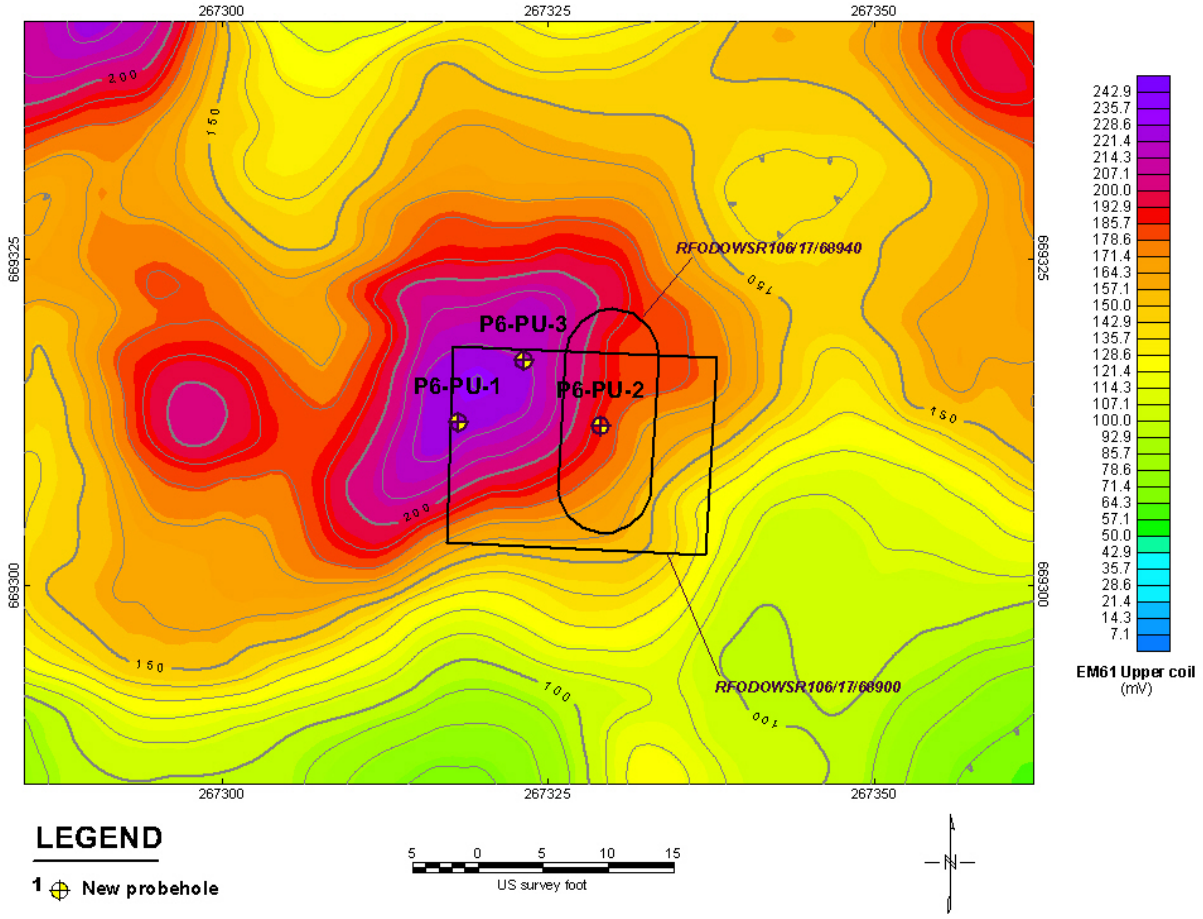

Figure 3-12. Map showing the location of Focus Area 5.

Tables 3-17 and 3-18 present summaries of the logged intervals and the detected contaminants for each Focus Area 5 probe. A logging data summary chart for each Focus Area 5 probe is included in Appendix B. Note that radionuclide levels are presented in units of activity concentration. These values should be understood as *apparent* concentrations, because the actual concentration is highly dependent on heterogeneity in the vicinity of the probehole.

Table 3-17. Logging completion summary showing depth intervals logged for each Focus Area 5 probe.

	Passive Neutron		Passive Gamma		N-gamma		Moisture	
Well_ID	Minimum (ft bgs)	Maximum (ft bgs)	Minimum (ft bgs)	Maximum (ft bgs)	Minimum (ft bgs)	Maximum (ft bgs)	Minimum (ft bgs)	Maximum (ft bgs)
P6-PU-1	4.25	19.59	4.00	19.92	4.00	18.82	0.25	19.92
P6-PU-2	4.25	19.43	4.00	20.06	4.00	19.02	0.25	20.05
P6-PU-3	4.25	7.38	4.00	7.80	4.00	6.74	0.25	7.88

Table 3-18. Radionuclide detection summary for Focus Area 5.[a]

Well_ID	Cs-137 662 keV (pCi/g)	Co-60 1,332 keV (pCi/g)	Pu-239 375 keV (pCi/g)	Am-241 662 keV (pCi/g)	Np-237 312 keV (pCi/g)	U-235 186 keV (pCi/g)	U-238 1,001 keV (pCi/g)	Chlorine 1,151 keV (counts/ second)
P6-PU-1	ND	ND	7,943,767.1	42,117,789.8	593.7	ND	573.8	5.3
P6-PU-2	ND	ND	1,590,915.7	1,129,598.6	12.1	ND	28.1	2.8
P6-PU-3	ND	ND	1,234,124.6	551,023.7	8.1	ND	ND	ND
MAX[b]	140.5	814.2	194,171,000	30,449,000	4,881	344.9	220,894	38
PROBE	741-04	P9-FI-05	P9-20	743-08-02	DU-08	743-08	743-08	P9-03

a. Concentration estimates obtained from geophysical logging measurements can be significantly affected by heterogeneous subsurface conditions; values presented in this table should be viewed as *apparent* concentration.
b. Maximum observed value of radionuclide or element from previous SDA logging.

NA = not applicable
ND = not detected
SDA = Subsurface Disposal Area

Probes P6-PU-1 and P6-PU-2 encountered high levels of americium, neptunium, and plutonium. Probe P6-PU-1 log data indicate the highest apparent Am-241 concentration observed anywhere in SDA logging to date. Uranium-238 and chlorine were observed to be sporadically associated with the americium-neptunium-plutonium radionuclide zones.

The apparent presence of a thick soil layer beneath the waste in probes P6-PU-1 and P6-PU-2 offers an opportunity to evaluate the possible migration of radionuclides into the underburden. Therefore, several long-count measurements were conducted in the underburden of these probes. The long-count data show that migration of radionuclides into underburden soils is very limited. Section 4.4 contains a further discussion of long-count data results.

Azimuthal logging was conducted in probeholes P6-PU-1 (seven depths), P6-PU-2 (six depths), and P6-PU-3 (one depth). Azimuthal data are presented in Section 4.5.

3.9 Focus Area 6: Pit 10 Plutonium Waste

Focus Area 6 probe targets are RFP drum shipments in Pit 10 suspected to contain plutonium contaminated waste. Three probes were installed based on combined evaluation of inventory records and surface geophysics (see Figure 3-13). Probes P10-PU-1 and P10-PU-2 met refusal at 5.5 and 10.0 ft respectively. Probe P10-PU-3 was installed to nearly 21.0 ft. These circumstances suggest that probe P10-PU-1 and P10-PU-2 may have struck impenetrable waste.

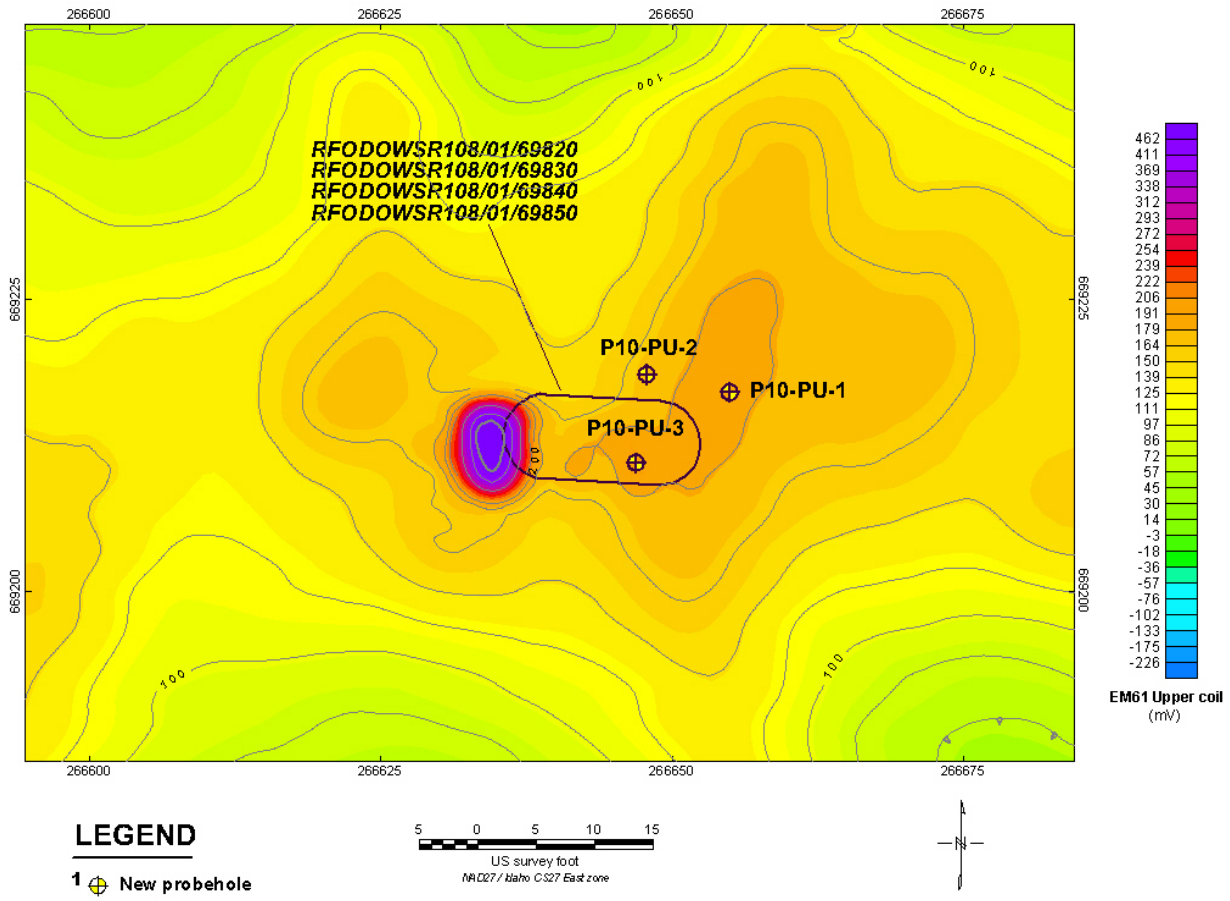

Figure 3-13. Map showing location of Focus Area 6 probes.

Tables 3-19 and 3-20 present summaries of the logged intervals and the detected contaminants for each of the Focus Area 6 probes. A logging data summary chart for each Area 6 probe is included in Appendix B. Note that radionuclide levels are presented in units of activity concentration. These values should be understood as *apparent* concentrations, since the actual concentration is highly dependent on heterogeneity in the vicinity of the probehole.

Table 3-19. Logging completion summary showing depth intervals logged for each Focus Area 6 probe.

	Passive Neutron		Passive Gamma		N-gamma		Moisture	
Well_ID	Minimum (ft bgs)	Maximum (ft bgs)	Minimum (ft bgs)	Maximum (ft bgs)	Minimum (ft bgs)	Maximum (ft bgs)	Minimum (ft bgs)	Maximum (ft bgs)
P10-PU-1	4.24	5.10	4.00	5.54	4.00	4.48	0.25	5.58
P10-PU-2	4.24	9.60	4.00	10.07	4.00	8.97	0.25	10.10
P10-PU-3	4.25	19.86	4.00	20.31	4.00	19.26	0.24	20.50

Table 3-20. Radionuclide detection summary for Focus Area 6.[a]

Well_ID	Cs-137 662 keV (pCi/g)	Co-60 1,332 keV (pCi/g)	Pu-239 375 keV (pCi/g)	Am-241 662 keV (pCi/g)	Np-237 312 keV (pCi/g)	U-235 186 keV (pCi/g)	U-238 1,001 keV (pCi/g)	Chlorine 1,151 keV (counts/ second)
P10-PU-1	ND	ND	ND	ND	ND	ND	ND	1.3
P10-PU-2	ND	ND	ND	ND	ND	ND	ND	14.6
P10-PU-3	ND	ND	21,301.0	ND	ND	ND	ND	8.7
MAX[b]	140.5	814.2	194,171,000	30,449,000	4,881	344.9	220,894	38
PROBE	741-04	P9-FI-05	P9-20	743-08-02	DU-08	743-08	743-08	P9-03

a. Concentration estimates obtained from geophysical logging measurements can be significantly affected by heterogeneous subsurface conditions;
values presented in this table should be viewed as *apparent* concentration.
b. Maximum observed value of radionuclide or element from previous SDA logging.

NA = not applicable
ND = not detected
SDA = Subsurface Disposal Area

No man-made radionuclides were detected in any of the Focus Area 6 probes, except for one low-level Pu-239 detection in Probe P10-PU-3. All three probes showed the presence of low-to-moderate levels of chlorine.

3.10 Focus Area 7: Pit 2 Concentrated Rocky Flats Plant Drums

Focus Area 7 targets are plutonium-contaminated graphite molds in Pit 2. Pit 2 inventory records were first evaluated to identify waste shipments that could potentially contain graphite molds. Search criteria were:

- Generator: Building 776
- Waste type: Type 5 (noncombustible)
- Weight: approximately 200 lb.

Figure 3-14 shows two areas found to contain the largest concentration of drums meeting the search criteria, using inventory data. Historical documents indicate that Pit 2 waste drums were carefully stacked in rows rather than randomly dumped as in later SDA disposal operations. The final position of the probes was adjusted to coincide with strong anomalies observed in surface geophysics data. These anomalies were interpreted to show the position of buried drums. Figure 3-14 also shows targeted drum concentrations, surface geophysics (magnetic field data), and the installed position of the six Pit 2 probes.

The probes were installed during December 2003, and the driller observed that the probes did not go in as smoothly as others have in the past. The drilling process experienced numerous stops and starts, suggesting alternating harder and softer zones in the subsurface. The driller also indicated that a screeching sound of metal on metal was heard during each probe installation.

Tables 3-21 and 3-22 present summaries of the logged intervals and the detected contaminants for each of the Focus Area 7 probes. A logging data summary chart for each Focus Area 7 probe is included in Appendix B. Note that radionuclide levels are presented in units of activity concentration. These values should be understood as *apparent* concentrations, because the actual concentration is highly dependent on heterogeneity in the vicinity of the probehole.

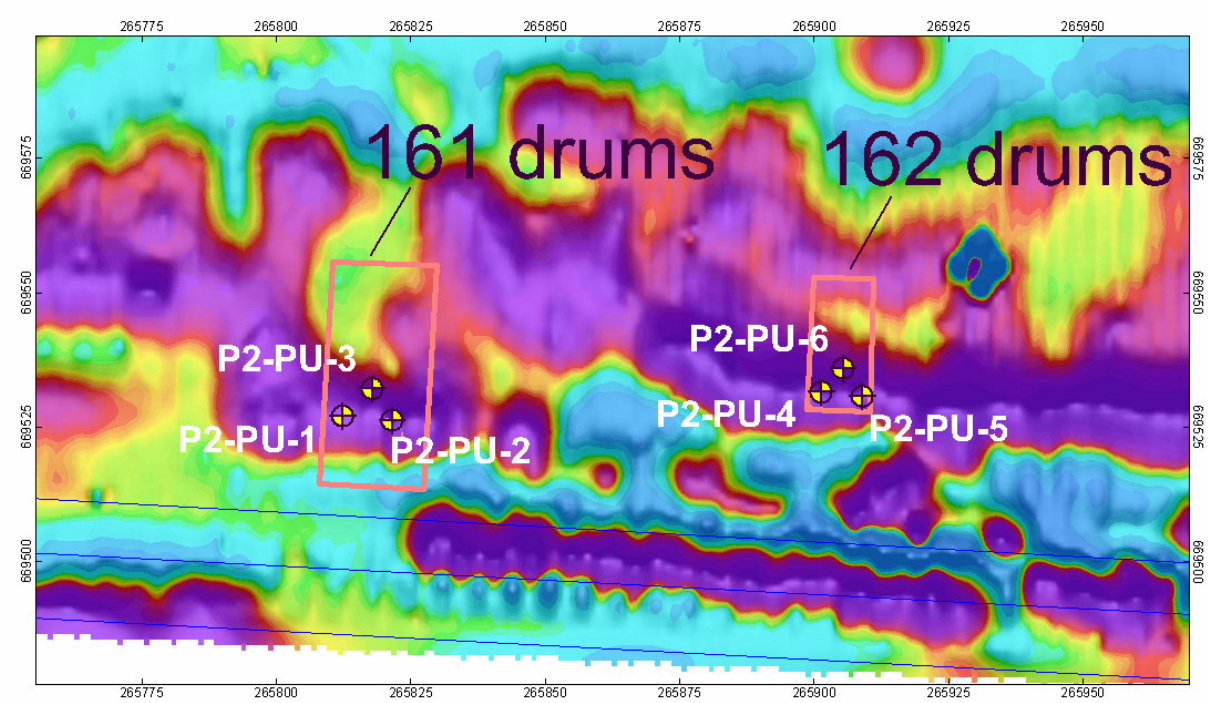

Figure 3-14. Targeted drum concentrations, surface geophysics (magnetic field data), and the installed position of the six Pit 2 probes.

Table 3-21. Logging completion summary for the new Pit 2 probes.

	Passive Neutron		Passive Gamma		N-gamma		Moisture	
Well_ID	Minimum (ft bgs)	Maximum (ft bgs)	Minimum (ft bgs)	Maximum (ft bgs)	Minimum (ft bgs)	Maximum (ft bgs)	Minimum (ft bgs)	Maximum (ft bgs)
P2-PU-1	9.76	18.09	2.00	18.47	2.00	17.49	0.25	18.61
P2-PU-2	2.25	13.83	2.00	14.29	2.00	13.14	0.25	14.33
P2-PU-3	11.25	20.14	2.00	20.52	2.00	19.46	0.25	20.59
P2-PU-4	4.25	12.18	2.00	12.63	2.00	11.58	0.25	12.66
P2-PU-5	2.25	12.04	2.00	12.49	2.00	11.45	0.25	12.52
P2-PU-6	2.25	14.62	2.00	15.11	2.00	14.00	0.25	15.13

Table 3-22. Radionuclide detection summary for Focus Area 7.[a]

Well_ID	Cs-137 662 keV (pCi/g)	Co-60 1,332 keV (pCi/g)	Pu-239 375 keV (pCi/g)	Am-241 662 keV (pCi/g)	Np-237 312 keV (pCi/g)	U-235 186 keV (pCi/g)	U-238 1,001 keV (pCi/g)	Chlorine 1,151 keV (counts/ second)
P2-PU-1	ND	ND	46,366,044.4	13,049,853.1	ND	6.3	ND	3.9
P2-PU-2	ND	ND	3,298,986.8	3,417,208.1	ND	ND	ND	5.7
P2-PU-3	ND	ND	ND	ND	ND	ND	2,216.8	2.2
P2-PU-4	ND	ND	330,830.6	120,077.6	ND	200.6	82,055.1	2.3
P2-PU-5	ND	ND	2,138,749.9	665,430.0	ND	78.8	21.8	13.6
P2-PU-6	ND	ND	2,046,223.8	607,892.8	ND	330.1	482.2	6.7

Table 3-22. (continued).

Well_ID	Cs-137 662 keV (pCi/g)	Co-60 1,332 keV (pCi/g)	Pu-239 375 keV (pCi/g)	Am-241 662 keV (pCi/g)	Np-237 312 keV (pCi/g)	U-235 186 keV (pCi/g)	U-238 1,001 keV (pCi/g)	Chlorine 1,151 keV (counts/ second)
MAX[a]	140.5	814.2	194,171,000	30,449,000	4,881	344.9	220,894	38
PROBE	741-04	P9-FI-05	P9-20	743-08-02	DU-08	743-08	743-08	P9-03

a. Concentration estimates obtained from geophysical logging measurements can be significantly affected by heterogeneous subsurface conditions; values presented in this table should be viewed as *apparent* concentration.
b. Maximum observed value of radionuclide or element from previous SDA logging.

NA = not applicable
ND = not detected
SDA = Subsurface Disposal Area

Moisture logs for these six probes show a dramatic decrease in soil moisture at depths from 3.5–7 ft bgs. The sudden decrease in the moisture log is believed to mark the transition from soil overburden into the underlying solid waste. Pit 2 moisture logs are somewhat unique in that the moisture log reading drops very nearly to zero and sustains near-zero readings over significant depth intervals. Probe P2-PU-3 exhibits the single exception to this pattern. This moisture log characteristic suggests a thick consistent waste zone that may exist because the drums are stacked, and little or no soil is between the stacked drums. Moisture curves for probes P2-PU-4, P2-PU-5, and P2-PU-6 also show a steep increase in overburden soil moisture content that reaches 50%, which may be due to the geomembrane on the surface. The base of the waste zone varies from 12.4–14 ft bgs.

Logging data show that Pit 2 probes penetrated zones with significant plutonium and americium. The measured plutonium levels in Probe P2-PU-1 are among the highest observed anywhere in the SDA. (Note that only probes P9-20, 743-12, and DU-15 showed higher apparent plutonium levels.) The zones with plutonium and americium occupy only a portion of the waste intervals (i.e., significant portions of the waste zones show no man-made radionuclides). Zones contaminated with U-235 and/or U-238 are observed in four of the six probes. Levels of U-238 in Probe P2-PU-4 are among the highest observed anywhere in the SDA. Ratios of U-235:U-238 in probes P2-PU-3 and P2-PU-4 suggest depleted uranium, and the ratios in P2-PU-5 and P2-PU-6 suggest enriched uranium (see Table 3-22). The zones containing uranium generally occur at distinctly different depths than the zones containing americium and plutonium. Also, some of the radionuclide zones occur in discrete 2-ft intervals, which are interpreted to correspond with individual drums.

Chlorine is prevalent throughout the waste layer, as is the case shown by most SDA probes that have been logged to date. Chlorine levels are moderate to low compared with results from other SDA probes.

Probes P2-PU-1, P2-PU-2, P2-PU-3, and P2-PU-5 show anomalously high levels of natural uranium.[a] Probes P2-PU-3 and P2-PU-4 show anomalously high levels of natural thorium. Dr. C. Koizumi of Stoller observed and discussed these anomalous peaks (see Appendix C) for probe P2-PU-3. He concludes that the thorium anomaly almost certainly points to Th-228 enrichment. One possible mechanism is alpha decay of U-232, but this could not be verified. Dr Koizumi suggests that the apparent excess of natural uranium is consistent with uranium mill tailings or concentrated radium. Neither possibility could be readily verified (see Appendix C).

a. Natural uranium is identified based on 1,764 keV gamma rays from the uranium daughter, Bi-214; man-made uranium is identified based on the 1,001 keV gamma rays emitted by the uranium daughter, Pa-234m.

4. OTHER ANALYSES

4.1 Evaluation of Logging Tool Calibration

During FY 2004, the probing project evaluated the calibration methodology used for converting Type A nuclear logging measurements into quantitative estimates of radionuclide concentration. This section provides a brief synopsis of that evaluation. For more details, refer to the complete report entitled *Evaluation of Nuclear Logging Tool Calibrations for Use in Type A Probes at the Idaho National Engineering and Environmental Laboratory Subsurface Disposal Area* (Giles, Josten, and Broomfield 2003).

4.1.1 Report Summary

This section explores the usefulness of recalibrating logging tools used during Type A probing investigations conducted within the SDA. In particular, limitations of the existing method of calibrating passive gamma ray tools are examined in detail to assess the cause of uncertainty in quantitative results.

The response of the passive gamma ray tool is known to depend on many factors, but the three most important are (1) the amount of radionuclide source present, (2) geometry of the radionuclide source distribution (i.e., anywhere between a compact point source and a homogenous distribution), and (3) density of the waste and soil matrix surrounding the source. Modeling exercises show that these three factors have roughly equal influence on the logging-tool response. As a consequence, the logging data cannot provide an unequivocal estimate for one factor unless the other factors are known. The existing calibration method handles this problem by making simplifying assumptions for the source geometry and soil-matrix density such that the third factor, the amount of radionuclide, can be estimated directly.

Radionuclide estimates produced by the existing calibration methodology have very limited utility because the underlying uniformity assumptions are indefensible. Inventory records, waste drum scan records, and logging data all indicate highly heterogeneous conditions within SDA waste. Furthermore, no known methods will independently measure the waste and soil matrix density. This section considers alternative methods for gamma ray tool calibration and data processing that acknowledge these limitations.

The proposed method would permit some non-TRU areas[b] to be directly identified from logging data, which may have some utility for remedial decision-making. However, this information could only be achieved at a very high monetary cost for probe installation, downhole logging, and data processing. The method is conservative by design, and therefore, would produce a large number of false-positive errors where non-TRU areas are incorrectly classified as TRU waste. Furthermore, no allowance is made for exotic conditions that could cause false-negative errors where TRU waste is incorrectly classified as non-TRU.

Finally, alternative radiation measurement technologies were investigated to determine their applicability for differentiating TRU waste. Several large-area, long-count-time detectors were considered for deployment on the SDA ground surface. As a class, these tools were found to have no utility at the SDA because of the limited penetration of alpha particles, gamma rays, and neutrons through soil. Emerging-technology radiation-logging tools may significantly improve sensitivity to radionuclides, thus allowing for much faster field operations. However, the new tools will suffer from the same ambiguity

---

b. Transuranic areas are defined as areas having greater than or equal to 100 nCi/g combined activity from all man-made alpha-emitting radionuclides with a mass number greater than 235 and half lives greater than 20 years.

issues that affect existing logging tools (i.e., uncertainties about source geometry and density of the soil and waste matrix).

4.2 Comparison of Moisture Sampling and Logging Data

4.2.1 Report Conclusions and Recommendations

Because of heterogeneous conditions in the SDA subsurface, most, if not all, Type A probeholes violate the spectral gamma ray logging tool calibration conditions that assume homogenous radionuclide distribution and homogenous waste and soil matrix density. Recalibration of the spectral gamma ray tool to a new standard condition is not recommended because no meaningful standard exists for radionuclide distribution or waste and soil matrix density. Furthermore, information concerning radionuclide distribution and waste and soil matrix density cannot be obtained by any known independent measurement method. Consequently, the spectral gamma ray measurements cannot be meaningfully corrected for heterogeneity.

An alternative approach to calibration and processing of Type A logging data was developed with the sole purpose of screening the subsurface for non-TRU waste. To implement this method, a set of standard conditions is defined under which a subsurface volume surrounded by probes may be categorized as either non-TRU or possible-TRU. Possible-TRU areas are subjected to additional processing steps by which some may be recategorized as non-TRU.

By the proposed method, subdivision of the entire SDA into non-TRU and possible-TRU subvolumes can be achieved. However, the method requires the installation, logging, and analysis of approximately 15,600 Type A probes per acre. Furthermore, both false-positive errors (non-TRU waste categorized as possible-TRU) and false-negative errors (TRU waste categorized as non-TRU) are possible. The proportion of the two error types depends on the choice of standard conditions. For example, if standard conditions are chosen conservatively, many false-negatives may be avoided, but a large number of false-positives will be generated.

Alternative radiation measurement technologies were investigated to determine their applicability for differentiating TRU waste. Several large-area, long-count-time detectors were considered for deployment on the SDA ground surface. As a class, these tools were found to have no utility at the SDA because of the limited penetration of alpha particles, gamma rays, and neutrons through soil. New emerging radiation logging tools may be very useful for TRU differentiation if employed in a high probe-density survey as described in the Giles, Josten, and Broomfield (2003) report. The primary benefit of these tools will be improved speed of operation. As proposed, the new tools implement more sophisticated data acquisition and processing schemes and may, therefore, produce more detailed radionuclide and elemental information that would provide additional constraints on three-dimensional modeling. However, these tools will not significantly improve the ability to directly identify non-TRU waste, because they will suffer from the same uncertainties about source geometry and density of the soil and waste matrix.

Despite the difficulties (improbabilities) associated with calibrating the tools for quantitative purposes, the existing data set and any logging data gathered in the future may be used qualitatively in identifying waste types, and waste zone composition, and in providing information directing quantitative investigations.

4.3 Comparison of Moisture Sampling and Logging Data in Focus Area 3

New neutron-neutron moisture logging data for Focus Area 3 were obtained in the shallow vadose zone (i.e., less than 20 ft) of the SDA during August and September 2003. The Type A neutron-neutron logging tool reports moisture content in excess of 30 volume percent (vol%) for Focus Area 3 probes P5-UEU-1, P5-UEU-3, P5-UEU-4, P5-UEU-5, P5-UEU-6, and P5-UEU-8. These moisture-content readings occur within the first few feet of the subsurface, despite the excessively dry summer conditions and long-term drought that has affected southeast Idaho. The readings are also anomalously high compared with other SDA probes including nearby probes in Pit 5 (see Figures 4-1 and 4-2).

4.3.1 Density Effect on Moisture Logging Data

The logging subcontractor made no density correction to the moisture data. However, their vendor data submittals discuss the density effect on moisture logging. In general, if the density of the formation is greater than the calibration density, the actual moisture vol% is less than the measured value. Moisture data for Focus Area 3 exhibits the opposite case (i.e., anomalously high moisture contents). Soil density in the UEU-probe area would have to be anomalously low for density effects to have produced anomalously high moisture contents. This seems implausible, because the probes in questions are located on a roadway and have been compacted by vehicle traffic over many years. Furthermore, it is physically impossible that densities could be low enough to change apparent moisture content by 10 vol% or more. Therefore, it is unlikely that the observed high moisture contents in the UEU probes are caused by density effects.

4.3.2 Field Verification of the Moisture Tool Calibration

The moisture logging tool that produced the new data was calibrated at Hanford by the logging subcontractor; however, no field results check had ever been performed. For this reason, a small soil-sampling effort was initiated to provide an independent evaluation of the tool performance and calibration.

Three locations were selected for soil sampling adjacent to Type A probes, HAL1, UD-01, and P5-UEU-4, representing low, medium, and high soil moisture respectively. Soil samples were collected within 6 in. of the probe locations, on the southwest side of the probe, at depths of 1.0, 2.0, and 3.0 ft bgs. Samples were analyzed on a gravimetric basis, using ASTM D2216-98, “Standard Test Method for Laboratory Determination of Water (Moisture) Content of Soil and Rock by Mass.”

Soil-sampling results in weight percent (wt%) are listed in Table 4-1, along with a computed value for the corresponding vol% to facilitate comparison with moisture-logging data. The conversion between wt% and vol% depends on the soil dry-bulk density, which was taken as 1.44 g/cc based on previous SDA soil sample data (McElroy and Hubbell 1990).

Figure 4-3 compares the soil-sample results with the moisture logging data for each probe. In general, the agreement between the two methods is good. Both data sets show the same trend of low, medium, and high soil moisture for the three probes. Small discrepancies occur at specific measurement points, but these may be attributed to various factors such as density variation, sampling location, or sampling effects. Overall, the sampling results validate the performance and calibration of the moisture logging tool. Additional information concerning the soil moisture-sampling program is provided in Appendix E.

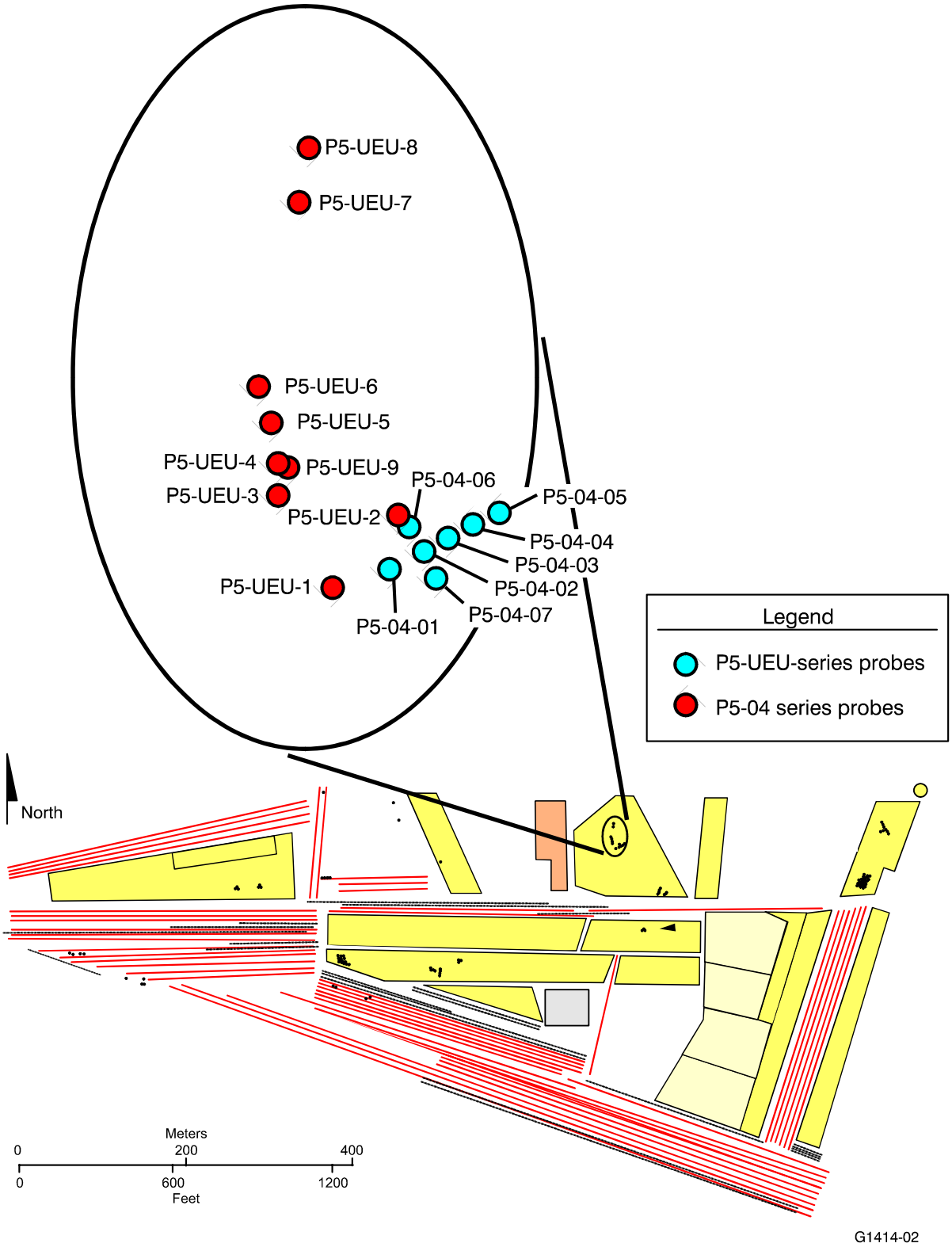

Figure 4-1. Sketch map showing location of Pit 5 P5-UEU-series and P5-04-series Type A probes.

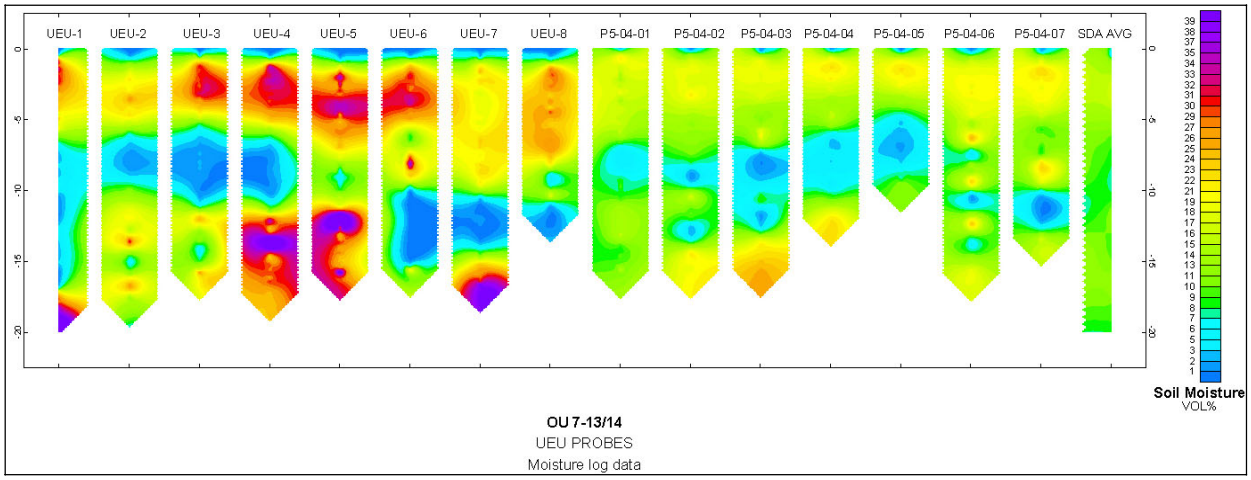

Figure 4-2. Diagram showing the depth variation of neutron-neutron soil moisture readings for the Pit 5 UEU-series and P5-04-series Type A probes.

Table 4-1. Summary of sampling and logging results. Sample volume percent values calculated assuming soil dry-bulk density of 1.44 g/cc.

Well_ID	Sample_ID	Depth	Wt%	Vol%[a]	Log Vol%
P5-UEU-4	SMV00601M7	1	19.5	28.1	19.2
P5-UEU-4	SMV00701M7	2	22.2	32.0	32.2
P5-UEU-4	SMV00801M7	3	24.5	35.3	32.0
UD-01	SMV00301M7	1	13.4	19.3	16.2
UD-01	SMV00401M7	2	16.6	23.9	22.2
UD-01	SMV00501M7	3	19.3	27.8	22.3
HAL1	SMV00001M7	1	8.4	12.1	7.0
HAL1	SMV00101M7	2	7.9	11.4	8.5
HAL1	SMV00201M7	3	6.8	9.8	11.5

a. Volume percent based on a dry bulk density of 1.4 g/cc (McElroy and Hubbell 1990).

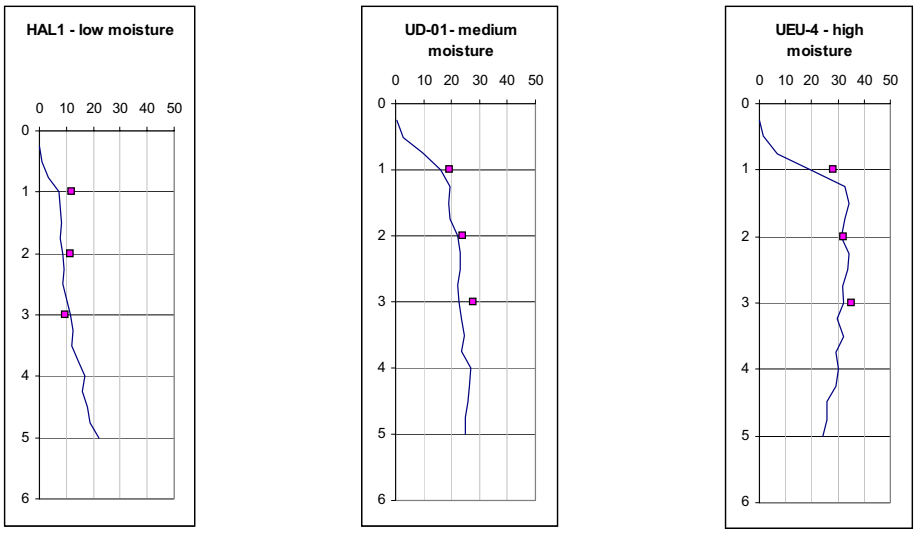

Figure 4-3. Comparison of neutron-neutron moisture logs (curves) and soil moisture sampling results (square point data for three depth locations for each of three probes). Sampling data were converted from weight percent to volume percent based on an assumed dry bulk density of 1.44 g/cc.

4.4 Results from the Long-count Gamma Ray Study

Four 3,000-second long-count spectral gamma ray measurements were performed during December 2003: two in Probehole P6-PU-1 and two in Probehole P6-PU-2. Ten 8-hour long-count measurements were performed in January 2004: five in Probehole P6-PU-1 and five in Probehole P6-PU-2. Measurements were performed within underburden soils beneath the waste zone. The purpose of the long-count measurements was to detect low-level radionuclides, which would indicate the downward migration of radionuclides from the waste zone into the soil. A comparison of the theoretical detection limits for these count times is given in Table 4-2.

Table 4-2. Comparison of theoretical detection limits for count times.

Radionuclide	Energy (keV)	Detection Limit at 300 Seconds[a] (pCi/g)	Detection Limit at 3,000 Seconds[b] (pCi/g)	Detection Limit at 8 Hours[b] (pCi/g)
Np-237	312	1	0.32	0.10
Pu-239	375	25,000	7,906	2,552
Am-241	662	43,000	13,598	4,389
Am-241	722	90,000	28,460	9,186
U-238	1,001	10	3.16	1.02

a. Based on minimum detection levels calculated for low-level radionuclide zones in Probehole P6-PU-1.
b. Scaled based on square root of count time.

4.4.1 Three-thousand-second Long-count Results

Figure 4-4a shows a detail of the depth range from 12–16 ft in Probehole P6-PU-1. The waste and soil interface is interpreted to occur at about 14 ft. Two 3,000-second measurements were conducted in soil just below the bottom of waste at 14.5 and 15.5 ft. Plutonium-239, Np-237, and U-238 were detected at 14.5 ft, but were not detected at 15.5 ft. Americium-241 was detected at both 14.5 ft and 15.5 ft, but the Am-241 apparent concentration decreases to just above the 3,000-second detection limit at 15.5 ft. These results suggest that contaminant migration into soils beneath the waste zone is extremely limited.

Figure 4-4b shows a detail of the waste and soil interface in Probehole P6-PU-2. The waste and soil interface is interpreted to occur near 14.5 ft. Low levels of Am-241, Pu-239, and U-238 were detected at 15.0 ft. No radionuclides were detected at 16.0 ft. As for Probehole P6-PU-1, these data suggest that contaminant migration into underburden soils is very limited.

Appendix D contains the subcontractor report describing data processing for the 3,000-second long-count measurements. Plots showing the long-count data are included in Appendix B.

4.4.2 Eight-hour Long-count Results

Five 8-hour long-count measurements were performed in Probehole P6-PU-2 (i.e., at depths of 14.5, 15.0, 15.5, 16.0, 20.06 ft), and five 8-hour long-count measurements were performed in Probehole P6-PU-1 (i.e., at depths of 14.5, 15.0, 15.5, 16.0, and 19.92 ft). The 8-hour long-count data support the conclusions determined from the 3,000-second data (i.e., that contaminant migration into underburden soils is very limited).

Appendix D contains the subcontractor report describing data processing for the 8-hour long-count measurements. Plots showing the long-count data are included in Appendix B.

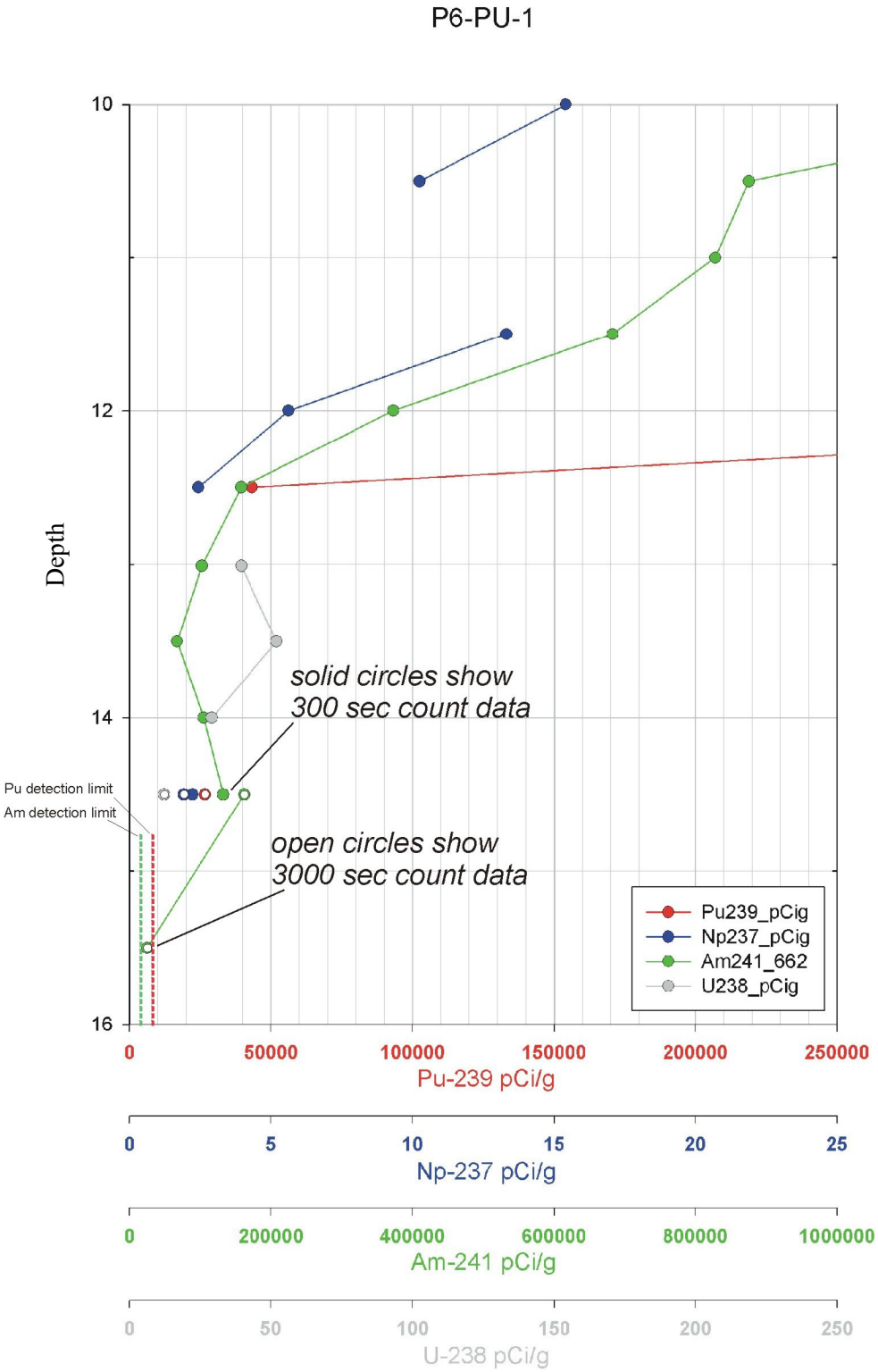

Figure 4-4a. Detail of the depth range from 12–16 ft in Probehole P6-PU-1.

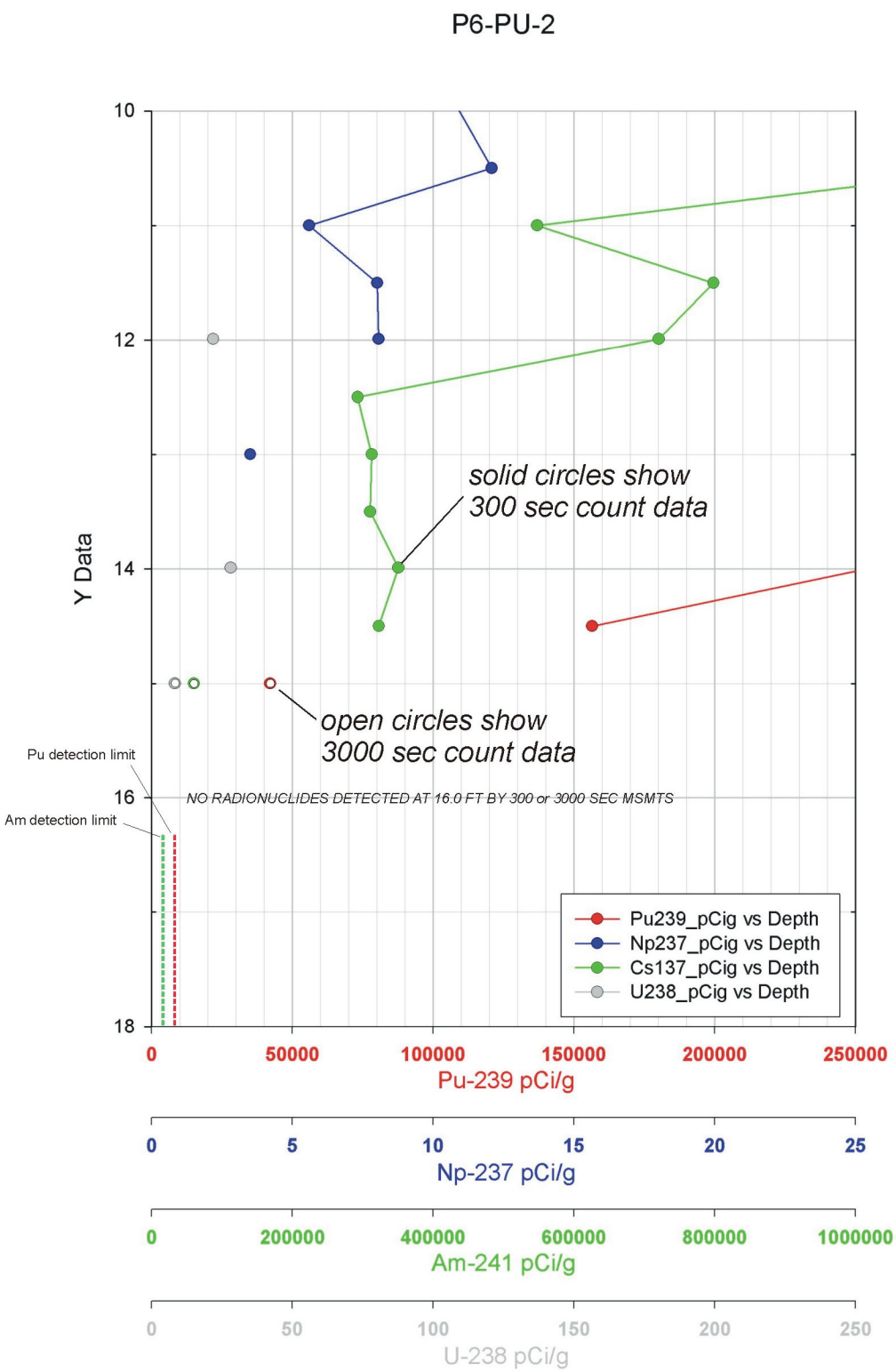

Figure 4-4b. Detail of the waste and soil interface in Probehole P6-PU-2.

4.5 Logging Data Analysis to Support Replacement Tensiometers

Several of the in situ tensiometers installed to investigate SDA subsurface radionuclide areas failed to produce useful data. It was believed that the tensiometers failed because of inadequate coupling with the surrounding media, possibly because the tensiometers were emplaced within solid waste rather than soil. Type A logging data were evaluated to choose locations for replacement tensiometers. Type A data were used to identify subsurface regions likely to contain soil rather than waste.

The original tensiometers that required replacement are listed in Table 4-3 along with the recommended locations for new tensiometers. Figures 4-5–4-9 show cross-section sketches compiled from Type A logging data in the vicinity of these locations.

Table 4-3. Tensiometers requiring replacement and recommended locations for new tensiometers.

Type A Probe	Tensiometer Number	Depth (ft bgs)	Recommended Location for Replacement Tensiometer	Figure Showing Area
DU-08	265	6.14	Between probes DU-08A and DU-08B and as close to Probe DU-08A as practical.	4-5
DU-08	269	11.50	Between probes DU-08A and DU-08B and as close to Probe DU-08A as practical.	4-5
DU-08	270	17.86	Between probes DU-08A and DU-08B and as close to Probe U-08A as practical.	4-5
DU-10	271	6.64	Between probes DU-10A and DU-10B, as close to Probe DU-10A as practical, and in the depth range from 4–6 ft bgs.	4-6
DU-14	278	9.83	No clear soil zones to target. Recommend attempt to emplace tensiometer in thin stringer as indicated in Figure 4-7. Install as close as possible to Probe DU-14A.	4-7
743-03	226	12.31	At depths and locations shown in Figure 4-8. Install as close as possible to the adjacent Type A probes.	4-8
743-03	237	19.09	At depths and locations shown in Figure 4-8. Install as close as possible to the adjacent Type A probes.	4-8
743-18	248	12.83	At depths and locations shown in Figure 4-9. Do not install toward Probe 743-20, because conditions change significantly in this direction.	4-9
743-18	236	19.00	At depths and locations shown in Figure 4-9. Do not install toward Probe 743-20, because conditions change significantly in this direction.	4-9

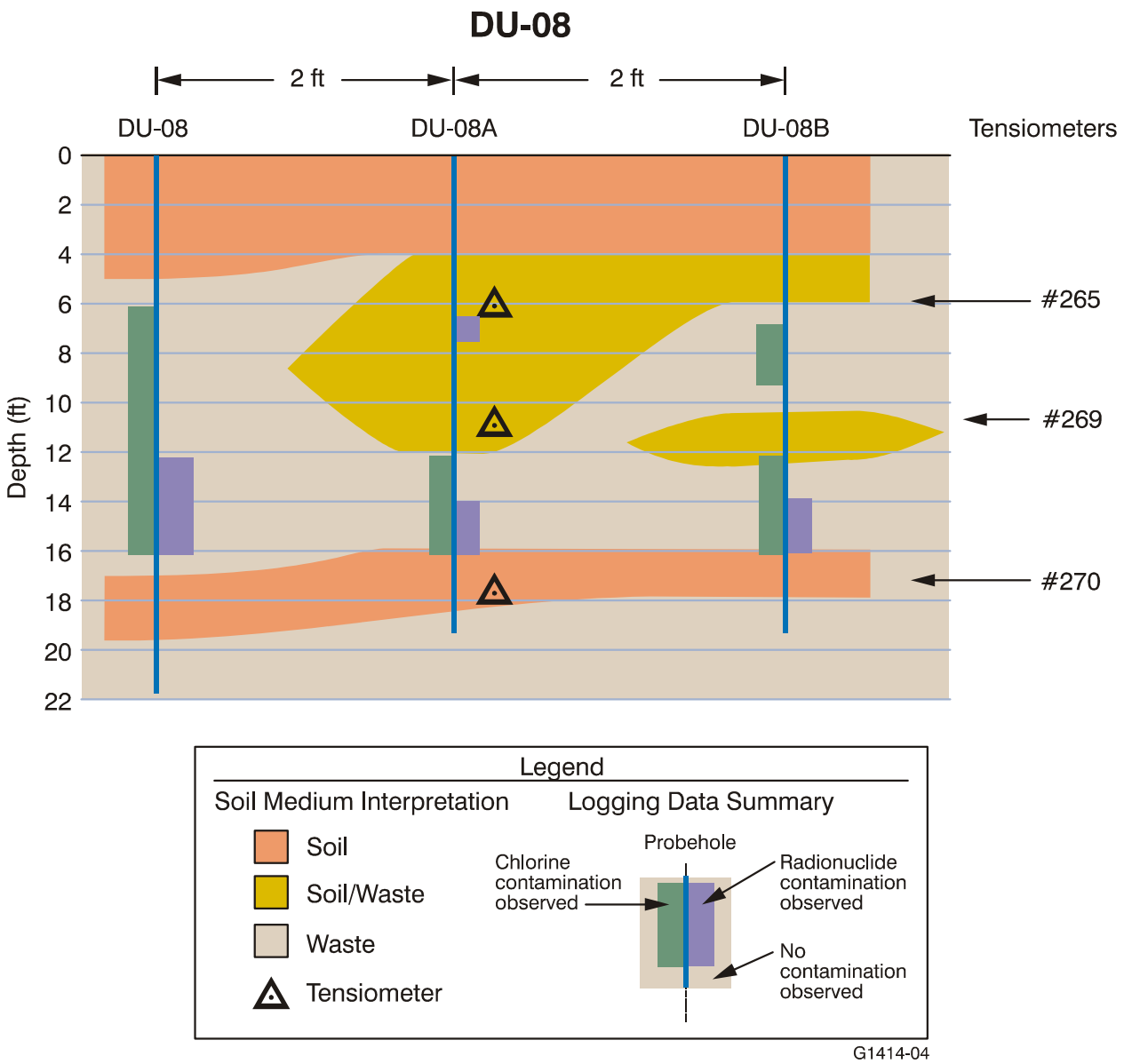

Figure 4-5. Cross-section sketches compiled from Type A logging data near Probe DU-08.

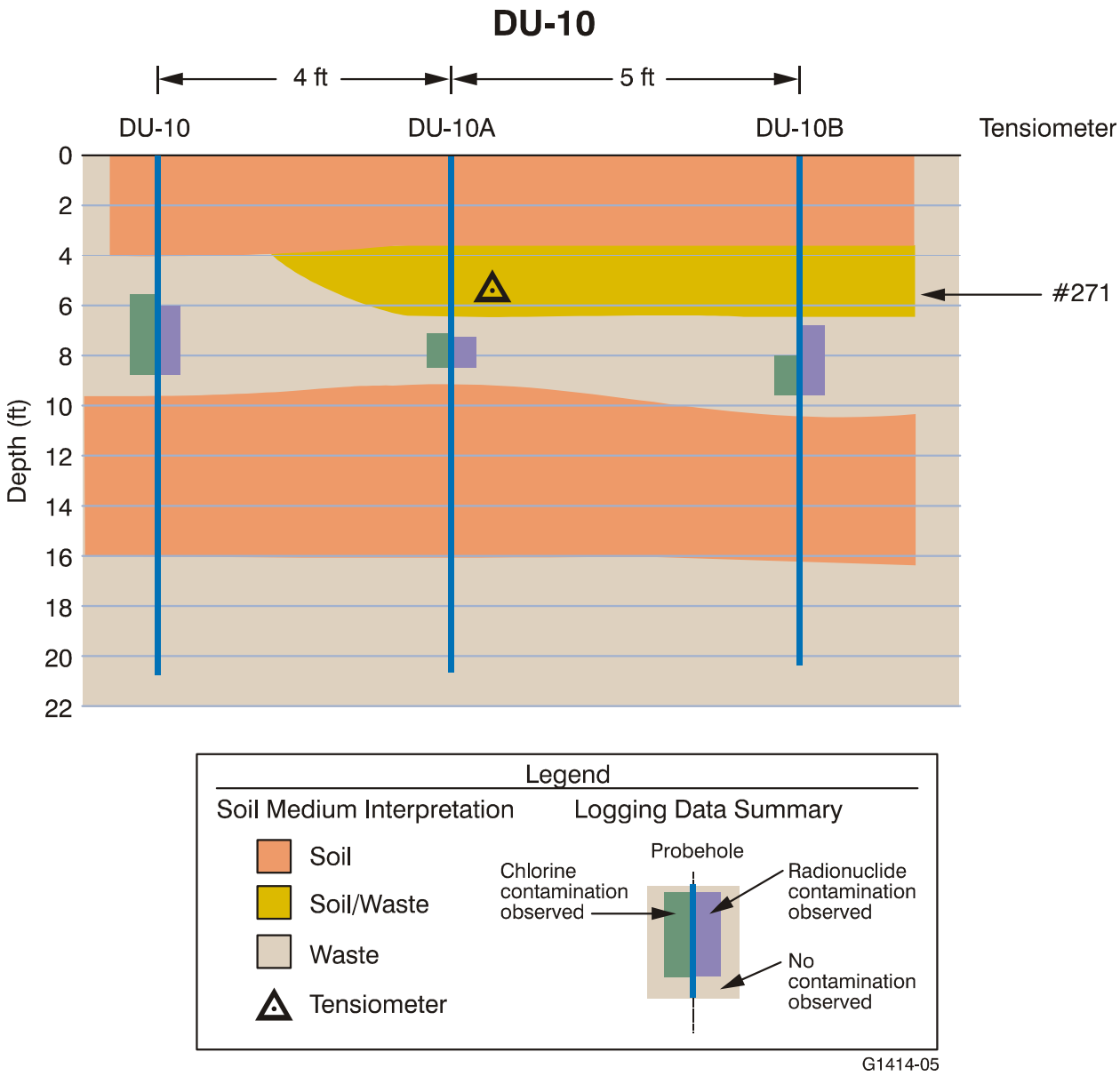

Figure 4-6. Cross-section sketches compiled from Type A logging data near Probe DU-10.

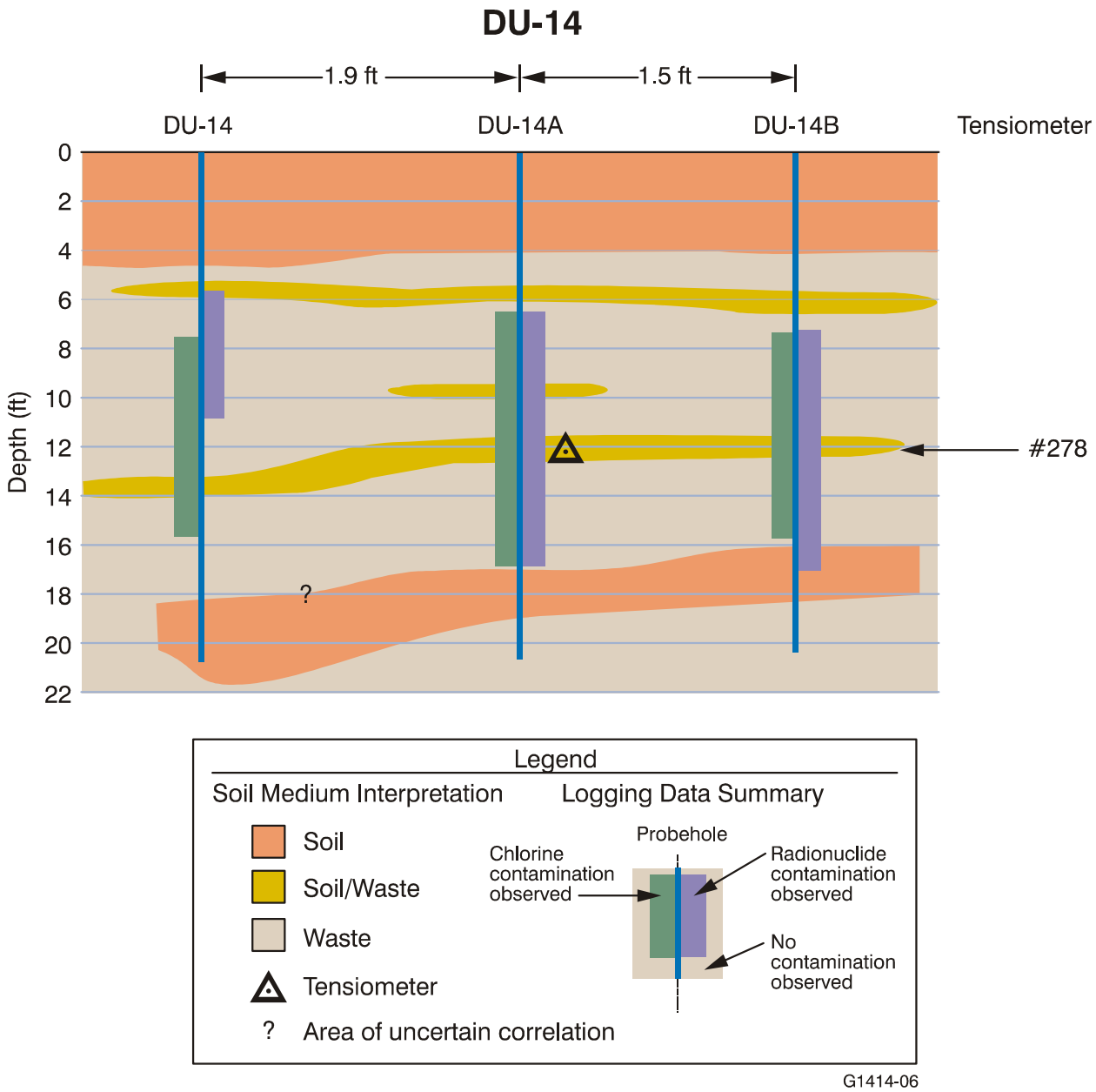

Figure 4-7. Cross-section sketches compiled from Type A logging data near Probe DU-14.

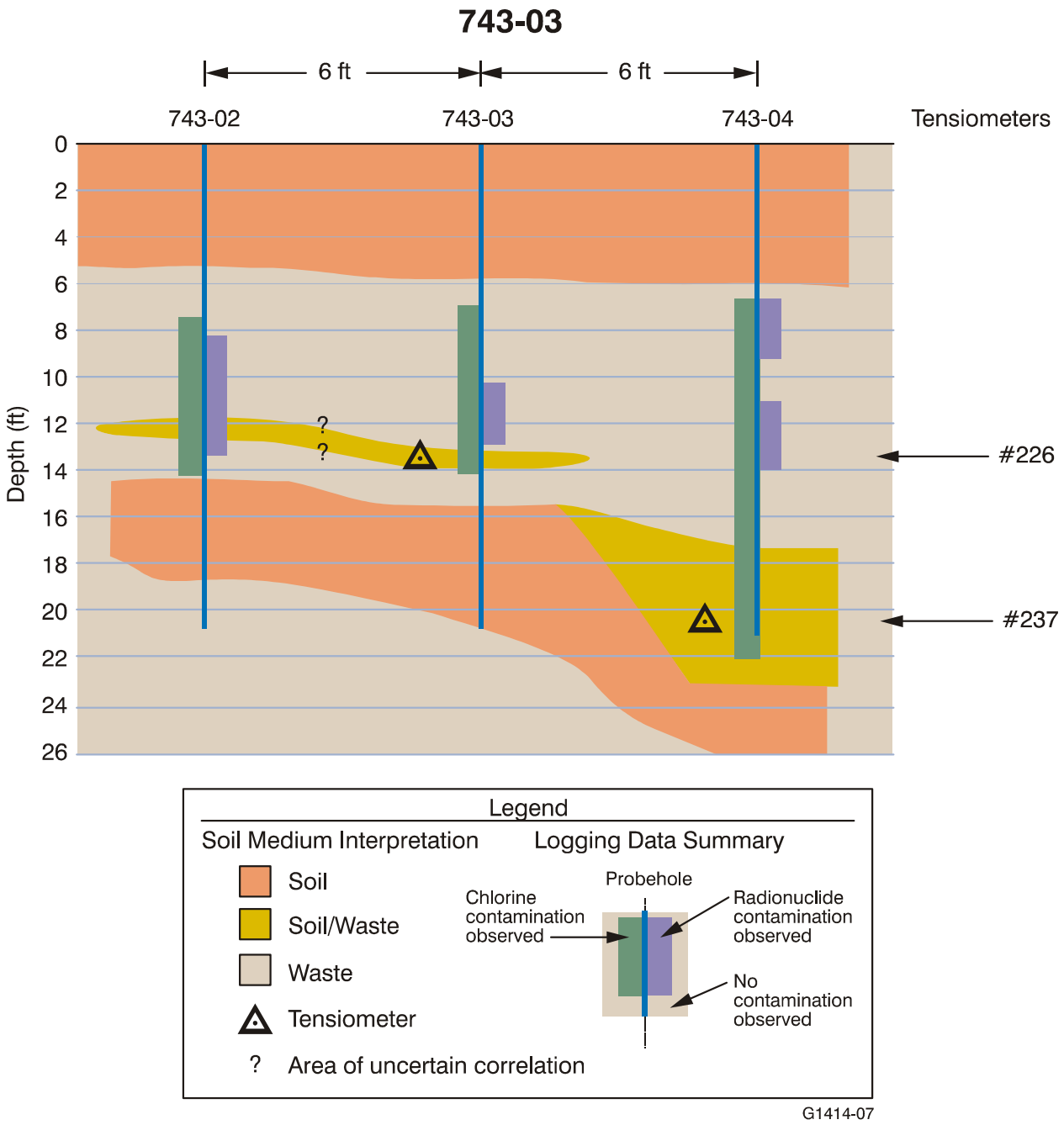

Figure 4-8. Cross-section sketches compiled from Type A logging data near Probe 743-03.

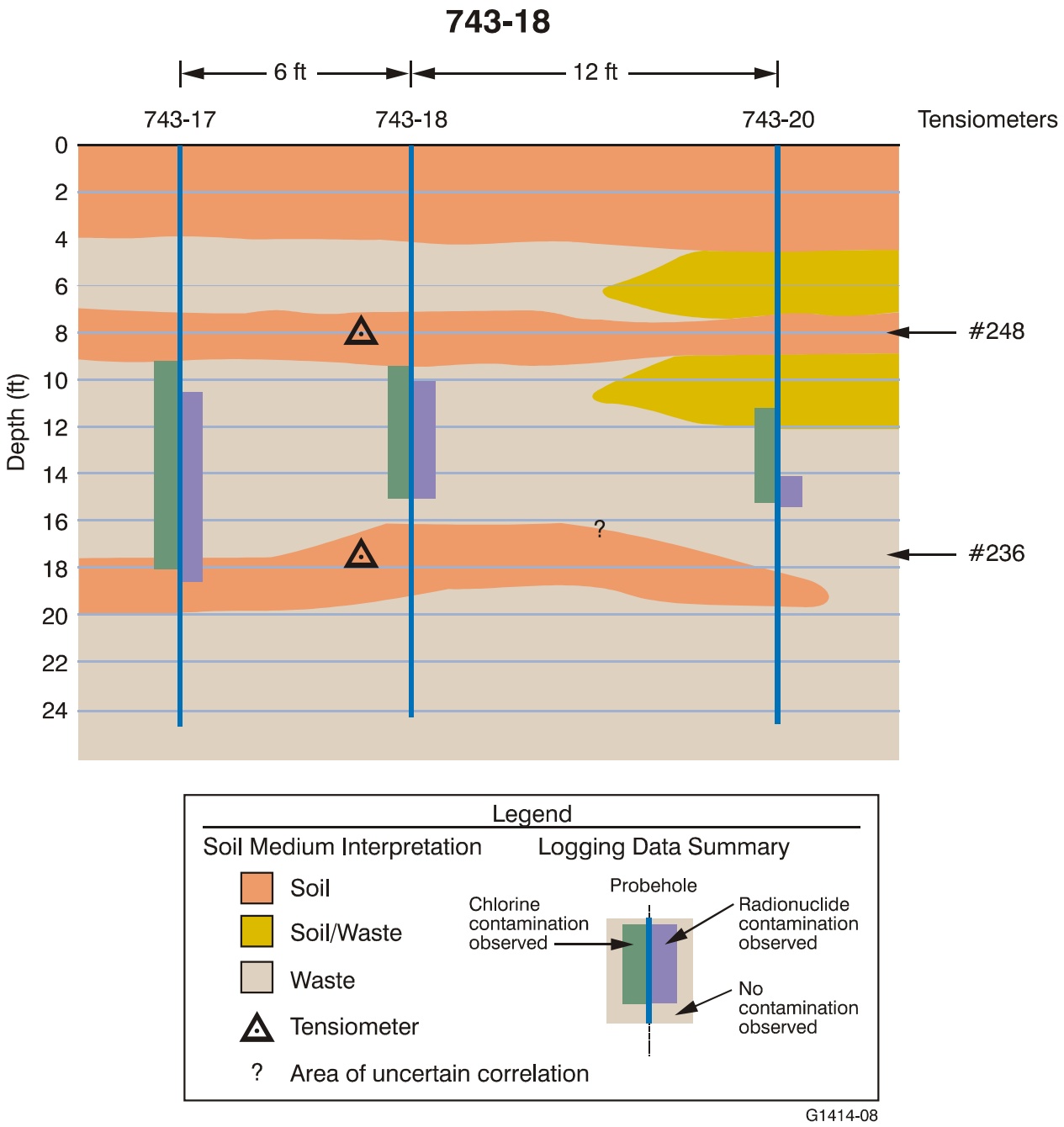

Figure 4-9. Cross-section sketches compiled from Type A logging data near Probe 743-18.

4.6 Analysis of Azimuthal Logging Data

Azimuthal logging was conducted in 13 probes during November–December 2003 (see Table 4-4). Azimuthal logging is conducted with a hyper-pure germanium gamma ray detector contained within a slotted shield. During logging, the tool (and the slot) are rotated through 360 degrees of azimuth, and a gamma ray spectrum is acquired at 22.5-degree increments. The purpose of azimuthal logging is to detect heterogeneous radionuclide distributions as indicated by variation in gamma ray flux with azimuthal direction. Logging depth is held constant during the azimuthal survey. In some cases, azimuthal surveys were conducted at multiple depths in a probehole. A total of 57 azimuthal surveys were conducted during the November–December 2003 logging effort.

Table 4-4. Azimuthal logging data acquisition summary (November–December 2003).

Focus Area	Pit or Trench	Target	Probe_ID	Depths Logged (ft bgs)
1A	Trench 3	Enriched uranium	T3-EU-02	8.0
1A	Trench 3	Enriched uranium	T3-EU-03	8.0
1B	Trench 47	Irradiated fuel	T47-IF-1	8.0
1B	Trench 47	Irradiated fuel	T47-IF-2	8.0, 10.0
2	Trench 24	Liquid waste	HAL2	12.0, 21.0
2	Trench 24	Liquid waste	HAL4	12.0
3	Pit 5	Uranium/enriched uranium	P5-UEU-1	8.0, 8.5, 9.0, 9.5, 10.0, 10.5, 11.0, 11.5, 12.0, 12.5, 13.0, 13.5, 14.0, 14.5, 15.0, 15.5, 16.0
3	Pit 5	Uranium/enriched uranium	P5-UEU-4	6.0, 7.0, 8.0, 9.0, 9.5, 10.0, 11.0, 12.0, 13.0, 14.0
3	Pit 5	Uranium/enriched uranium	P5-UEU-5	11.0, 12.0, 13.0
3	Pit 5	Uranium/enriched uranium	P5-UEU-7	10.0, 11.0, 12.0, 13.0, 14.0
5	Pit 6	Plutonium waste	P6-PU-1	6.0, 7.0, 8.0, 9.0, 10.0, 11.0, 12.0
5	Pit 6	Plutonium waste	P6-PU-2	9.0, 10.0, 11.0, 12.0, 13.0, 14.0
5	Pit 6	Plutonium waste	P6-PU-3	7.74

Azimuthal logging results are presented as polar plots that show the variation in gamma ray flux with azimuthal direction (see Appendix B). Two examples are shown in Figure 4-10. In the left-hand example, a clear Cs-137-flux peak occurs at approximately 295 degrees azimuth. In the right-hand example, a faint U-238-flux peak occurs at approximately 68 degrees azimuth. As these examples show, the distinctness of azimuthal peaks can vary significantly. The precise azimuth of peaks is also uncertain owing to the asymmetry of the flux variation and the coarse measurement interval (22.5 degrees). Table 4-5 lists interpreted azimuthal peaks for the logs covered by this summary. The nuclides causing the azimuthal peaks and the quality of the peak are indicated, along with the interpreted azimuth direction. Where azimuthal peaks are observed to span several adjacent logging depths, the azimuth is interpreted from the depth corresponding to the strongest gamma ray flux.

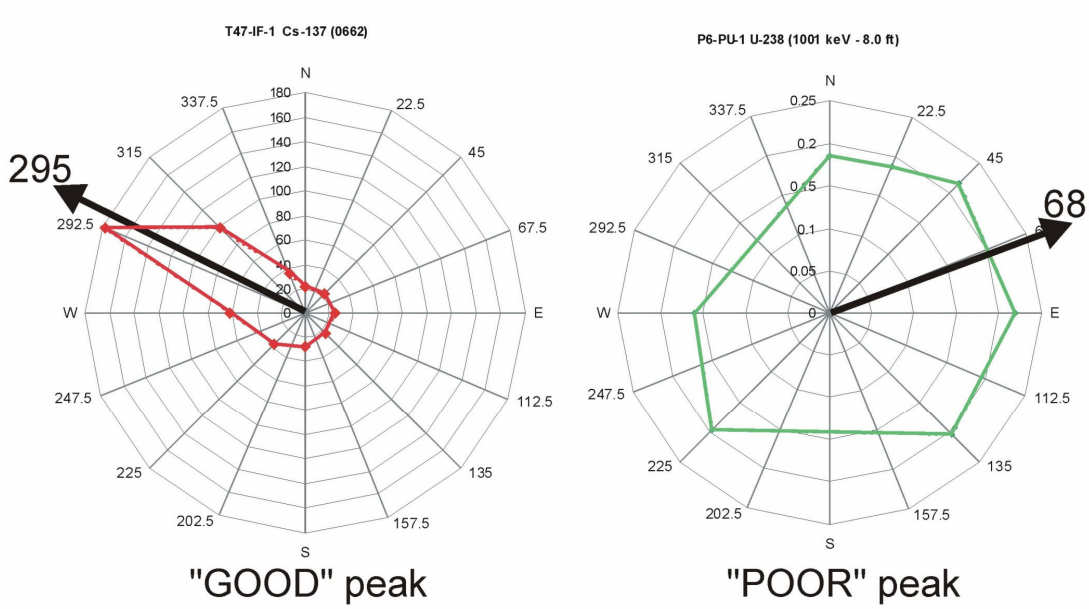

Figure 4-10. Azimuthal data plots showing examples of a highly directional gamma ray flux (left) and marginally directional gamma ray flux (right).

Table 4-5. Azimuthal logging data results summary.

Probe_ID	Depth (ft bgs)	Azimuth (degrees)	Nuclide	Peak Quality
T3-EU-02	8.0	169	U-238	Fair
T3-EU-03	8.0	None	U-238	Poor
T47-IF-1	8.0	290	Cs, minor Co	Good
T47-IF-2	8.0	290	Cs, minor Co	Good
T47-IF-2	10.0	124	Cs, minor Co	Good
HAL2	12.0	191	Cs, minor Co	Good
HAL2	21.0	90	Cs, minor Co	Fair
HAL4	12.0	90	Cs, Co	Fair
P5-UEU-1	9.0	280	Pu	Good
P5-UEU-1	14.5	45	Pu	Fair
P5-UEU-4	9.0	11	Pu, Am	Good
P5-UEU-4	10.0	90	Pu, Am	Good
P5-UEU-4	12.0	0	Am	Poor
P5-UEU-4	14.0	135	U-238	Poor
P5-UEU-5	12.0	236	Pu, Am, Np	Fair
P5-UEU-7	11.0	68	Pu	Fair
P6-PU-1	8.0	34	Am, Np, Pu	Good
P6-PU-1	8.0	68	U-238	Poor
P6-PU-1	10.0	90	Pu	Fair
P6-PU-2	10.0	168	Am	Fair
P6-PU-2	10.0	338	Am	Poor
P6-PU-2	13.0	260	Pu	Fair
P6-PU-3	7.74	185	Pu, Np	Good

The shape of azimuthal peaks, even for ideal point sources, varies for different radionuclides depending on gamma ray energy. This variation is because some gamma rays will always penetrate through the azimuthal shield, even when the shield's window is pointed directly away from the radionuclide source. Backside gamma ray penetration is greater for high-energy gamma rays (e.g., U-238 1,001 keV) than for lower-energy gamma rays (e.g., Pu-239 375 keV). Thus azimuthal peaks tend to be more subdued for the higher energy radionuclides. Azimuthal results should be corrected for this effect if it becomes important to make comparisons between the distribution of different radionuclides.

4.6.1 Subsurface Waste Heterogeneity as Observed from Azimuthal Logging Data

Azimuthal logs were collected at 0.5-ft intervals from 8.0–16.0 ft in Probehole P5-UEU-1. These logs provide some useful insight into the heterogeneity of the SDA subsurface. Probe P5-UEU-1 azimuthal plots for total gamma ray flux are presented in Figure 4-11. Homogenous conditions would be indicated by constant gamma ray flux in all azimuthal directions (i.e., roughly circular plots). Figure 4-11 shows that approximate homogenous conditions occur at a few depths, but most depths indicate heterogeneous conditions. Heterogeneity may be caused by nonuniform radionuclide distribution or nonuniform density distribution in the vicinity in the probehole. Probehole P5-UEU-1 data also show that the location and character of the heterogeneity changes gradually with depth.

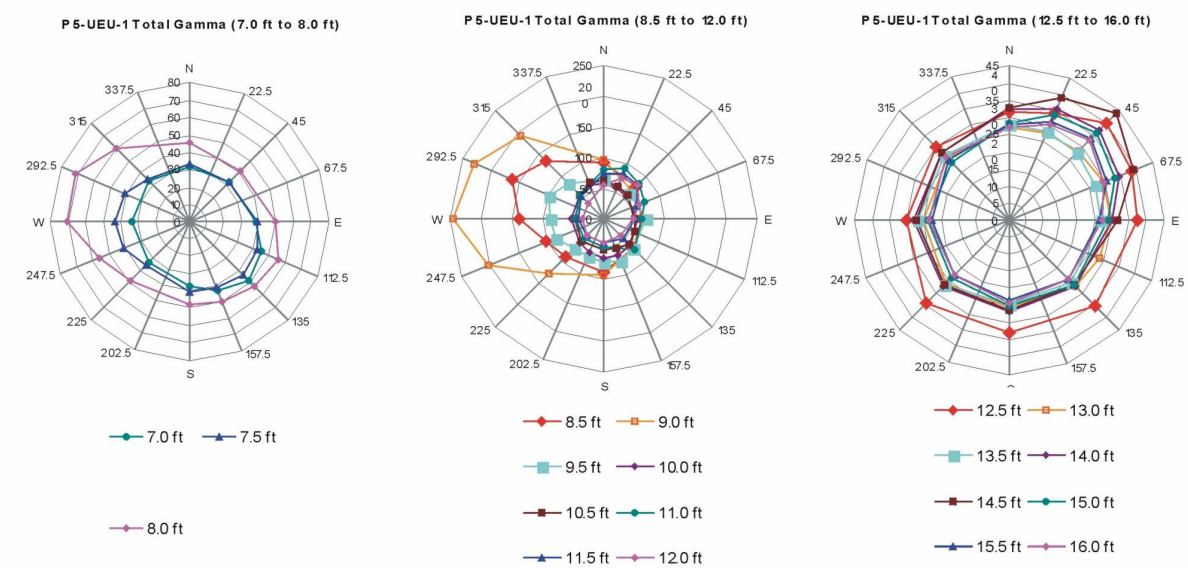

Figure 4-11. Azimuthal plots for total gamma ray flux in Probe P5-UEU-1.

4.7 Geophysics Database Compilation

During FY 2004, the probing project completed a compilation of surface and borehole geophysical data into the comprehensive Nuclear Logging and Surface Geophysics Database. Information about the structure, use, and maintenance of this data base may be found in PLN-1709.

The PLN-1709 provides documentation for the Nuclear Logging and Surface Geophysics Database, including software documentation, resource descriptions, and assumptions. The data-flow analysis, the logical software design, the physical system design, and data access module design documents are included as sections in this document.

4.8 Beryllium Block Investigation

The Early Actions Beryllium Block Encapsulation Project encapsulated buried beryllium reflector blocks and related reactor components within an injected grout material. Grout injection is accomplished via an injection well array that is installed surrounding the targeted beryllium block disposal site. Grout is injected throughout the depth interval containing the target shipment. Thus, the horizontal and vertical location of the beryllium block disposals is a prerequisite for engineering design of the grout injection system.

The "Determination of Beryllium Block Disposal Locations for the OU 7-13/14 Early Actions Beryllium Encapsulation Project" (EDF-4899), discusses the combined use of waste disposal inventory records, surface geophysical data, and tritium gas surveys to estimate the horizontal and vertical location of disposed beryllium blocks in the SDA. Beryllium disposals were evaluated in Trench 52, Trench 54, Trench 57, Trench 58, and Soil Vault Row 17.

4.9 Volatile Organic Compound Analysis using n-Gamma Logging Data

During FY 2004, the probing project completed an evaluation of methods for estimating VOC mass remaining within the SDA. Details of this investigation may be found Sondrup et al. (2004). A summary of the report findings is discussed below.

The purpose of the Sondrup et al. (2004) study was to provide an estimate of the mass fraction of carbon tetrachloride and VOCs remaining in the waste disposal pits at the SDA. Both OU 7-08 and 7-13/14 could use this information for estimating risk and making remediation decisions. The estimate initially was based on a comparison of the mass of VOCs originally buried at select locations in the SDA to the mass that currently remains at the same location, which is based on neutron-gamma logging of probeholes. However, a defensible estimate was not possible because of the inability to quantify uncertainty around the original estimate of chlorine mass per probehole and the inadequacy of the neutron-gamma logging-tool calibration function.

A revised strategy that also relied on neutron-gamma logging data was also unsuccessful because of (1) the inability to distinguish Series 743 sludge from other media (e.g., soil and debris) and (2) the inability to develop a tool-response function capable of predicting all observed neutron-gamma data. In addition, even if an adequate tool-response function were developed, it would remain difficult to defensibly estimate the mass of VOCs remaining in SDA pits without the ability to independently characterize both the matrix composition and the distribution of the chlorine-containing material around the neutron-gamma tool.

A simpler, alternative approach was used to approximate the amount of VOC mass remaining without any attempt to quantify the uncertainty. Based on the approach, an estimate of 50 percent VOC mass remaining is recommended as a starting point for numerical modeling to predict risk and remediation goals for OU 7-08 and OU 7-13/14. An estimate of 75 percent mass remaining is recommended as an upper bound. The lack of uncertainty surrounding these estimates should be carefully considered when interpreting any results derived from their use.

Because more precise estimates will almost certainly involve nuclear logging data, any further attempts to estimate the fraction of remaining mass should involve redesigning the neutron-gamma tool or performing a comprehensive calibration to conditions and materials that are more likely to be encountered in the waste pits. A broad-based, technically defensible strategy should be developed to logically ensure

the objectives of the project could be achieved. This strategy would likely involve redesigning the neutron-gamma tool so that it would (1) interrogate a volume of material that more closely approximates homogeneous conditions and (2) maximize sensitivity of the tool in the region of interest to the project (50 wt% chlorine in this case). It also should include a recalibration of the tool to constituents, other than chlorine, that are unique to Series 743 waste or be able, by some other means, to distinguish between Series 743 sludge and other media. In addition, the tool also will require a thorough calibration to conditions and materials that are more likely to be encountered in the waste pits or, alternatively, a model-based tool response developed for the same conditions and materials.

5. REFERENCES

ASTM-D2216-98, 1998, "Standard Test Method for Laboratory Determination of Water (Moisture) Content of Soil and Rock by Mass," ASTM International.

Beitel, G. A., P. Kuan, C. W. Bishop, and N. E. Josten, 2000, *Evaluation of OU 7-10 Stage I Soil Moisture Readings*, INEEL/EXT-00-00651, Rev. 0, Idaho National Laboratory.

EDF-4899, 2004, "Determination of Beryllium Block Disposal Locations for the OU 7-13/14 Early Actions Beryllium Encapsulation Project," Rev. 1, Idaho Completion Project.

GE, 1989, *Chart of the Nuclides*, 14th edition, General Electric Company.

Giles, John R., Nick Josten, and Barbara J. Broomfield, 2003, *Evaluation of Nuclear Logging Tool Calibrations for use in Type A Probes at the INEEL Subsurface Disposal Area, OU 7-13/14*, INEEL/EXT-03-00118, Rev. 0, Idaho National Laboratory.

Holdren, K. Jean, Bruce H. Becker, Nancy L. Hampton, L. Don Koeppen, Swen O. Magnuson, T. J. Meyer, Gail L. Olson, and A. Jeffrey Sondrup, 2002, *Ancillary Basis for Risk Analysis of the Subsurface Disposal Area,* INEEL/EXT-02-01125, Rev. 0, Idaho National Laboratory.

INL, 2002, *Type A Nuclear Logging Data Acquisition and Processing for Operable Units 7- 13/14 and 7-10*, INEEL/EXT-02-00558, Rev. 1, Idaho National Laboratory.

Jewell, James K., L. Reber Edward, and C. Hertzog Russell, 2002, *Estimating the Mass of Pu-239 Waste Near P9-20 Probe Hole for the OU 7-10 Glovebox Excavator Method Project*, INEEL/EXT-02-01189, Rev. 0, Idaho National Laboratory.

Josten, N. E. and J. C. Okeson, 2000, *OU 7-10 Initial Probing Campaign Downhole Logging Results*, INEEL/EXT-2000-00526, EDF-ER-207, Rev., Idaho National Laboratory.

Josten, Nicholas E., 2002, *Compilation of Analytical Notes and Data Analyses for the Integrated Probing Project 1999-2002*, INEEL/EXT-02-01306, Rev. 0, Idaho National Laboratory.

McElroy, D. L. and J. M. Hubbell, 1990, *Hydrologic and Physical Properties of Sediments at the Radioactive Waste Management Complex*, EGG-BG-9147, Idaho National Laboratory.

PLN-1709, 2004, "Software Documentation for the Nuclear Logging and Surface Geophysics Database," Rev. 0, Idaho Completion Project.

SOW-561, 2003, "Statement of Work for Nuclear Geophysical Logging," Rev. 0, Idaho National Laboratory.

Sondrup, A. Jeffrey, Eric C. Miller, Edward H. Seabury, and Nick Josten, 2004, *Estimating Carbon Tetrachloride and Total Volatile Organic Compound Mass Remaining in Subsurface Disposal Area Pits*, ICP/EXT-04-00396, Idaho Completion Project.

Appendix A

Sage Earth Science Report

Appendix A
Sage Earth Science Report

Two surface geophysical studies were performed by Sage Earth Science at the Subsurface Disposal Area (SDA) within the Idaho National Laboratory Radioactive Waste Management Complex from FY 2003 through 2004. These studies were conducted to support analysis of remedial alternatives and future environmental restoration needs for the SDA, with the exception of Pit 9 and the low-level waste pit. The FY 2004 survey produced comprehensive, high-resolution geophysical data for most of the SDA. The Sage Earth Science report for this survey comprises this appendix.

SAGE EARTH SCIENCE

May 24, 2004

BBWI
P.O. Box 1625
Idaho Falls, ID 83415

RE: DATA DELIVERY / FINAL REPORT
GEOPHYSICAL LAND SURVEY OF SDA AT RWMC
SUBCONTRACT NO. 00029560

INTRODUCTION

Locating buried objects including drums, underground storage tanks, and other waste is among the most popular applications of geophysics in the environmental industry. Basic questions relating to the location and distribution objects, pits, and trenches can be addressed in a straightforward manner with confident results. Most often, magnetic field and/or electromagnetic induction surveys are performed depending on the project objective and site conditions. Over the period of March 8 thru April 29, 2004 magnetic field and time domain electromagnetic induction (TDEMI) surveys were performed at the Subsurface Disposal Area (SDA) of the Radioactive Waste Management Complex (RWMC) located at the Idaho National Engineering and Environmental Laboratory (INEEL). Included in this report are the results of the geophysical surveys covering the approximate 80-acre landfill site.

TECHNICAL APPROACH

Given project needs and site conditions, proposals to conduct high-resolution metal detection surveys were sought. To meet these objectives, magnetic field and TDEMI surveys were proposed. Of critical importance in the design of a geophysical survey is the selection of the appropriate survey method, data station, and profile spacing. Typically, the data spacing is based on a number of factors including:

1. target size
2. the degree which it is necessary to place a location or boundary
3. the degree which it is necessary to distinguish between closely spaced boundaries or individual objects
4. interference from small scattered surface or near surface objects
5. interference from surface features (e.g. fences, buildings, utilities, wells, posts etc.)
6. requirements for size/depth estimates
7. properties of the measurement equipment

Based on these parameters, the magnetic field data were collected on a 6-inch by 20-inch station/profile spacing. The TDEMI data were collected on an 8-inch by 40-inch station/profile spacing.

Magnetics Field Measurements

Magnetic objects such a steel drums, rebar, underground storage tanks, and other ferrous/magnetic objects produce localized variations in the earth's magnetic field. By mapping those variations, the location, size, and depth of magnetic objects can be determined. In typical burial settings, mapping the distribution of magnetic objects will clearly delineate the location of fill areas, pits, and trenches

The magnetic field data for this task were acquired using the Rapid Geophysical Surveyor (RGS), a proprietary magnetic field mapping system jointly developed by Sage Earth Science and the INEEL. Using high precision fluxgate gradiometers, vertical gradient of the vertical magnetic field data were collected on a 6-inch by 20-inch station/profile spacing (50,000 points/acre) over the approximate 80-acre site totaling nearly 4 million data points.

The RGS employs two fluxgate magnetic gradient sensors spaced 20 inches apart; therefore collecting two data profiles simultaneously during each pass of the mapping system across the site. An optical encoder integrated with the system wheel drives the data acquisition. The wheel and encoder serve as an odometer to located each data point along profile. Data profiles were positioned by referencing a 200-foot by 200-foot control grid placed at the site by the INEEL. Each profile is located by placing a visual marker at end of each 200-foot pass. The visual marker is used to guide the operator in a straight line across each 200-foot grid cell.

A fluxgate magnetometer consists of a "sensing" coil surrounding an inner "drive" coil that is wound around a ring-shaped core material. An alternating current is applied to the drive coil that induces a current in the sensing coil. Without an external magnetic field, the total flux seen by the sensing coil is zero. When an external magnetic field is present, the flux is switched to saturation. The voltage induced in the sensing coil is proportional to the rate of change of the flux with respect to time. Because of the effect of the external magnetic field on the changing magnetic permeability of the core, the voltage induced in the sensing coil contains even harmonics of the drive current frequency. The strength of the induced harmonics is proportional to the strength of the external magnetic field.

The Billingsley Magnetics GRAD-12 sensor used in the RGS is a single axis fluxgate gradiometer. The sensor consists of two single axis magnetometers spaced 12 inches apart along a common vertical axis. Each magnetometer provides an analog output corresponding to the component of the magnetic field along its axis. The gradient is derived by measuring and

510 East 17th Street, Suite 110, Idaho Falls, ID 83404
telephone: (208)522-5049, Fax: (208)528-6200, email: ses@srv.net
http://www.srv.net/~ses/SES.HTM

logging the difference between the two closely spaced magnetometers. The property measured is therefore the vertical gradient of the vertical magnetic field reported in nanoTesla per meter.

Time Domain Electromagnetic Induction Survey (Geonics EM-61)

Electrically conductive objects such a steel drums, rebar, underground storage tanks, and other metallic objects can be located by inducing electrical currents into the subsurface and measuring the response at the surface. By mapping this response, the location, size, and depth of conductive objects can be determined. In typical burial settings, mapping the distribution of metallic objects will clearly delineate the location of fill areas, pits, and trenches

The TDEMI response data were acquired using a Geonics EM-61 metal detector. The EM-61 is a high sensitivity, high-resolution time-domain metal detector. The system consists of a transmitter coil that generates a pulsed primary magnetic field, which induces eddy currents in nearby metallic objects. Two separate receiver coils mounted on a trailer assembly measure the decay of the induced current. The response curve is a single well defined positive peak centered over the conductive body facilitating an accurate location and from which a depth can be estimated based on the width of the anomaly or the relative response of the two receiver coils.

The upper coil and lower coil, response data were recorded on an 8-inch by 40-inch station/profile spacing (20,000 points/acre) over the 80-acre site totaling an approximate 1.4 million data points. An optical encoder integrated with the system wheel drives the data acquisition. The encoder and wheel serve as an odometer to locate each data point along profile. Data profiles were positioned by referencing a 200-foot by 200-foot control grid place at the site by the INEEL. Each profile was located by placing a visual marker at the end point of each 200-foot pass. The visual markers were used to guide the operator in a straight line across each grid cell. The logged responses are reported in millivolts.

TECHNICAL REQUIREMENTS

All data were acquired in accordance with INEEL TTP 154 and Sage Earth Science Standard Operating Procedures *3.1 Magnetic Field Mapping (RGS)* or *4.3 Time Domain Electromagnetic Induction.*

All locations are provided in State Plane, Idaho East Zone (1101), U.S. Survey Feet, horizontal datum NAD27. The data were acquired on the dates between March 8, 2004 and April 29, 2004. Depth estimates derived from this data should be reference to the ground surface elevation between those dates.

510 East 17th Street, Suite 110, Idaho Falls, ID 83404
telephone: (208)522-5049, Fax: (208)528-6200, email: ses@srv.net
http://www.srv.net/~ses/SES.HTM

DATA PRESENTATION

The following figures show the results of each survey: vertical gradient of the magnetic field in nanoTesla per meter and EM-61 bottom coil response in millivolts each in State Plane, Idaho East Zone (1101), U.S. Survey Feet, horizontal datum NAD27.

Magnetic field map

For the purposes of interpretation, every magnetic object can be considered to be a small bar magnet with both a north and south pole. These areas are represented as an area of positive gradient (reds/purples) and negative gradient (blues/greens). Low field areas are represented with yellow.

The character of a magnetic anomaly is related to the magnetic properties of the object as well as its size and depth of burial. In general, a large object or groups of magnetic objects will produce a high amplitude field. However, the amplitude as measured at the surface, is strongly influenced by distance to the object or its depth of burial. The way in which the amplitude changes laterally or as the system passes over a buried object is related to the depth of burial.

Those pits that are populated with high volumes of ferrous metal are well expressed; in particular pits 1-6, 8, 10, 13, 14, and 15. Pits 11, 12, and acid pit are poorly expressed in the magnetic field data.

A number of the trenches and soil vault rows are well expressed. In general, the rows and trenches on the west end of the SDA are more clearly expressed due the contents of the trench and the depth of burial. Many of trenches and rows are not well expressed most likely due to the nature of the material received in those trenches. These areas will require an extensive interpretation effort to delineate or could be handled on a case-by-case basis as project needs arise.

TDEMI Map

For the purposes of interpretation, every electrically conductive object will produce a single well defined positive peak centered over the conductive body facilitating an accurate location and from which a depth can be estimated based on the width of the anomaly or the relative response of the two receiver coils.

The amplitude of a TDEMI anomaly is related to the surface area of the metallic object as well as its depth of burial. In general, a large object or groups of metallic objects will produce a high amplitude response. However, the amplitude as measured at the surface, is strongly influenced by the distance to the object or its depth of burial. Therefore, the way in which the amplitude changes laterally is closely related to the depth of burial of the object. Similarly, because of the influence of distance, the difference in response between the upper and lower coil is related to the depth of burial.

Those pits that are populated with high volumes of metal are well expressed; in particular pits 1-6, 8, 10, 13, 14, and 15. Pits 11, 12, and acid pit are poorly expressed in the TDEMI data.

A number of the trenches and soil vault rows are well expressed. In general, the rows and trenches on the west end of the SDA are more clearly expressed due to the contents of the trench. Many of trenches and rows are not well expressed likely due to the nature of the material received in those trenches. These areas will require an extensive interpretation effort to delineate or could be handled on a case-by-case basis as project needs arise.

DATA PROCESSING SEQUENCE

The following data processing steps were applied to each of the data sets.

TDEMI data

1. Transformation of field/local grid coordinates to State Plane, Idaho East Zone (1101), U.S. Survey Feet, horizontal datum NAD27.
2. Inline spline fit to establish regularly spaced inline data
3. line by line leveling (instrument drift correction)
4. Instrument Lag correction – 2 fiducials
5. (X,Y,Z1,Z2) ASCII output (easting, northing, top coil, bottom coil)
6. 3.28 ft by 3.28 ft gridding - minimum curvature algorithm – for report graphics
7. 0.5 ft by 0.5 ft gridding – minimum curvature algorithm – for INEEL GIS

Magnetic field data

1. Transformation of field/local grid coordinates to State Plane, Idaho East Zone (1101), U.S. Survey Feet, horizontal datum NAD27.
2. Inline spline fit to establish regularly spaced inline data
3. line by line leveling (instrument drift and magnetometer orientation correction)
4. (X,Y,Z1) ASCII output (easting, northing, magnetic gradient)
5. 3.28 ft by 3.28 ft gridding - minimum curvature algorithm – for report graphics
6. 0.5 ft by 0.5 ft gridding – minimum curvature algorithm – for INEEL GIS

DIGITAL DATA FORMATS

The full geophysical data sets are included on the accompanying compact data disk. The data have been provided in two formats, ASCII (x,y,z) and ARCVIEW raster grid for inclusion into the INEEL GIS data system.

EM_BOTTOM_COIL.flt	89,947 KB	ARCVIEW FLT File	Raster grid
EM_BOTTOM_COIL.flt	4 KB	ARCVIEW GI File	Registration file
EM_BOTTOM_COIL.hdr	1 KB	ARCVIEW HDR File	Header file
EM_TOP_COIL.flt	89,947 KB	ARCVIEW FLT File	Raster grid
EM_TOP_COIL.flt	4 KB	ARCVIEW GI File	Registration file
EM_TOP_COIL.hdr	1 KB	ARCVIEW HDR File	Header file
Sda-em-out	52,511KB	ASCII (X,Y,Top,Bottom)	ASCII data file
Sda-mag.flt	90,331 KB	ARCVIEW FLT File	Raster grid
Sda-mag.flt	4 KB	ARCVIEW GI File	Registration file
Sda-mag.hdr	1 KB	ARCVIEW HDR File	Header file
Sda-mag-out	106,313 KB	ASCII (X,Y,Mag gradient)	ASCII data file

Appendix A
Geophysical Survey Maps
(color contour)

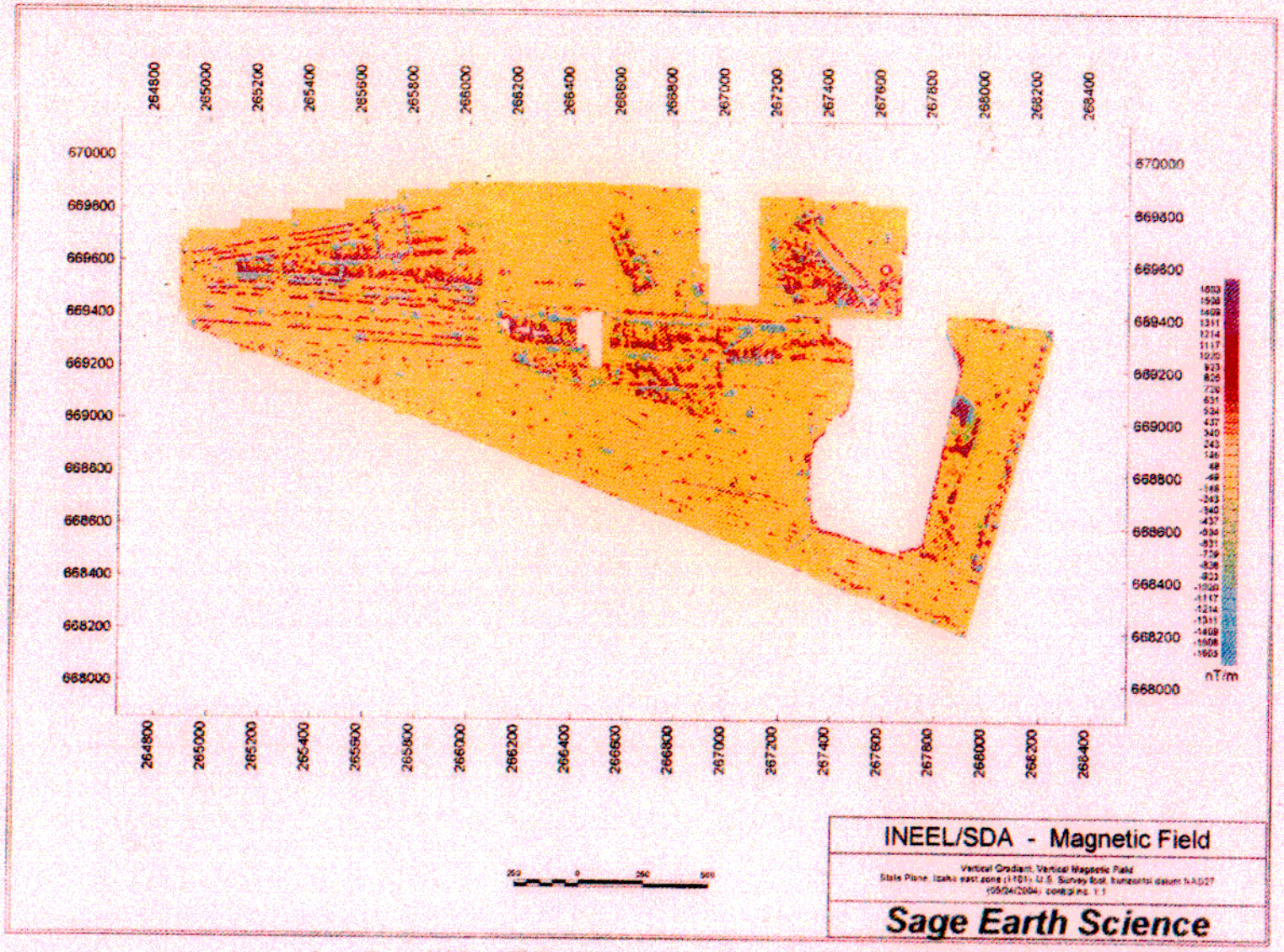

510 East 17th Street, Suite 110, Idaho Falls, ID 83404
telephone: (208)522-5049, Fax: (208)528-6200, email: sec@srv.net
http://www.srv.net/~sec/SES.HTM

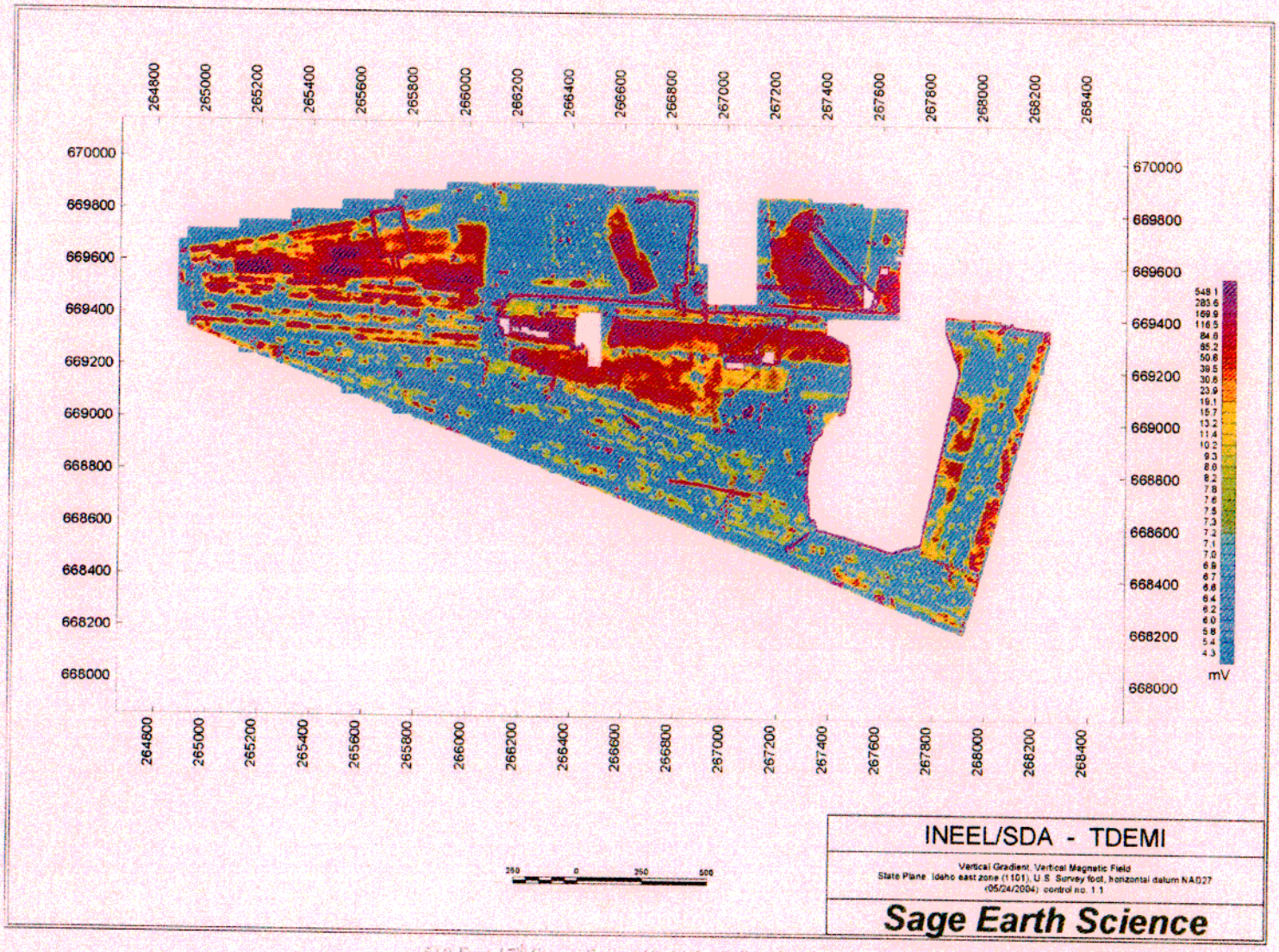

510 East 17th Street, Suite 110, Idaho Falls, ID 83404
telephone: (208)522-5049, Fax: (208)528-6200, email: ses@srv.net
http://www.srv.net/~ses/SES.HTM

Appendix B
Geophysical Survey Maps
(shaded relief)

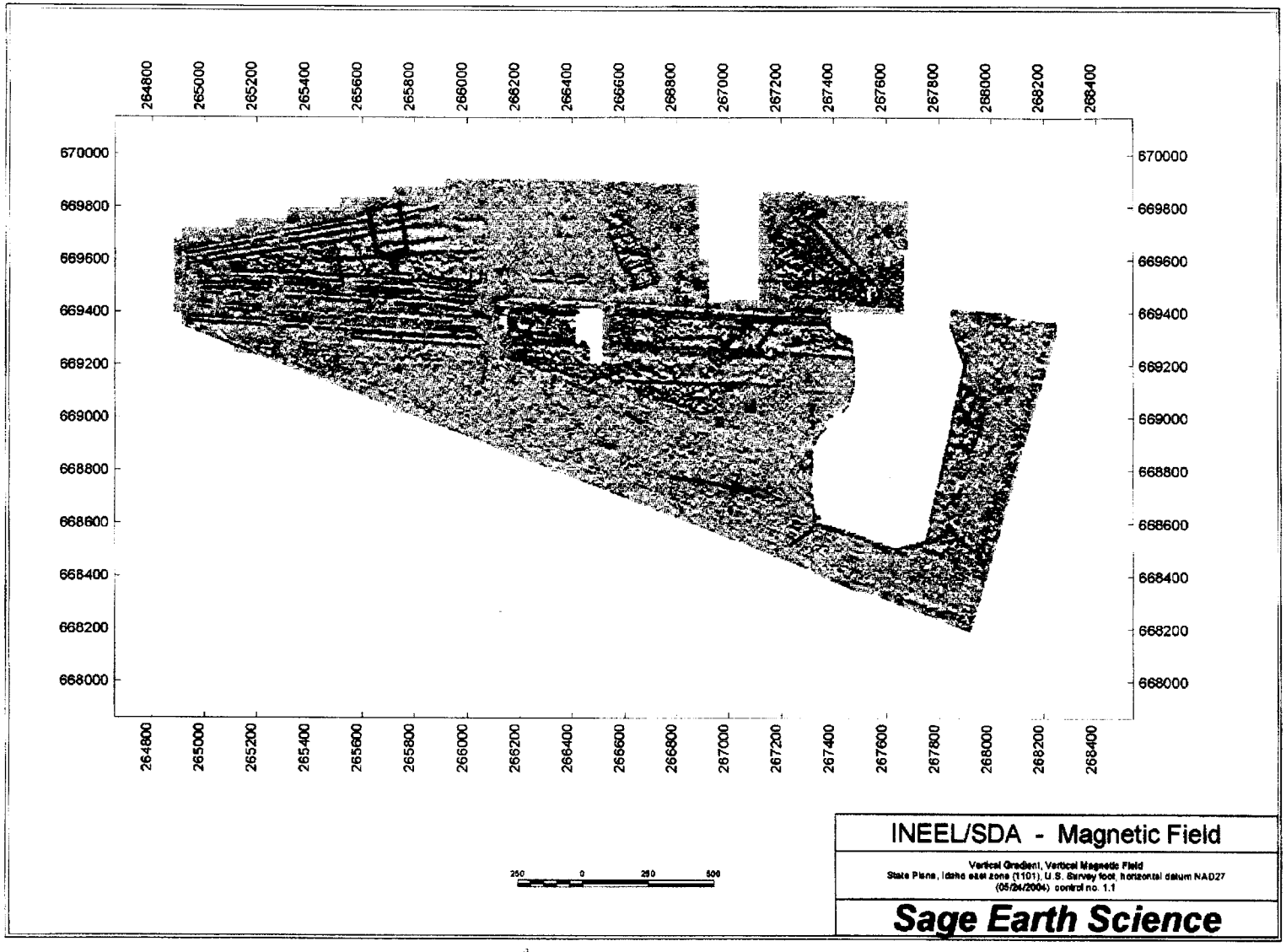

510 East 17th Street, Suite 110, Idaho Falls, ID 83404
telephone: (208)522-5049, Fax: (208)528-6200, email: ses@srv.net
http://www.srv.net/~ses/SES.HTM

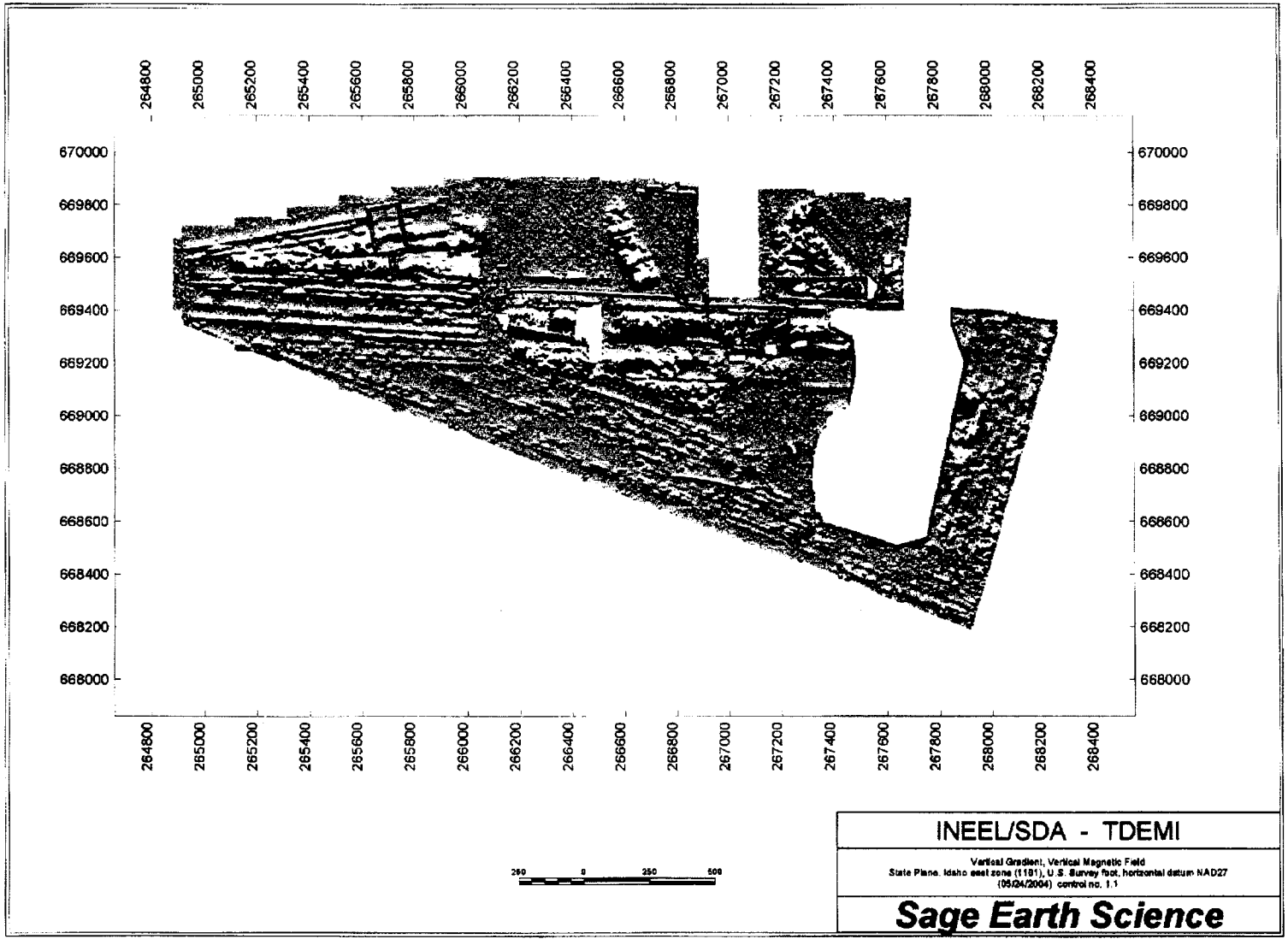

510 East 17th Street, Suite 110, Idaho Falls, ID 83404
telephone: (208)522-5049, Fax: (208)528-6200, email: ses@srv.net
http://www.srv.net/~ses/SES.HTM

Appendix C
Geophysical Survey Maps
(combination color contour/shaded relief maps)

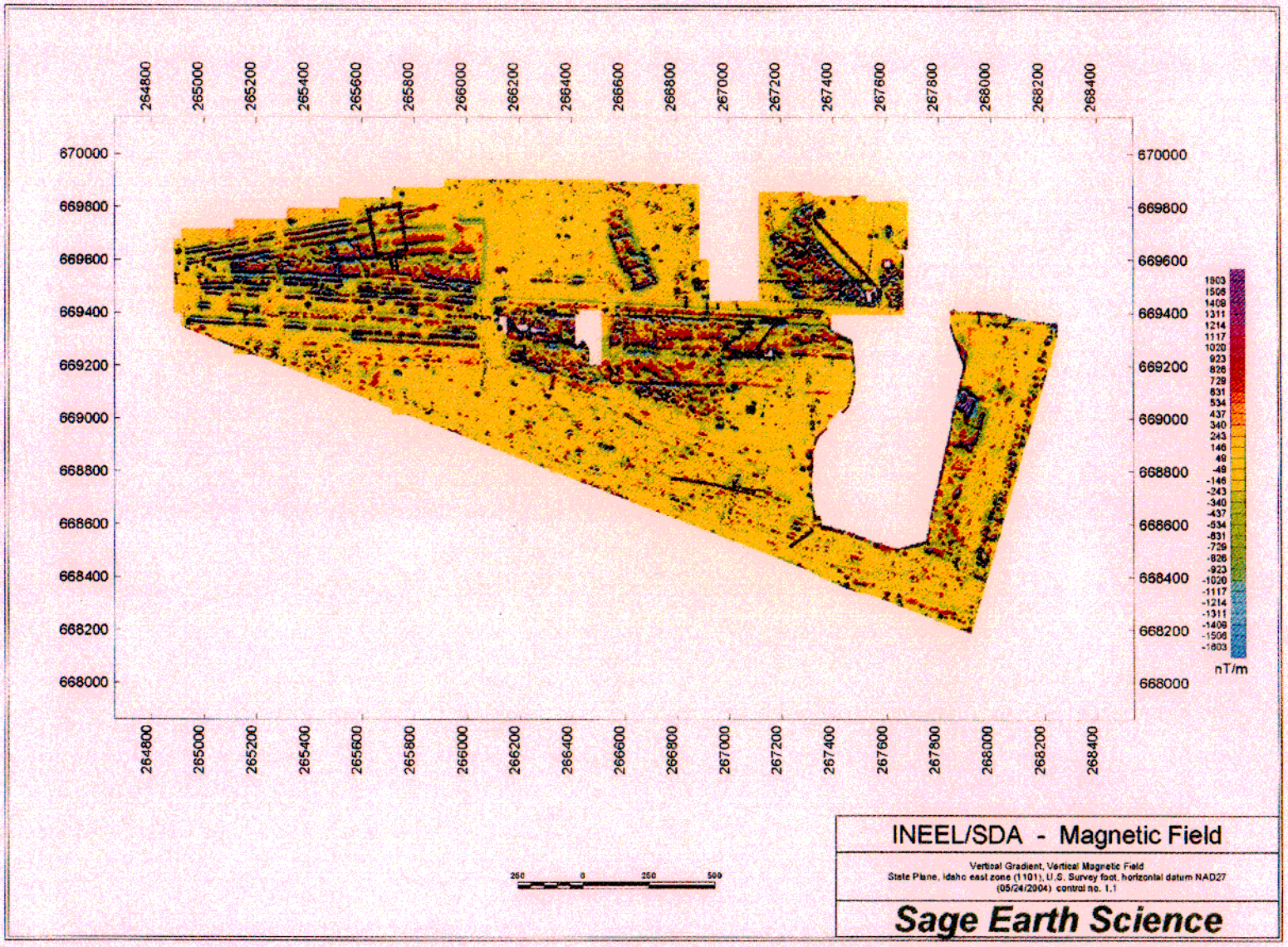

510 East 17th Street, Suite 110, Idaho Falls, ID 83404
telephone: (208)522-5049, Fax: (208)528-6200, email: ses@srv.net
http://www.srv.net/~ses/SES.HTM

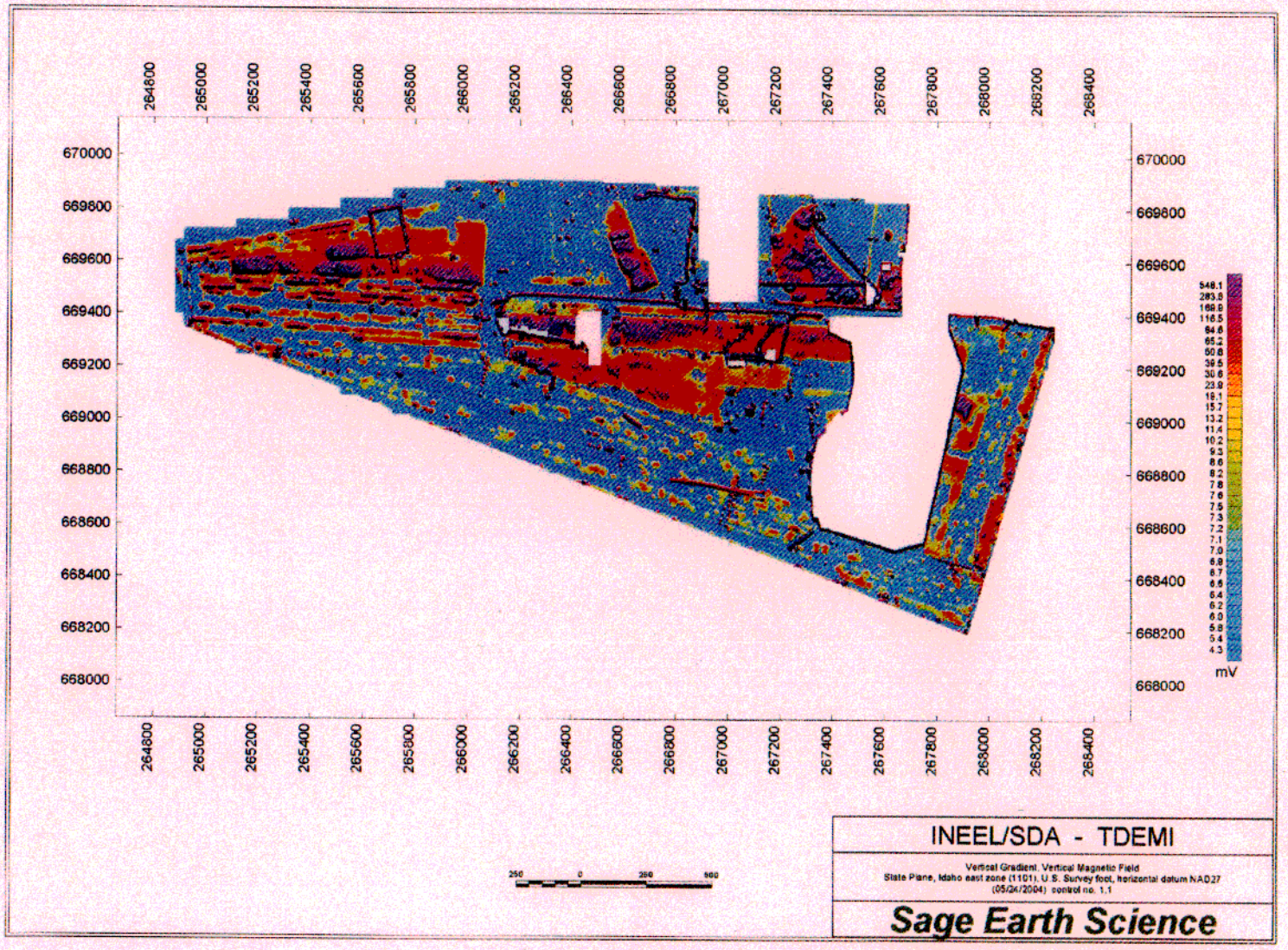

510 East 17th Street, Suite 110, Idaho Falls, ID 83404
telephone: (208)522-5049, Fax: (208)528-6200, email: ses@srv.net
http://www.srv.net/~ses/SES.HTM

Appendix B

Stoller Logging Data — Stripcharts

Appendix B

Stoller Logging Data — Stripcharts

Appendix B contains a complete record of subcontractor-submitted logging stripcharts for Type A Subsurface Disposal Area logging data collected between September 2003 and August 2004. Because of the heterogeneity of the buried waste and the suite of contaminants associated with a given waste stream (or mixture of waste streams), the passive gamma ray spectra acquired at any given location in the waste zones are complex. Proper identification of radionuclides is further complicated by interference issues due to similar energy gamma rays from multiple, potential radionuclides. A detailed knowledge of the composition of the waste being interrogated is required to provide correct interpretations of the gamma ray spectra.

Results presented in these stripcharts represent the logging subcontractor's interpretation of the nuclear data and are, in some cases, subject to alternate interpretations. The following alternative interpretations of the passive gamma ray data are particularly noted:

1. Europium-154 was identified in numerous probeholes based on the 1,274-keV gamma ray. The presence of Eu-154 in Subsurface Disposal Area waste material is strongly questioned. Both Eu-152 and Eu-154 are formed through neutron capture reactions, by Eu-151 and Eu-152 respectively, which occur in roughly equal amounts as impurities in metal. Europium-151 has a capture cross section 10 times greater than Eu-153, and Eu-152 has a half-life of 13.48 years compared with 8.59 years for Eu-154. These properties indicate that Eu-152 should be present. Additionally, consultation with Idaho Completion Project staff, who have extensive experience in neutron activation analysis, corroborates the fact that Eu-152 and Eu-154 should be identified together and not exclusive of each other. Europium-152 has several lines that would be measurable in the presence of large activities of Co-60, Cs-137, and transuranic (TRU) material. If Eu-154 was identified, then Eu-152 would almost certainly be present as well. However, Eu-152 was not reported by the subcontractor (except in the single case discussed below).

2. The 1,274-keV gamma ray also was reported extensively by the previous Type A logging subcontractor, but was not associated with Eu-154. It was suggested by Idaho National Laboratory subject matter experts that this gamma ray is most likely due to an (α n) reaction on fluorine. It is notable that most of the Eu-154 reported in this appendix correlates closely with Am-241, which is an alpha-emitter. This calls the identification of Eu-154 into question.

3. Stripcharts for probeholes P2-PU-1 and P2-PU-2 identify Eu-152 through the 344-keV and 1,408-keV lines; however, the data are marked as suspect because an alternate source for the 344-keV line could not be identified. There is a strong argument that the 344-keV line is actually from Pu-239, and the 1,408-keV line is attributed to naturally occurring radioactive material. Taking the ratio of the branching ratios of the 344-keV line from Pu-239 to that from Eu-152, a value of 4,666.667 is obtained. If this value is then multiplied by the apparent Eu-152 concentration calculated from the 344-keV line, a value is obtained that agrees very well with the apparent concentration for Pu-239 as reported using the 375-keV and 414-keV lines. This also is supported by detailed analysis of the long-count data, demonstrating that the spectral analysis software continuously misidentified the 1,408-keV peak from Bi-214 as the 1,408-keV peak from Eu-152. Further, because of the nature of the targeted waste, it is highly unlikely that europium contamination would be associated with the plutonium-contaminated graphite waste.

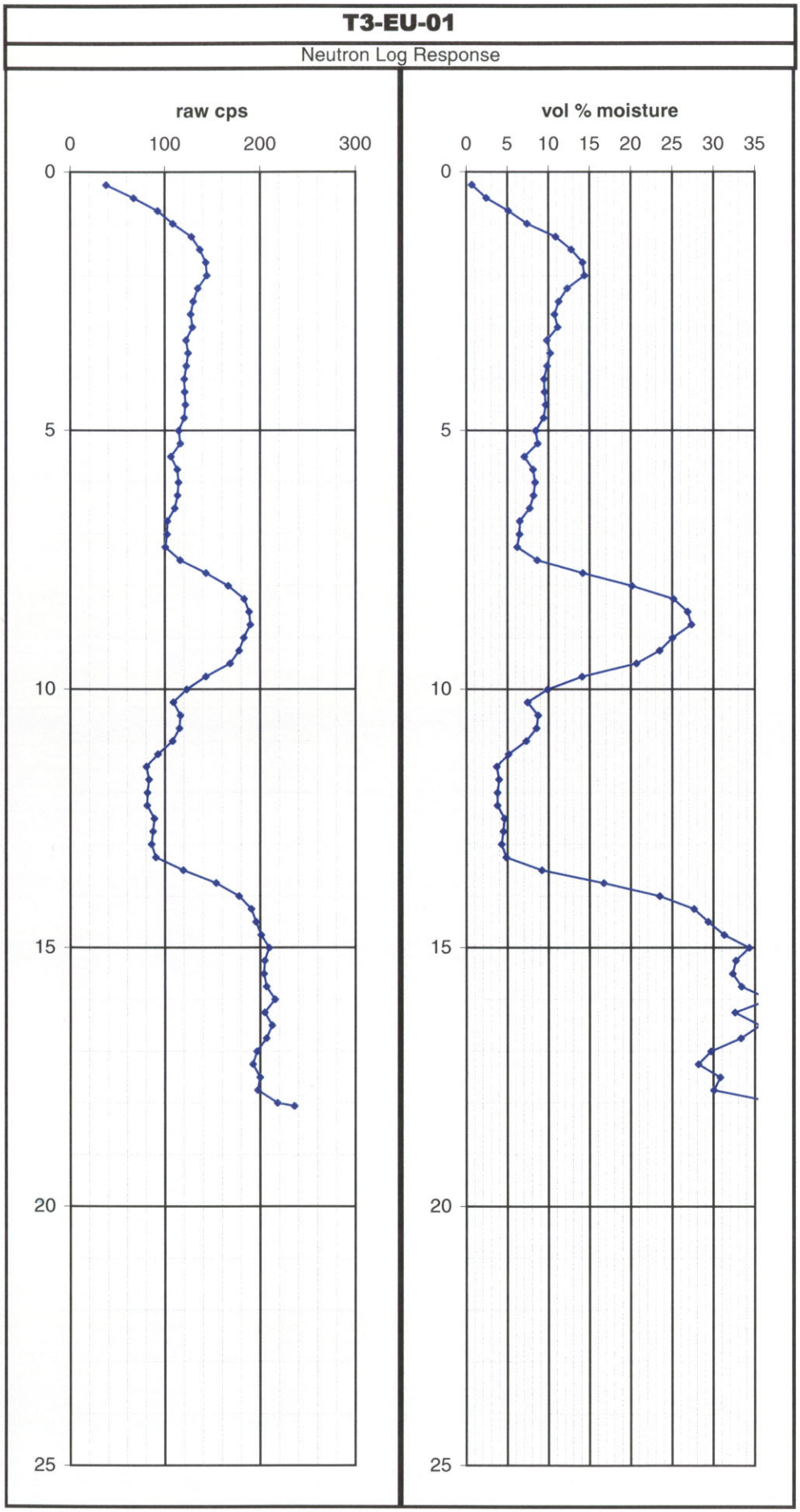
T3-EU-01
Neutron Log Response
raw cps
0
100
200
300
0
5
10
15
20
25
vol % moisture
0
5
10
15
20
25
30
35
0
5
10
15
20
25

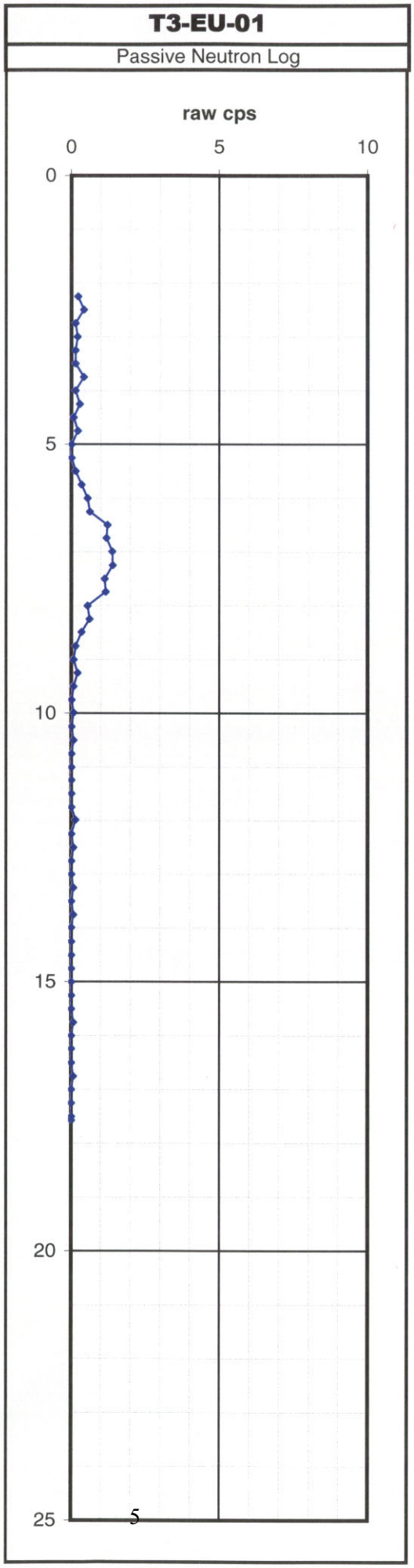
T3-EU-01
Passive Neutron Log
raw cps
0
5
10
0
5
10
15
20
25

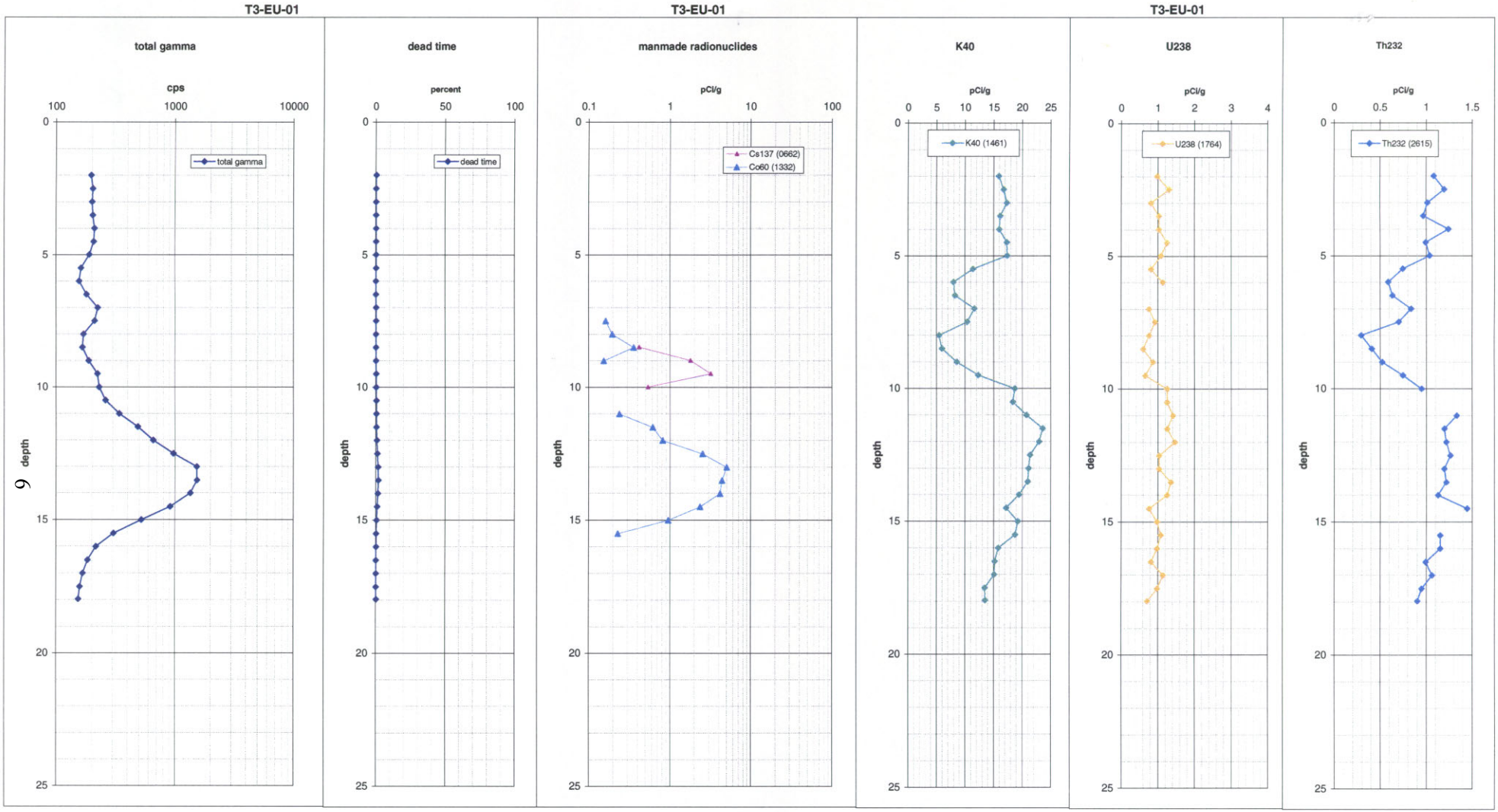
T3-EU-01
total gamma
cps
100
1000
10000
total gamma
depth
0
5
10
15
20
25
T3-EU-01
dead time
percent
0
50
100
dead time
depth
T3-EU-01
manmade radionuclides
pCi/g
0.1
1
10
100
Cs137 (0662)
Co60 (1332)
depth
T3-EU-01
K40
pCi/g
0
5
10
15
20
25
K40 (1461)
depth
U238
pCi/g
0
1
2
3
4
U238 (1764)
depth
Th232
pCi/g
0
0.5
1
1.5
Th232 (2615)
depth

T3-EU-01

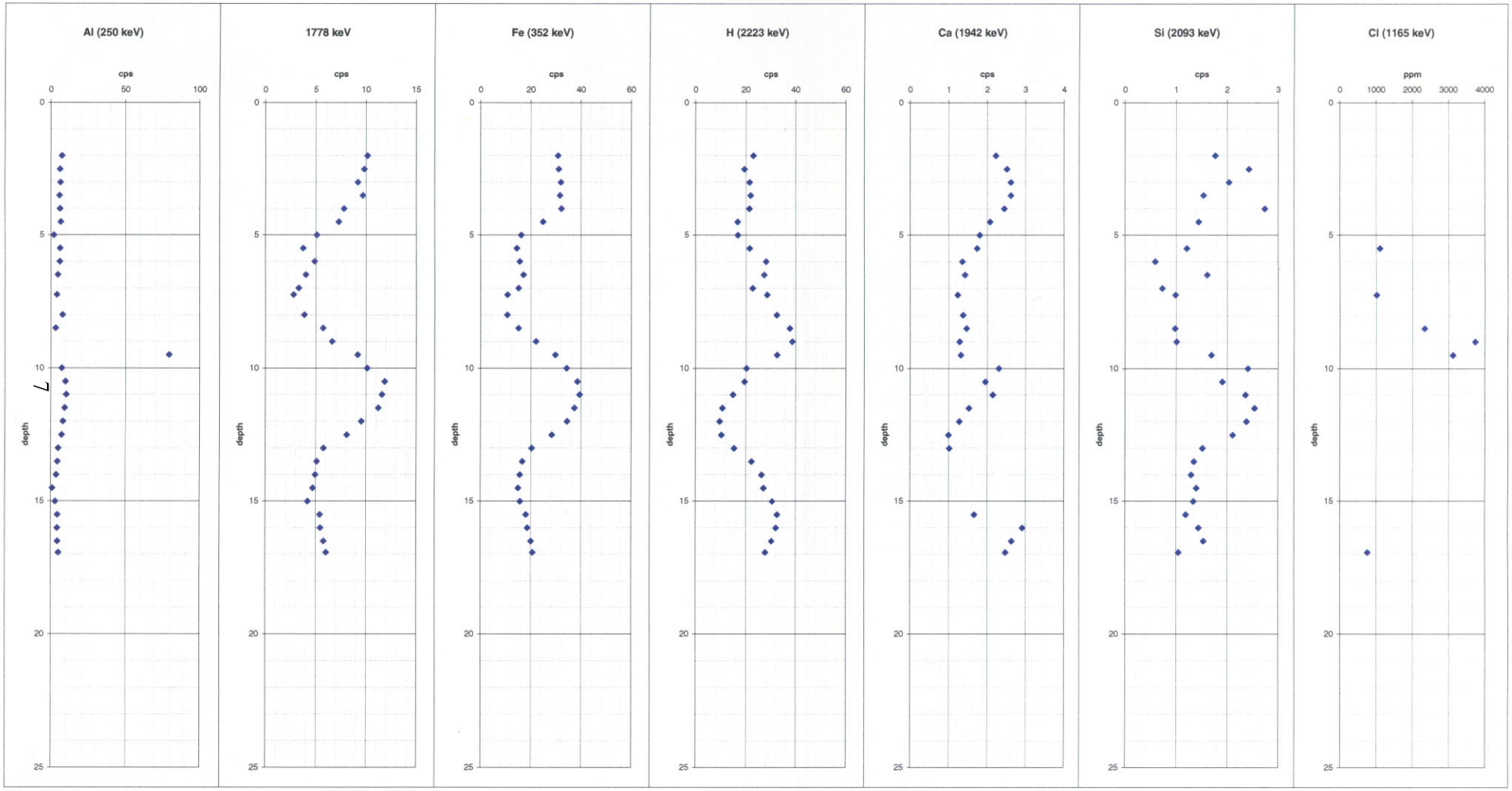
Al (250 keV)
1778 keV
Fe (352 keV)
H (2223 keV)
Ca (1942 keV)
Si (2093 keV)
Cl (1165 keV)
cps
ppm
depth
0
5
10
15
20
25
50
100
1
2
3
4
1000
2000
3000
4000

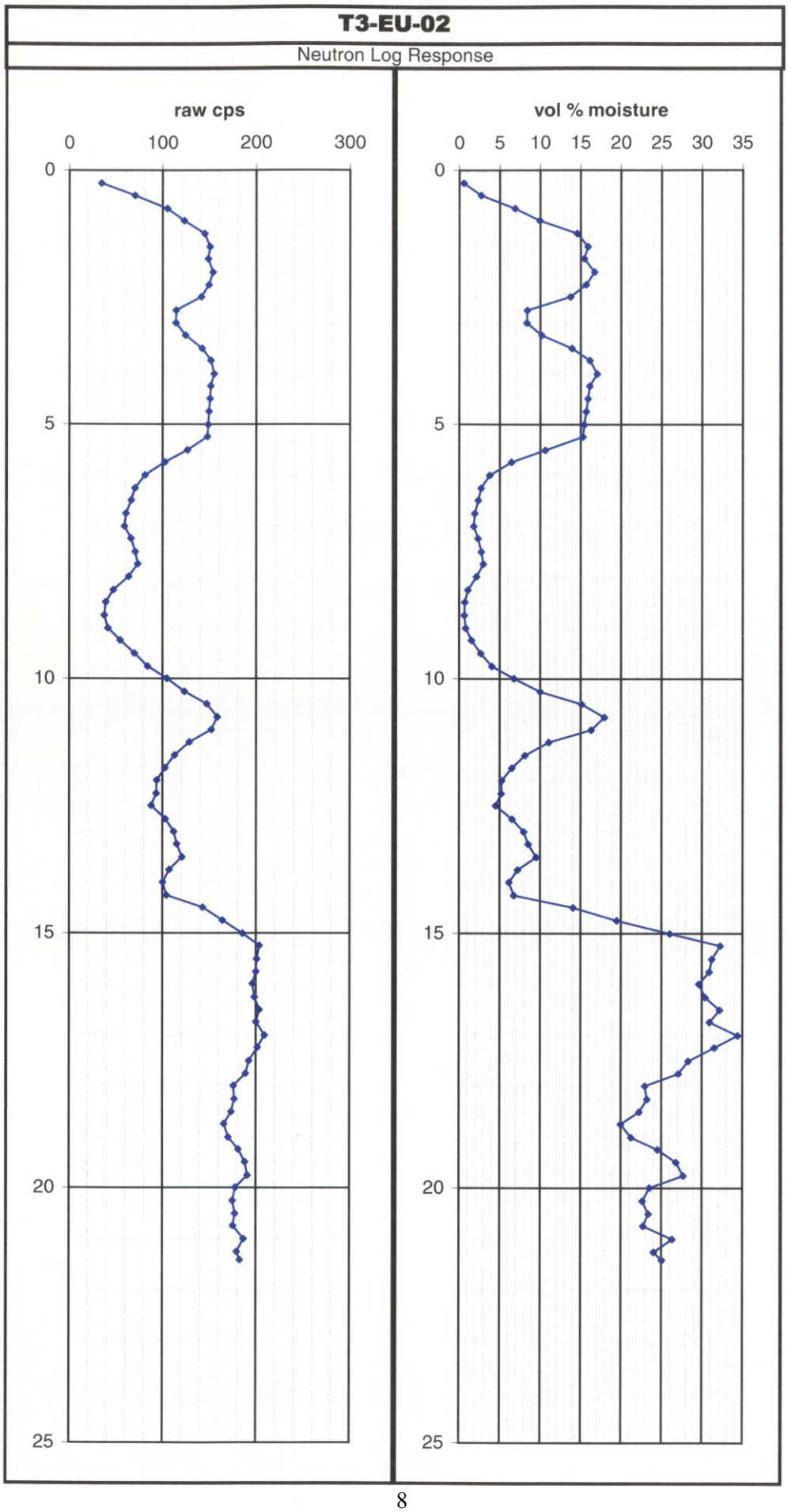
T3-EU-02
Neutron Log Response
raw cps
0
100
200
300
0
5
10
15
20
25
vol % moisture
0
5
10
15
20
25
30
35
0
5
10
15
20
25

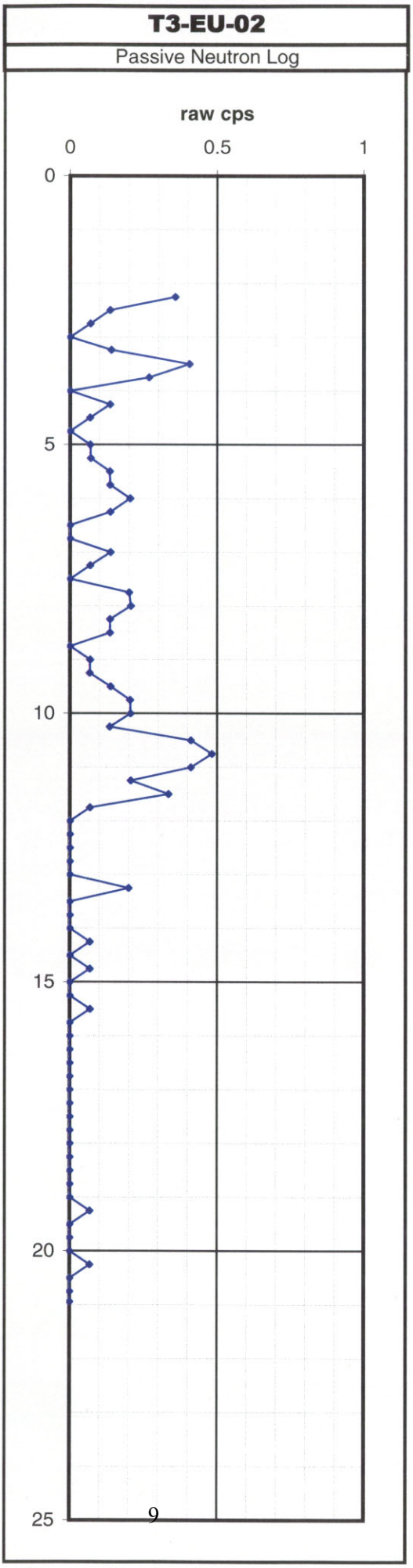
T3-EU-02
Passive Neutron Log
raw cps
0
0.5
1
0
5
10
15
20
25

T3-EU-02

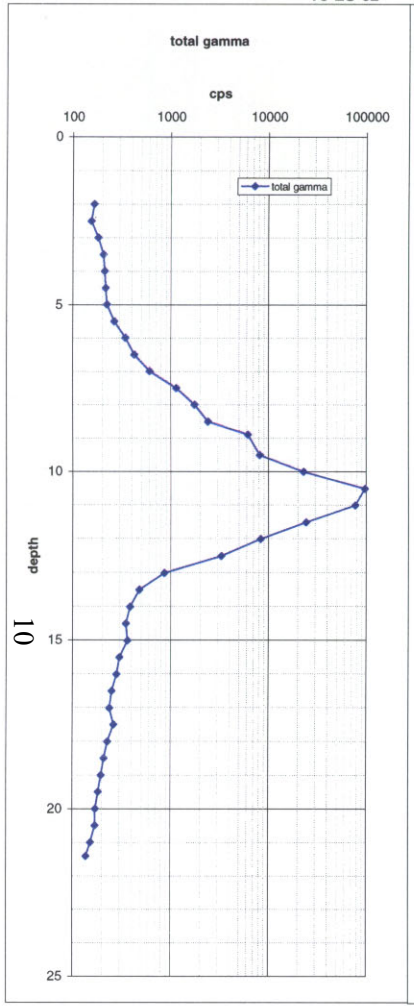

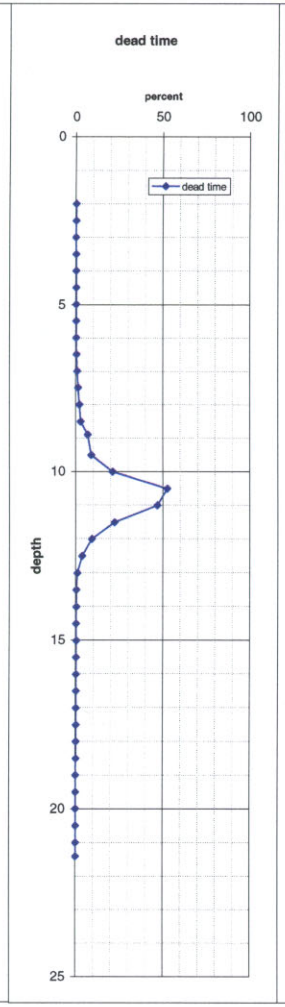

T3-EU-02

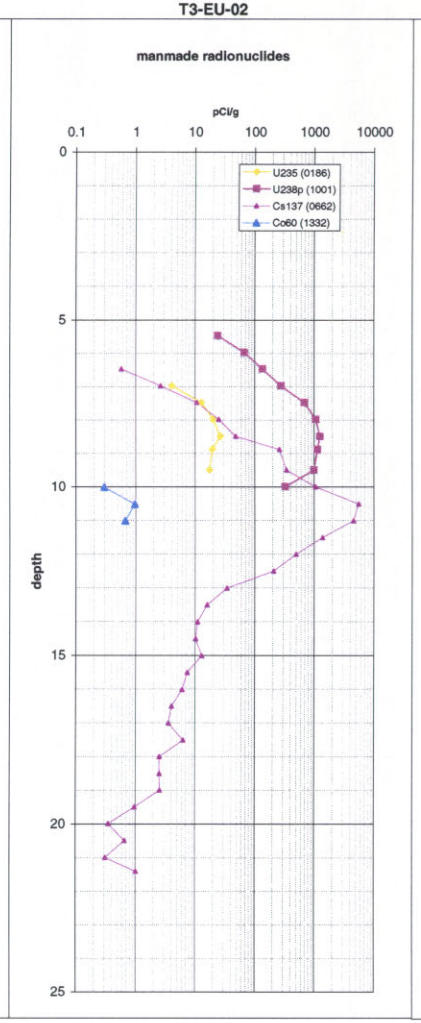

T3-EU-02

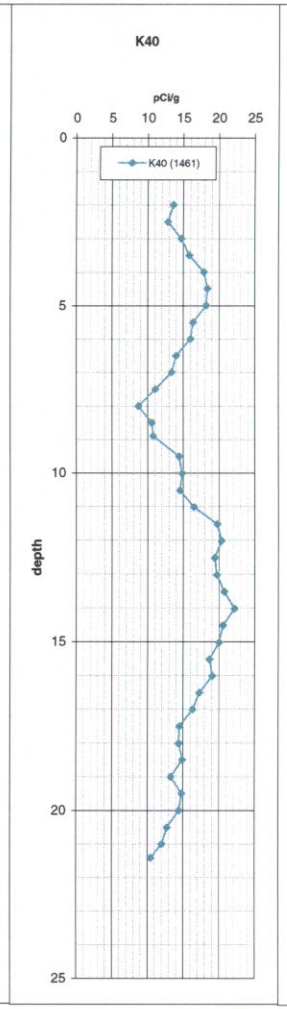

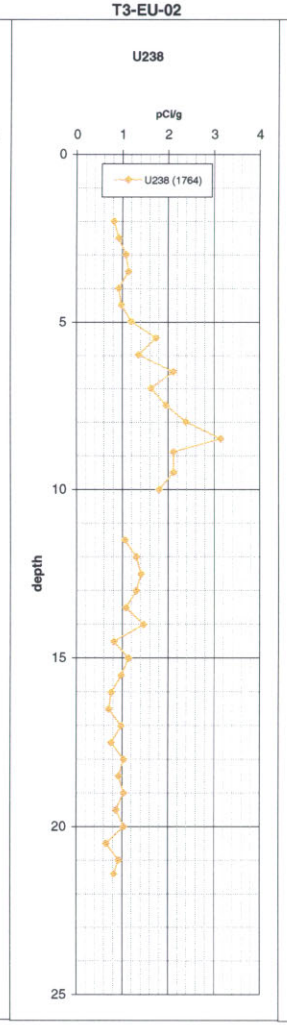

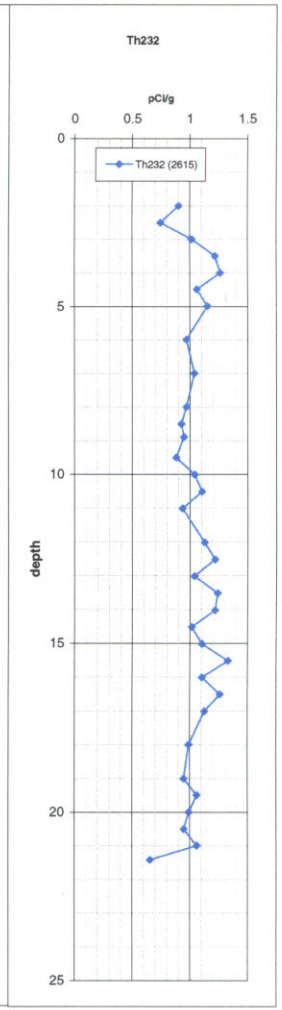

T3-EU-02

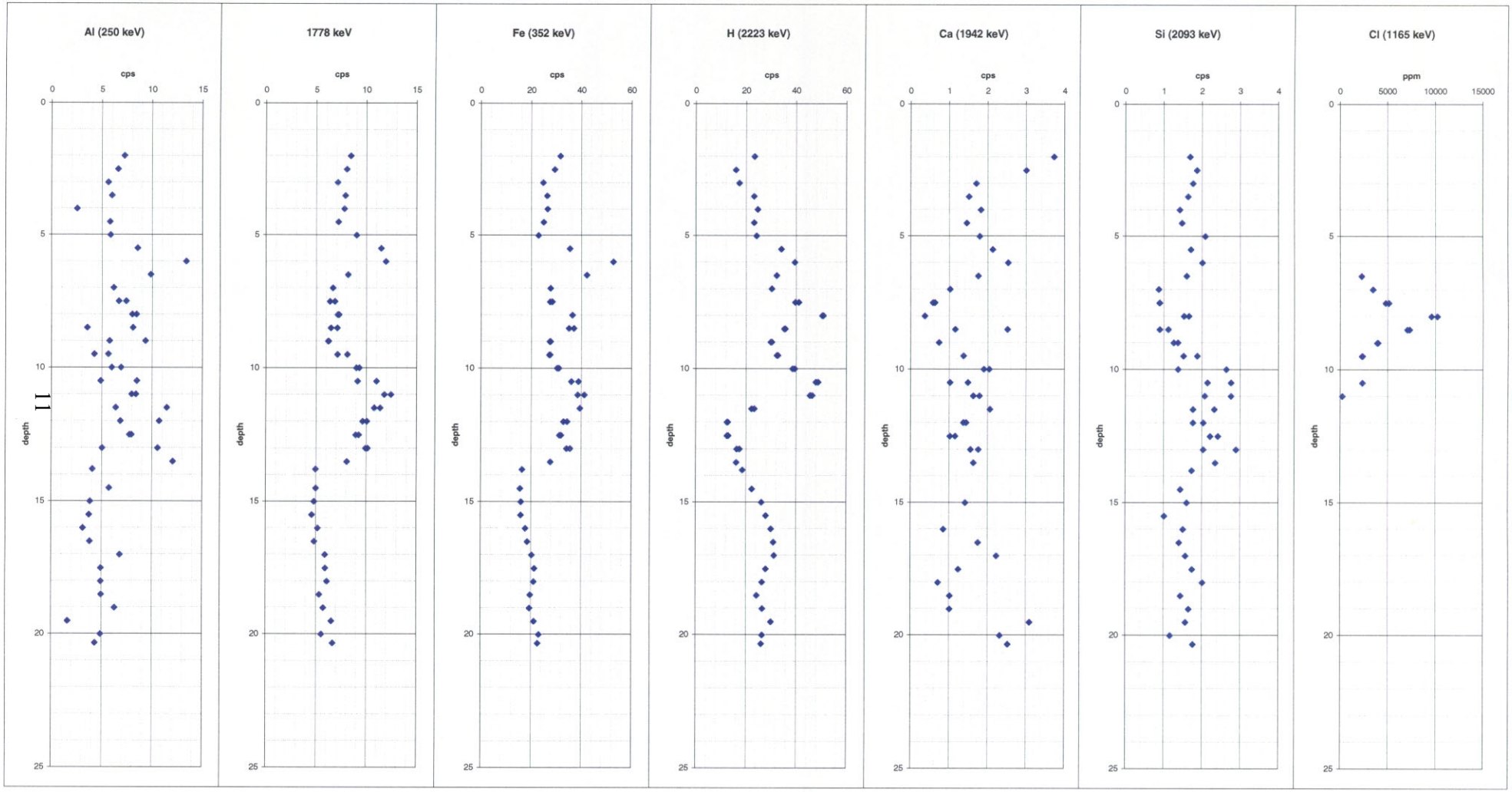
Al (250 keV)
1778 keV
Fe (352 keV)
H (2223 keV)
Ca (1942 keV)
Si (2093 keV)
Cl (1165 keV)
cps
ppm
depth

T3-EU-02 (Total Gamma)

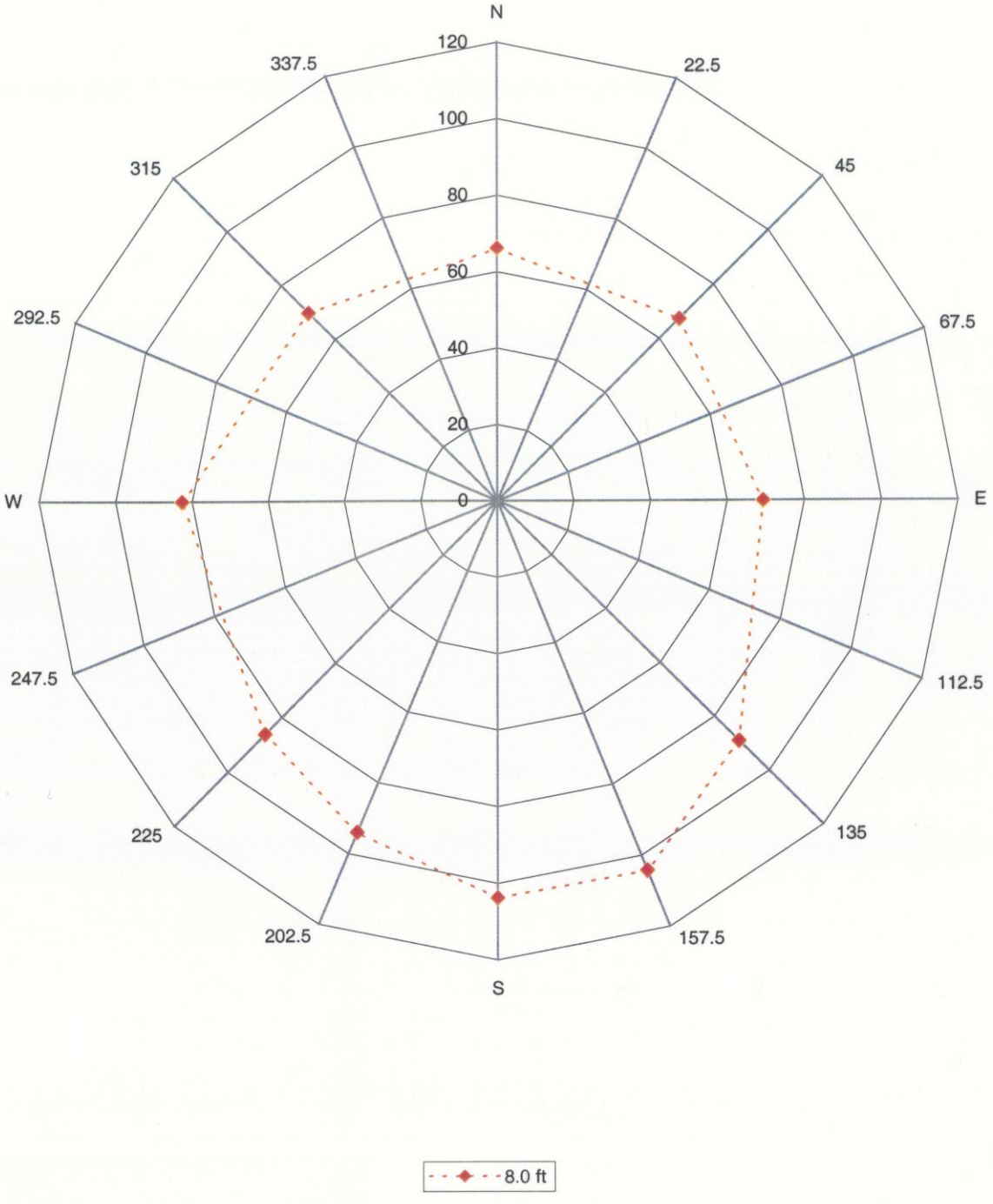

T3-EU-02 U-238p (1001 keV)

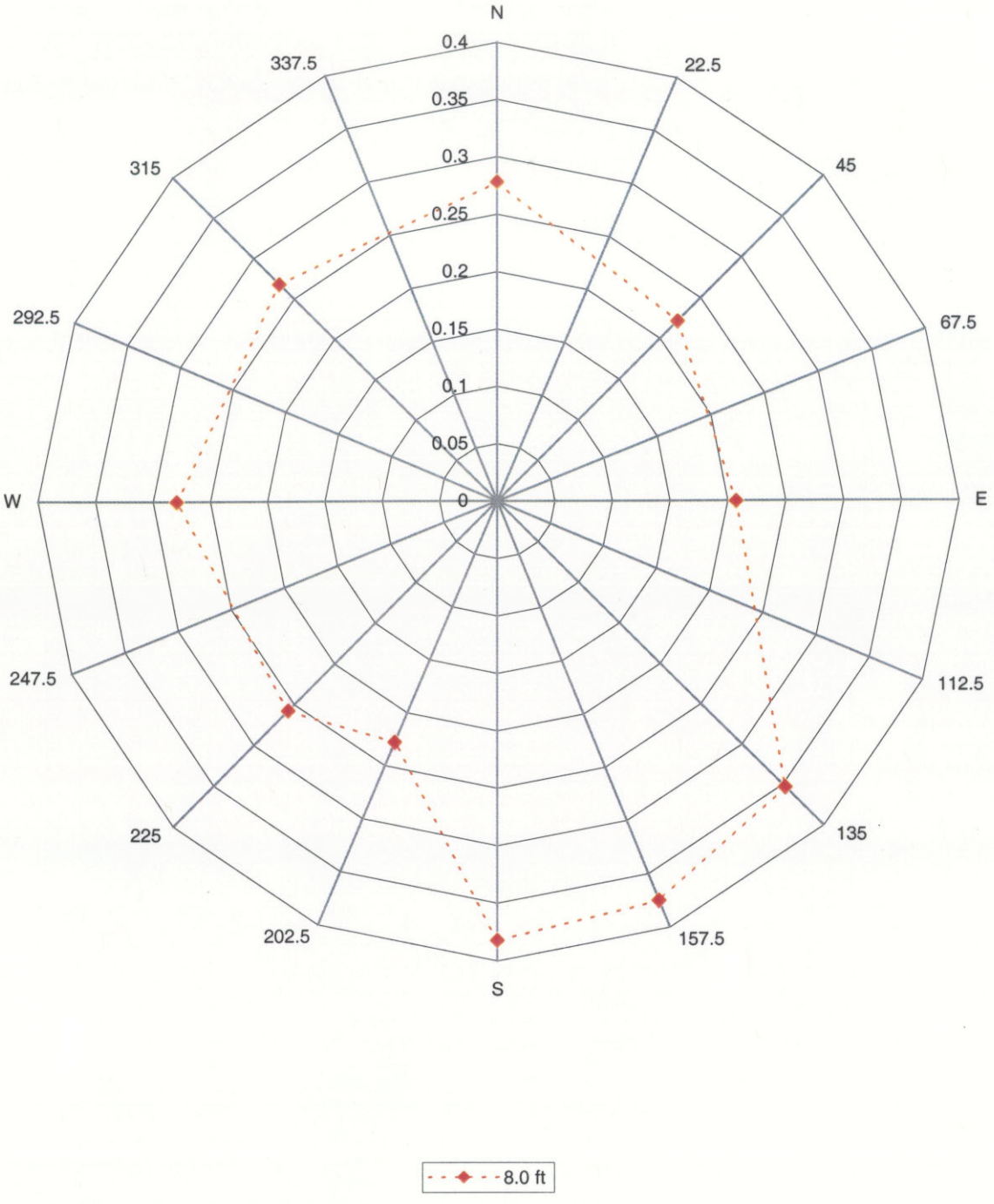

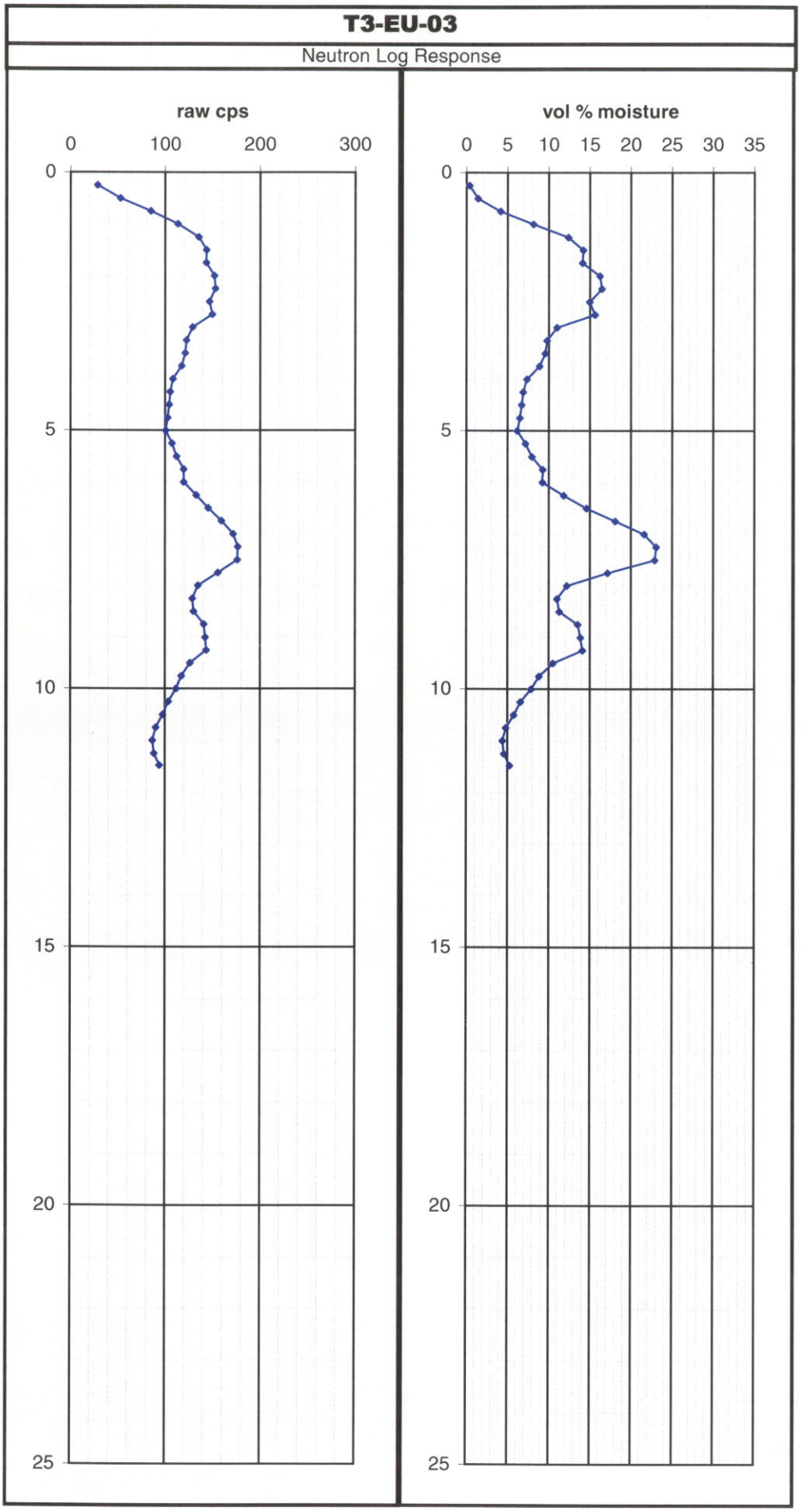
T3-EU-03
Neutron Log Response
raw cps
0
100
200
300
0
5
10
15
20
25
vol % moisture
0
5
10
15
20
25
30
35
0
5
10
15
20
25

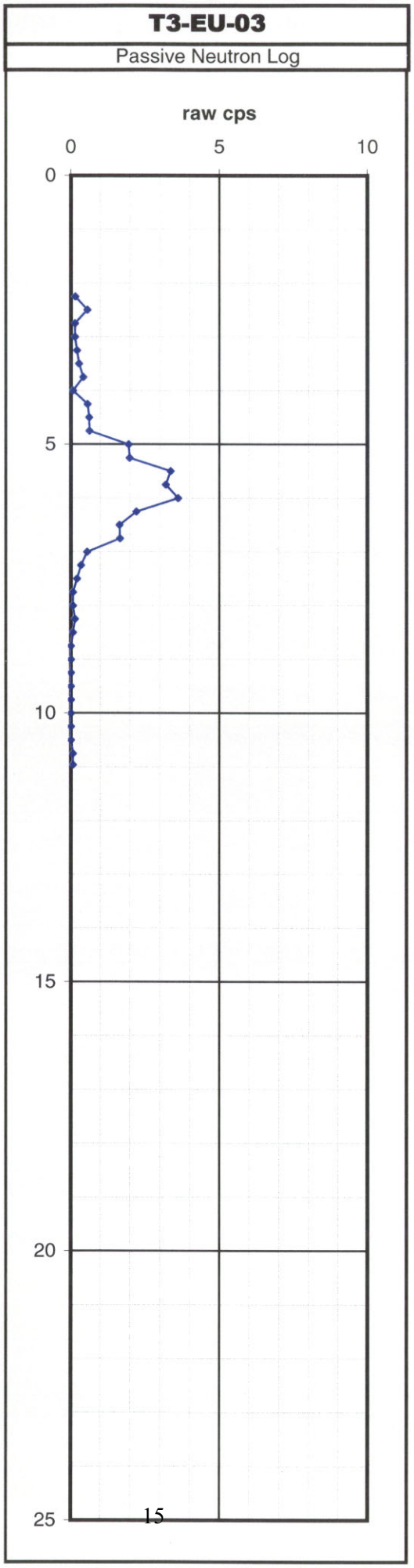
T3-EU-03
Passive Neutron Log
raw cps
0
5
10
0
5
10
15
20
25

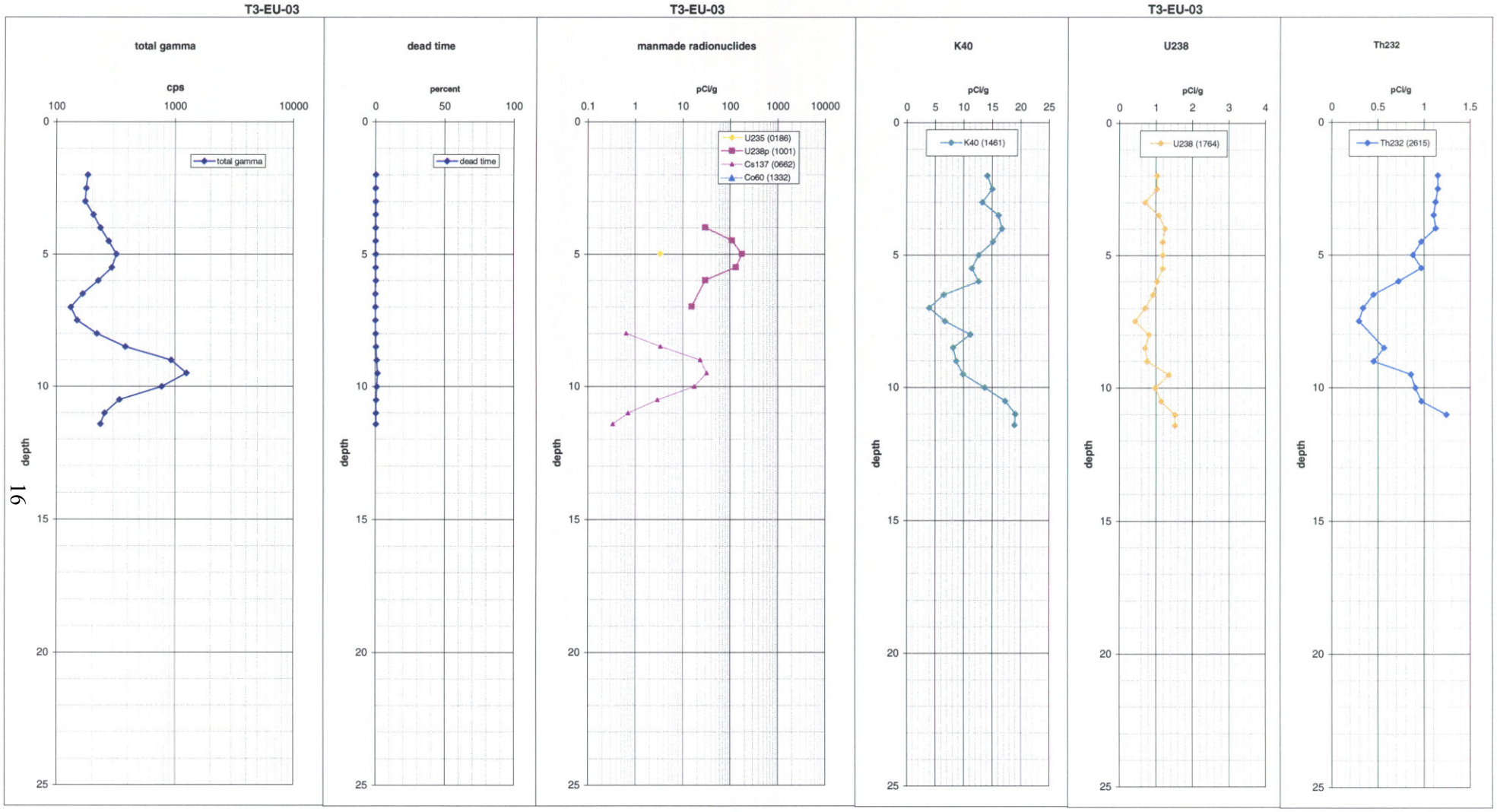
T3-EU-03
total gamma
cps
100
1000
10000
total gamma
depth
0
5
10
15
20
25
T3-EU-03
dead time
percent
0
50
100
dead time
depth
T3-EU-03
manmade radionuclides
pCi/g
0.1
1
10
100
1000
10000
U235 (0186)
U238p (1001)
Cs137 (0662)
Co60 (1332)
depth
T3-EU-03
K40
pCi/g
0
5
10
15
20
25
K40 (1461)
depth
U238
pCi/g
0
1
2
3
4
U238 (1764)
depth
Th232
pCi/g
0
0.5
1
1.5
Th232 (2615)
depth

T3-EU-03

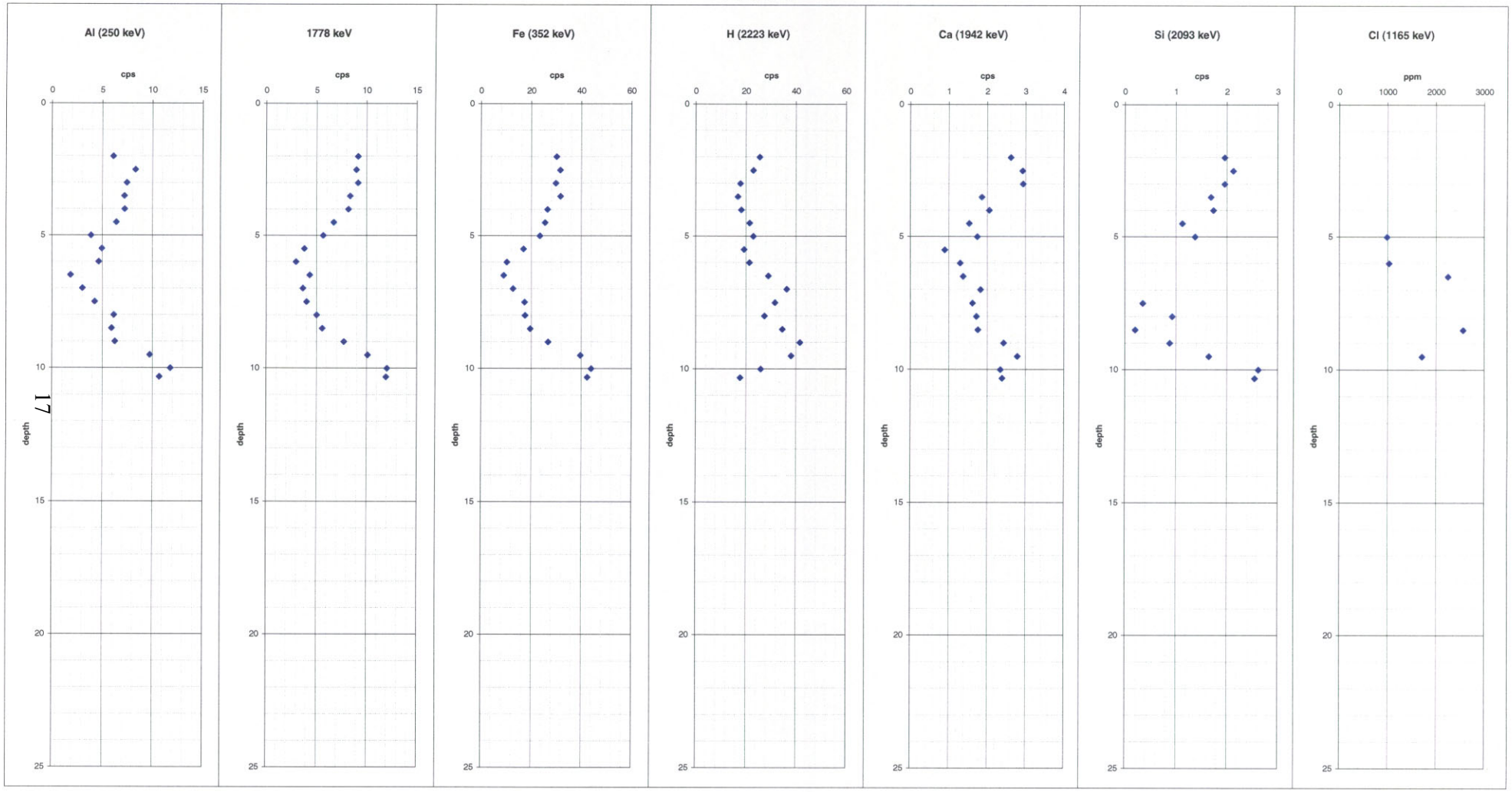
Al (250 keV)
1778 keV
Fe (352 keV)
H (2223 keV)
Ca (1942 keV)
Si (2093 keV)
Cl (1165 keV)
cps
ppm
depth

T3-EU-03 (Total Gamma)

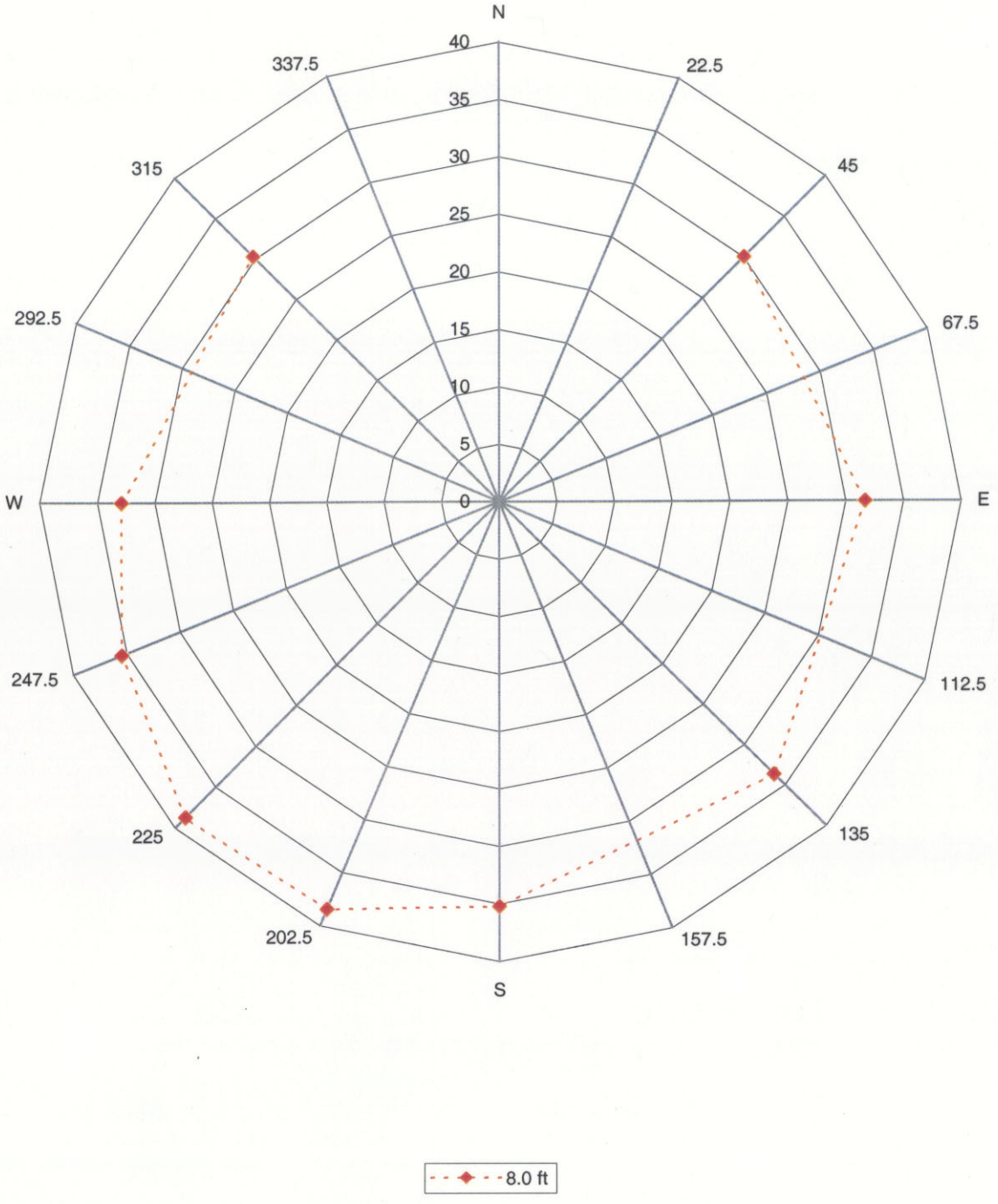

T3-EU-03 U-238p (1001 keV)

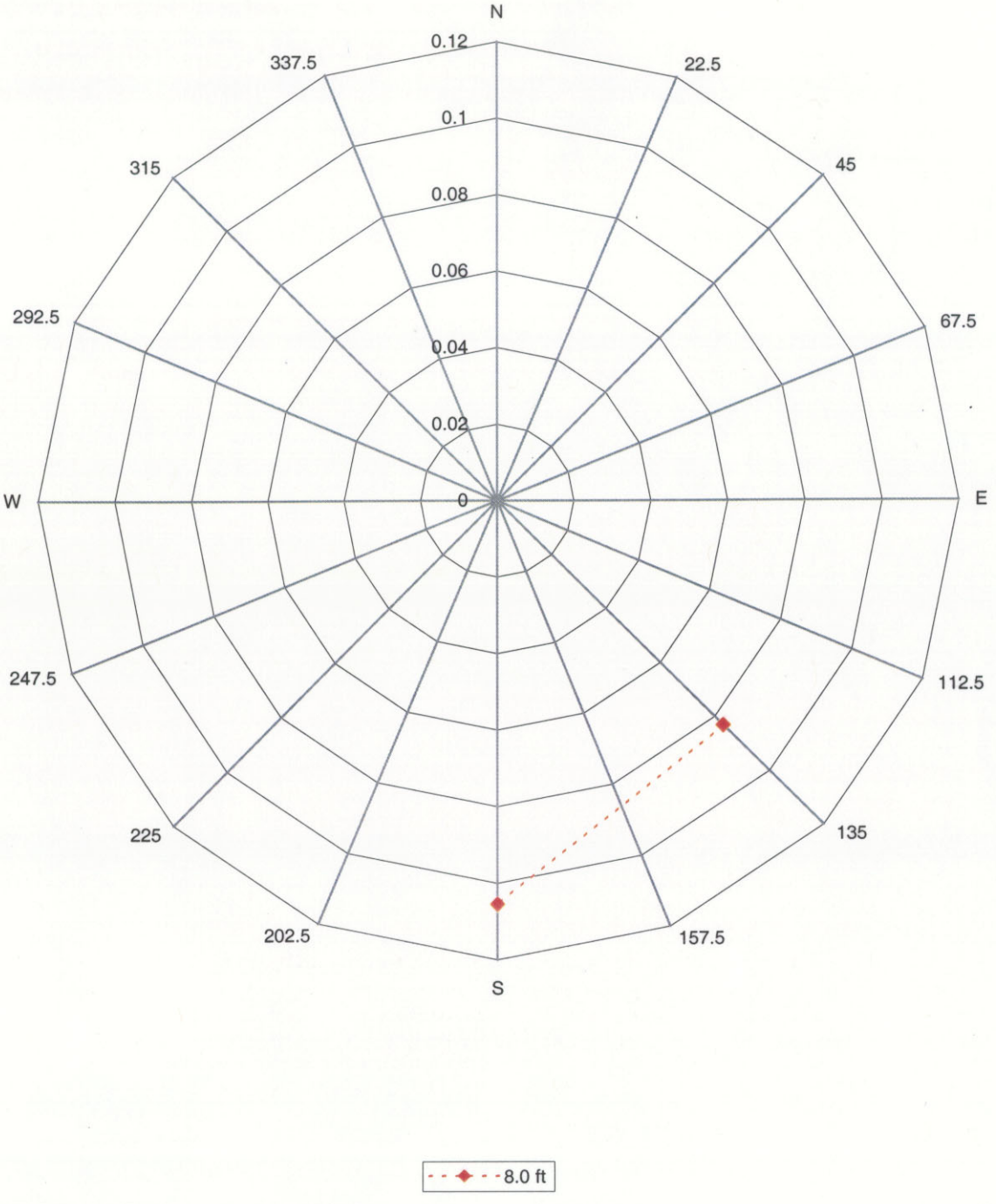

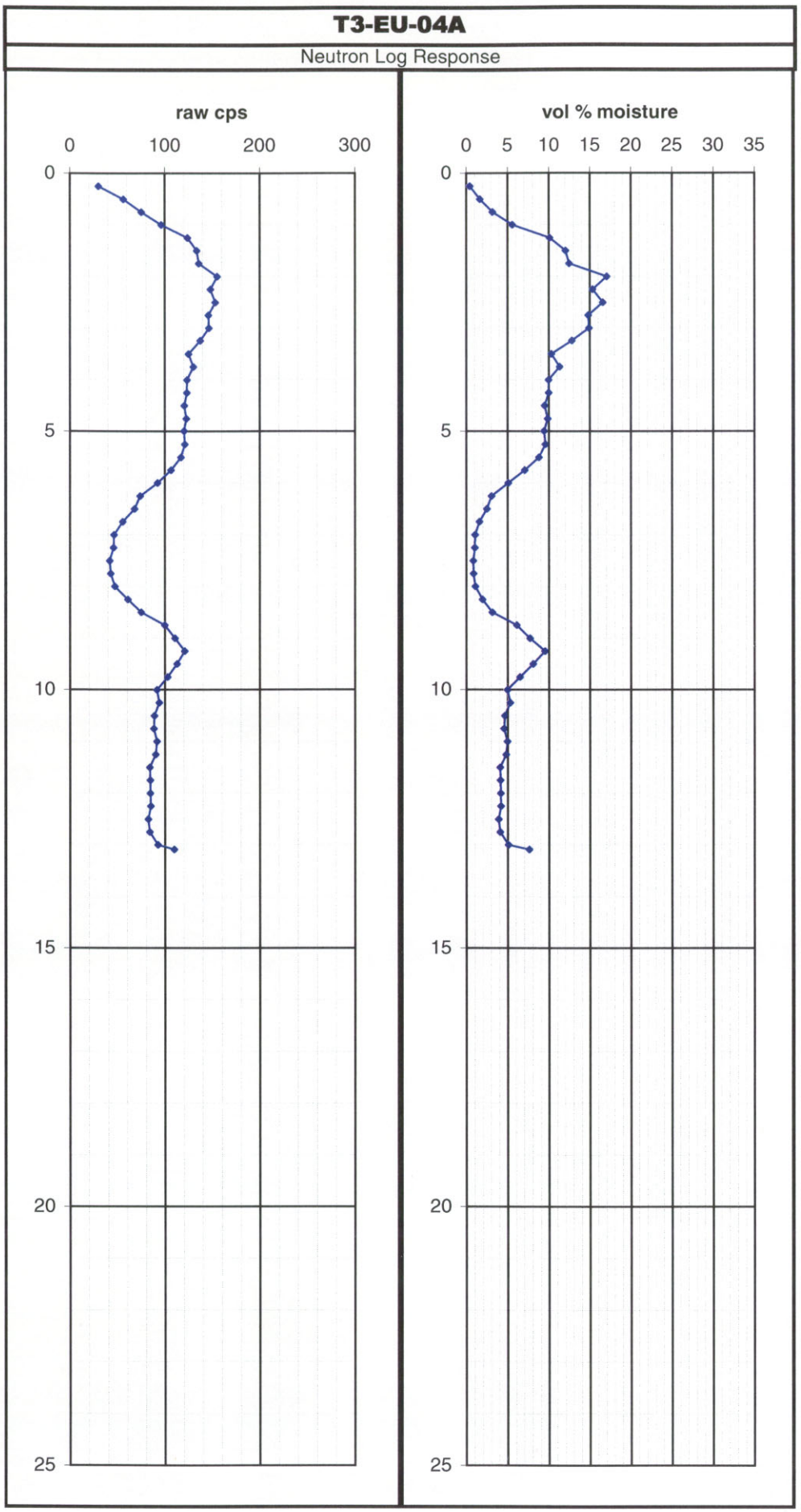
T3-EU-04A
Neutron Log Response
raw cps
0
100
200
300
vol % moisture
0
5
10
15
20
25
30
35
0
5
10
15
20
25

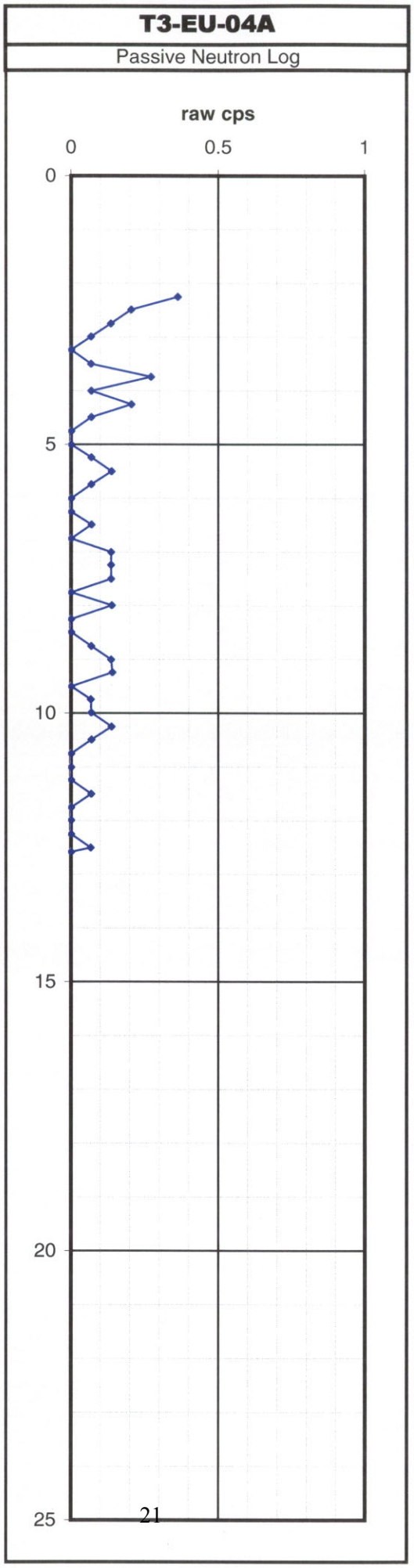
T3-EU-04A
Passive Neutron Log
raw cps
0
0.5
1
0
5
10
15
20
25

T3-EU-04a

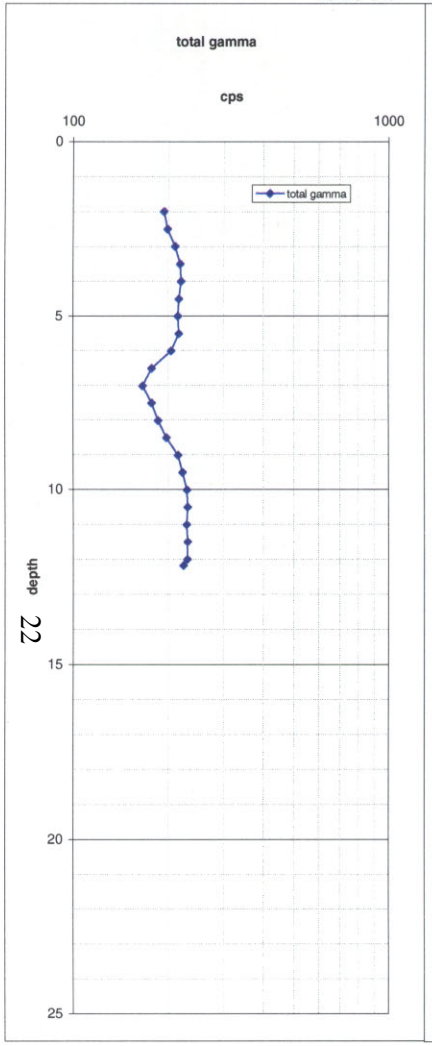

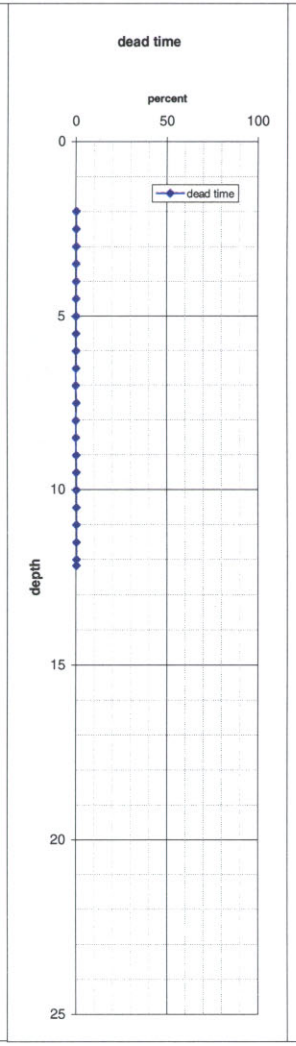

T3-EU-04a

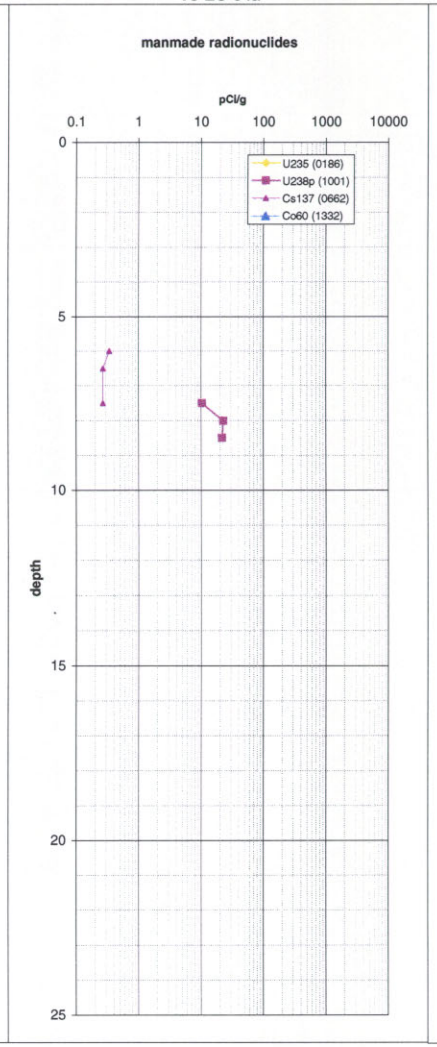

T3-EU-04a

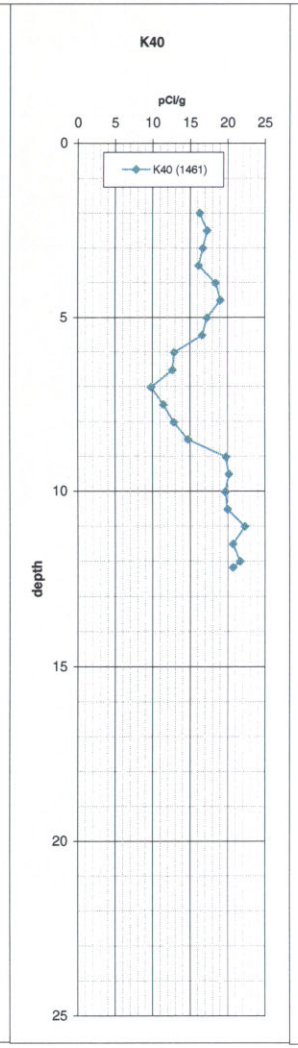

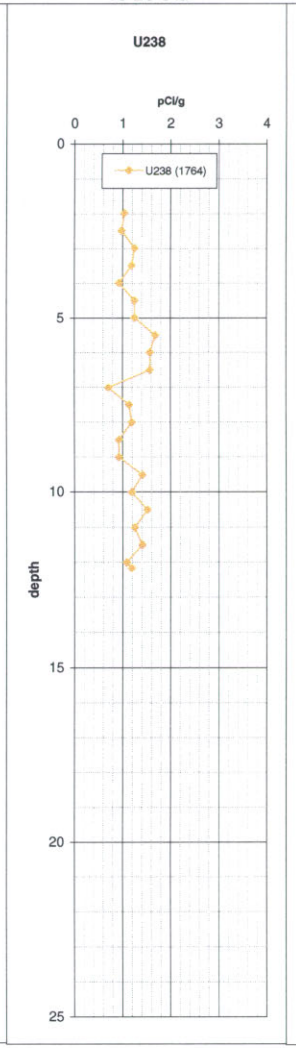

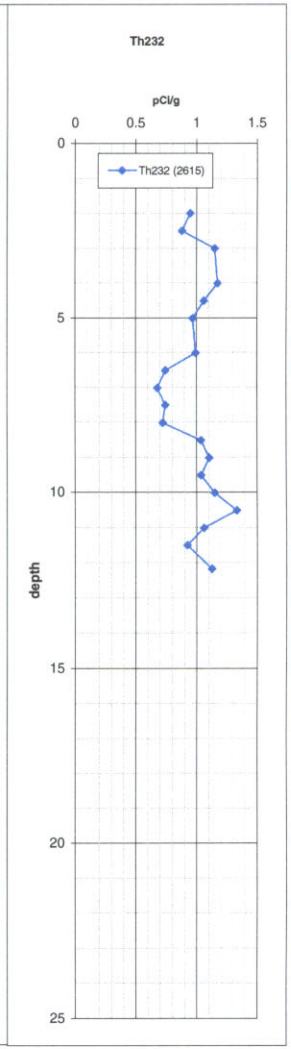

T3-EU-04a

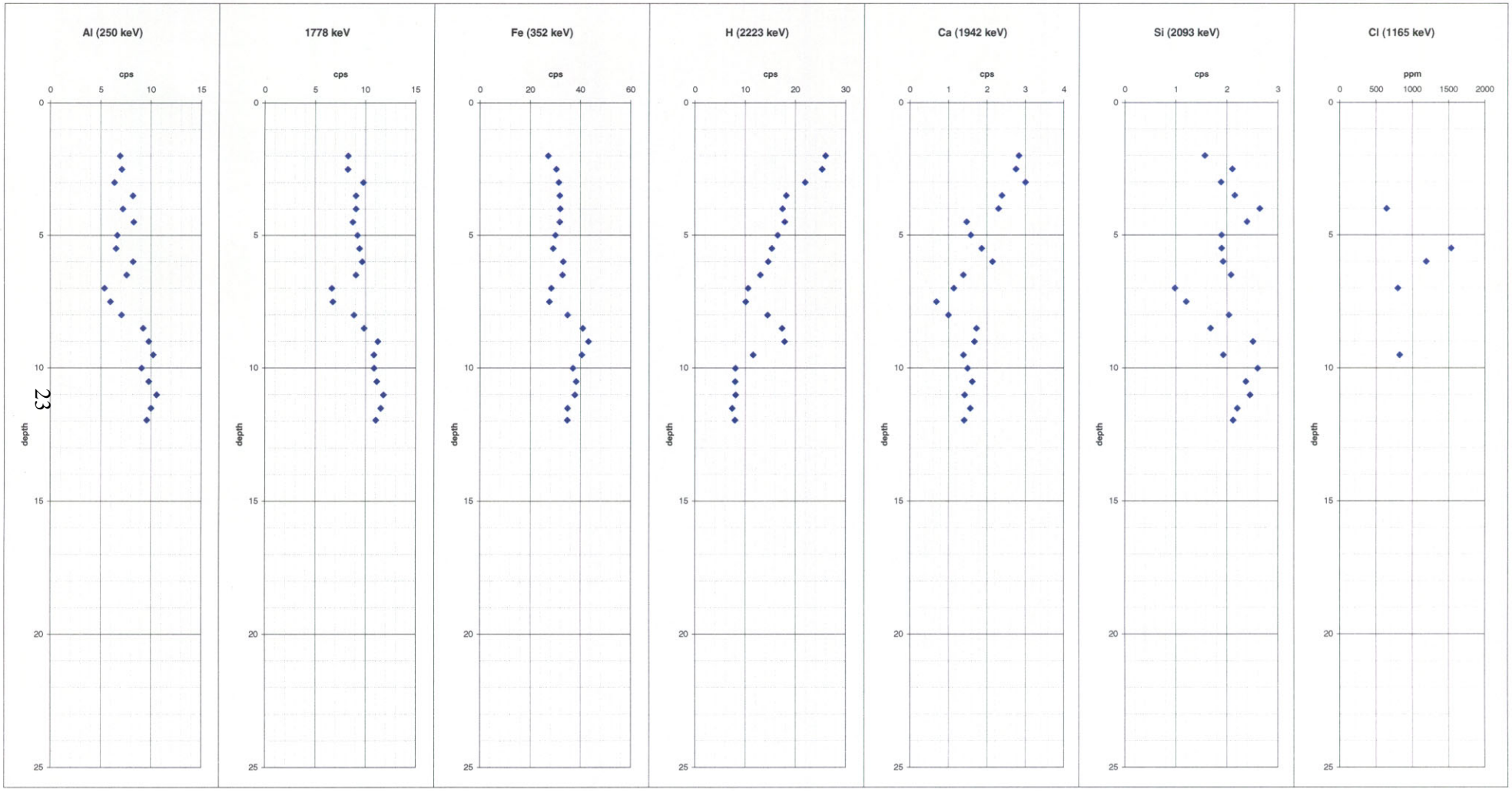
Al (250 keV)
1778 keV
Fe (352 keV)
H (2223 keV)
Ca (1942 keV)
Si (2093 keV)
Cl (1165 keV)
cps
ppm
depth

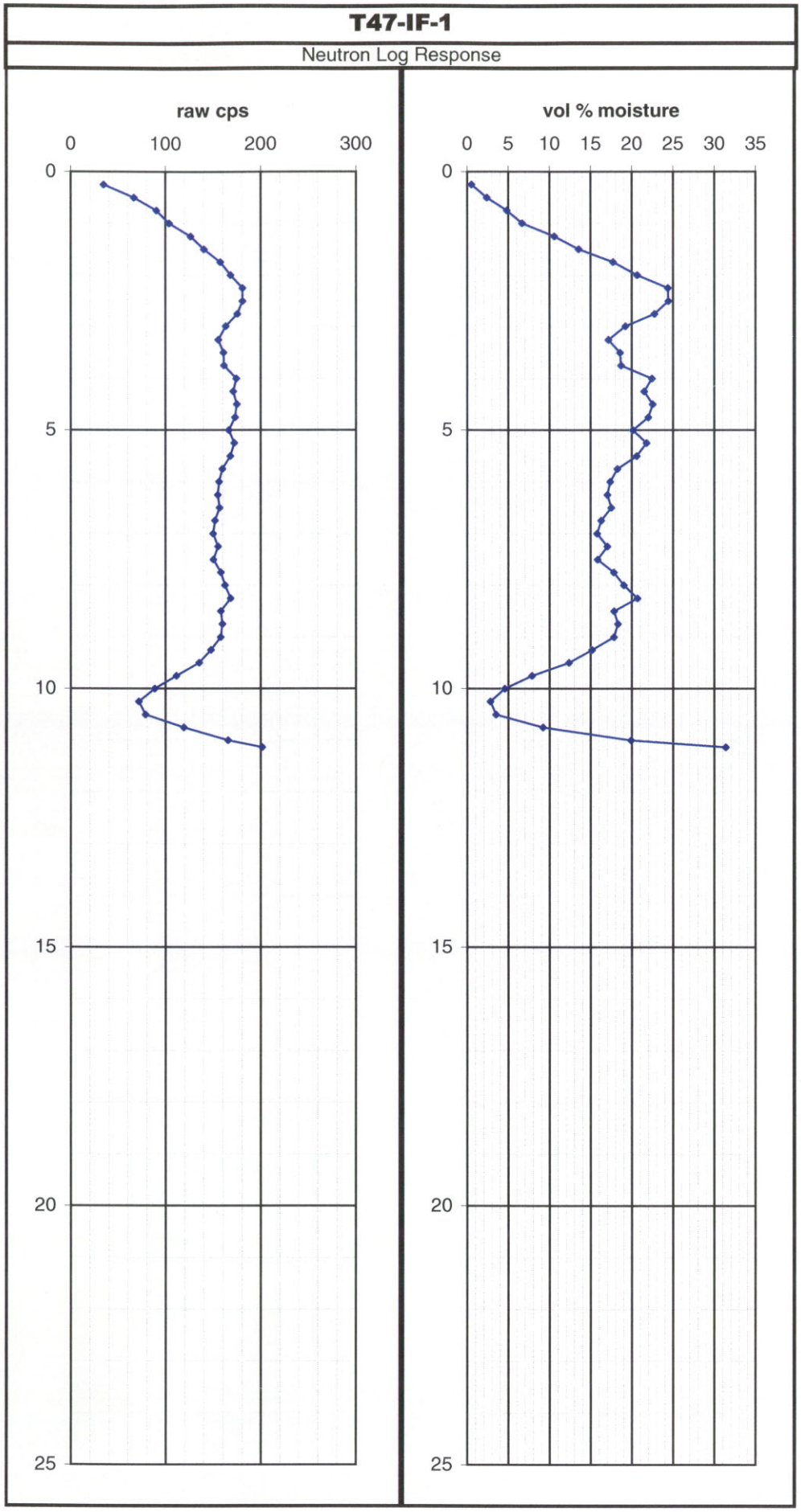
T47-IF-1
Neutron Log Response
raw cps
0
100
200
300
vol % moisture
0
5
10
15
20
25
30
35

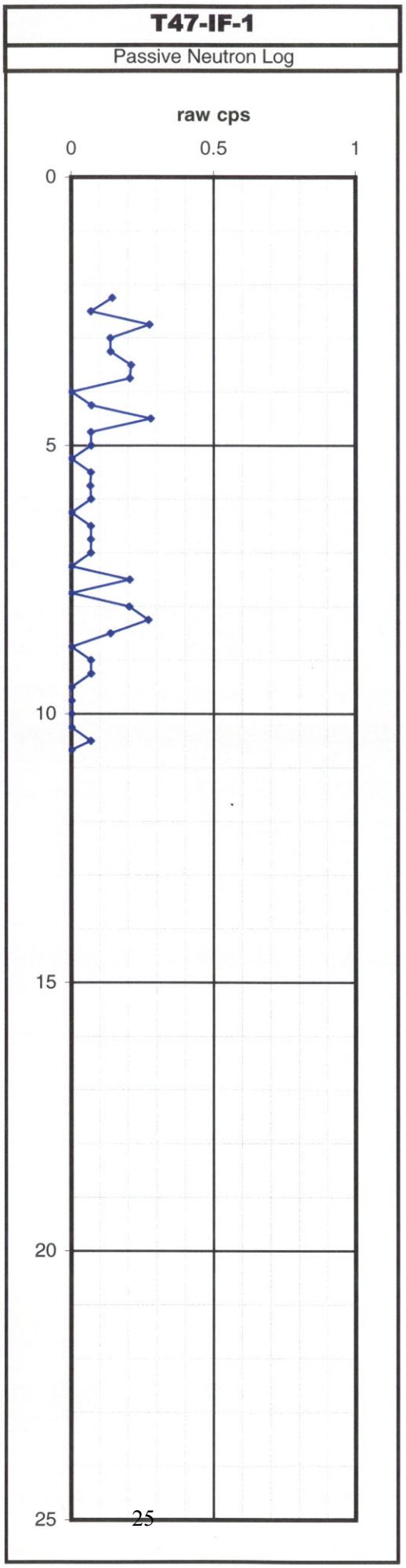
T47-IF-1
Passive Neutron Log
raw cps
0
0.5
1
0
5
10
15
20
25

T47-IF-1

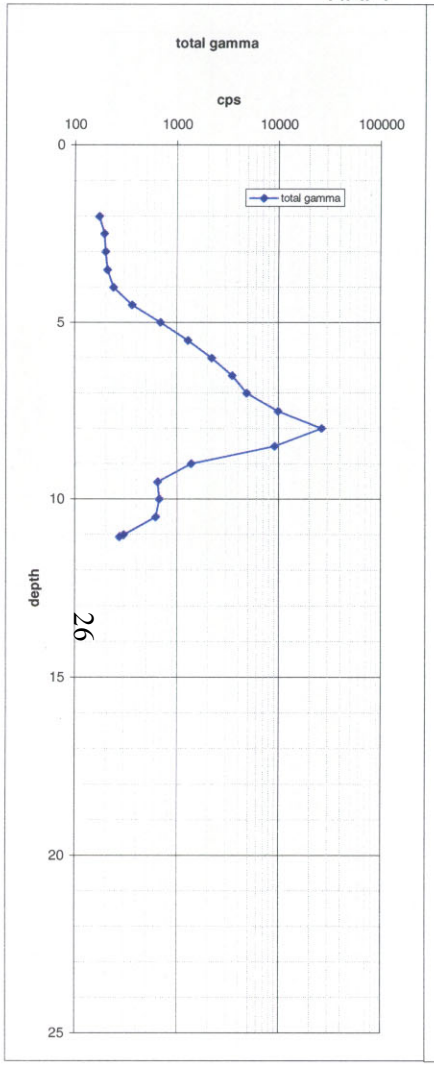

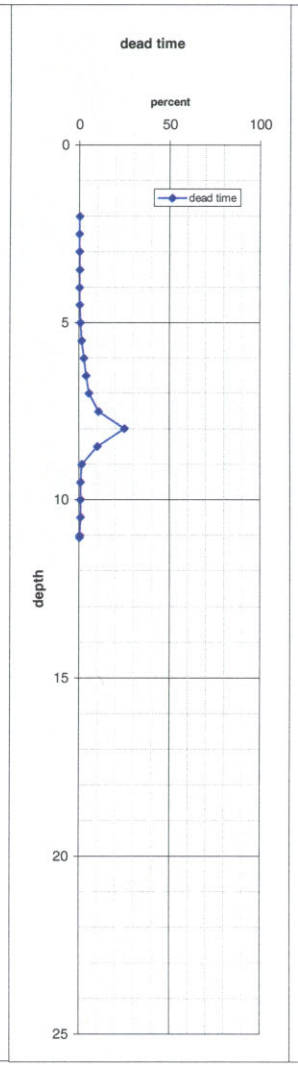

T47-IF-1

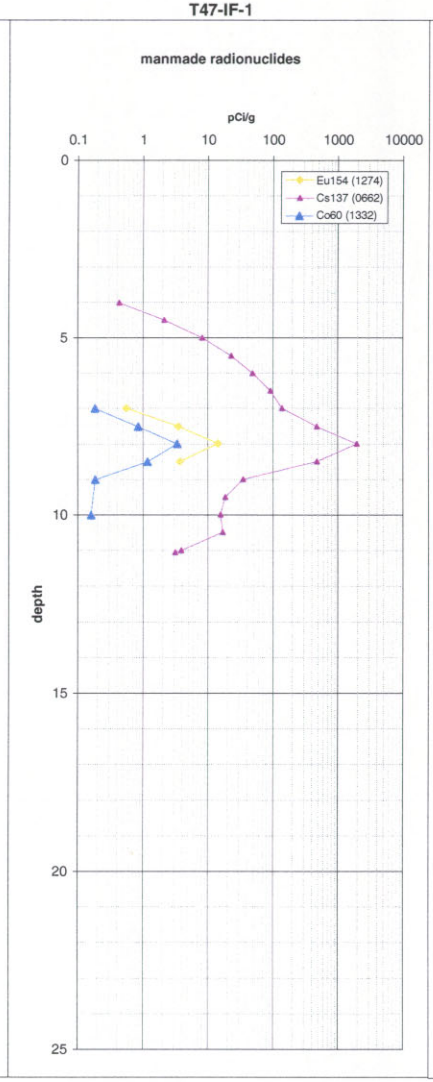

T47-IF-1

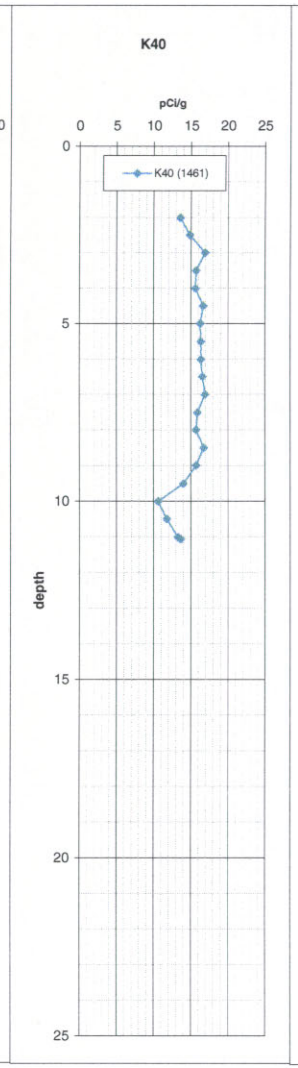

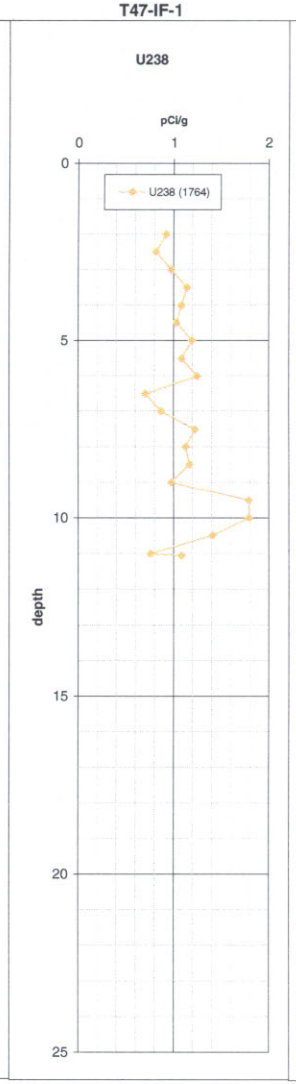

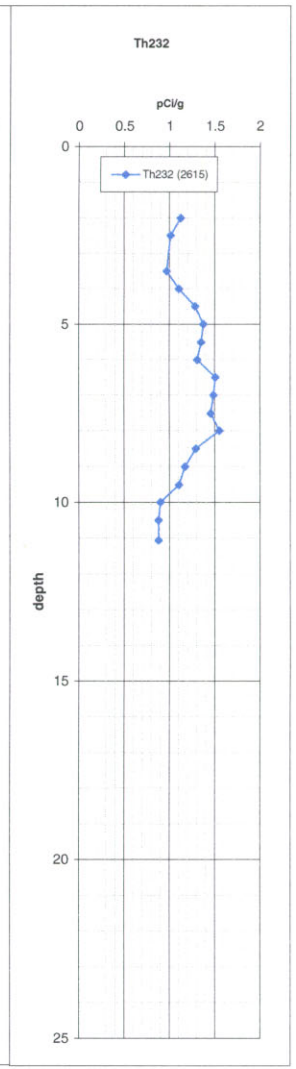

T47-IF-1

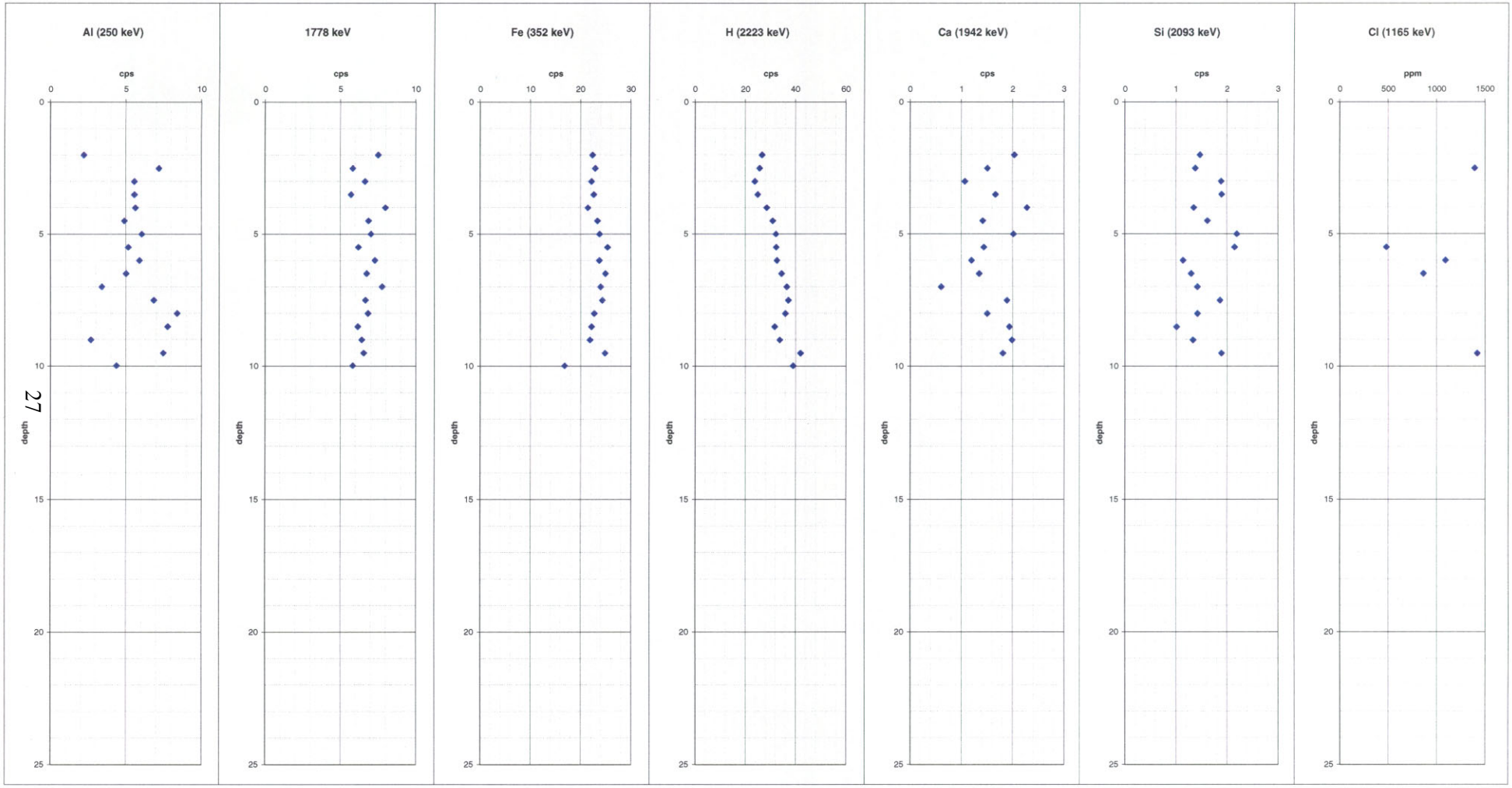
Al (250 keV)
1778 keV
Fe (352 keV)
H (2223 keV)
Ca (1942 keV)
Si (2093 keV)
Cl (1165 keV)
cps
ppm
depth

T47-IF-1 (Total Gamma)

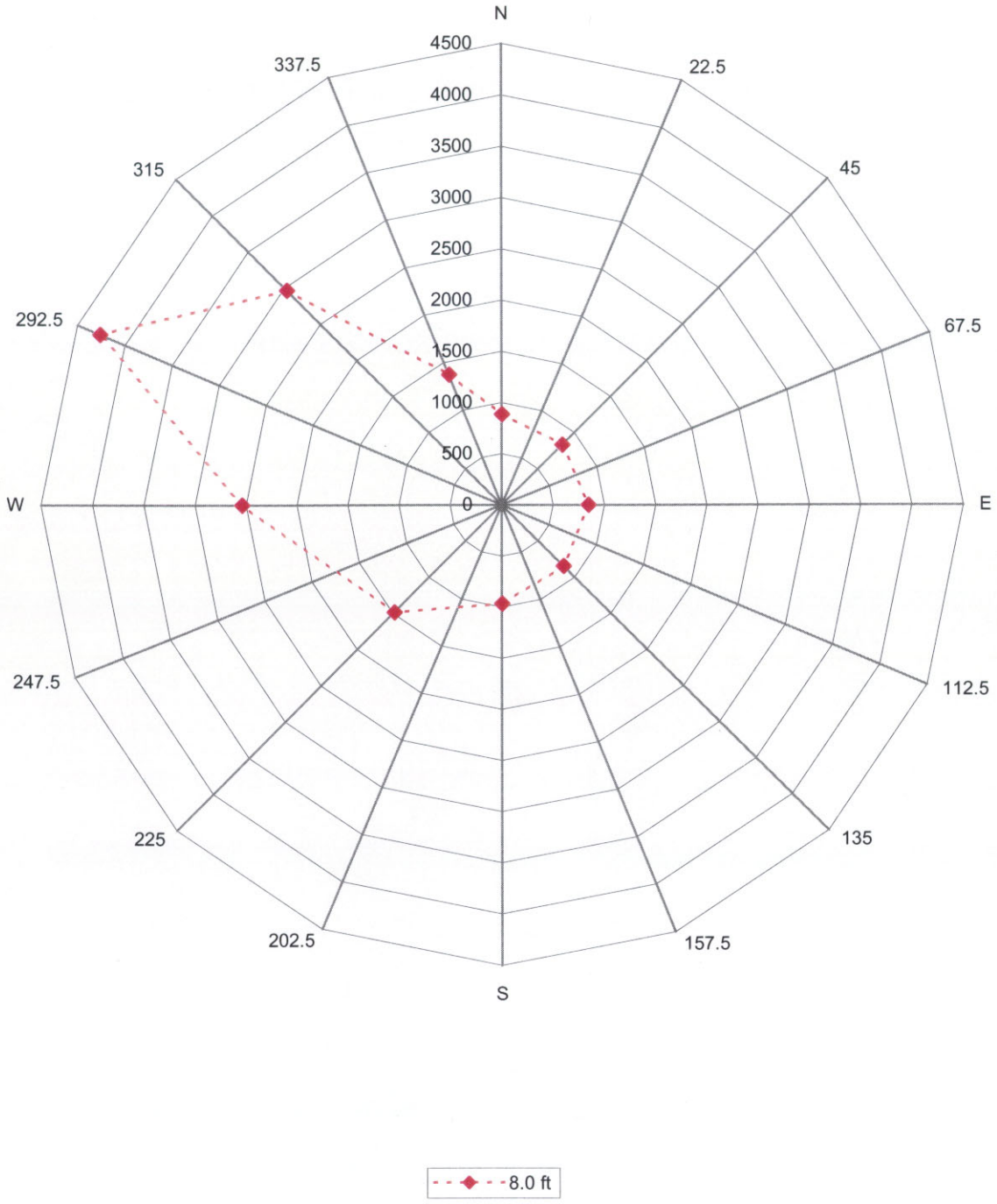

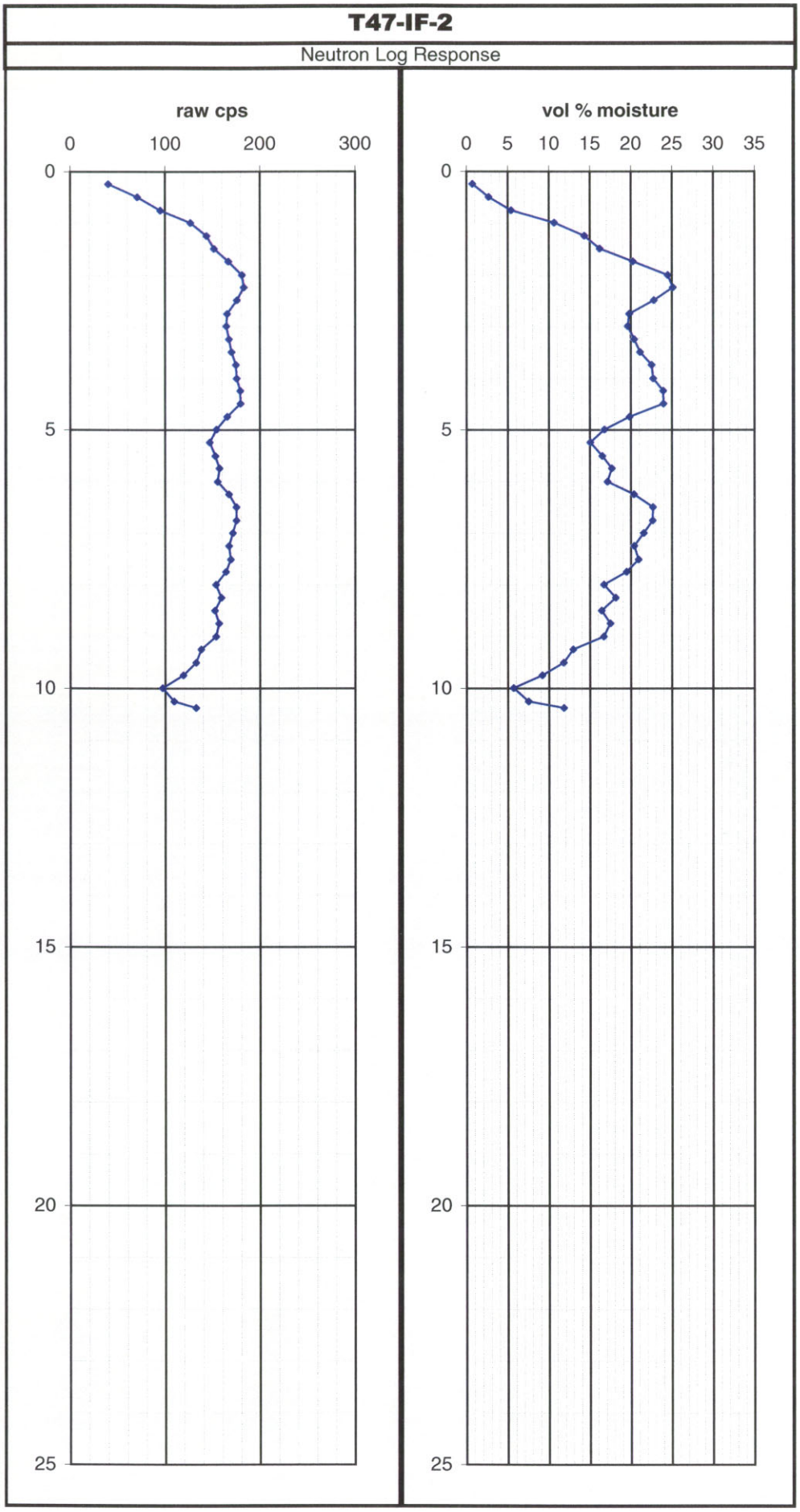
T47-IF-2
Neutron Log Response
raw cps
0
100
200
300
vol % moisture
0
5
10
15
20
25
30
35
0
5
10
15
20
25

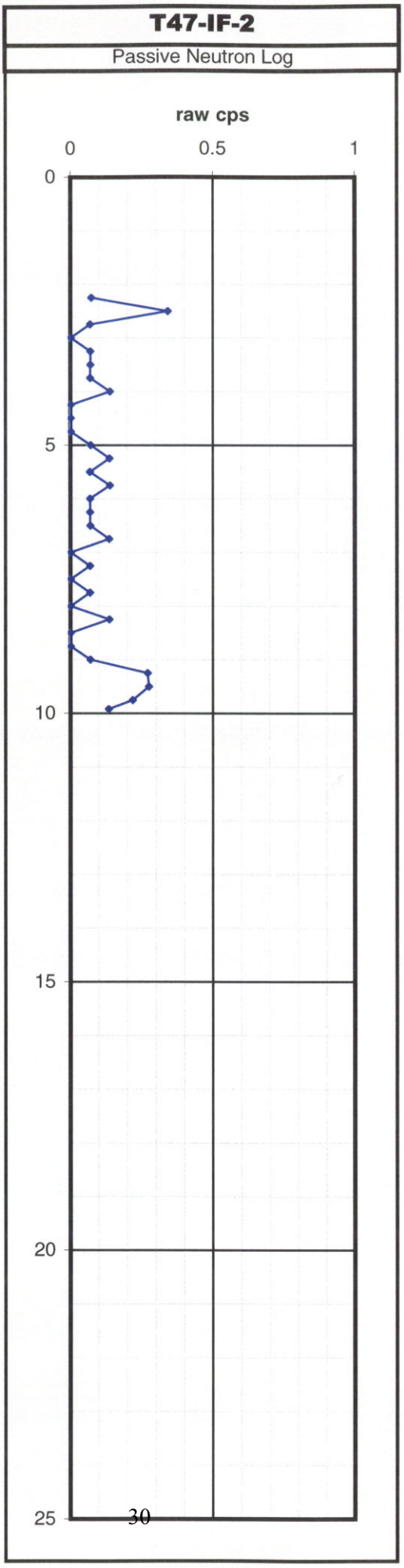
T47-IF-2
Passive Neutron Log
raw cps
0
0.5
1
0
5
10
15
20
25

T47-IF-2

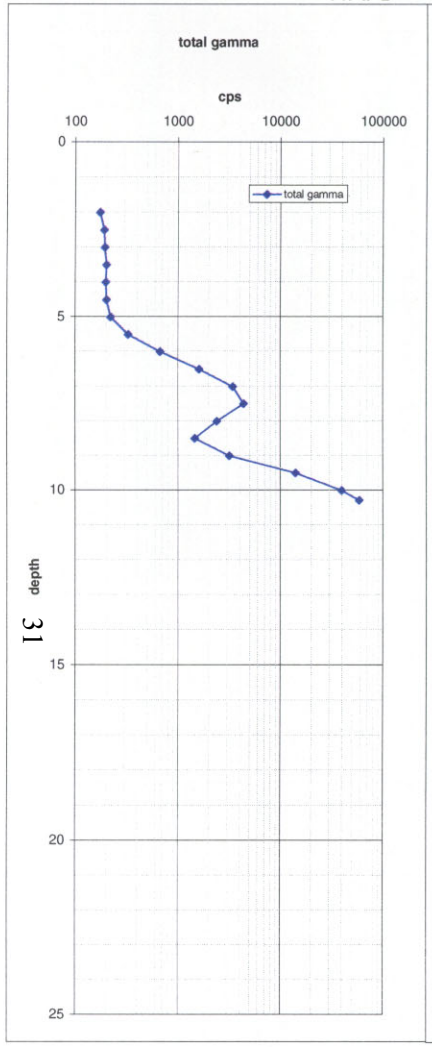

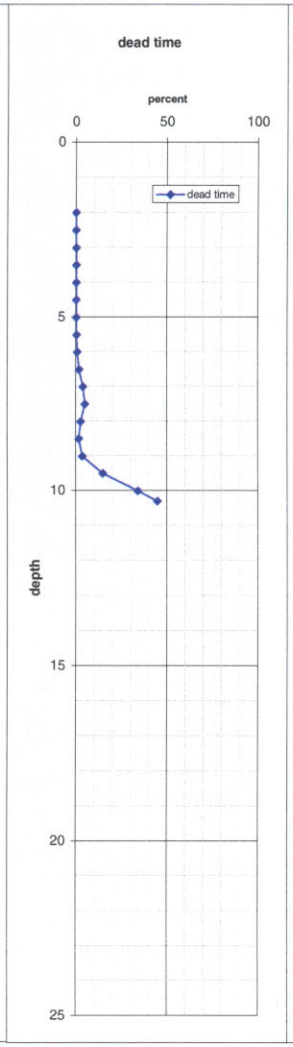

T47-IF-2

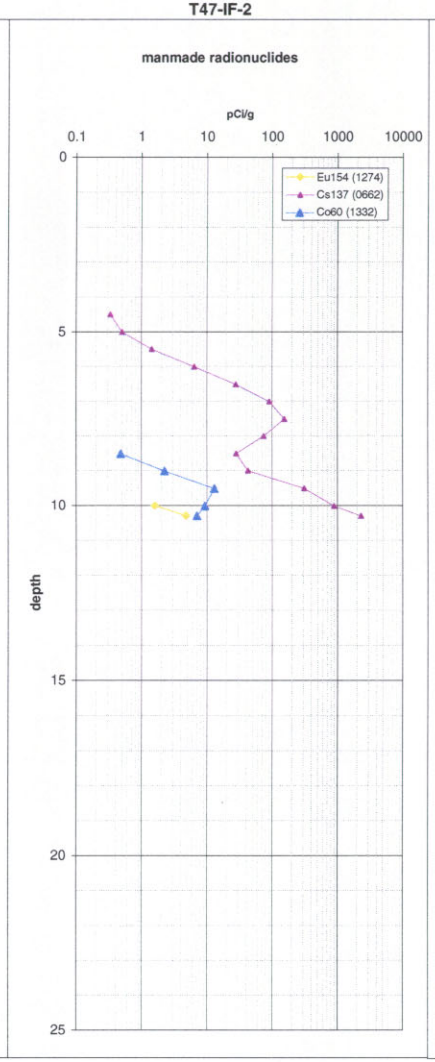

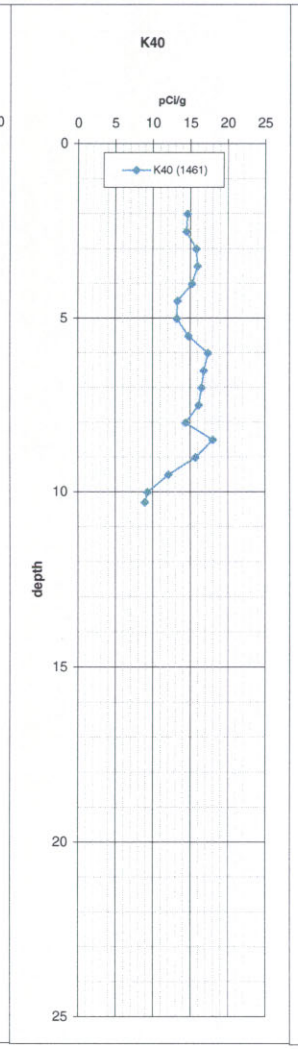

T47-IF-2

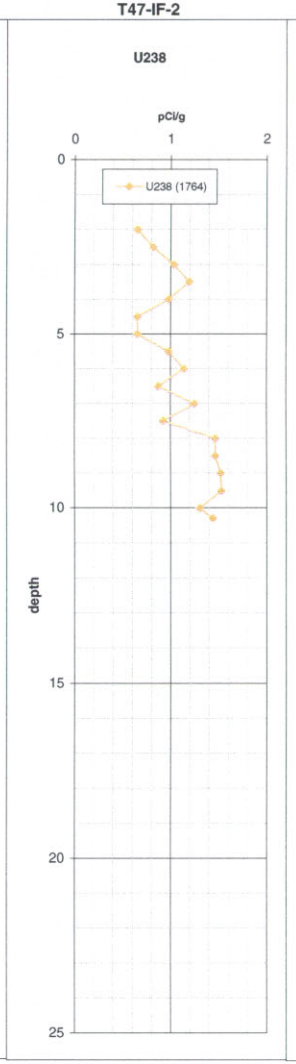

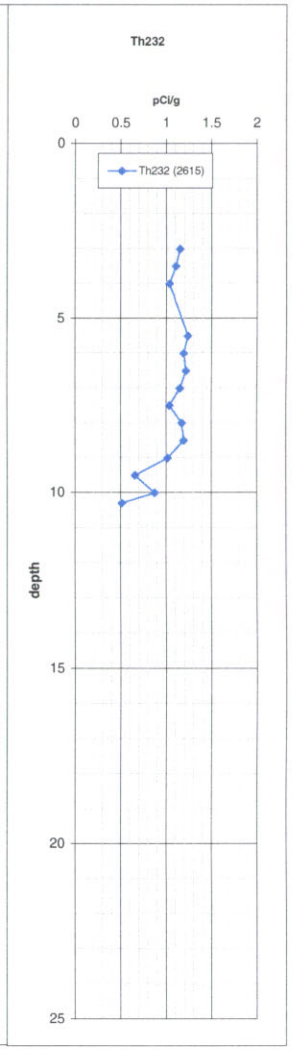

T47-IF-2

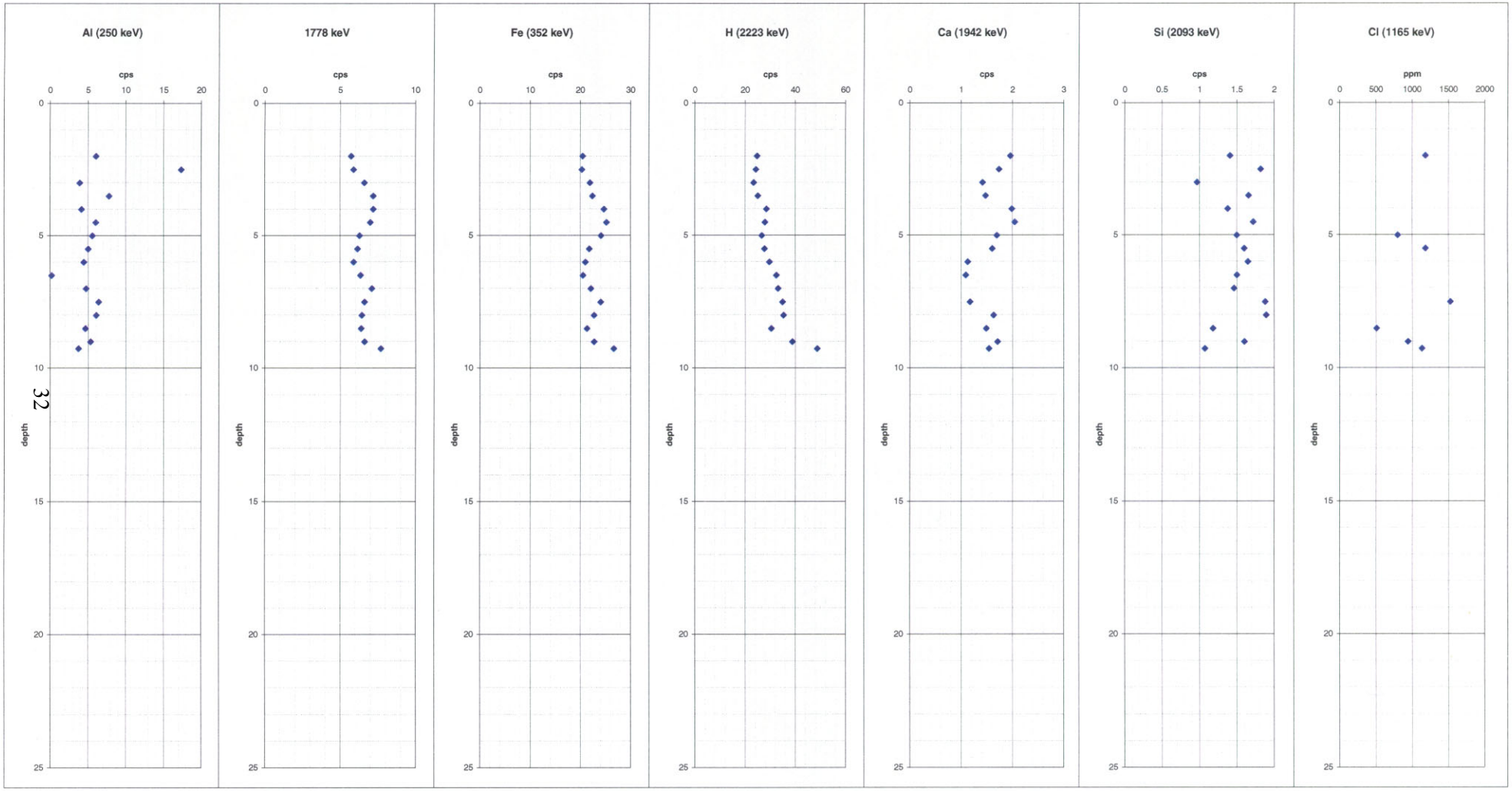
Al (250 keV)
cps
0 5 10 15 20
1778 keV
cps
0 5 10
Fe (352 keV)
cps
0 10 20 30
H (2223 keV)
cps
0 20 40 60
Ca (1942 keV)
cps
0 1 2 3
Si (2093 keV)
cps
0 0.5 1 1.5 2
Cl (1165 keV)
ppm
0 500 1000 1500 2000
depth
0 5 10 15 20 25

T47-IF-2 (Total Gamma)

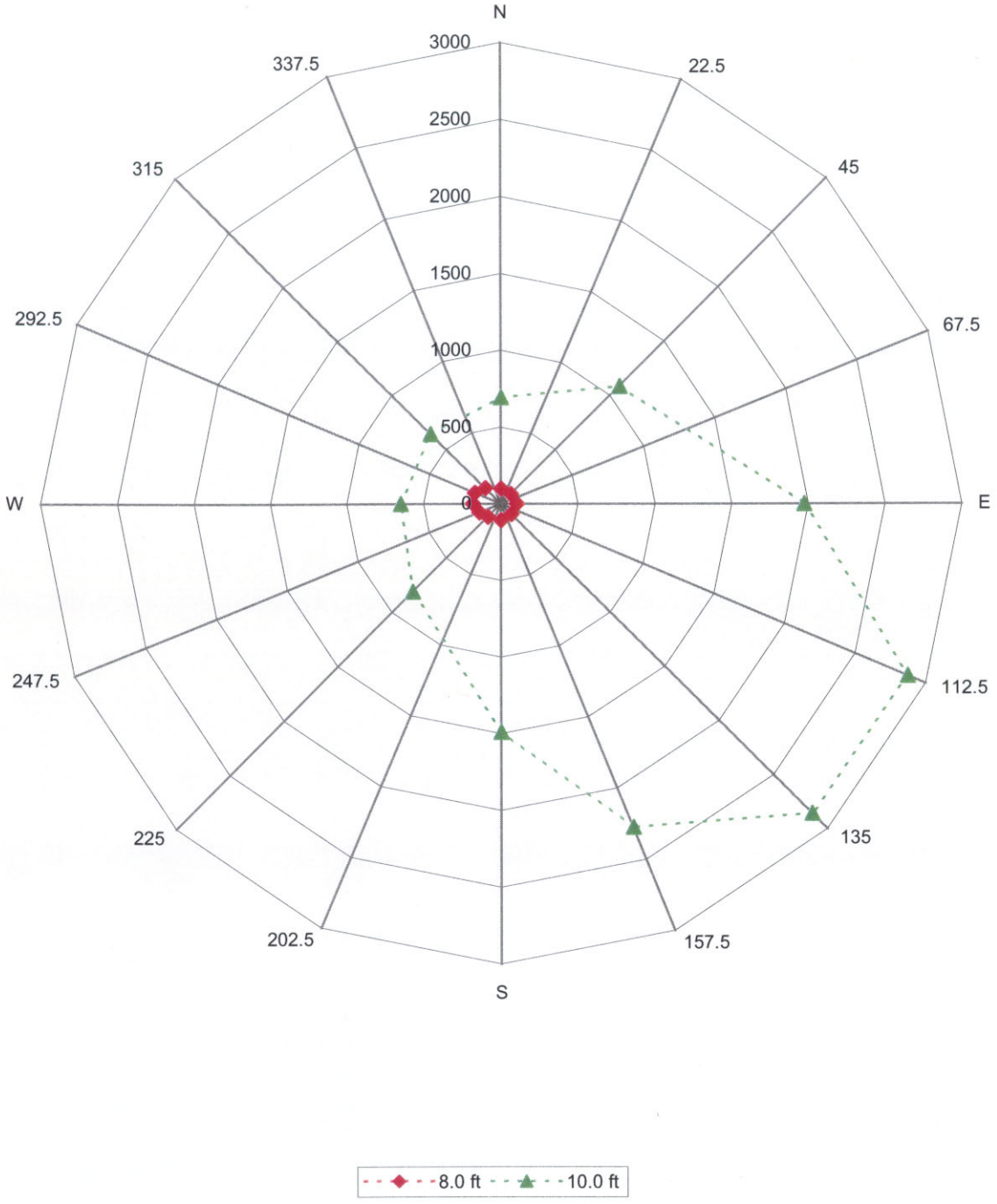

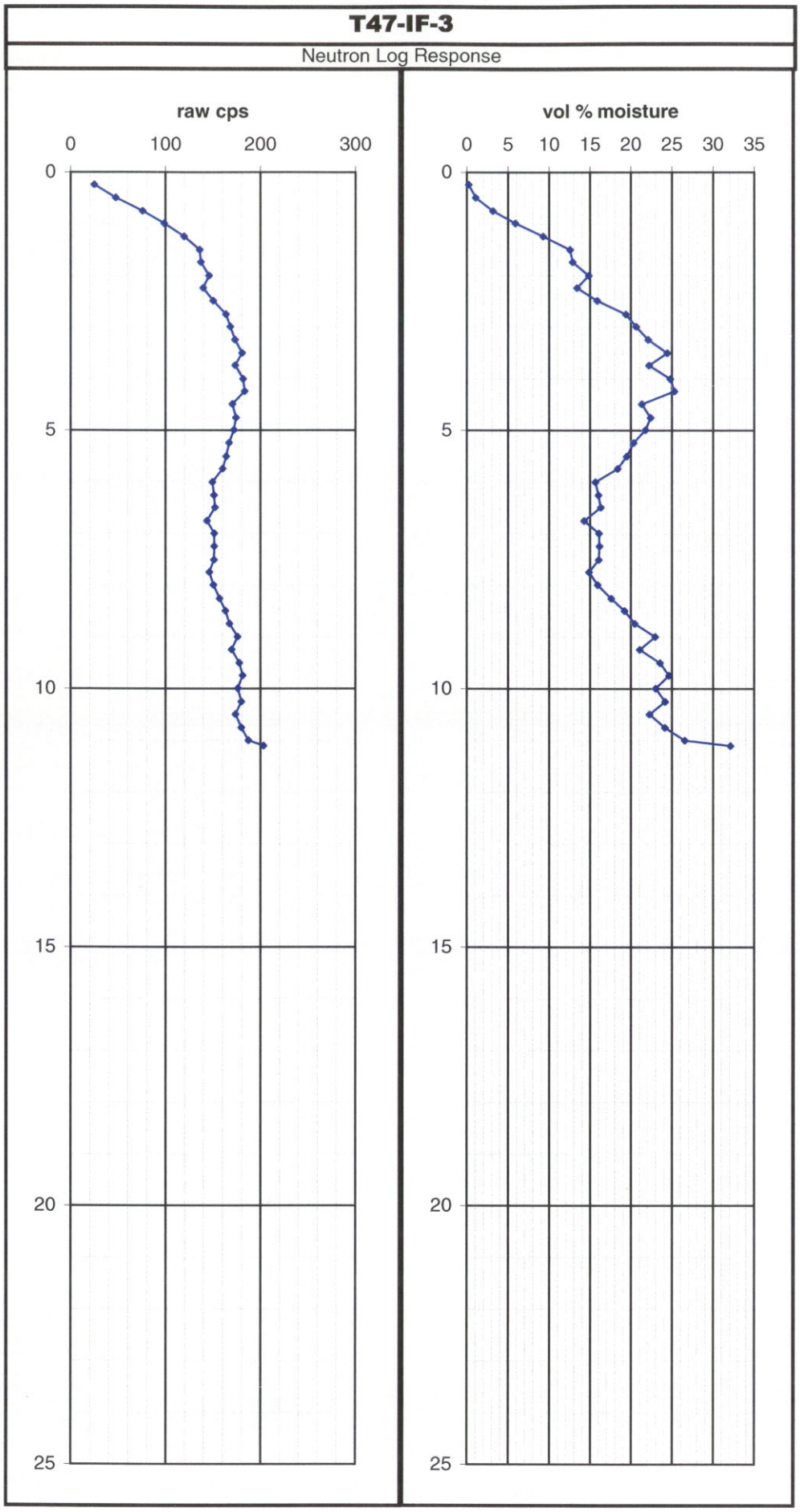
T47-IF-3
Neutron Log Response
raw cps
0
100
200
300
vol % moisture
0
5
10
15
20
25
30
35

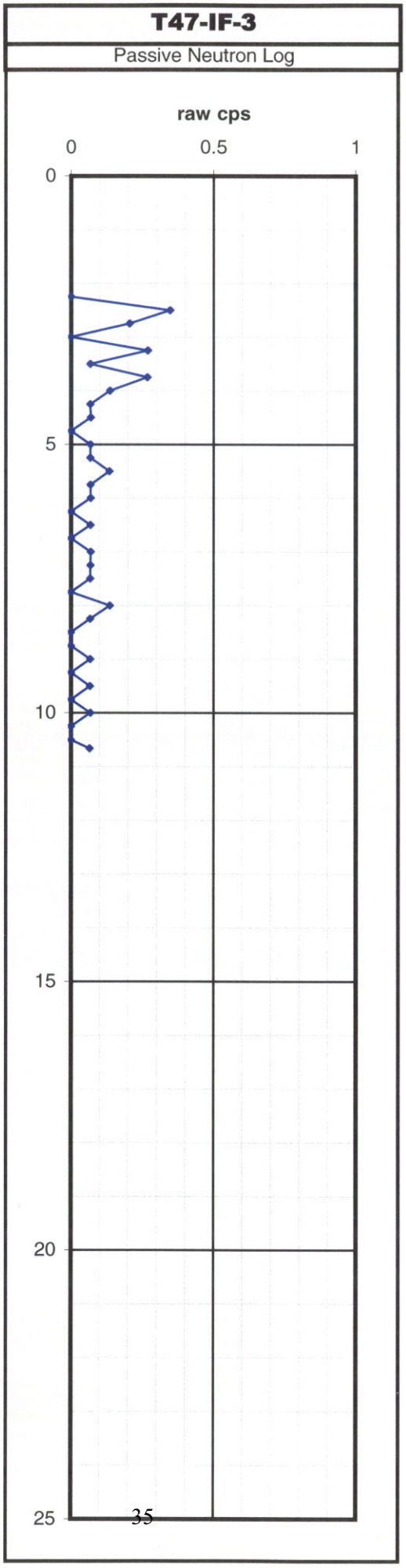
T47-IF-3
Passive Neutron Log
raw cps
0
0.5
1
0
5
10
15
20
25

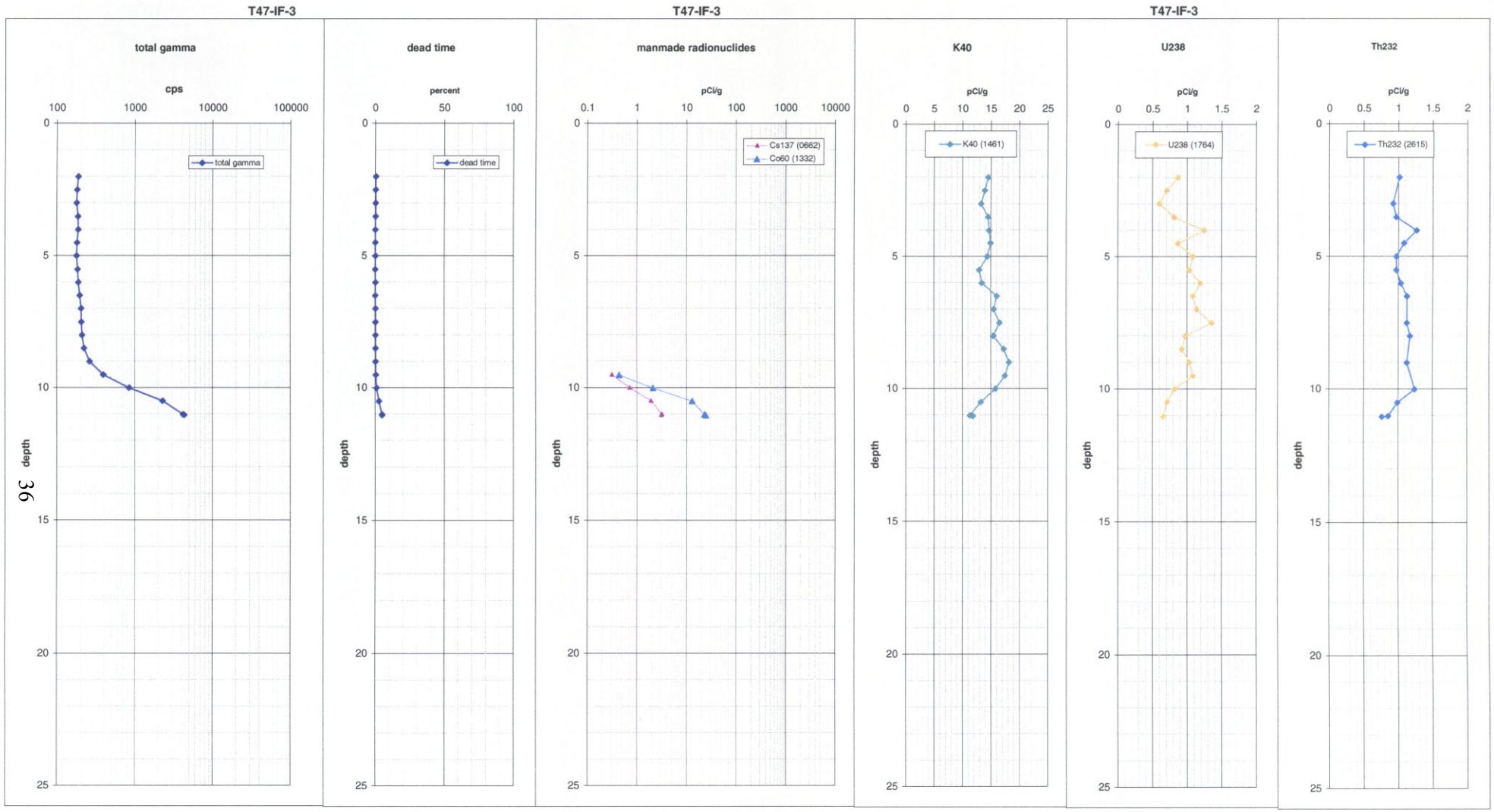
T47-IF-3
total gamma
cps
100
1000
10000
100000
total gamma
depth
0
5
10
15
20
25
T47-IF-3
dead time
percent
0
50
100
dead time
depth
T47-IF-3
manmade radionuclides
pCi/g
0.1
1
10
100
1000
10000
Cs137 (0662)
Co60 (1332)
depth
K40
pCi/g
0
5
10
15
20
25
K40 (1461)
depth
T47-IF-3
U238
pCi/g
0
0.5
1
1.5
2
U238 (1764)
depth
Th232
pCi/g
0
0.5
1
1.5
2
Th232 (2615)
depth

T47-IF-3

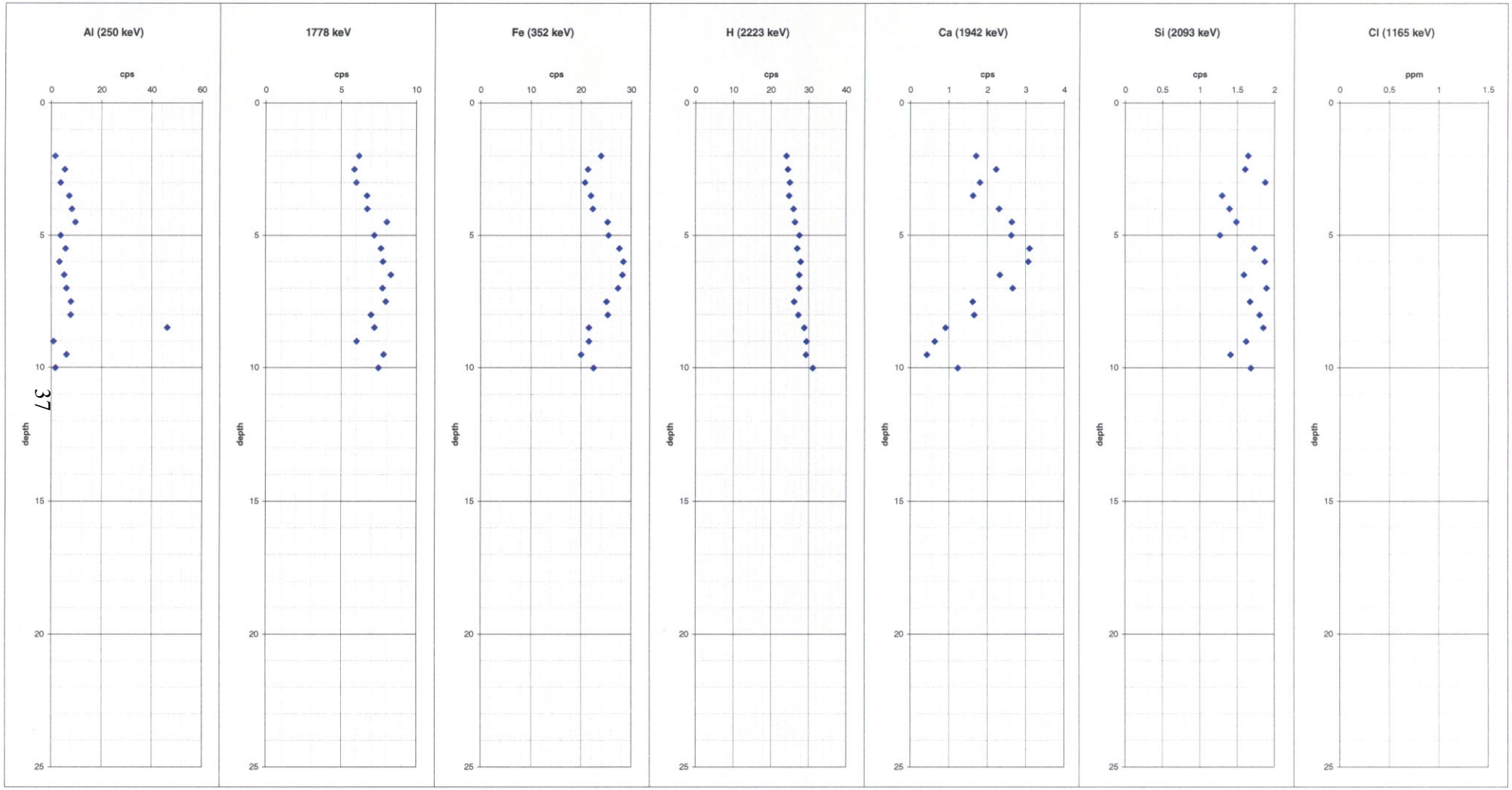
Al (250 keV)
cps
0 20 40 60
1778 keV
cps
0 5 10
Fe (352 keV)
cps
0 10 20 30
H (2223 keV)
cps
0 10 20 30 40
Ca (1942 keV)
cps
0 1 2 3 4
Si (2093 keV)
cps
0 0.5 1 1.5 2
Cl (1165 keV)
ppm
0 0.5 1 1.5
depth
0 5 10 15 20 25

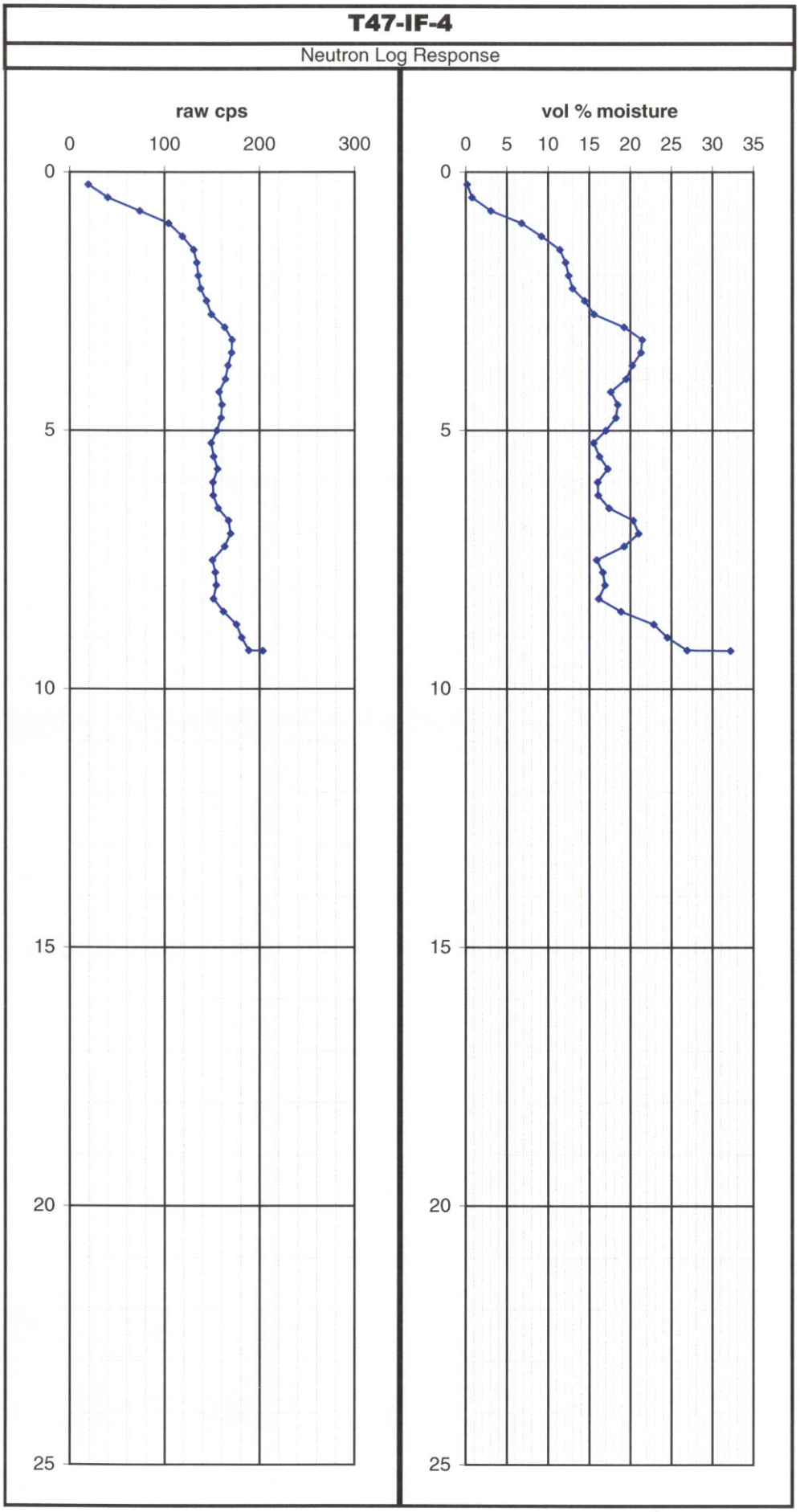
T47-IF-4
Neutron Log Response
raw cps
0
100
200
300
vol % moisture
0
5
10
15
20
25
30
35
0
5
10
15
20
25

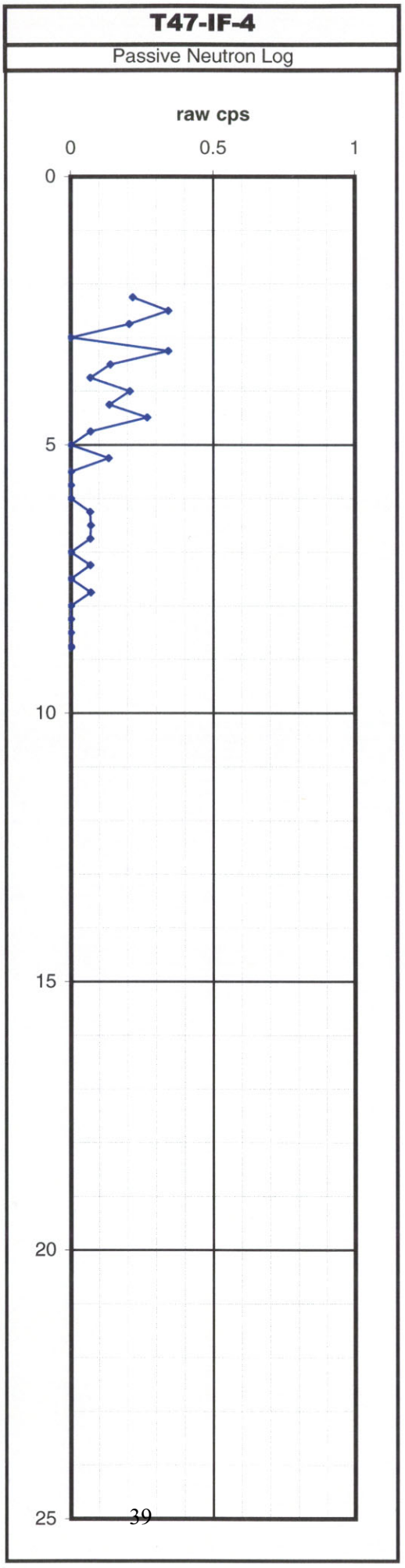
T47-IF-4
Passive Neutron Log
raw cps
0
0.5
1
0
5
10
15
20
25

T47-IF-4

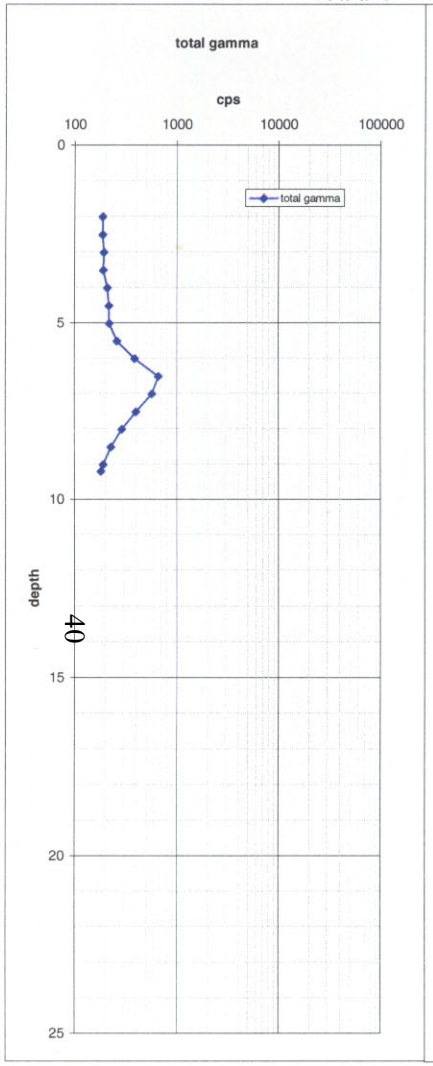

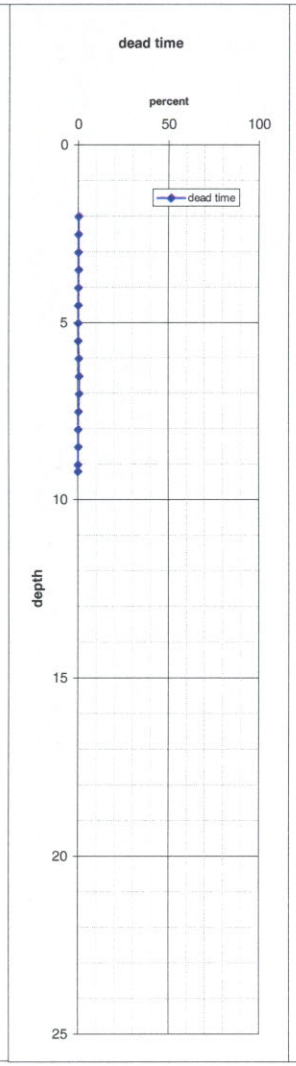

T47-IF-4

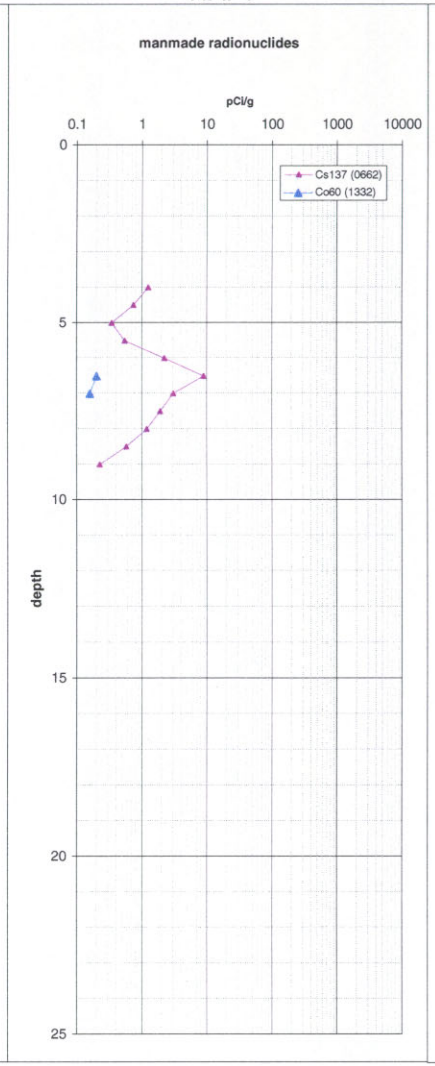

T47-IF-4

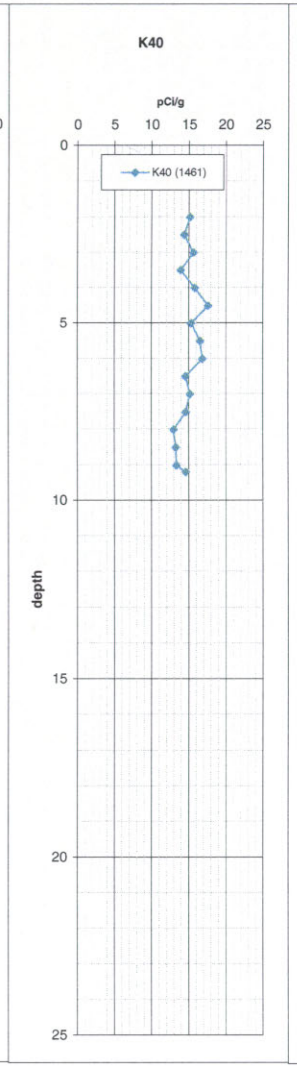

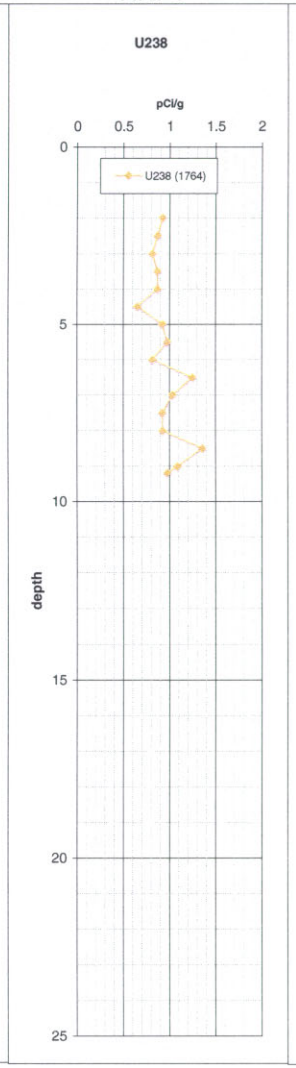

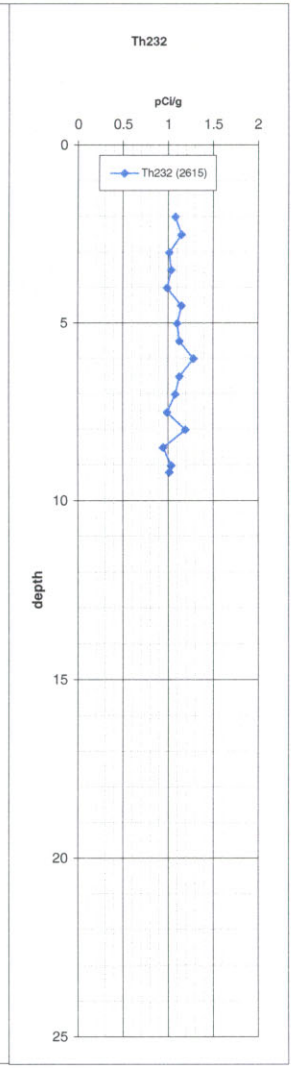

T47-IF-4

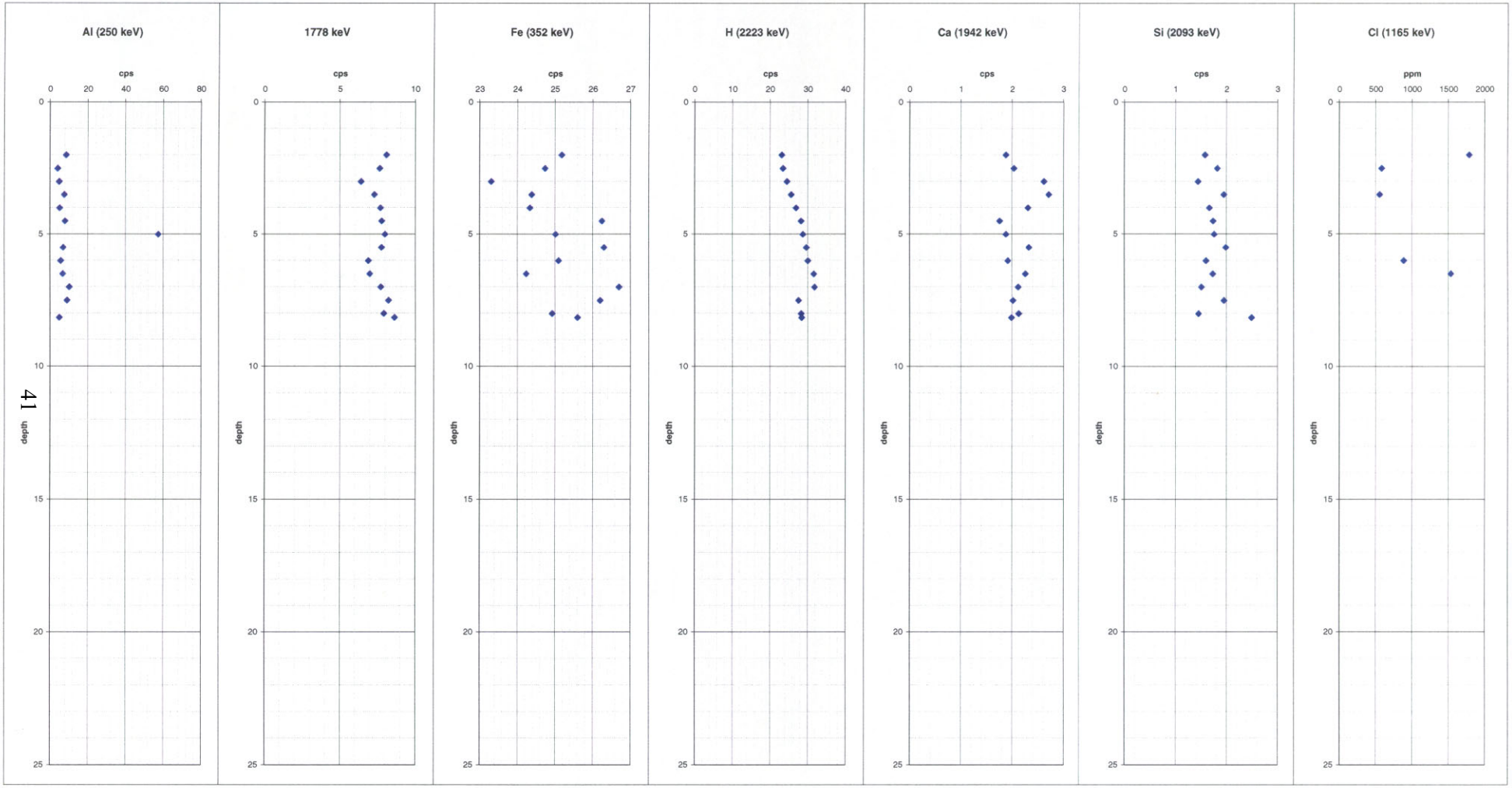
Al (250 keV)
cps
0 20 40 60 80
1778 keV
cps
0 5 10
Fe (352 keV)
cps
23 24 25 26 27
H (2223 keV)
cps
0 10 20 30 40
Ca (1942 keV)
cps
0 1 2 3
Si (2093 keV)
cps
0 1 2 3
Cl (1165 keV)
ppm
0 500 1000 1500 2000
depth
0 5 10 15 20 25

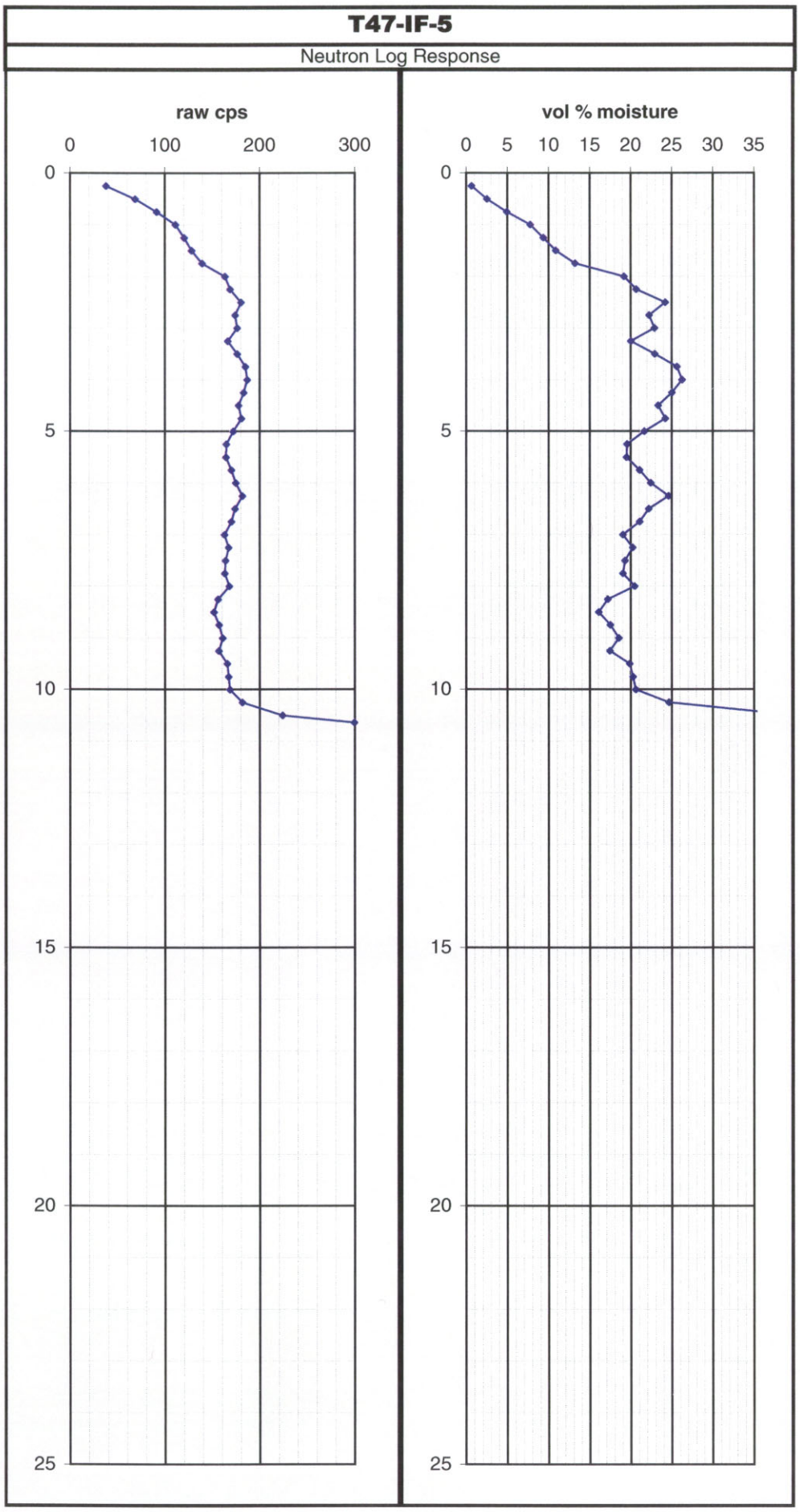
T47-IF-5
Neutron Log Response
raw cps
0
100
200
300
vol % moisture
0
5
10
15
20
25
30
35
0
5
10
15
20
25

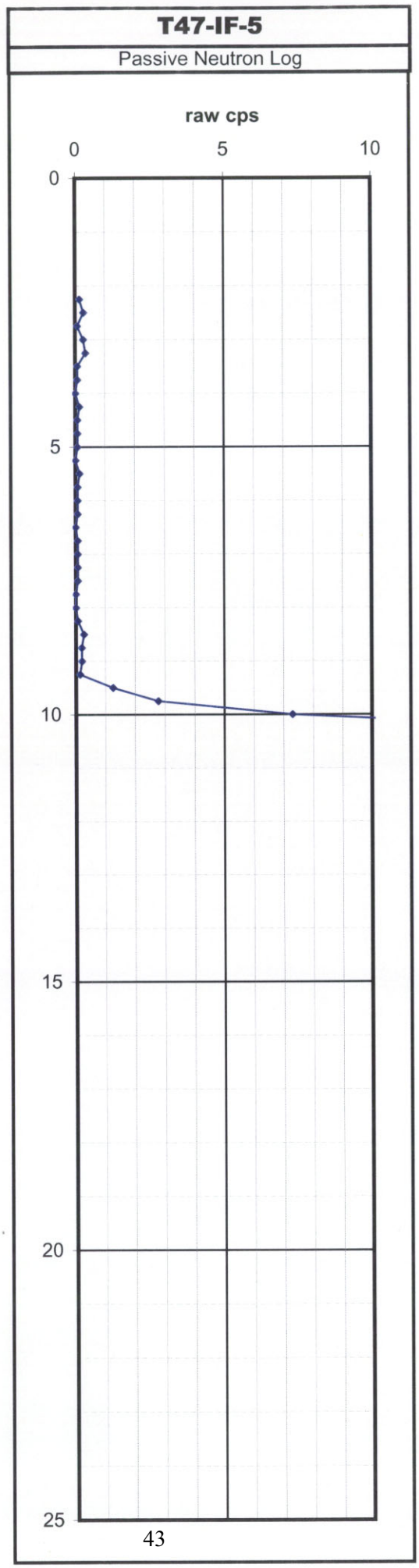
T47-IF-5
Passive Neutron Log
raw cps
0
5
10
0
5
10
15
20
25

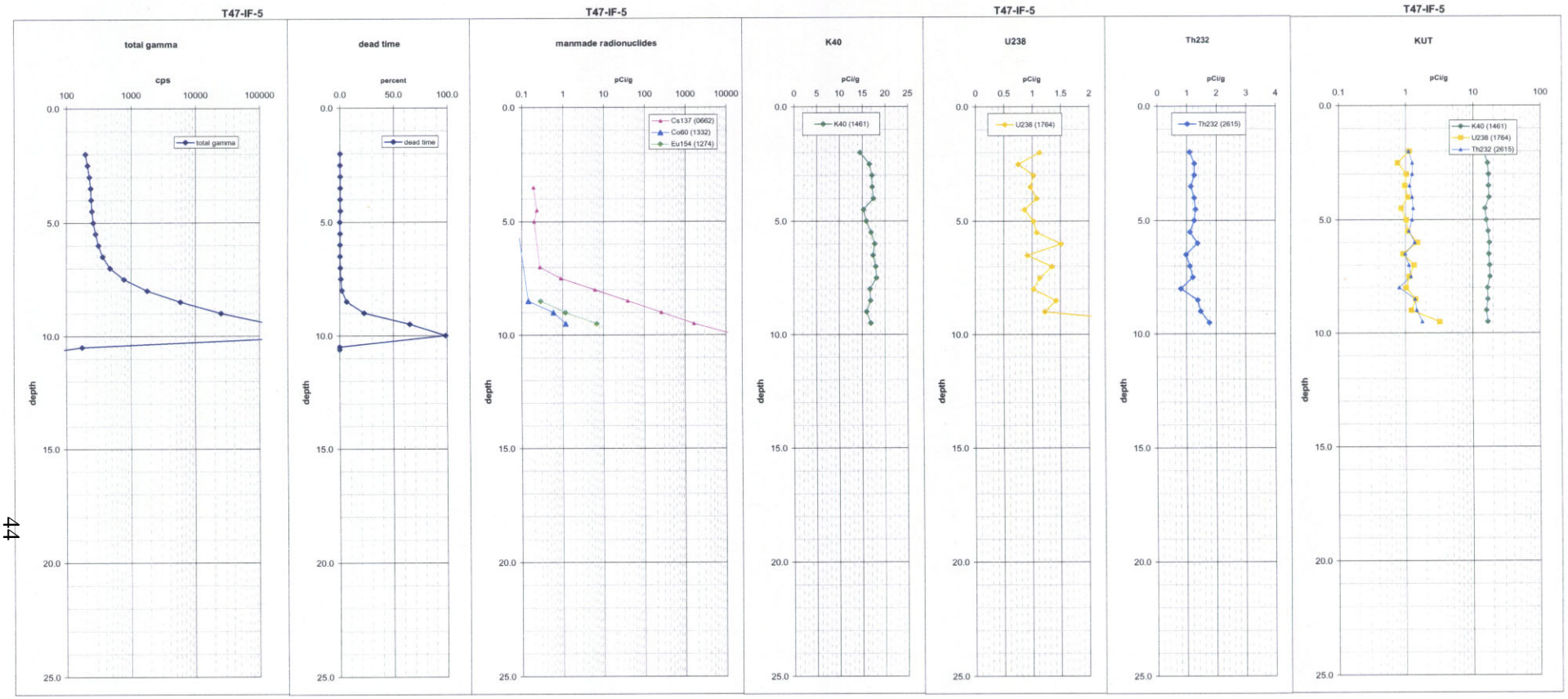
T47-IF-5
total gamma
cps
100
1000
10000
100000
total gamma
dead time
percent
0.0
50.0
100.0
dead time
manmade radionuclides
pCi/g
0.1
1
10
100
1000
10000
Cs137 (0662)
Co60 (1332)
Eu154 (1274)
K40
0
5
10
15
20
25
K40 (1461)
U238
0.5
1.5
2
U238 (1764)
Th232
3
4
Th232 (2615)
KUT
K40 (1461)
U238 (1764)
Th232 (2615)
depth
0.0
5.0
10.0
15.0
20.0
25.0

T47-IF-5

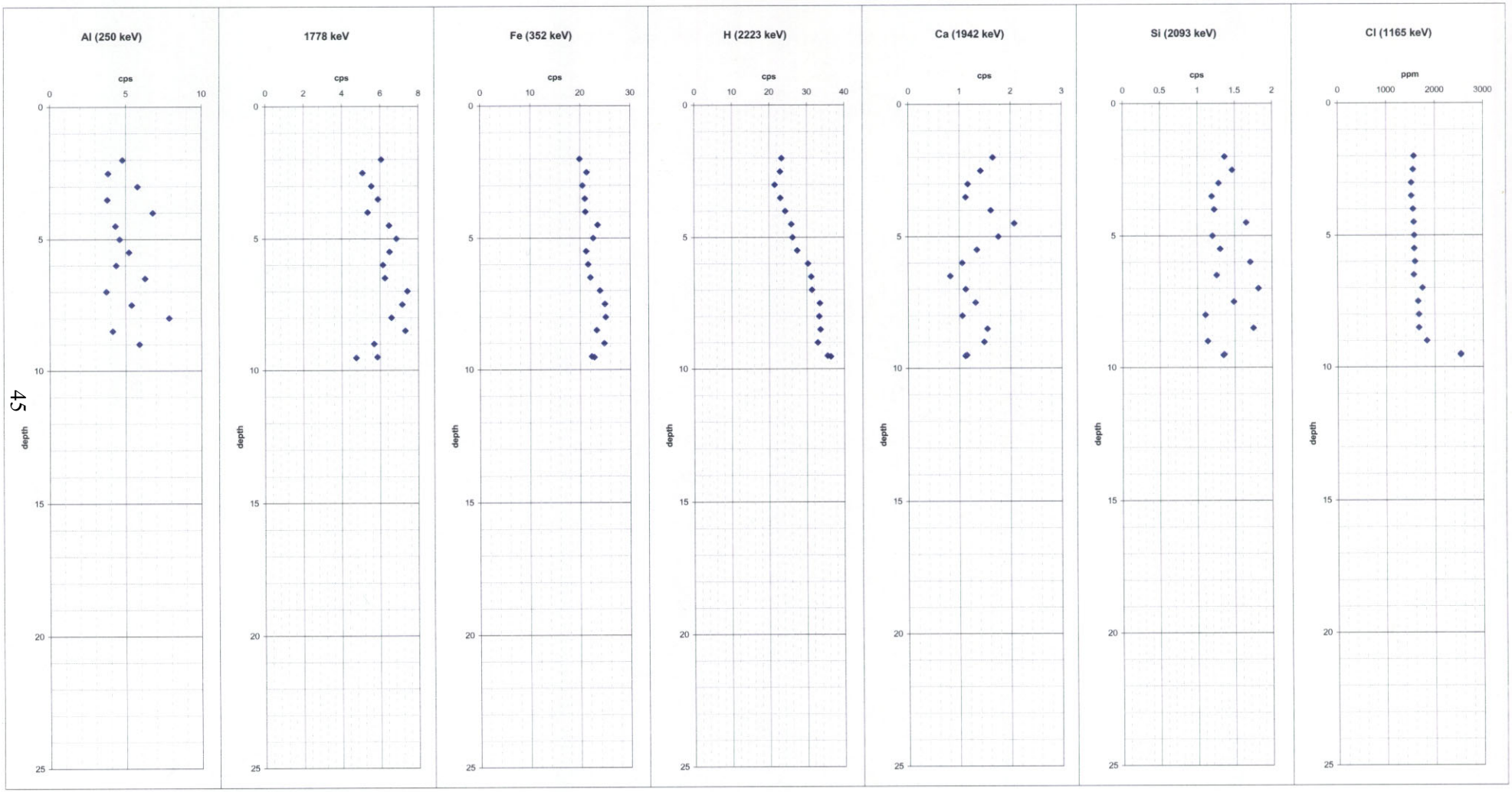
Al (250 keV)
1778 keV
Fe (352 keV)
H (2223 keV)
Ca (1942 keV)
Si (2093 keV)
Cl (1165 keV)
cps
ppm
depth

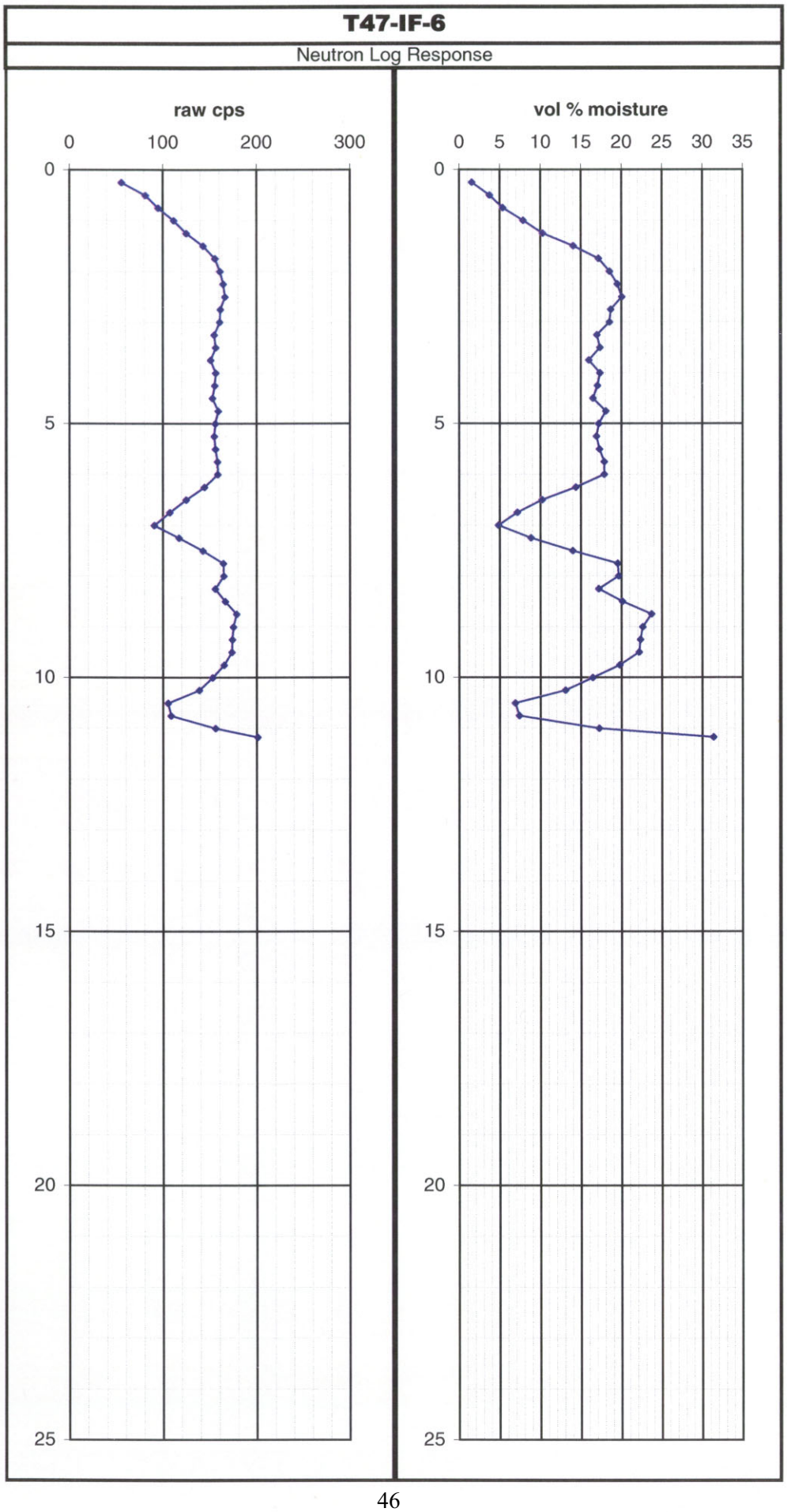
T47-IF-6
Neutron Log Response
raw cps
0
100
200
300
vol % moisture
0
5
10
15
20
25
30
35
0
5
10
15
20
25

T47-IF-6

Passive Neutron Log

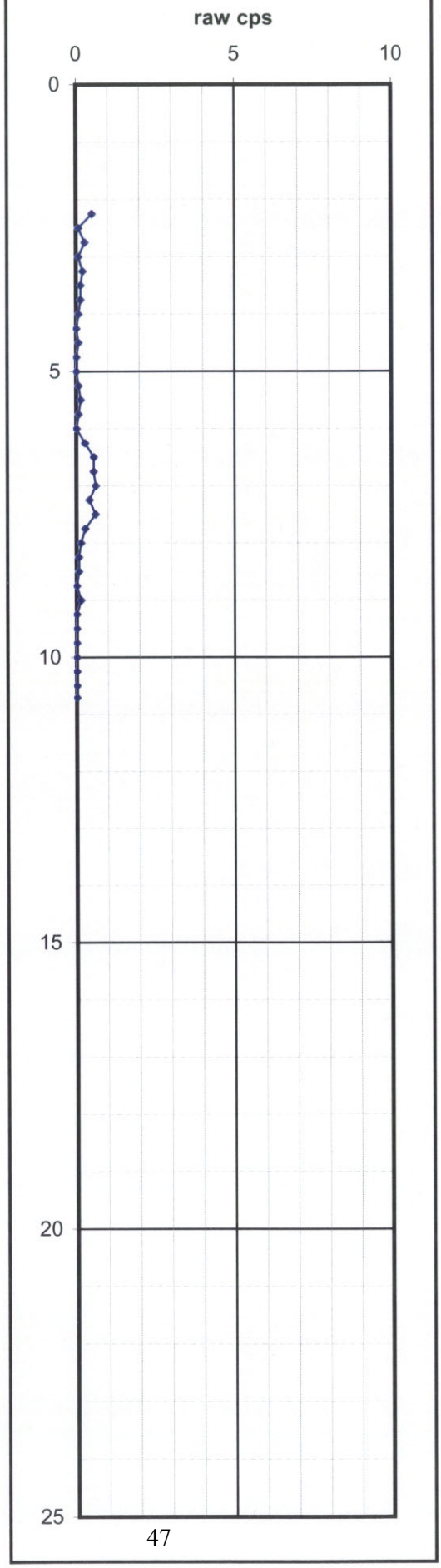

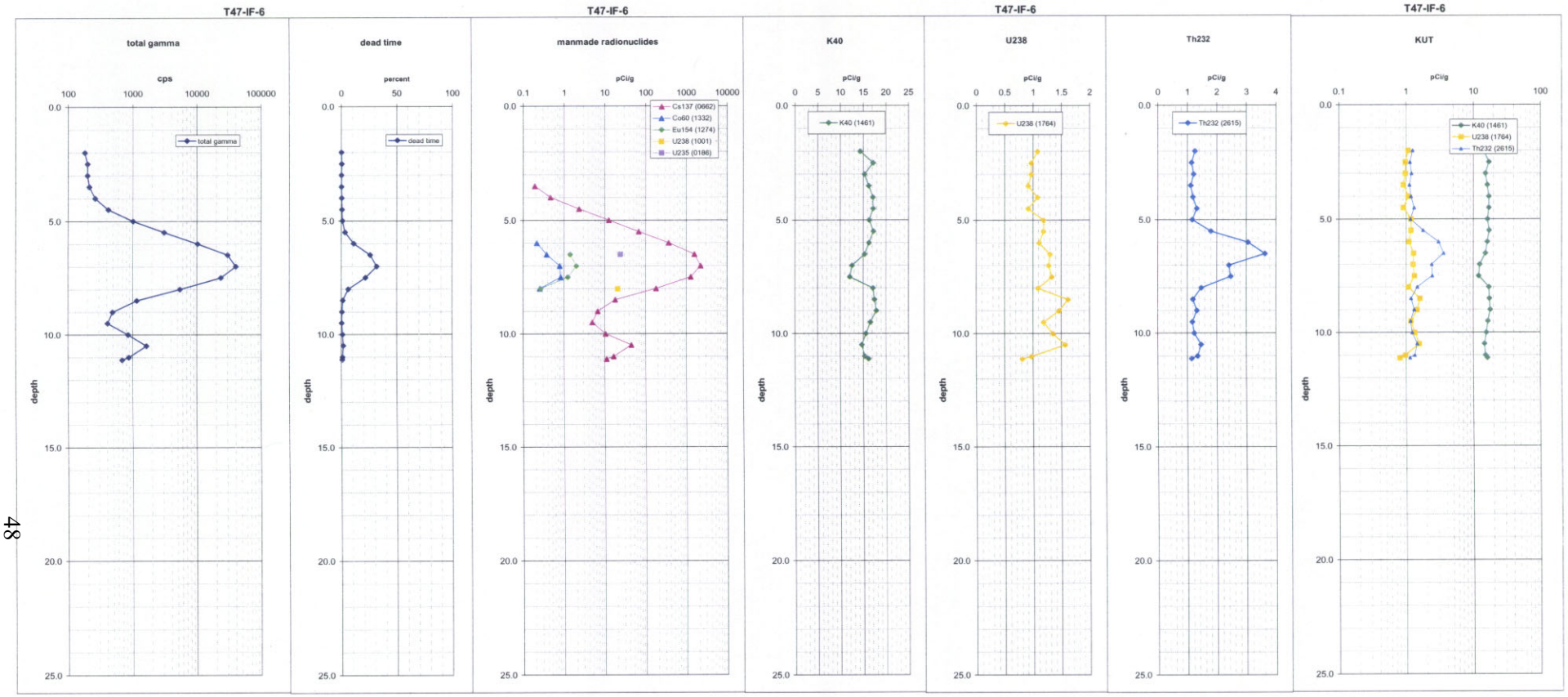
T47-IF-6
total gamma
cps
100
1000
10000
100000
total gamma
depth
0.0
5.0
10.0
15.0
20.0
25.0
T47-IF-6
dead time
percent
0
50
100
dead time
depth
T47-IF-6
manmade radionuclides
pCi/g
0.1
1
10
100
1000
10000
Cs137 (0662)
Co60 (1332)
Eu154 (1274)
U238 (1001)
U235 (0186)
depth
T47-IF-6
K40
pCi/g
0
5
10
15
20
25
K40 (1461)
depth
T47-IF-6
U238
pCi/g
0
0.5
1
1.5
2
U238 (1764)
depth
T47-IF-6
Th232
pCi/g
0
1
2
3
4
Th232 (2615)
depth
T47-IF-6
KUT
pCi/g
0.1
1
10
100
K40 (1461)
U238 (1764)
Th232 (2615)
depth

T47-IF-6

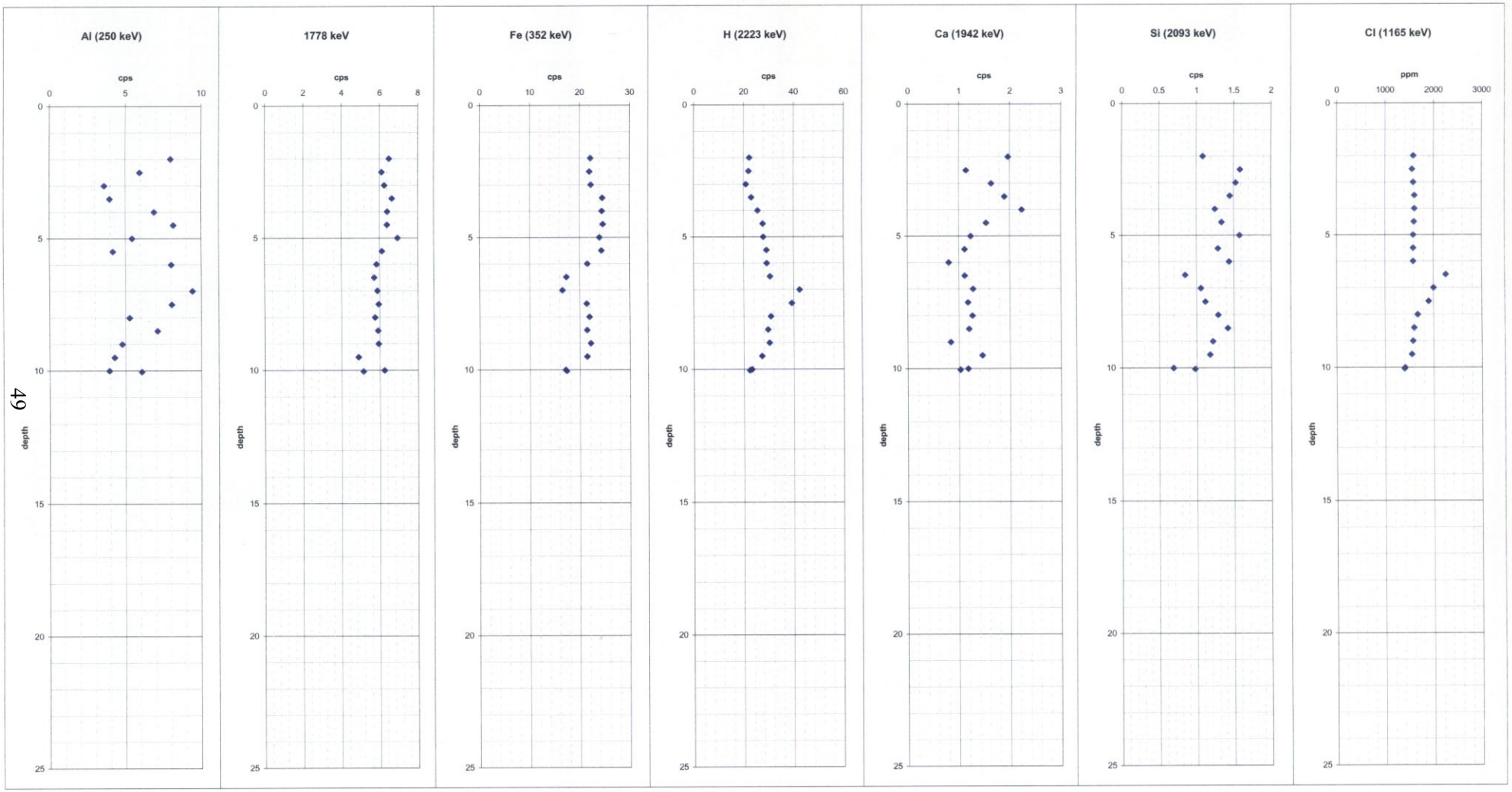
Al (250 keV)
1778 keV
Fe (352 keV)
H (2223 keV)
Ca (1942 keV)
Si (2093 keV)
Cl (1165 keV)
cps
ppm
depth

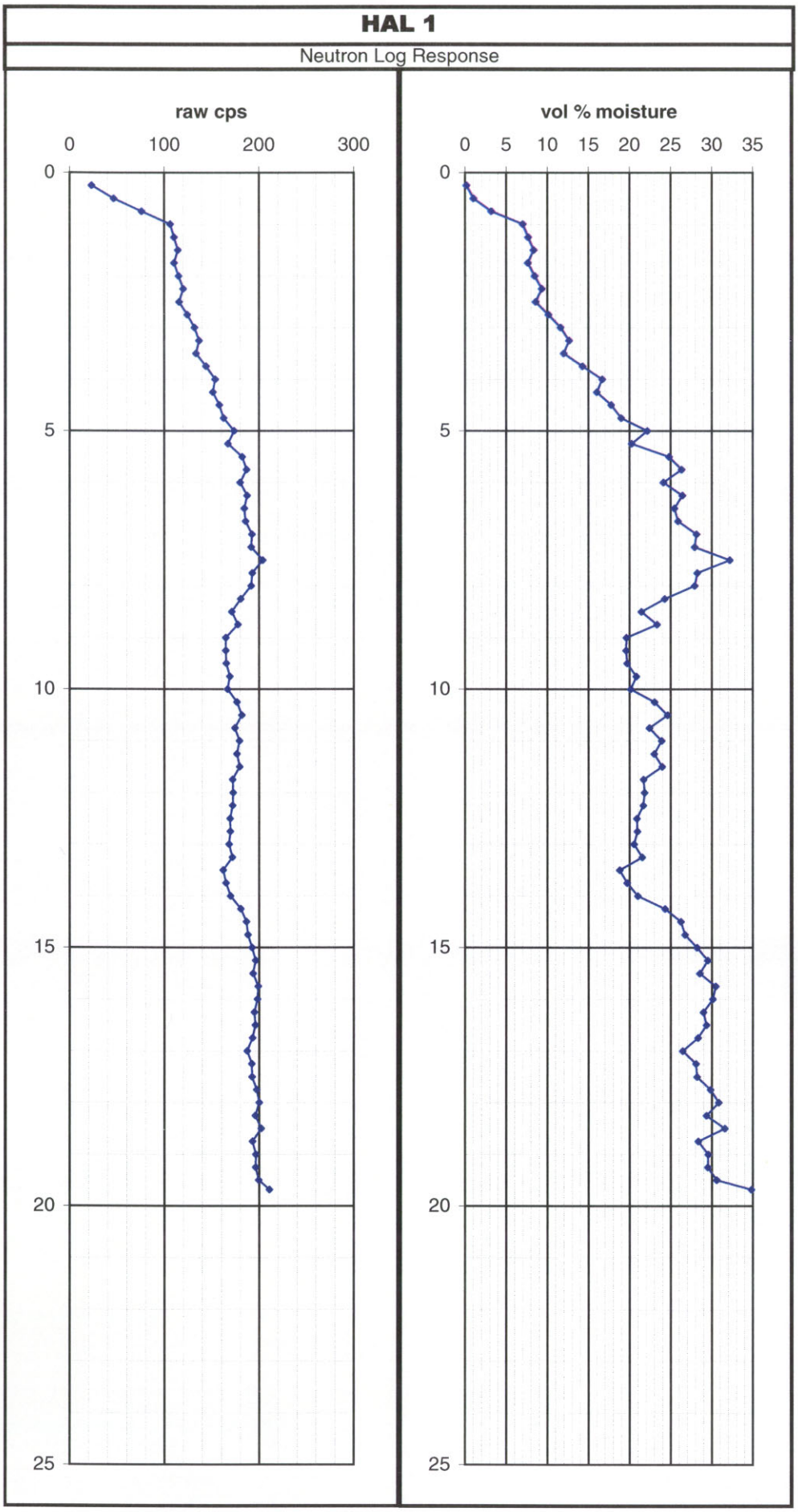
HAL 1
Neutron Log Response
raw cps
0
100
200
300
0
5
10
15
20
25
vol % moisture
0
5
10
15
20
25
30
35
0
5
10
15
20
25

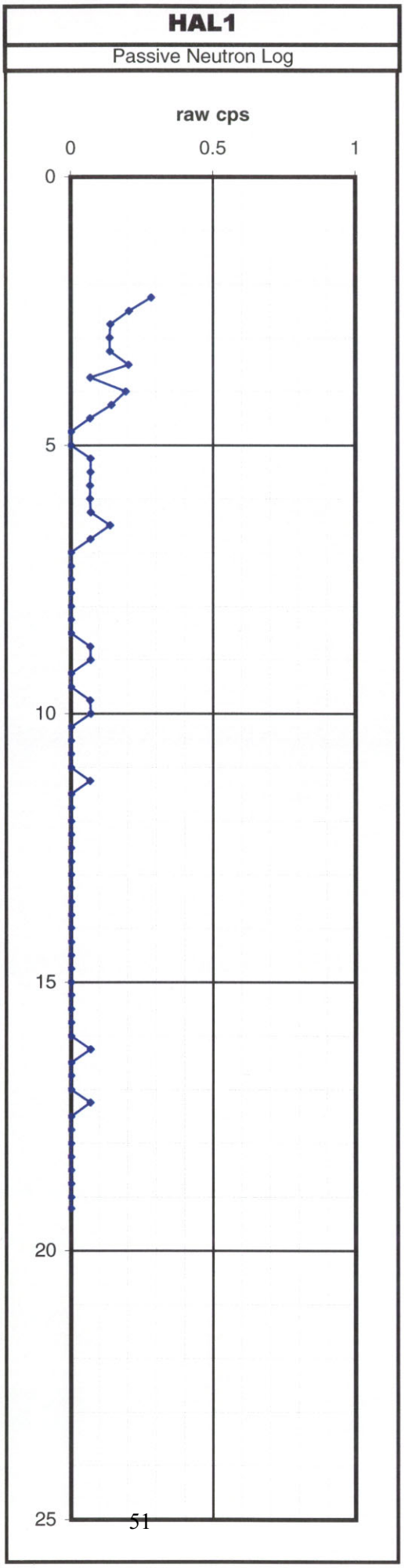
HAL1
Passive Neutron Log
raw cps
0
0.5
1
0
5
10
15
20
25

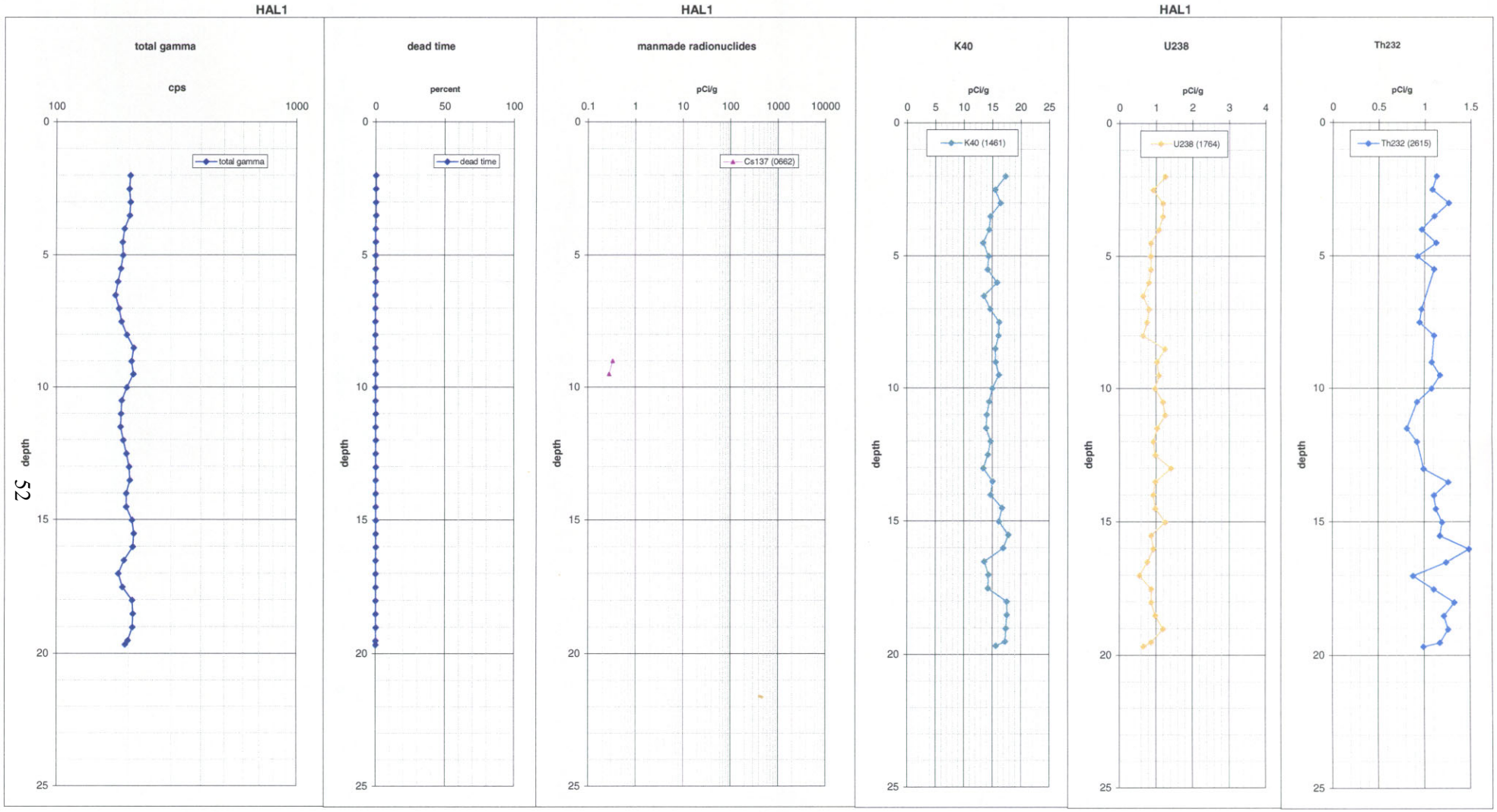
HAL1
total gamma
cps
100
1000
total gamma
depth
0
5
10
15
20
25
HAL1
dead time
percent
0
50
100
dead time
depth
HAL1
manmade radionuclides
pCi/g
0.1
1
10
100
1000
10000
Cs137 (0662)
depth
HAL1
K40
pCi/g
0
5
10
15
20
25
K40 (1461)
depth
U238
pCi/g
0
1
2
3
4
U238 (1764)
depth
Th232
pCi/g
0
0.5
1
1.5
Th232 (2615)
depth

HAL 1

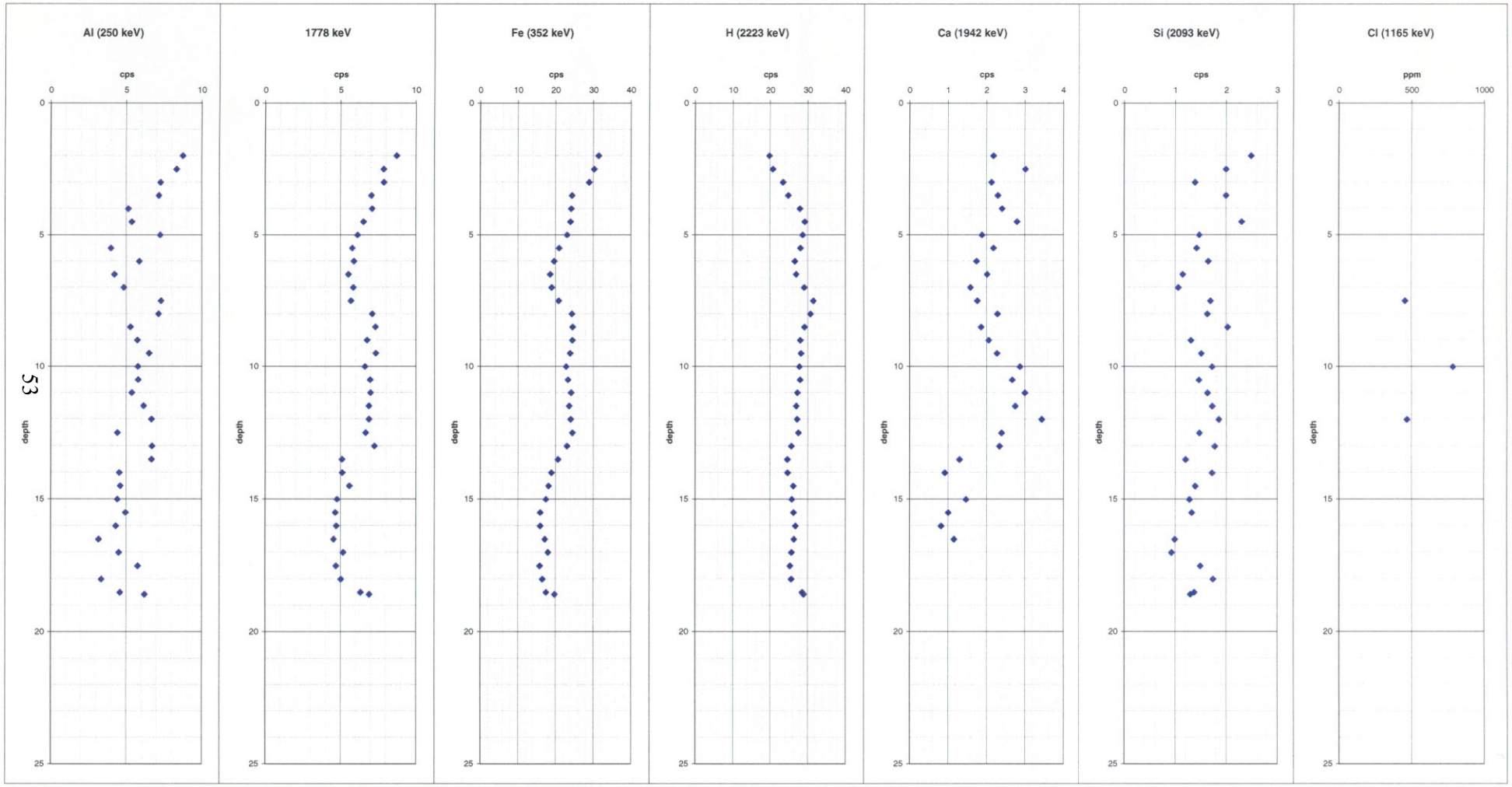
Al (250 keV)
1778 keV
Fe (352 keV)
H (2223 keV)
Ca (1942 keV)
Si (2093 keV)
Cl (1165 keV)
cps
ppm
depth

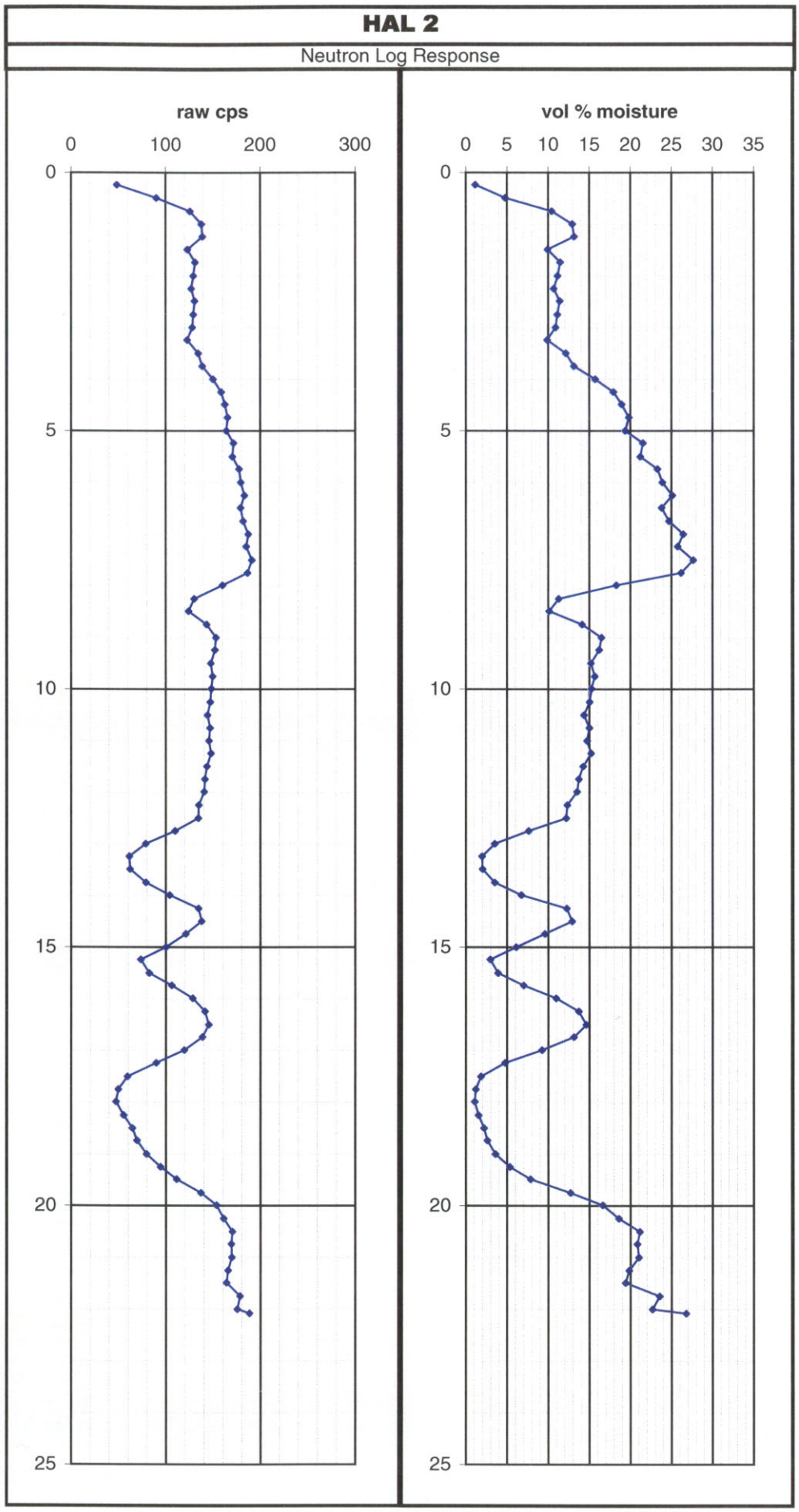
HAL 2
Neutron Log Response
raw cps
0
100
200
300
vol % moisture
0
5
10
15
20
25
30
35

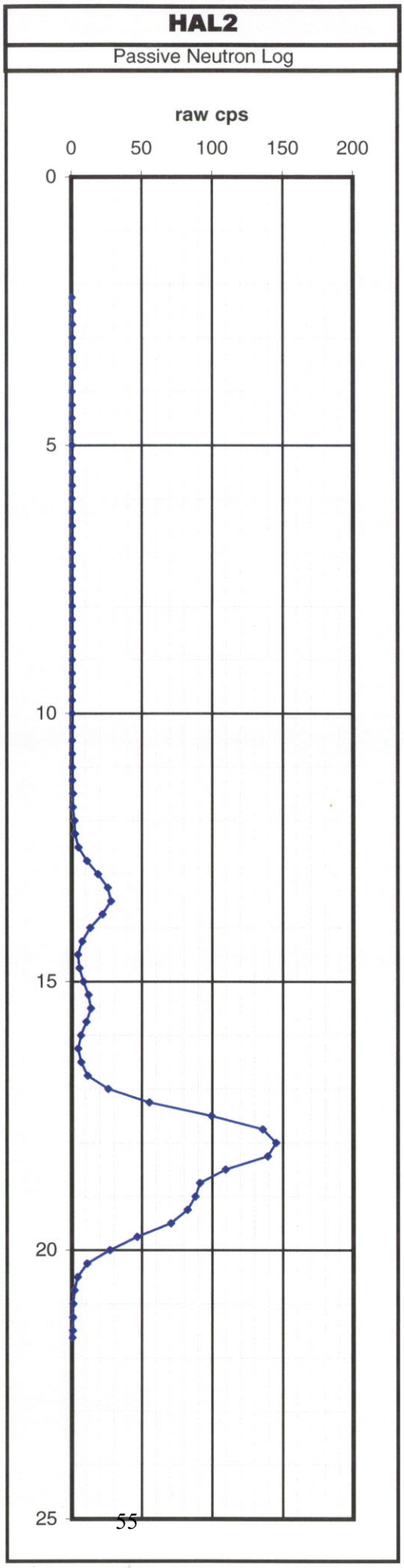
HAL2
Passive Neutron Log
raw cps
0
50
100
150
200
0
5
10
15
20
25

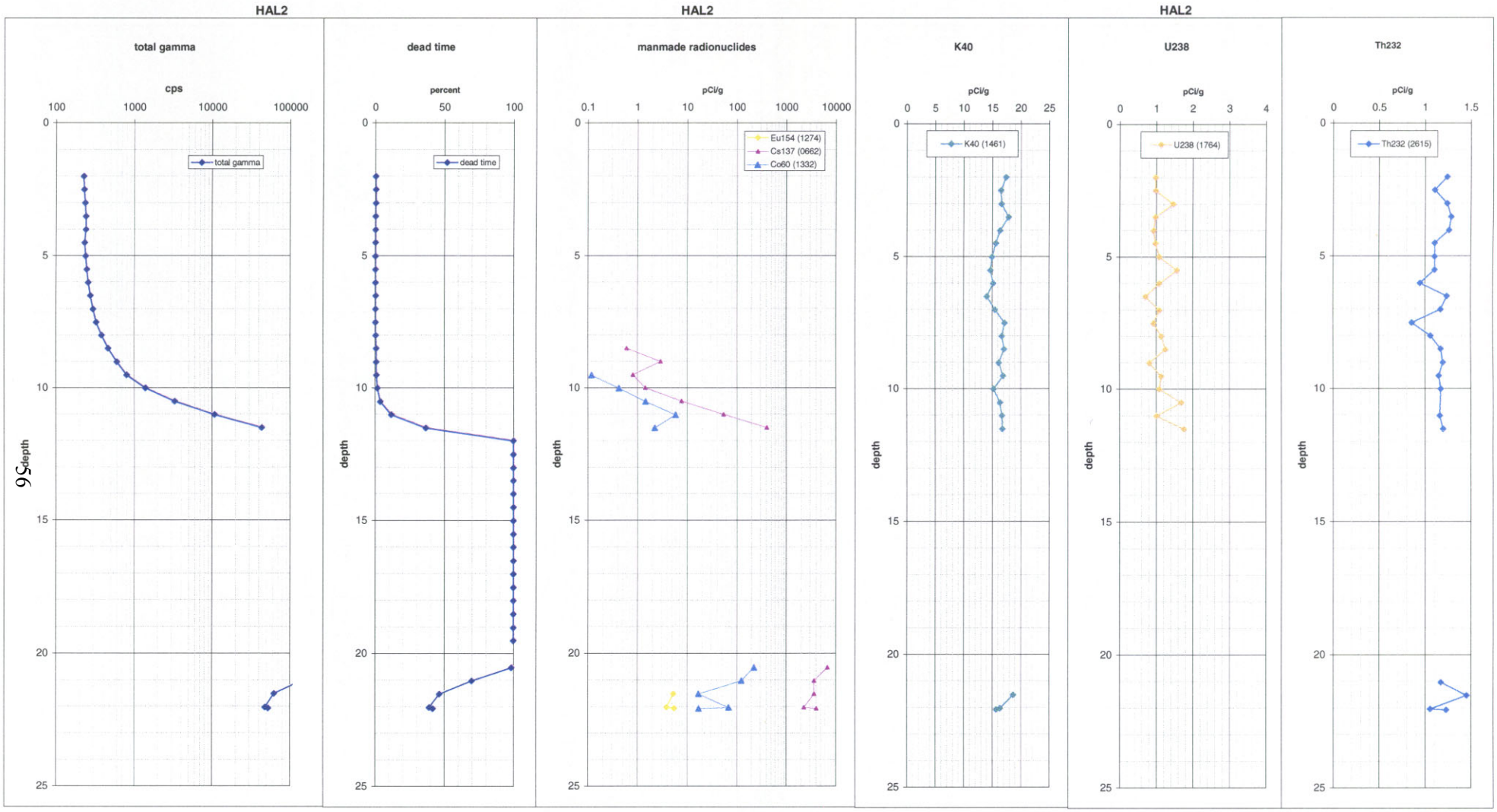
HAL2
total gamma
cps
100
1000
10000
100000
total gamma
depth
0
5
10
15
20
25
HAL2
dead time
percent
0
50
100
dead time
depth
HAL2
manmade radionuclides
pCi/g
0.1
1
10
100
1000
10000
Eu154 (1274)
Cs137 (0662)
Co60 (1332)
depth
K40
pCi/g
0
5
10
15
20
25
K40 (1461)
depth
U238
pCi/g
0
1
2
3
4
U238 (1764)
depth
Th232
pCi/g
0
0.5
1
1.5
Th232 (2615)
depth

HAL 2

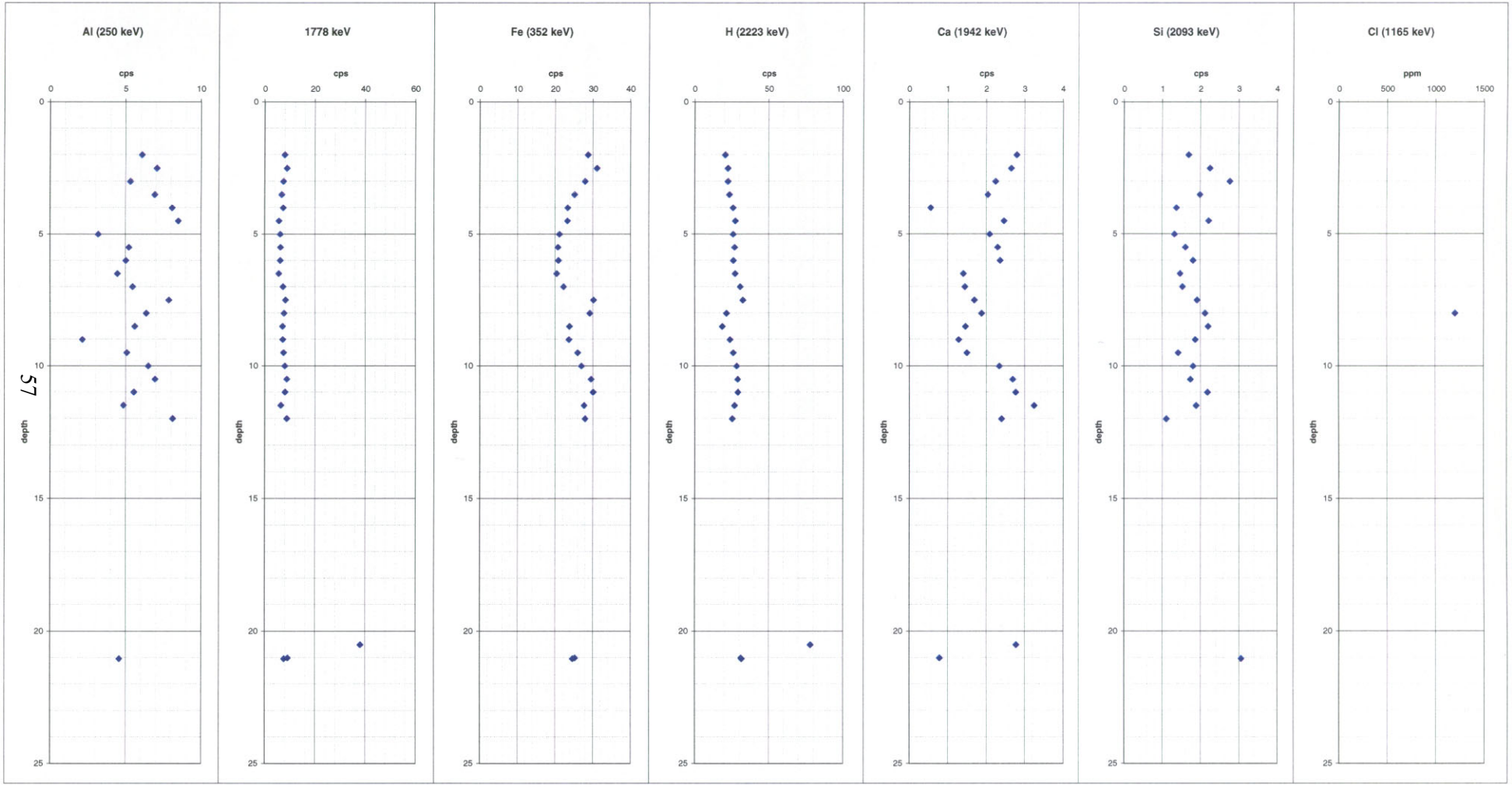
Al (250 keV)
1778 keV
Fe (352 keV)
H (2223 keV)
Ca (1942 keV)
Si (2093 keV)
Cl (1165 keV)
cps
ppm
depth

HAL 2 (Total Gamma)

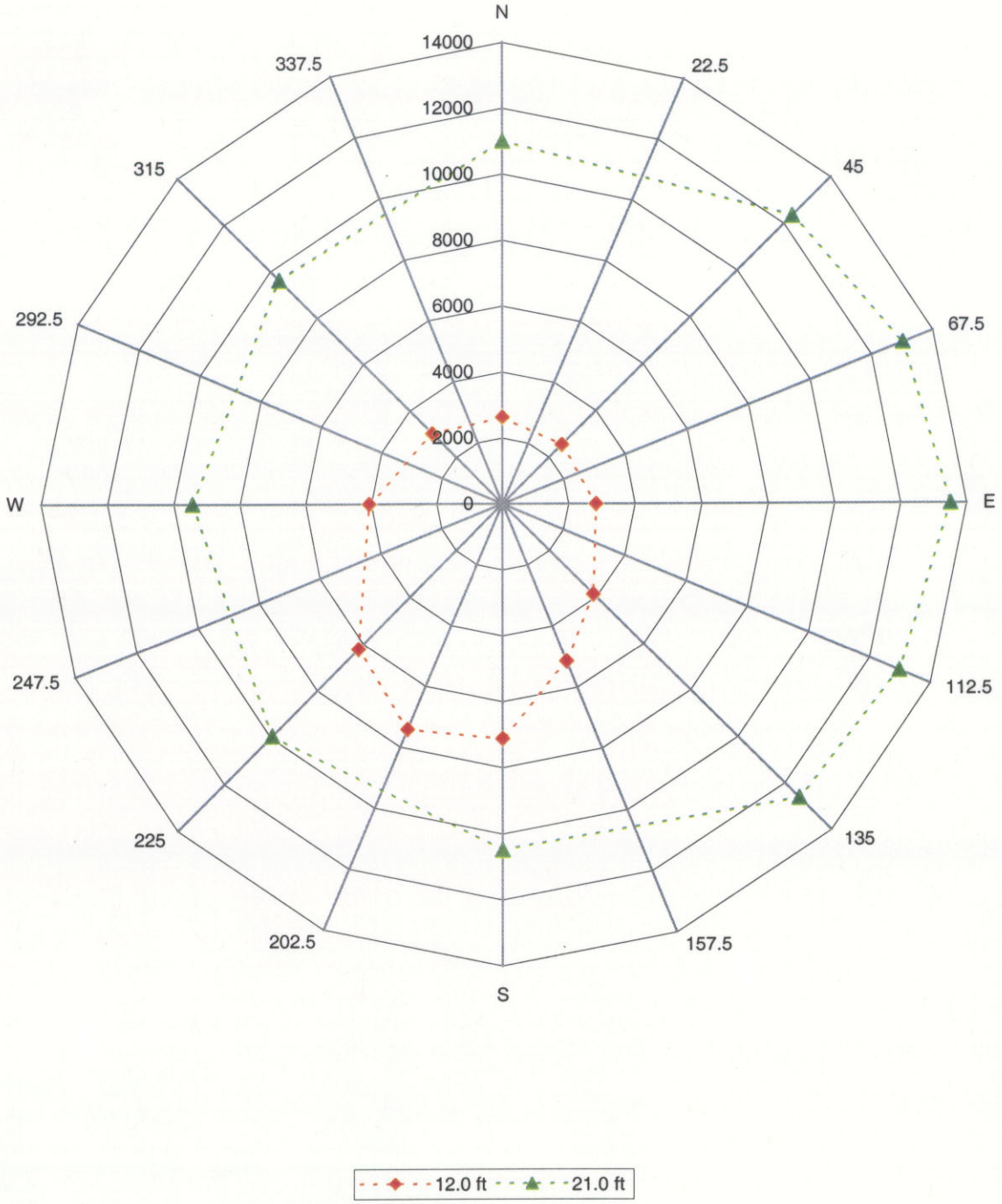

HAL 2 Cs-137 (0662)

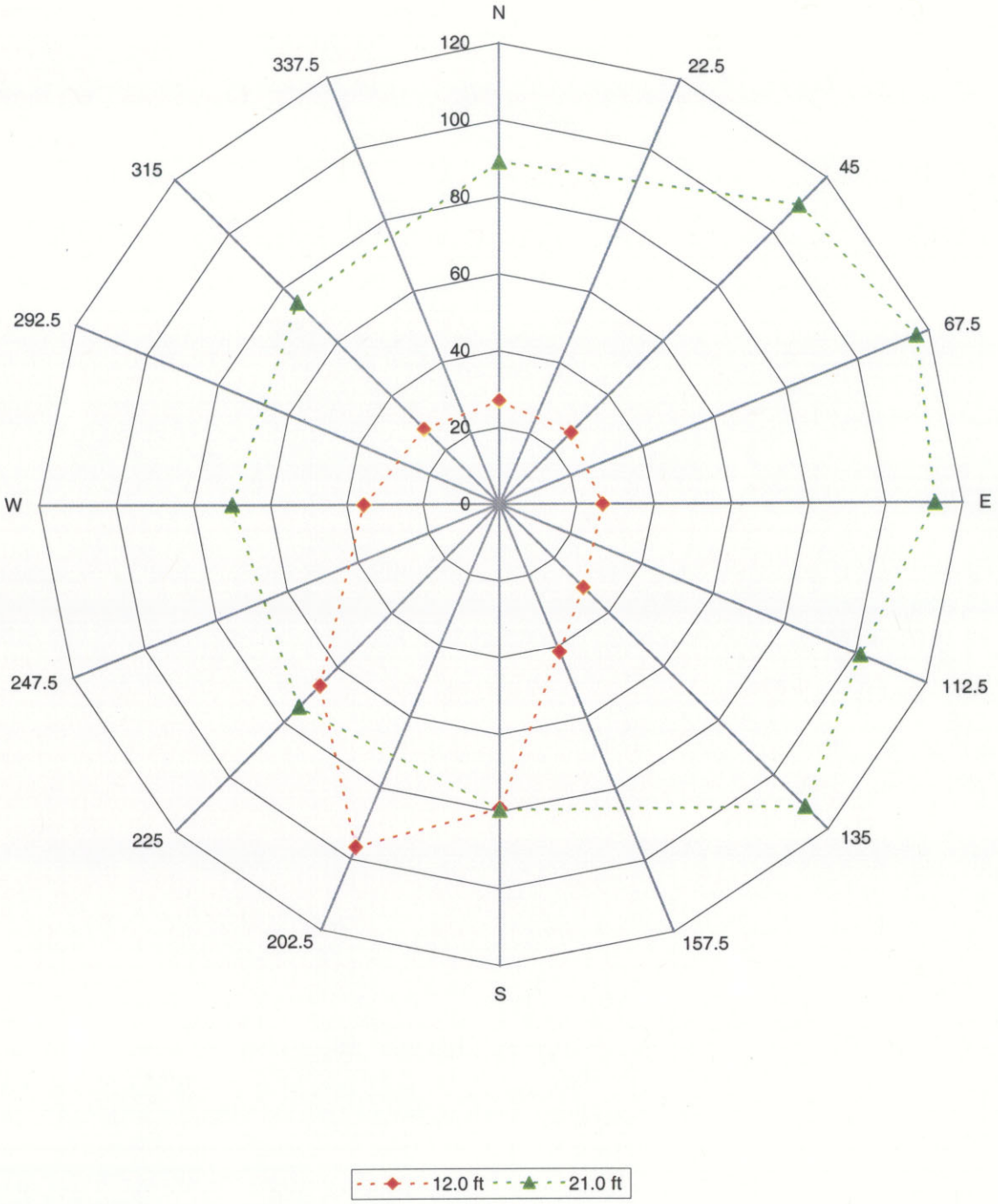

HAL 2 Co-60 (1332)

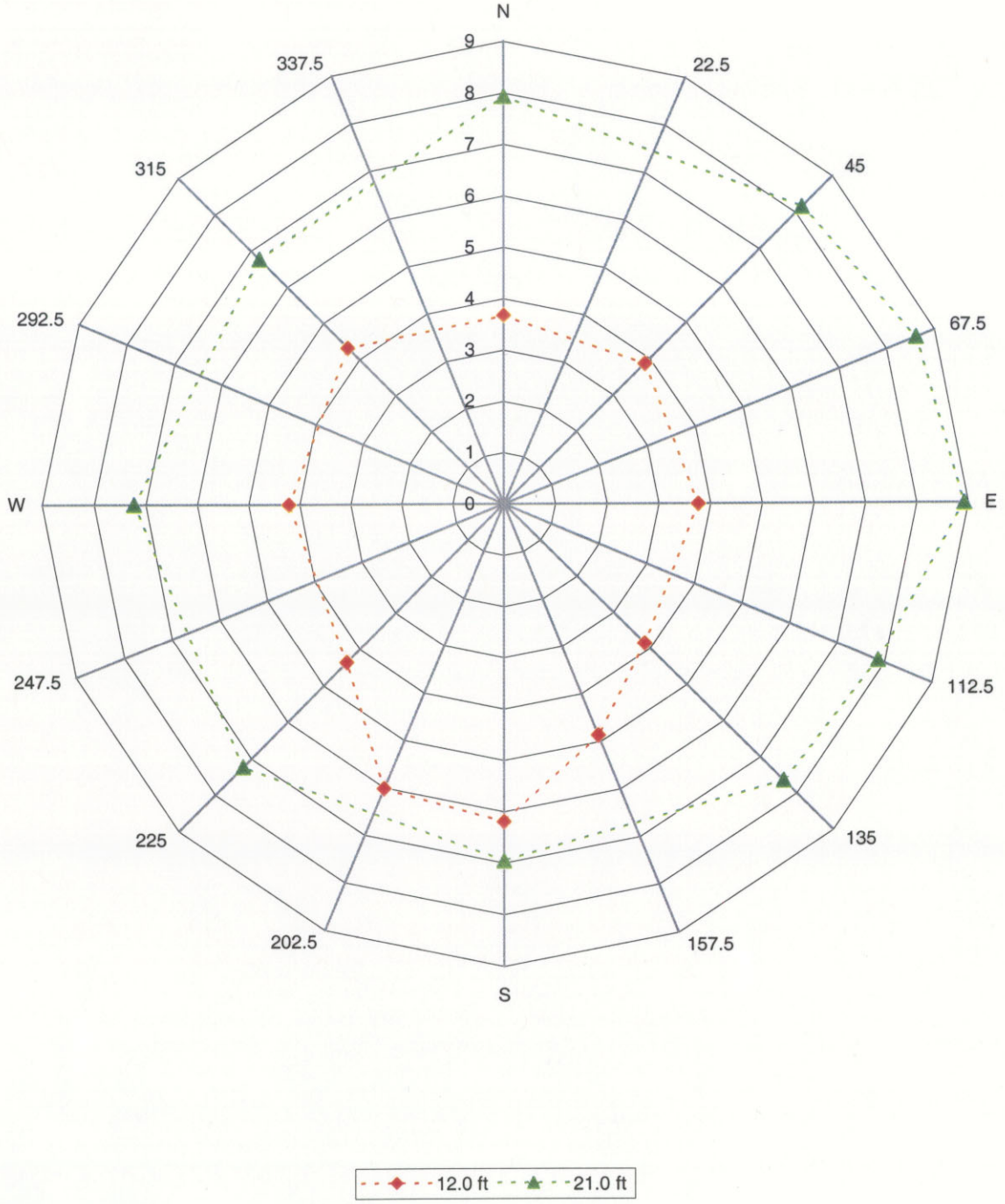

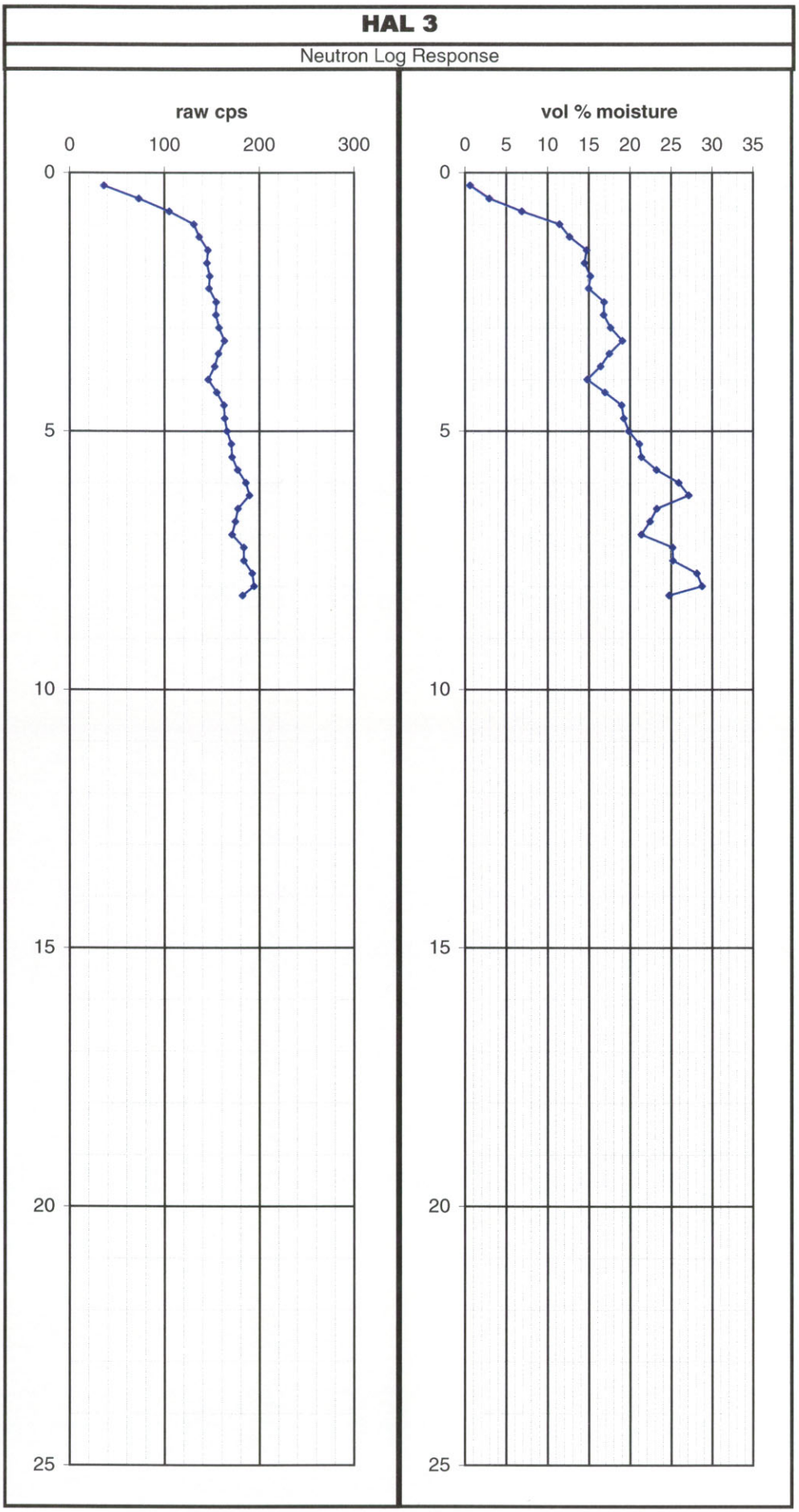
HAL 3
Neutron Log Response
raw cps
0
100
200
300
vol % moisture
0
5
10
15
20
25
30
35
0
5
10
15
20
25

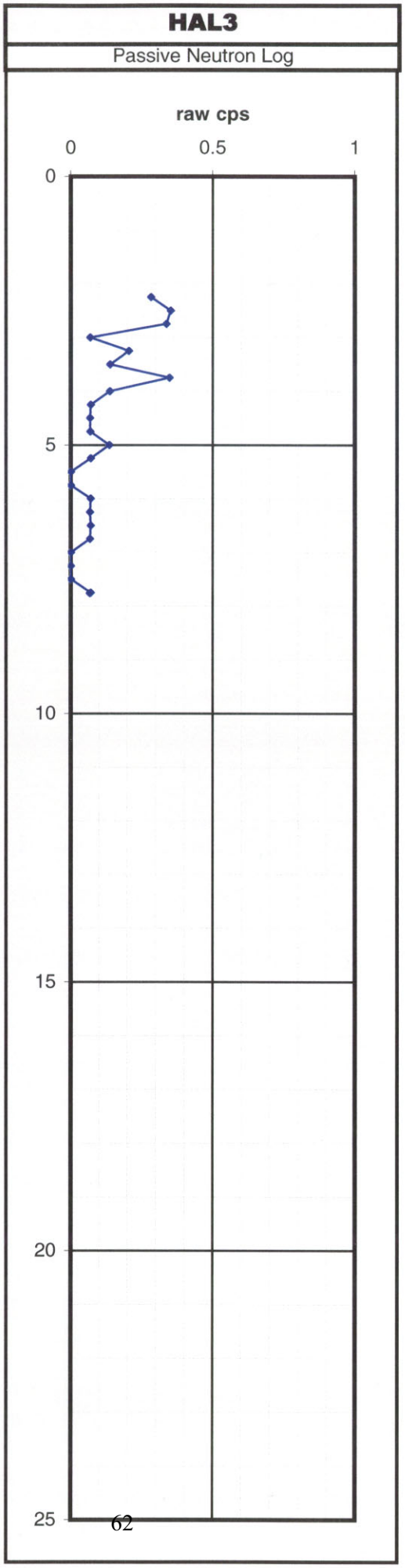
HAL3
Passive Neutron Log
raw cps
0
0.5
1
0
5
10
15
20
25

HAL3

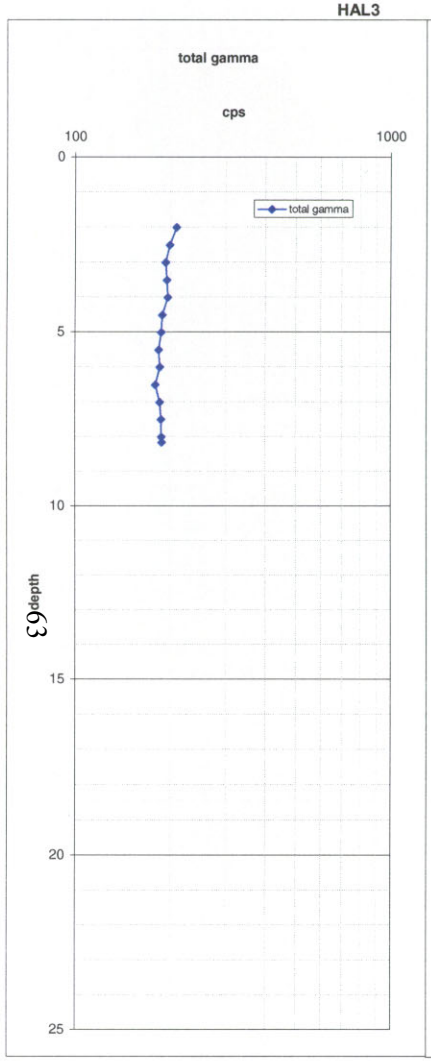

HAL3

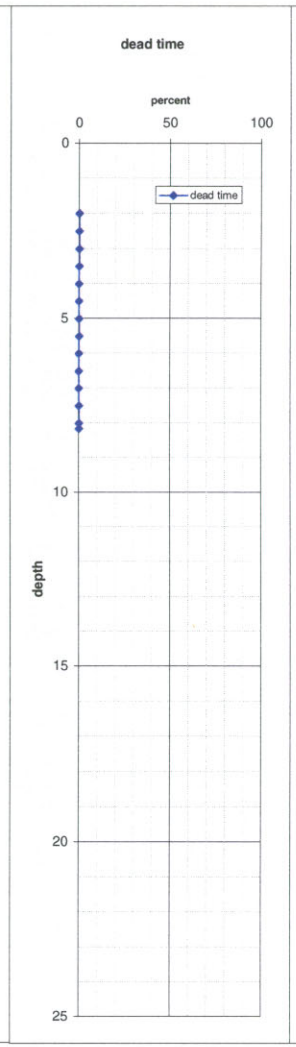

HAL3

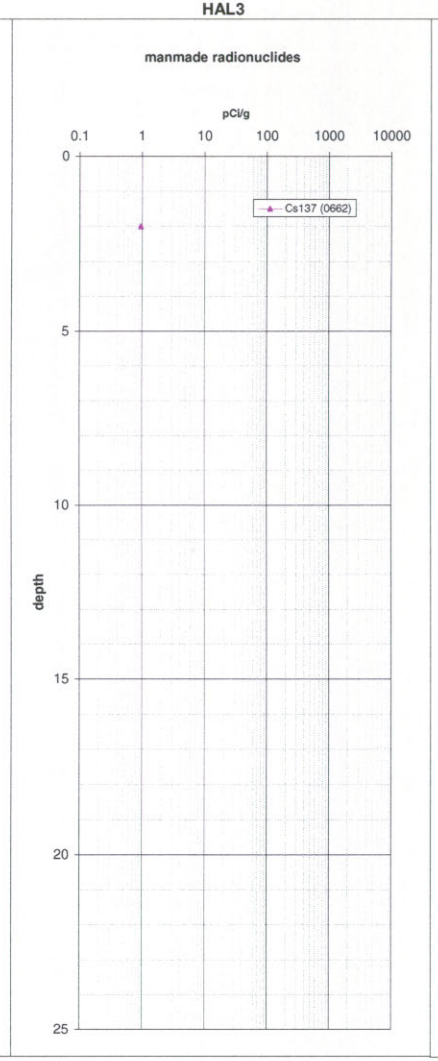

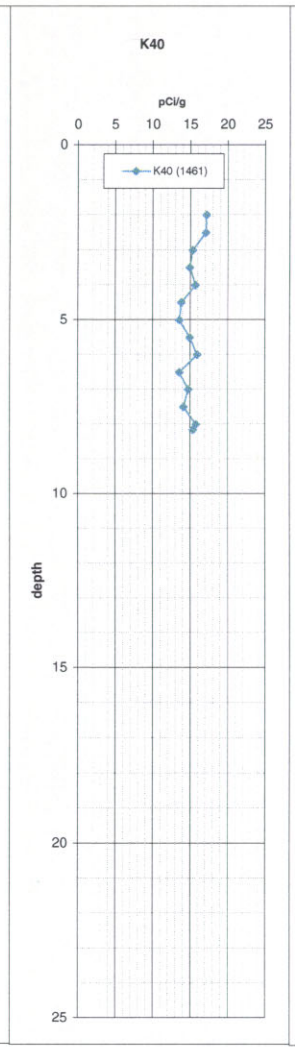

HAL3

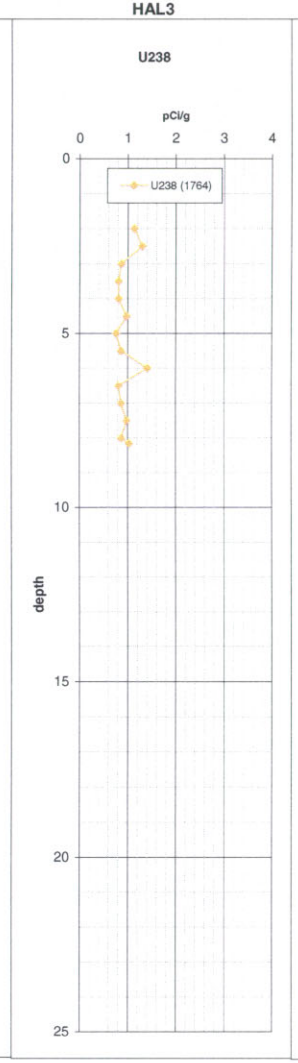

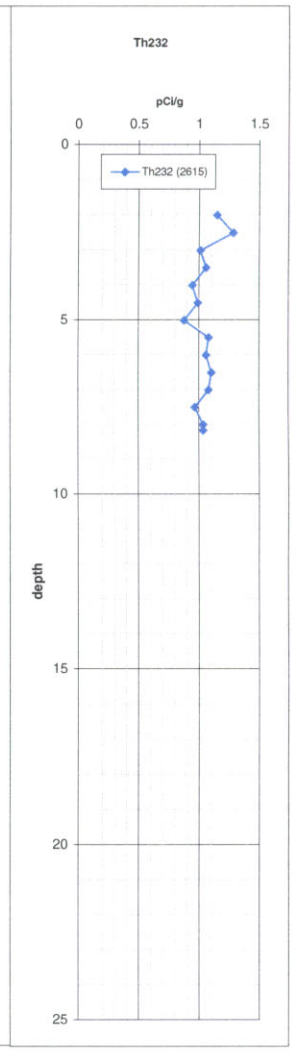

HAL 3

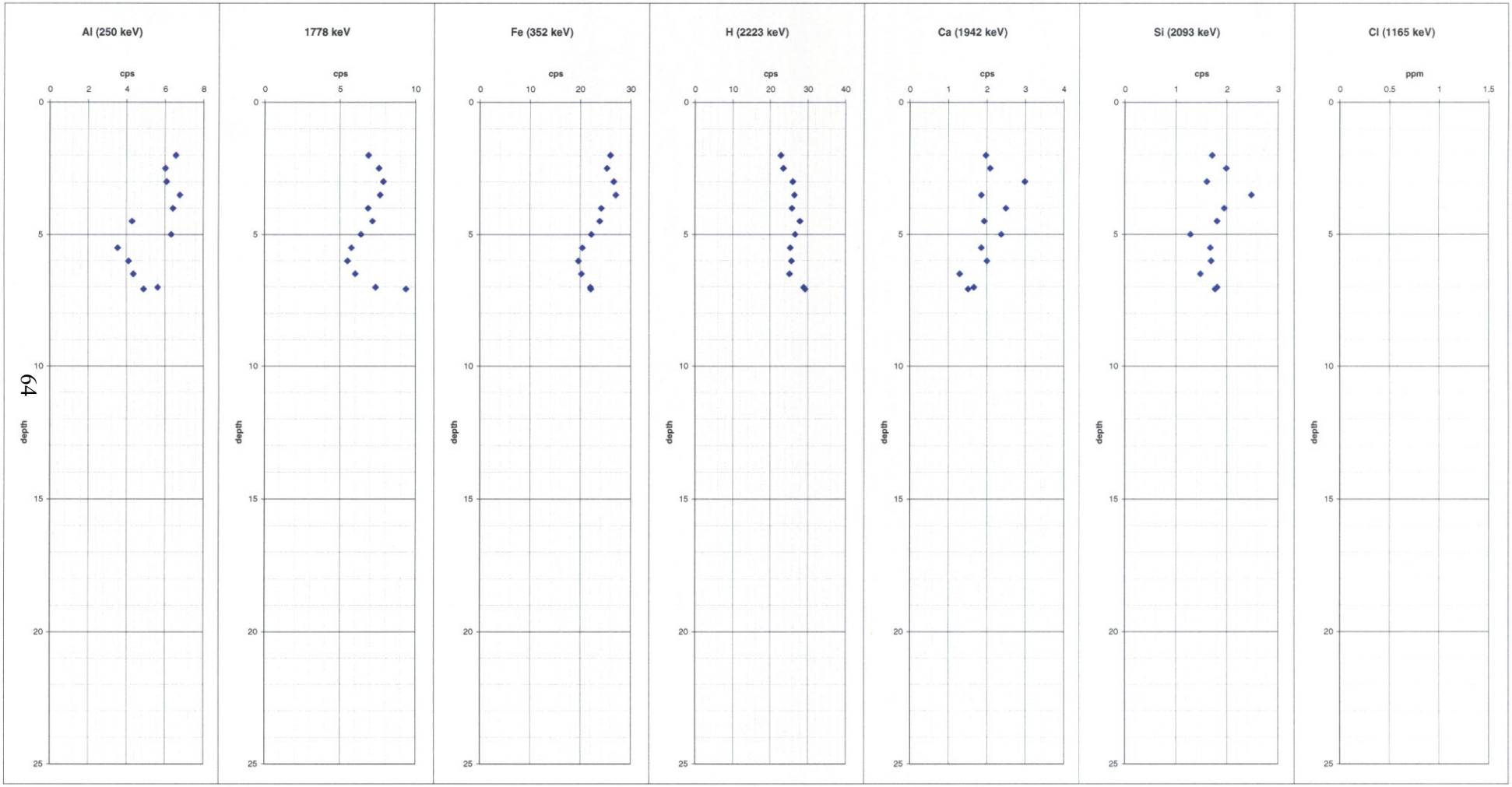
Al (250 keV)
1778 keV
Fe (352 keV)
H (2223 keV)
Ca (1942 keV)
Si (2093 keV)
Cl (1165 keV)
cps
ppm
depth

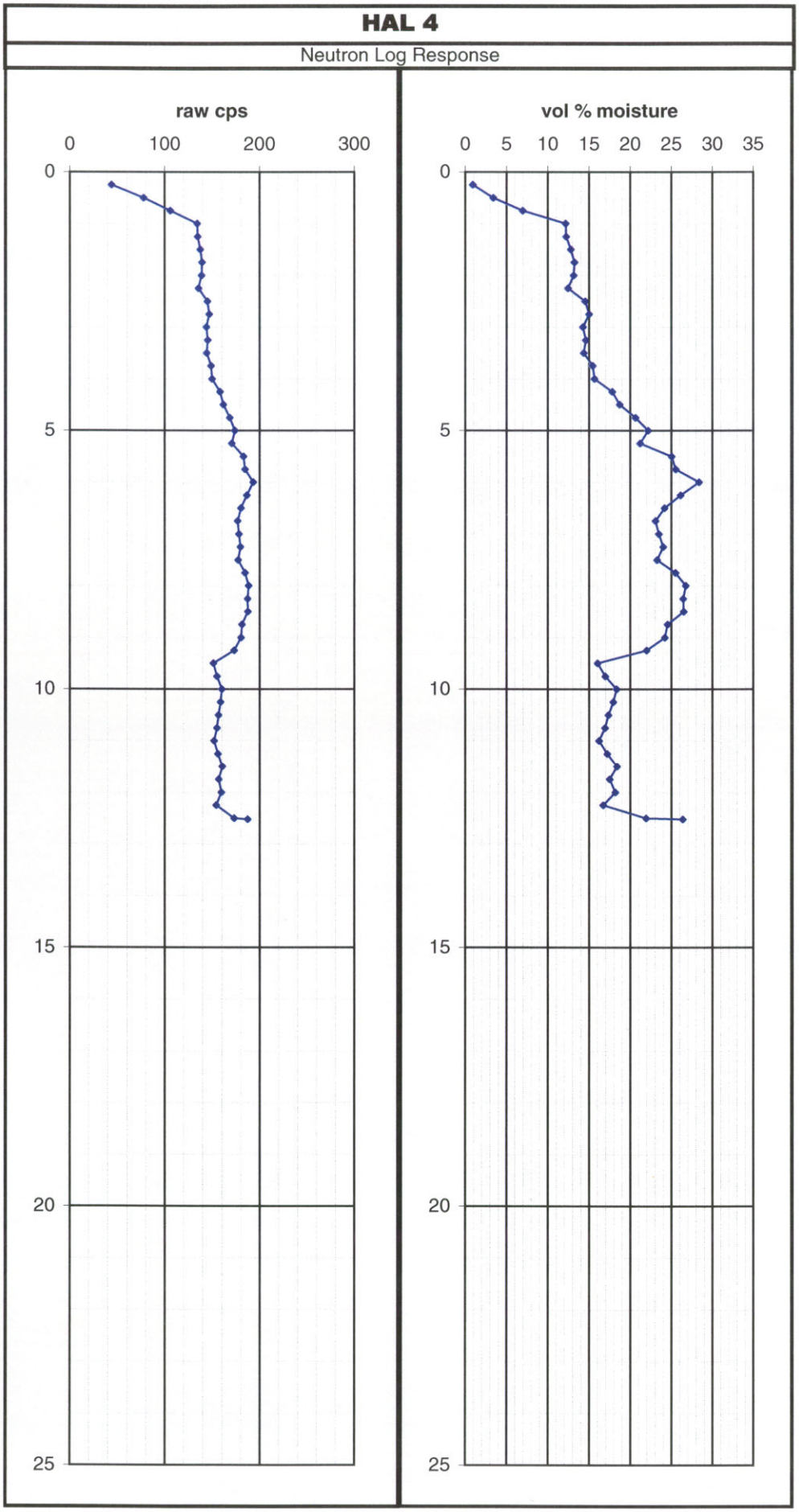
HAL 4
Neutron Log Response
raw cps
0
100
200
300
vol % moisture
0
5
10
15
20
25
30
35
0
5
10
15
20
25

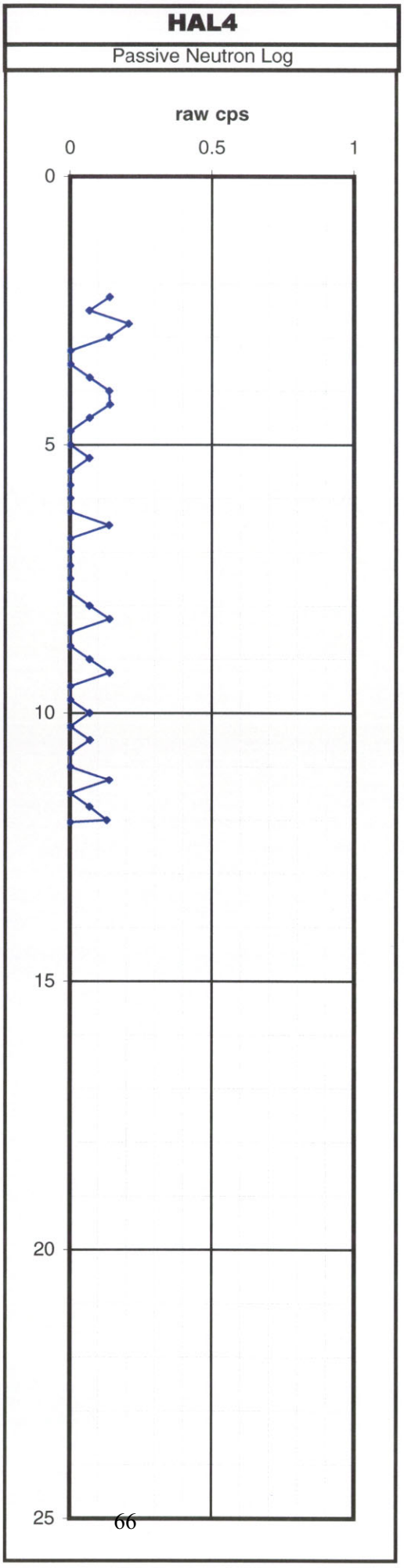
HAL4
Passive Neutron Log
raw cps
0
0.5
1
0
5
10
15
20
25

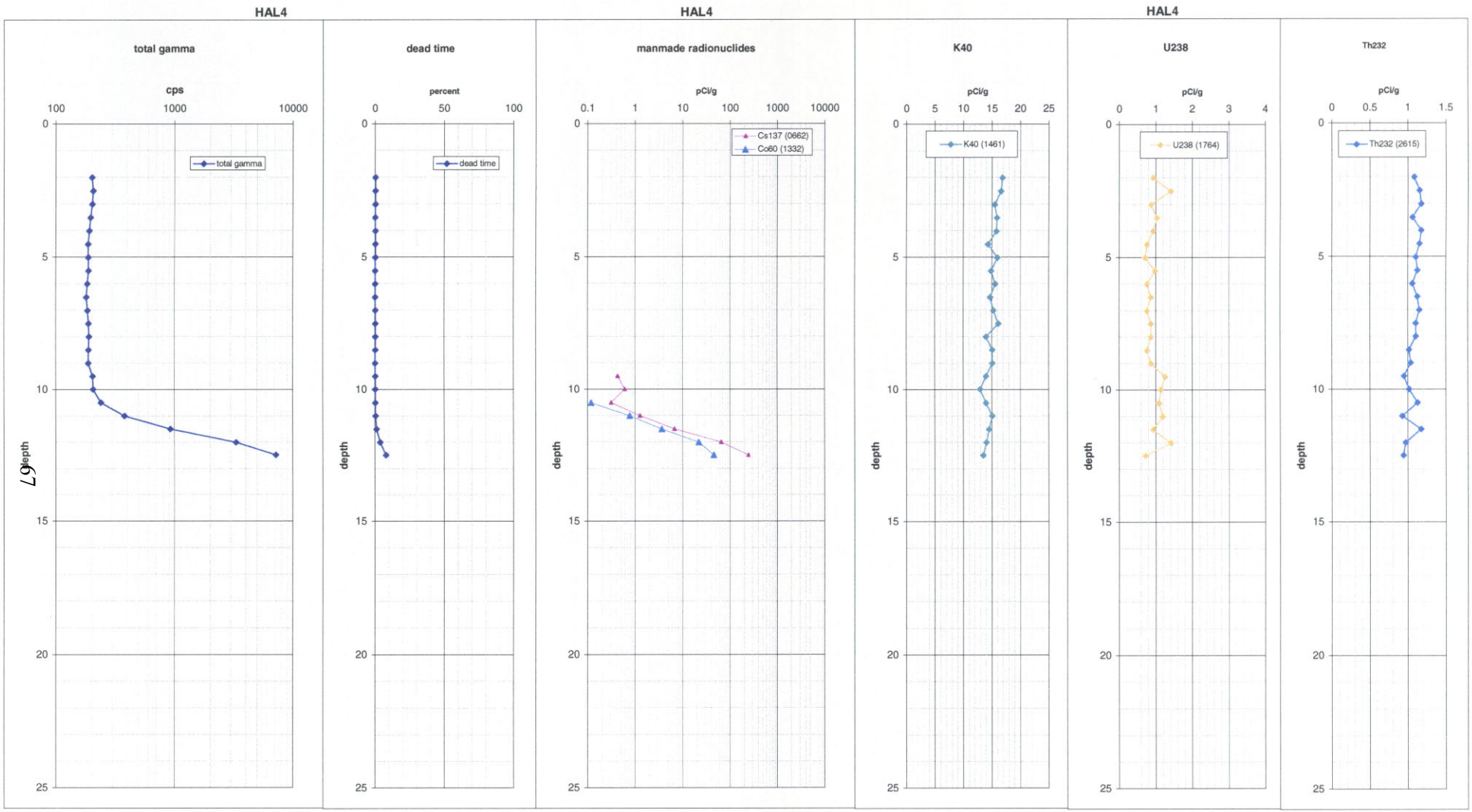
HAL4
total gamma
cps
100
1000
10000
total gamma
depth
0
5
10
15
20
25
HAL4
dead time
percent
0
50
100
dead time
depth
HAL4
manmade radionuclides
pCi/g
0.1
1
10
100
1000
10000
Cs137 (0662)
Co60 (1332)
depth
K40
pCi/g
0
5
10
15
20
25
K40 (1461)
depth
U238
pCi/g
0
1
2
3
4
U238 (1764)
depth
Th232
pCi/g
0
0.5
1
1.5
Th232 (2615)
depth

HAL 4

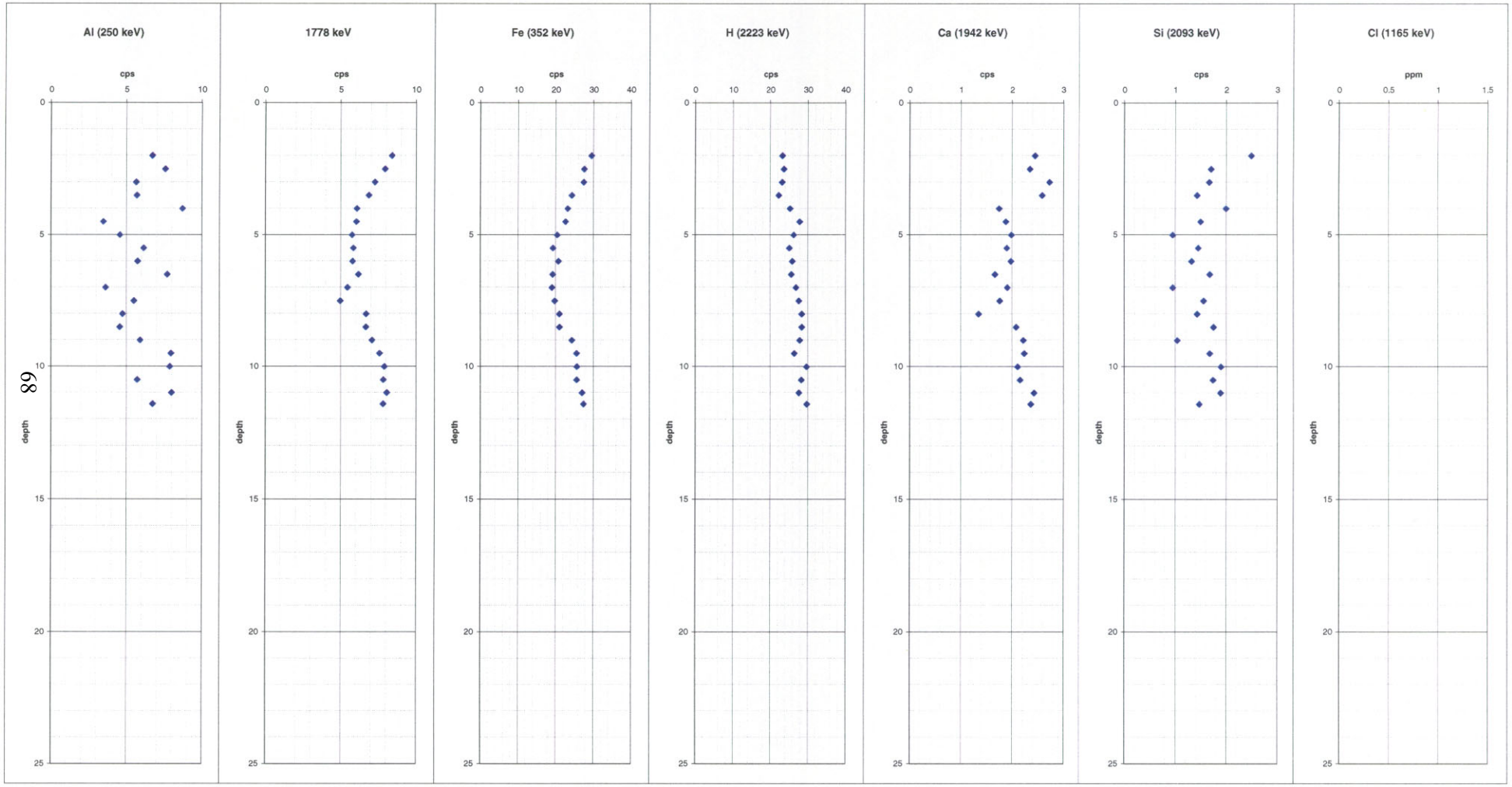
Al (250 keV)
1778 keV
Fe (352 keV)
H (2223 keV)
Ca (1942 keV)
Si (2093 keV)
Cl (1165 keV)
cps
ppm
depth

HAL 4 (Total Gamma)

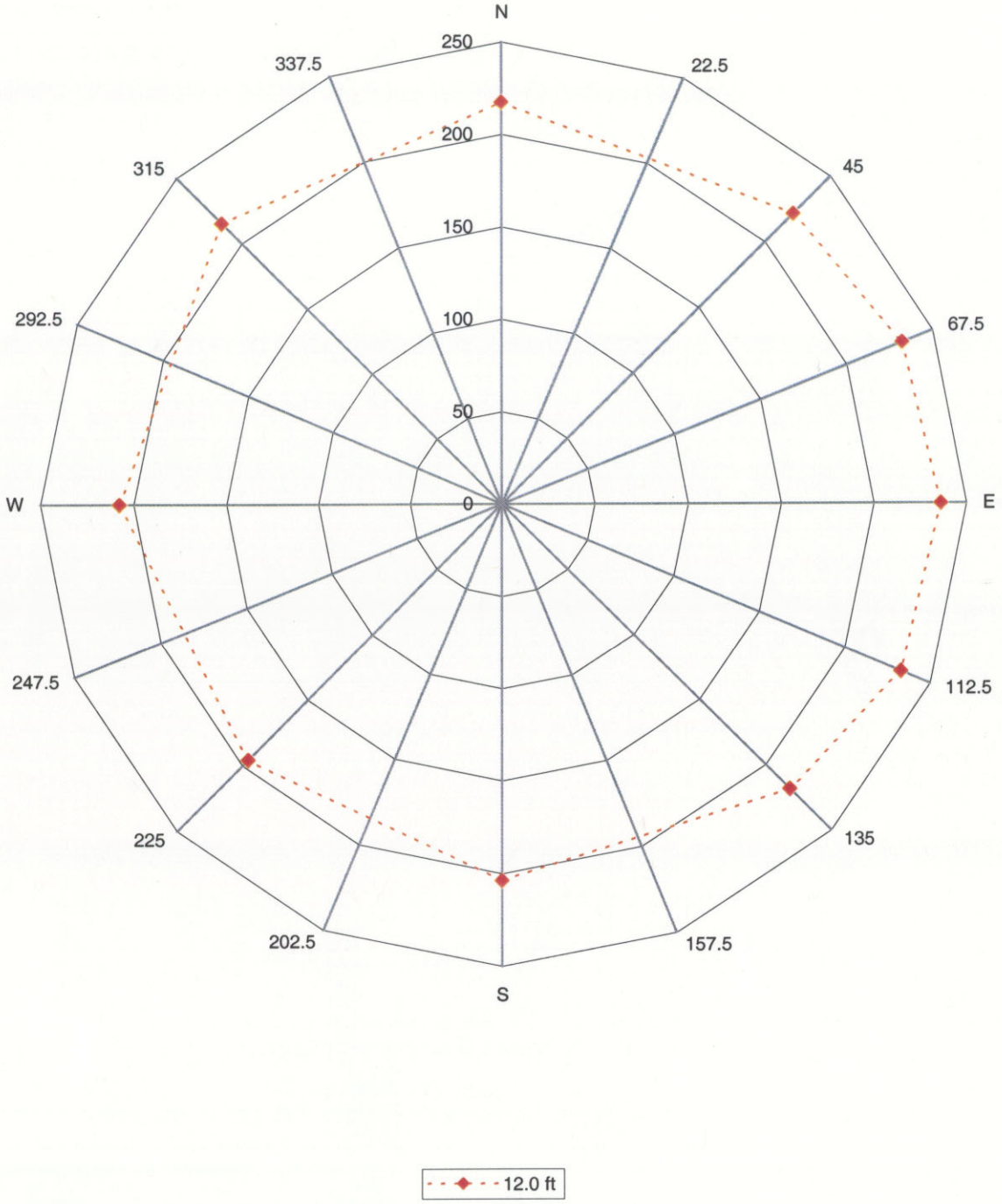

HAL 4 Cs-137 (0662)

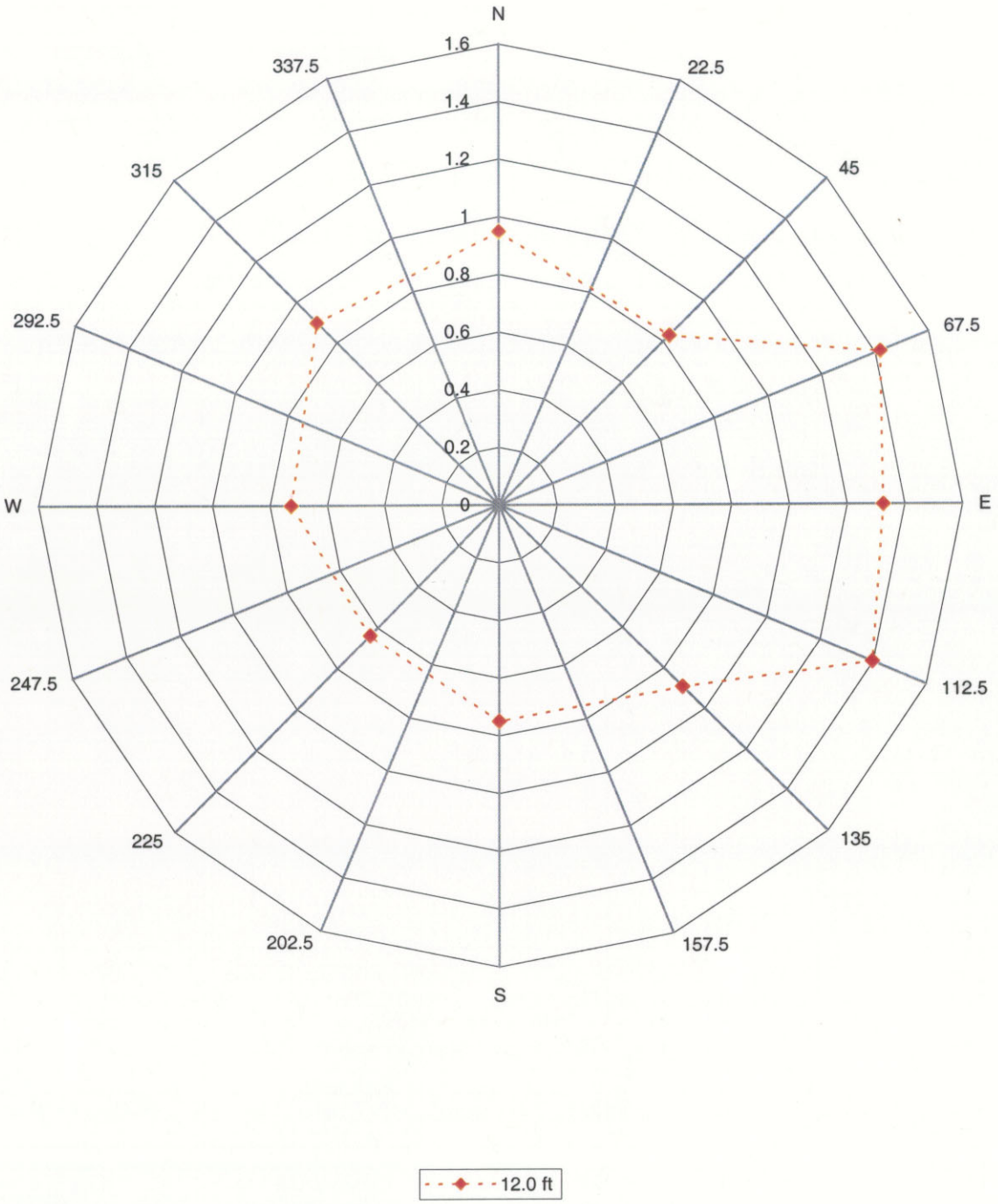

HAL 4 Co-60 (1332)

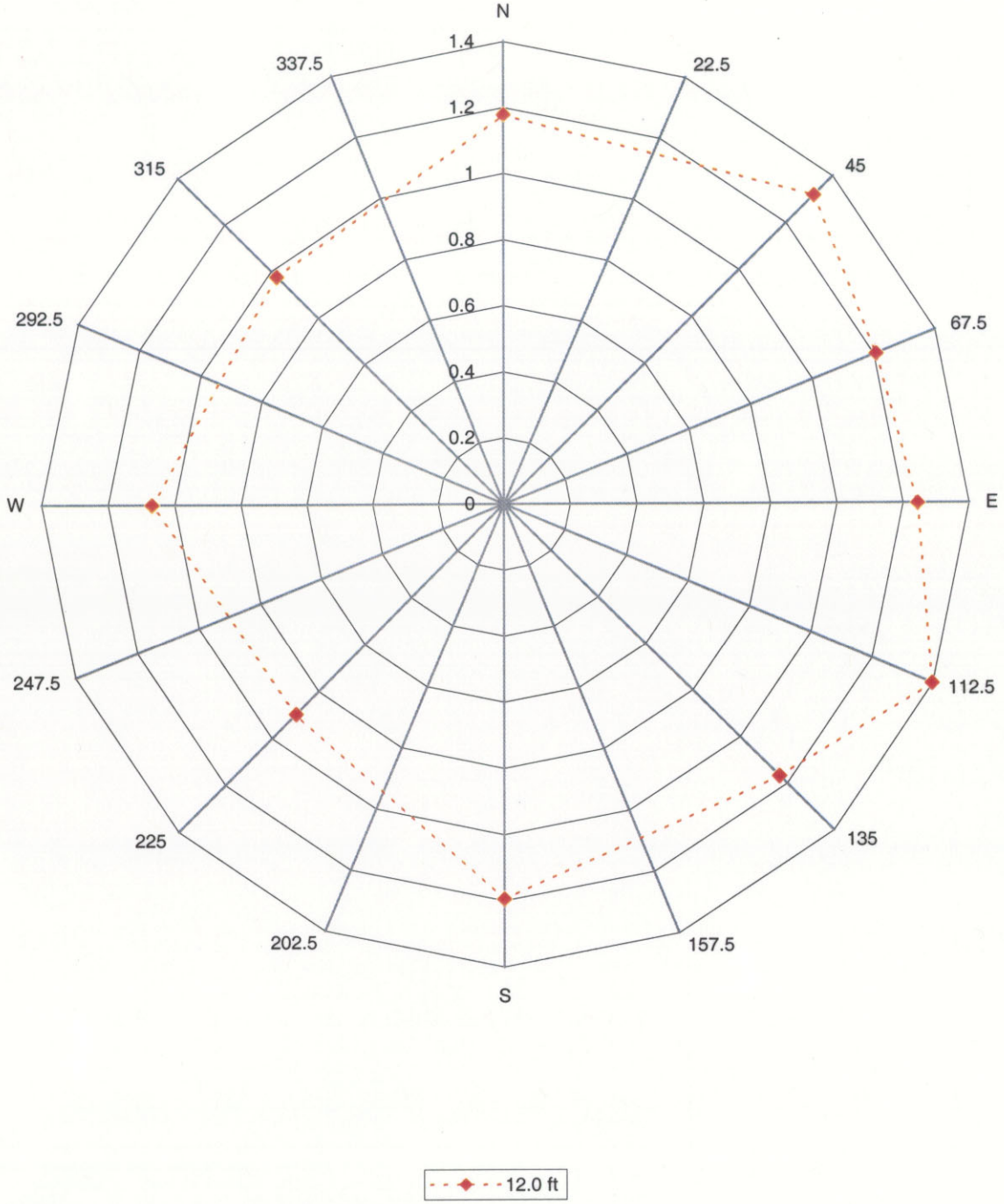

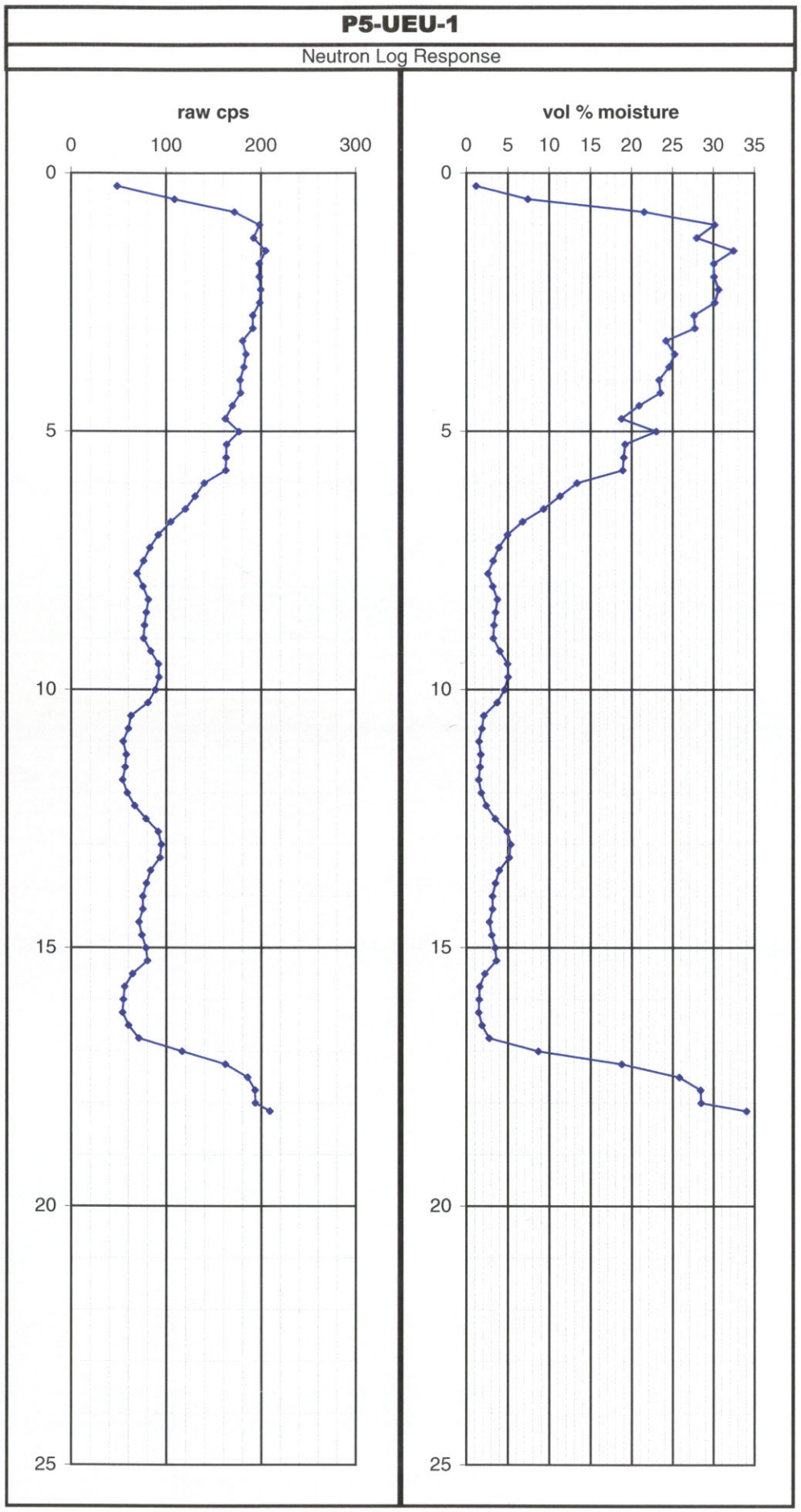
P5-UEU-1
Neutron Log Response
raw cps
0
100
200
300
vol % moisture
0
5
10
15
20
25
30
35
0
5
10
15
20
25

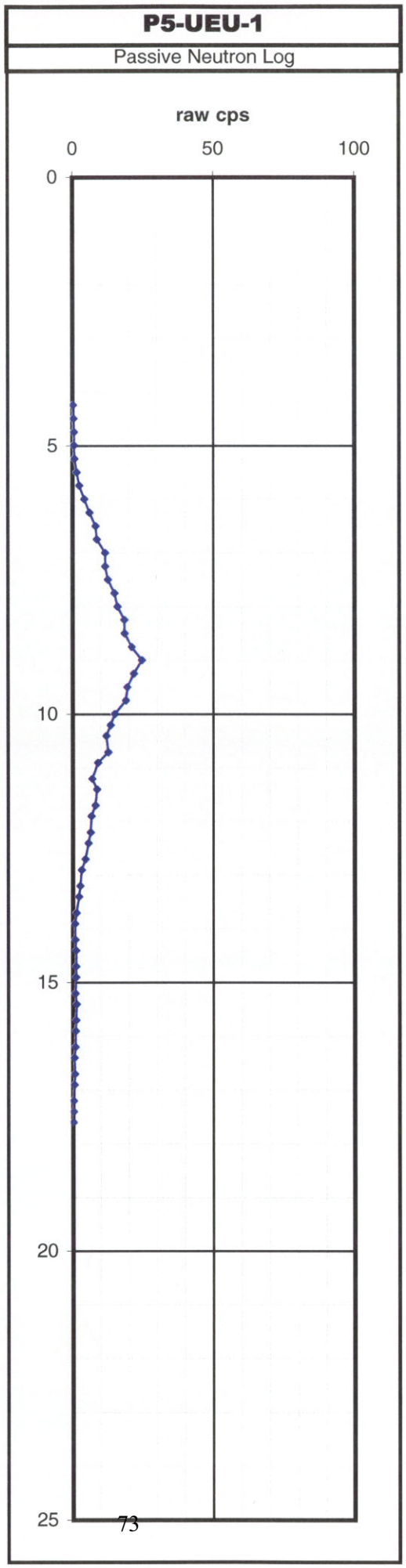
P5-UEU-1
Passive Neutron Log
raw cps
0
50
100
0
5
10
15
20
25

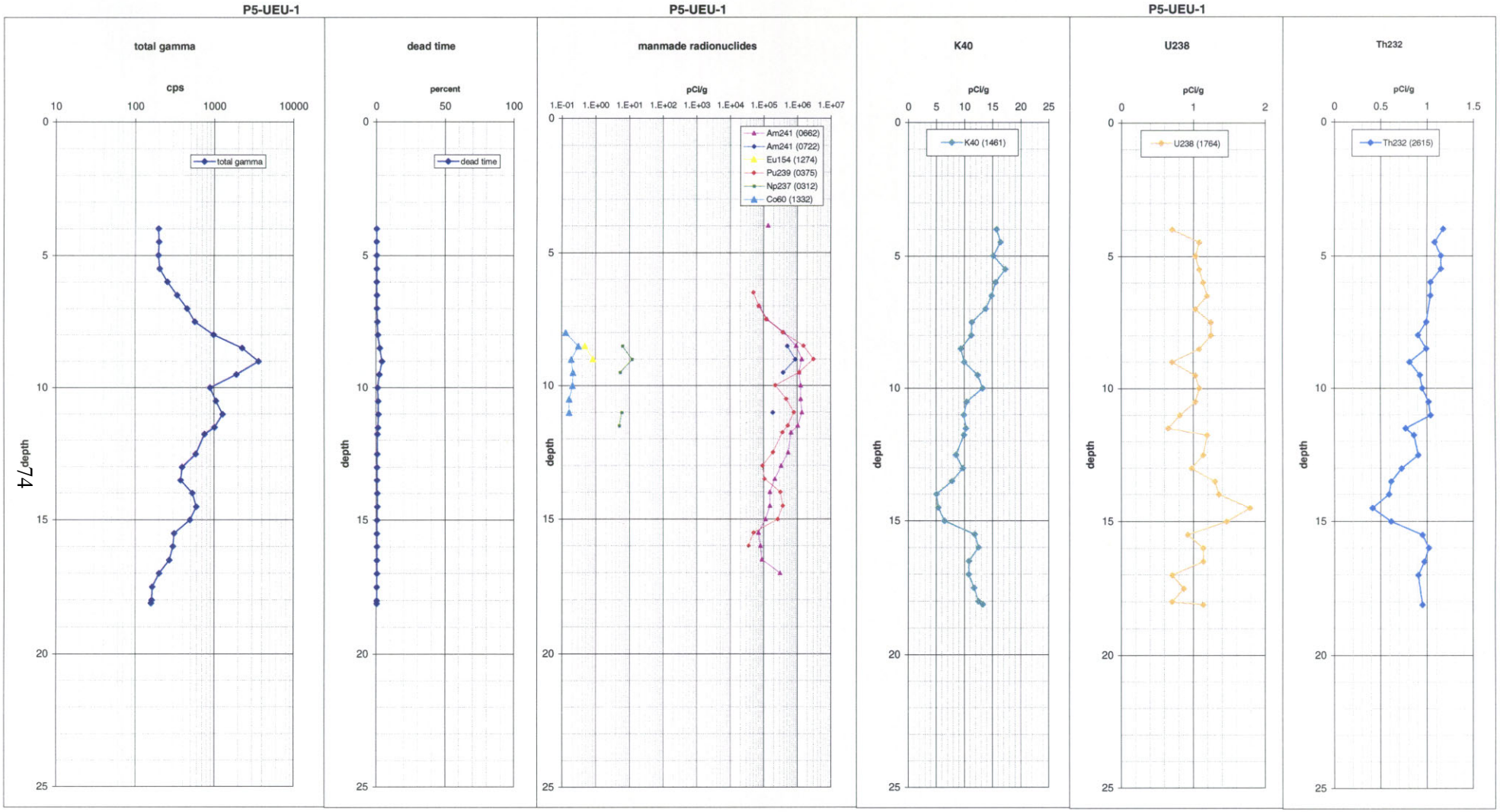
P5-UEU-1
total gamma
cps
10
100
1000
10000
total gamma
depth
0
5
10
15
20
25
P5-UEU-1
dead time
percent
0
50
100
dead time
depth
P5-UEU-1
manmade radionuclides
pCi/g
1.E-01
1.E+00
1.E+01
1.E+02
1.E+03
1.E+04
1.E+05
1.E+06
1.E+07
Am241 (0662)
Am241 (0722)
Eu154 (1274)
Pu239 (0375)
Np237 (0312)
Co60 (1332)
depth
P5-UEU-1
K40
pCi/g
0
5
10
15
20
25
K40 (1461)
depth
U238
pCi/g
0
1
2
U238 (1764)
depth
Th232
pCi/g
0
0.5
1
1.5
Th232 (2615)
depth

P5-UEU-1

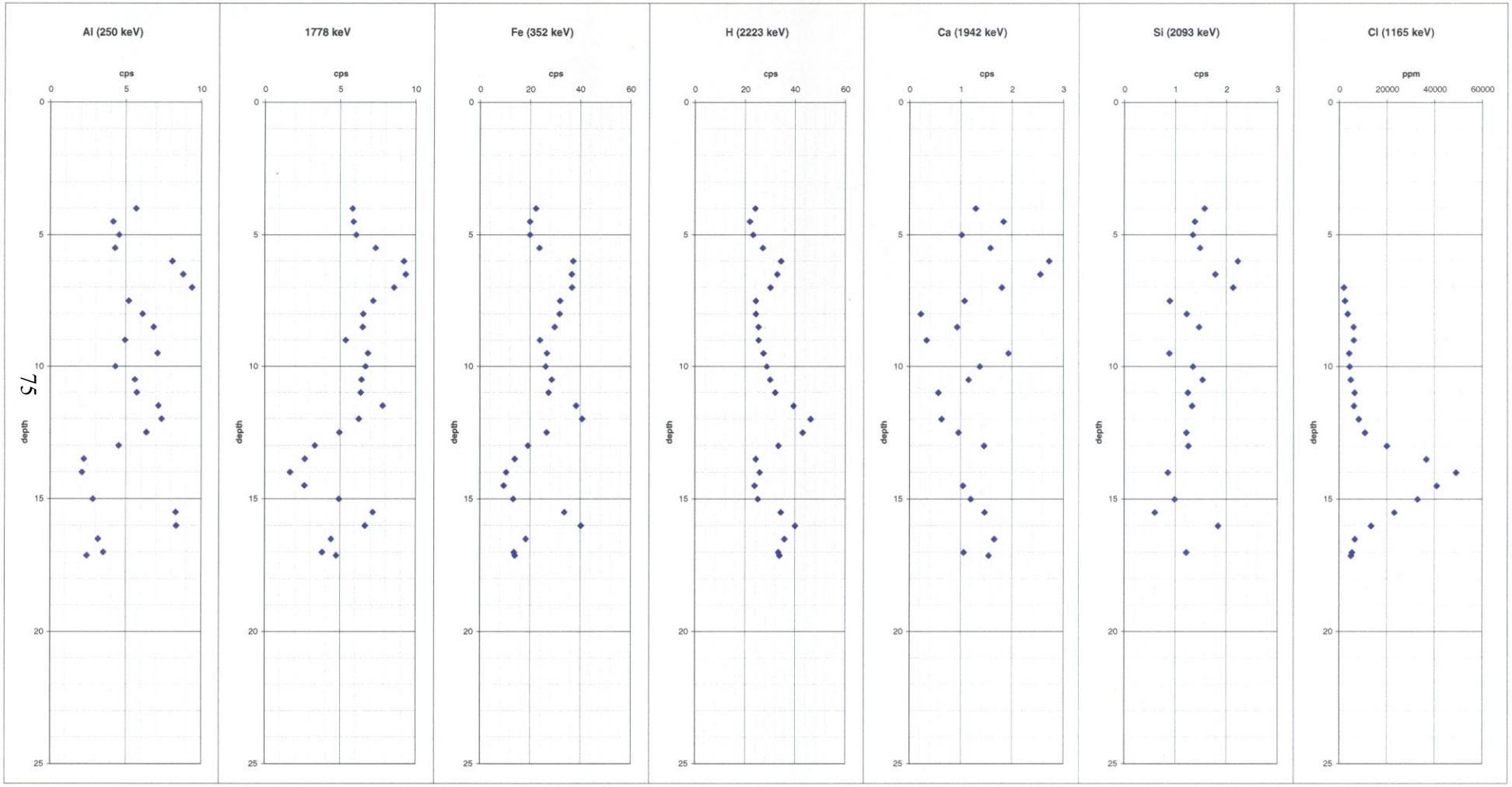
Al (250 keV)
1778 keV
Fe (352 keV)
H (2223 keV)
Ca (1942 keV)
Si (2093 keV)
Cl (1165 keV)
cps
ppm
depth

P5-UEU-1 Total Gamma (7.0 ft to 16.0 ft)

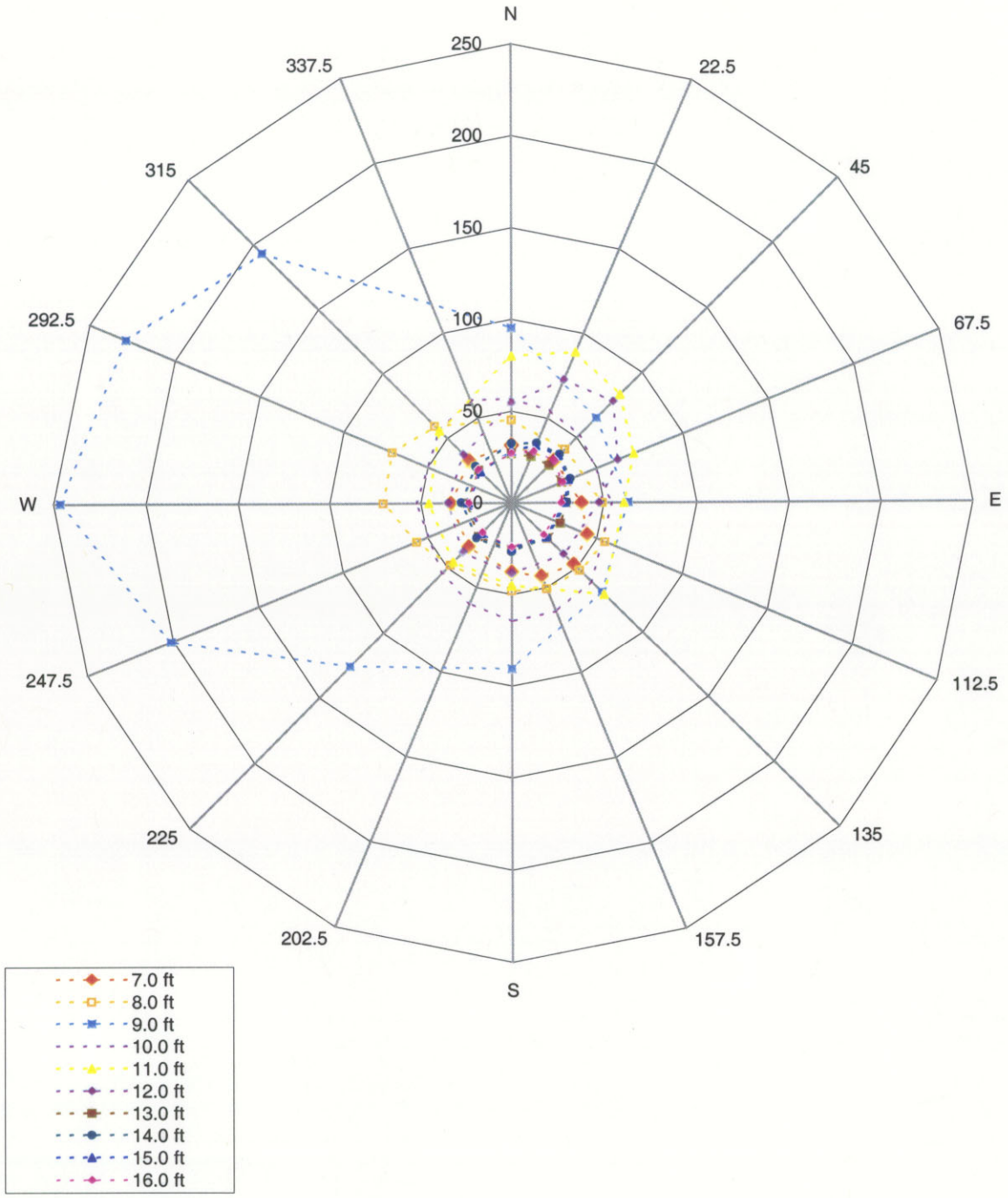

P5-UEU-1 Total Gamma (7.0 ft to 8.0 ft)

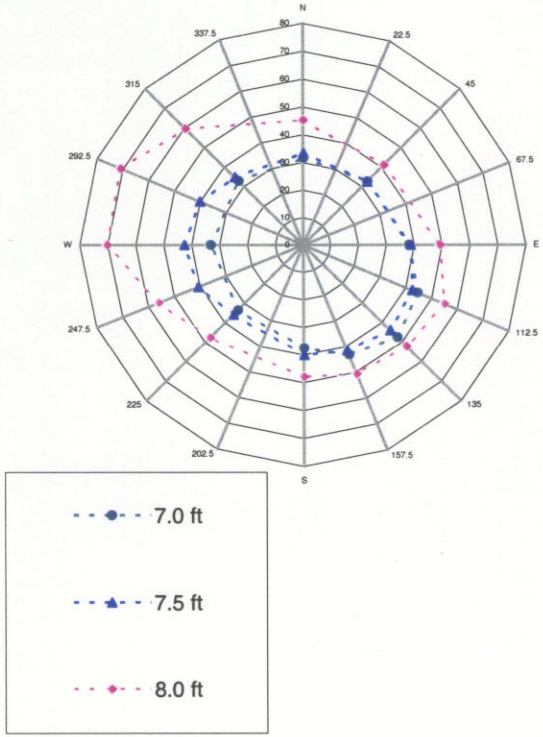

P5-UEU-1 Total Gamma (8.5 ft to 12.0 ft)

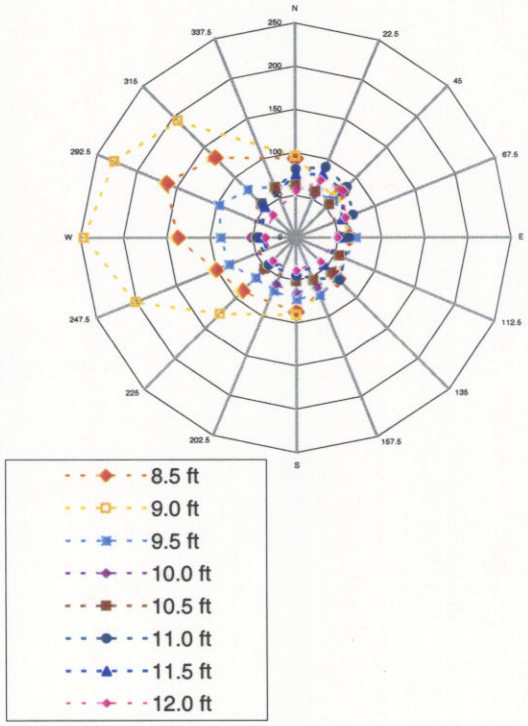

P5-UEU-1 Total Gamma (12.5 ft to 16.0 ft)

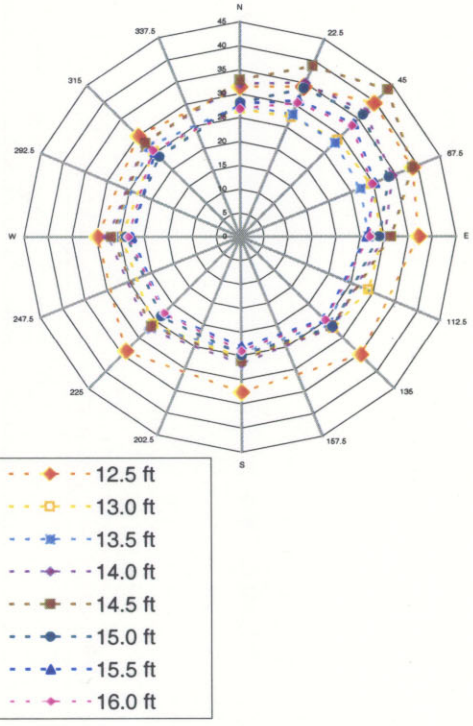

P5-UEU-1 Pu-239 (375 keV - 8.0 ft to 15.0 ft)

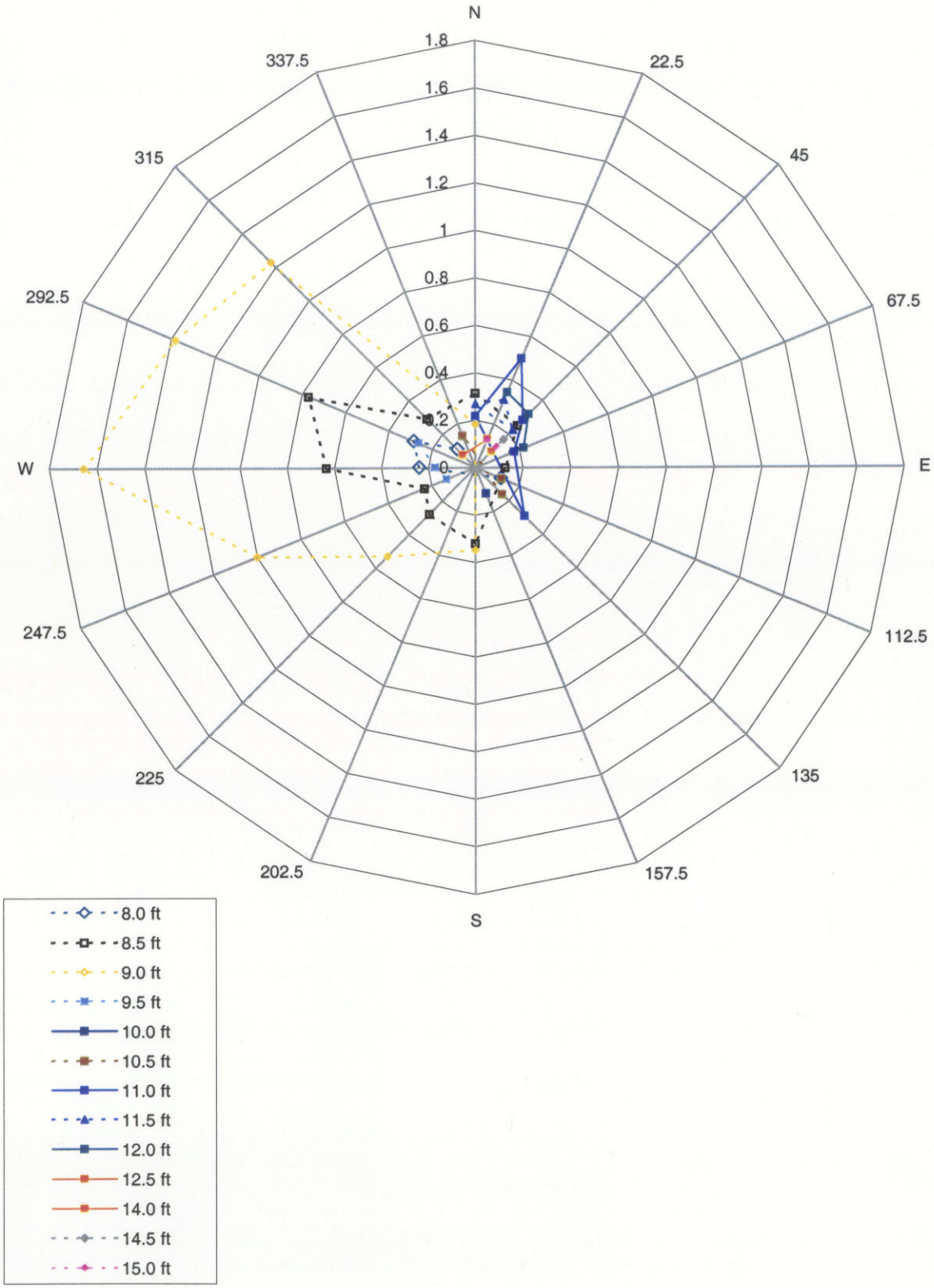

P5-UEU-1 Am-241 (662 keV - 9.0 ft)

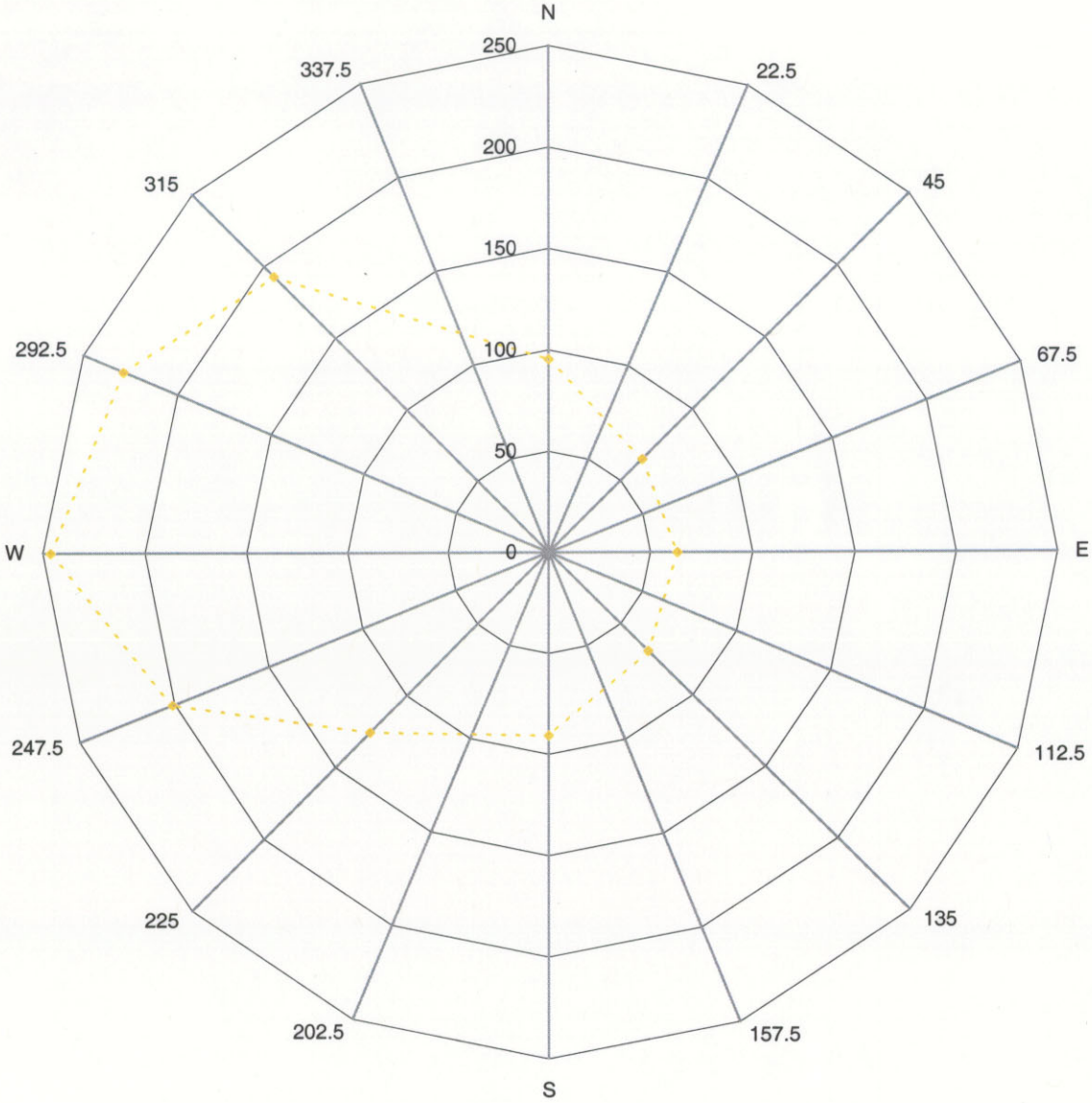

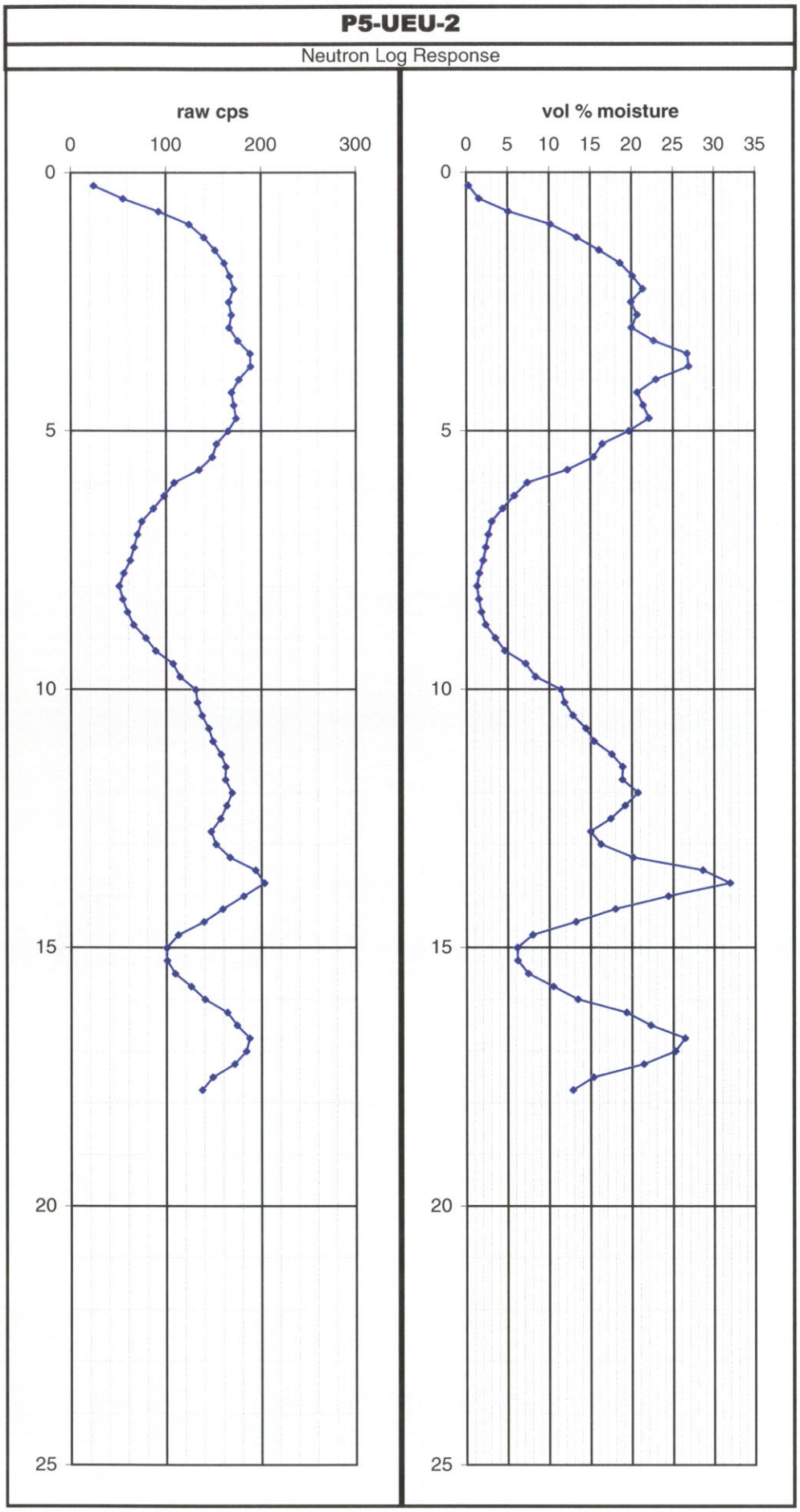
P5-UEU-2
Neutron Log Response
raw cps
0
100
200
300
0
5
10
15
20
25
vol % moisture
0
5
10
15
20
25
30
35
0
5
10
15
20
25

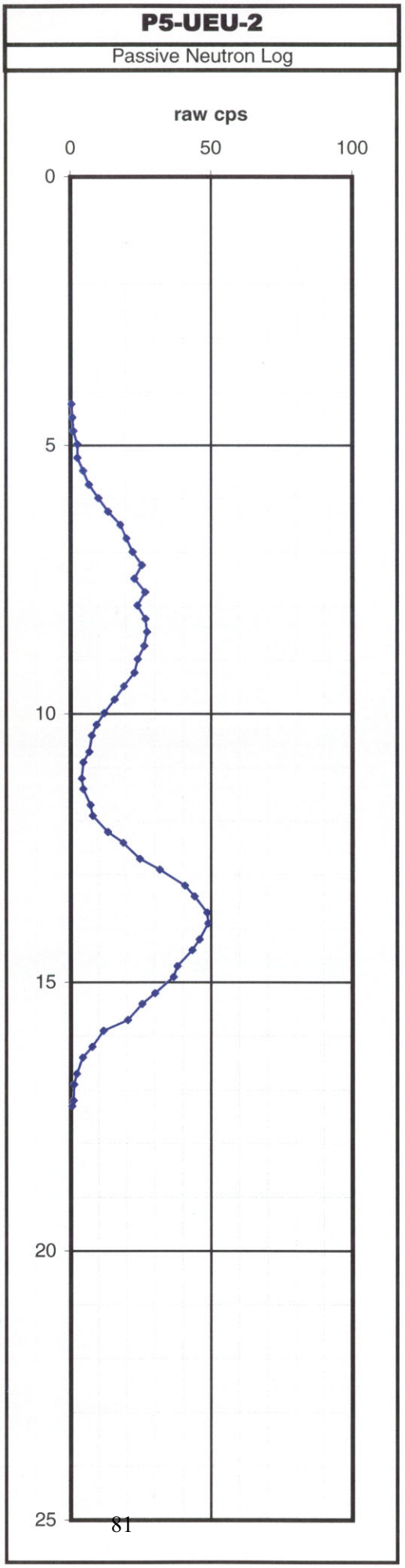
P5-UEU-2
Passive Neutron Log
raw cps
0
50
100
0
5
10
15
20
25

P5-UEU-2

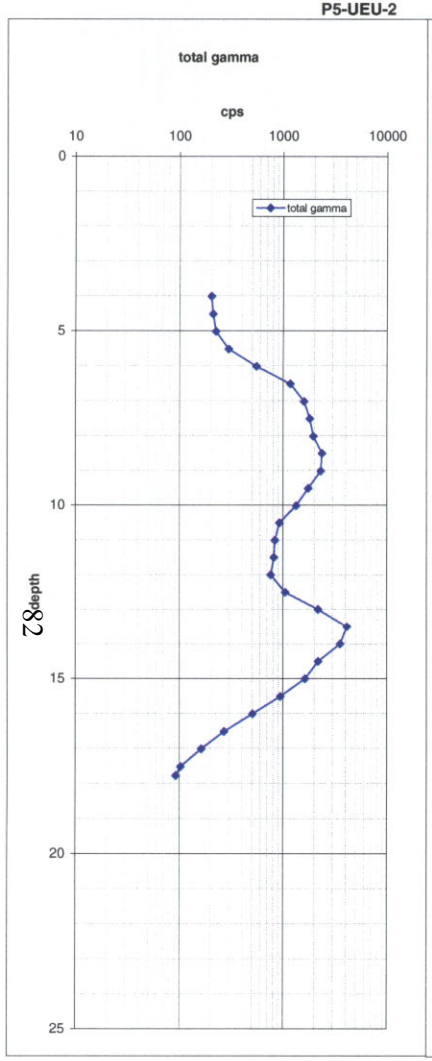

P5-UEU-2

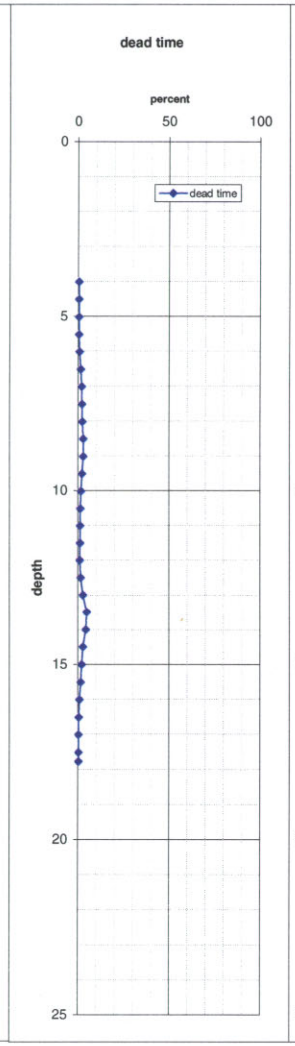

P5-UEU-2

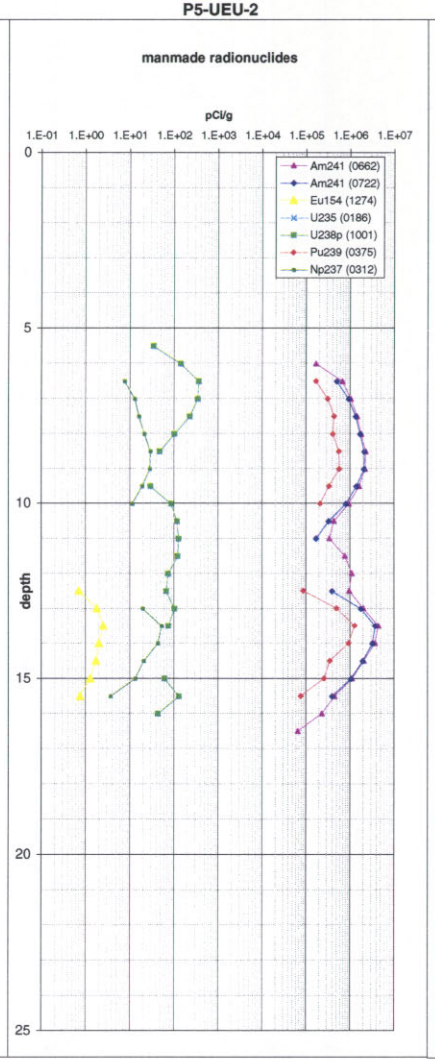

P5-UEU-2

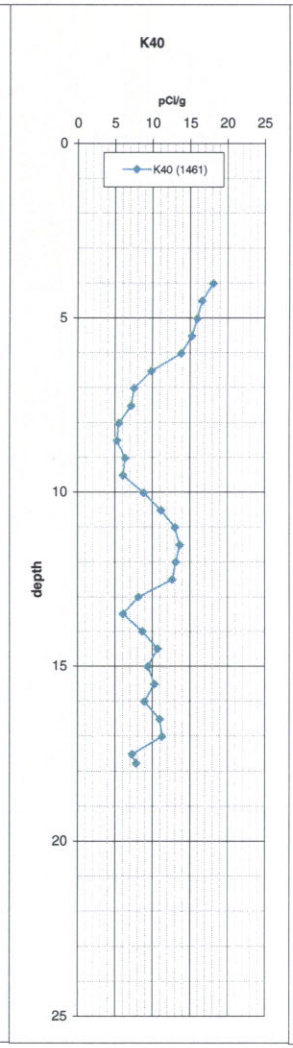

P5-UEU-2

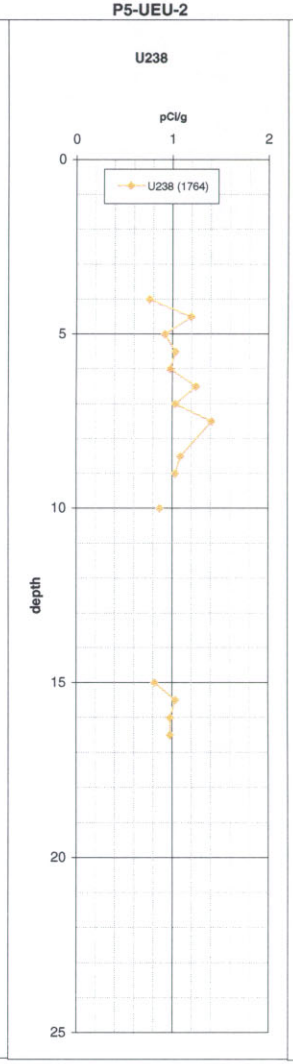

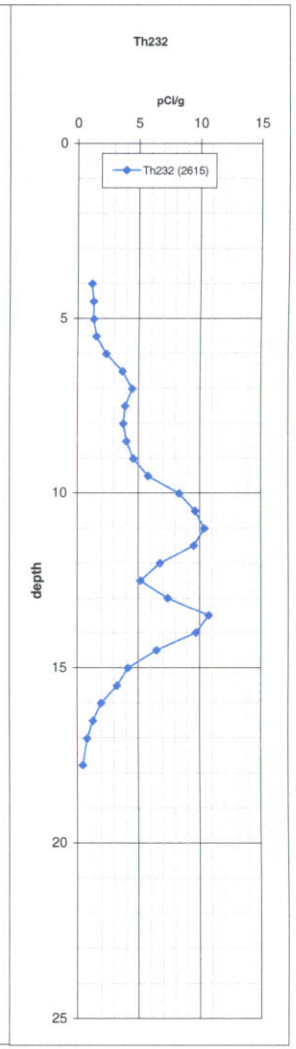

P5-UEU-2

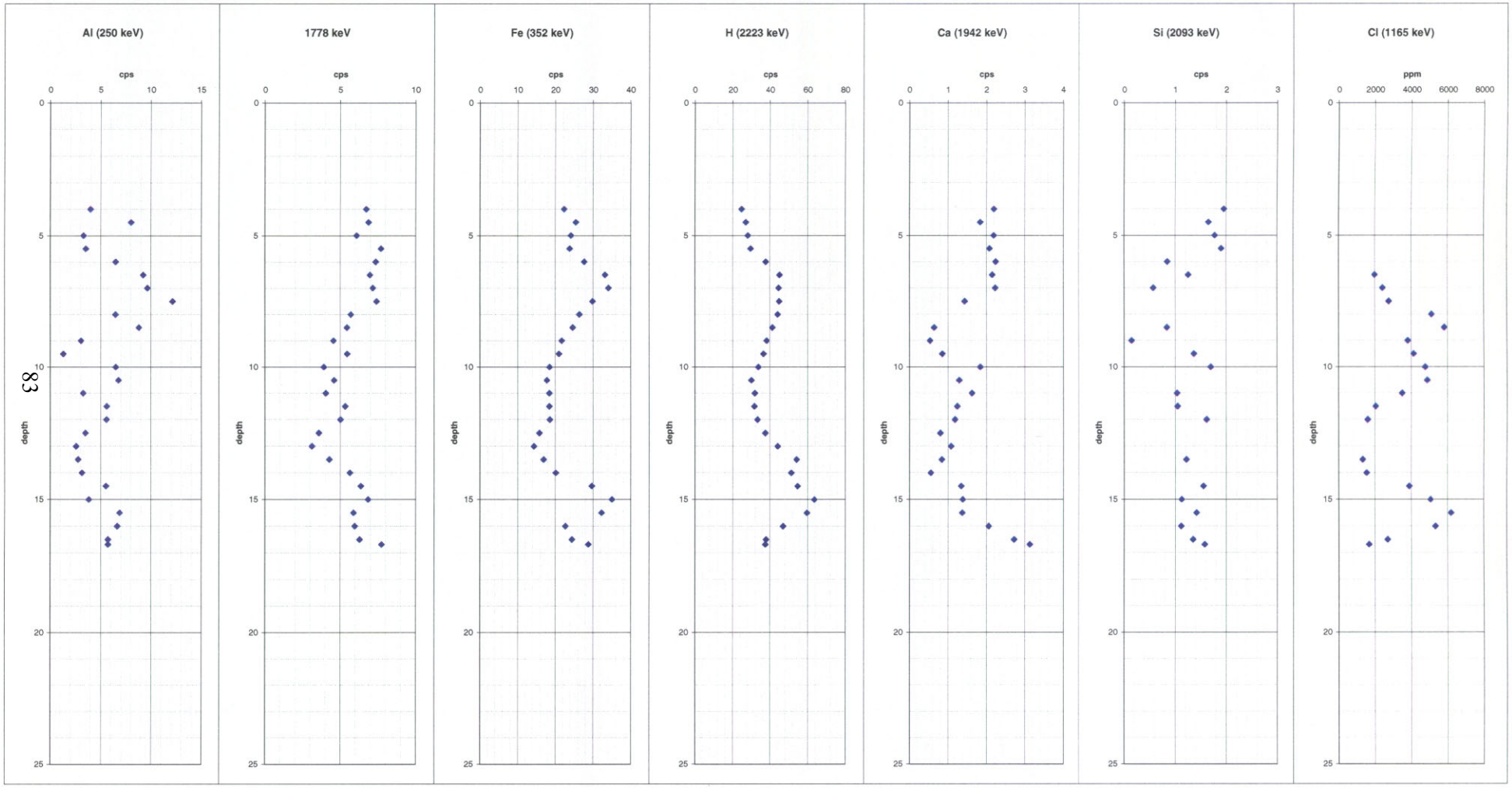
Al (250 keV)
1778 keV
Fe (352 keV)
H (2223 keV)
Ca (1942 keV)
Si (2093 keV)
Cl (1165 keV)
cps
ppm
depth

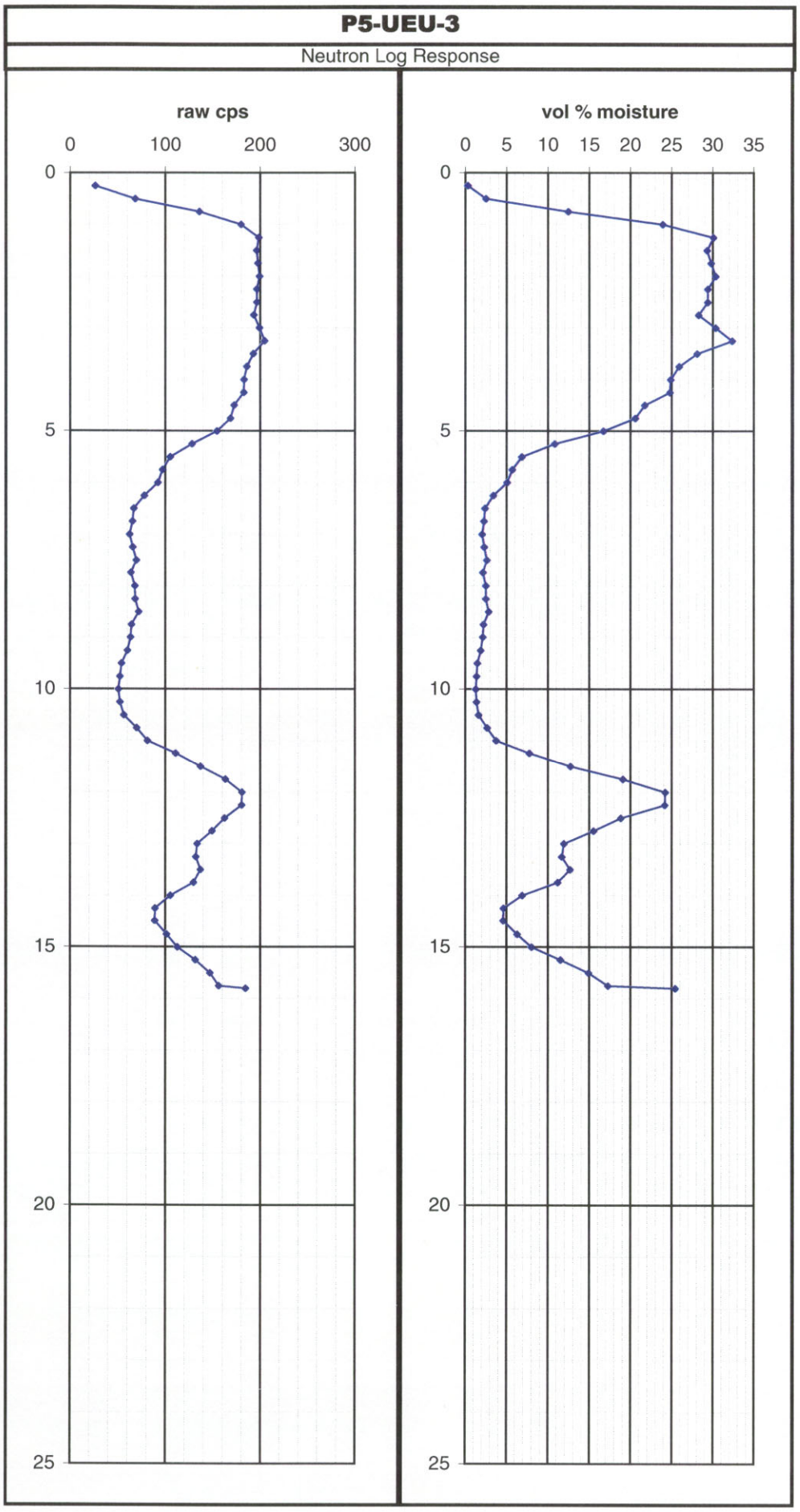
P5-UEU-3
Neutron Log Response
raw cps
0
100
200
300
vol % moisture
0
5
10
15
20
25
30
35
0
5
10
15
20
25

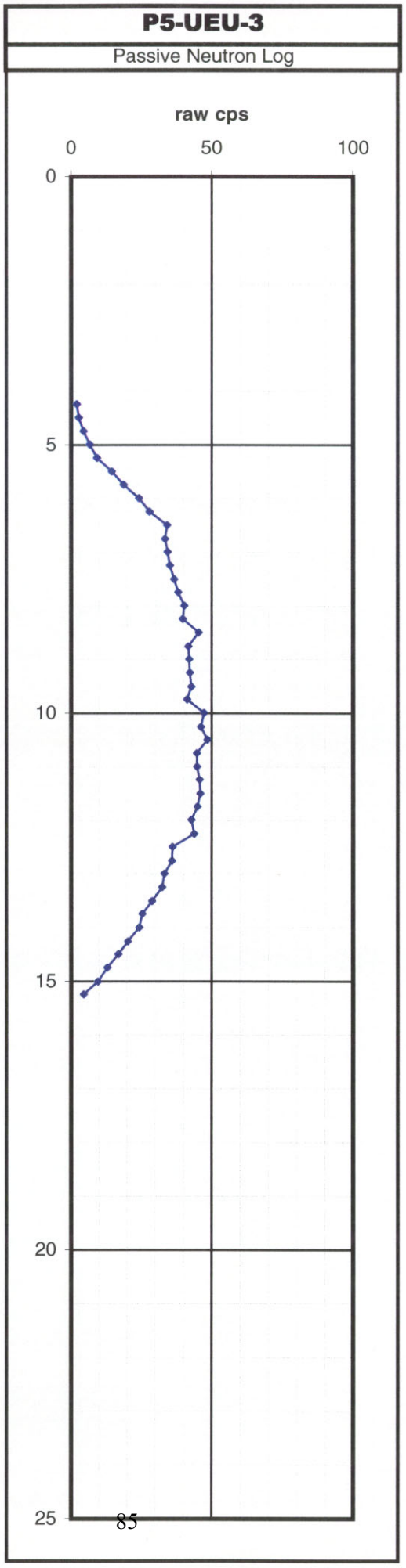
P5-UEU-3
Passive Neutron Log
raw cps
0
50
100
0
5
10
15
20
25

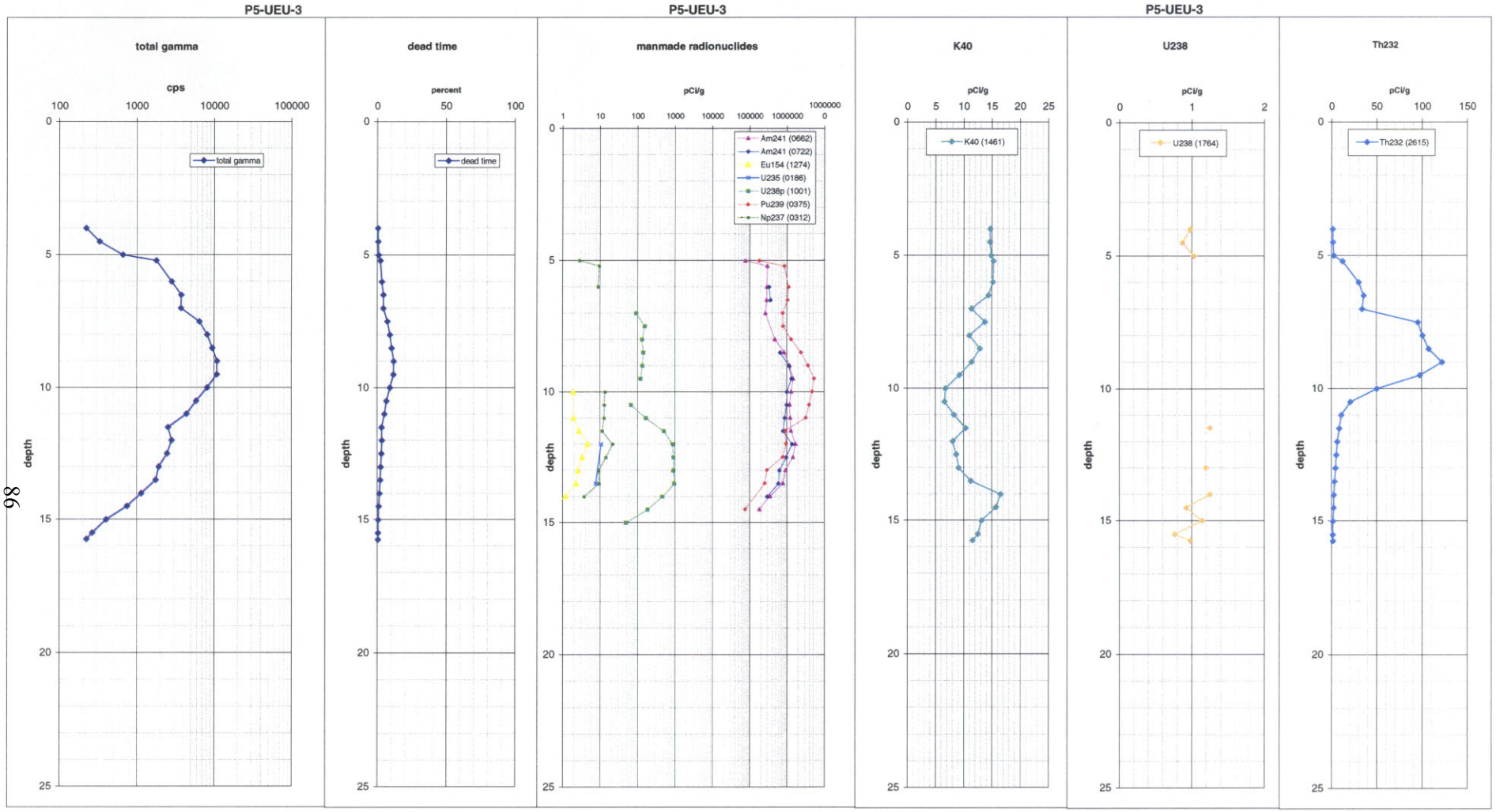
P5-UEU-3
total gamma
cps
100
1000
10000
100000
total gamma
depth
0
5
10
15
20
25
P5-UEU-3
dead time
percent
0
50
100
dead time
depth
P5-UEU-3
manmade radionuclides
pCi/g
1
10
100
1000
10000
100000
1000000
Am241 (0662)
Am241 (0722)
Eu154 (1274)
U235 (0186)
U238p (1001)
Pu239 (0375)
Np237 (0312)
depth
K40
pCi/g
0
5
10
15
20
25
K40 (1461)
depth
U238
pCi/g
0
1
2
U238 (1764)
depth
Th232
pCi/g
0
50
100
150
Th232 (2615)
depth

P5-UEU-3

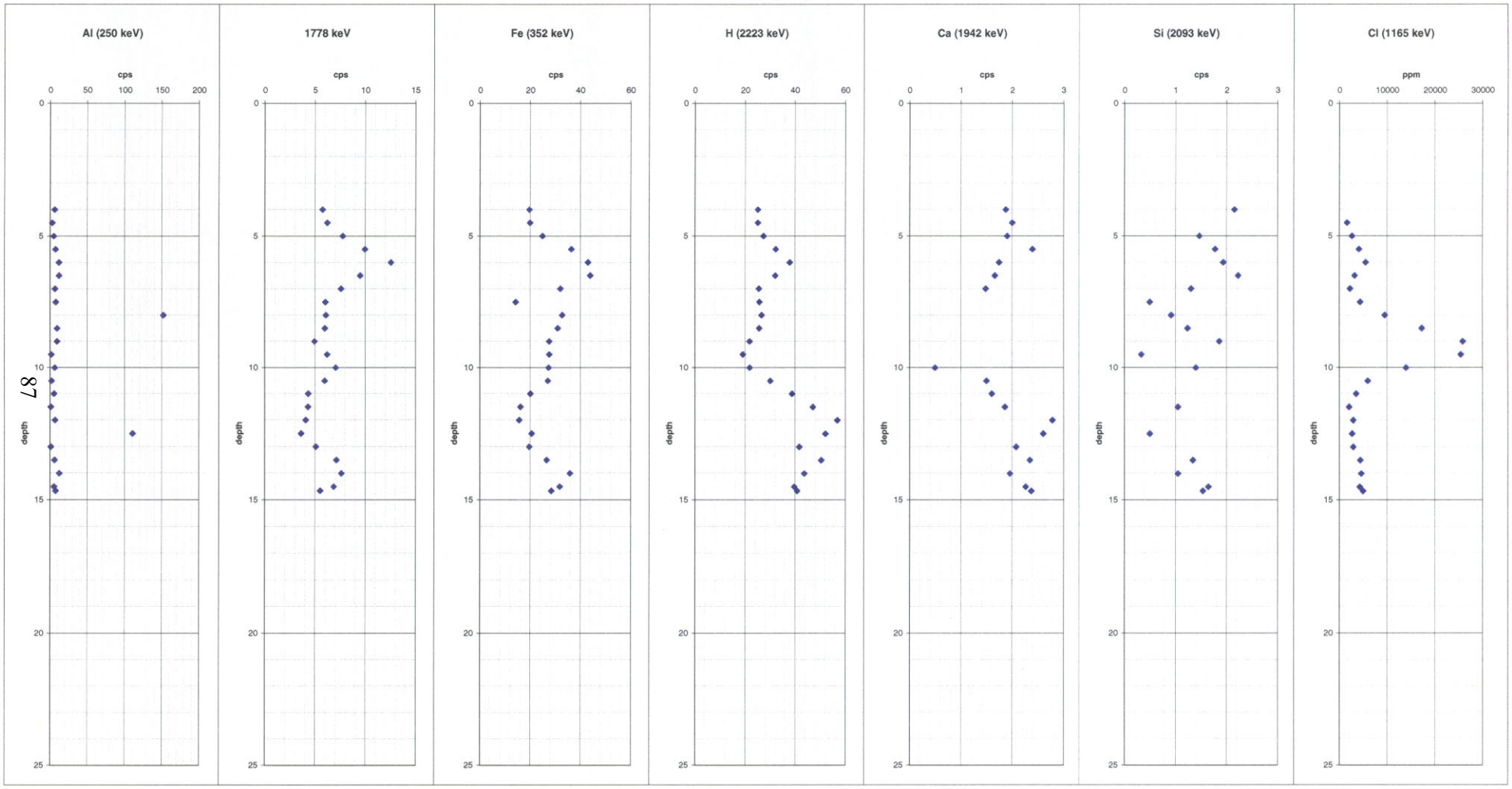
Al (250 keV)
1778 keV
Fe (352 keV)
H (2223 keV)
Ca (1942 keV)
Si (2093 keV)
Cl (1165 keV)
cps
ppm
depth
0
5
10
15
20
25
0 50 100 150 200
0 5 10 15
0 20 40 60
0 20 40 60
0 1 2 3
0 1 2 3
0 10000 20000 30000

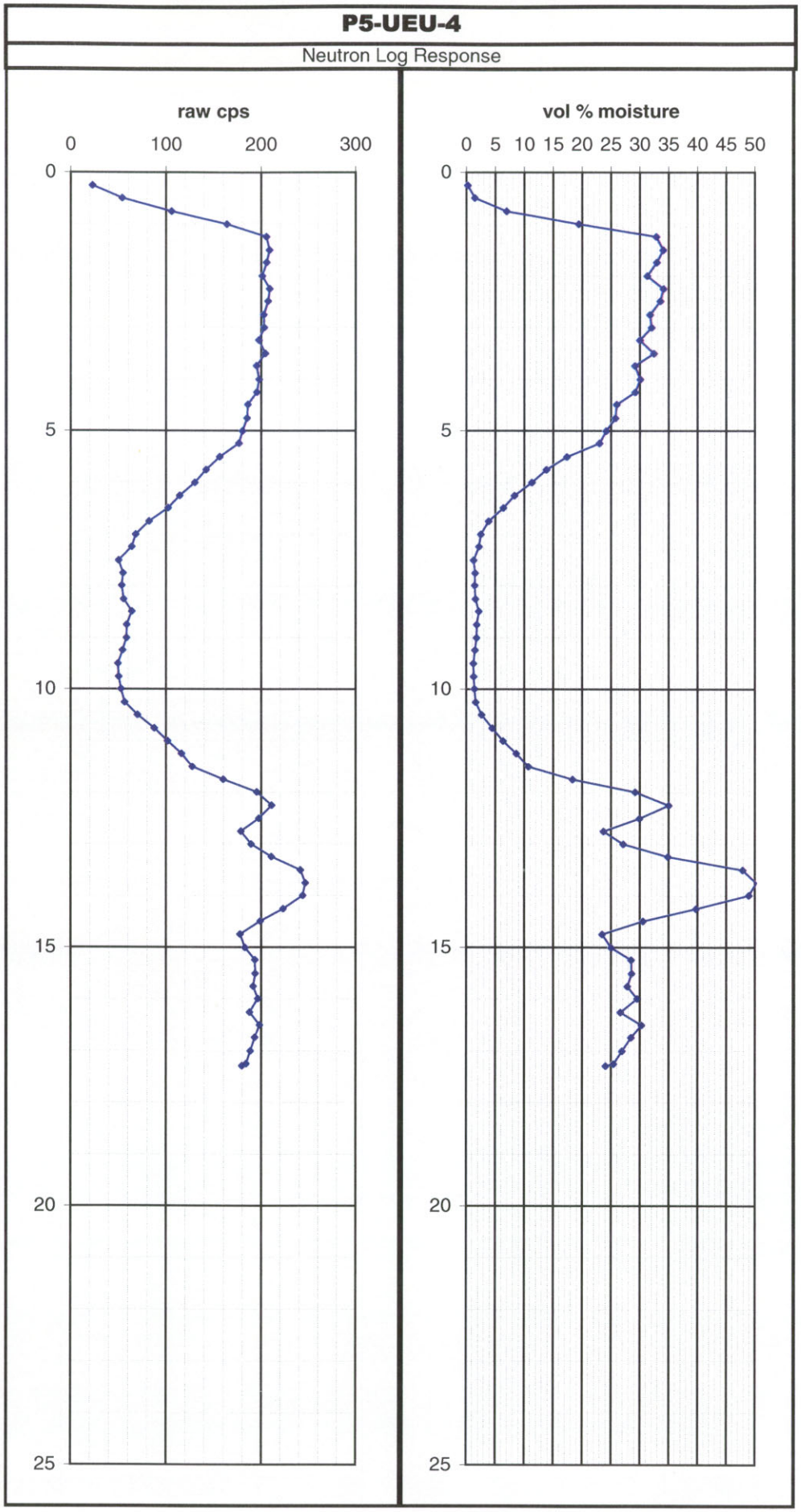
P5-UEU-4
Neutron Log Response
raw cps
0
100
200
300
vol % moisture
0 5 10 15 20 25 30 35 40 45 50
0
5
10
15
20
25

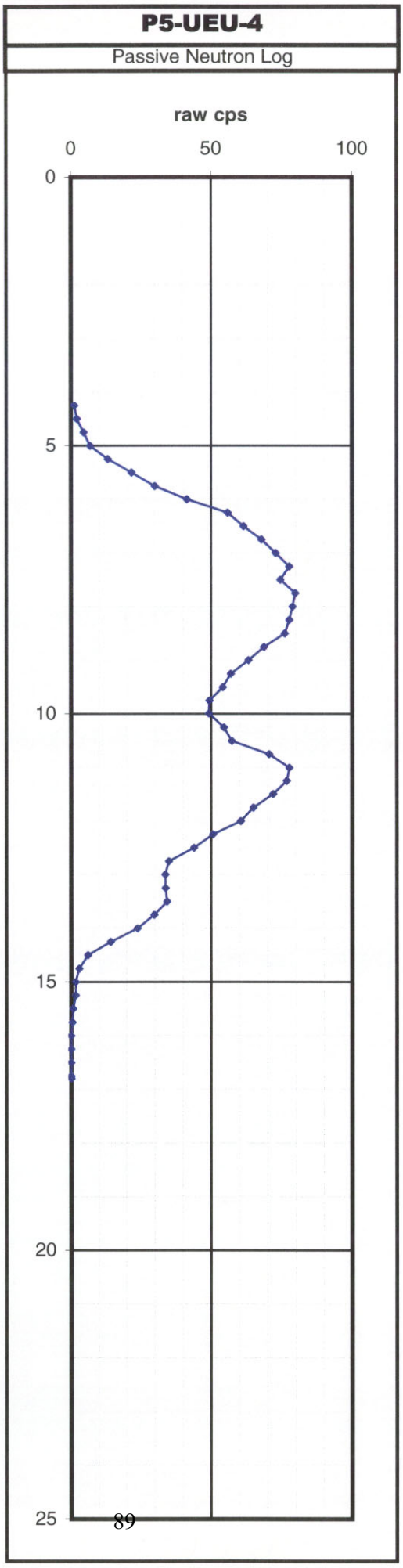
P5-UEU-4
Passive Neutron Log
raw cps
0
50
100
0
5
10
15
20
25

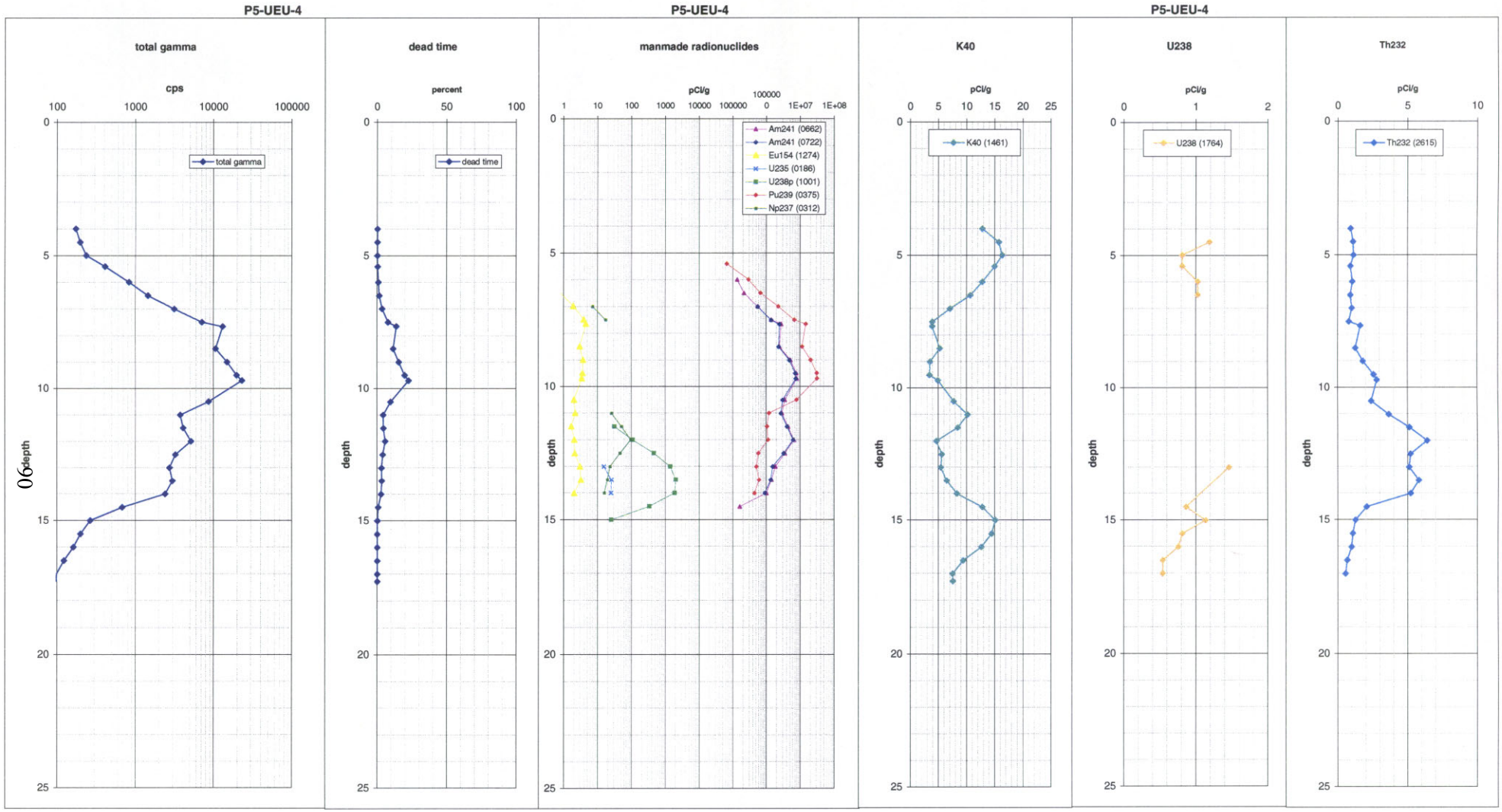
P5-UEU-4
total gamma
cps
total gamma
depth
dead time
percent
dead time
P5-UEU-4
manmade radionuclides
pCi/g
Am241 (0662)
Am241 (0722)
Eu154 (1274)
U235 (0186)
U238p (1001)
Pu239 (0375)
Np237 (0312)
P5-UEU-4
K40
pCi/g
K40 (1461)
U238
pCi/g
U238 (1764)
Th232
pCi/g
Th232 (2615)

P5-UEU-4

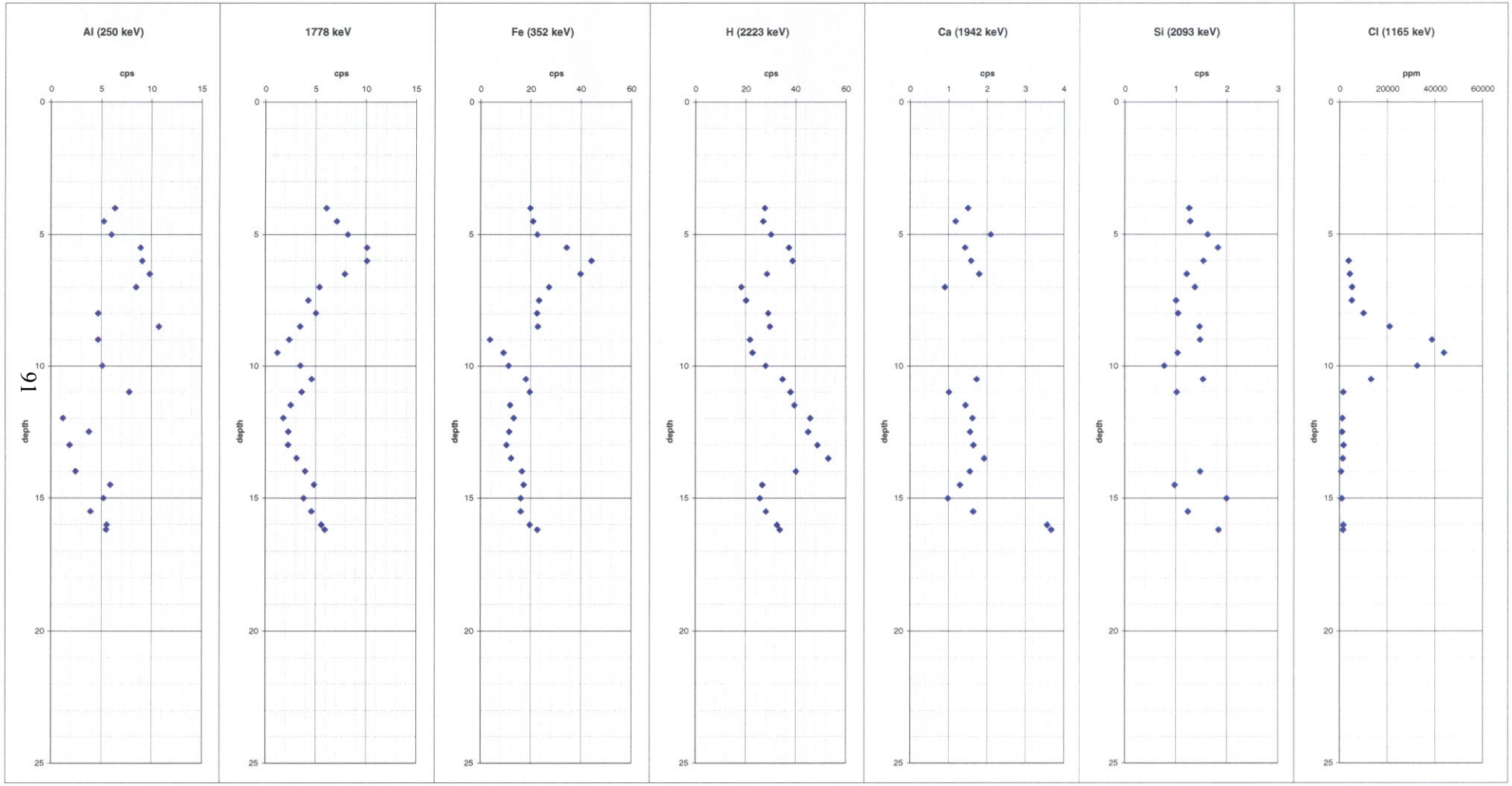
Al (250 keV)
1778 keV
Fe (352 keV)
H (2223 keV)
Ca (1942 keV)
Si (2093 keV)
Cl (1165 keV)
cps
ppm
depth

P5-UEU-4 Total Gamma (9.0 ft to 14.0 ft)

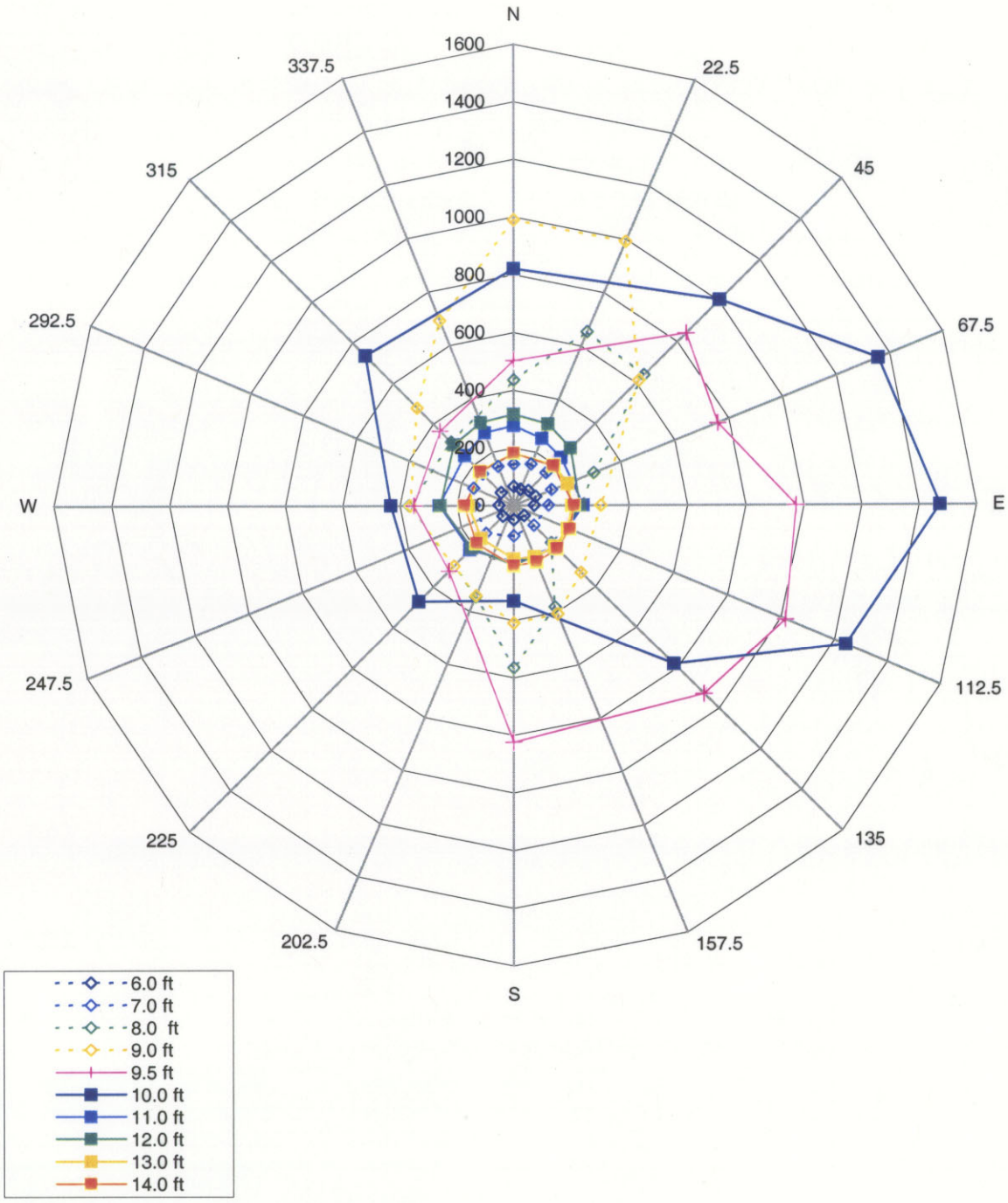

P5-UEU-4 Am-241 (662 keV - 9.0ft to 14.0 ft)

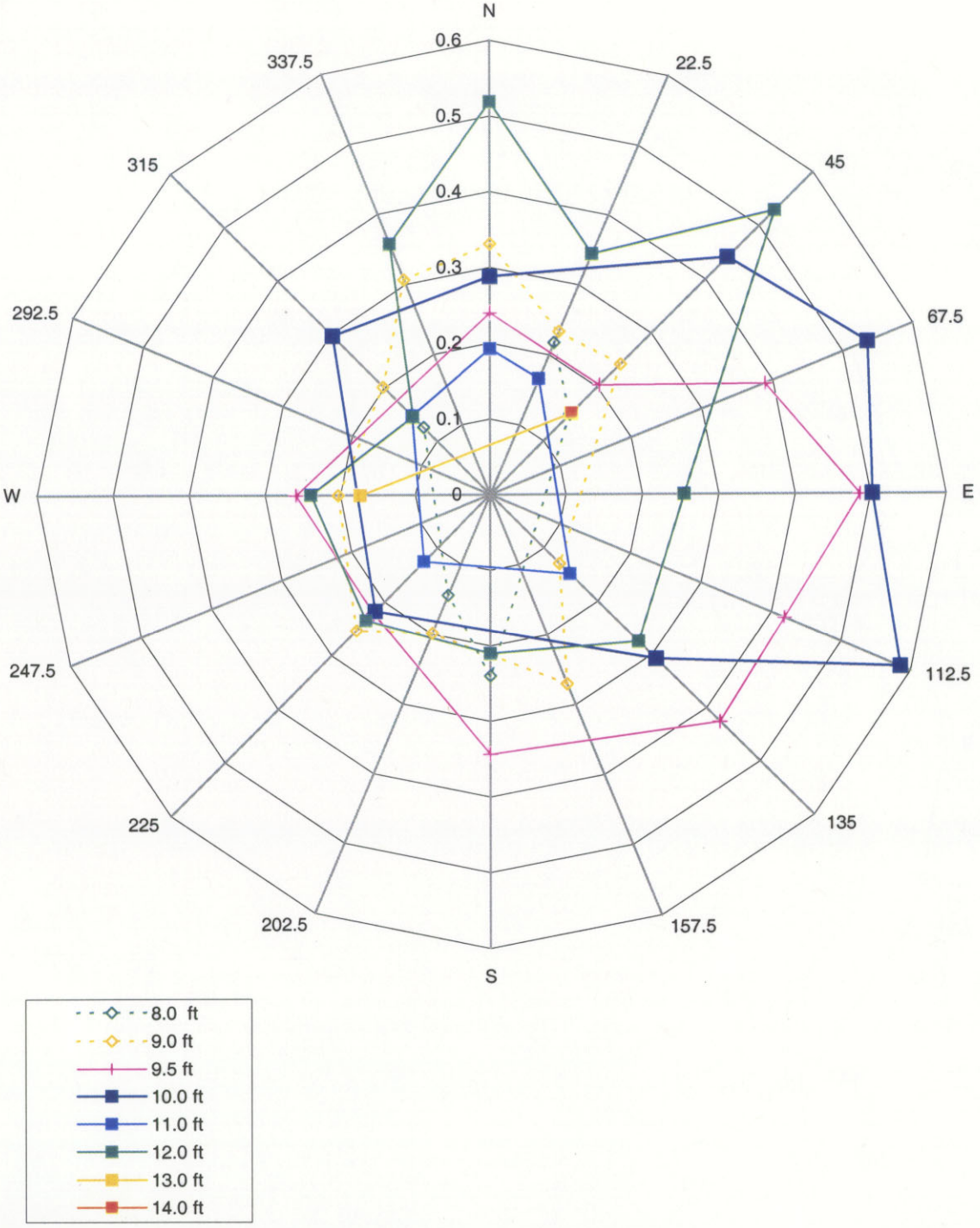

P5-UEU-4 Pu-239 (375 keV - 9.0 ft to 14.0 ft)

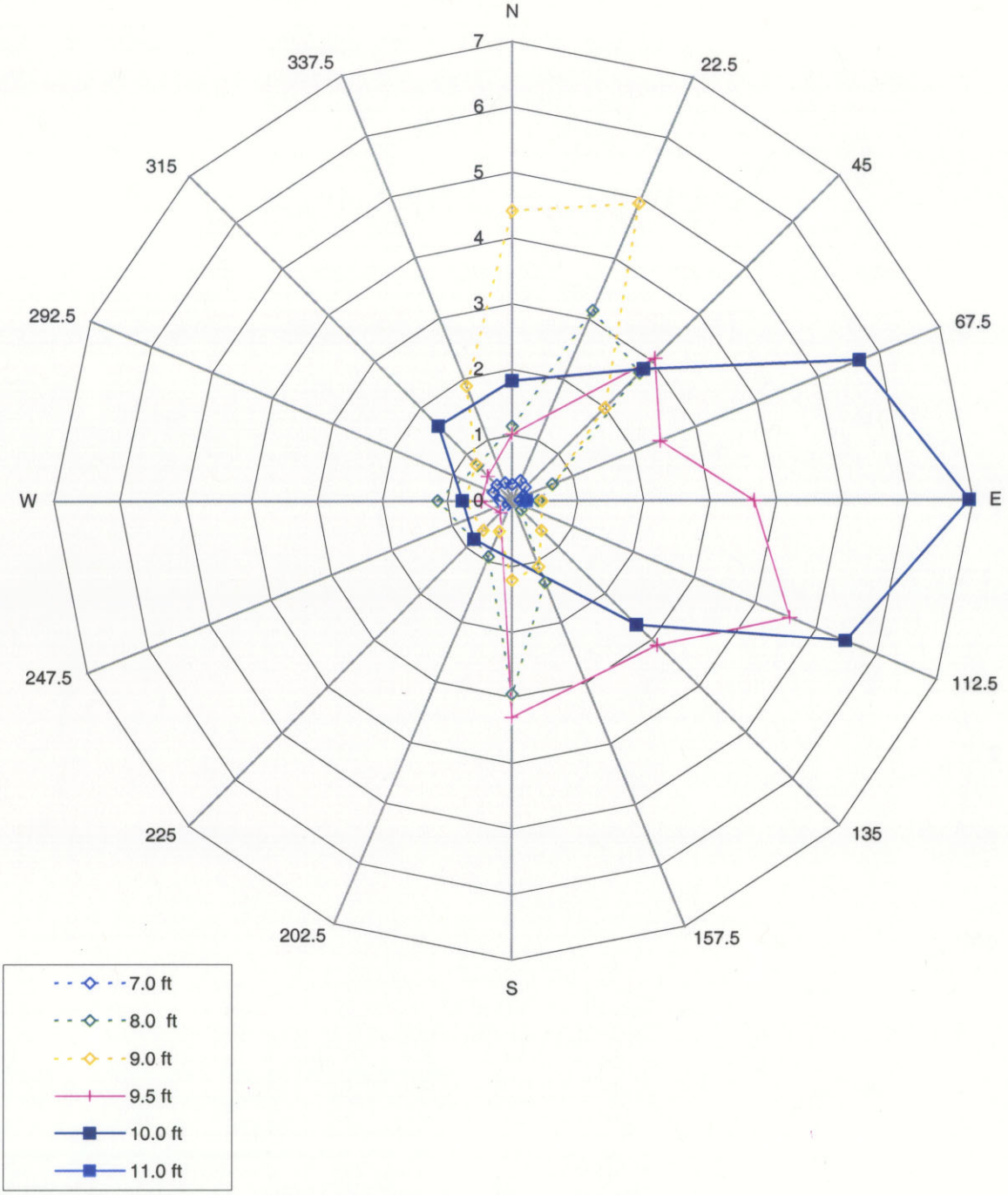

P5-UEU-4 U-238 (1001 keV - 9.0 ft to 14.0 ft)

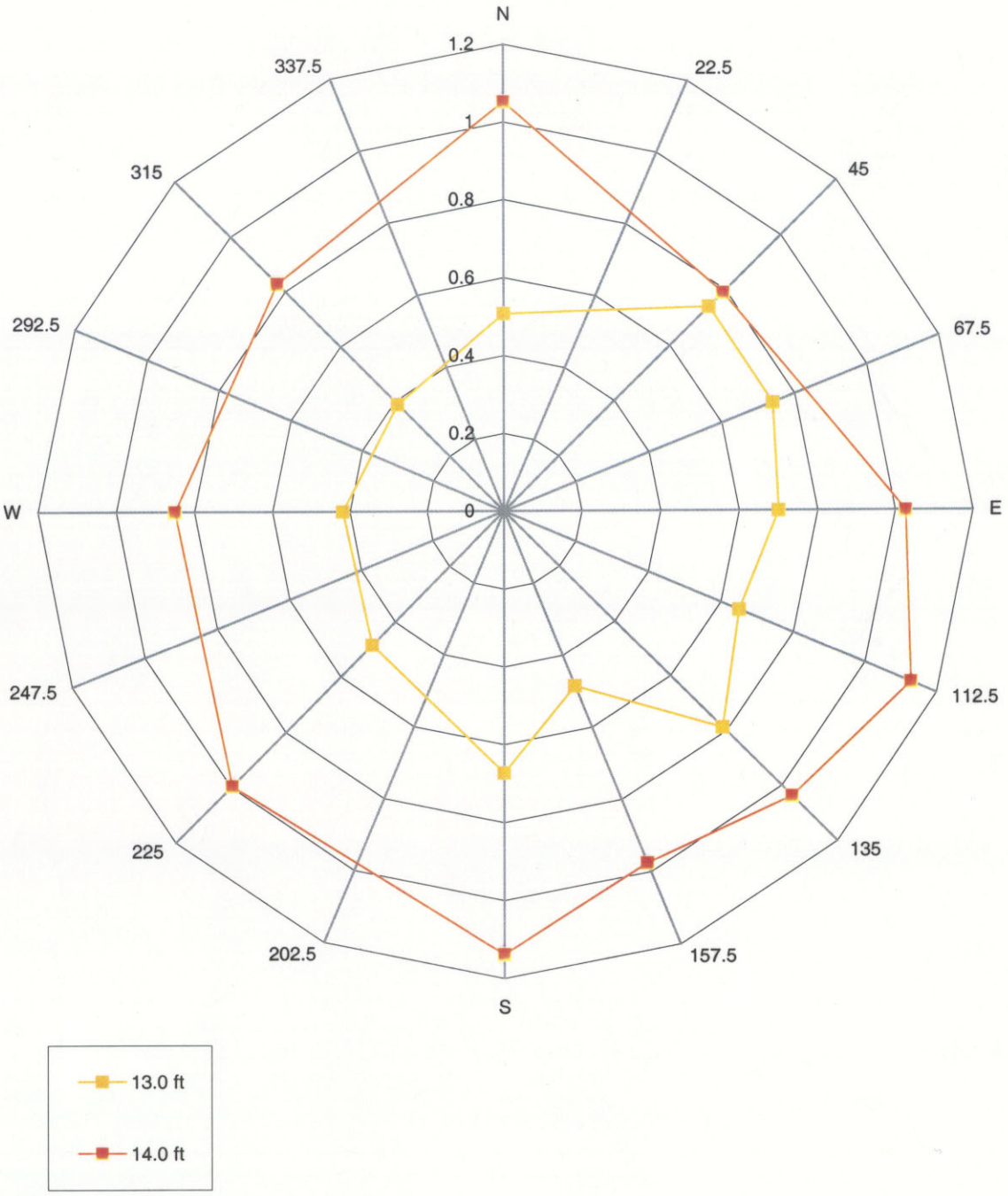

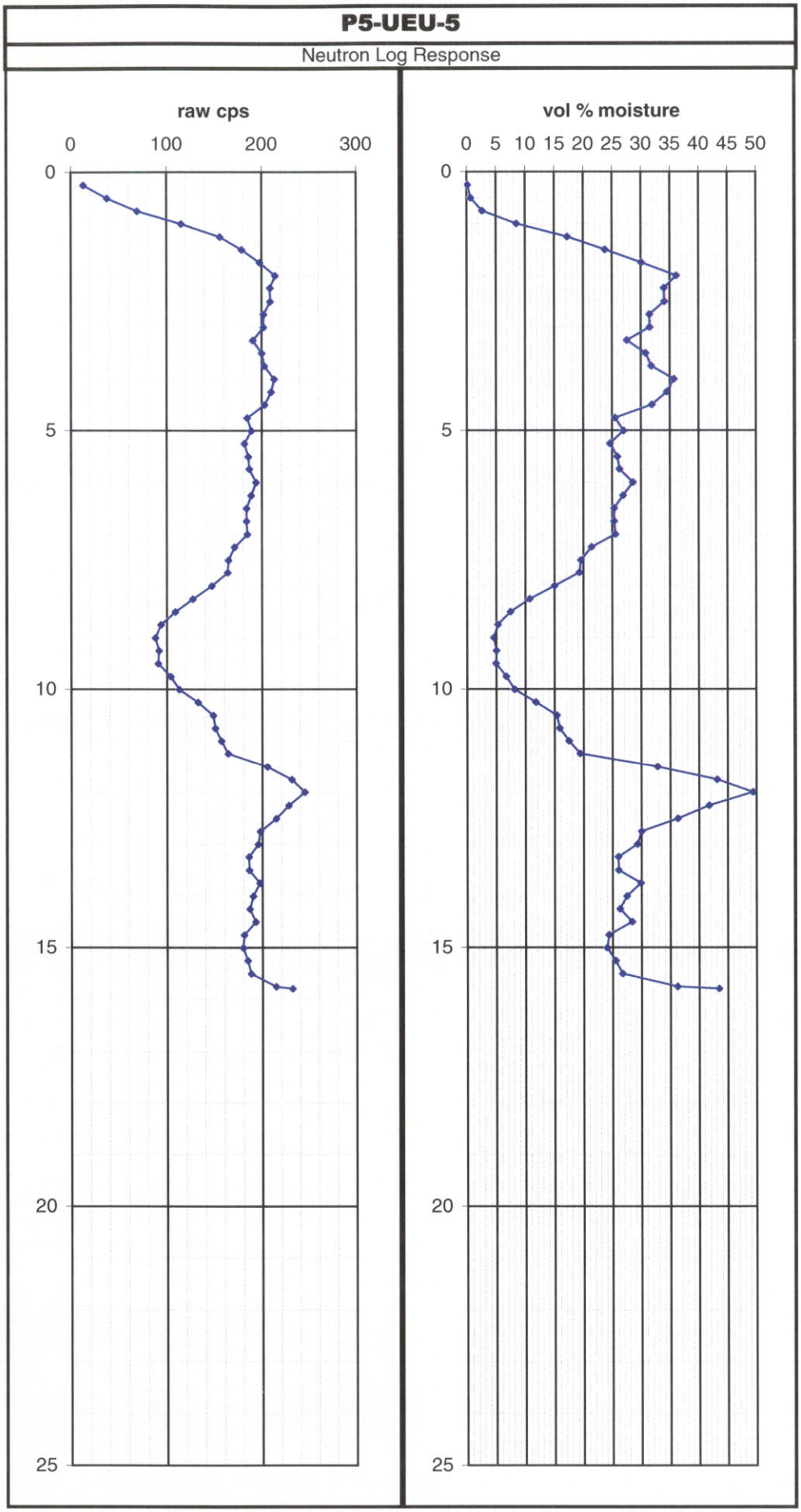
P5-UEU-5
Neutron Log Response
raw cps
0
100
200
300
vol % moisture
0 5 10 15 20 25 30 35 40 45 50
0
5
10
15
20
25

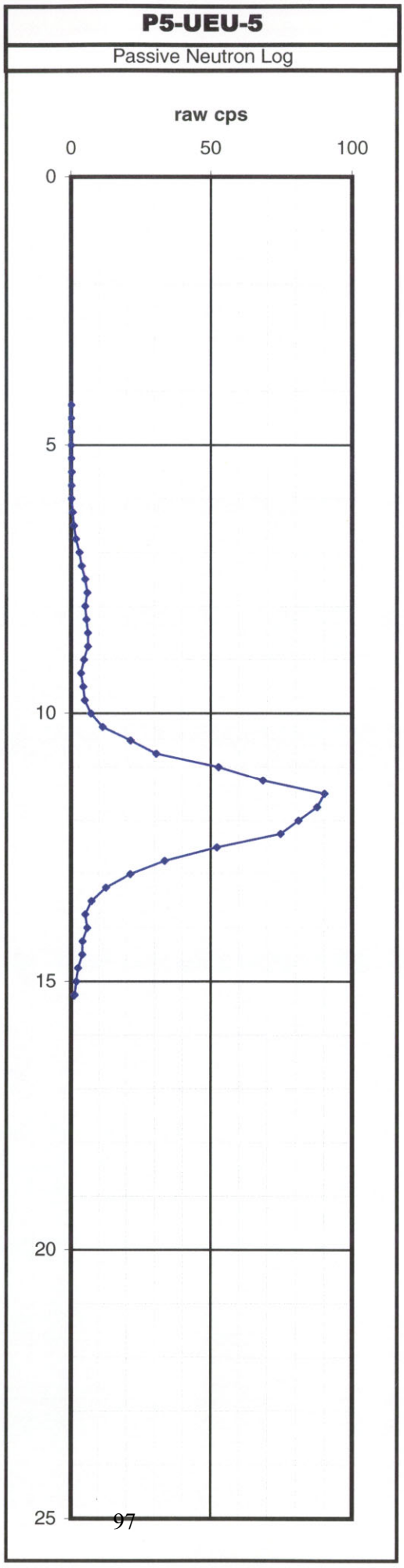
P5-UEU-5
Passive Neutron Log
raw cps
0
50
100
0
5
10
15
20
25

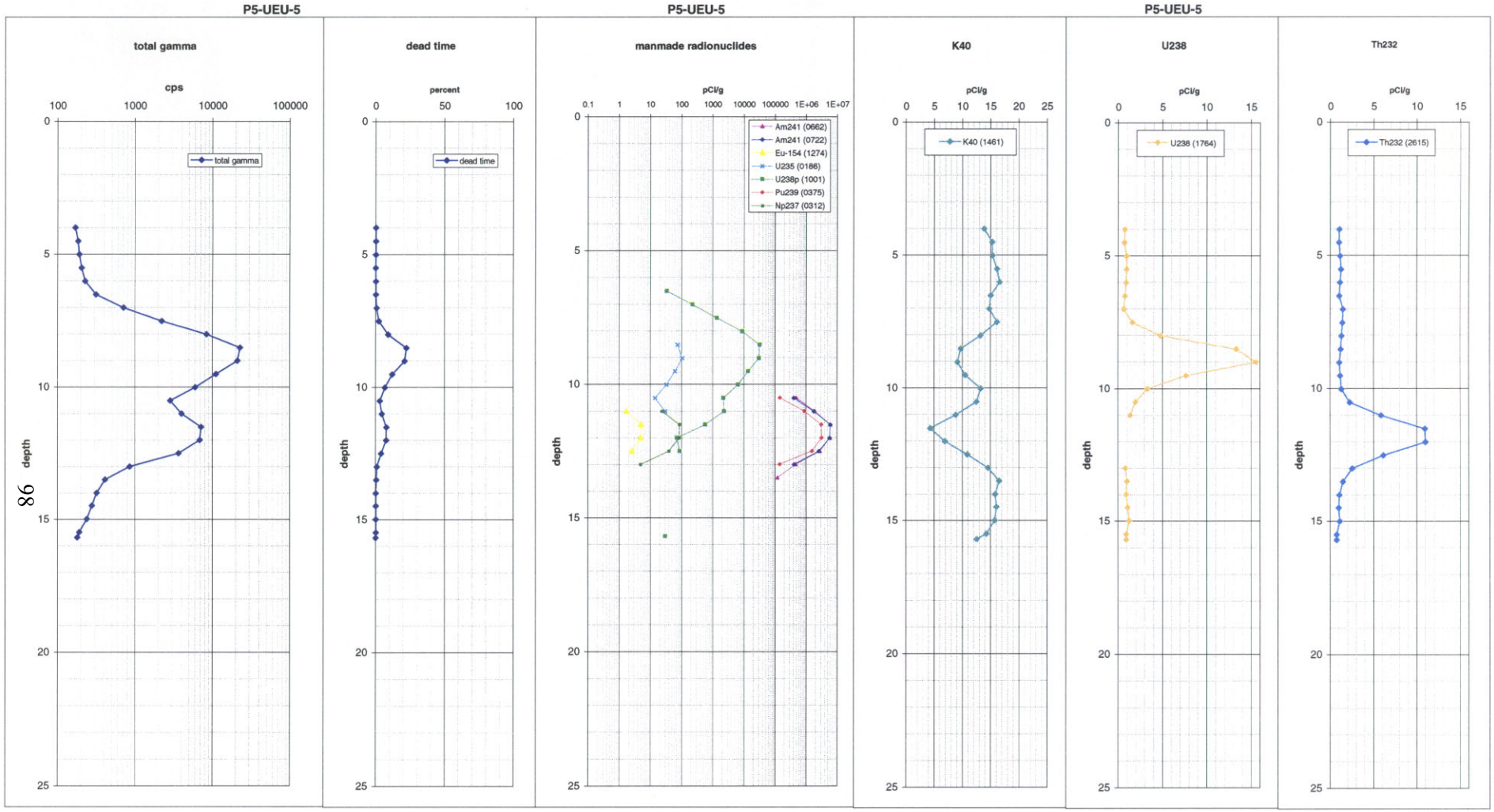
P5-UEU-5
total gamma
cps
100
1000
10000
100000
total gamma
depth
0
5
10
15
20
25
P5-UEU-5
dead time
percent
0
50
100
dead time
depth
P5-UEU-5
manmade radionuclides
pCi/g
0.1
1
10
100
1000
10000
100000
1E+06
1E+07
Am241 (0662)
Am241 (0722)
Eu-154 (1274)
U235 (0186)
U238p (1001)
Pu239 (0375)
Np237 (0312)
depth
K40
pCi/g
0
5
10
15
20
25
K40 (1461)
depth
U238
pCi/g
U238 (1764)
depth
Th232
pCi/g
Th232 (2615)
depth

P5-UEU-5

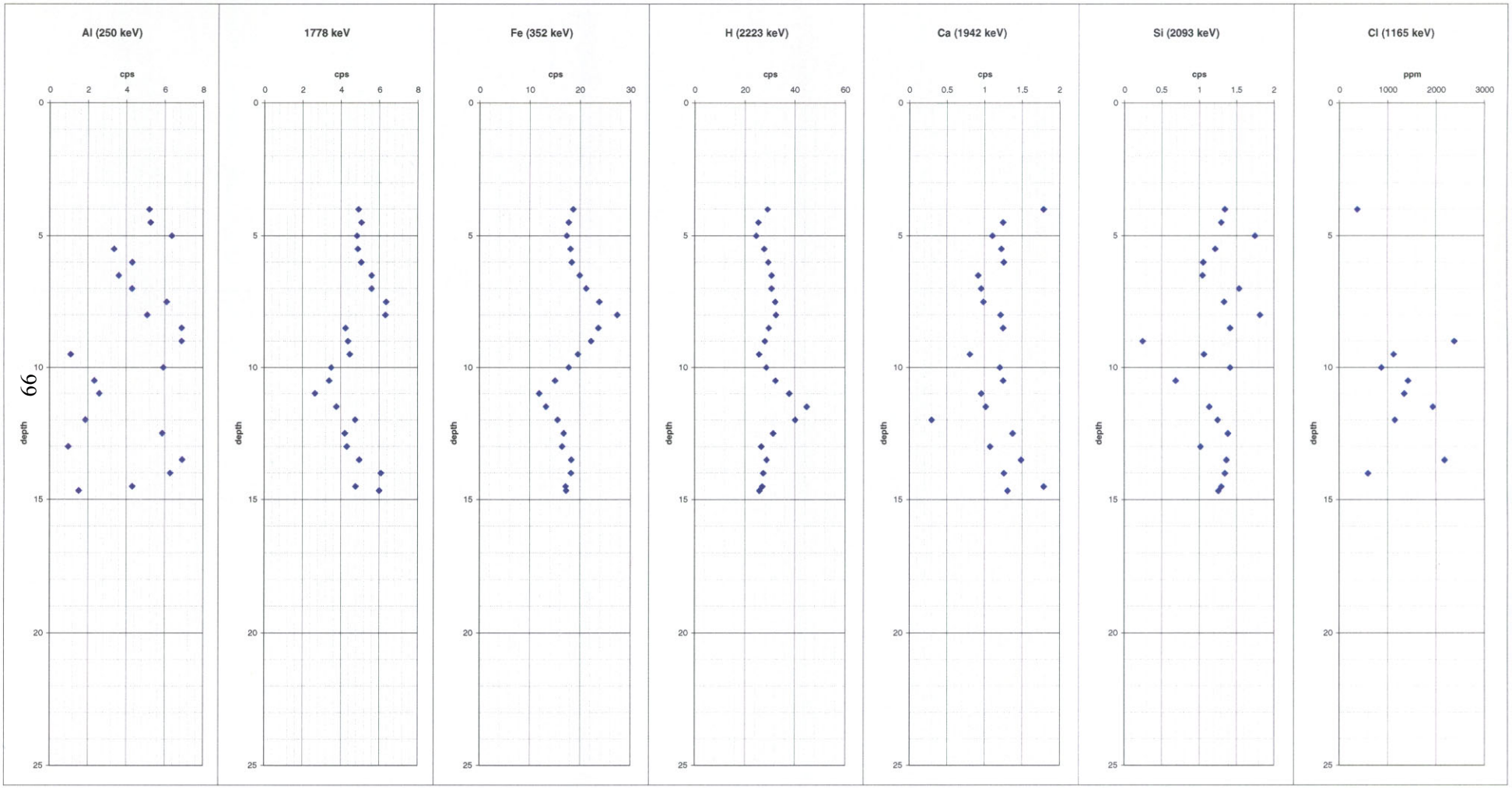
Al (250 keV)
1778 keV
Fe (352 keV)
H (2223 keV)
Ca (1942 keV)
Si (2093 keV)
Cl (1165 keV)
cps
ppm
depth

P5-UEU-5 Total Gamma (11.0 ft to 13.0 ft)

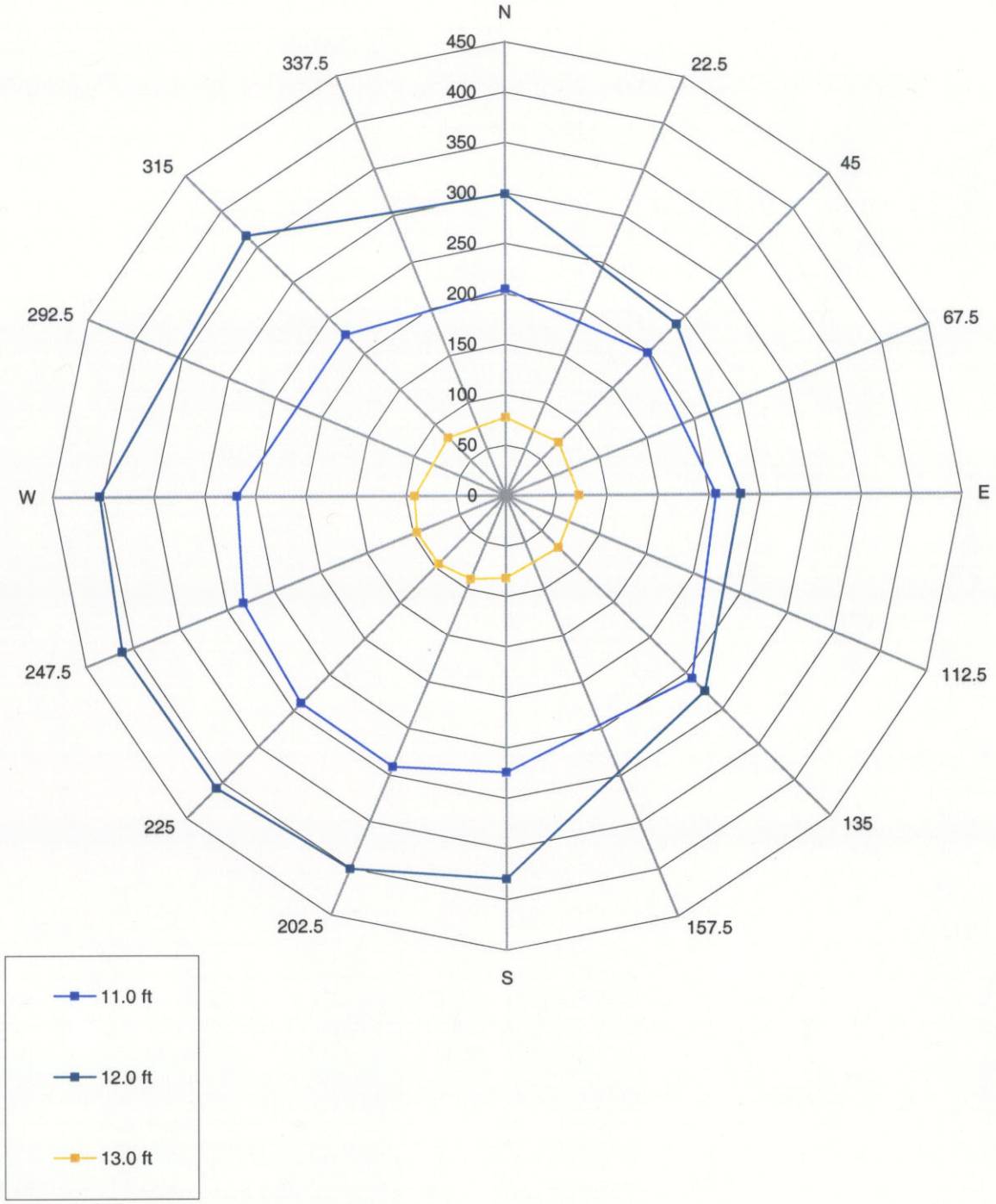

P5-UEU-5 Pu-239 (375 keV - 11.0 ft to 12.0 ft)

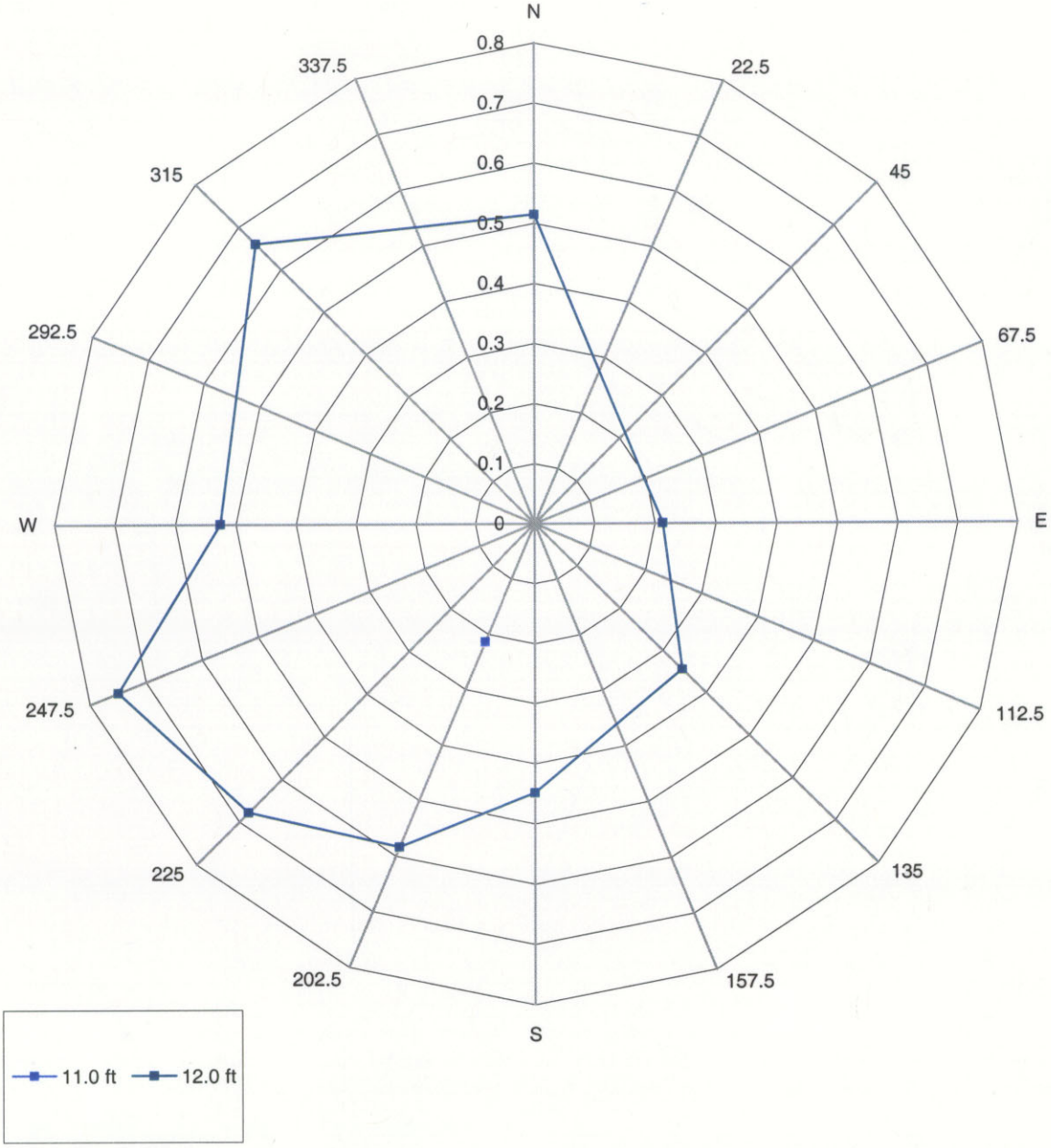

P5-UEU-5 Am-241 (662 keV - 12.0 ft)

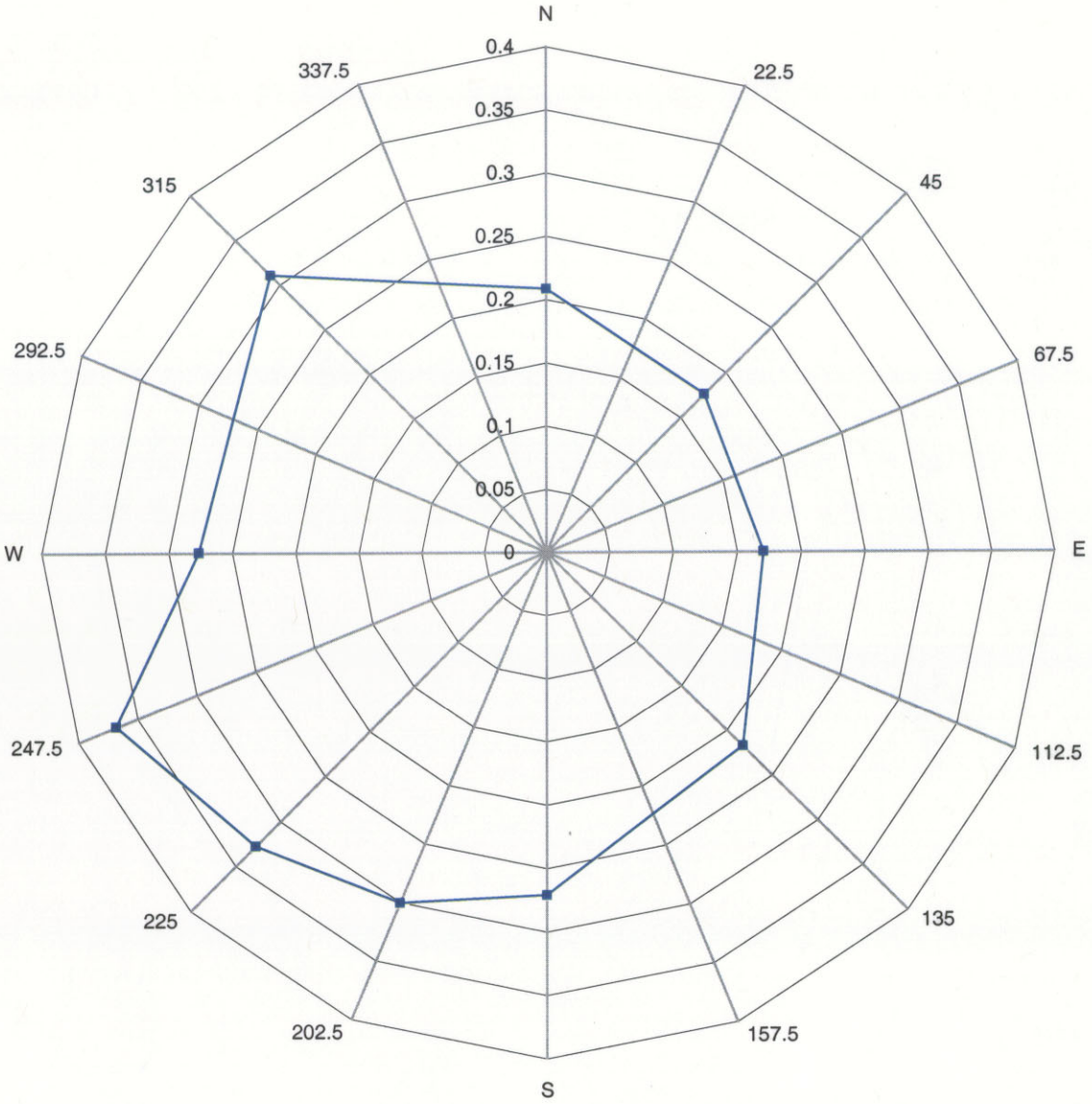

P5-UEU-5 Np-237 (312 keV - 12.0 ft)

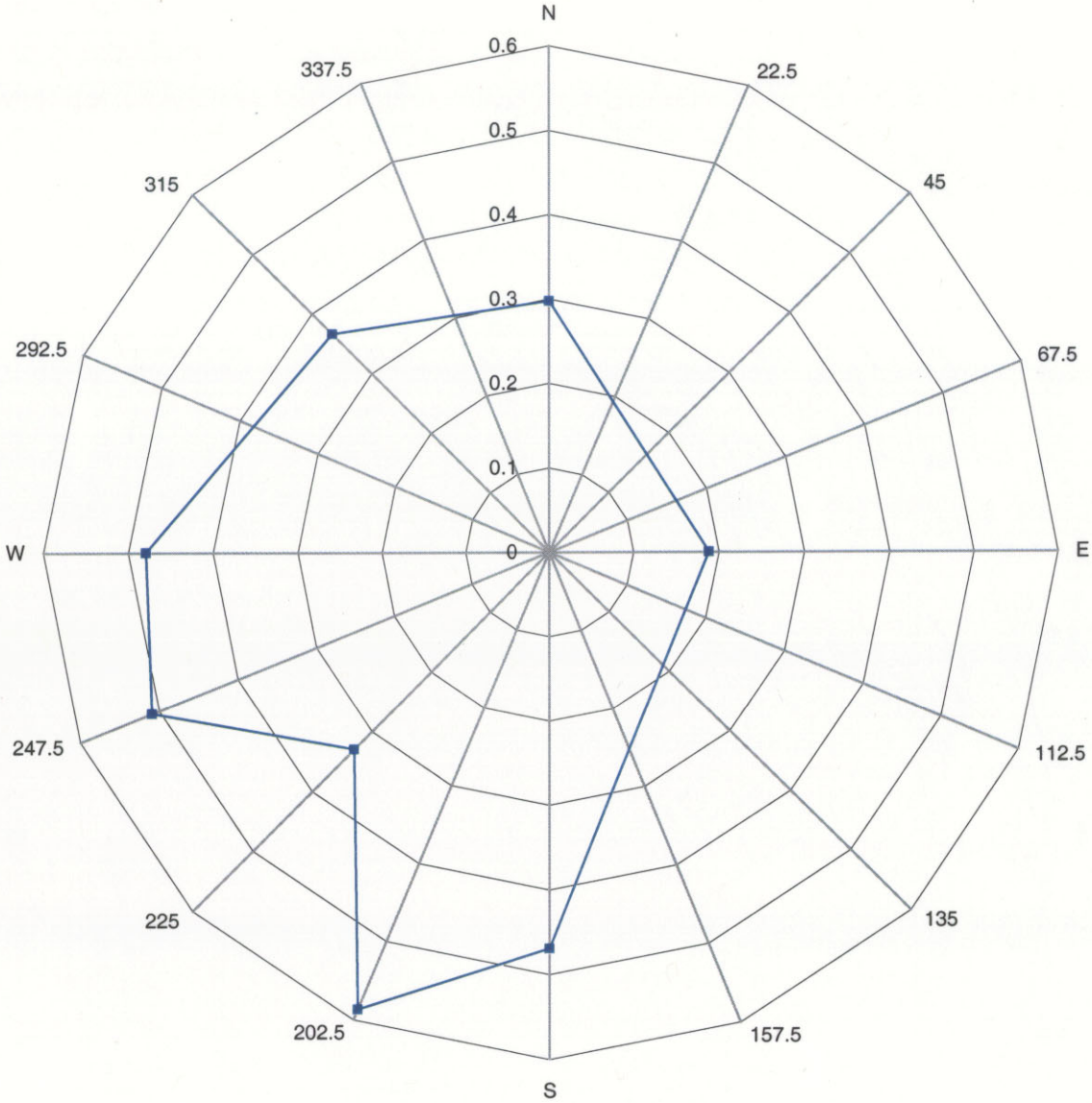

P5-UEU-5 U-238 (1001 keV - 11.0 ft to 13.0 ft)

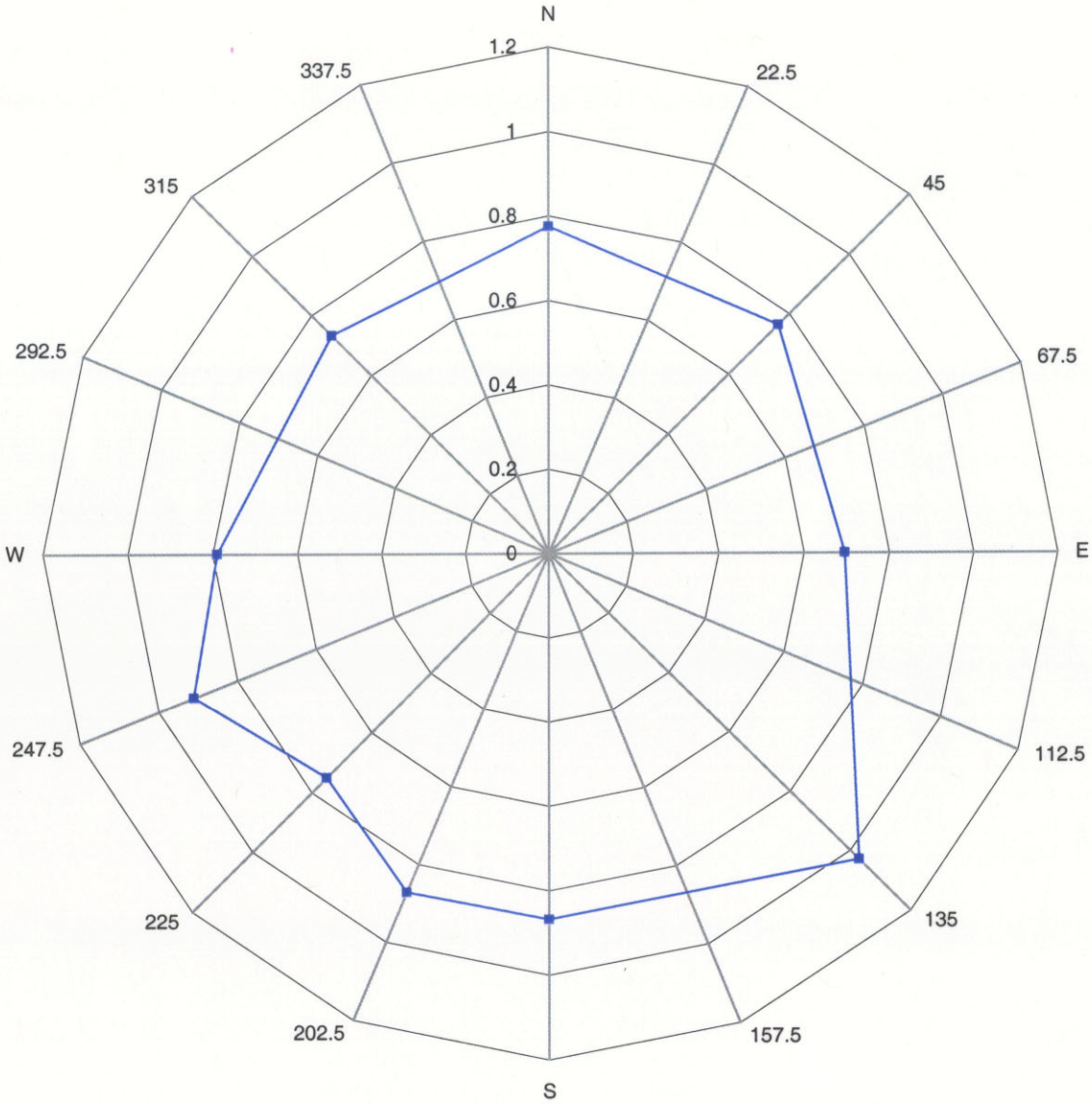

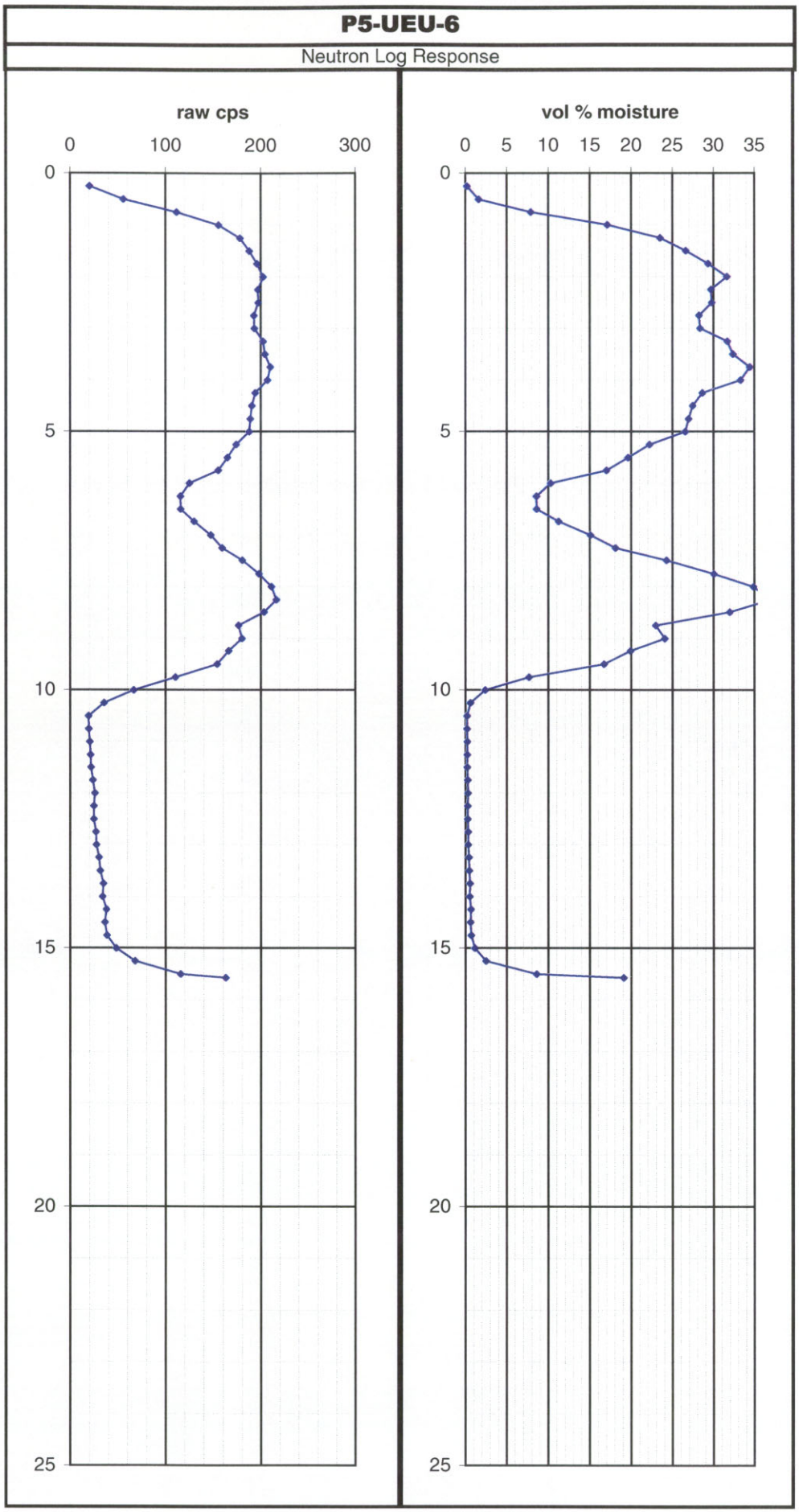
P5-UEU-6
Neutron Log Response
raw cps
0
100
200
300
vol % moisture
0
5
10
15
20
25
30
35
0
5
10
15
20
25

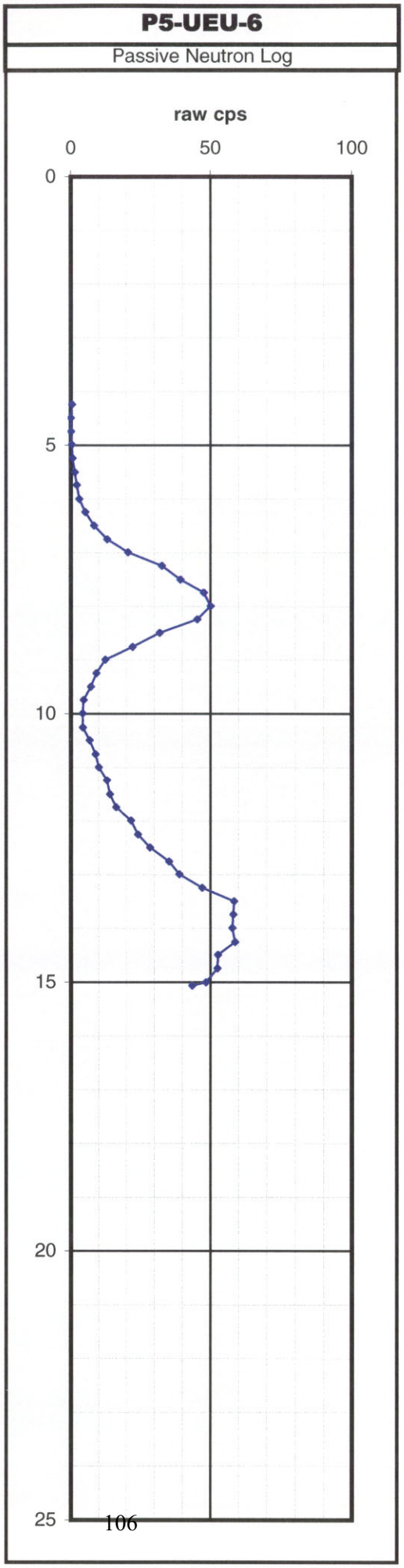
P5-UEU-6
Passive Neutron Log
raw cps
0
50
100
0
5
10
15
20
25

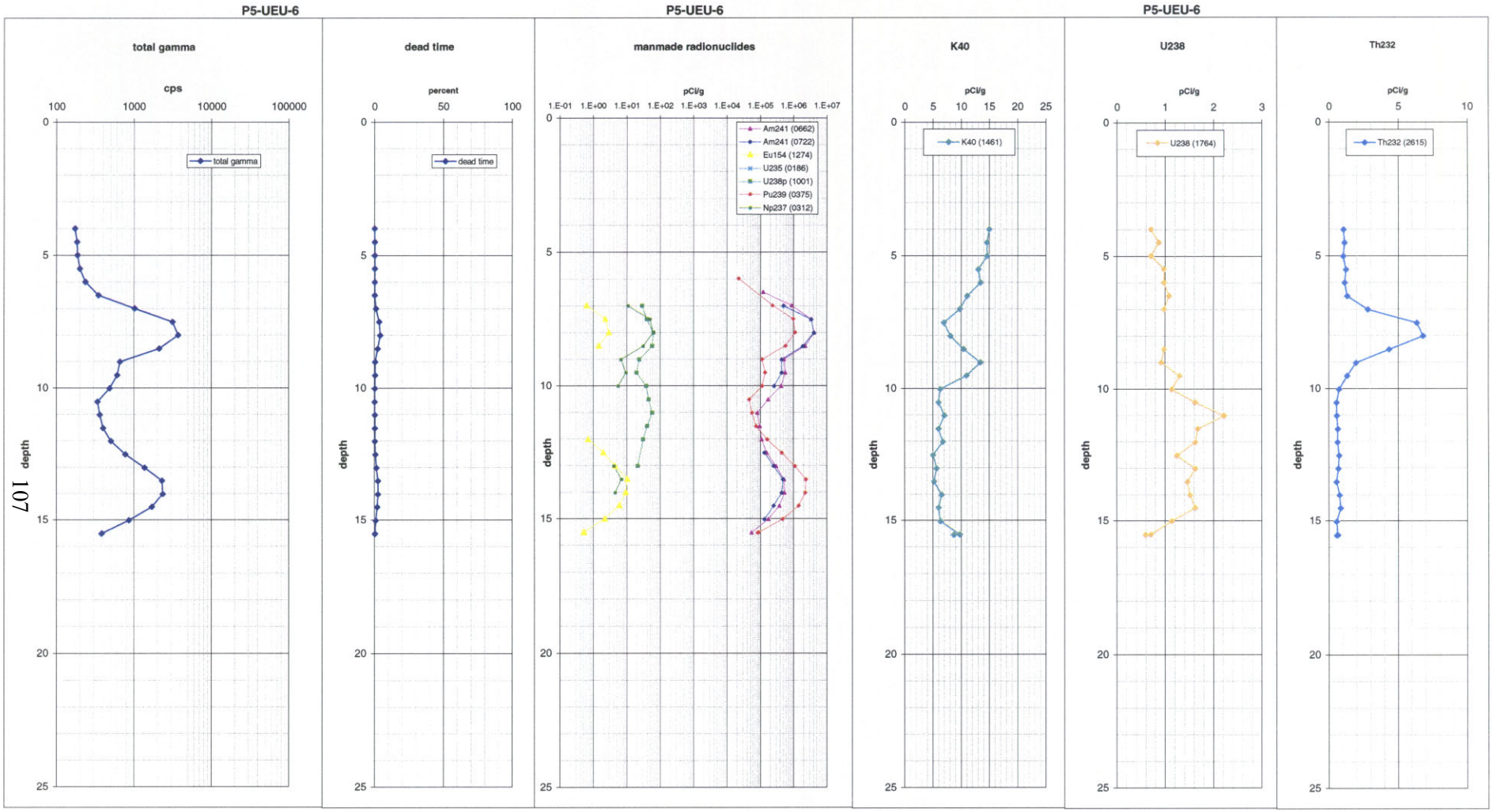
P5-UEU-6
total gamma
cps
100
1000
10000
100000
total gamma
depth
0
5
10
15
20
25
P5-UEU-6
dead time
percent
0
50
100
dead time
depth
P5-UEU-6
manmade radionuclides
pCi/g
1.E-01
1.E+00
1.E+01
1.E+02
1.E+03
1.E+04
1.E+05
1.E+06
1.E+07
Am241 (0662)
Am241 (0722)
Eu154 (1274)
U235 (0186)
U238p (1001)
Pu239 (0375)
Np237 (0312)
depth
P5-UEU-6
K40
pCi/g
0
5
10
15
20
25
K40 (1461)
depth
U238
pCi/g
0
1
2
3
U238 (1764)
depth
Th232
pCi/g
0
5
10
Th232 (2615)
depth

P5-UEU-6

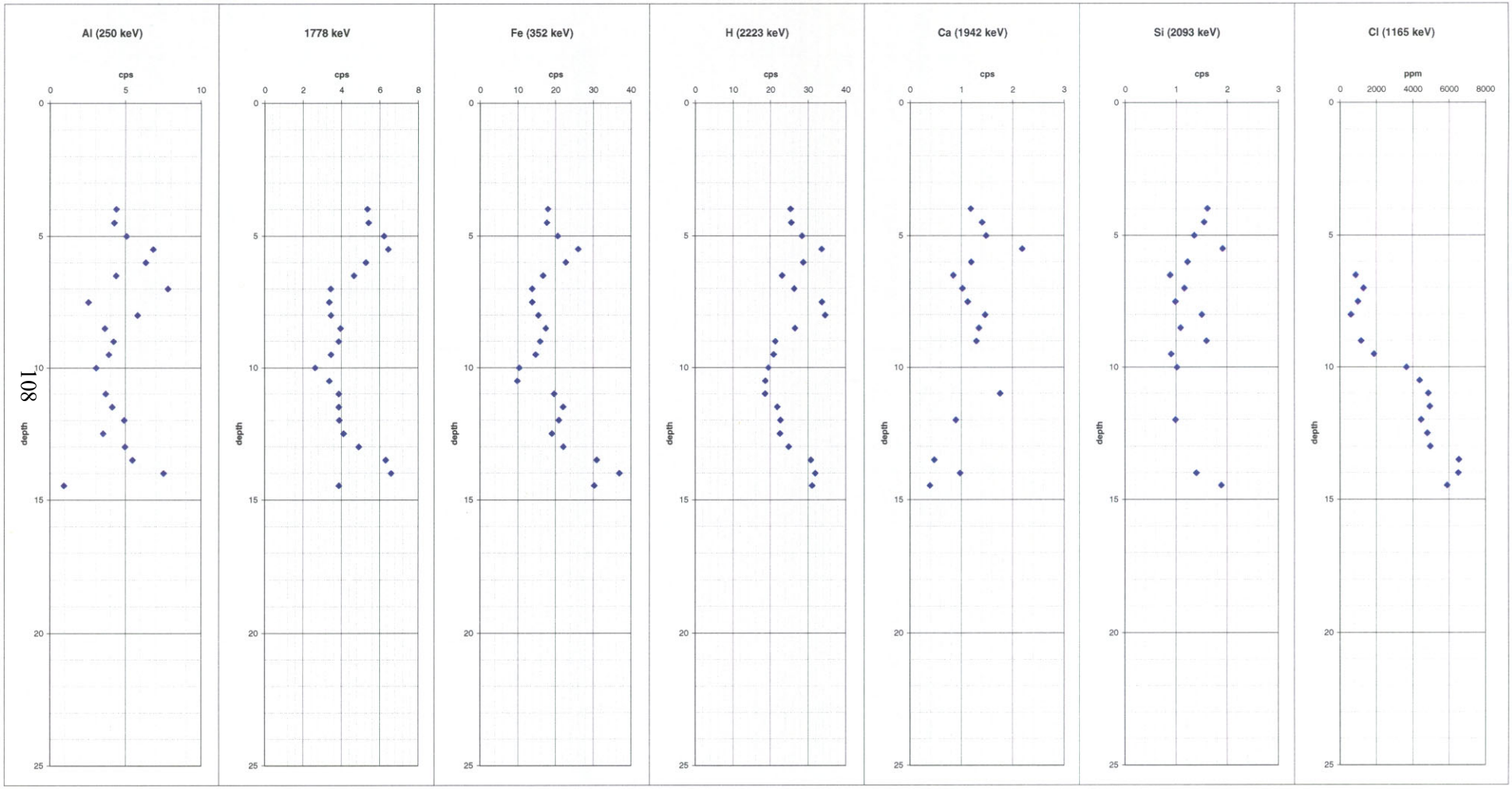
Al (250 keV)
1778 keV
Fe (352 keV)
H (2223 keV)
Ca (1942 keV)
Si (2093 keV)
Cl (1165 keV)
cps
ppm
depth

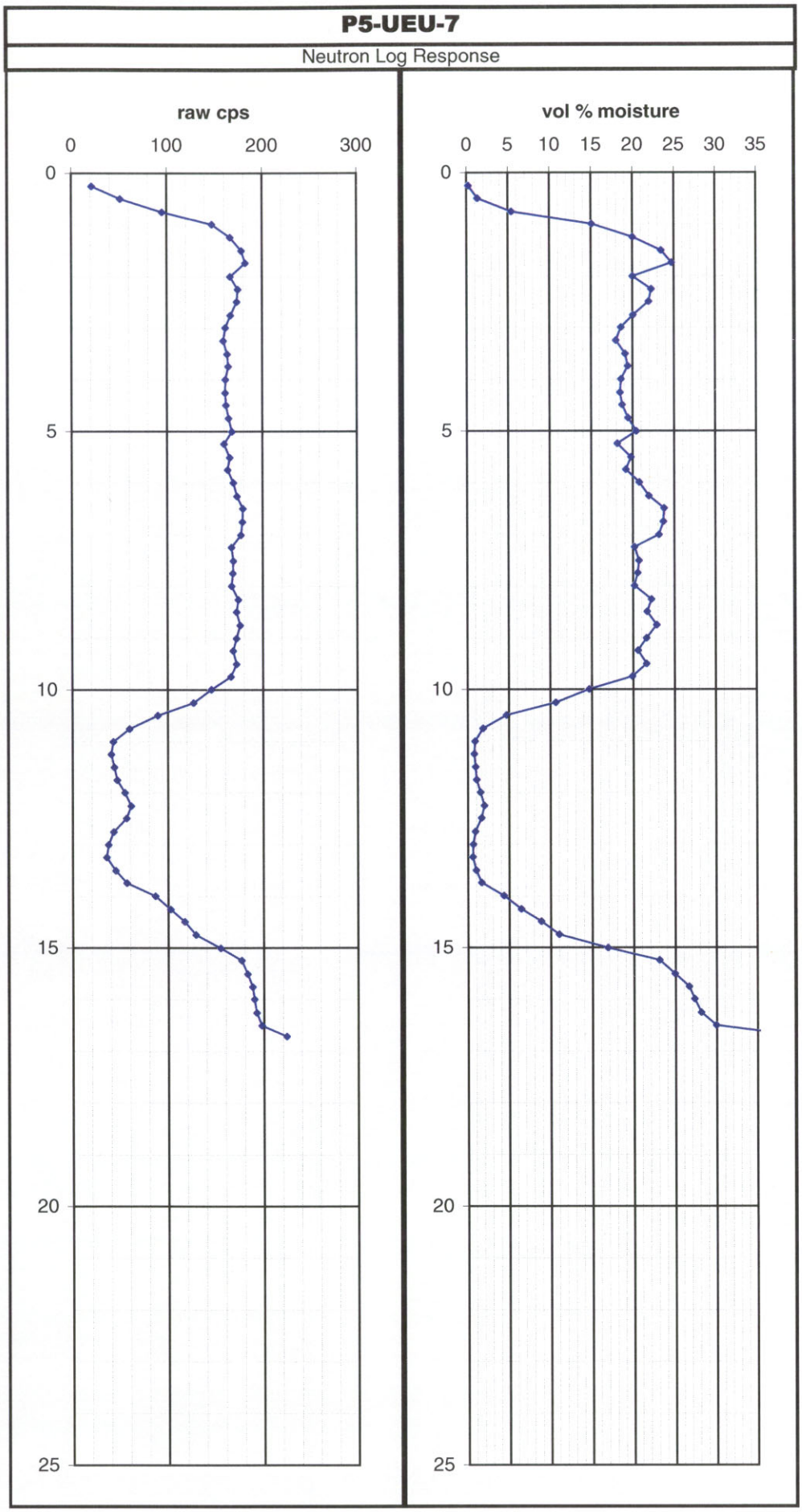
P5-UEU-7
Neutron Log Response
raw cps
0
100
200
300
vol % moisture
0
5
10
15
20
25
30
35
0
5
10
15
20
25

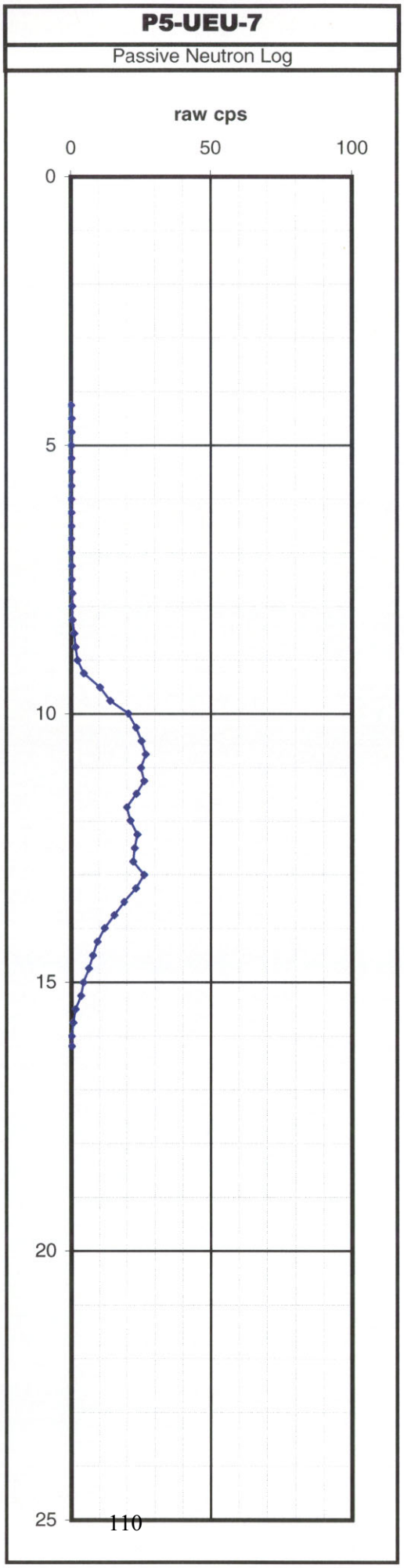
P5-UEU-7
Passive Neutron Log
raw cps
0
50
100
0
5
10
15
20
25

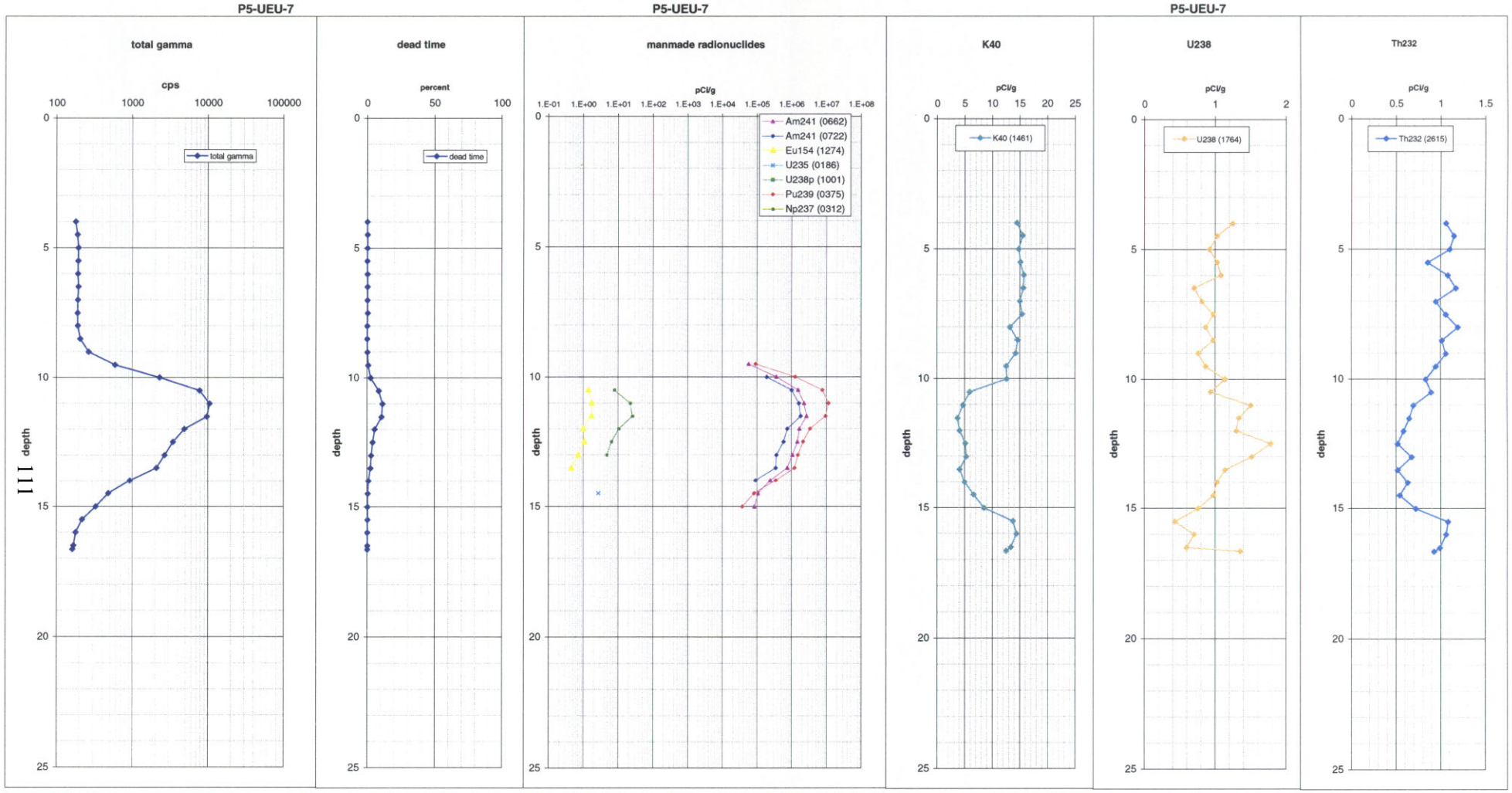
P5-UEU-7
total gamma
cps
100
1000
10000
100000
total gamma
depth
0
5
10
15
20
25
P5-UEU-7
dead time
percent
0
50
100
dead time
depth
P5-UEU-7
manmade radionuclides
pCi/g
1.E-01
1.E+00
1.E+01
1.E+02
1.E+03
1.E+04
1.E+05
1.E+06
1.E+07
1.E+08
Am241 (0662)
Am241 (0722)
Eu154 (1274)
U235 (0186)
U238p (1001)
Pu239 (0375)
Np237 (0312)
depth
K40
pCi/g
0
5
10
15
20
25
K40 (1461)
depth
U238
pCi/g
0
1
2
U238 (1764)
depth
Th232
pCi/g
0
0.5
1
1.5
Th232 (2615)
depth

P5-UEU-7

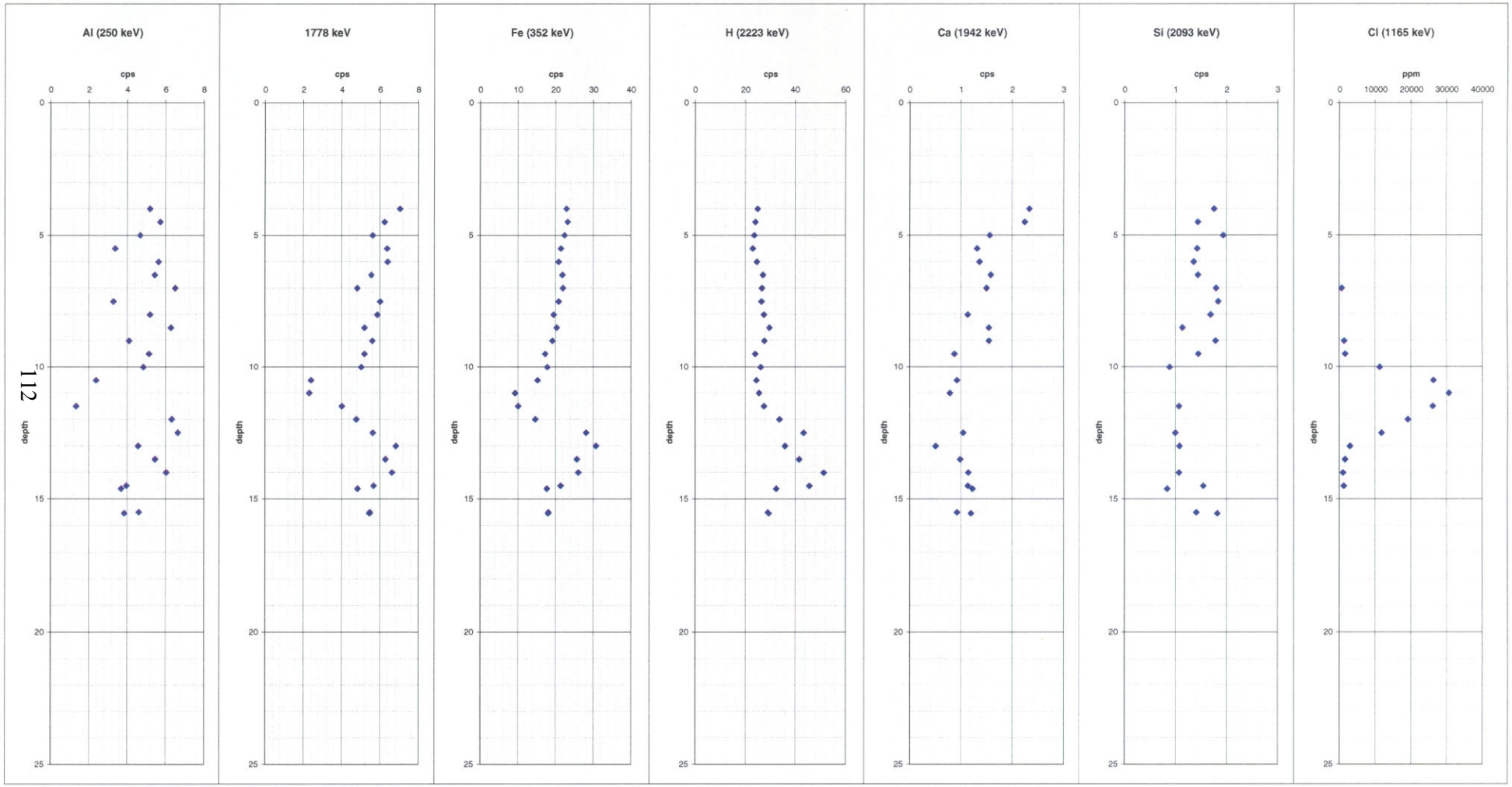
Al (250 keV)
1778 keV
Fe (352 keV)
H (2223 keV)
Ca (1942 keV)
Si (2093 keV)
Cl (1165 keV)
cps
ppm
depth

P5-UEU-7 Total Gamma (10.0 ft to 14.0 ft)

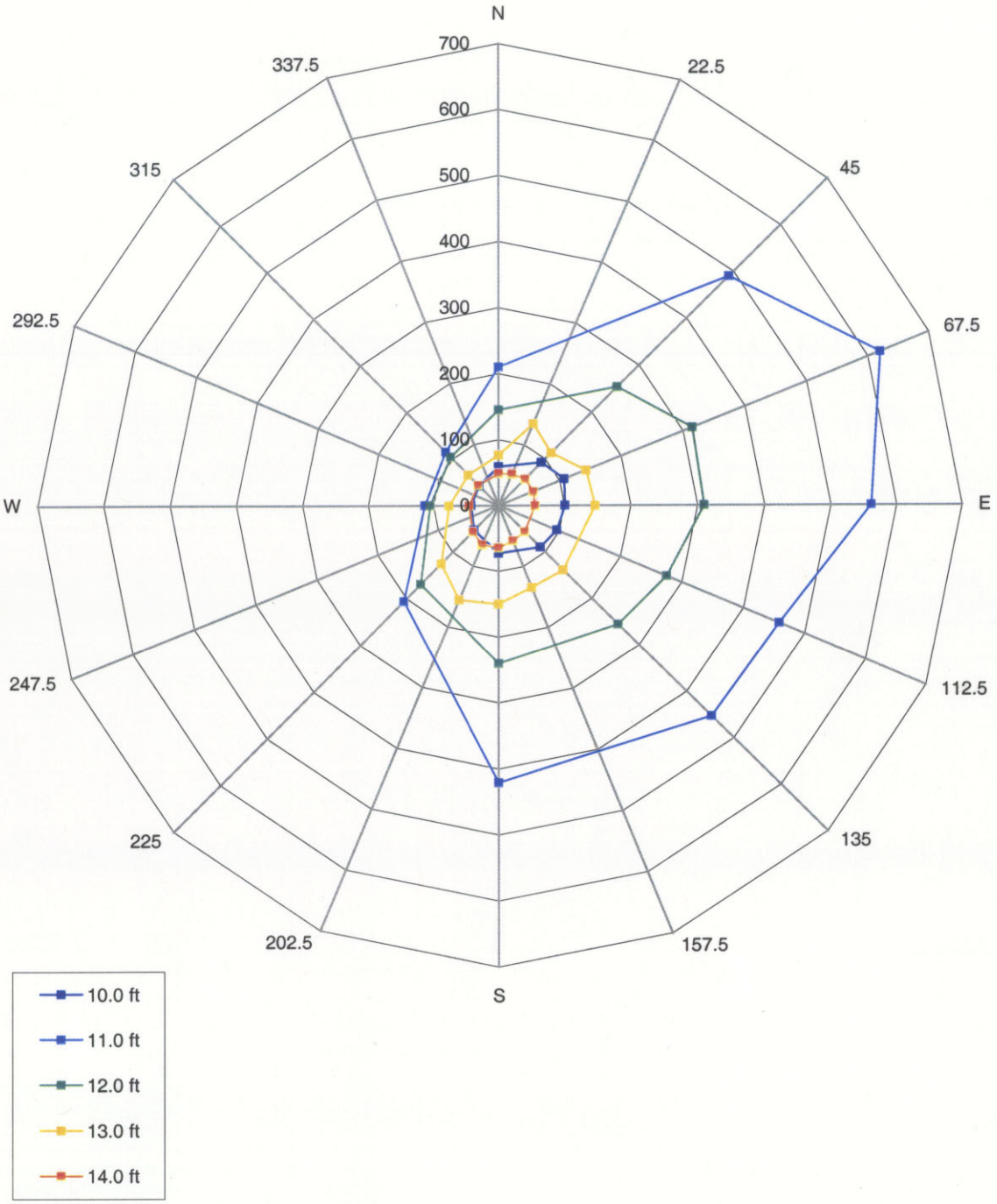

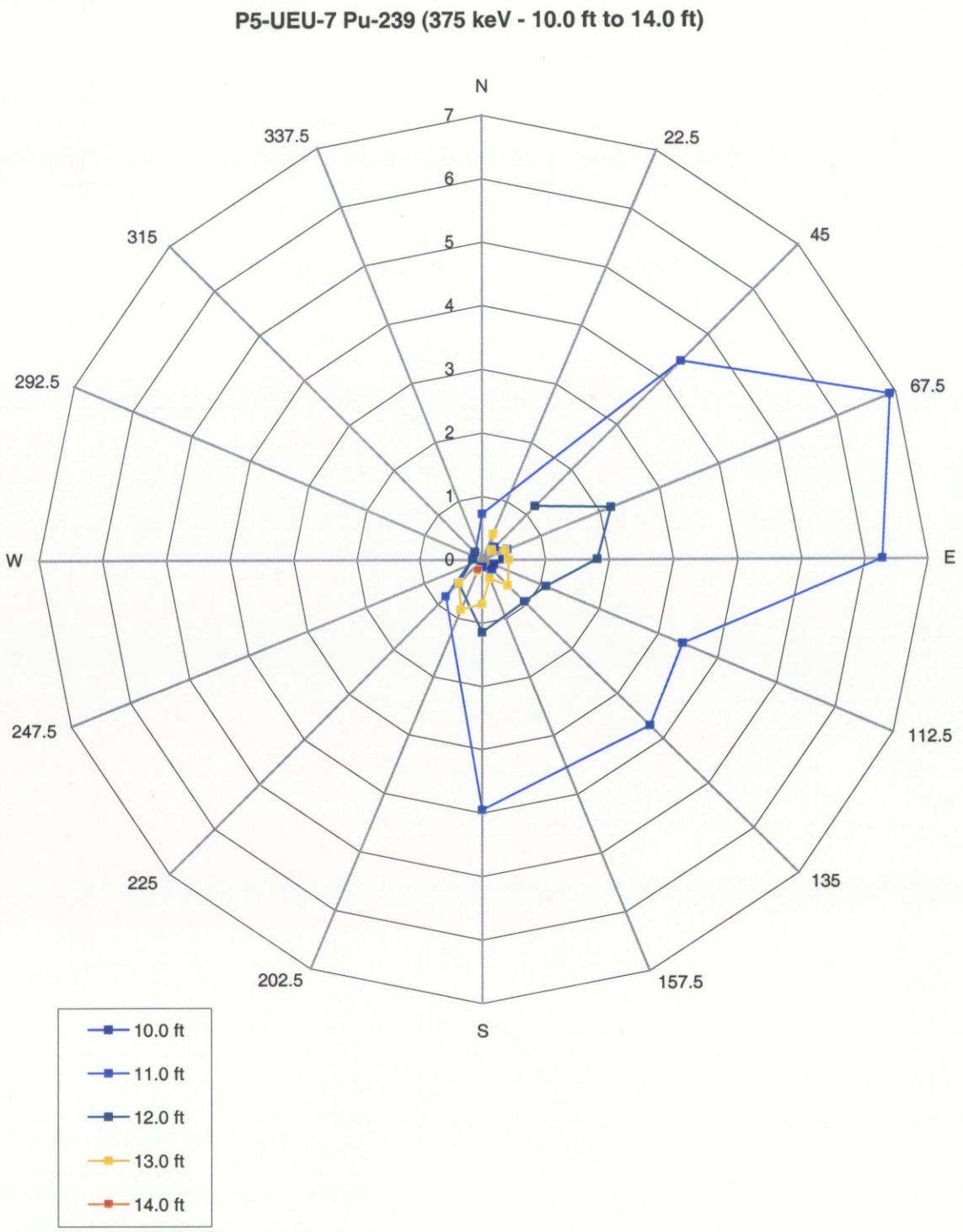
P5-UEU-7 Pu-239 (375 keV - 10.0 ft to 14.0 ft)
N
22.5
45
67.5
E
112.5
135
157.5
S
202.5
225
247.5
W
292.5
315
337.5
0
1
2
3
4
5
6
7
10.0 ft
11.0 ft
12.0 ft
13.0 ft
14.0 ft

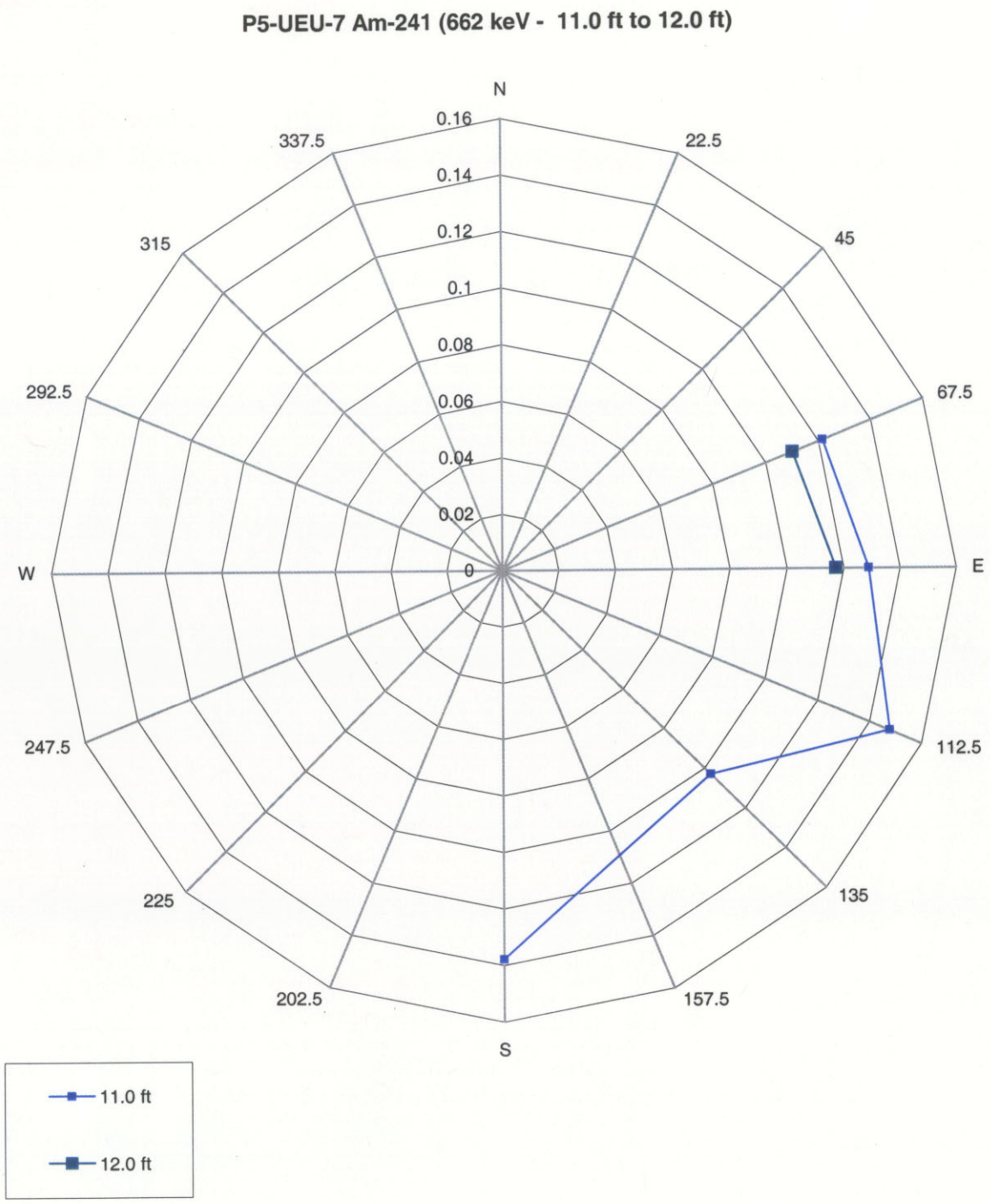
P5-UEU-7 Am-241 (662 keV - 11.0 ft to 12.0 ft)
N
22.5
45
67.5
E
112.5
135
157.5
S
202.5
225
247.5
W
292.5
315
337.5
0.16
0.14
0.12
0.1
0.08
0.06
0.04
0.02
0
11.0 ft
12.0 ft

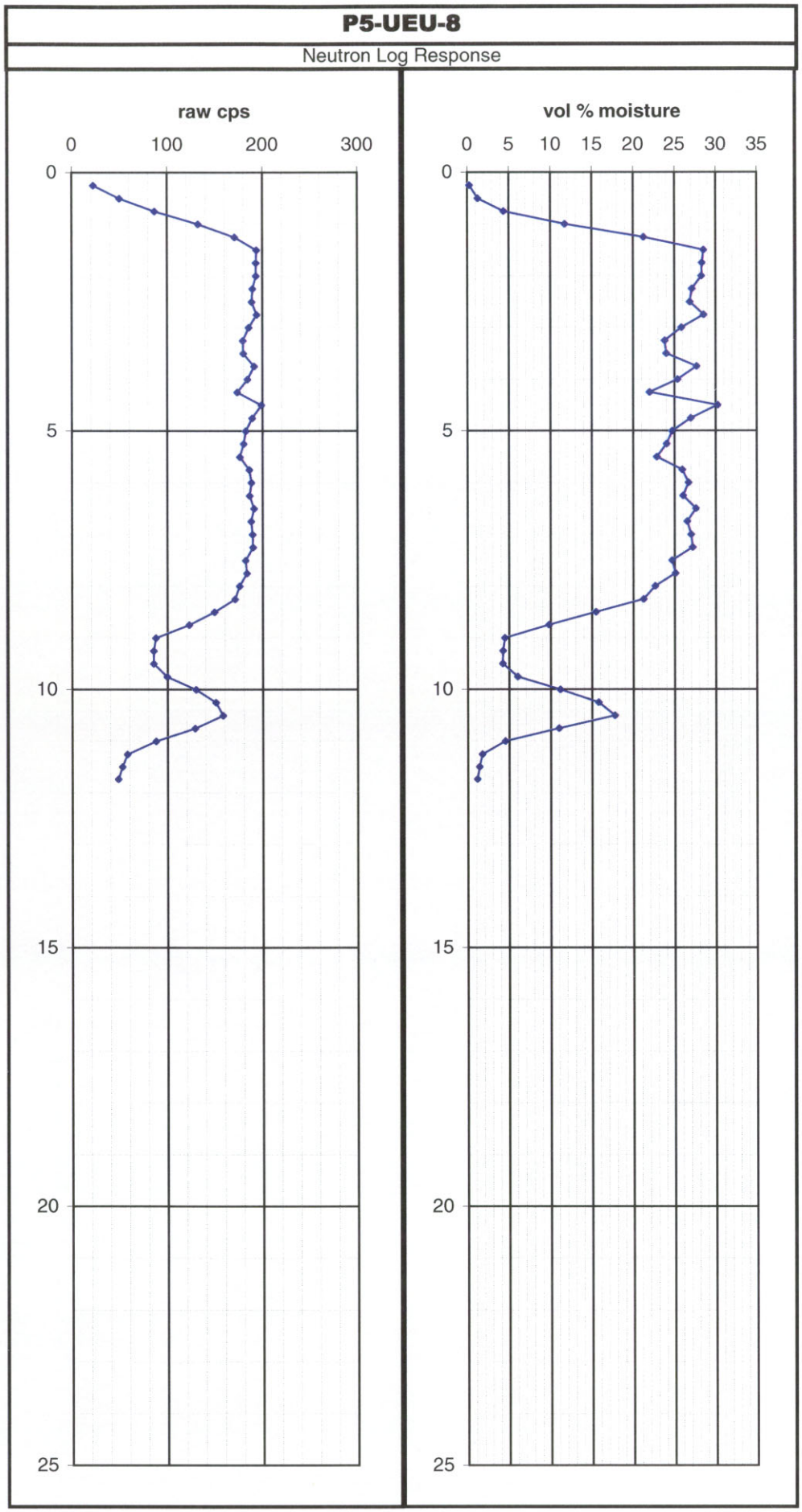
P5-UEU-8
Neutron Log Response
raw cps
0
100
200
300
vol % moisture
0
5
10
15
20
25
30
35
0
5
10
15
20
25

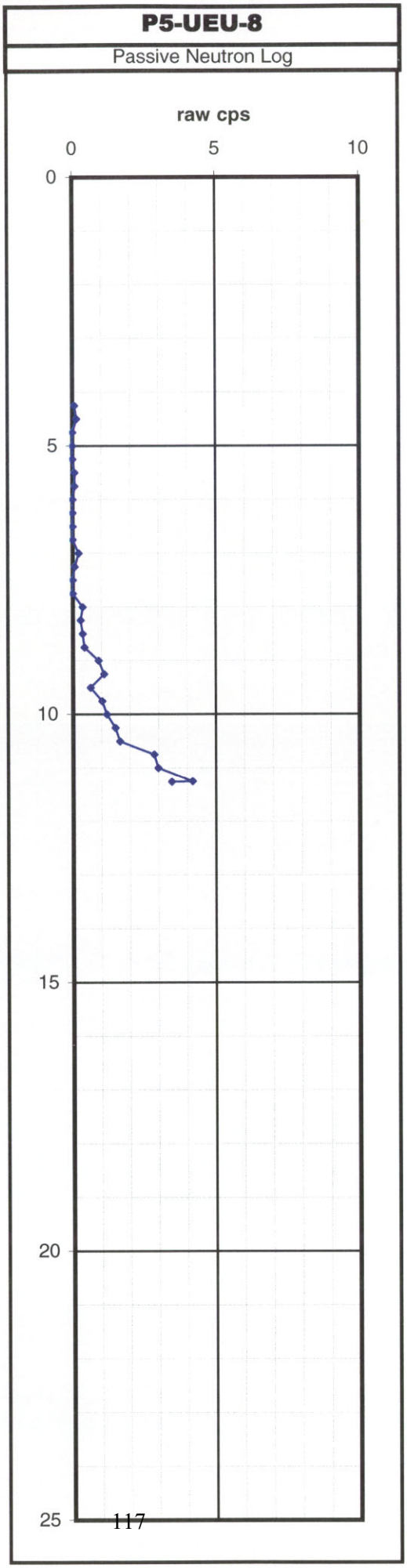
P5-UEU-8
Passive Neutron Log
raw cps
0
5
10
0
5
10
15
20
25

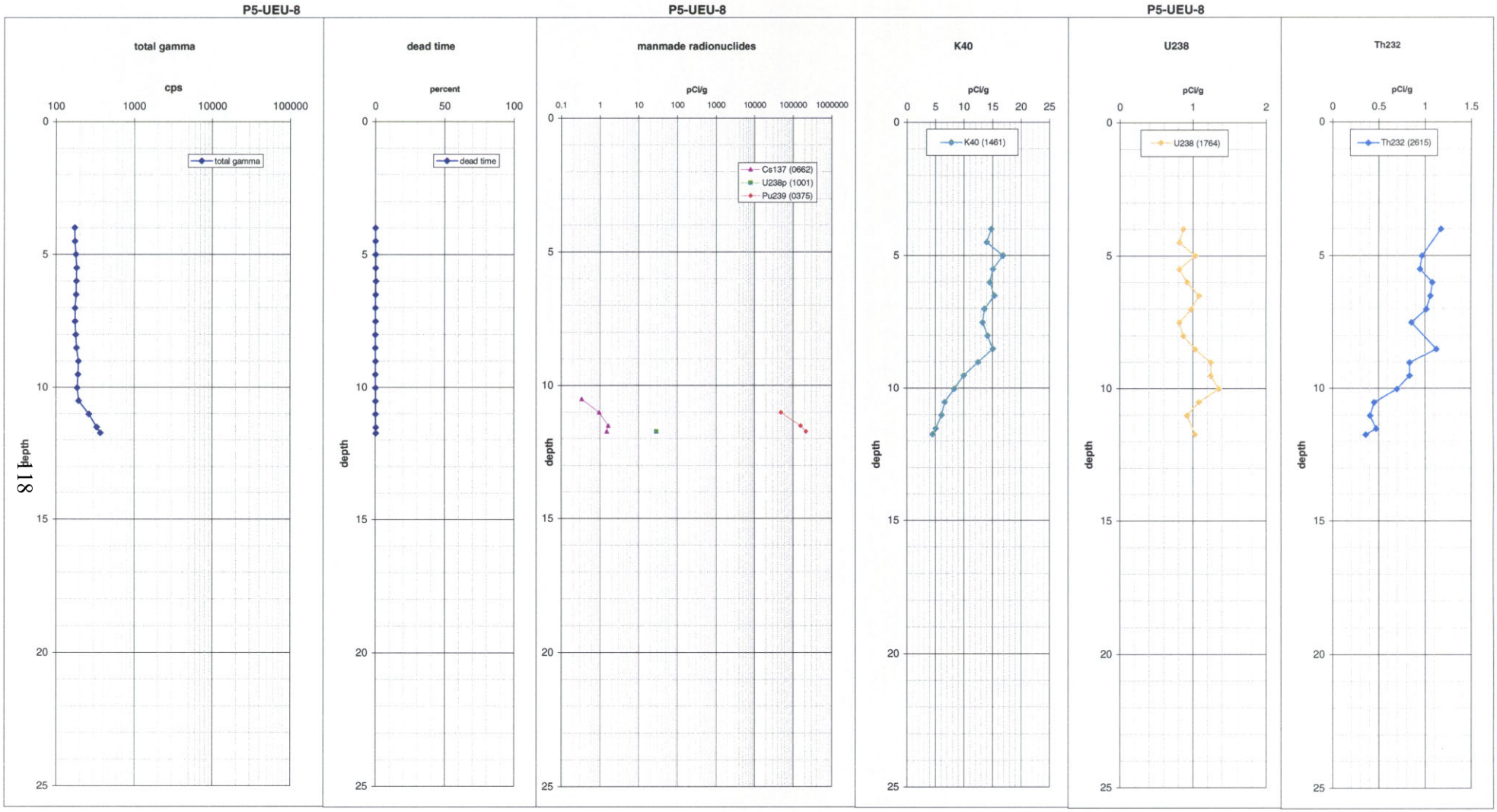
P5-UEU-8
total gamma
cps
100
1000
10000
100000
total gamma
depth
0
5
10
15
20
25
P5-UEU-8
dead time
percent
0
50
100
dead time
depth
P5-UEU-8
manmade radionuclides
pCi/g
0.1
1
10
100
1000
10000
100000
1000000
Cs137 (0662)
U238p (1001)
Pu239 (0375)
depth
P5-UEU-8
K40
pCi/g
0
5
10
15
20
25
K40 (1461)
depth
U238
pCi/g
0
1
2
U238 (1764)
depth
Th232
pCi/g
0
0.5
1
1.5
Th232 (2615)
depth

P5-UEU-8

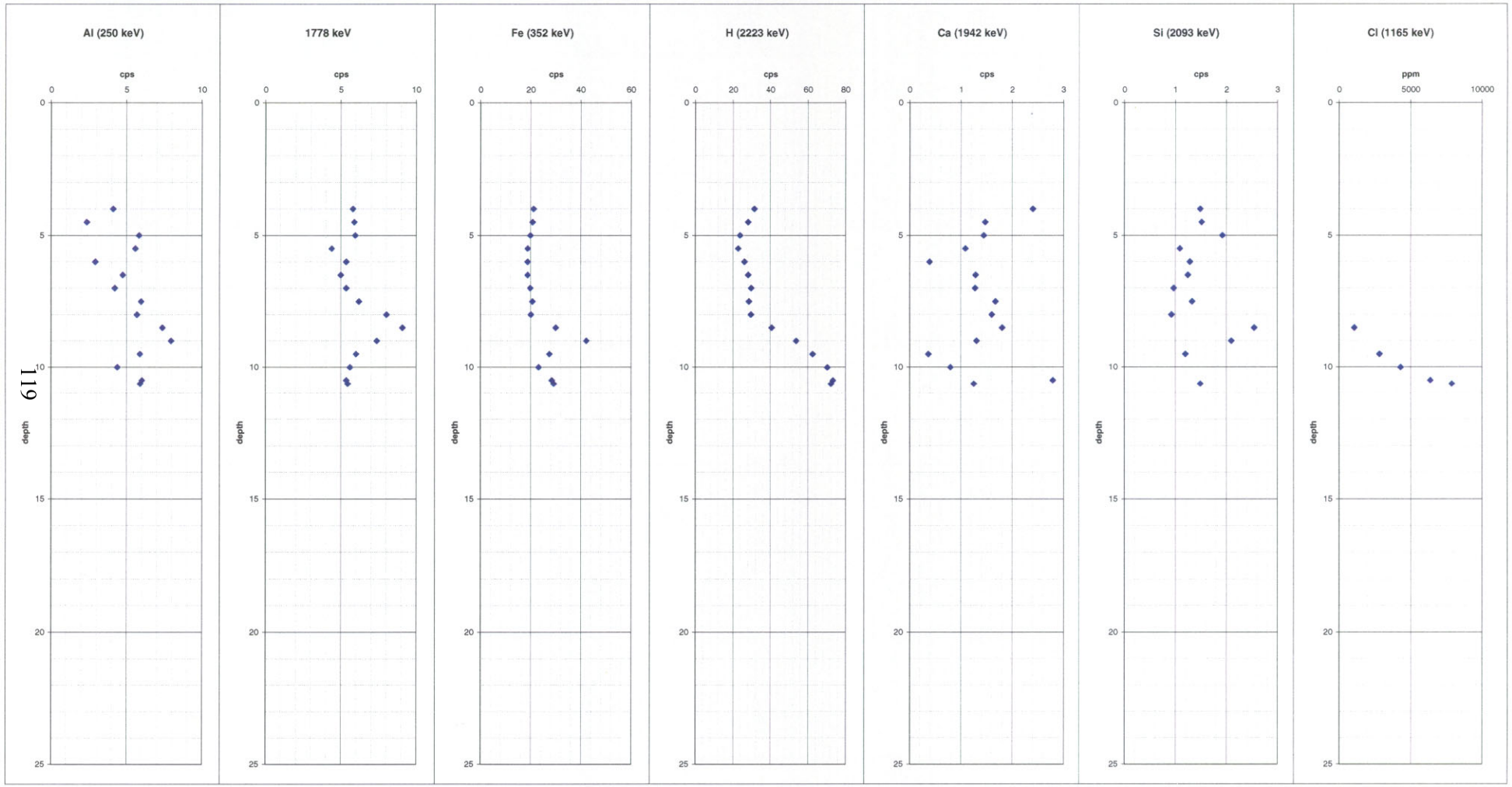
Al (250 keV)
1778 keV
Fe (352 keV)
H (2223 keV)
Ca (1942 keV)
Si (2093 keV)
Cl (1165 keV)
cps
ppm
depth

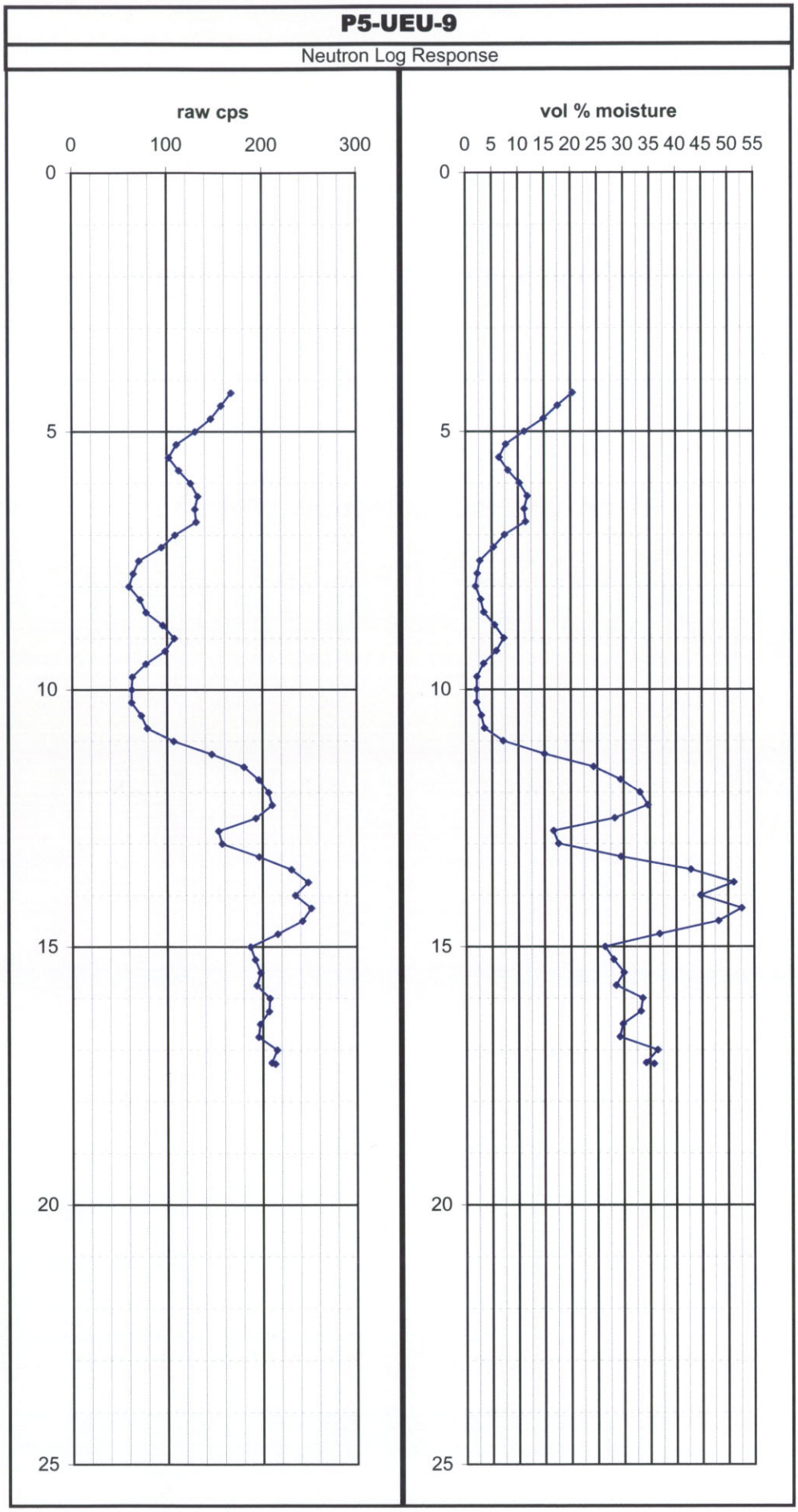
P5-UEU-9
Neutron Log Response
raw cps
0
100
200
300
vol % moisture
0 5 10 15 20 25 30 35 40 45 50 55
0
5
10
15
20
25

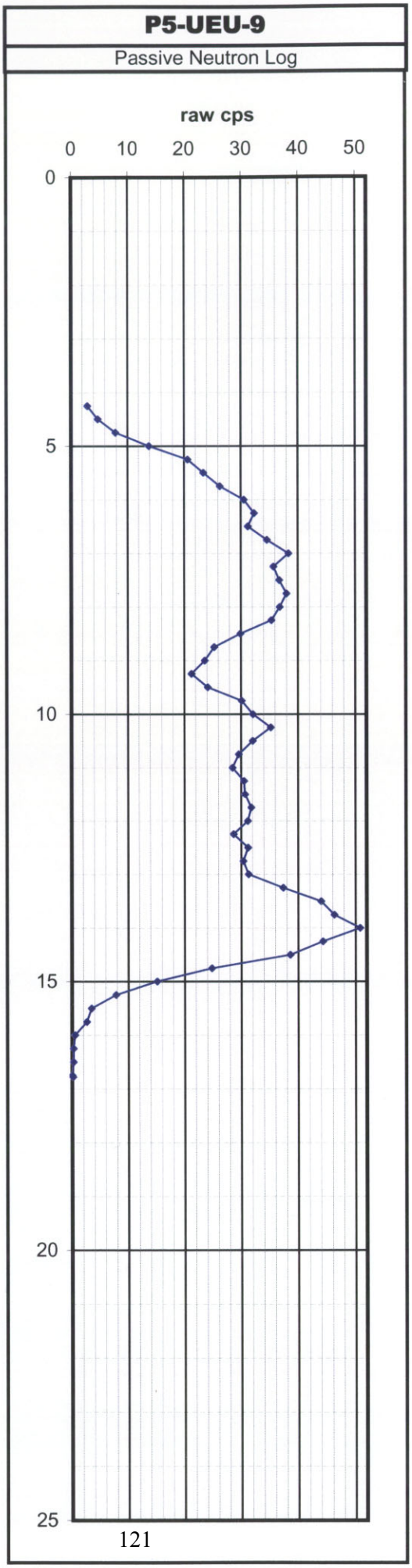
P5-UEU-9
Passive Neutron Log
raw cps
0
10
20
30
40
50
0
5
10
15
20
25

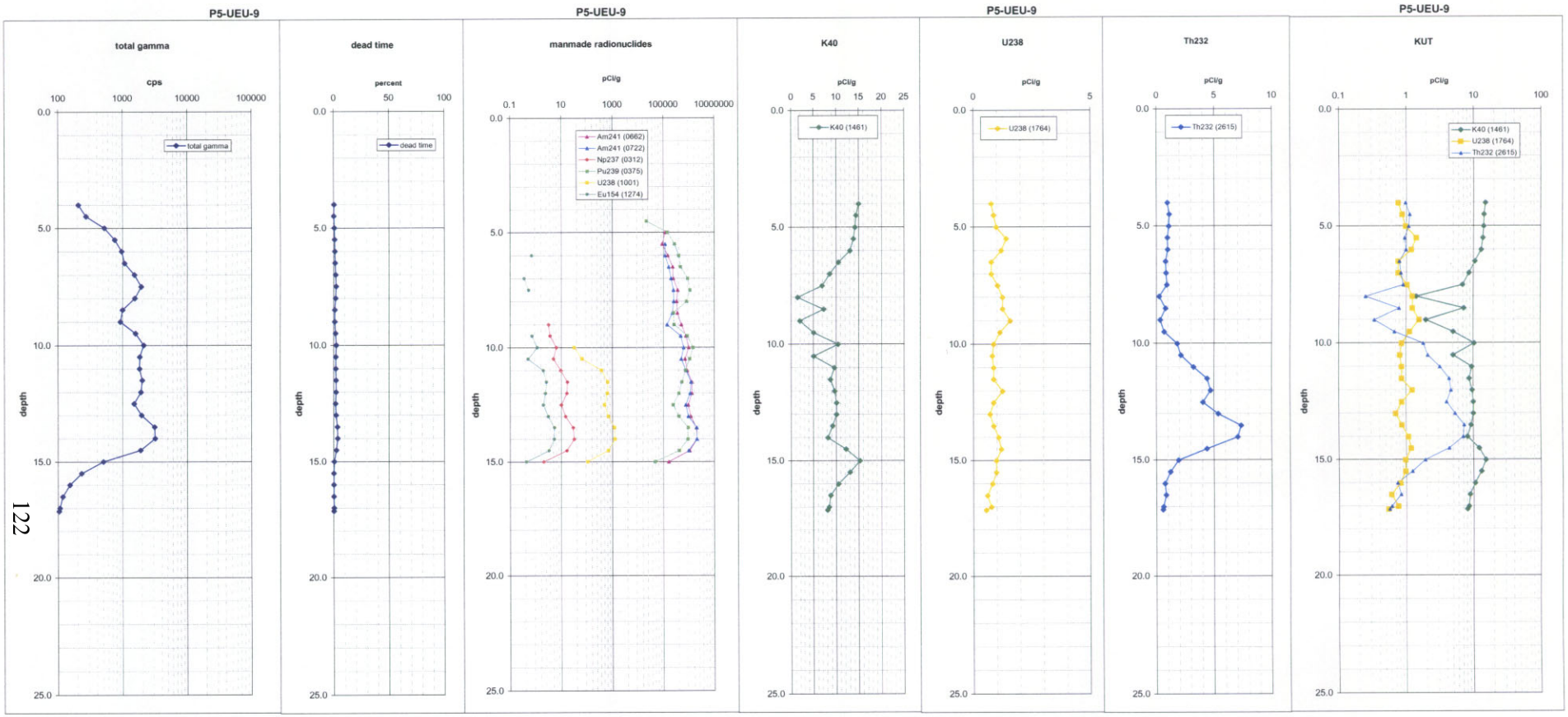
P5-UEU-9
total gamma
cps
100
1000
10000
100000
total gamma
depth
0.0
5.0
10.0
15.0
20.0
25.0
P5-UEU-9
dead time
percent
0
50
100
dead time
P5-UEU-9
manmade radionuclides
pCi/g
0.1
10
1000
100000
10000000
Am241 (0662)
Am241 (0722)
Np237 (0312)
Pu239 (0375)
U238 (1001)
Eu154 (1274)
P5-UEU-9
K40
pCi/g
0
5
10
15
20
25
K40 (1461)
P5-UEU-9
U238
pCi/g
0
5
U238 (1764)
P5-UEU-9
Th232
pCi/g
0
5
10
Th232 (2615)
P5-UEU-9
KUT
pCi/g
0.1
1
10
100
K40 (1461)
U238 (1764)
Th232 (2615)

P5-UEU-9

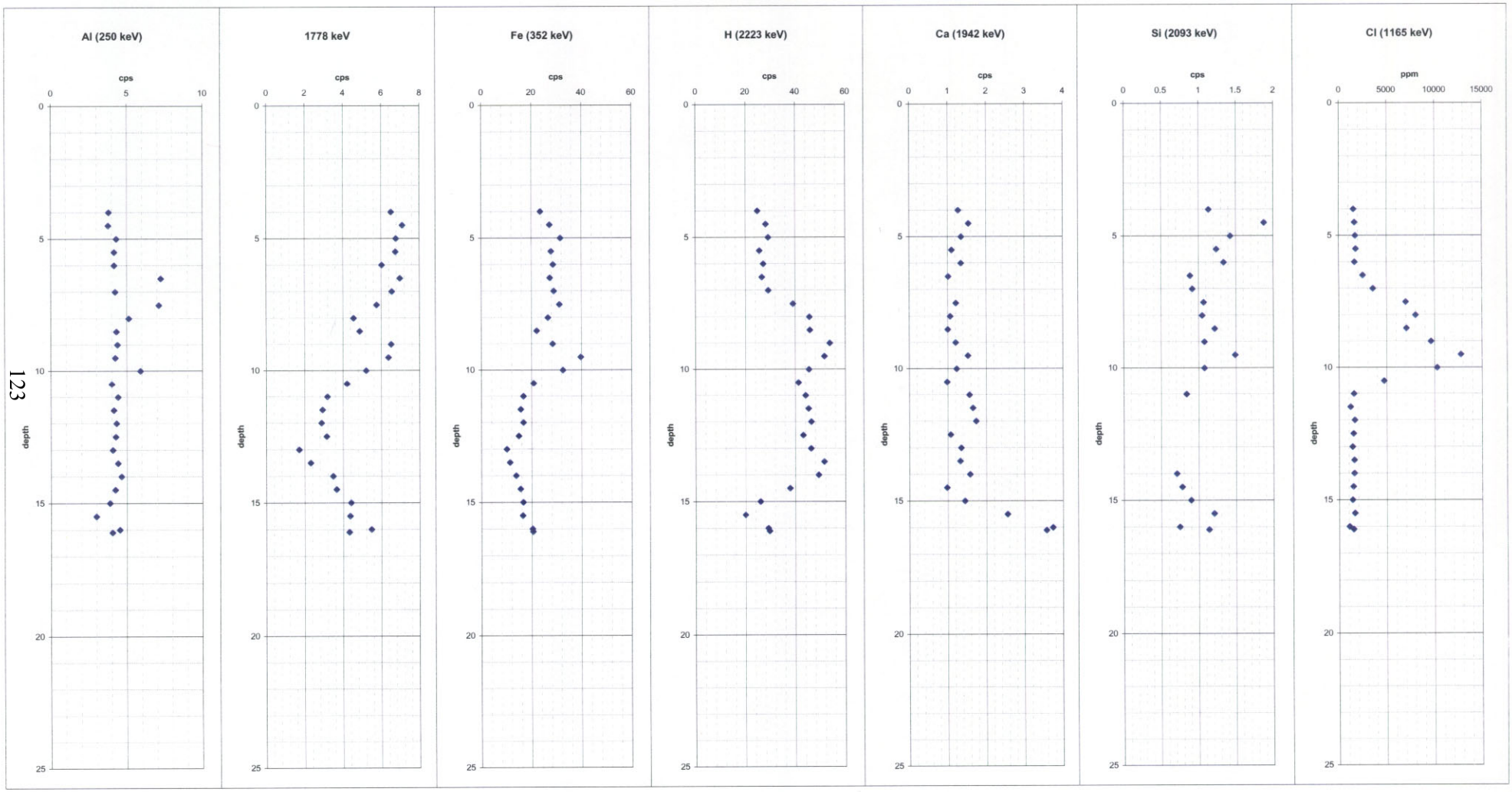
Al (250 keV)
1778 keV
Fe (352 keV)
H (2223 keV)
Ca (1942 keV)
Si (2093 keV)
Cl (1165 keV)
cps
ppm
depth

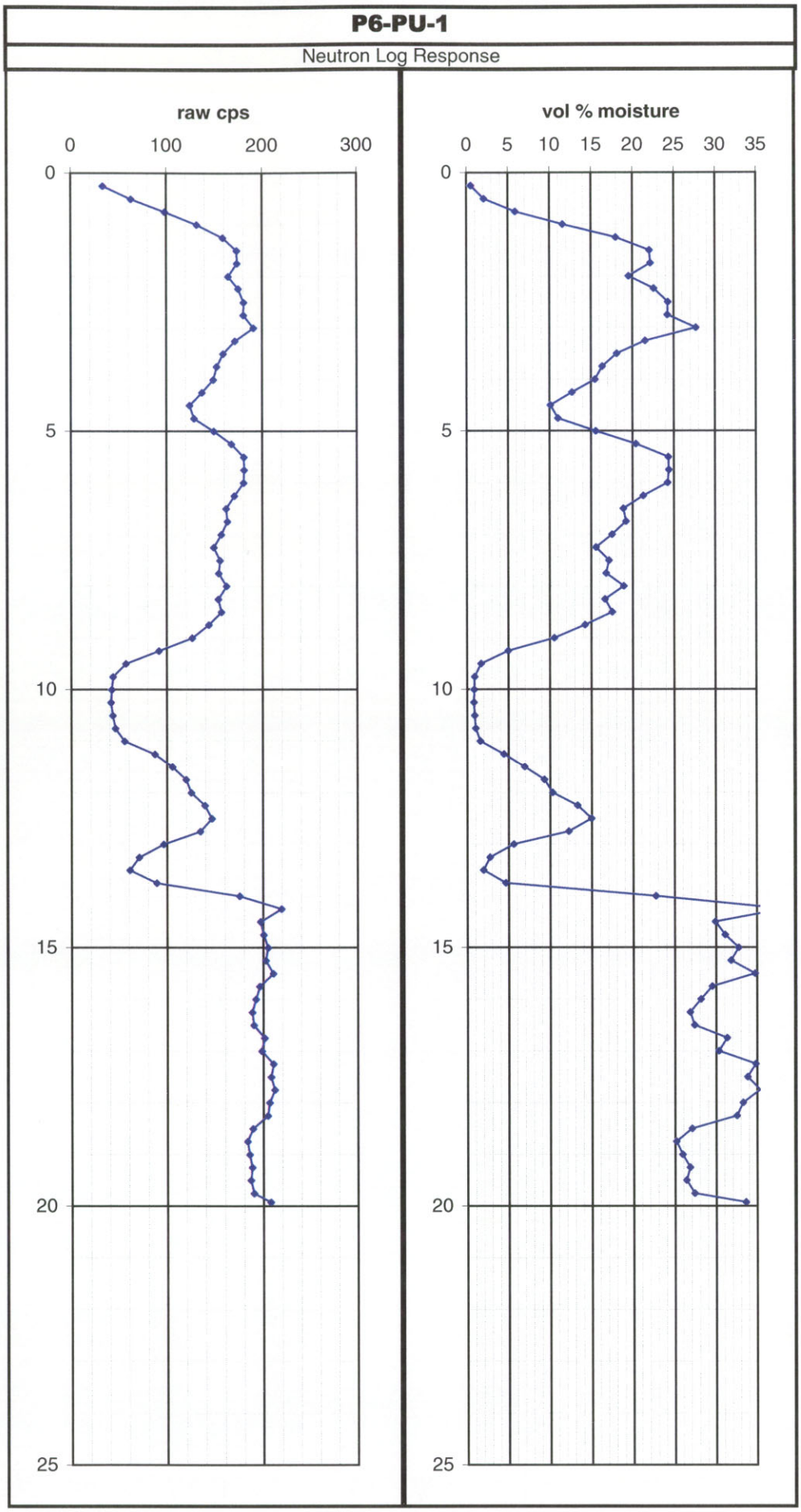
P6-PU-1
Neutron Log Response
raw cps
0
100
200
300
vol % moisture
0
5
10
15
20
25
30
35
0
5
10
15
20
25

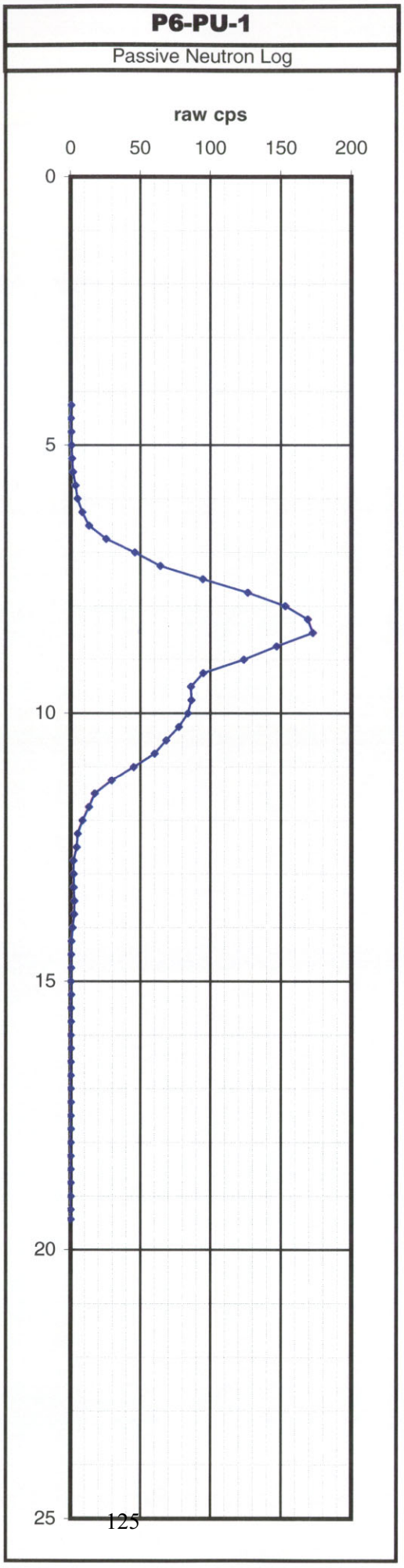
P6-PU-1
Passive Neutron Log
raw cps
0
50
100
150
200
0
5
10
15
20
25

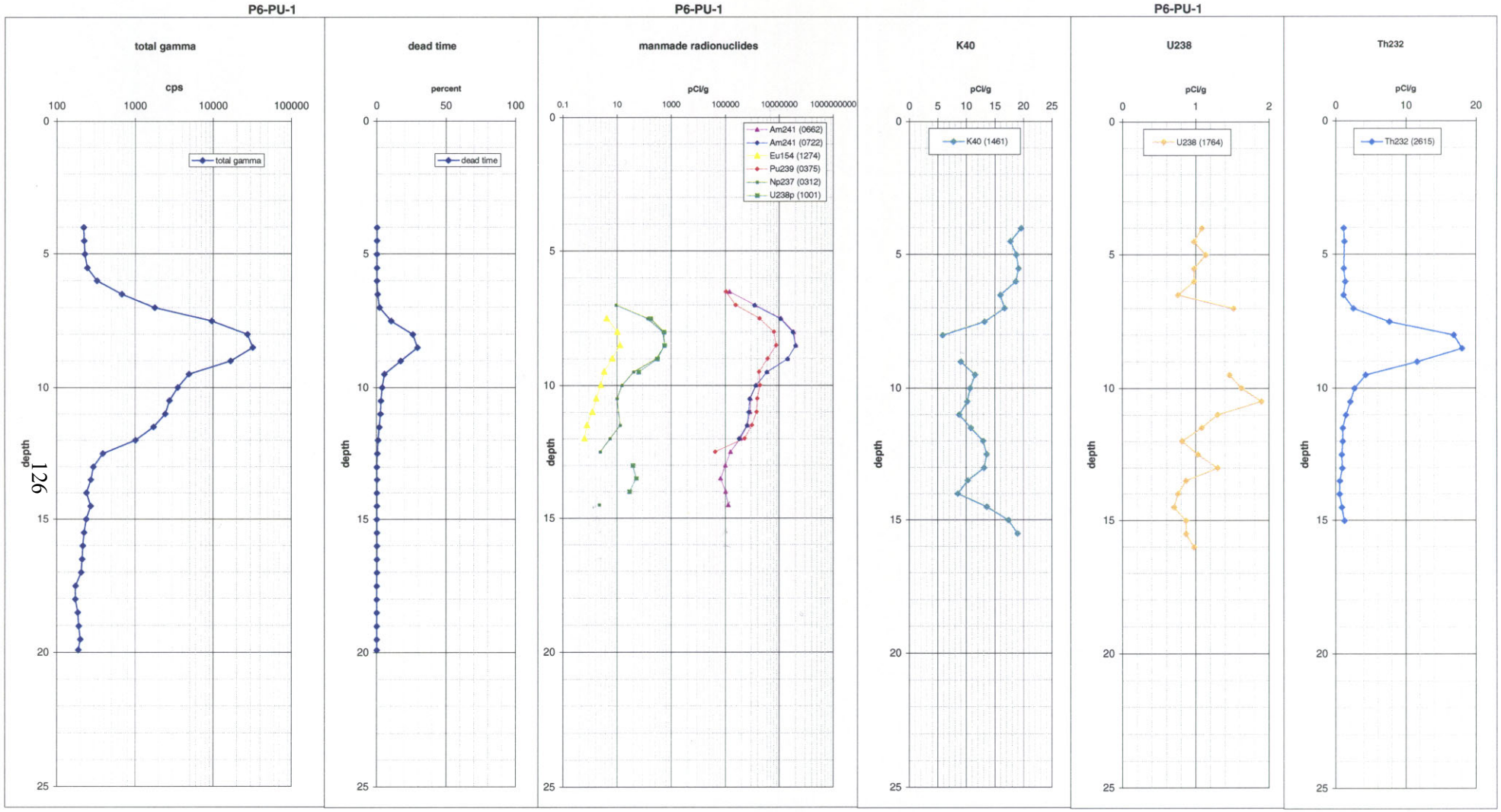
P6-PU-1
total gamma
cps
100
1000
10000
100000
total gamma
depth
0
5
10
15
20
25
P6-PU-1
dead time
percent
0
50
100
dead time
depth
P6-PU-1
manmade radionuclides
pCi/g
0.1
10
1000
100000
10000000
1000000000
Am241 (0662)
Am241 (0722)
Eu154 (1274)
Pu239 (0375)
Np237 (0312)
U238p (1001)
depth
P6-PU-1
K40
pCi/g
0
5
10
15
20
25
K40 (1461)
depth
U238
pCi/g
0
1
2
U238 (1764)
depth
Th232
pCi/g
0
10
20
Th232 (2615)
depth

P6-PU-1

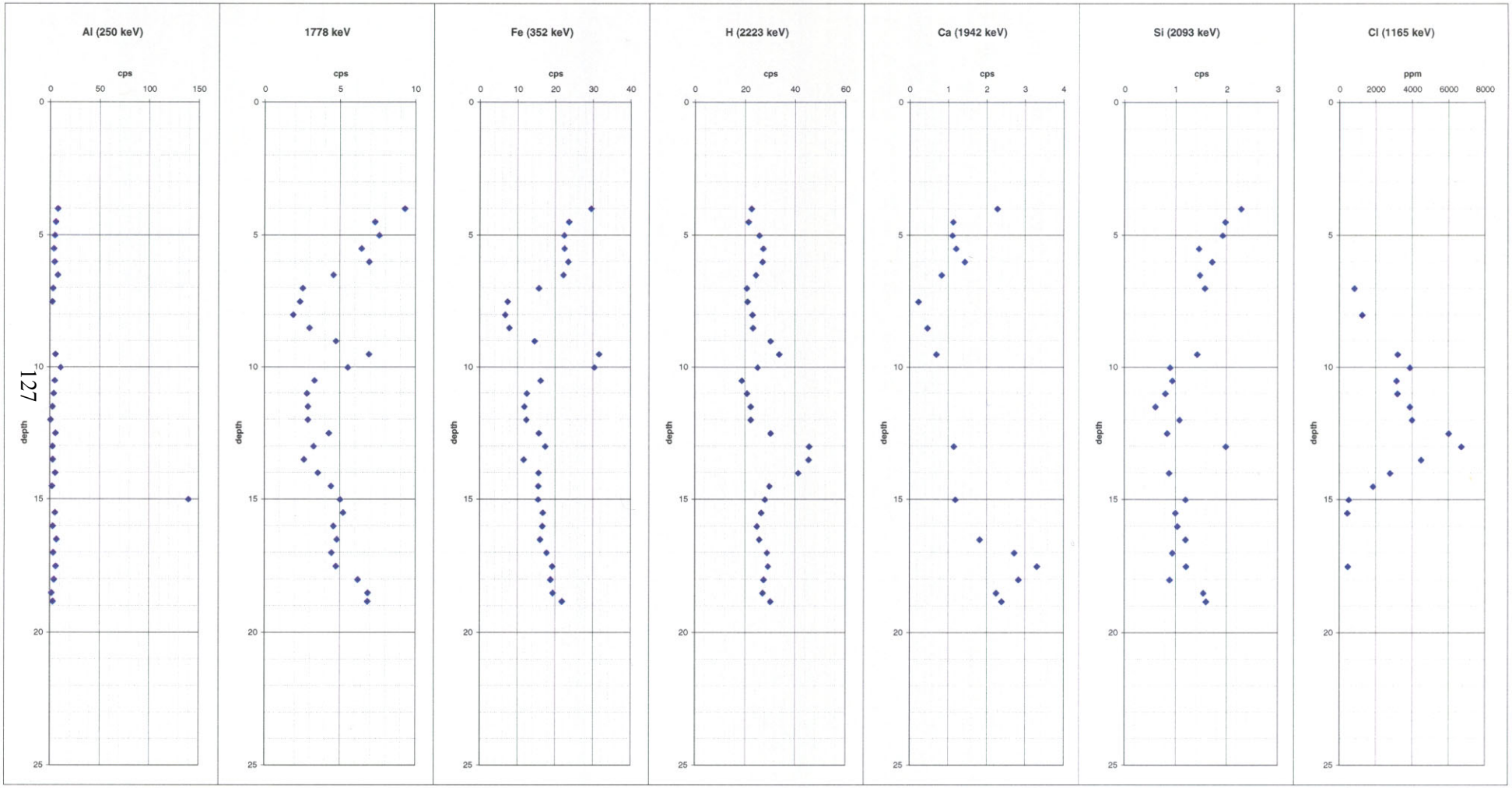
Al (250 keV)
1778 keV
Fe (352 keV)
H (2223 keV)
Ca (1942 keV)
Si (2093 keV)
Cl (1165 keV)
cps
ppm
depth

P6-PU-1 Total Gamma (6.0 ft to 12.0 ft)

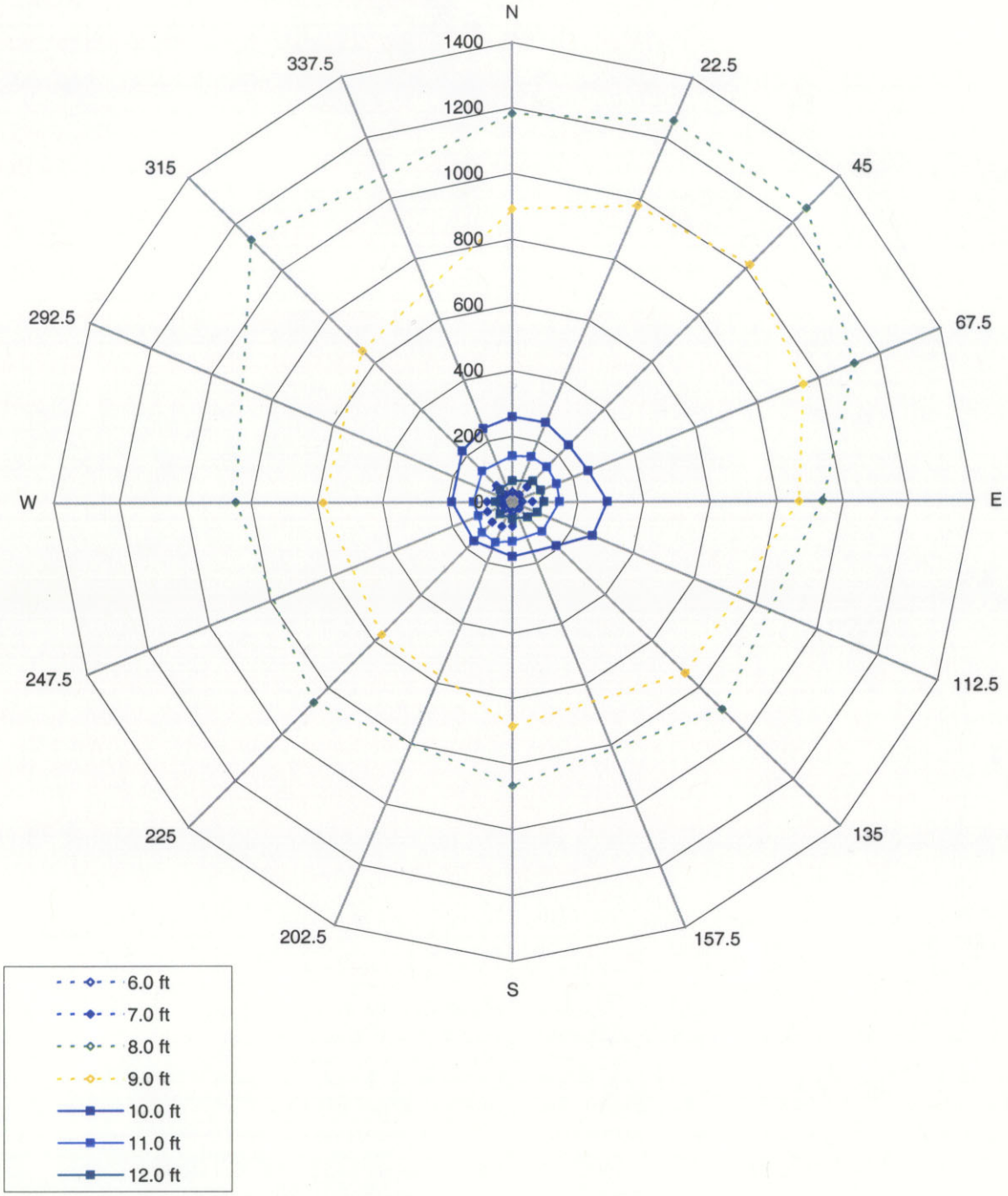

P6-PU-1 Pu-239 (375 keV - 8.0 ft to 12.0 ft)

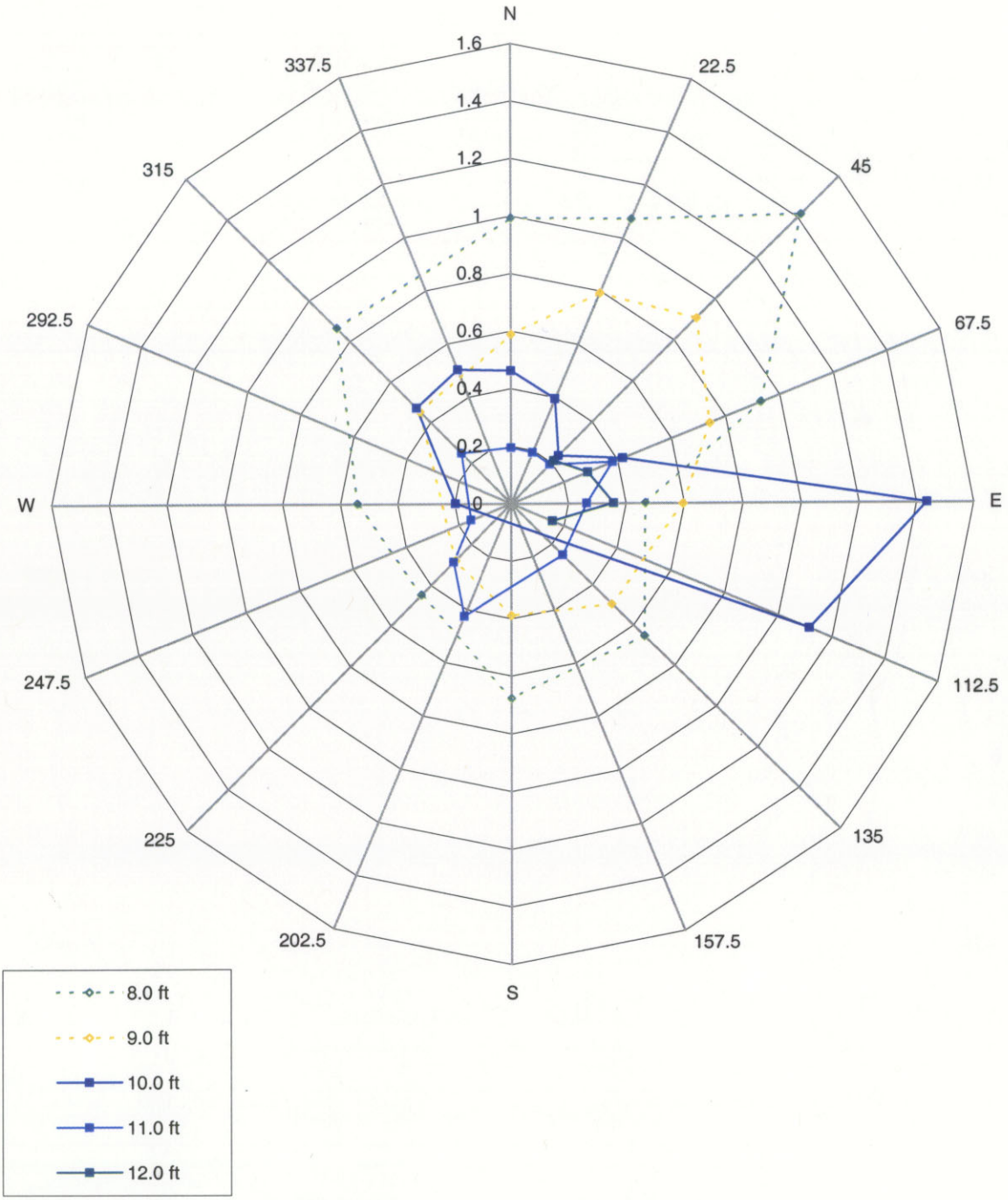

P6-PU-1 Am-241 (662 keV - 8.0 ft to 11.0 ft)

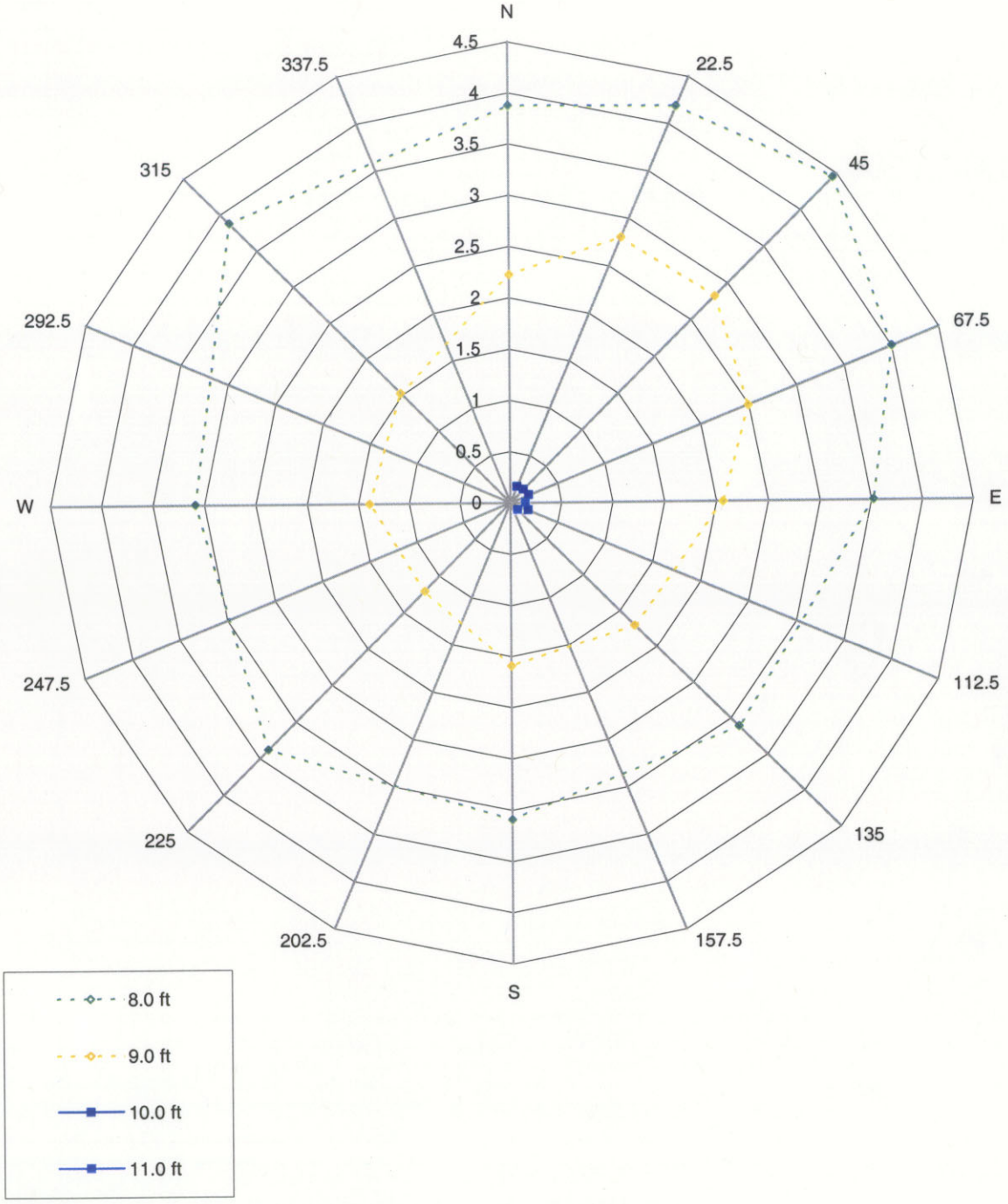

P6-PU-1 Np-237 (313 keV - 8.0 ft and 9.0 ft)

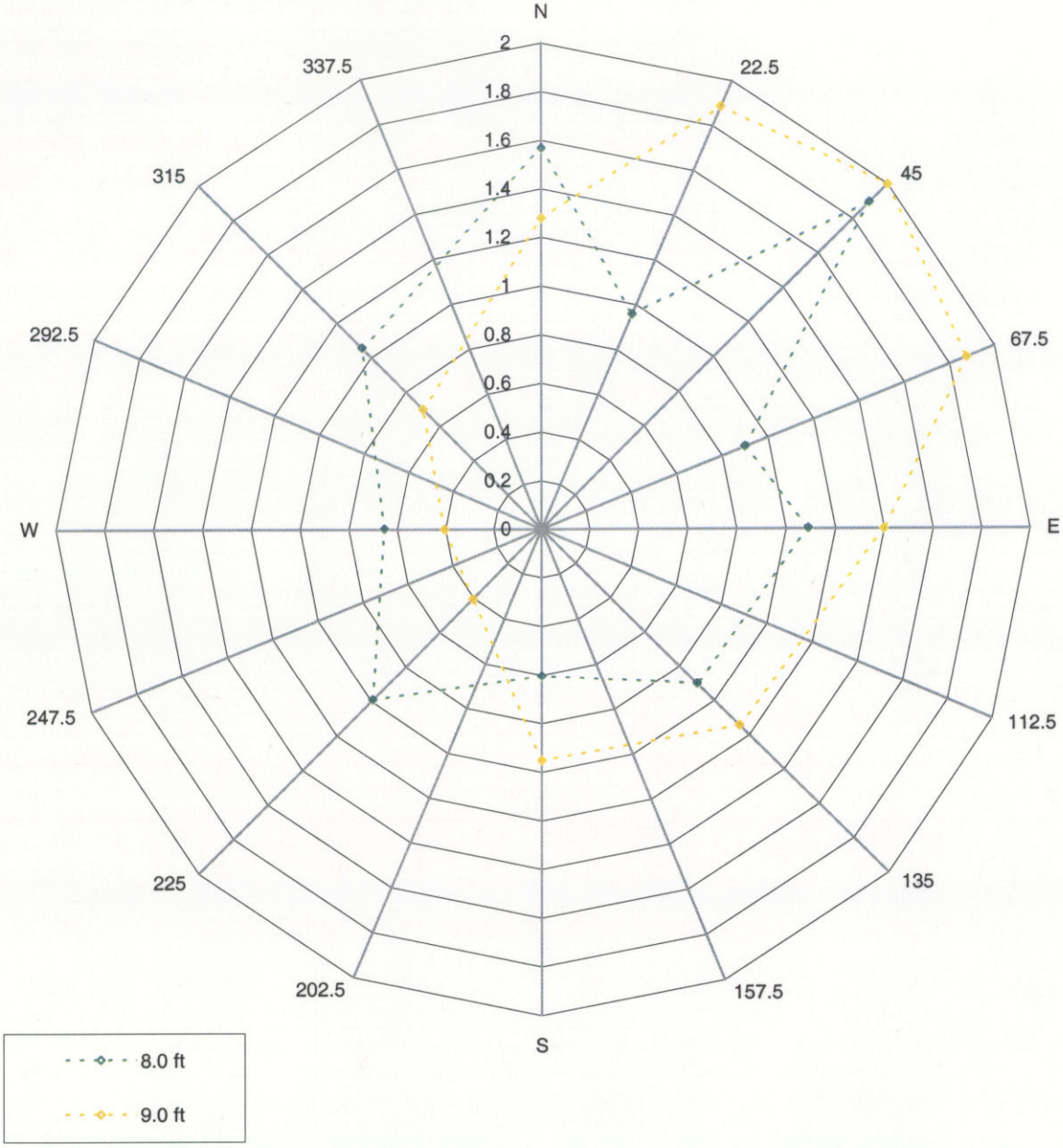

P6-PU-1 U-238 (1001 keV - 8.0 ft and 9.0 ft)

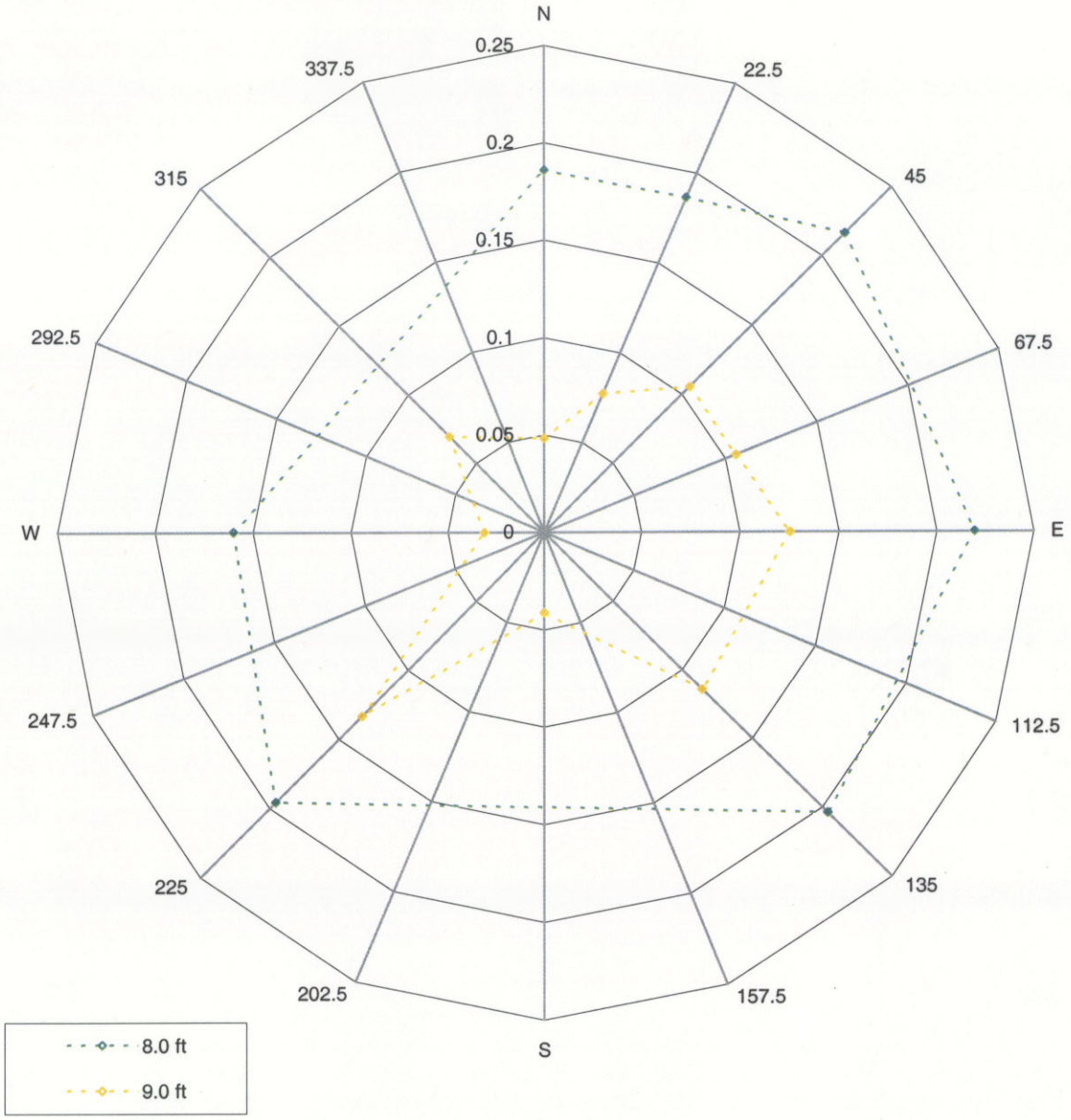

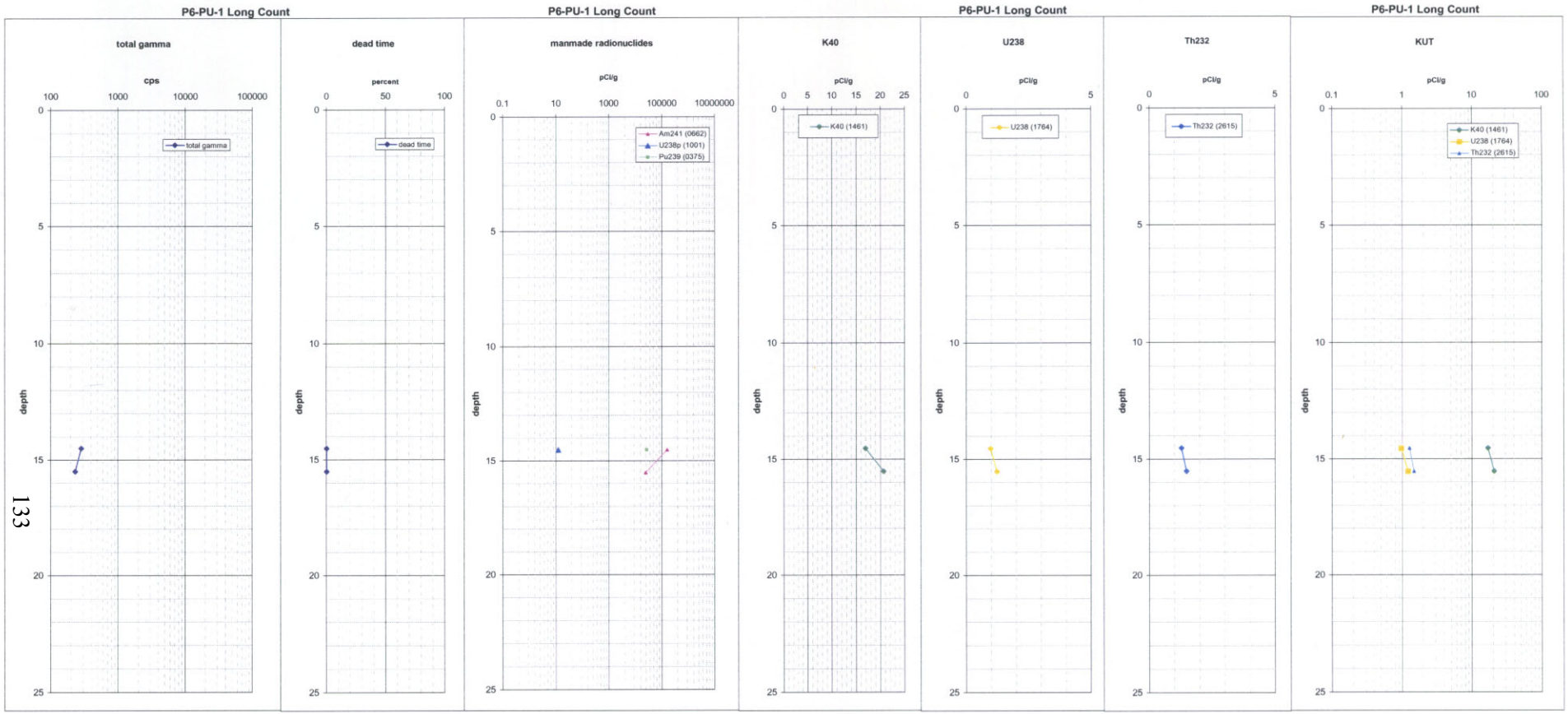
P6-PU-1 Long Count
total gamma
cps
100
1000
10000
100000
total gamma
dead time
percent
0
50
100
dead time
manmade radionuclides
pCi/g
0.1
10
1000
100000
10000000
Am241 (0662)
U238p (1001)
Pu239 (0375)
K40
pCi/g
0
5
10
15
20
25
K40 (1461)
U238
pCi/g
U238 (1764)
Th232
pCi/g
Th232 (2615)
KUT
pCi/g
0.1
1
10
100
K40 (1461)
U238 (1764)
Th232 (2615)
depth
0
5
10
15
20
25

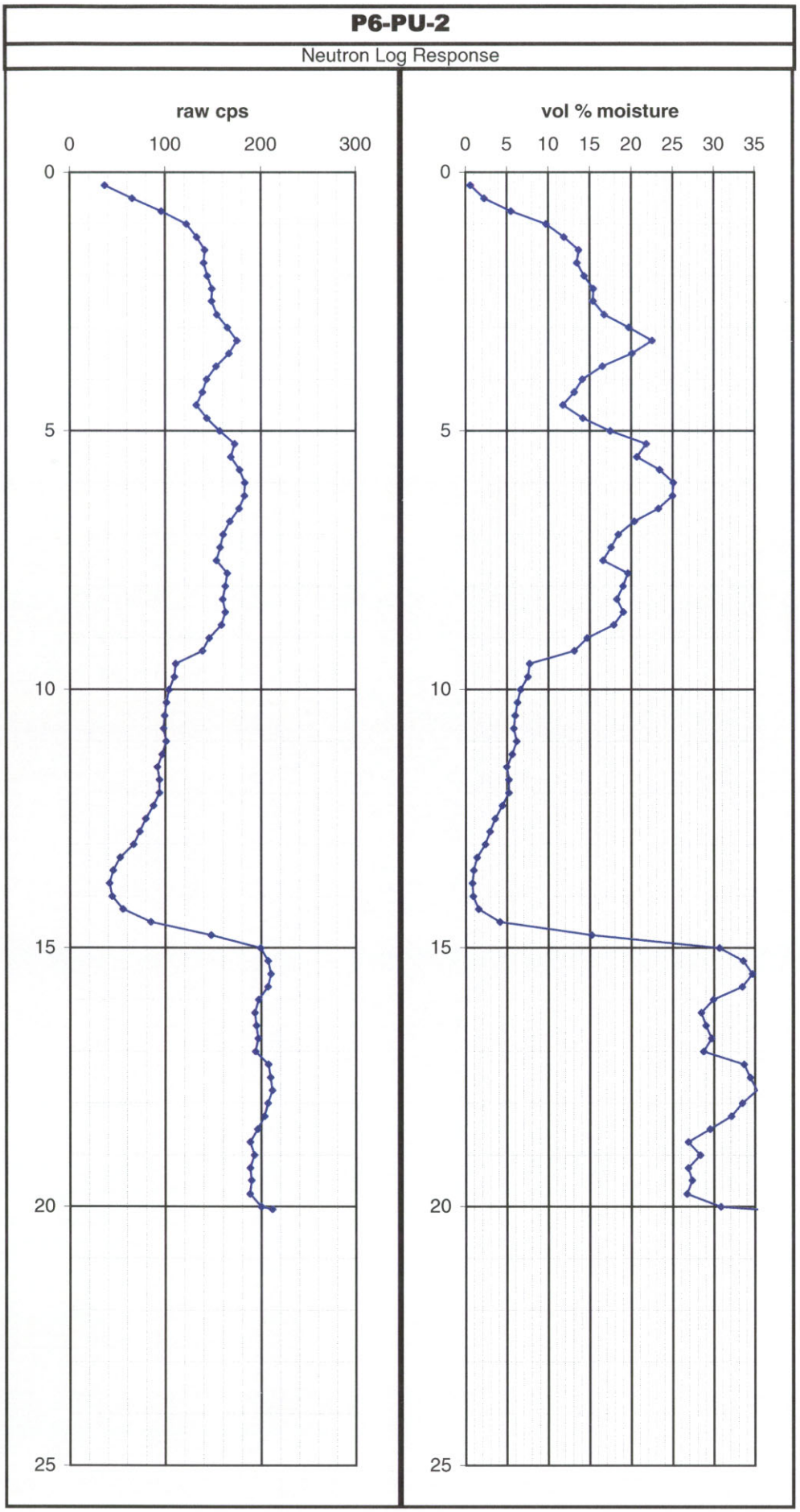
P6-PU-2
Neutron Log Response
raw cps
0
100
200
300
vol % moisture
0
5
10
15
20
25
30
35
0
5
10
15
20
25

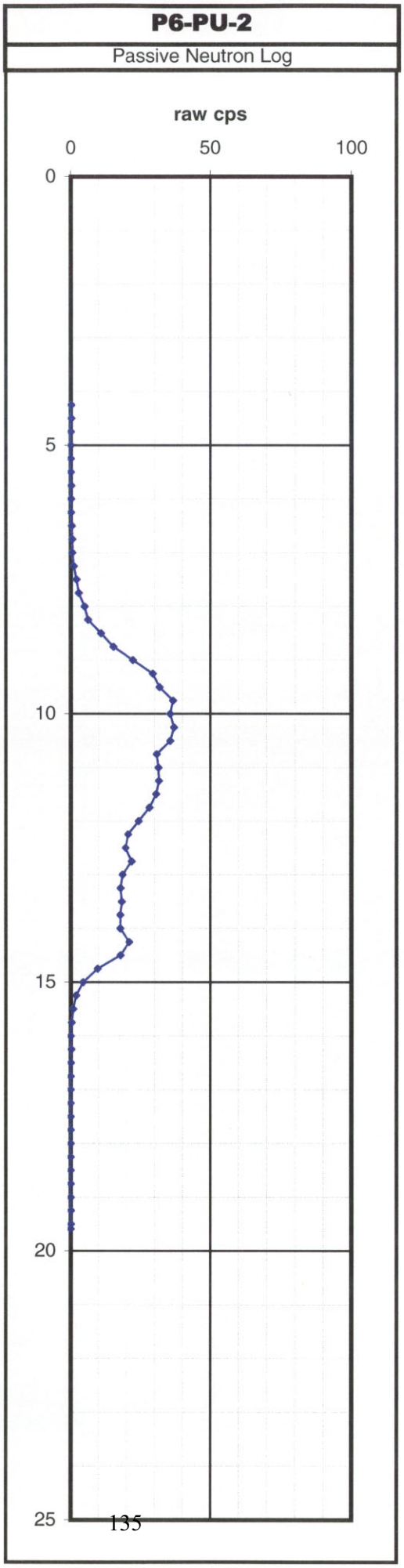
P6-PU-2
Passive Neutron Log
raw cps
0
50
100
0
5
10
15
20
25

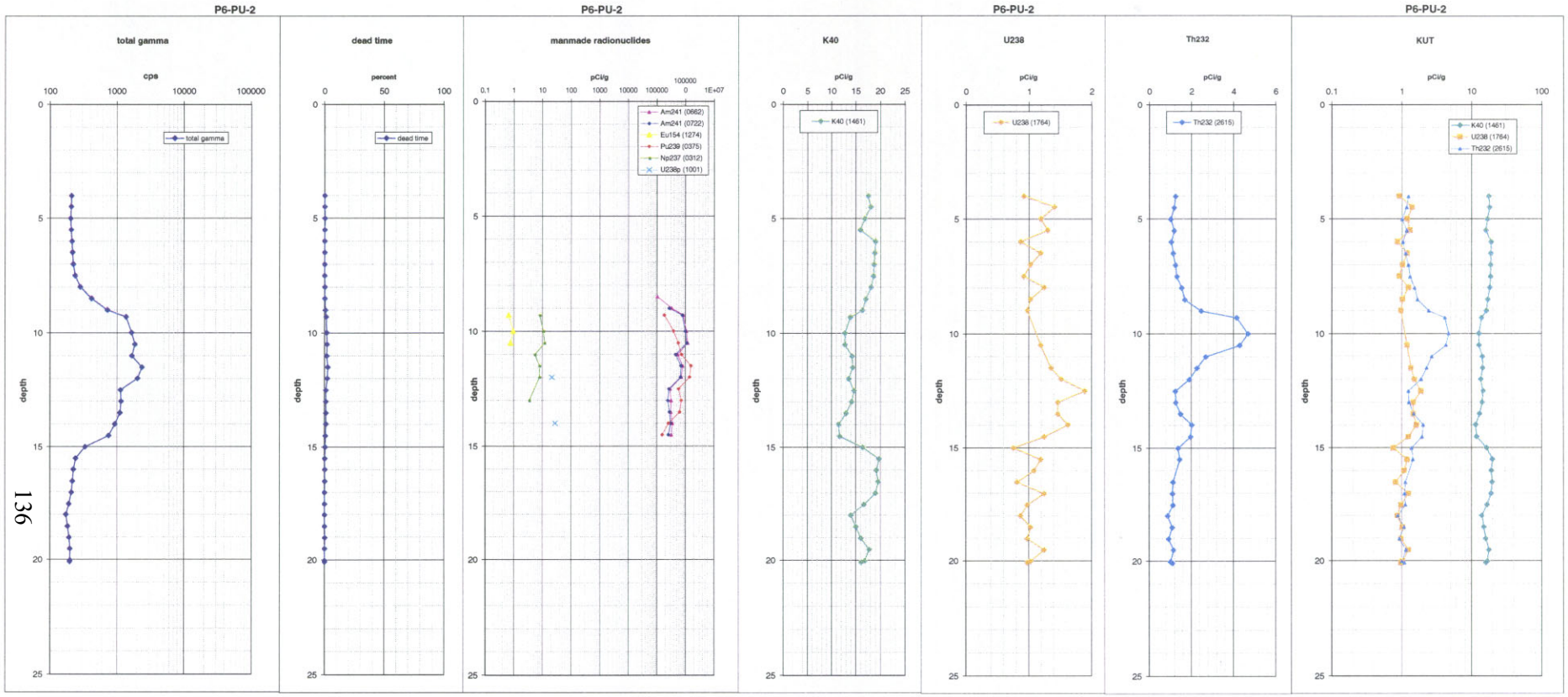
P6-PU-2
total gamma
cps
total gamma
dead time
percent
dead time
manmade radionuclides
pCi/g
Am241 (0662)
Am241 (0722)
Eu154 (1274)
Pu239 (0375)
Np237 (0312)
U238p (1001)
K40
pCi/g
K40 (1461)
U238
pCi/g
U238 (1764)
Th232
pCi/g
Th232 (2615)
KUT
pCi/g
K40 (1461)
U238 (1764)
Th232 (2615)
depth

P6-PU-2

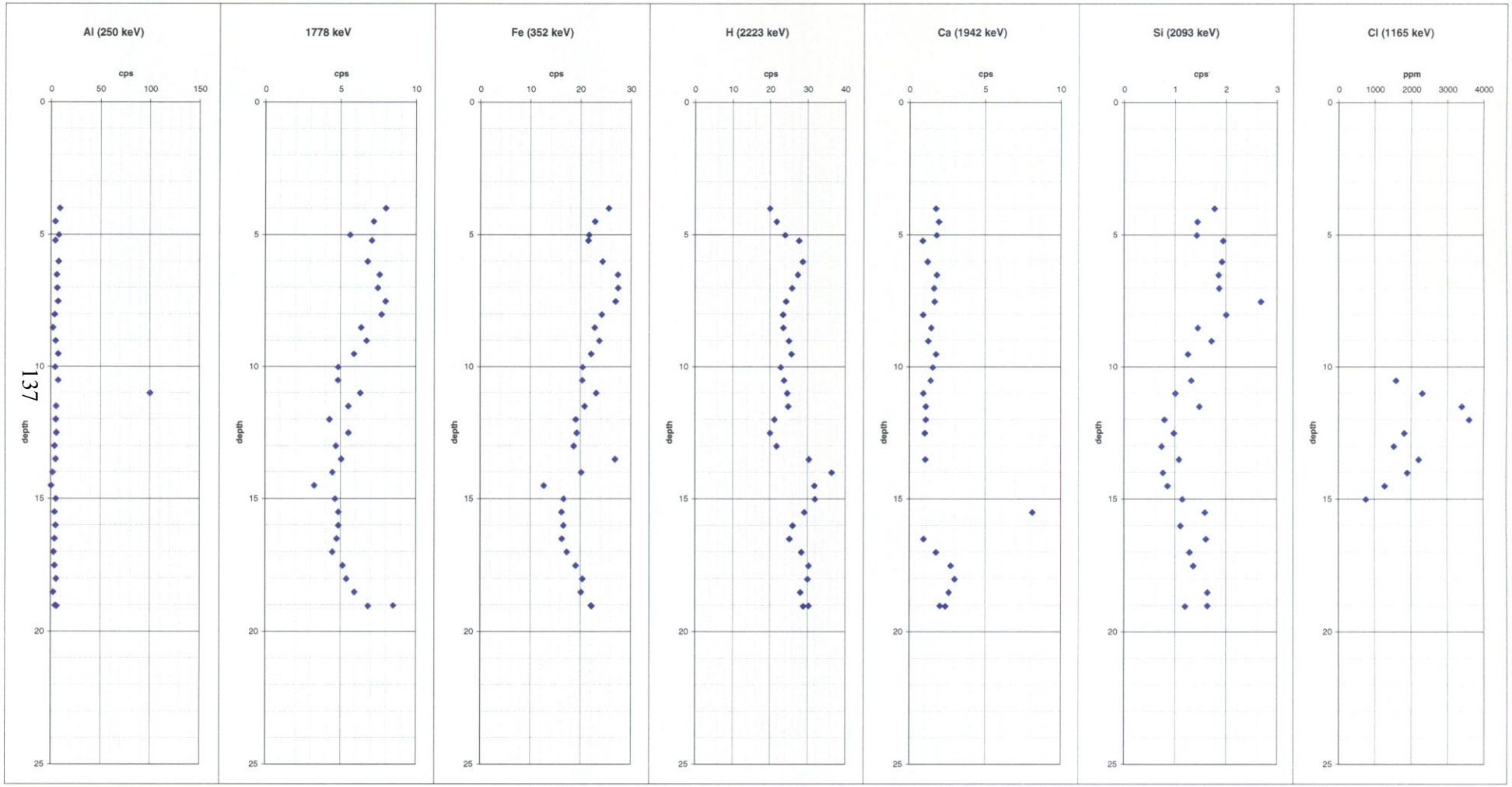
Al (250 keV)
1778 keV
Fe (352 keV)
H (2223 keV)
Ca (1942 keV)
Si (2093 keV)
Cl (1165 keV)
cps
ppm
depth

P6-PU-2 Total Gamma (9.0 ft to 14.0 ft)

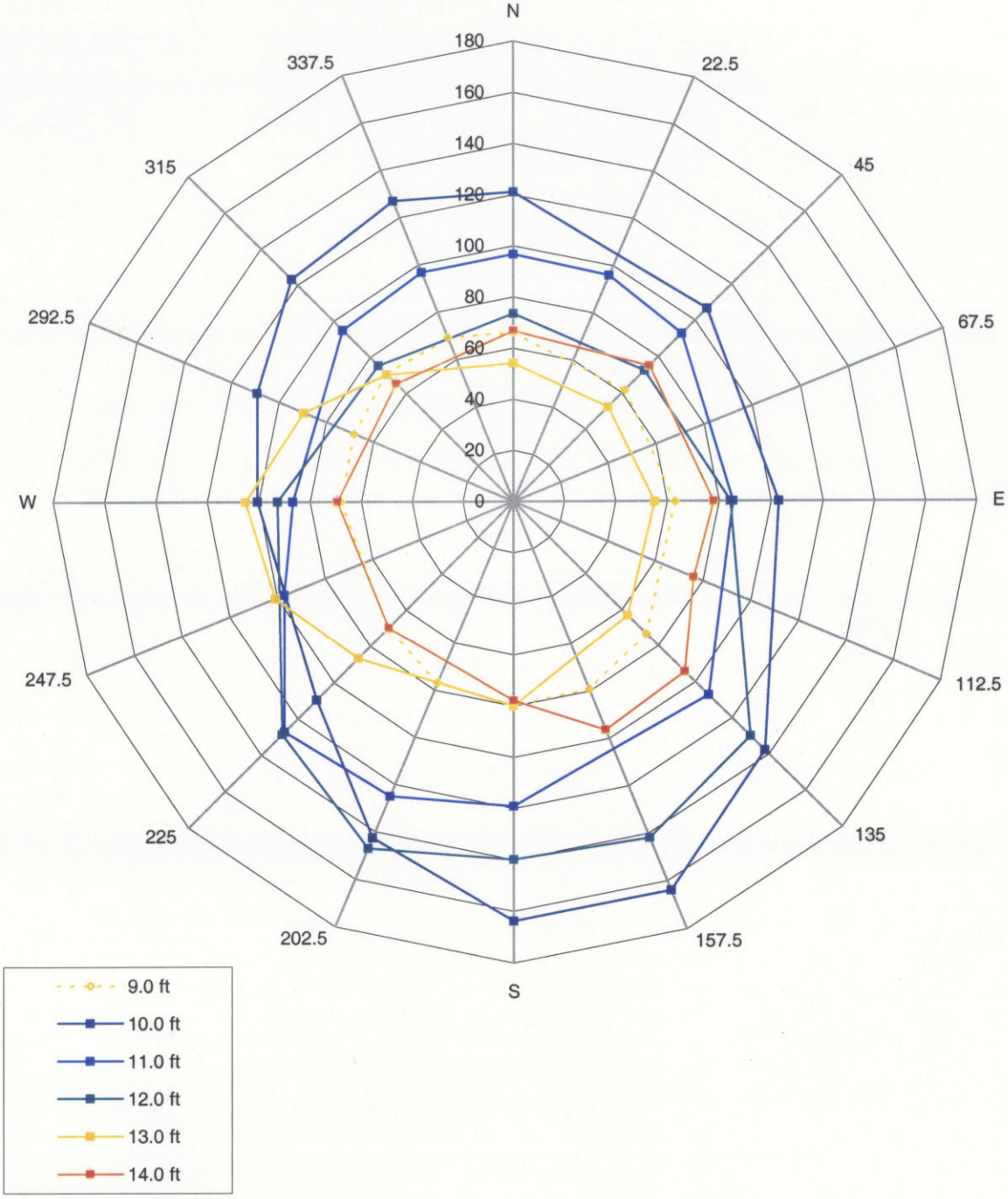

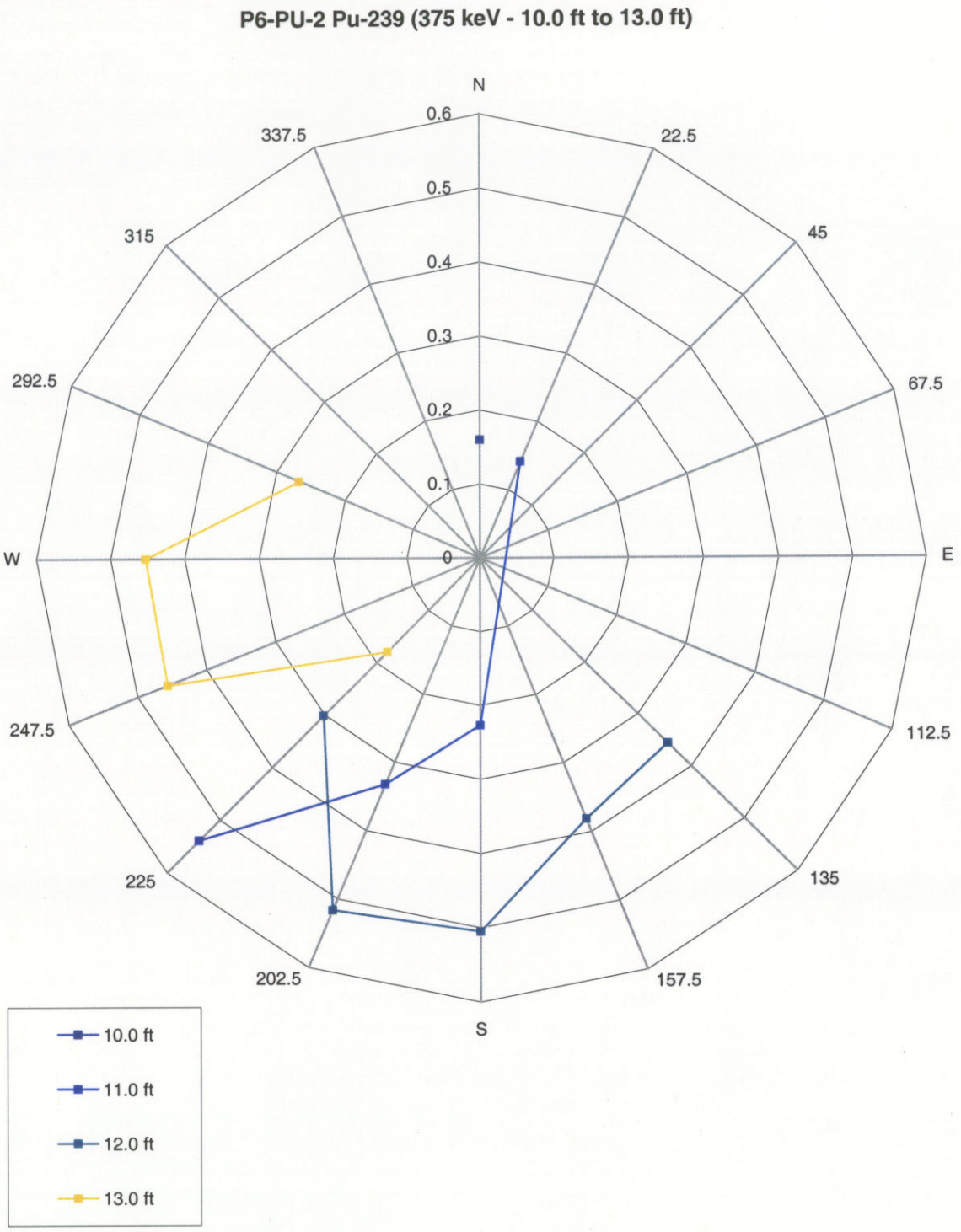
P6-PU-2 Pu-239 (375 keV - 10.0 ft to 13.0 ft)
N
22.5
45
67.5
E
112.5
135
157.5
S
202.5
225
247.5
W
292.5
315
337.5
0.6
0.5
0.4
0.3
0.2
0.1
0
10.0 ft
11.0 ft
12.0 ft
13.0 ft

P6-PU-2 Am-241 (662 keV - 10.0 ft and 14.0 ft)

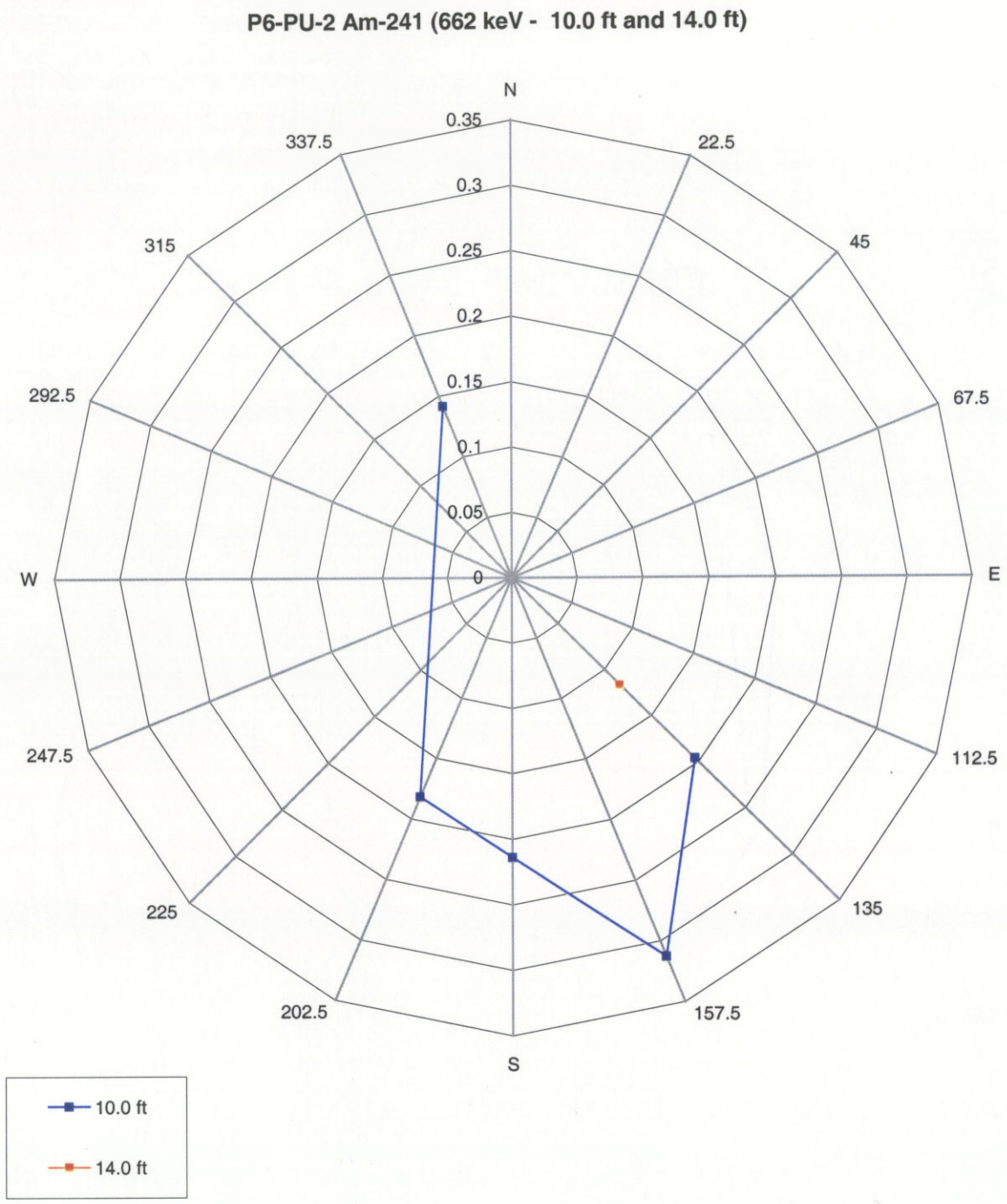

P6-PU-2 Long Count

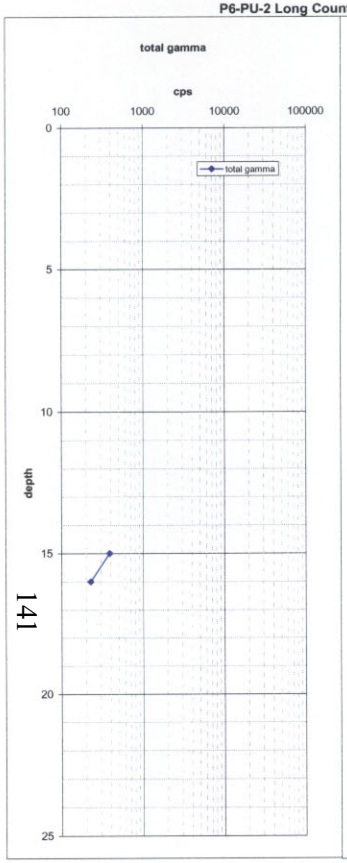

P6-PU-2 Long Count

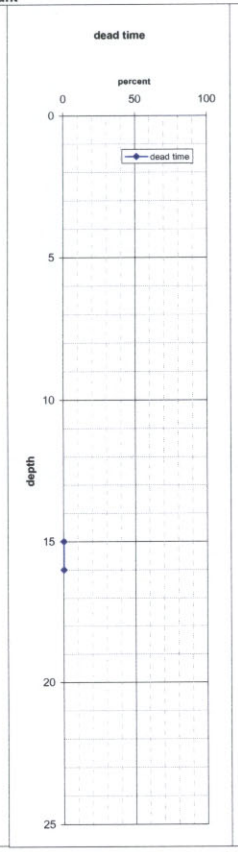

P6-PU-2 Long Count

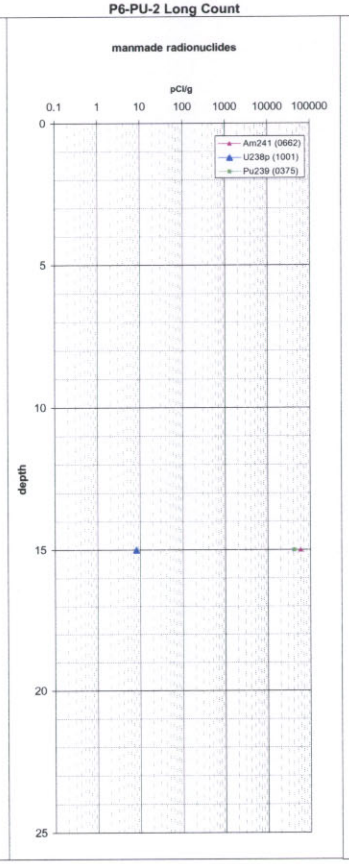

P6-PU-2 Long Count

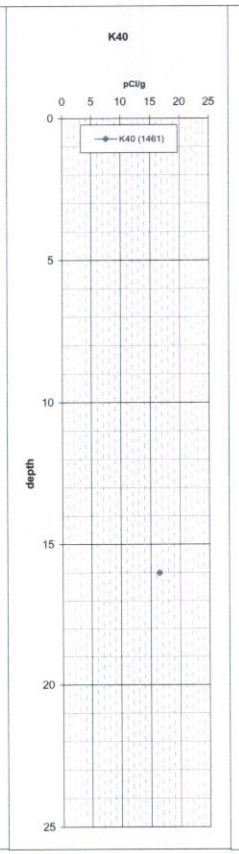

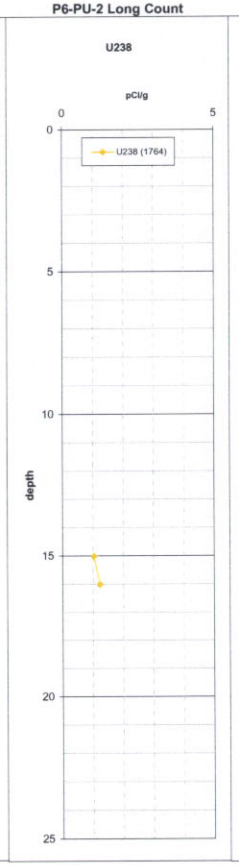

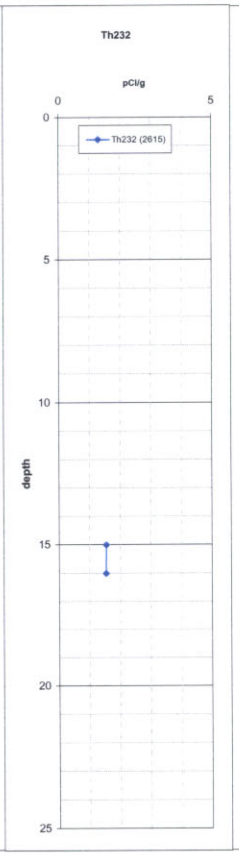

P6-PU-2 Long Count

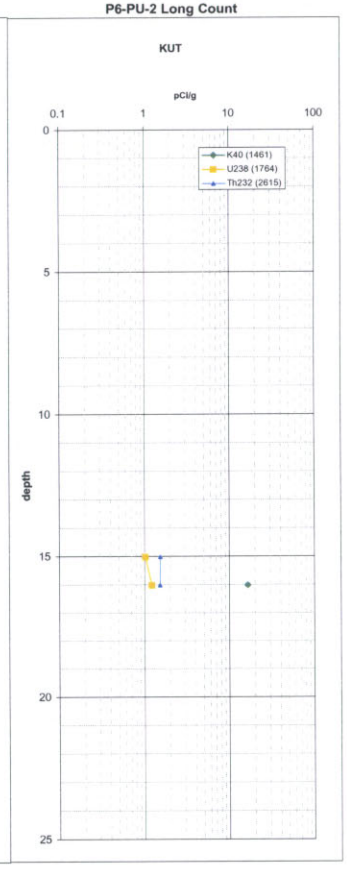

P6-PU-3

Neutron Log Response

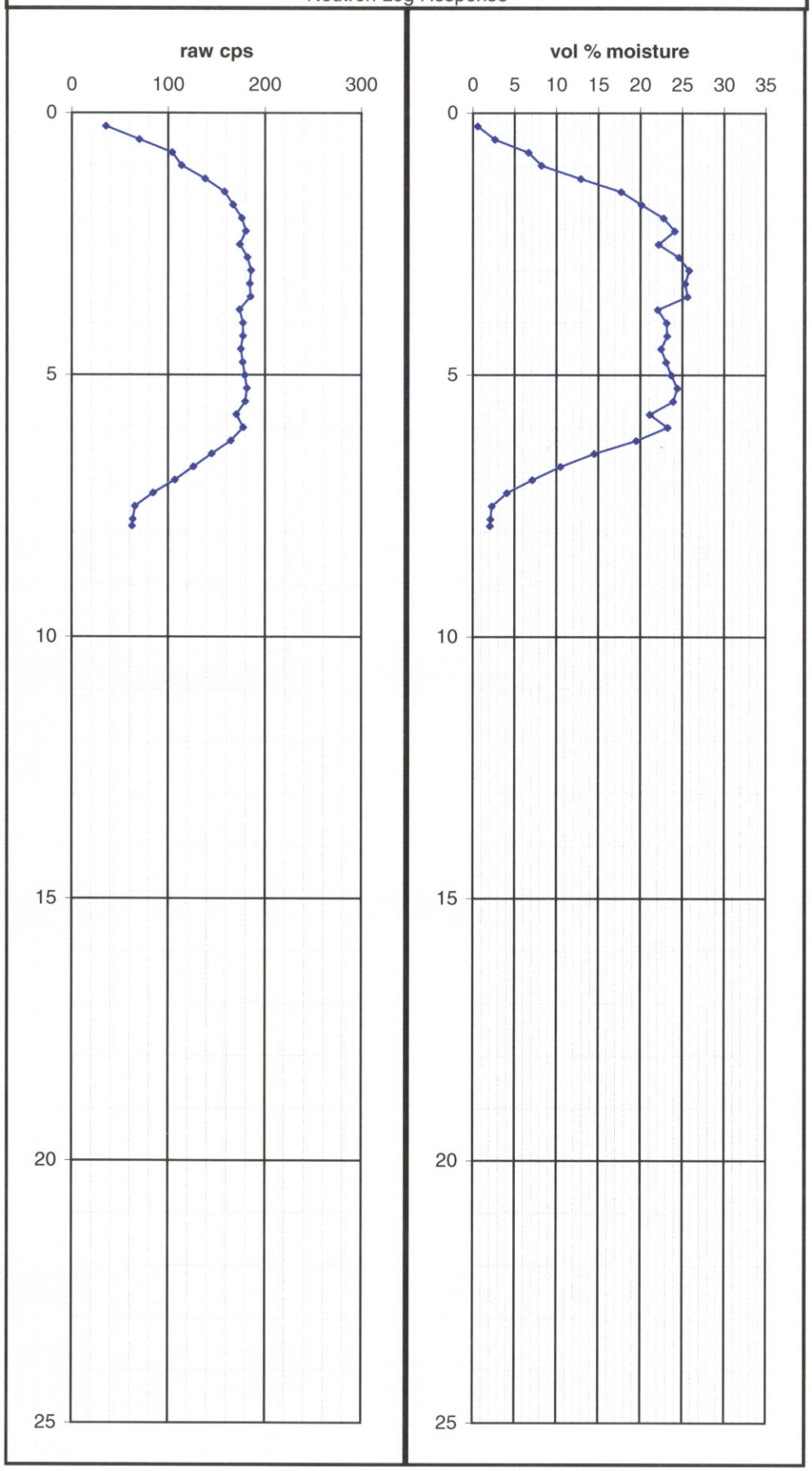

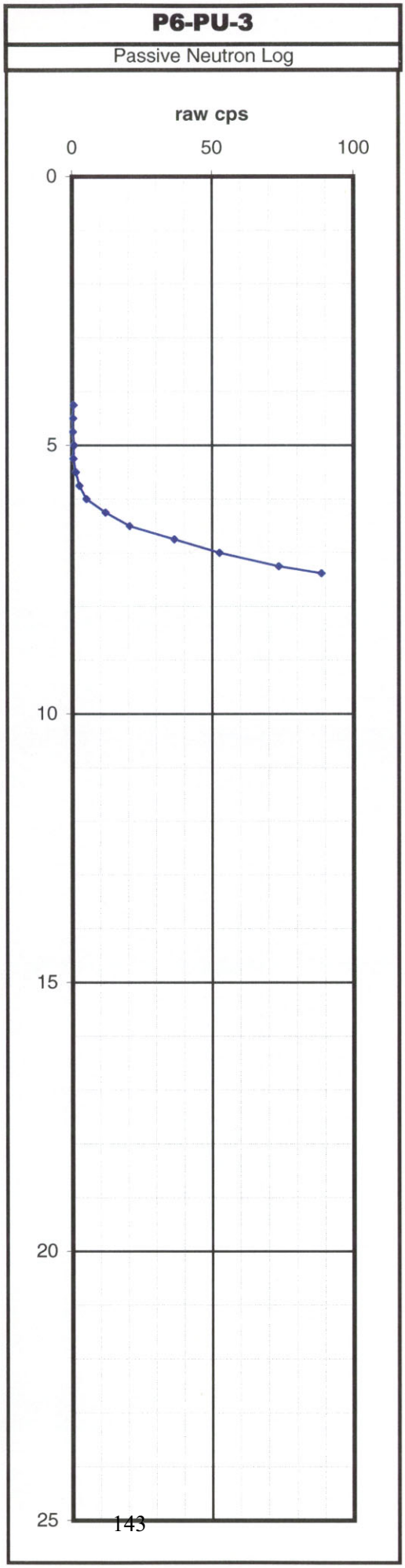
P6-PU-3
Passive Neutron Log
raw cps
0
50
100
0
5
10
15
20
25

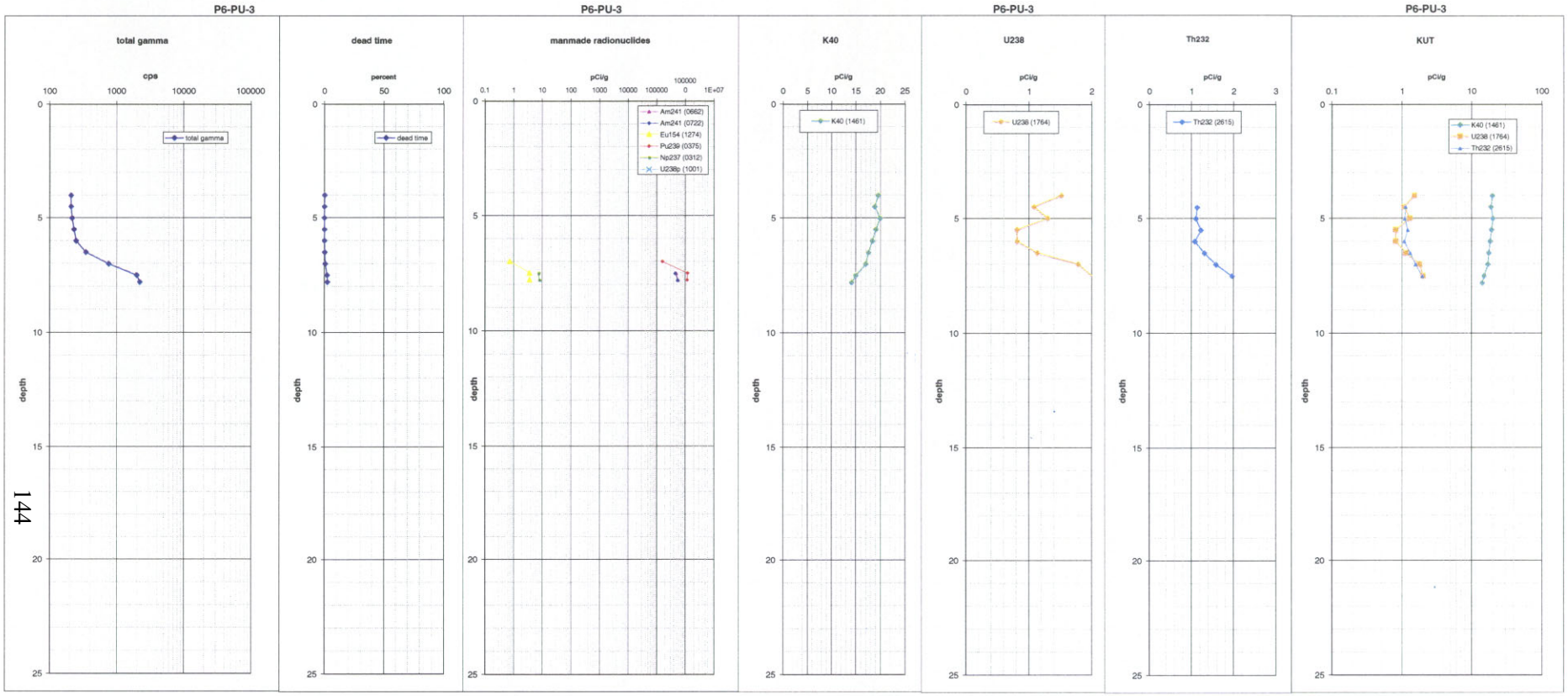
P6-PU-3
total gamma
cps
total gamma
dead time
percent
dead time
manmade radionuclides
pCi/g
Am241 (0662)
Am241 (0722)
Eu154 (1274)
Pu239 (0375)
Np237 (0312)
U238p (1001)
K40
pCi/g
K40 (1461)
U238
pCi/g
U238 (1764)
Th232
pCi/g
Th232 (2615)
KUT
pCi/g
K40 (1461)
U238 (1764)
Th232 (2615)
depth

P6-PU-3

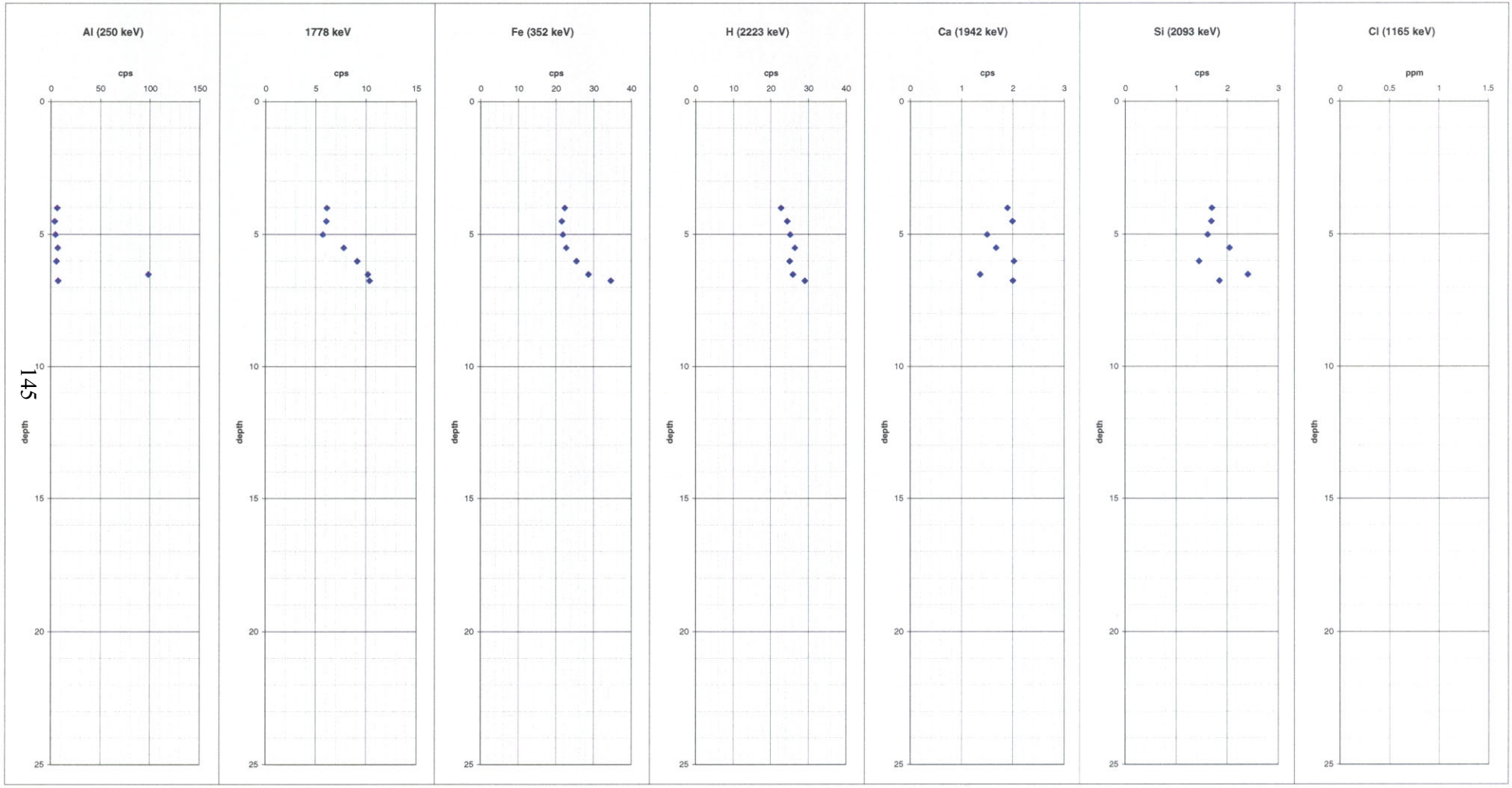
Al (250 keV)
1778 keV
Fe (352 keV)
H (2223 keV)
Ca (1942 keV)
Si (2093 keV)
Cl (1165 keV)
cps
ppm
depth

P6-PU-3 Total Gamma (7.74 ft)

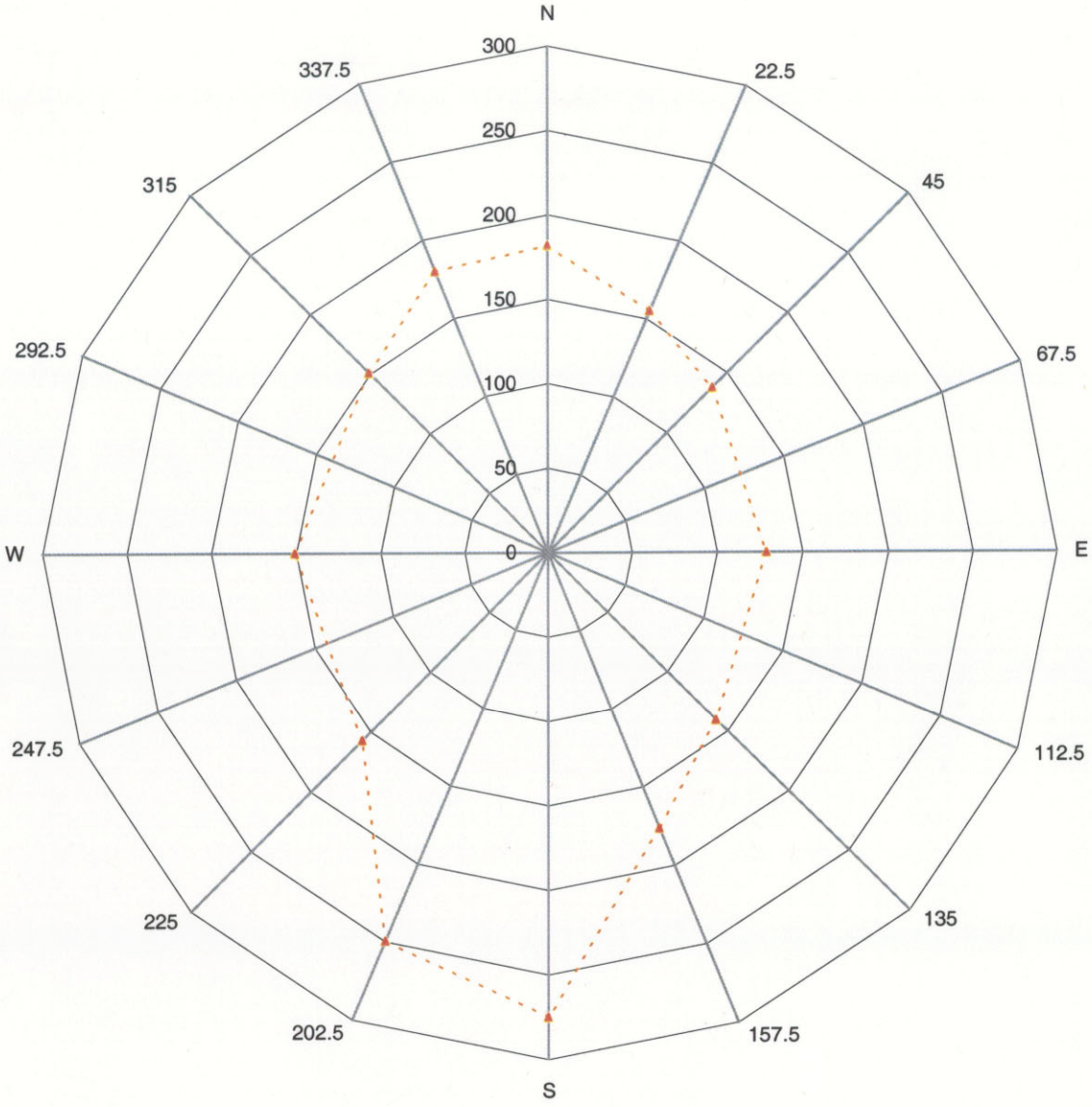

P6-PU-3 Pu-239 (375 keV - 7.74 ftt)

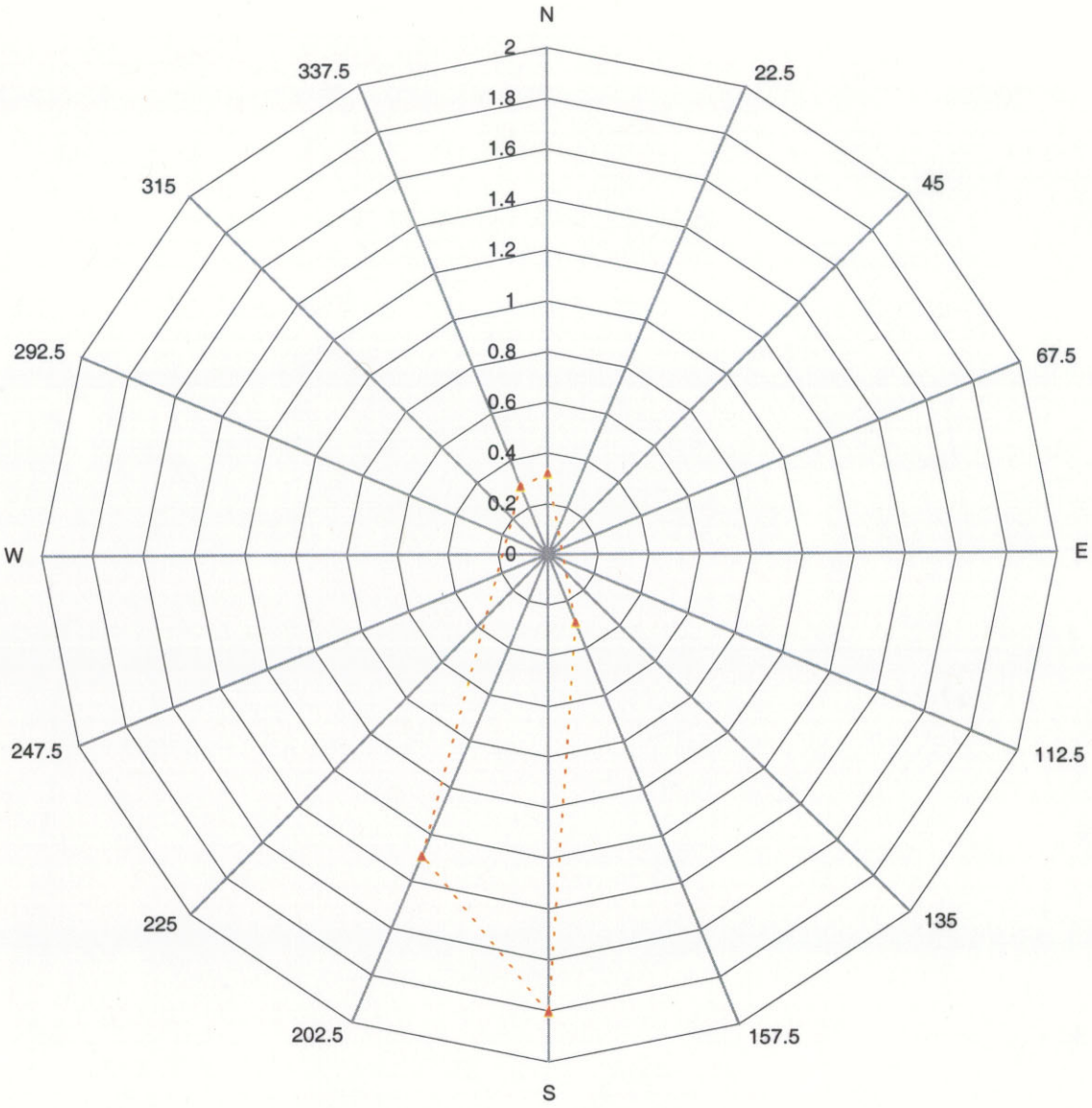

P6-PU-3 Np-237 (313 keV - 7.74 ftt)

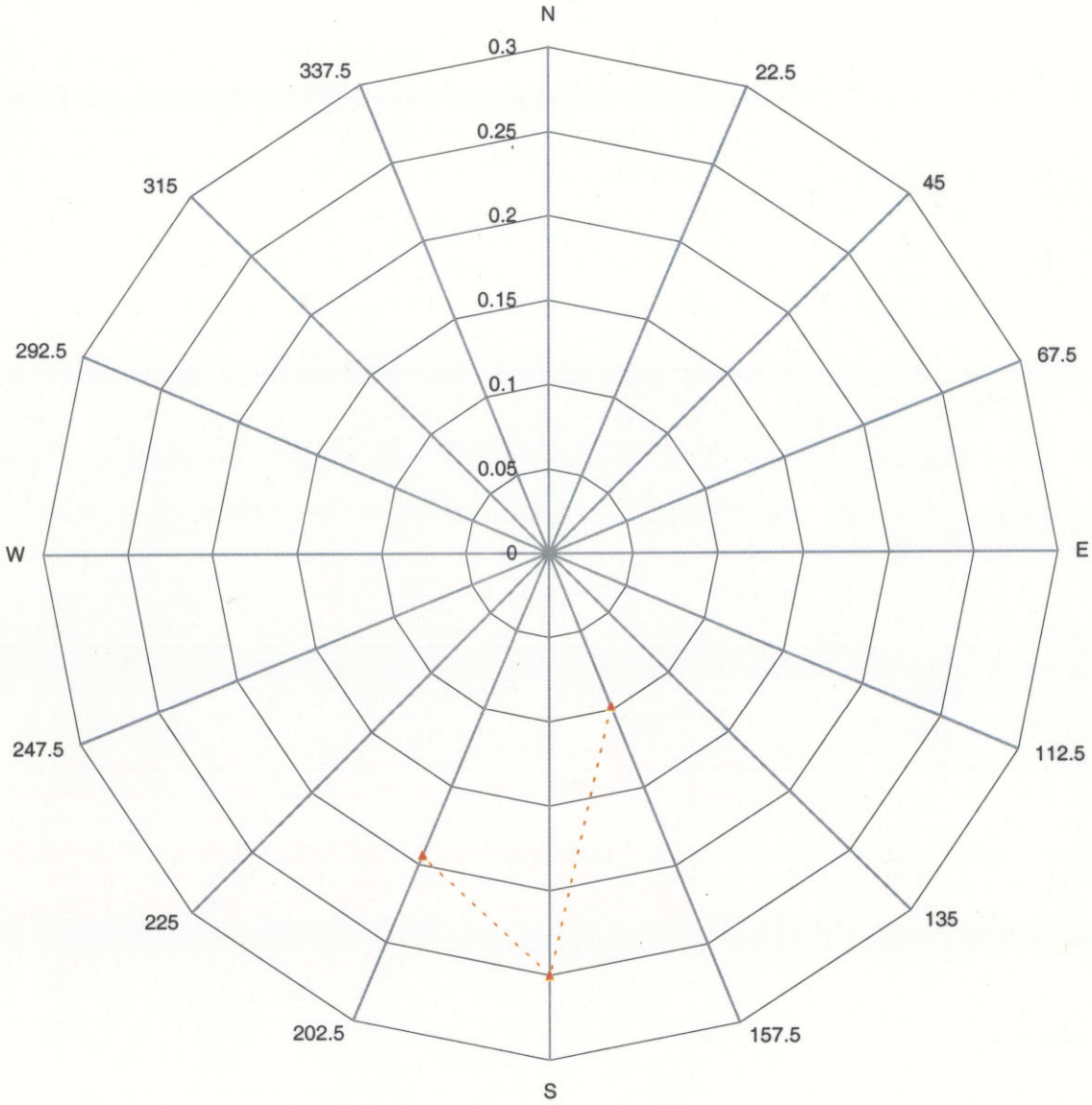

P10-PU-1

Neutron Log Response

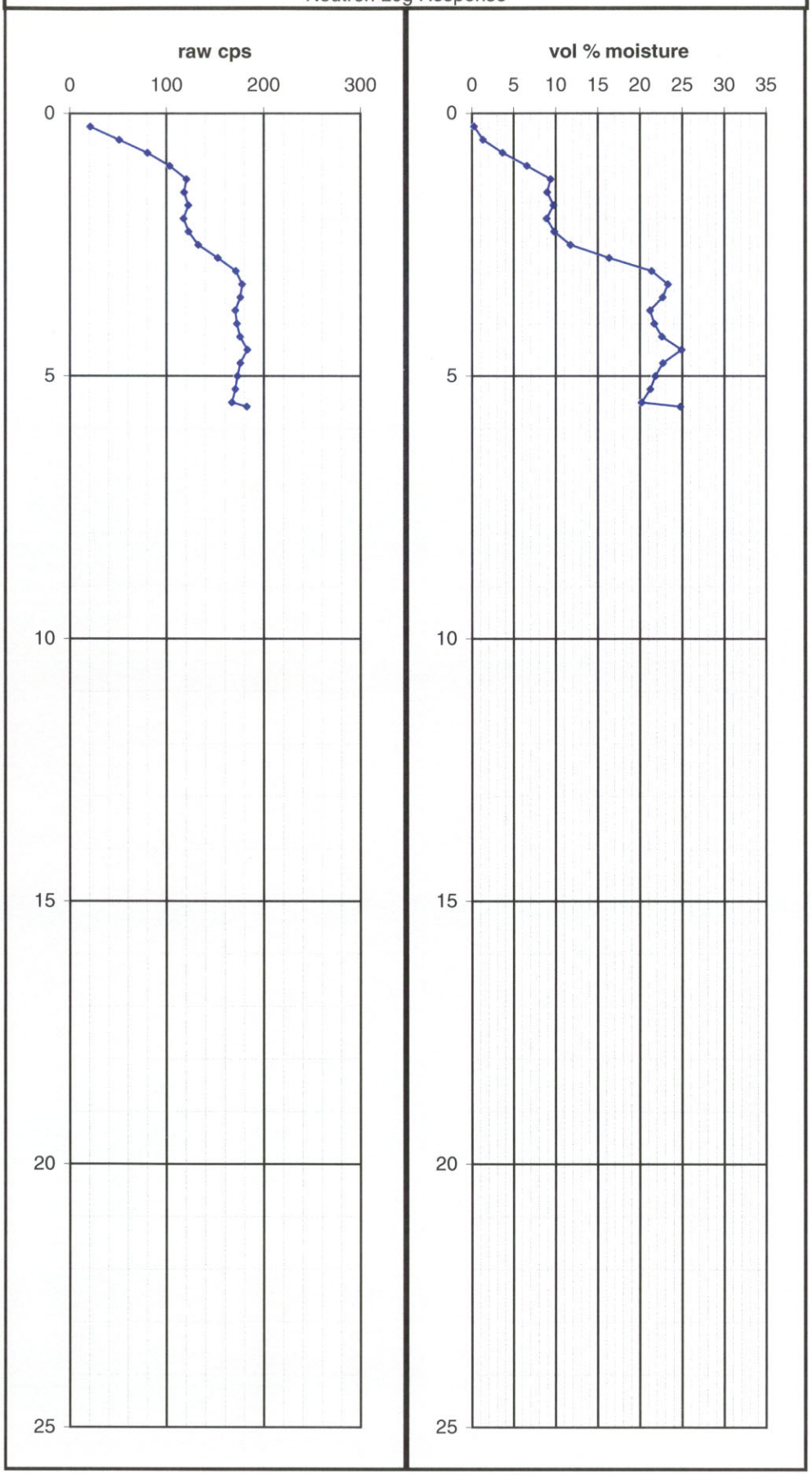

P10-PU-1

Passive Neutron Log

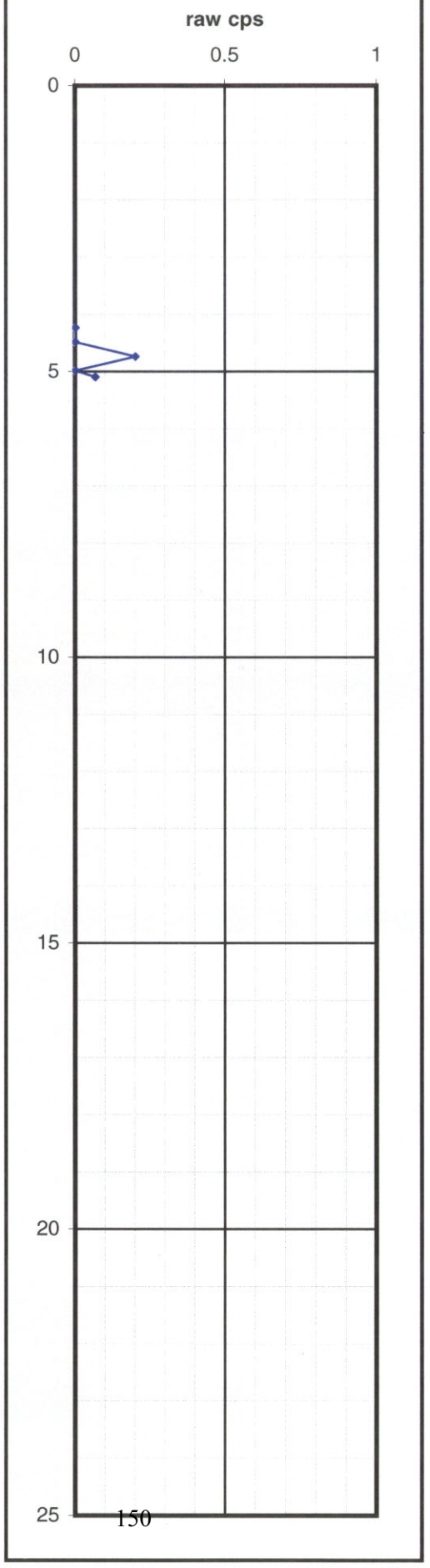

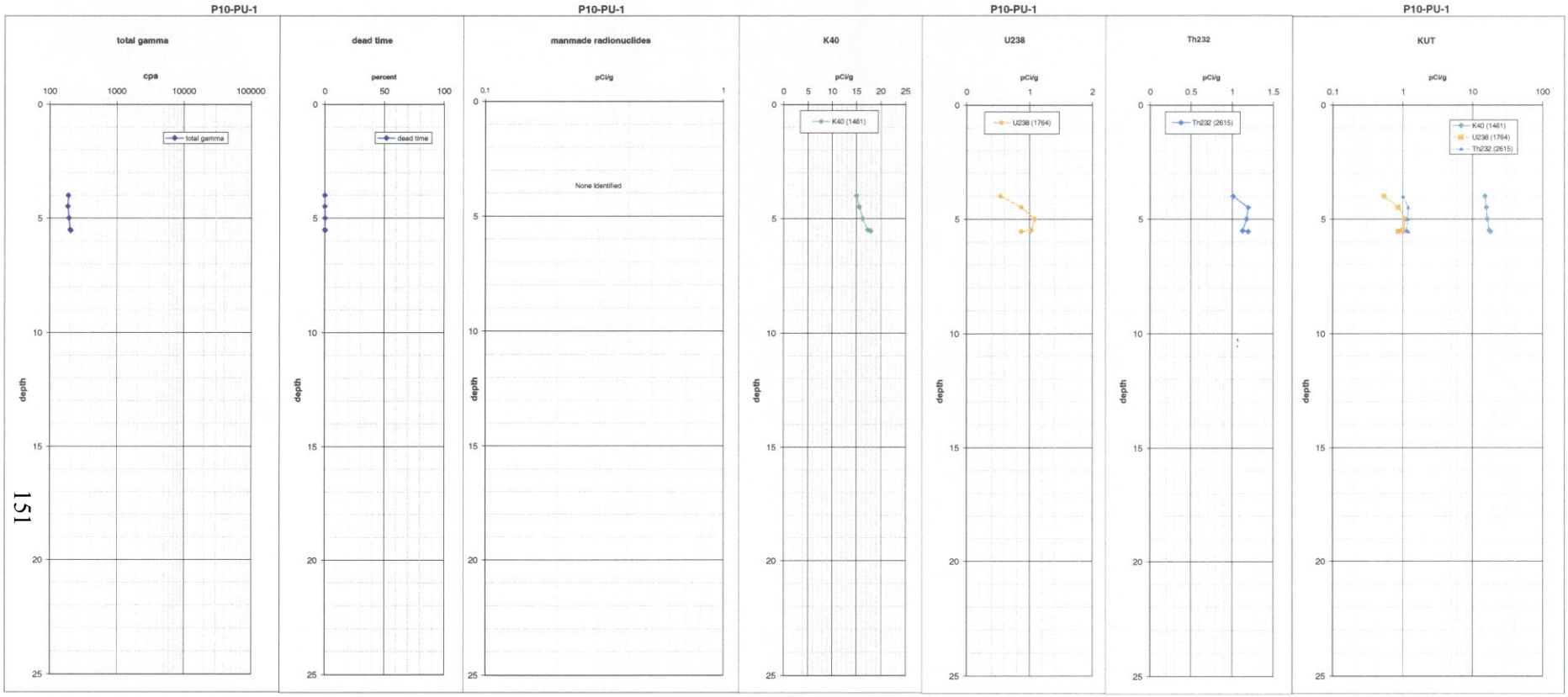
P10-PU-1
total gamma
cps
100
1000
10000
100000
total gamma
dead time
percent
0
50
100
dead time
manmade radionuclides
pCi/g
0.1
1
None Identified
K40
pCi/g
0
5
10
15
20
25
K40 (1461)
U238
pCi/g
0
1
2
U238 (1764)
Th232
pCi/g
0
0.5
1
1.5
Th232 (2615)
KUT
pCi/g
0.1
1
10
100
K40 (1461)
U238 (1764)
Th232 (2615)
depth
0
5
10
15
20
25

P10-PU-1

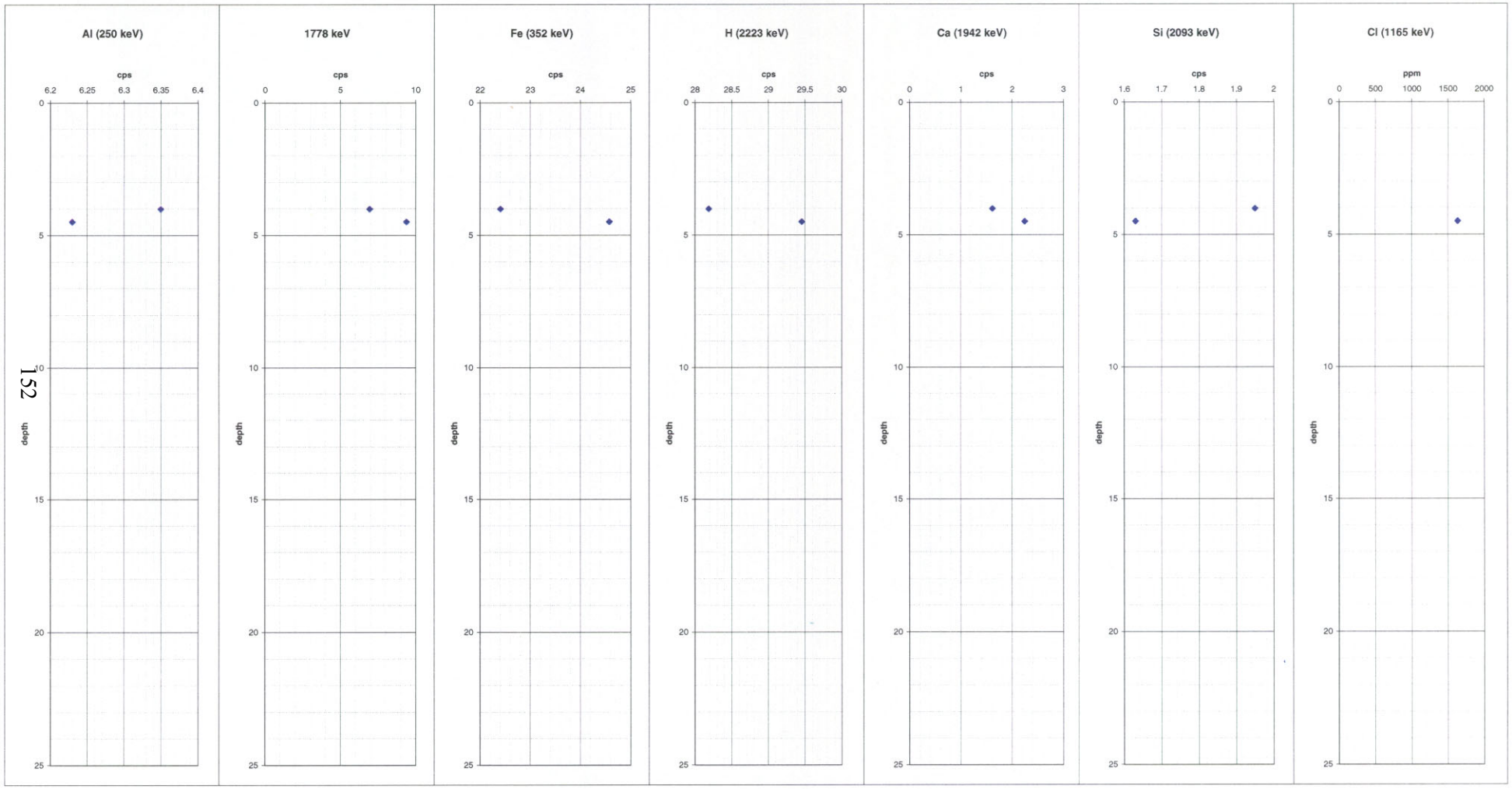
Al (250 keV)
cps
6.2 6.25 6.3 6.35 6.4
1778 keV
cps
0 5 10
Fe (352 keV)
cps
22 23 24 25
H (2223 keV)
cps
28 28.5 29 29.5 30
Ca (1942 keV)
cps
0 1 2 3
Si (2093 keV)
cps
1.6 1.7 1.8 1.9 2
Cl (1165 keV)
ppm
0 500 1000 1500 2000
depth
0 5 10 15 20 25

P10-PU-2

Neutron Log Response

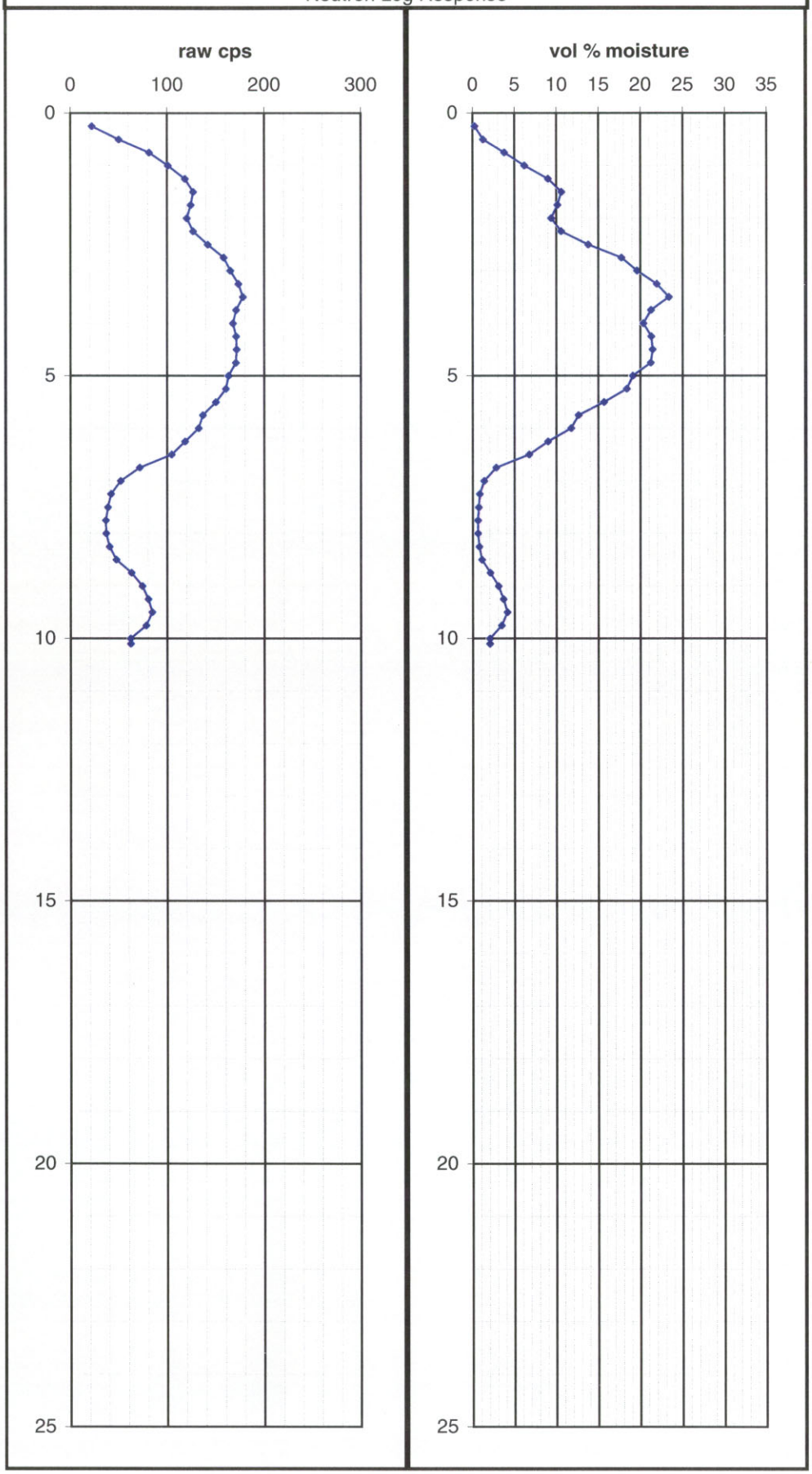

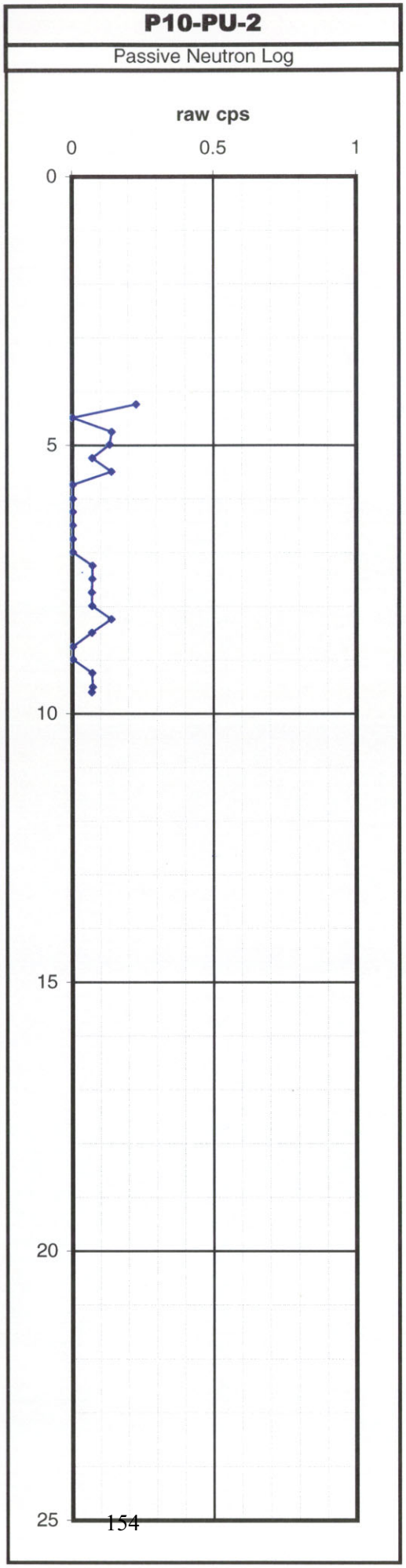
P10-PU-2
Passive Neutron Log
raw cps
0
0.5
1
0
5
10
15
20
25

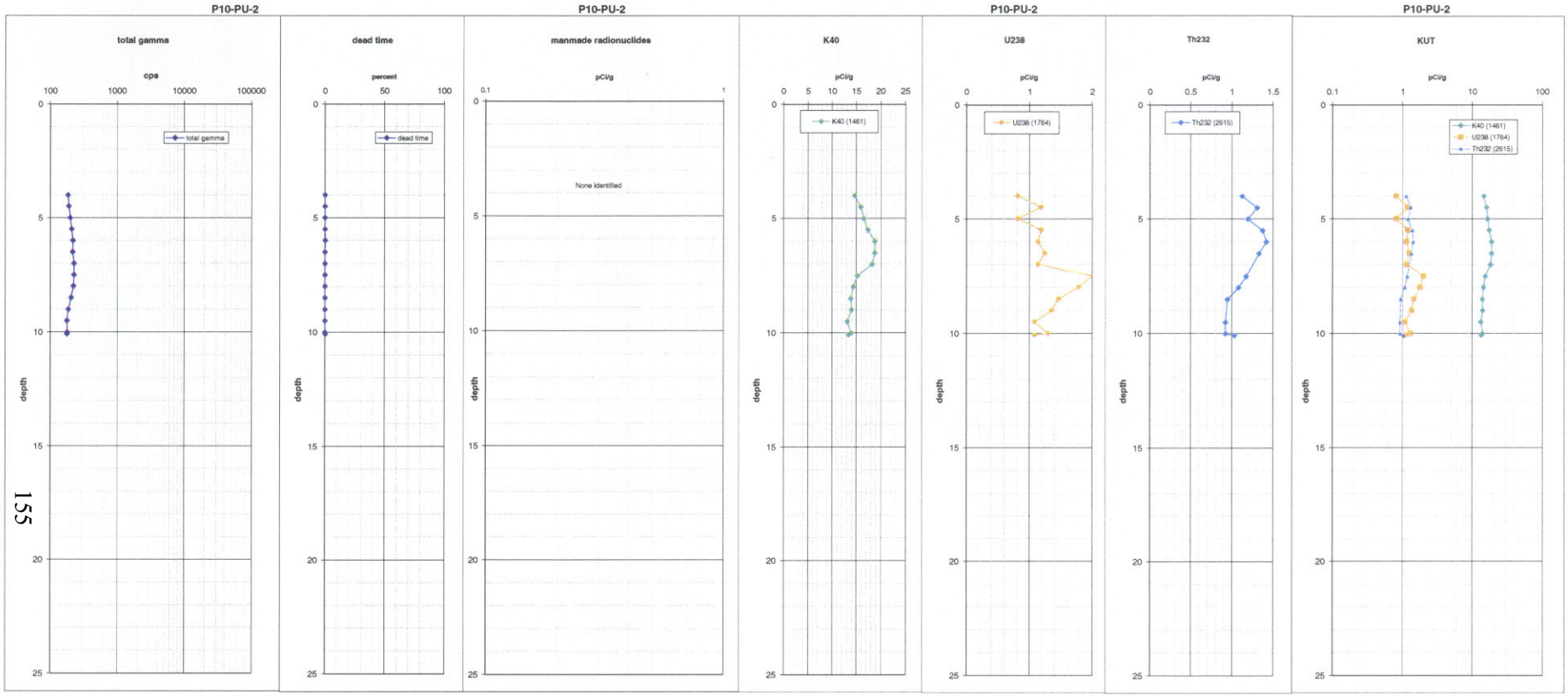
P10-PU-2
total gamma
cps
total gamma
dead time
percent
dead time
manmade radionuclides
pCi/g
None identified
K40
pCi/g
K40 (1461)
U238
pCi/g
U238 (1764)
Th232
pCi/g
Th232 (2615)
KUT
pCi/g
K40 (1461)
U238 (1764)
Th232 (2615)
depth

P10-PU-2

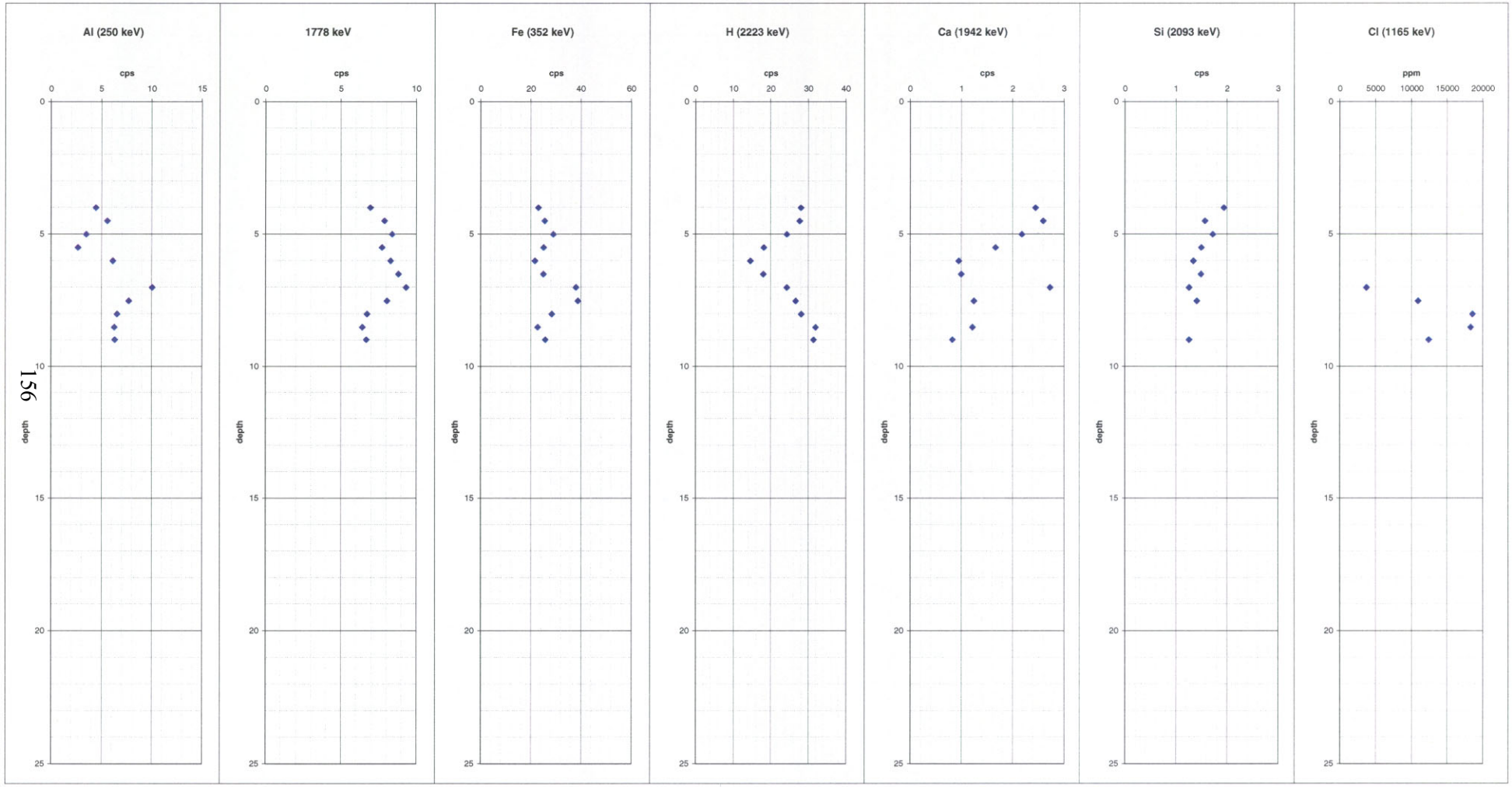
Al (250 keV)
1778 keV
Fe (352 keV)
H (2223 keV)
Ca (1942 keV)
Si (2093 keV)
Cl (1165 keV)
cps
ppm
depth

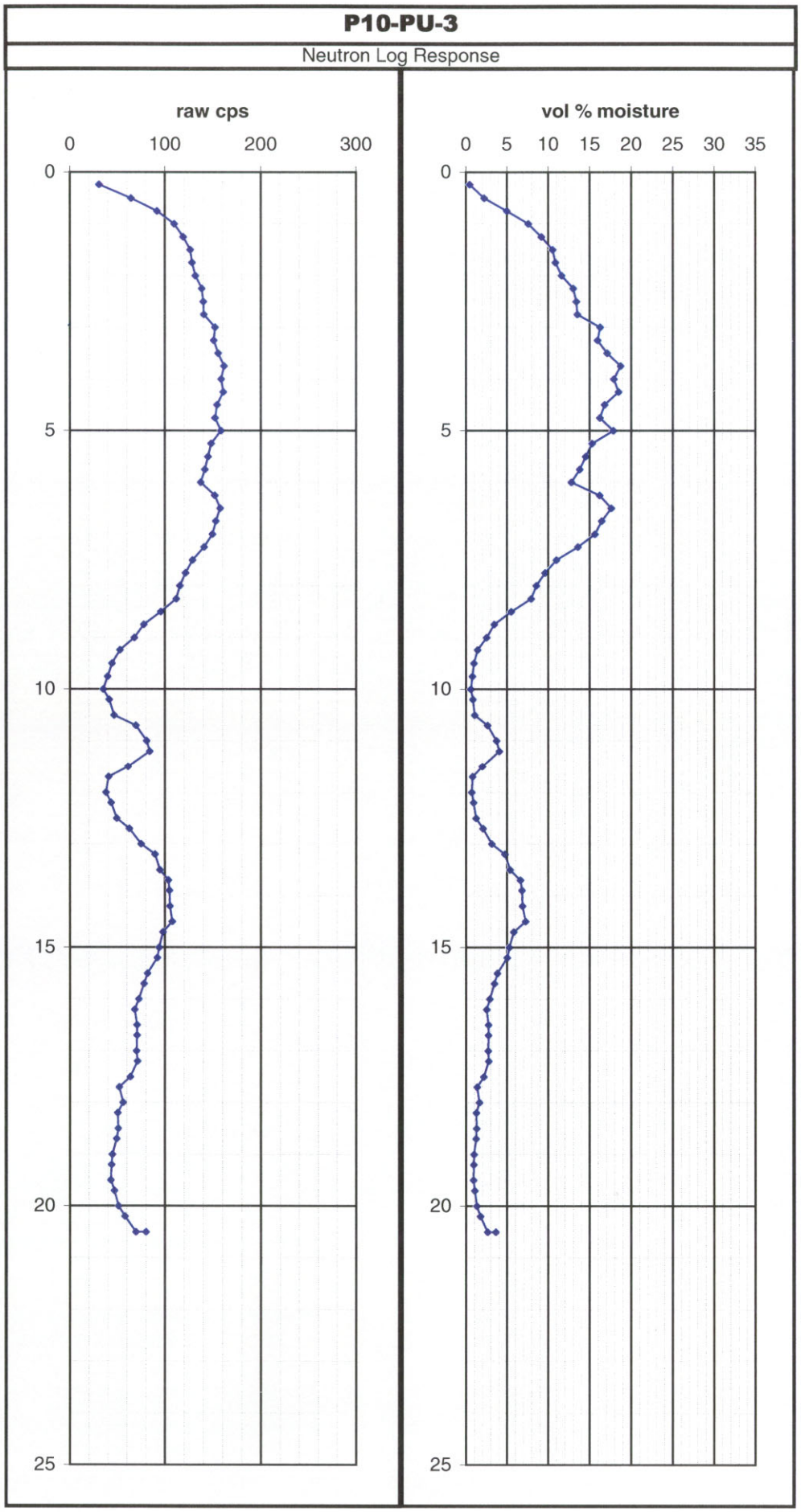
P10-PU-3
Neutron Log Response
raw cps
0
100
200
300
0
5
10
15
20
25
vol % moisture
0
5
10
15
20
25
30
35
0
5
10
15
20
25

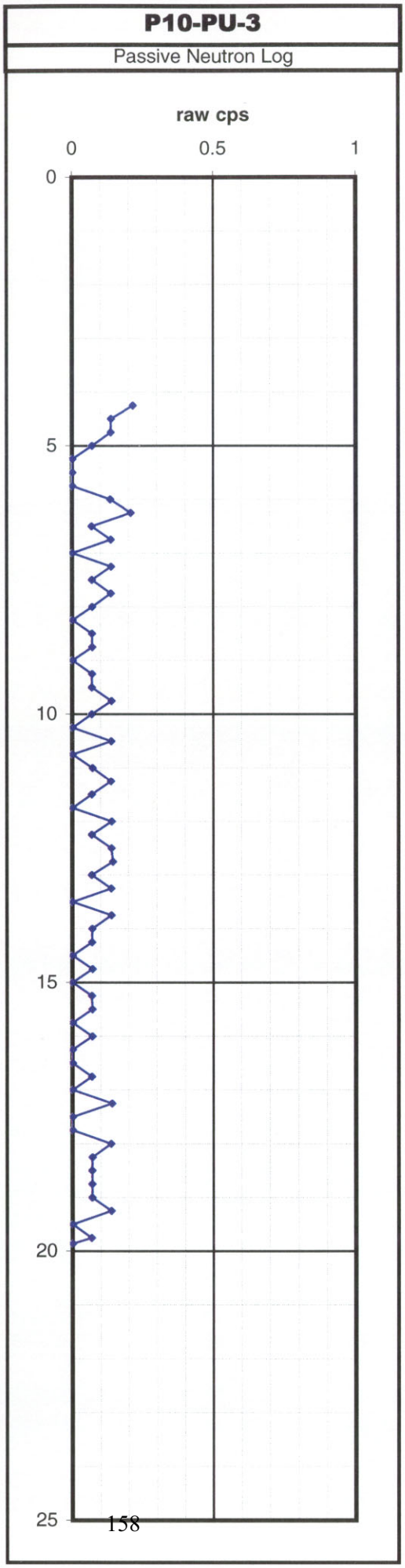
P10-PU-3
Passive Neutron Log
raw cps
0
0.5
1
0
5
10
15
20
25

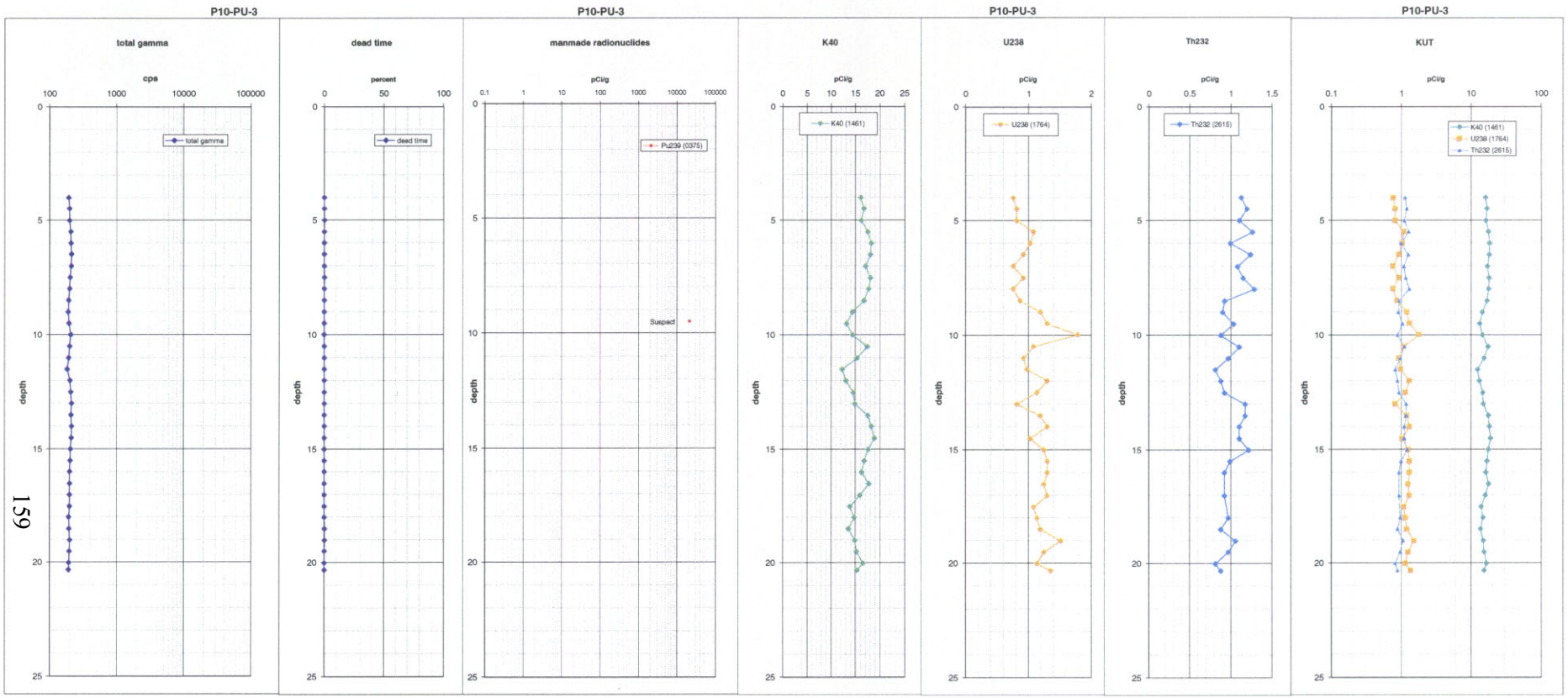
P10-PU-3
total gamma
cps
total gamma
dead time
percent
dead time
manmade radionuclides
pCi/g
Pu239 (0375)
Suspect
K40
pCi/g
K40 (1461)
U238
pCi/g
U238 (1764)
Th232
pCi/g
Th232 (2615)
KUT
pCi/g
K40 (1461)
U238 (1764)
Th232 (2615)
depth

P10-PU-3

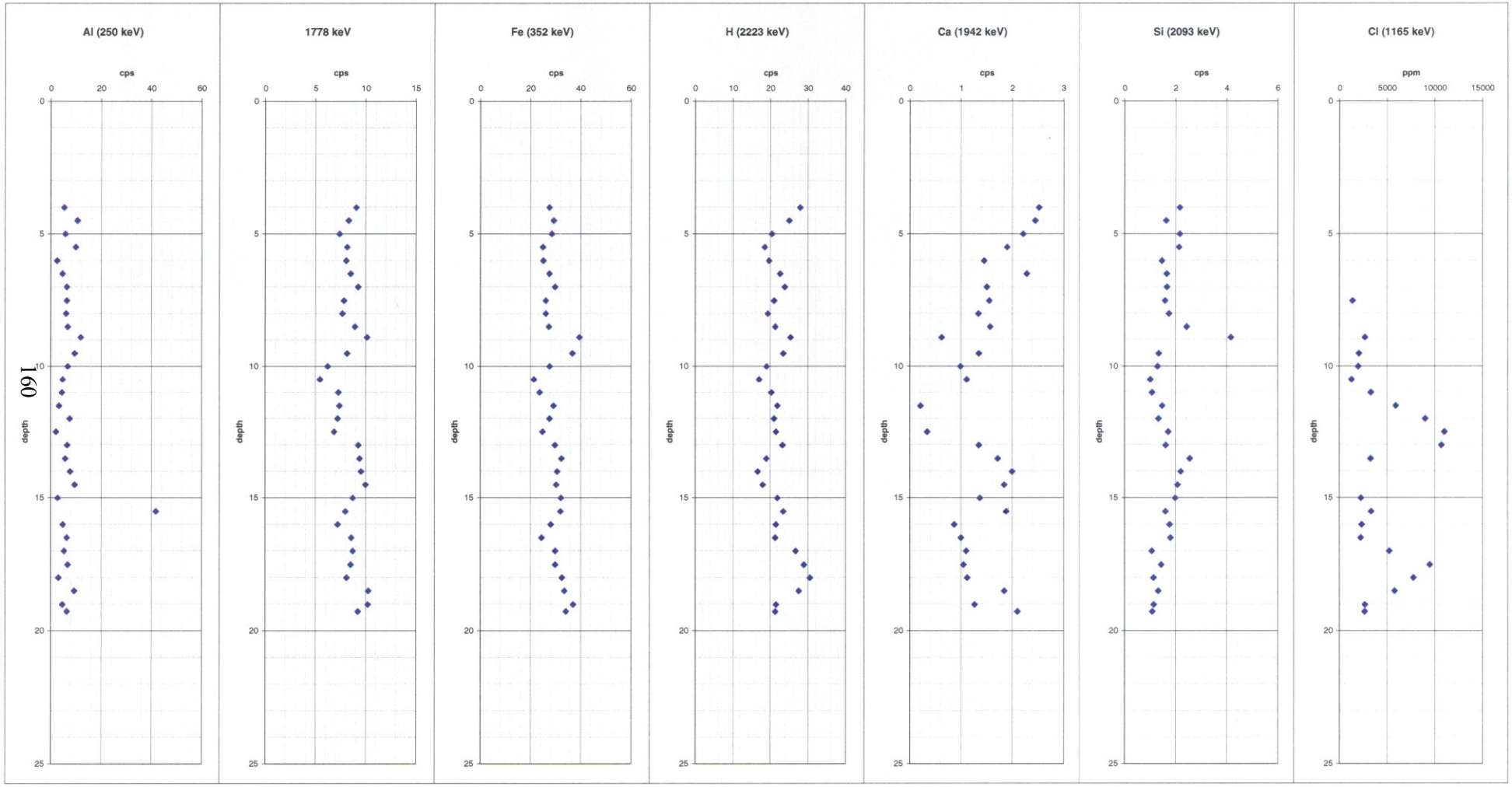
Al (250 keV)
1778 keV
Fe (352 keV)
H (2223 keV)
Ca (1942 keV)
Si (2093 keV)
Cl (1165 keV)
cps
ppm
depth

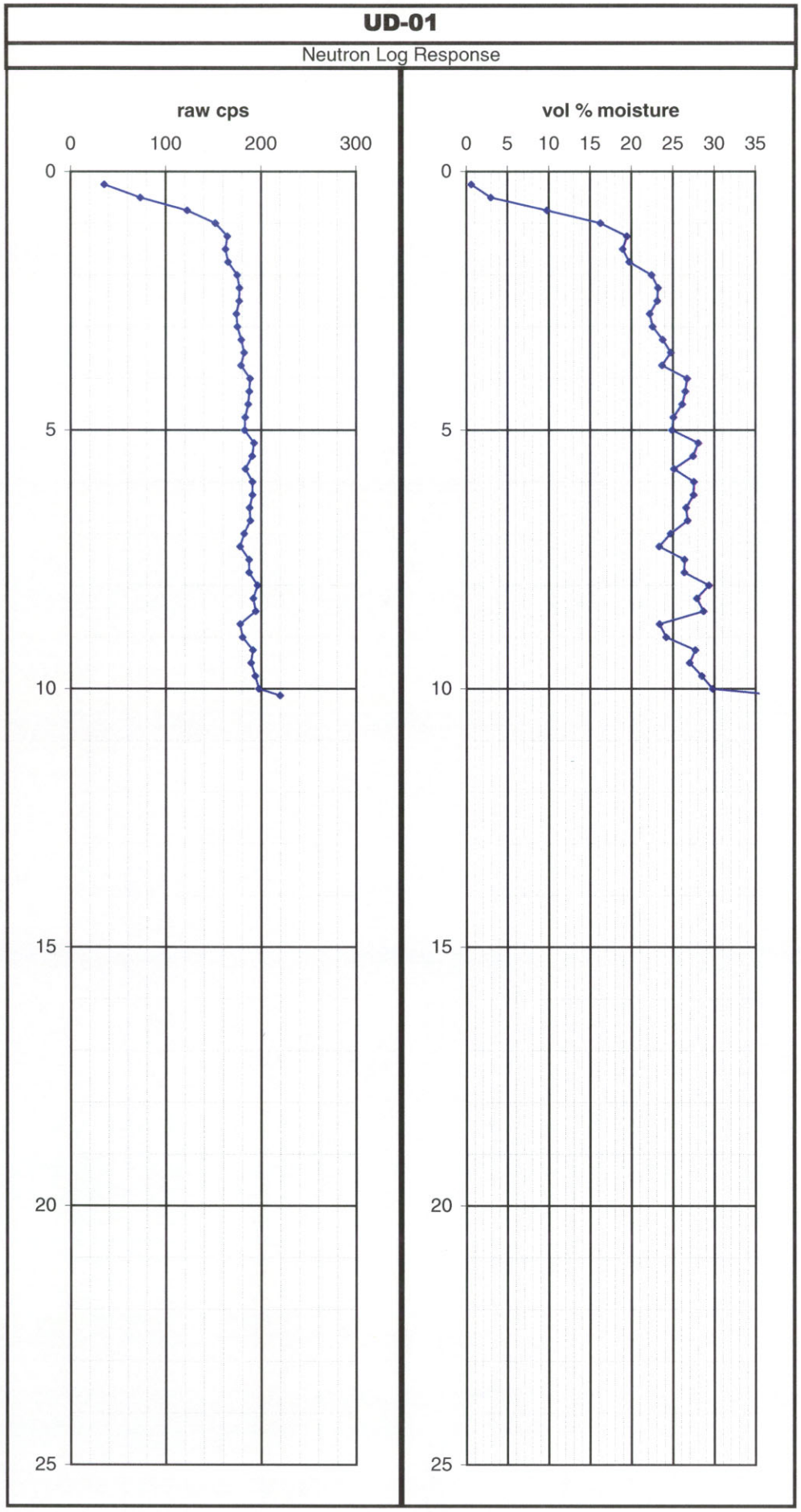
UD-01
Neutron Log Response
raw cps
0
100
200
300
vol % moisture
0
5
10
15
20
25
30
35
0
5
10
15
20
25

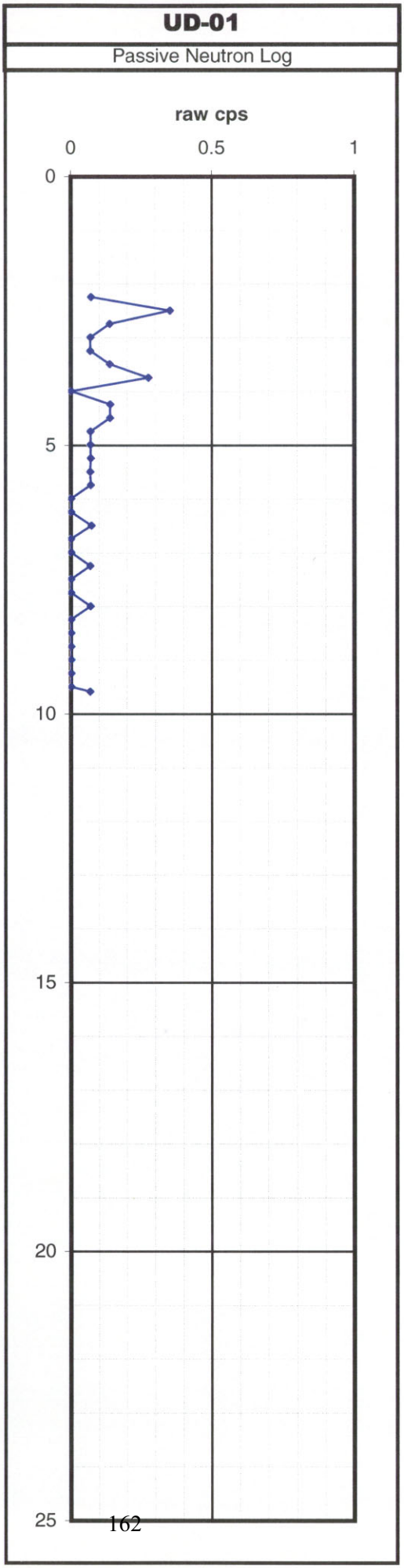
UD-01
Passive Neutron Log
raw cps
0
0.5
1
0
5
10
15
20
25

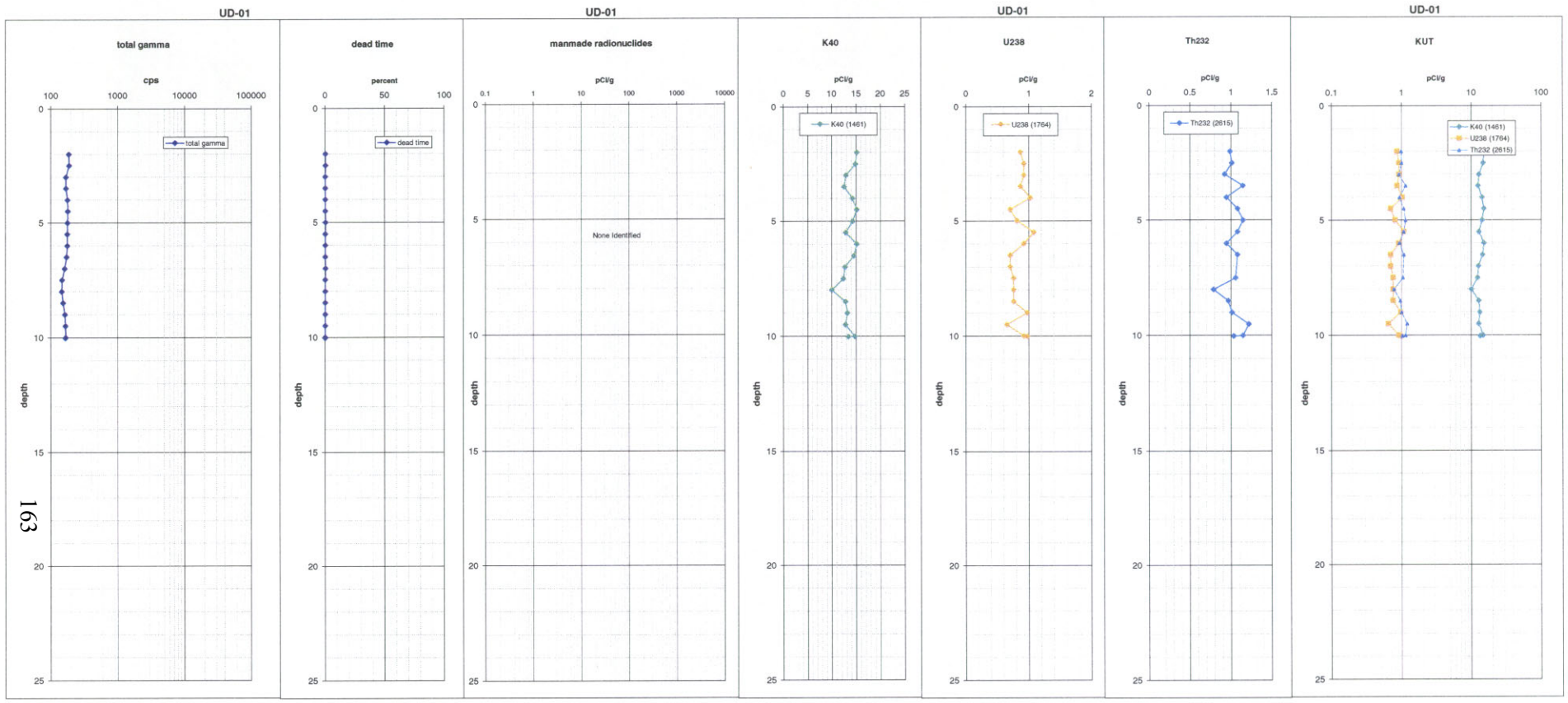
UD-01
total gamma
cps
100
1000
10000
100000
total gamma
depth
UD-01
dead time
percent
0
50
100
dead time
depth
UD-01
manmade radionuclides
pCi/g
0.1
1
10
100
1000
10000
None Identified
depth
UD-01
K40
pCi/g
0
5
10
15
20
25
K40 (1461)
depth
UD-01
U238
pCi/g
0
1
2
U238 (1764)
depth
UD-01
Th232
pCi/g
0
0.5
1
1.5
Th232 (2615)
depth
UD-01
KUT
pCi/g
0.1
1
10
100
K40 (1461)
U238 (1764)
Th232 (2615)
depth
0
5
10
15
20
25

UD-01

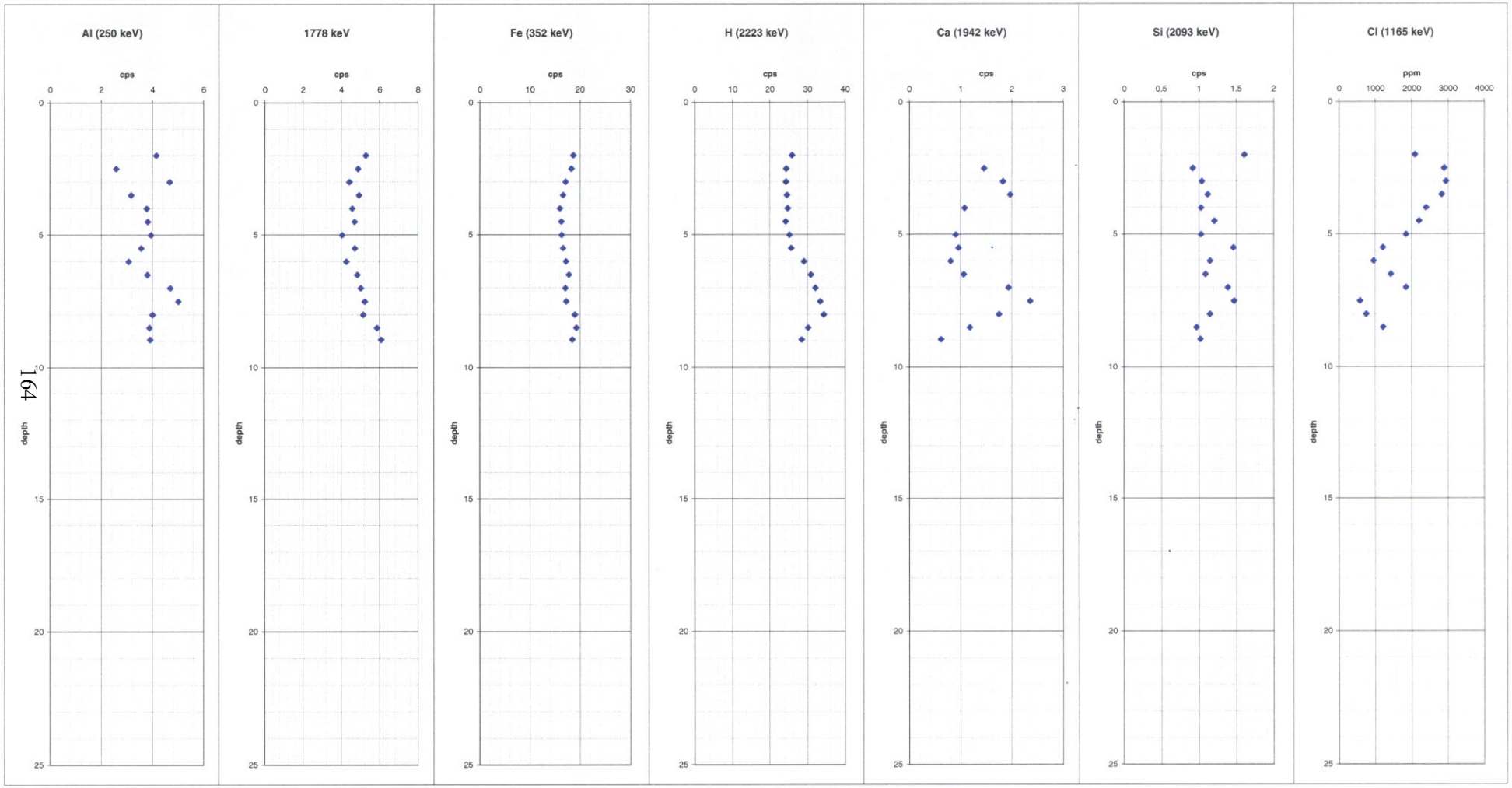
Al (250 keV)
1778 keV
Fe (352 keV)
H (2223 keV)
Ca (1942 keV)
Si (2093 keV)
Cl (1165 keV)
cps
ppm
depth

UD-03

Neutron Log Response

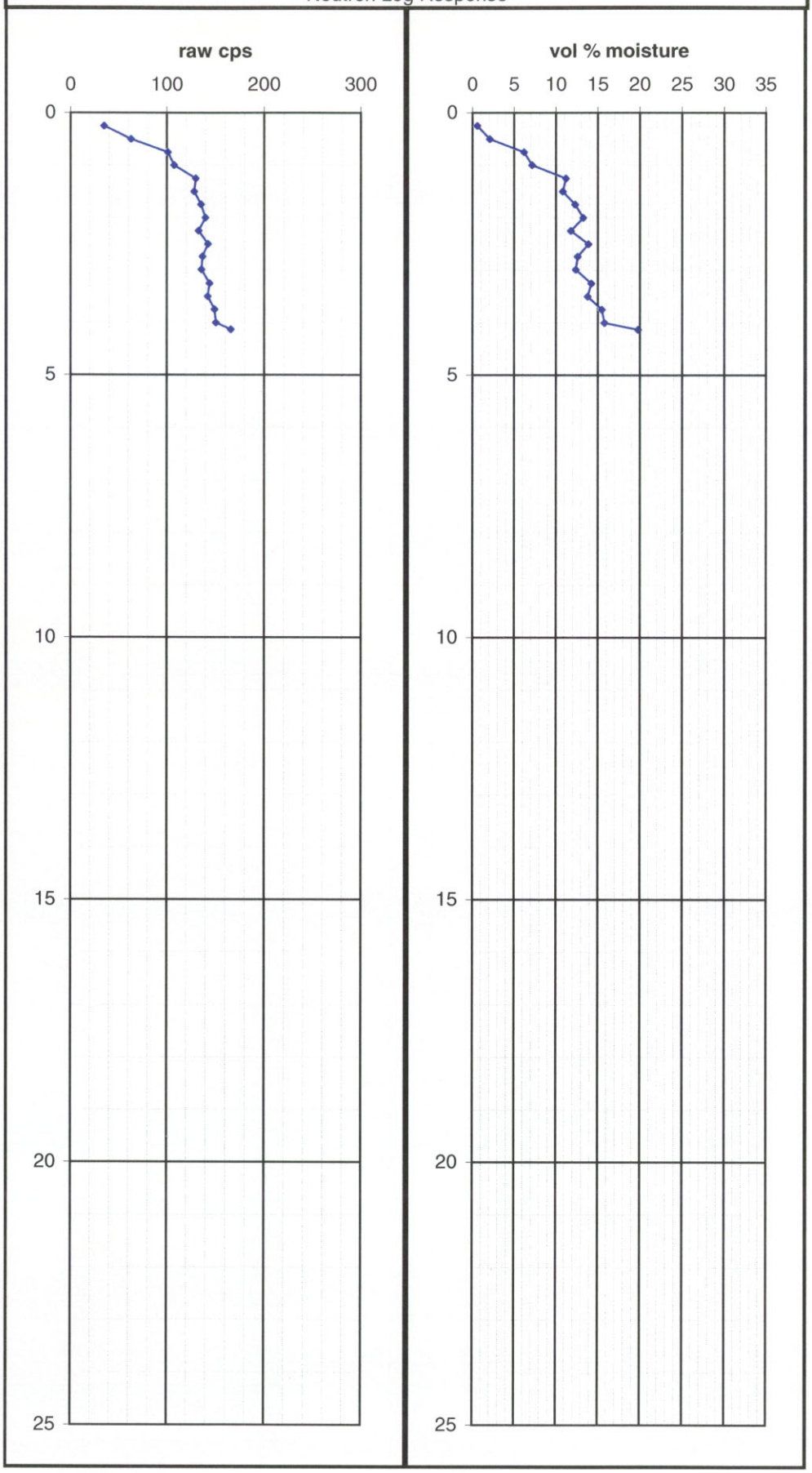

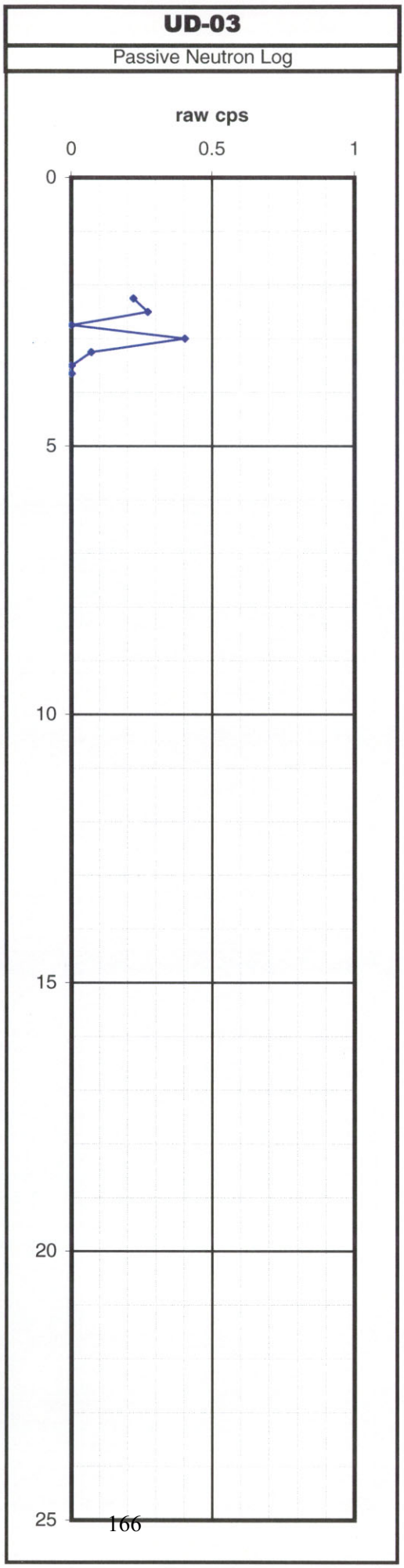
UD-03
Passive Neutron Log
raw cps
0
0.5
1
0
5
10
15
20
25

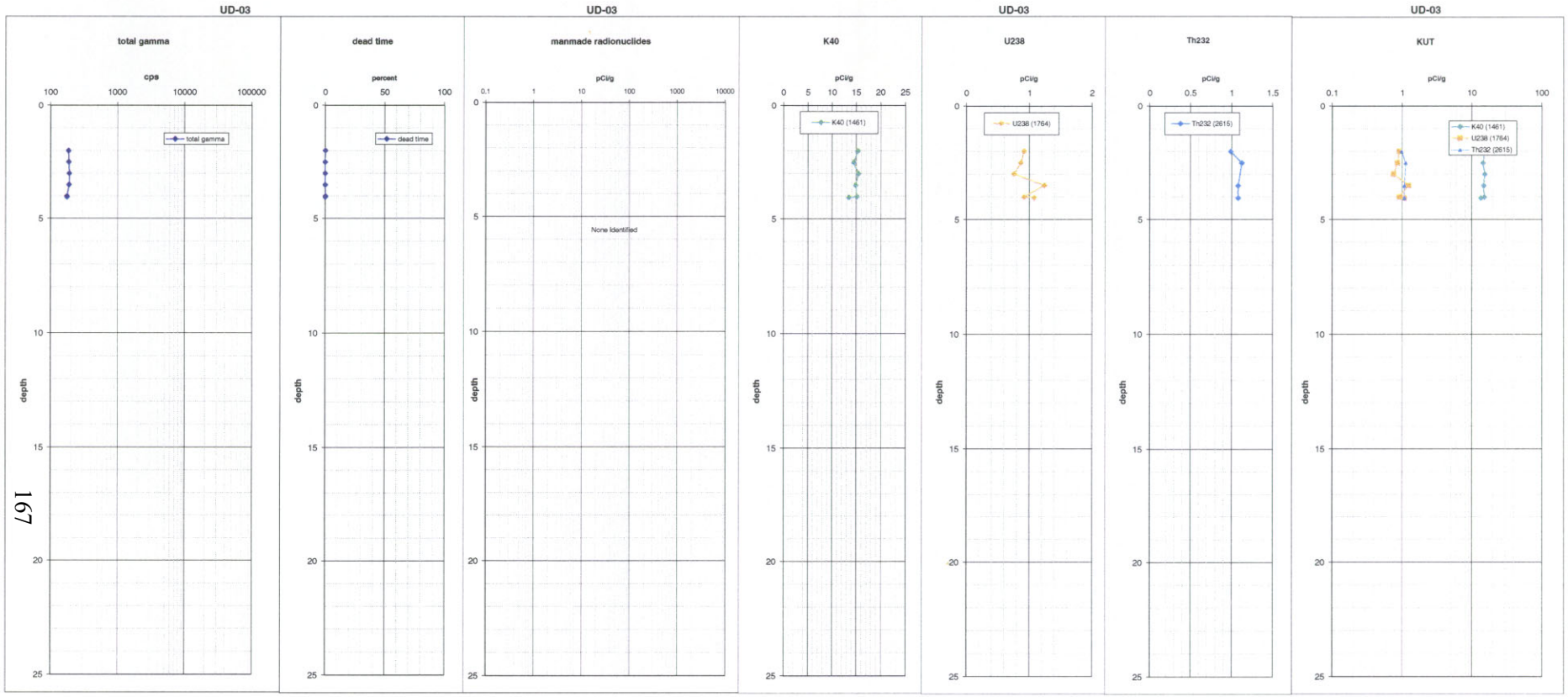
UD-03
total gamma
cps
total gamma
depth
UD-03
dead time
percent
dead time
depth
UD-03
manmade radionuclides
pCi/g
None Identified
depth
UD-03
K40
pCi/g
K40 (1461)
depth
UD-03
U238
pCi/g
U238 (1764)
depth
UD-03
Th232
pCi/g
Th232 (2615)
depth
UD-03
KUT
pCi/g
K40 (1461)
U238 (1764)
Th232 (2615)
depth

UD-03

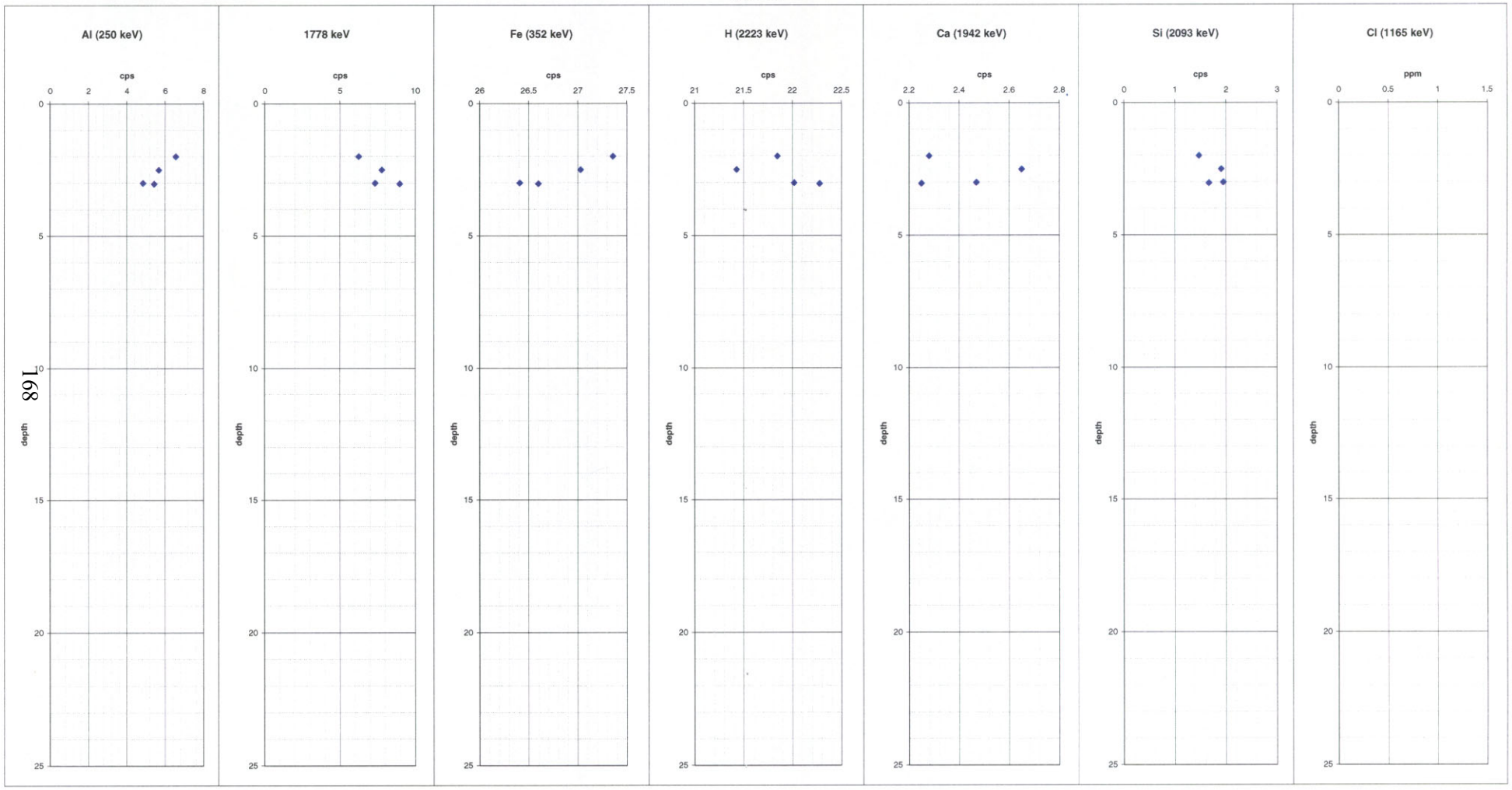
Al (250 keV)
cps
0 2 4 6 8
1778 keV
cps
0 5 10
Fe (352 keV)
cps
26 26.5 27 27.5
H (2223 keV)
cps
21 21.5 22 22.5
Ca (1942 keV)
cps
2.2 2.4 2.6 2.8
Si (2093 keV)
cps
0 1 2 3
Cl (1165 keV)
ppm
0 0.5 1 1.5
depth
0 5 10 15 20 25

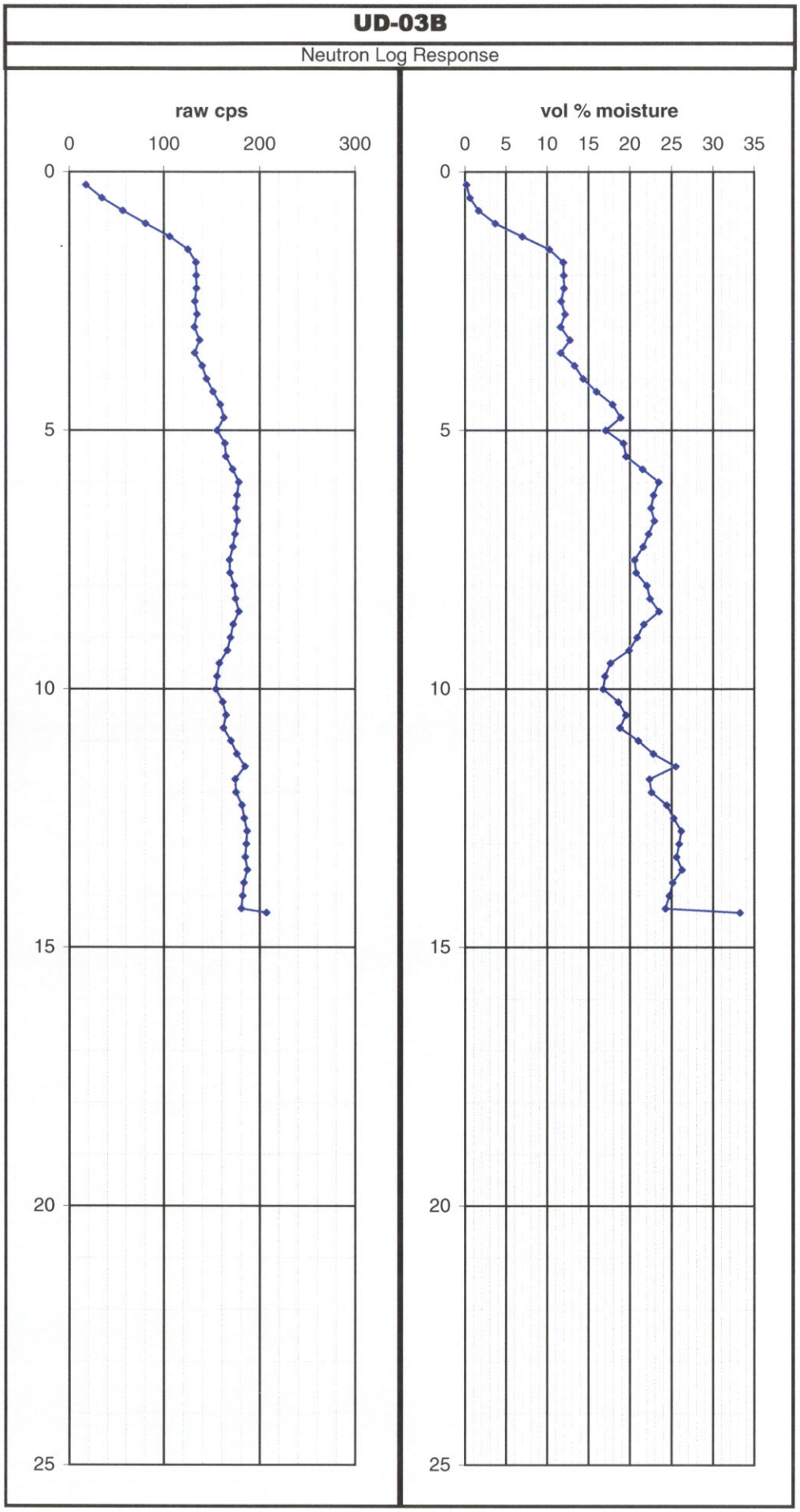
UD-03B
Neutron Log Response
raw cps
0
100
200
300
vol % moisture
0
5
10
15
20
25
30
35
0
5
10
15
20
25

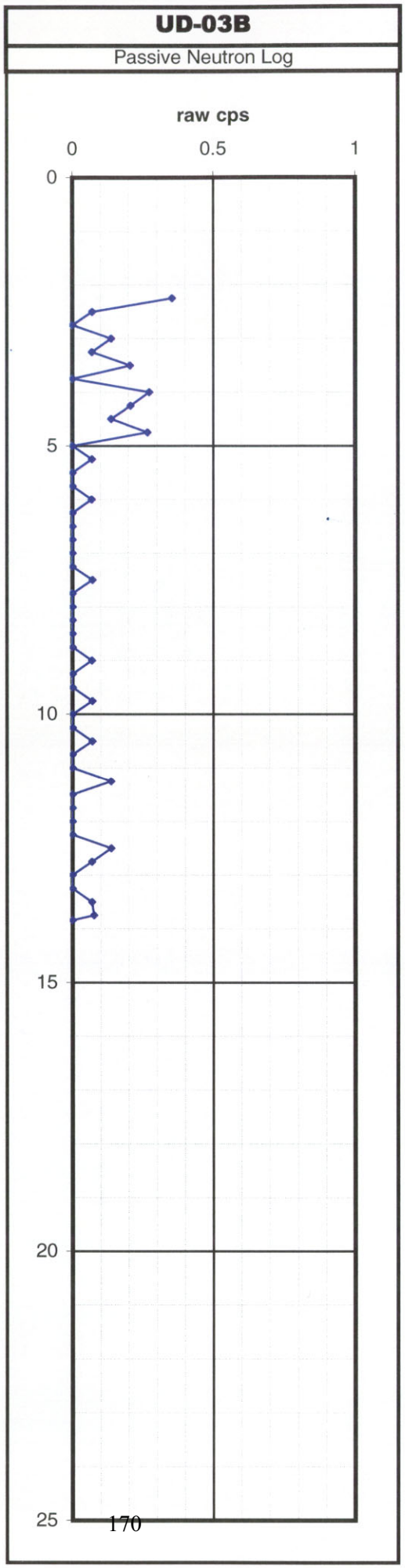
UD-03B
Passive Neutron Log
raw cps
0
0.5
1
0
5
10
15
20
25

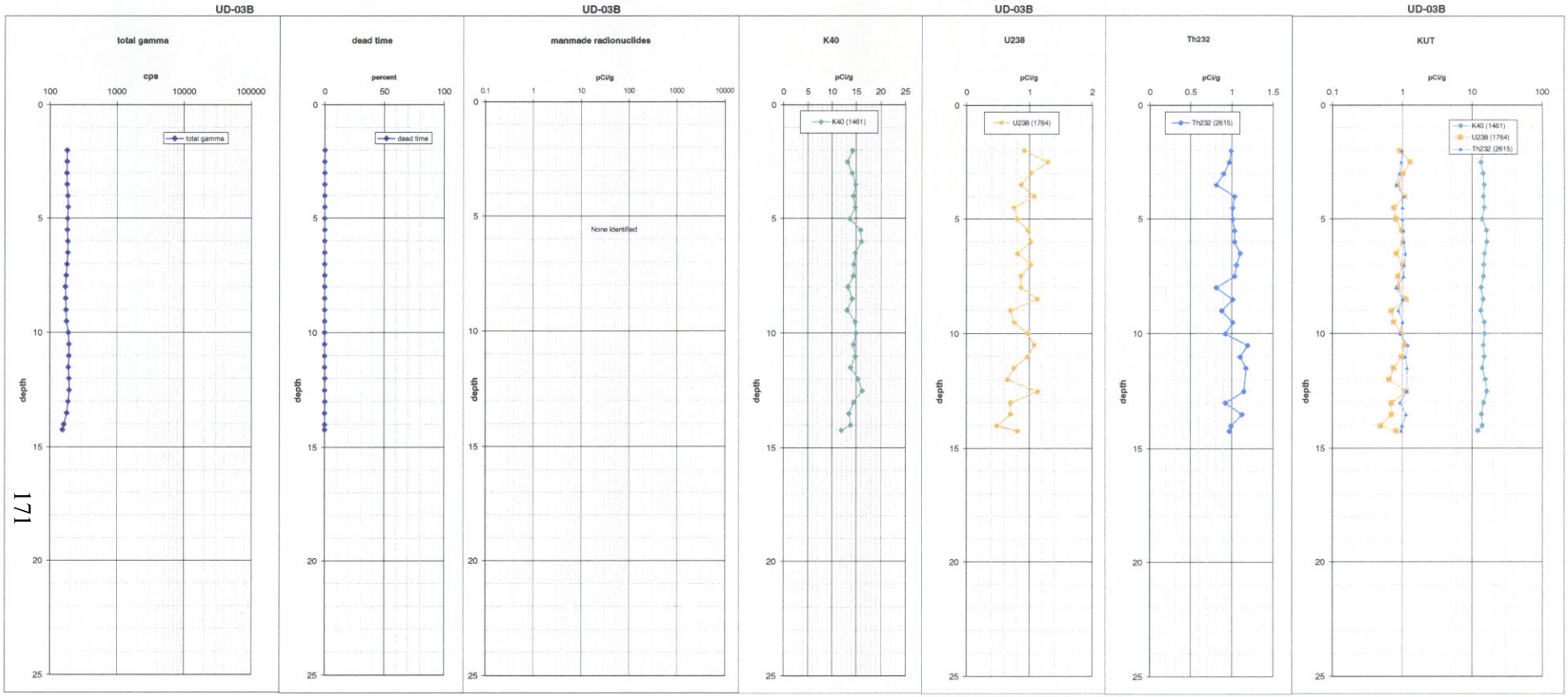
UD-03B
total gamma
cps
100
1000
10000
100000
total gamma
depth
0
5
10
15
20
25
UD-03B
dead time
percent
0
50
100
dead time
depth
UD-03B
manmade radionuclides
pCi/g
0.1
1
10
100
1000
10000
None Identified
depth
UD-03B
K40
pCi/g
0
5
10
15
20
25
K40 (1461)
depth
UD-03B
U238
pCi/g
0
1
2
U238 (1764)
depth
UD-03B
Th232
pCi/g
0
0.5
1
1.5
Th232 (2615)
depth
UD-03B
KUT
pCi/g
0.1
1
10
100
K40 (1461)
U238 (1764)
Th232 (2615)
depth

UD-03B

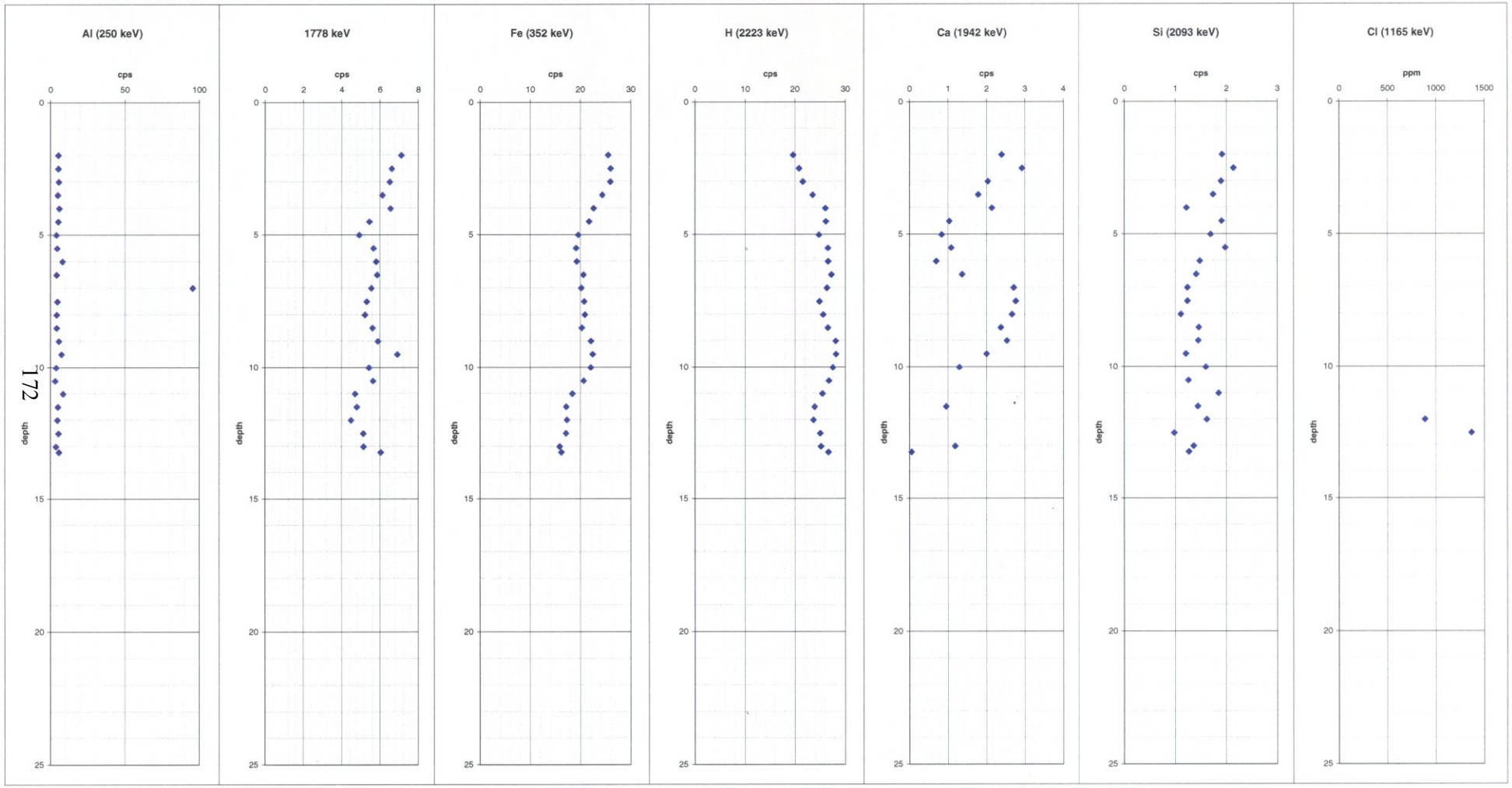
Al (250 keV)
1778 keV
Fe (352 keV)
H (2223 keV)
Ca (1942 keV)
Si (2093 keV)
Cl (1165 keV)
cps
ppm
depth

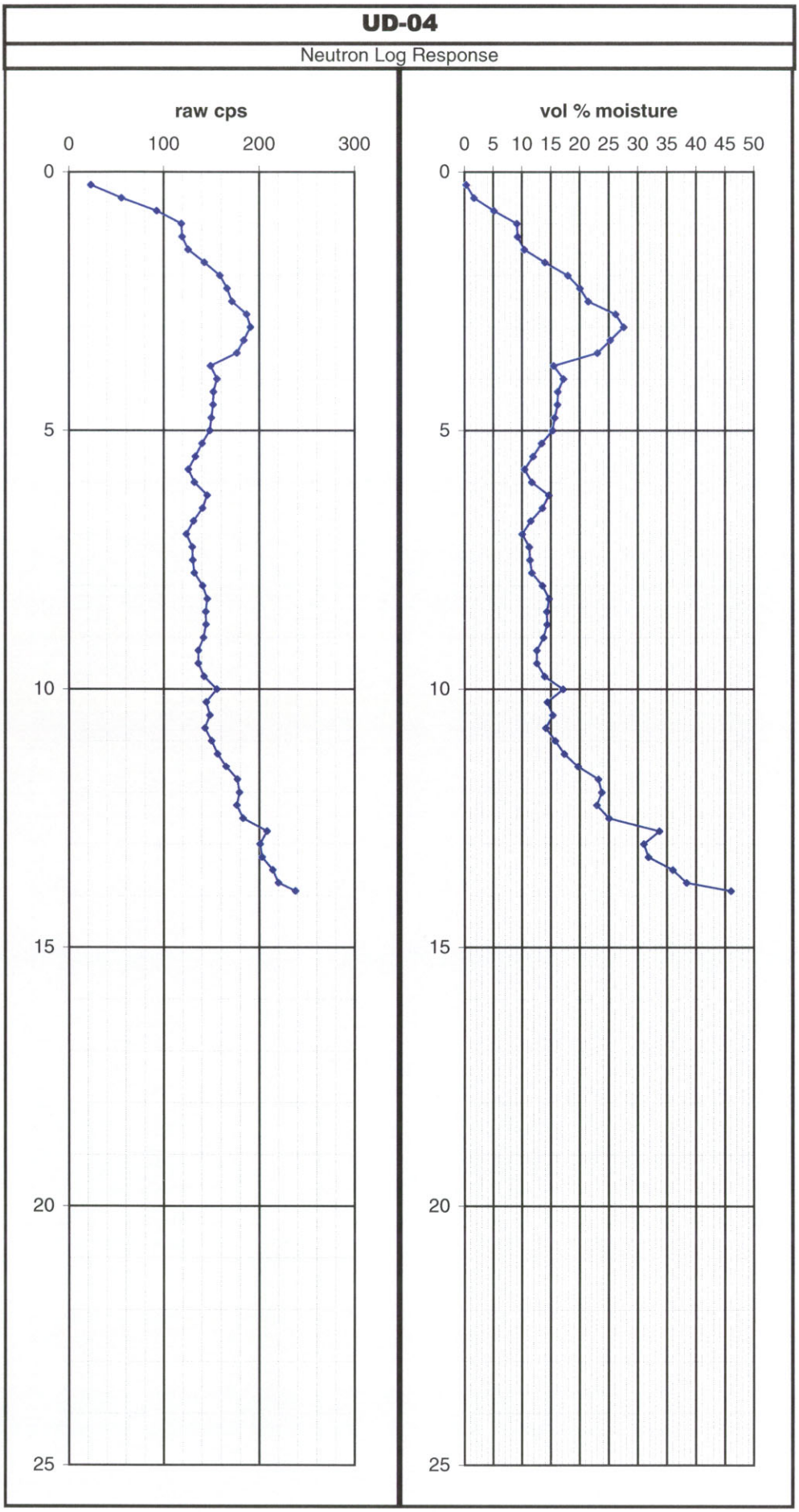
UD-04
Neutron Log Response
raw cps
0
100
200
300
vol % moisture
0
5
10
15
20
25
30
35
40
45
50

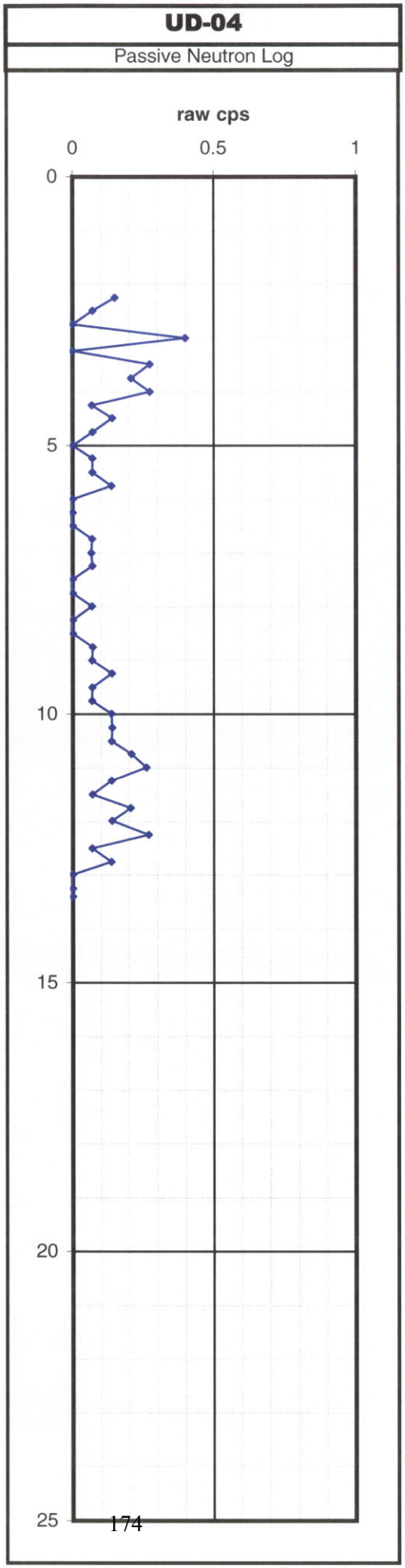
UD-04
Passive Neutron Log
raw cps
0
0.5
1
0
5
10
15
20
25

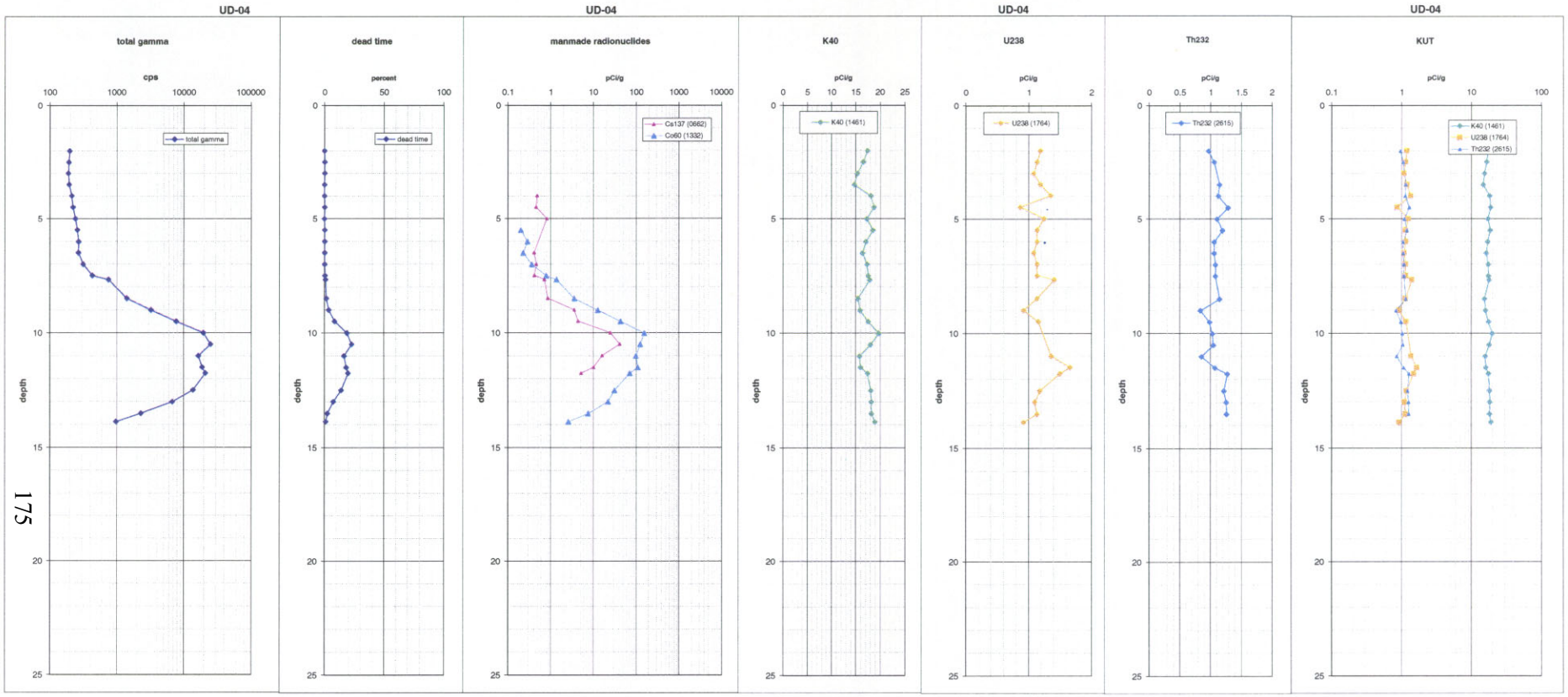
UD-04
total gamma
cps
total gamma
depth
UD-04
dead time
percent
dead time
depth
UD-04
manmade radionuclides
pCi/g
Cs137 (0662)
Co60 (1332)
depth
UD-04
K40
pCi/g
K40 (1461)
depth
UD-04
U238
pCi/g
U238 (1764)
depth
UD-04
Th232
pCi/g
Th232 (2615)
depth
UD-04
KUT
pCi/g
K40 (1461)
U238 (1764)
Th232 (2615)
depth

UD-04

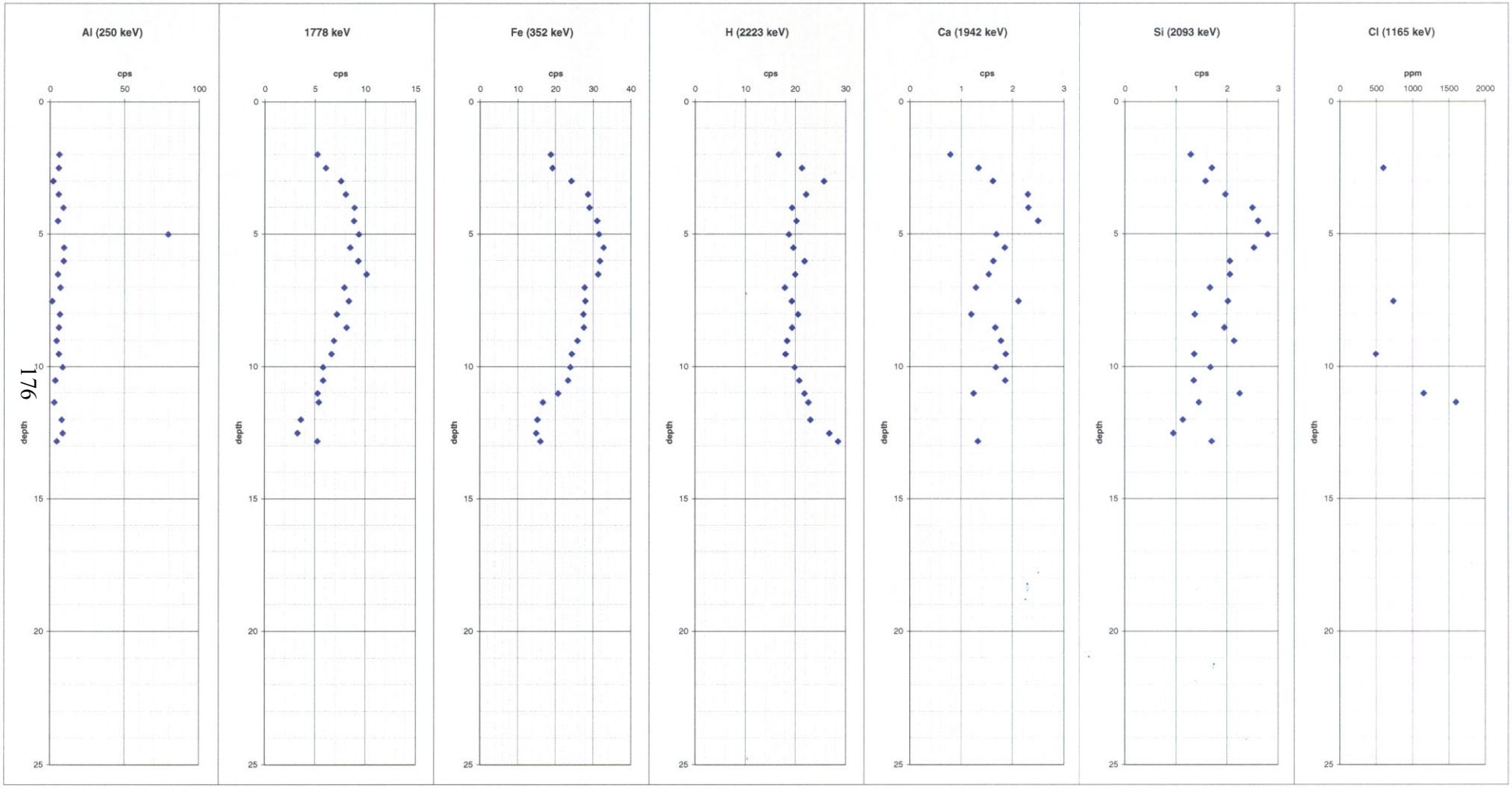
Al (250 keV)
1778 keV
Fe (352 keV)
H (2223 keV)
Ca (1942 keV)
Si (2093 keV)
Cl (1165 keV)
cps
ppm
depth

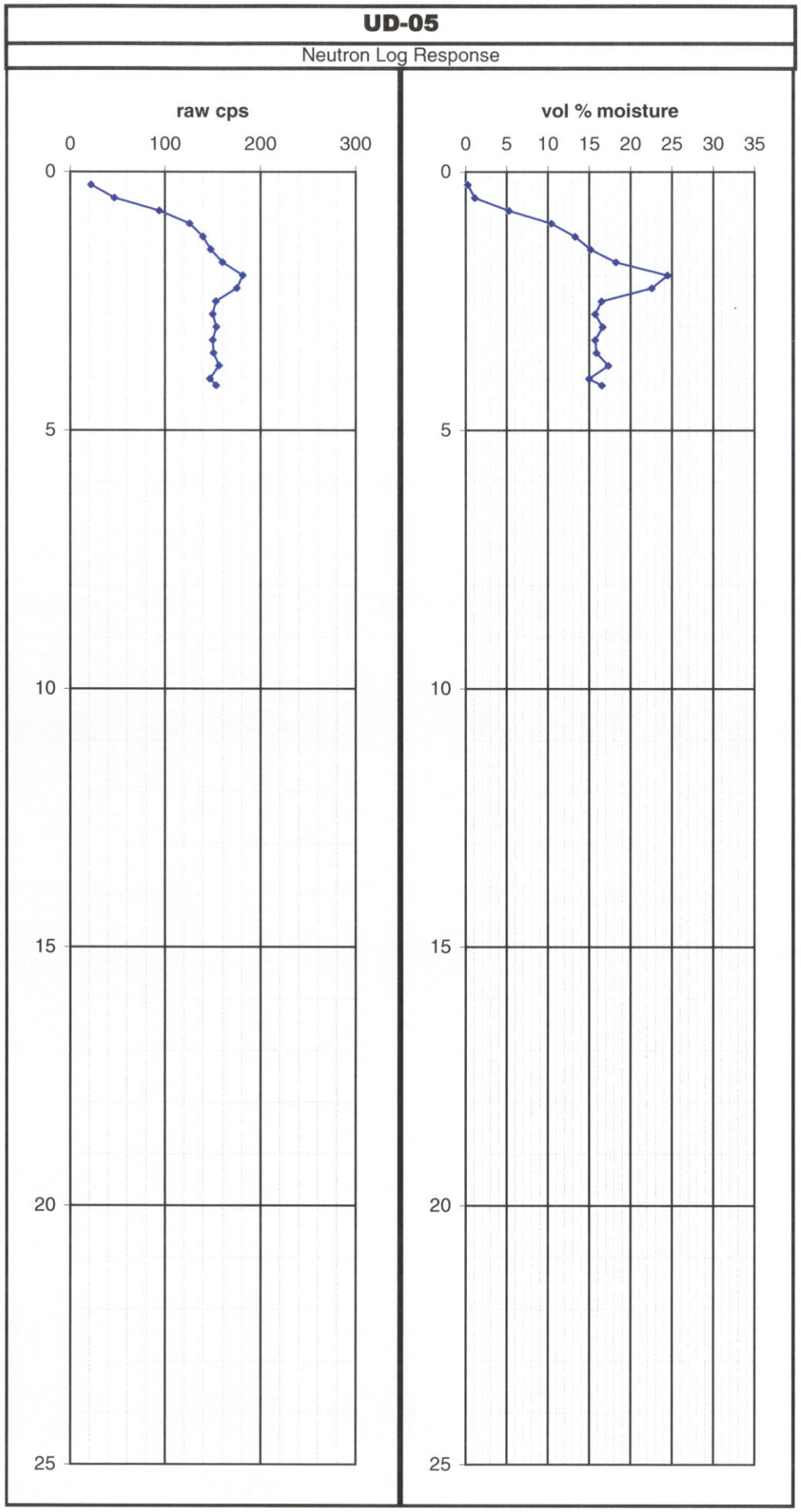
UD-05
Neutron Log Response
raw cps
0
100
200
300
vol % moisture
0
5
10
15
20
25
30
35
0
5
10
15
20
25

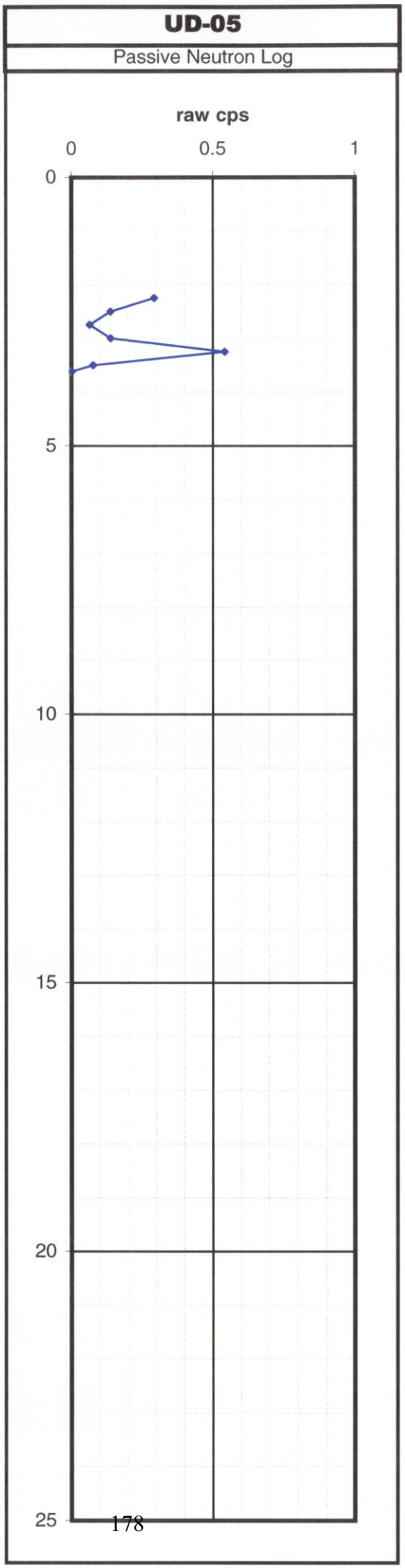
UD-05
Passive Neutron Log
raw cps
0
0.5
1
0
5
10
15
20
25

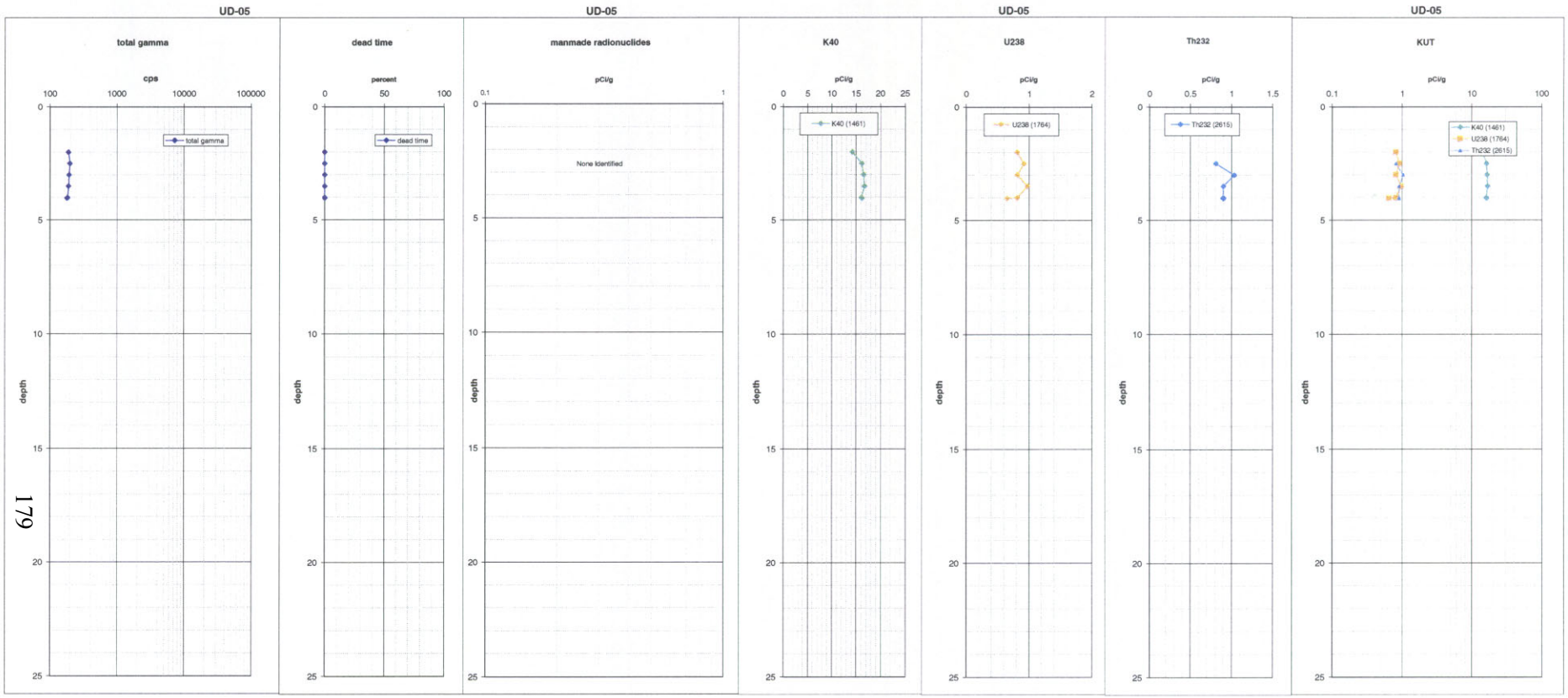
UD-05
total gamma
cps
100
1000
10000
100000
total gamma
depth
UD-05
dead time
percent
0
50
100
dead time
depth
UD-05
manmade radionuclides
pCi/g
0.1
1
None Identified
depth
UD-05
K40
pCi/g
0
5
10
15
20
25
K40 (1461)
depth
UD-05
U238
pCi/g
0
1
2
U238 (1764)
depth
UD-05
Th232
pCi/g
0
0.5
1
1.5
Th232 (2615)
depth
UD-05
KUT
pCi/g
0.1
1
10
100
K40 (1461)
U238 (1764)
Th232 (2615)
depth
0
5
10
15
20
25

UD-05

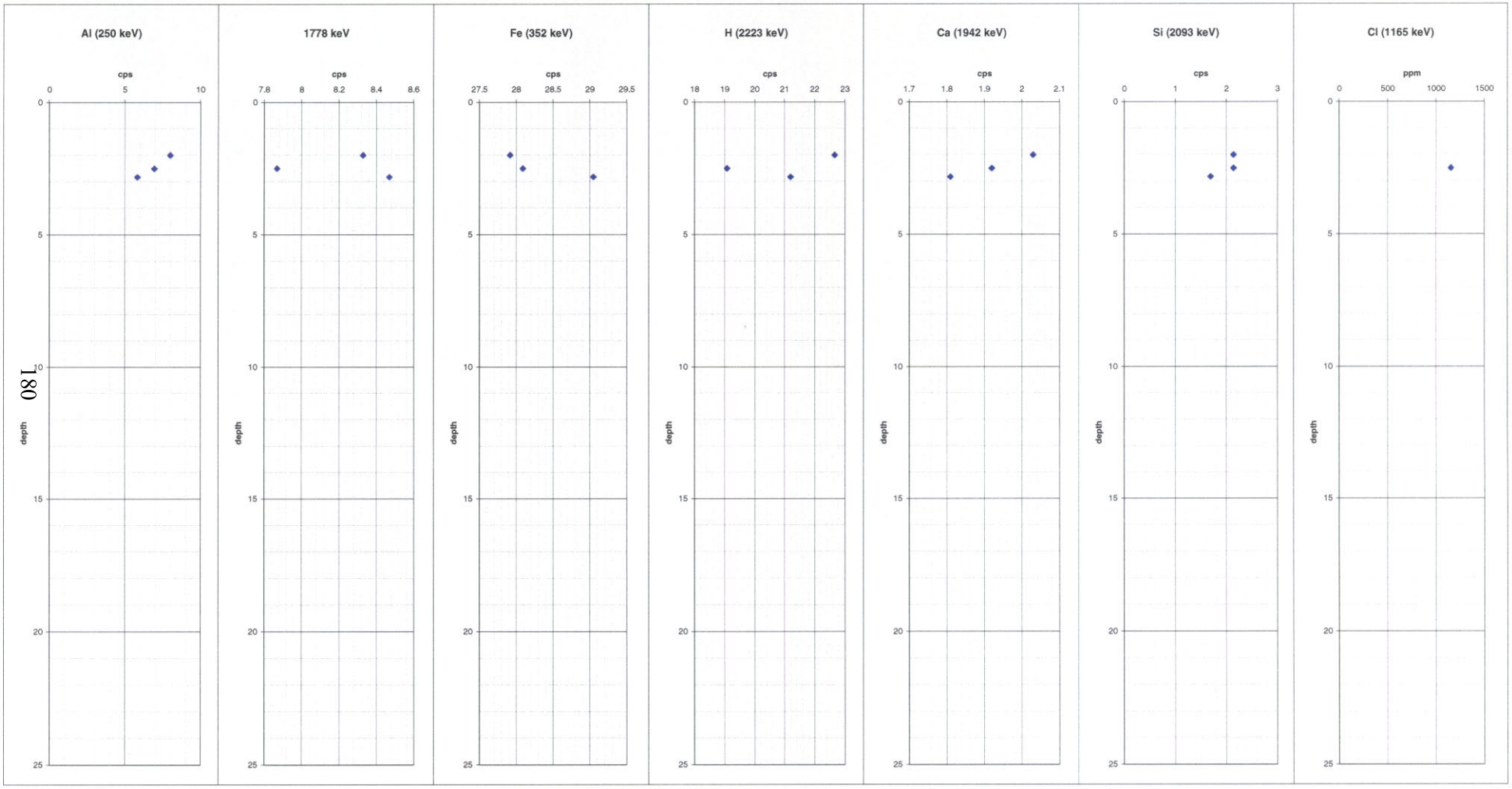
Al (250 keV)
cps
0 5 10
1778 keV
cps
7.8 8 8.2 8.4 8.6
Fe (352 keV)
cps
27.5 28 28.5 29 29.5
H (2223 keV)
cps
18 19 20 21 22 23
Ca (1942 keV)
cps
1.7 1.8 1.9 2 2.1
Si (2093 keV)
cps
0 1 2 3
Cl (1165 keV)
ppm
0 500 1000 1500
depth
0 5 10 15 20 25

UD-05B

Neutron Log Response

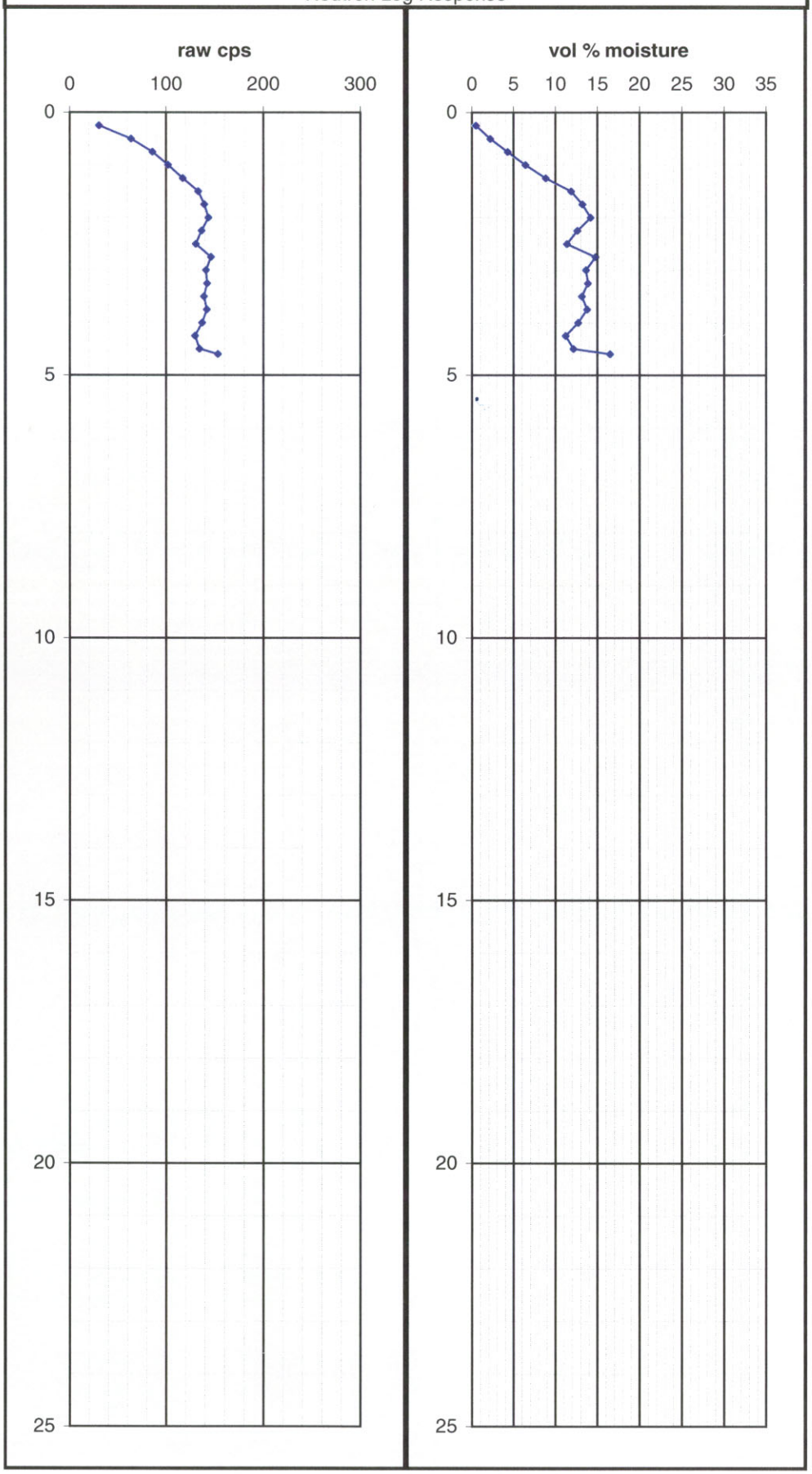

UD-05b

Passive Neutron Log

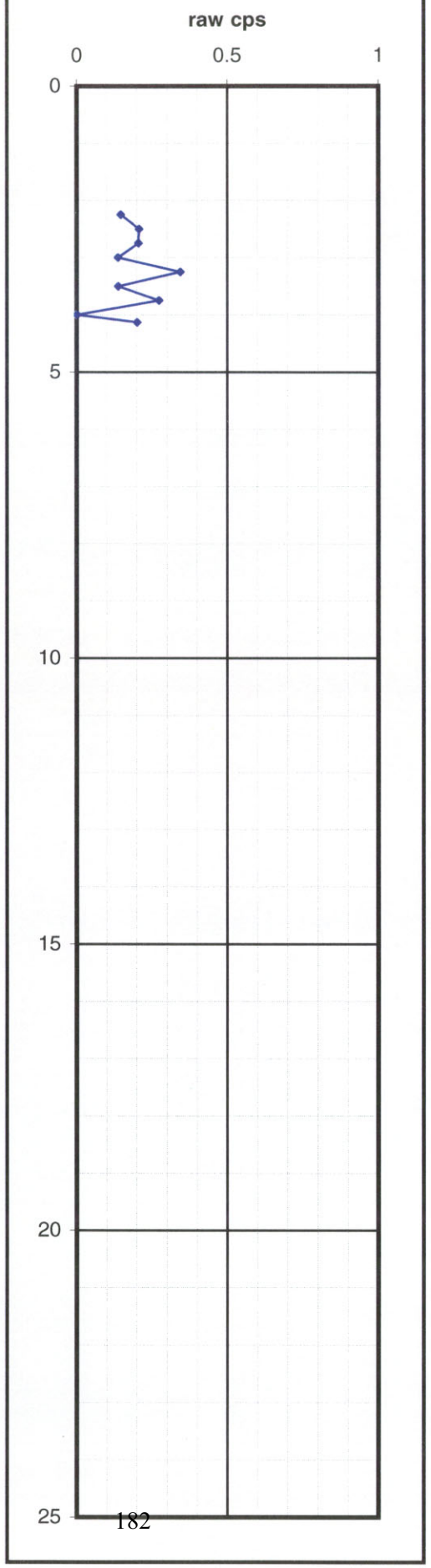

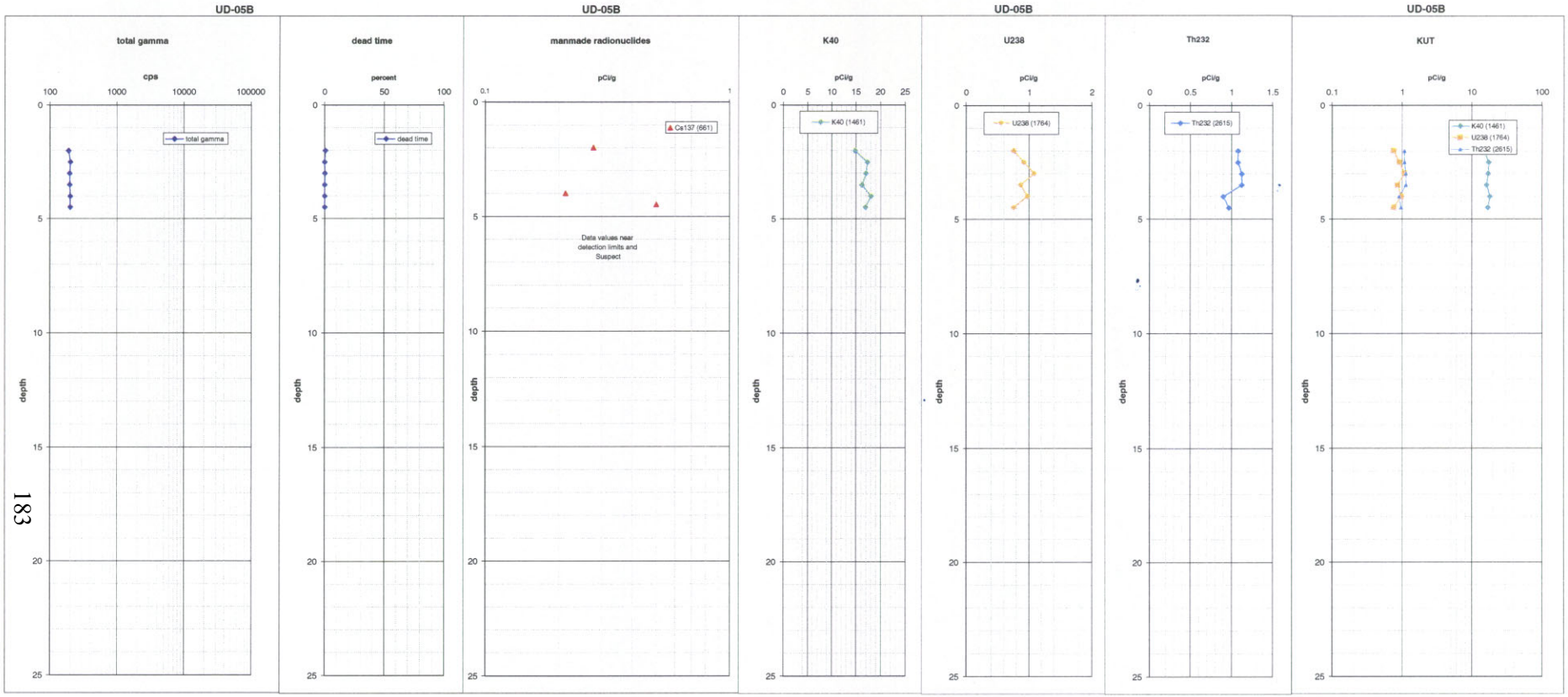
UD-05B
total gamma
cps
100
1000
10000
100000
total gamma
depth
0
5
10
15
20
25
UD-05B
dead time
percent
0
50
100
dead time
depth
UD-05B
manmade radionuclides
pCi/g
0.1
1
Cs137 (661)
Data values near detection limits and Suspect
depth
UD-05B
K40
pCi/g
0
5
10
15
20
25
K40 (1461)
depth
UD-05B
U238
pCi/g
0
1
2
U238 (1764)
depth
UD-05B
Th232
pCi/g
0
0.5
1
1.5
Th232 (2615)
depth
UD-05B
KUT
pCi/g
0.1
1
10
100
K40 (1461)
U238 (1764)
Th232 (2615)
depth

UD-05B

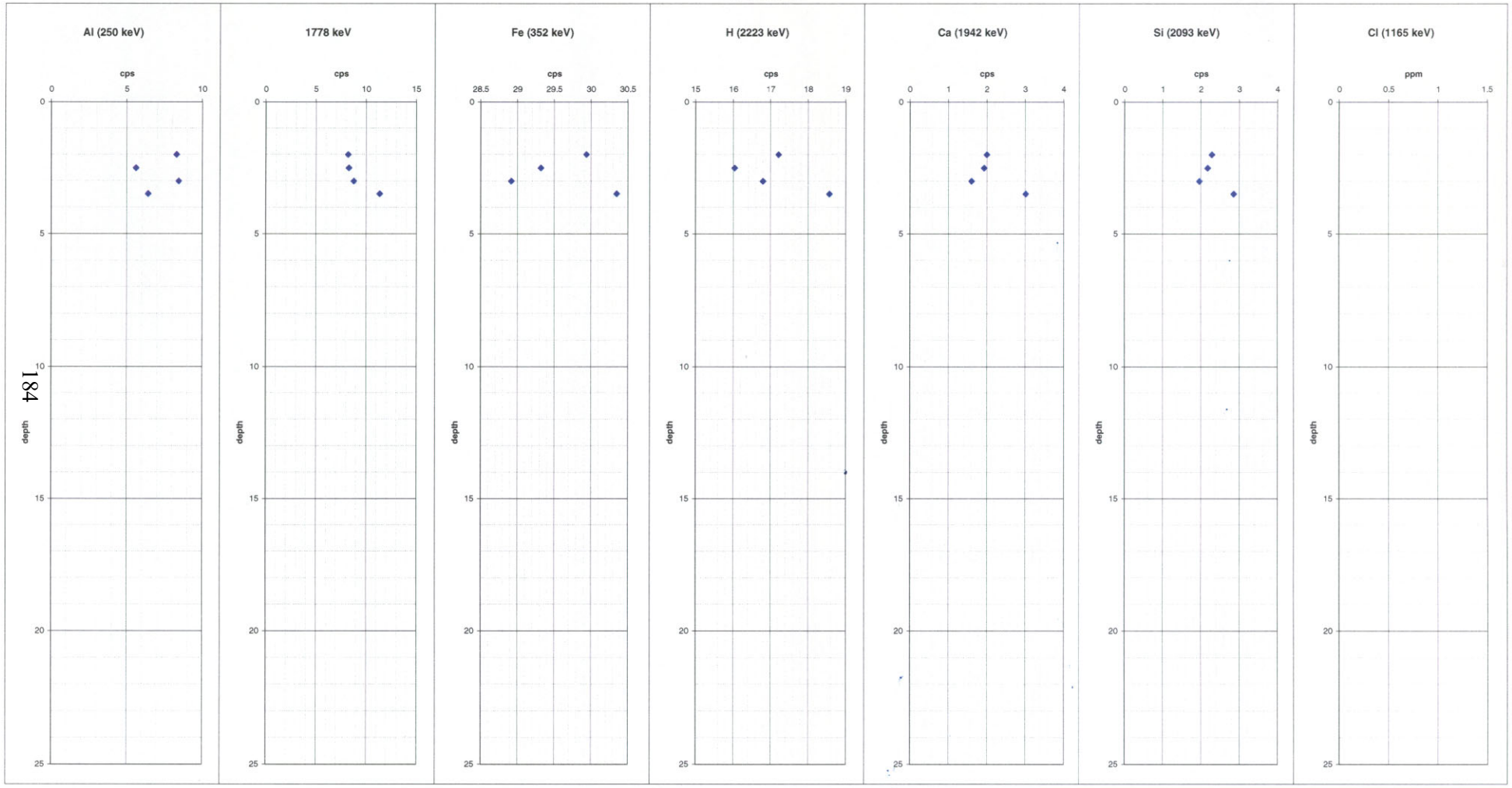
Al (250 keV)
cps
0 5 10
1778 keV
cps
0 5 10 15
Fe (352 keV)
cps
28.5 29 29.5 30 30.5
H (2223 keV)
cps
15 16 17 18 19
Ca (1942 keV)
cps
0 1 2 3 4
Si (2093 keV)
cps
0 1 2 3 4
Cl (1165 keV)
ppm
0 0.5 1 1.5
depth
0 5 10 15 20 25

UD-05C

Neutron Log Response

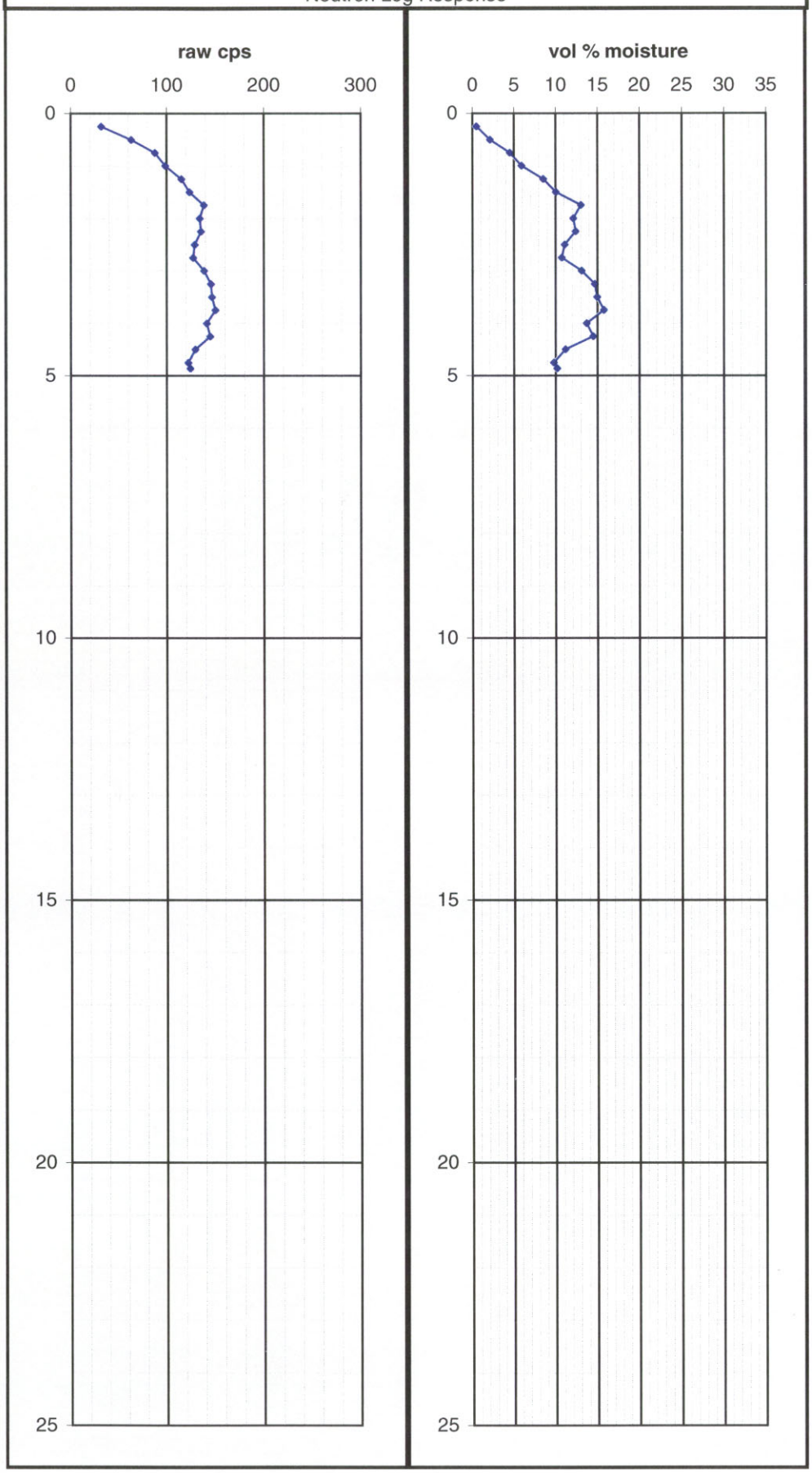

UD-05c

Passive Neutron Log

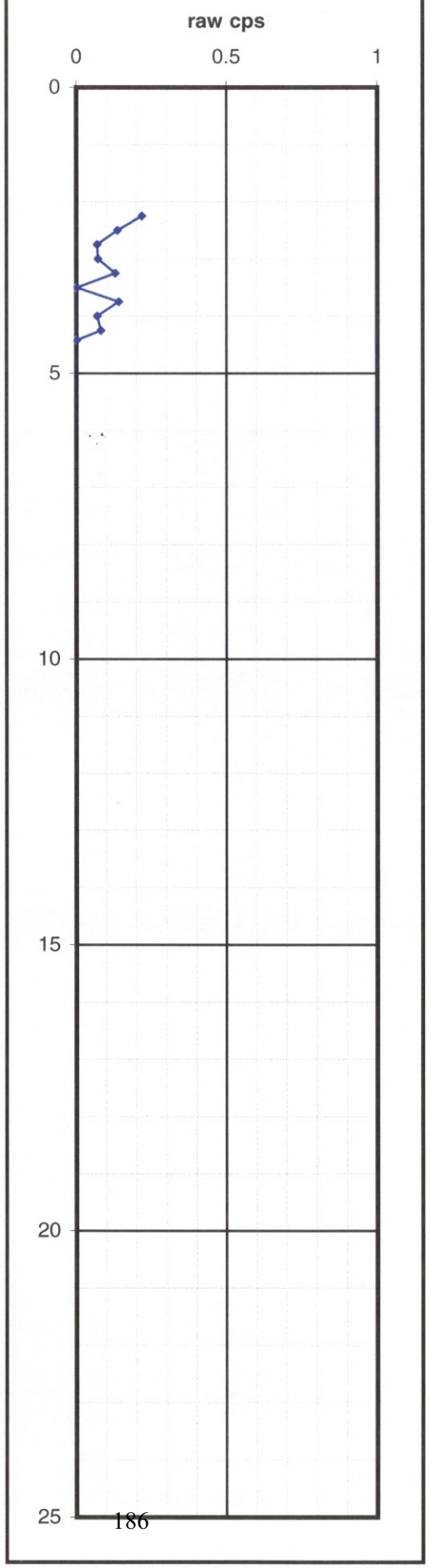

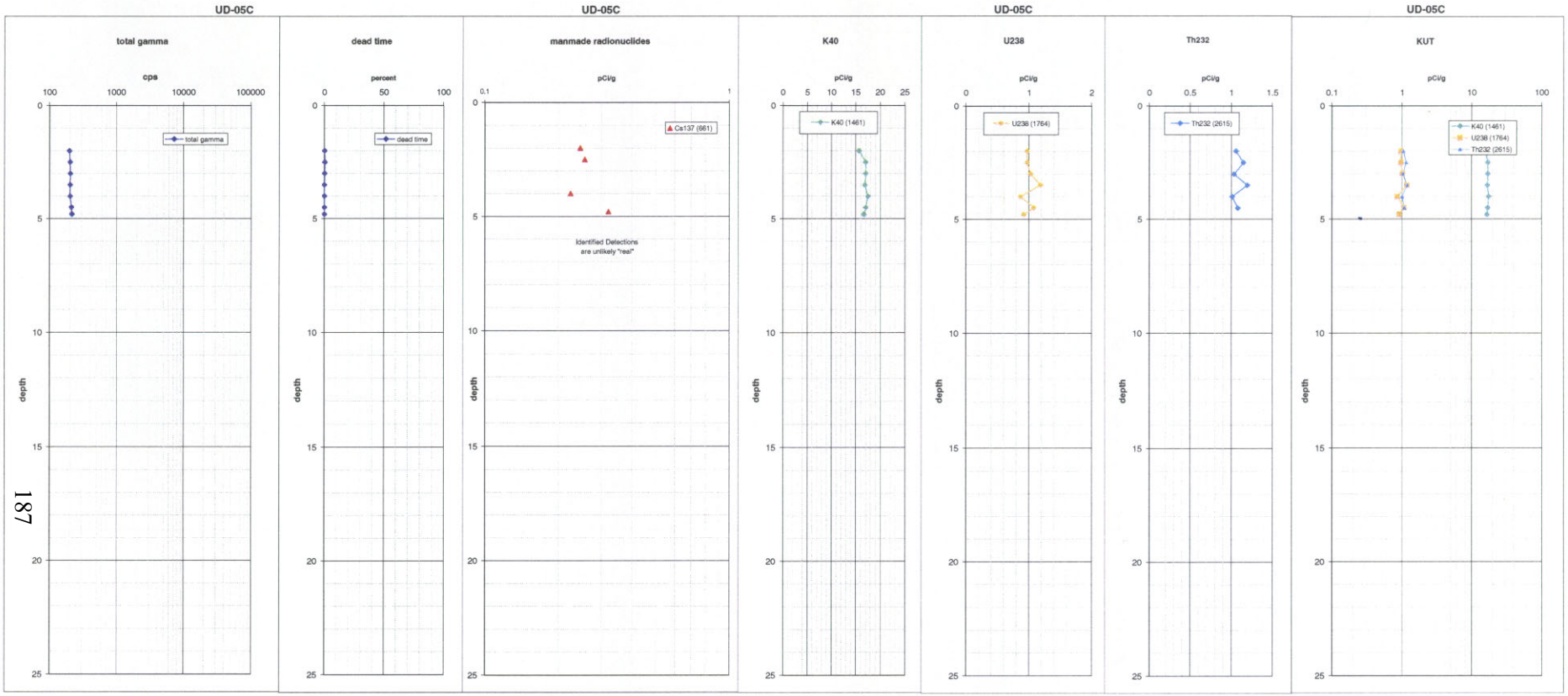
UD-05C
total gamma
cps
100
1000
10000
100000
total gamma
depth
UD-05C
dead time
percent
0
50
100
dead time
depth
UD-05C
manmade radionuclides
pCi/g
0.1
1
Cs137 (661)
Identified Detections
are unlikely "real"
depth
UD-05C
K40
pCi/g
0
5
10
15
20
25
K40 (1461)
depth
UD-05C
U238
pCi/g
0
1
2
U238 (1764)
depth
UD-05C
Th232
pCi/g
0
0.5
1
1.5
Th232 (2615)
depth
UD-05C
KUT
pCi/g
0.1
1
10
100
K40 (1461)
U238 (1764)
Th232 (2615)
depth

UD-05C

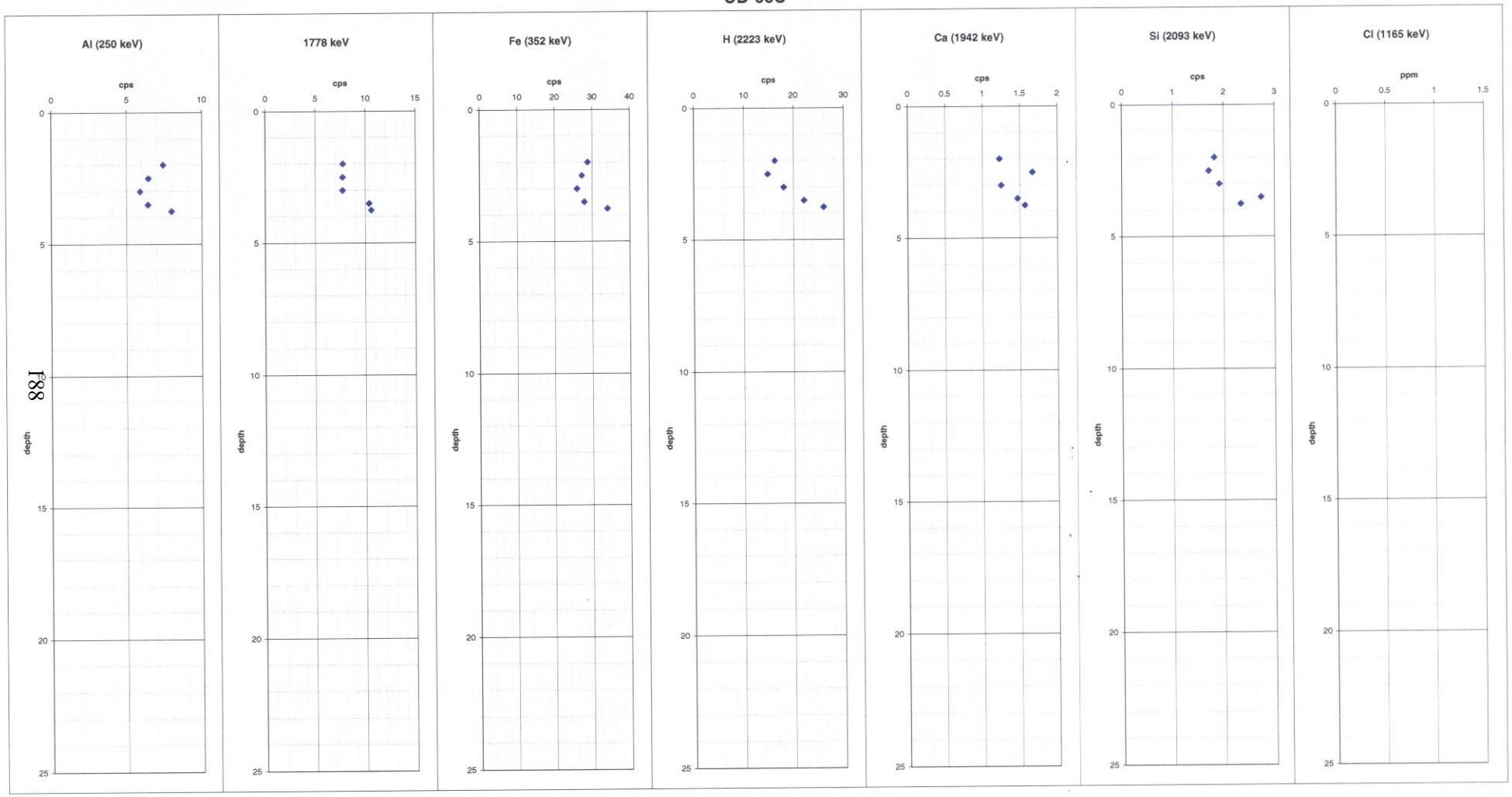
Al (250 keV)
cps
0 5 10
1778 keV
cps
0 5 10 15
Fe (352 keV)
cps
0 10 20 30 40
H (2223 keV)
cps
0 10 20 30
Ca (1942 keV)
cps
0 0.5 1 1.5 2
Si (2093 keV)
cps
0 1 2 3
Cl (1165 keV)
ppm
0 0.5 1 1.5
depth
0 5 10 15 20 25

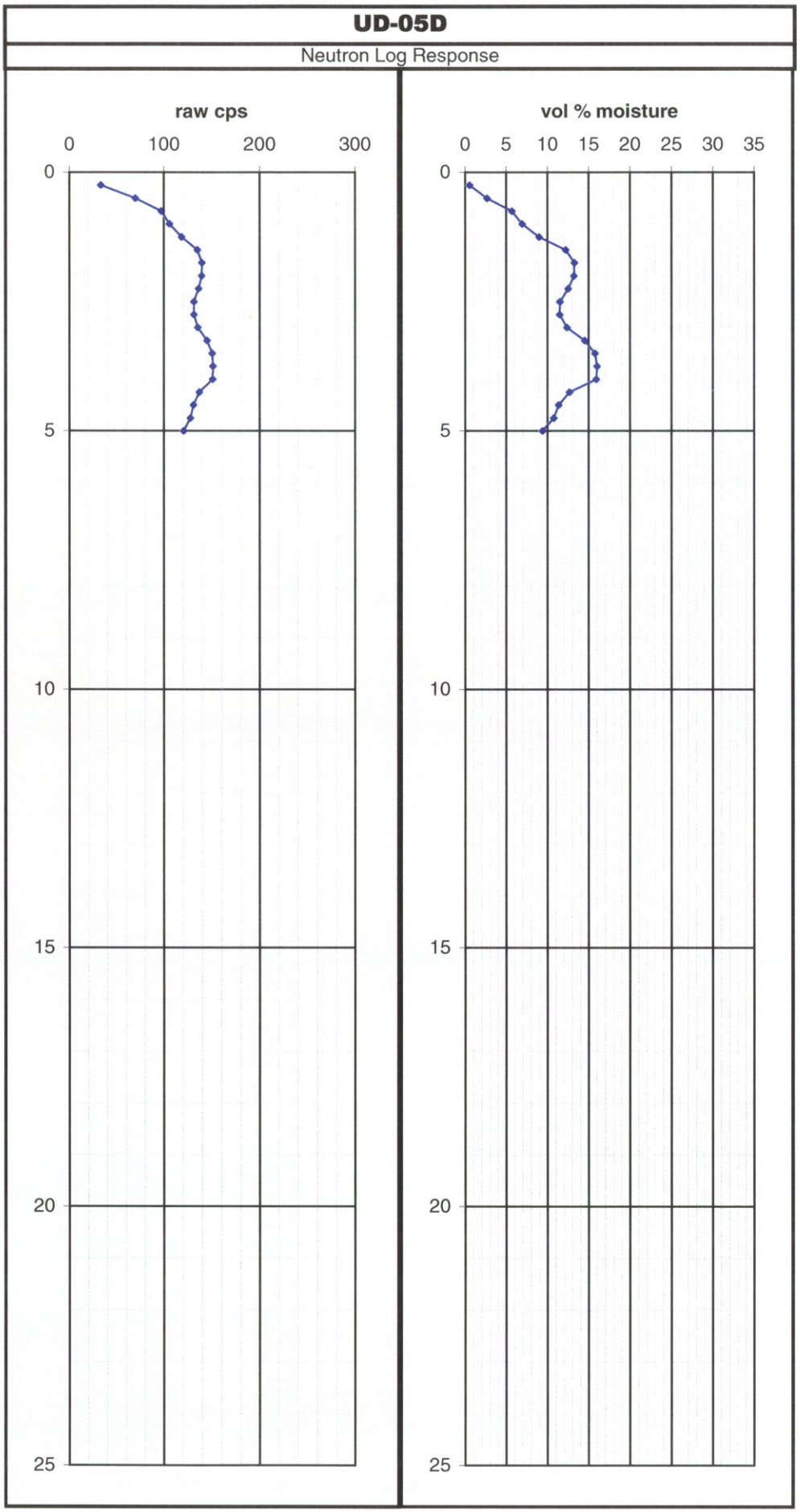
UD-05D
Neutron Log Response
raw cps
0
100
200
300
vol % moisture
0
5
10
15
20
25
30
35
0
5
10
15
20
25

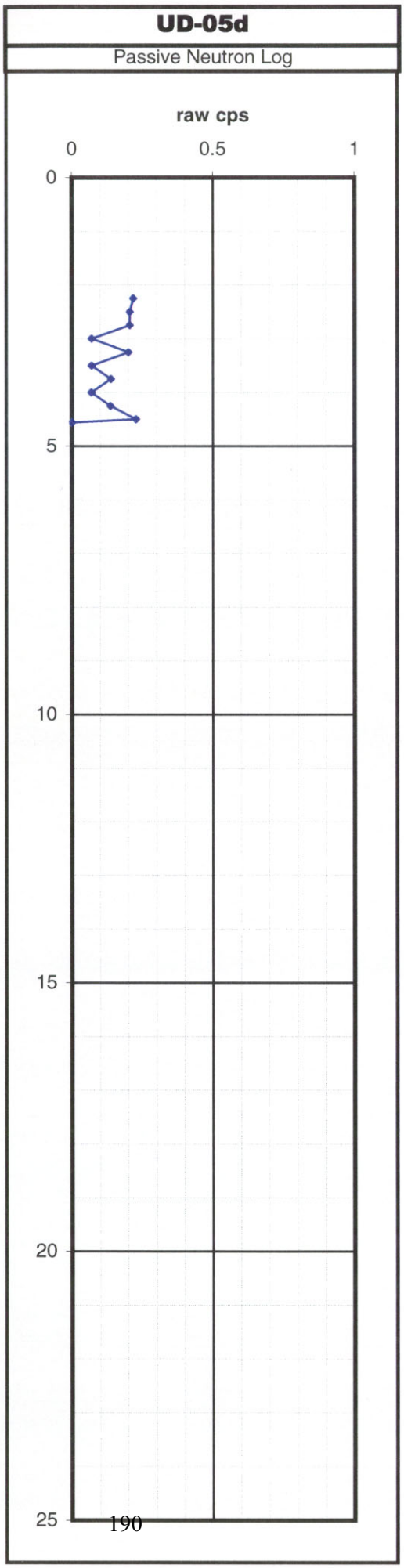
UD-05d
Passive Neutron Log
raw cps
0
0.5
1
0
5
10
15
20
25

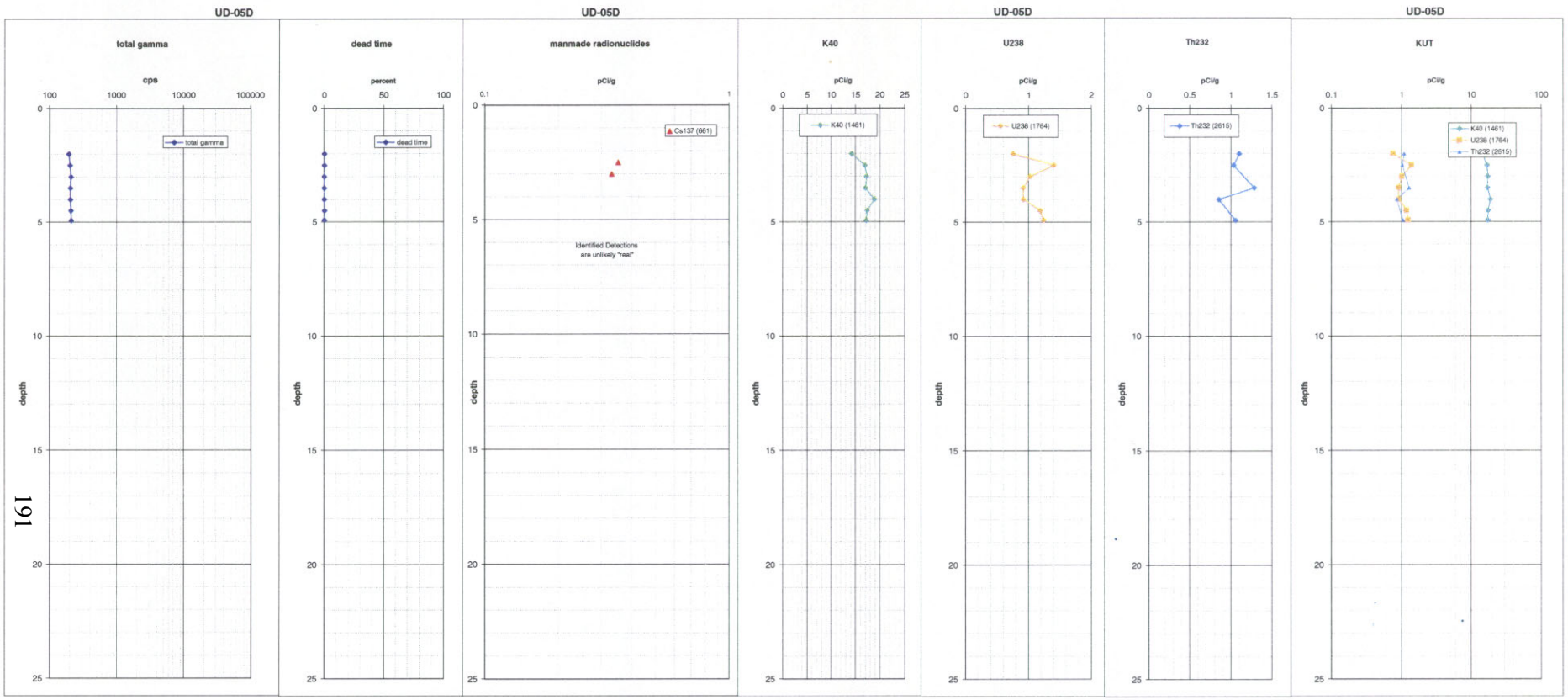
UD-05D
total gamma
cps
100
1000
10000
100000
total gamma
dead time
percent
0
50
100
dead time
manmade radionuclides
pCi/g
0.1
1
Cs137 (661)
Identified Detections
are unlikely "real"
K40
pCi/g
0
5
10
15
20
25
K40 (1461)
U238
pCi/g
0
1
2
U238 (1764)
Th232
pCi/g
0
0.5
1
1.5
Th232 (2615)
KUT
pCi/g
0.1
1
10
100
K40 (1461)
U238 (1764)
Th232 (2615)
depth
0
5
10
15
20
25

UD-05D

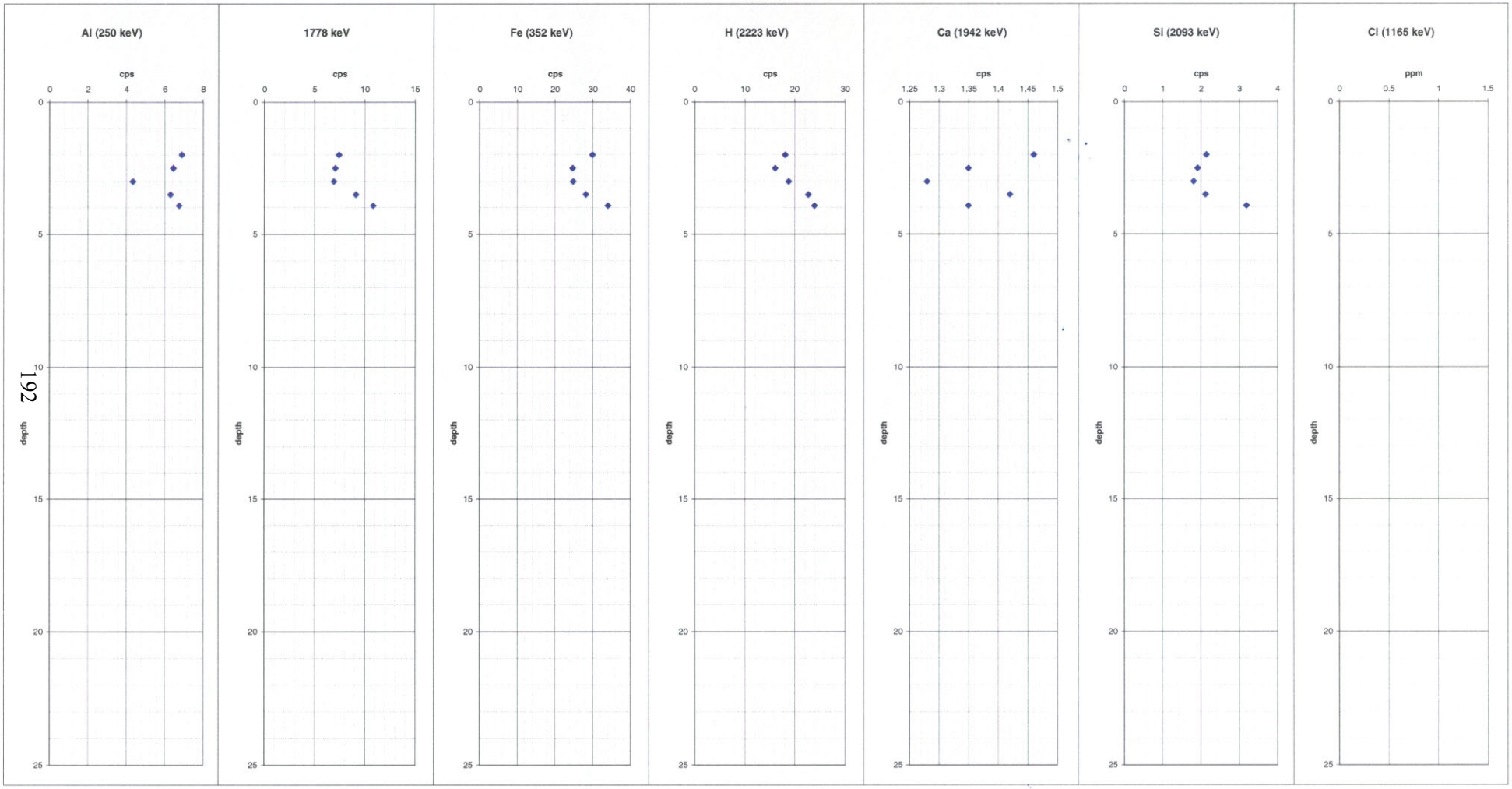
Al (250 keV)
cps
0 2 4 6 8
1778 keV
cps
0 5 10 15
Fe (352 keV)
cps
0 10 20 30 40
H (2223 keV)
cps
0 10 20 30
Ca (1942 keV)
cps
1.25 1.3 1.35 1.4 1.45 1.5
Si (2093 keV)
cps
0 1 2 3 4
Cl (1165 keV)
ppm
0 0.5 1 1.5
depth
0 5 10 15 20 25

UD-05E

Neutron Log Response

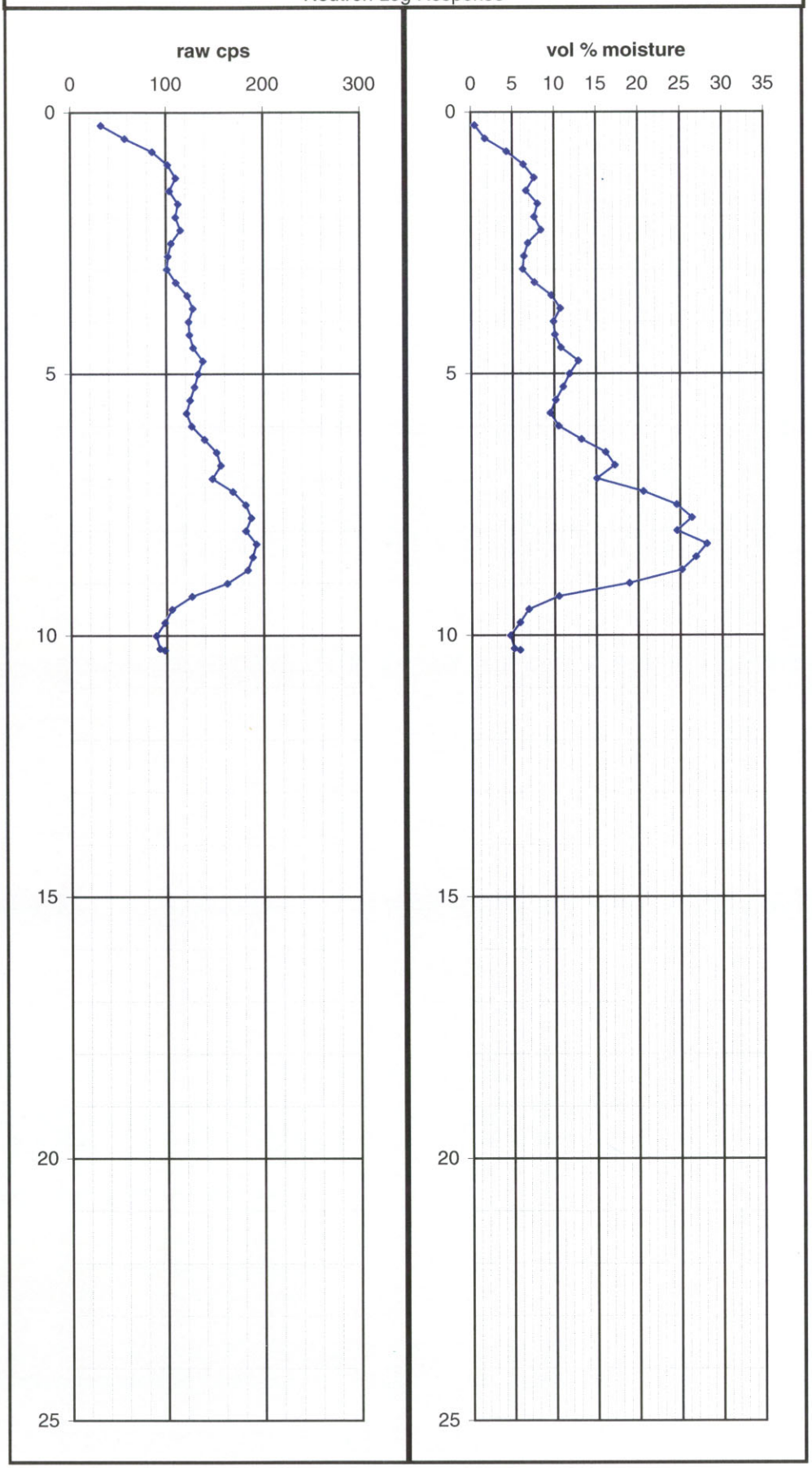

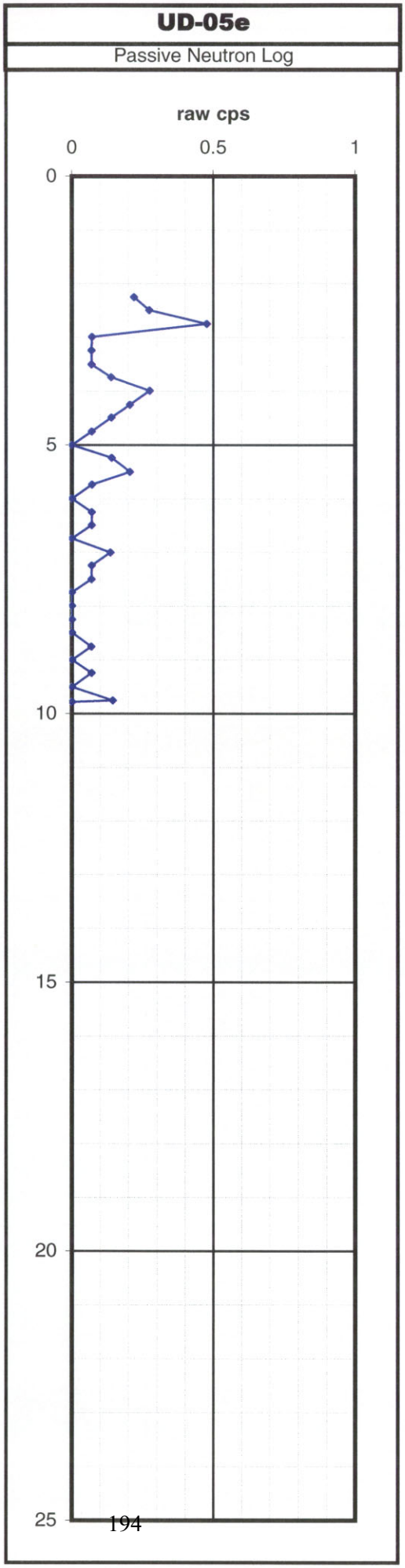
UD-05e
Passive Neutron Log
raw cps
0
0.5
1
0
5
10
15
20
25

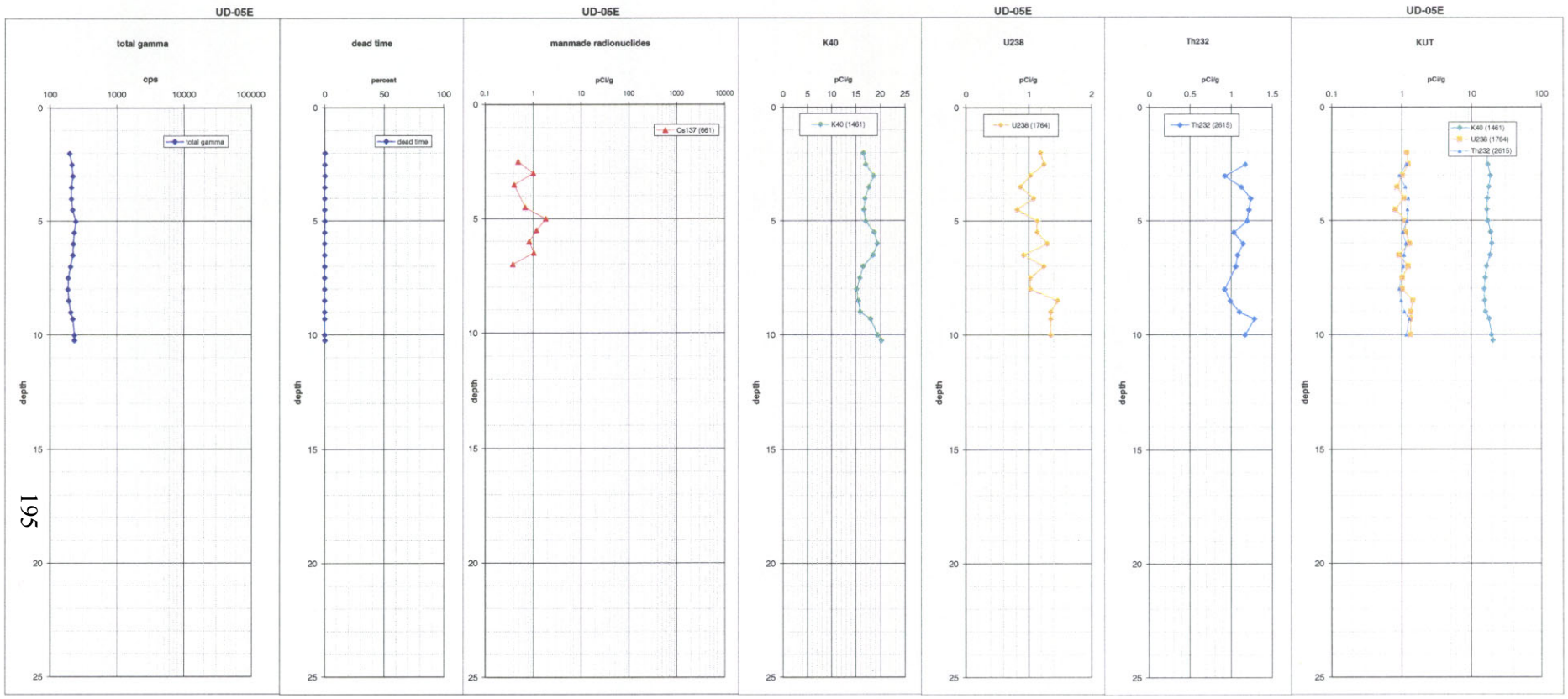
UD-05E
total gamma
cps
100
1000
10000
100000
total gamma
depth
UD-05E
dead time
percent
0
50
100
dead time
depth
UD-05E
manmade radionuclides
pCi/g
0.1
1
10
100
1000
10000
Cs137 (661)
depth
UD-05E
K40
pCi/g
0
5
10
15
20
25
K40 (1461)
depth
UD-05E
U238
pCi/g
0
1
2
U238 (1764)
depth
UD-05E
Th232
pCi/g
0
0.5
1
1.5
Th232 (2615)
depth
UD-05E
KUT
pCi/g
0.1
1
10
100
K40 (1461)
U238 (1764)
Th232 (2615)
depth

UD-05E

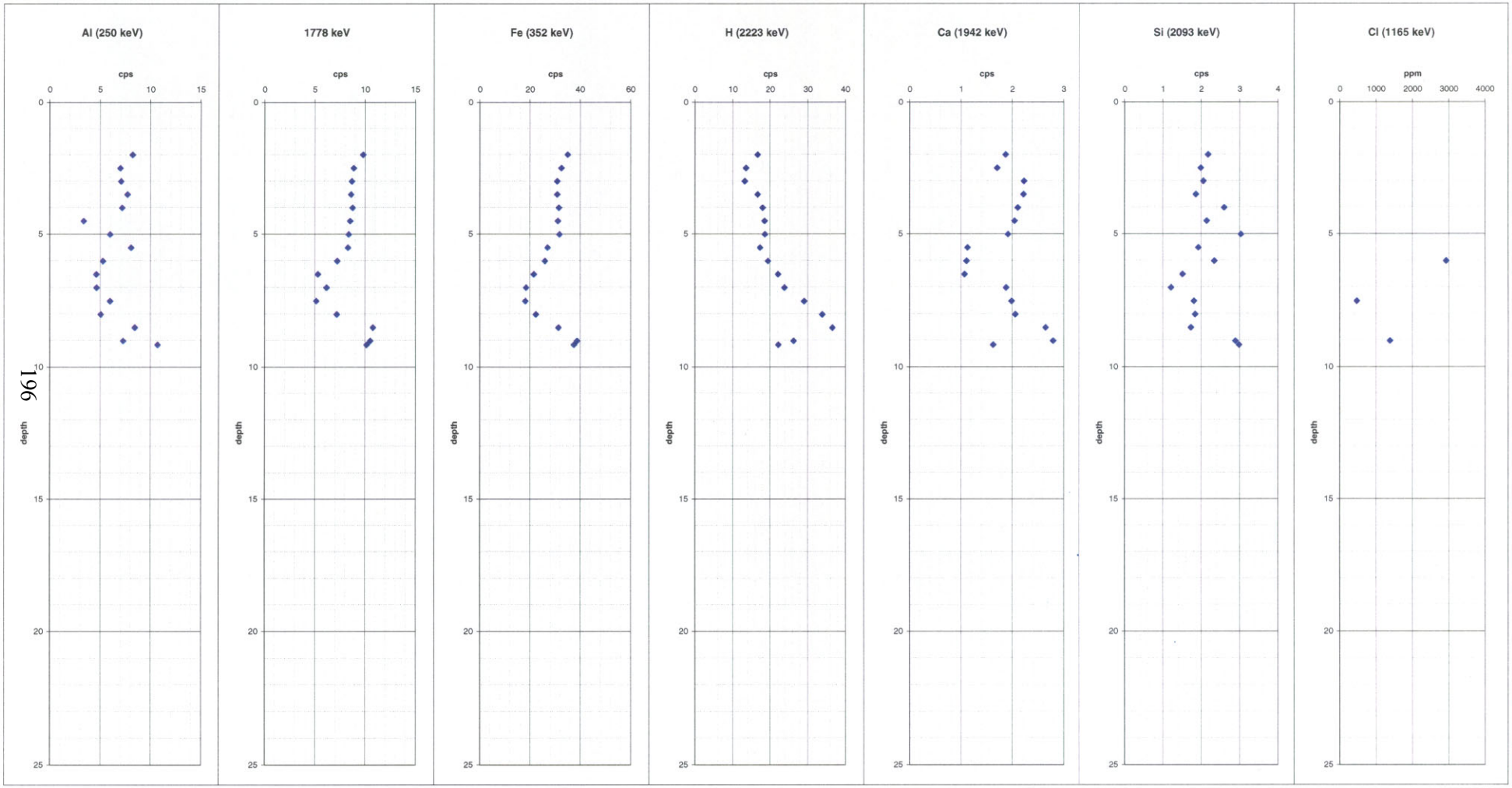
Al (250 keV)
1778 keV
Fe (352 keV)
H (2223 keV)
Ca (1942 keV)
Si (2093 keV)
Cl (1165 keV)
cps
ppm
depth

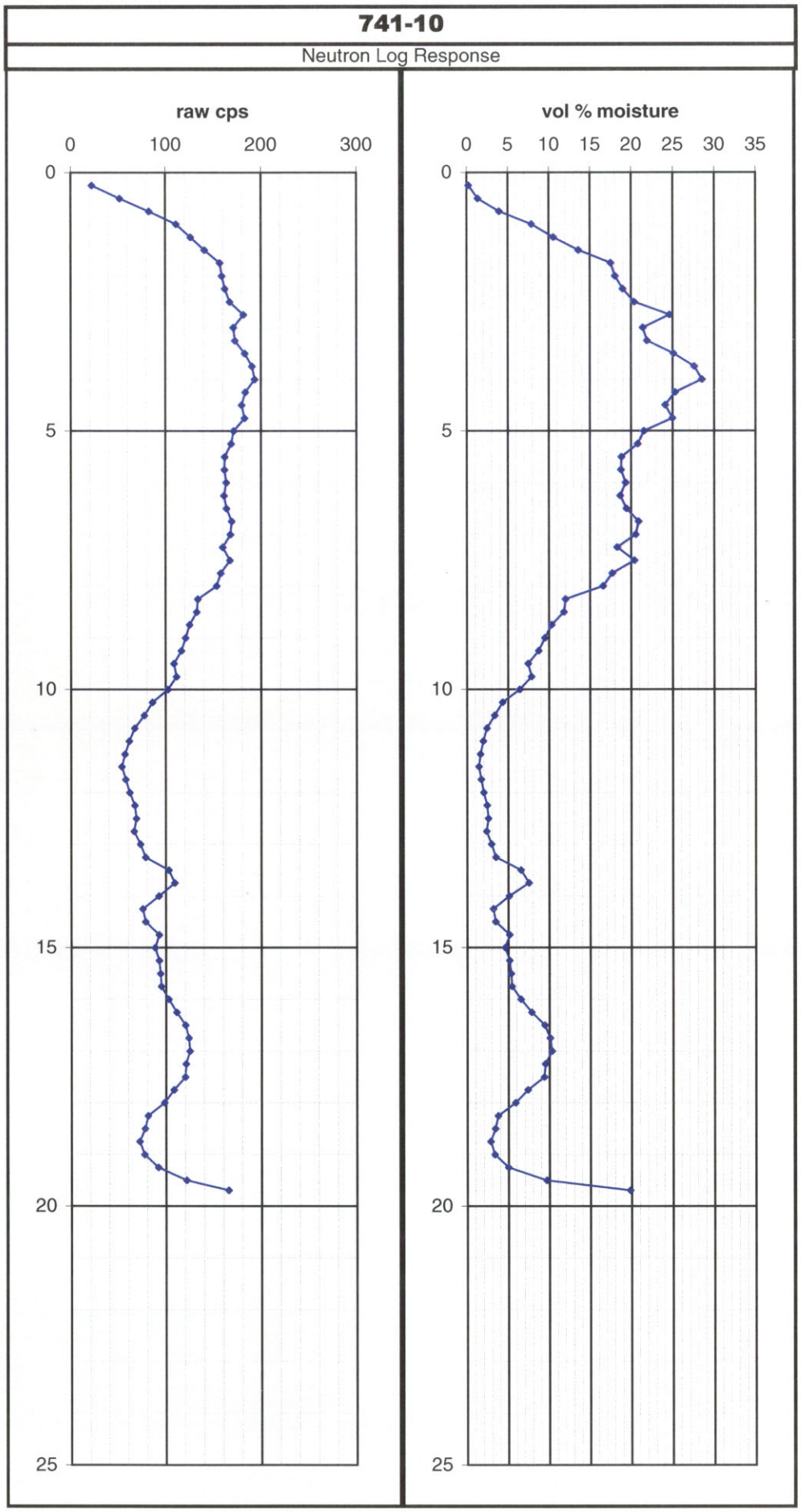
741-10
Neutron Log Response
raw cps
0
100
200
300
vol % moisture
0
5
10
15
20
25
30
35
0
5
10
15
20
25

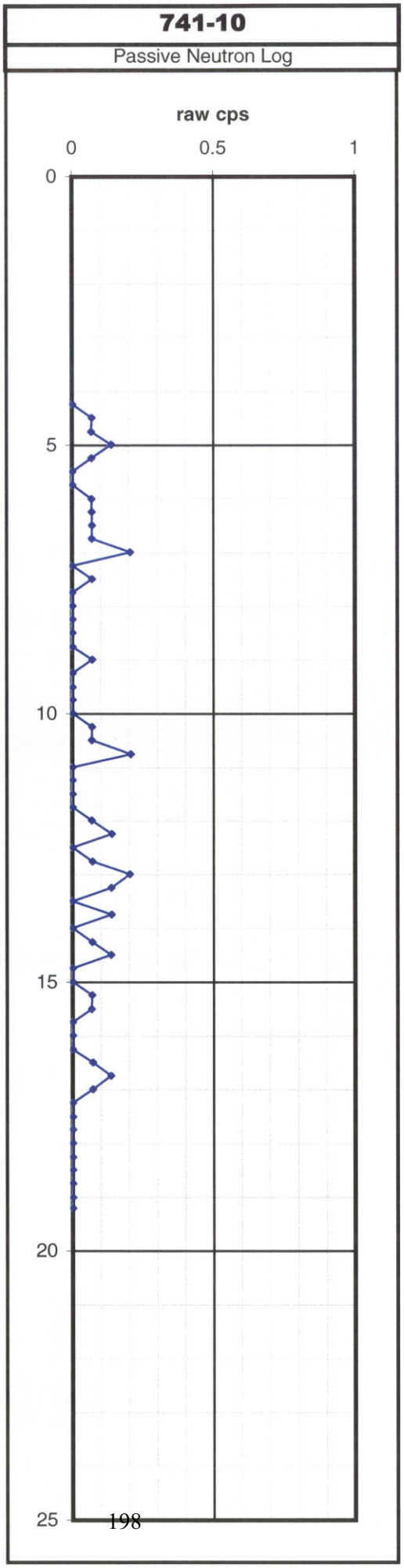
741-10
Passive Neutron Log
raw cps
0
0.5
1
0
5
10
15
20
25

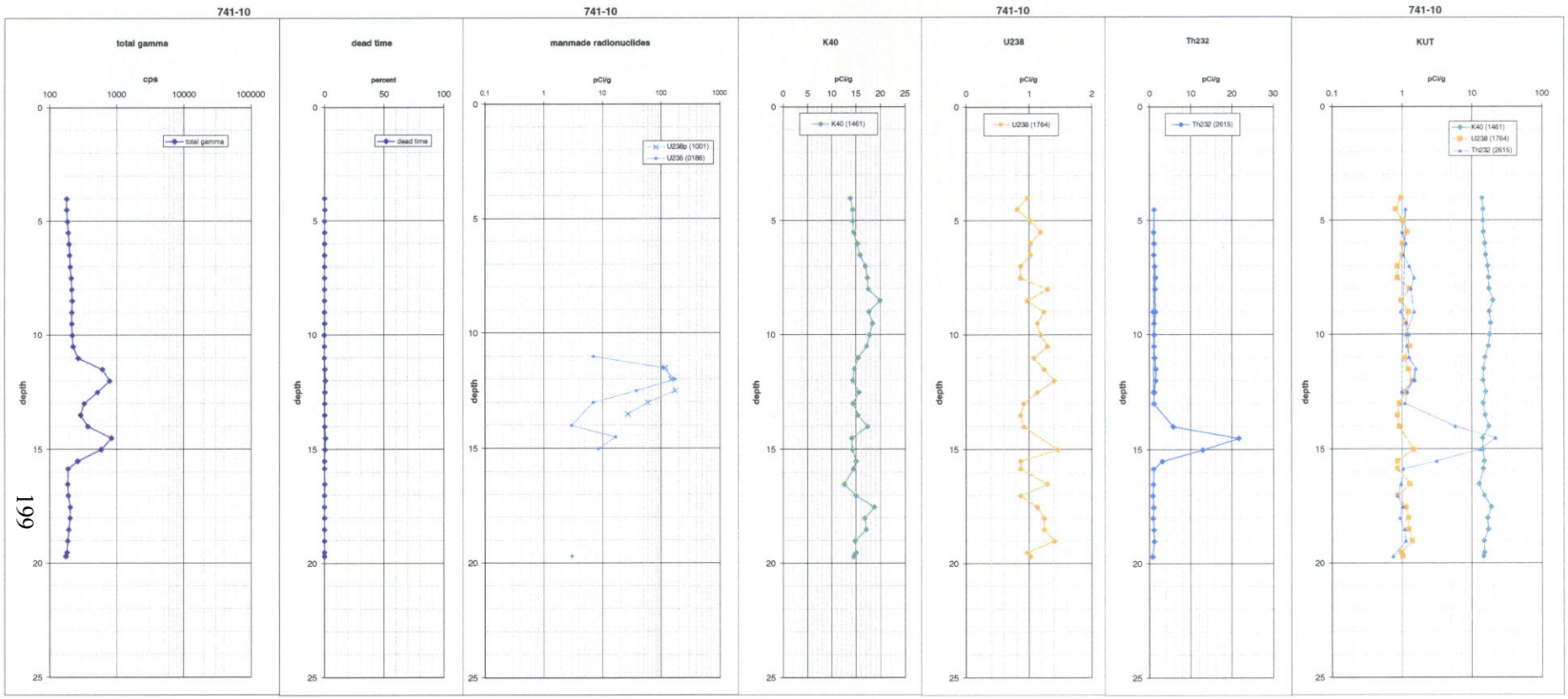
741-10
total gamma
cps
total gamma
depth
741-10
dead time
percent
dead time
depth
741-10
manmade radionuclides
pCi/g
U238p (1001)
U235 (0186)
depth
741-10
K40
pCi/g
K40 (1461)
depth
741-10
U238
pCi/g
U238 (1764)
depth
741-10
Th232
pCi/g
Th232 (2615)
depth
741-10
KUT
pCi/g
K40 (1461)
U238 (1764)
Th232 (2615)
depth

741-10

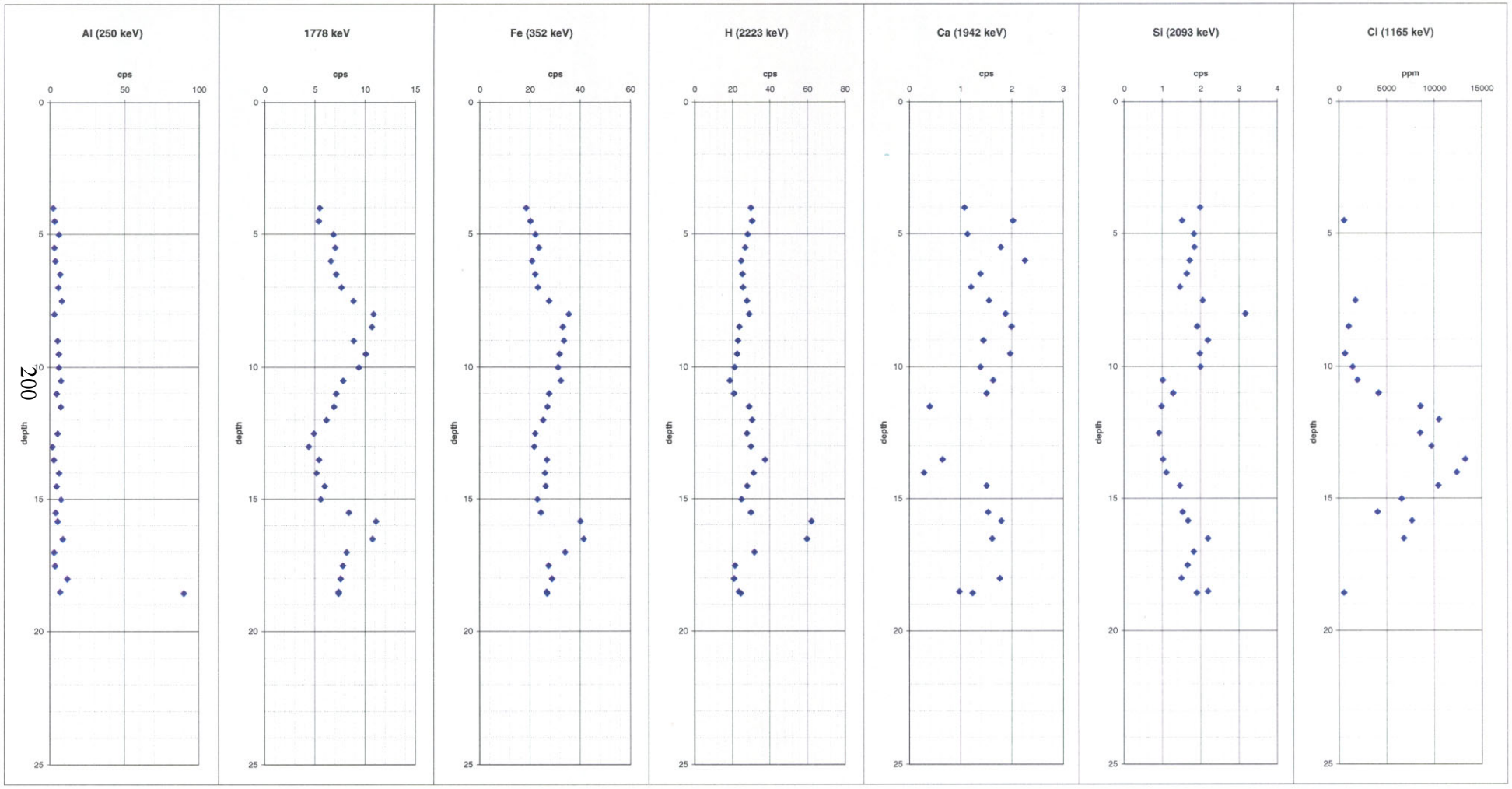
Al (250 keV)
1778 keV
Fe (352 keV)
H (2223 keV)
Ca (1942 keV)
Si (2093 keV)
Cl (1165 keV)
cps
ppm
depth

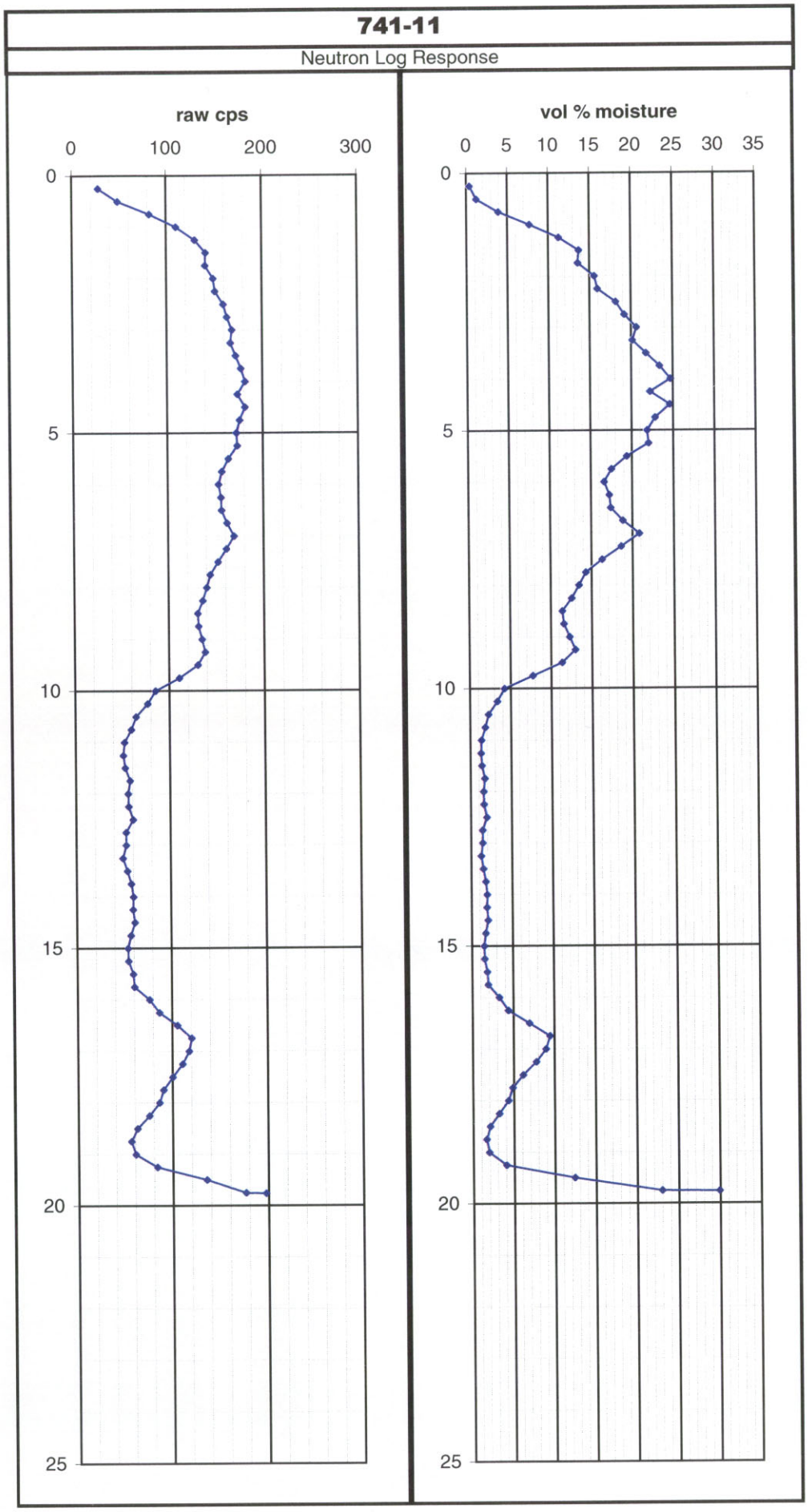
741-11
Neutron Log Response
raw cps
0
100
200
300
0
5
10
15
20
25
vol % moisture
0
5
10
15
20
25
30
35
0
5
10
15
20
25

741-11

Passive Neutron Log

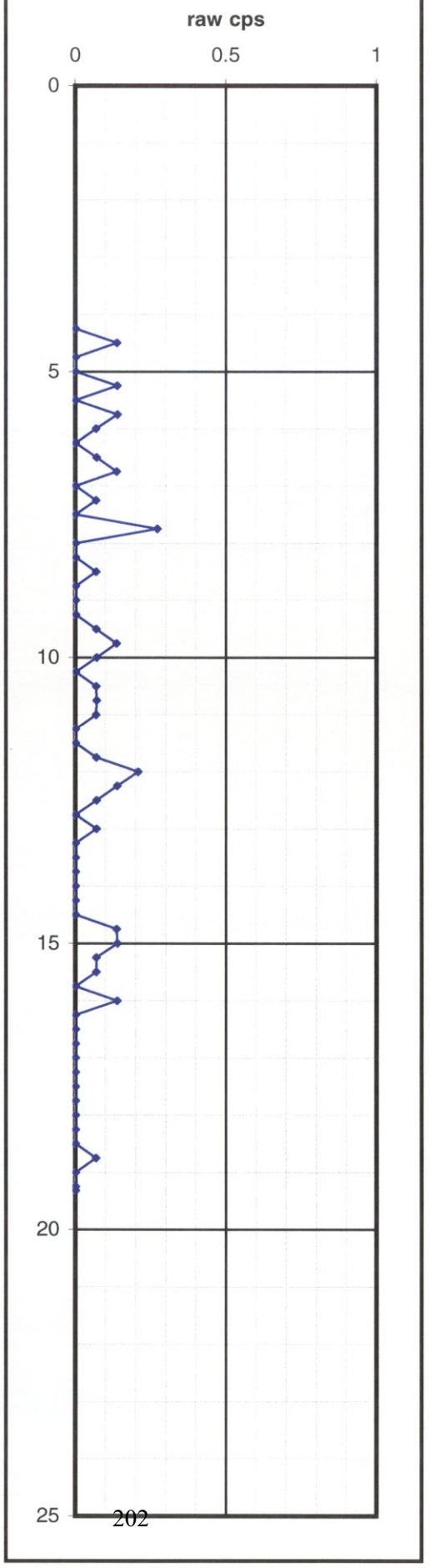

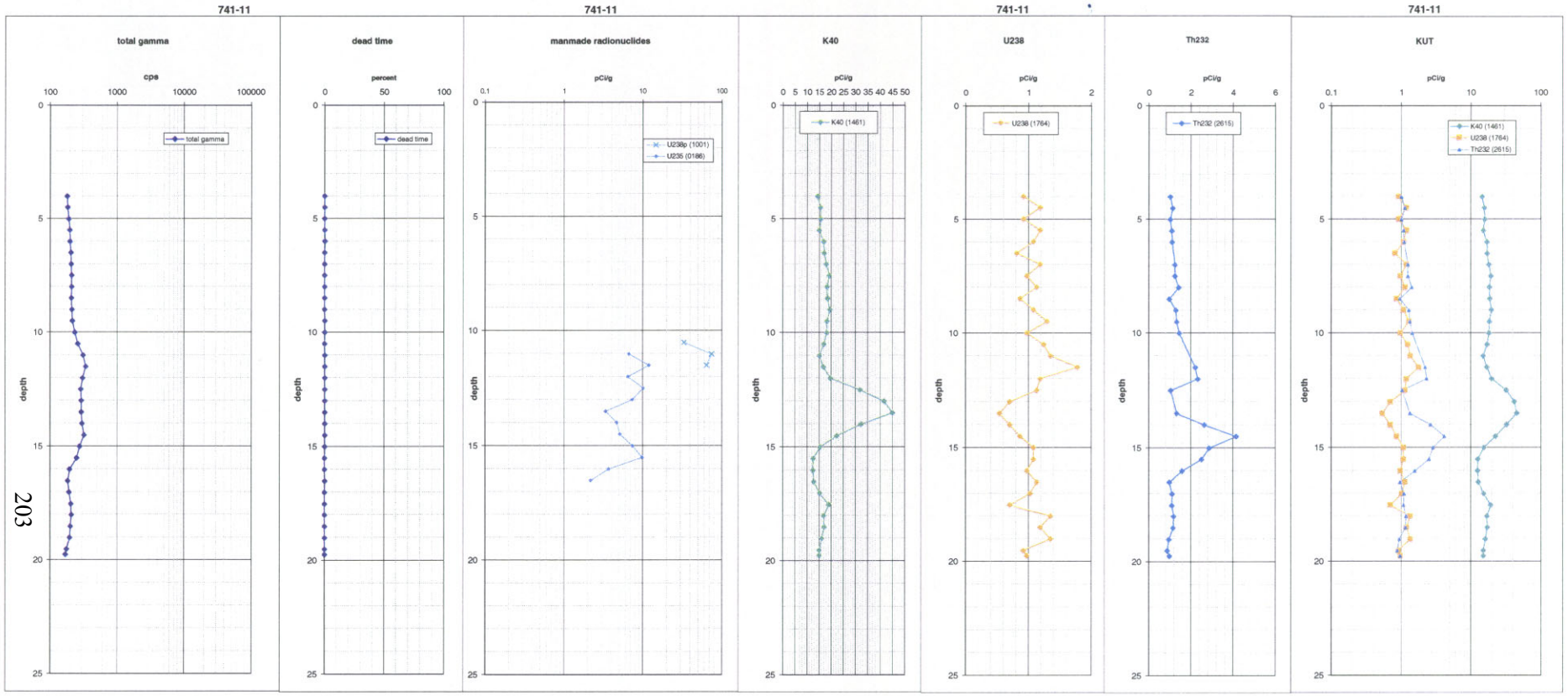
741-11
total gamma
cps
100
1000
10000
100000
total gamma
depth
741-11
dead time
percent
0
50
100
dead time
depth
741-11
manmade radionuclides
pCi/g
0.1
1
10
100
U238p (1001)
U235 (0186)
depth
741-11
K40
pCi/g
0 5 10 15 20 25 30 35 40 45 50
K40 (1461)
depth
741-11
U238
pCi/g
0
1
2
U238 (1764)
depth
741-11
Th232
pCi/g
0
2
4
6
Th232 (2615)
depth
741-11
KUT
pCi/g
0.1
1
10
100
K40 (1461)
U238 (1764)
Th232 (2615)
depth

741-11

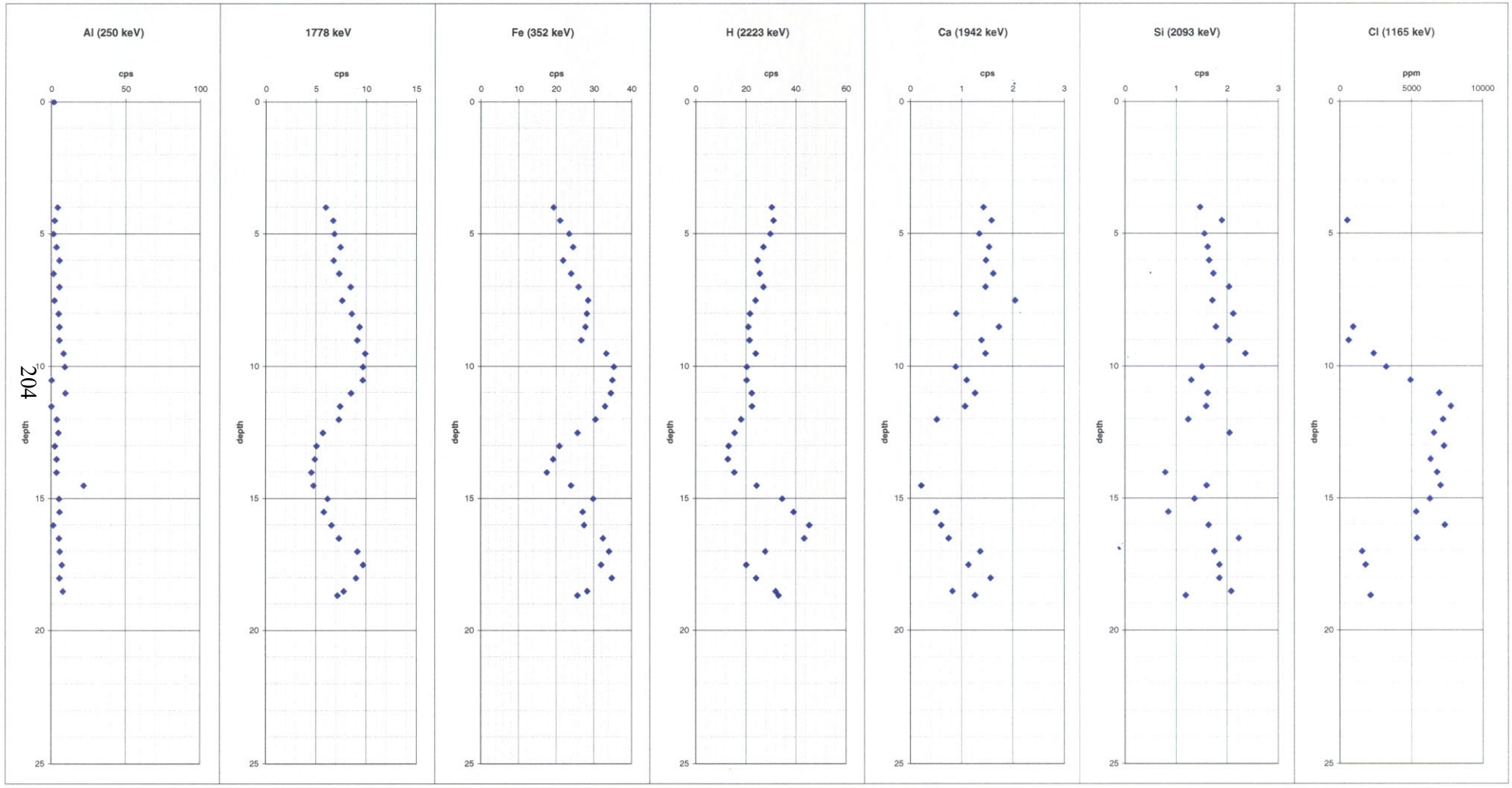
Al (250 keV)
1778 keV
Fe (352 keV)
H (2223 keV)
Ca (1942 keV)
Si (2093 keV)
Cl (1165 keV)
cps
ppm
depth

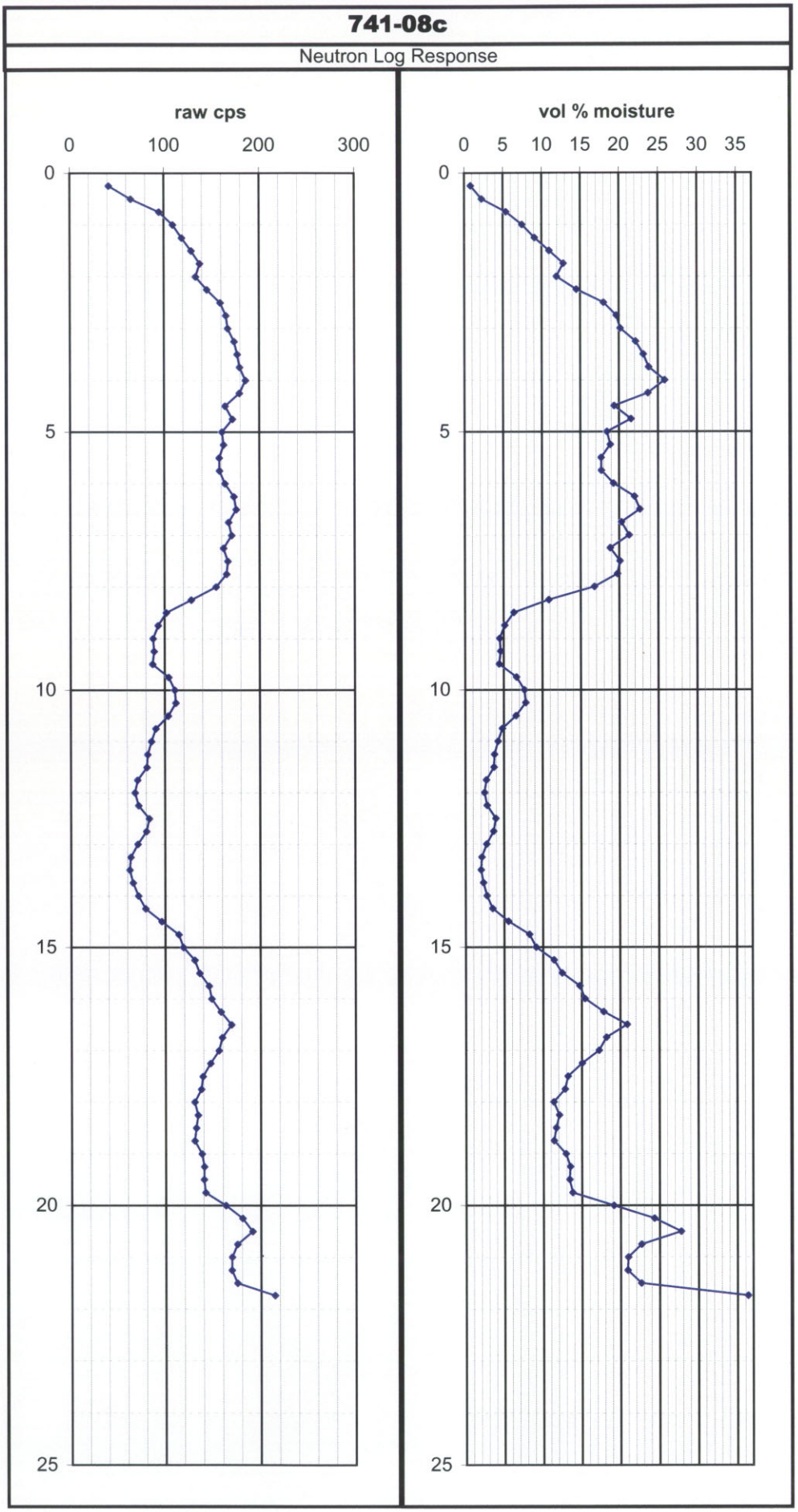
741-08c
Neutron Log Response
raw cps
0
100
200
300
0
5
10
15
20
25
vol % moisture
0
5
10
15
20
25
30
35
0
5
10
15
20
25

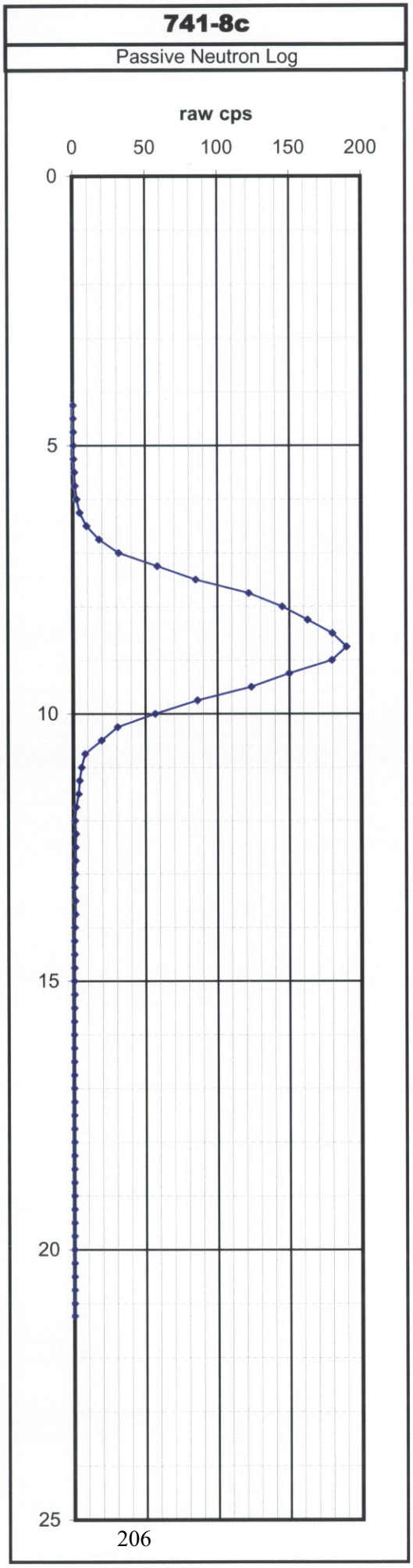
741-8c
Passive Neutron Log
raw cps
0
50
100
150
200
0
5
10
15
20
25

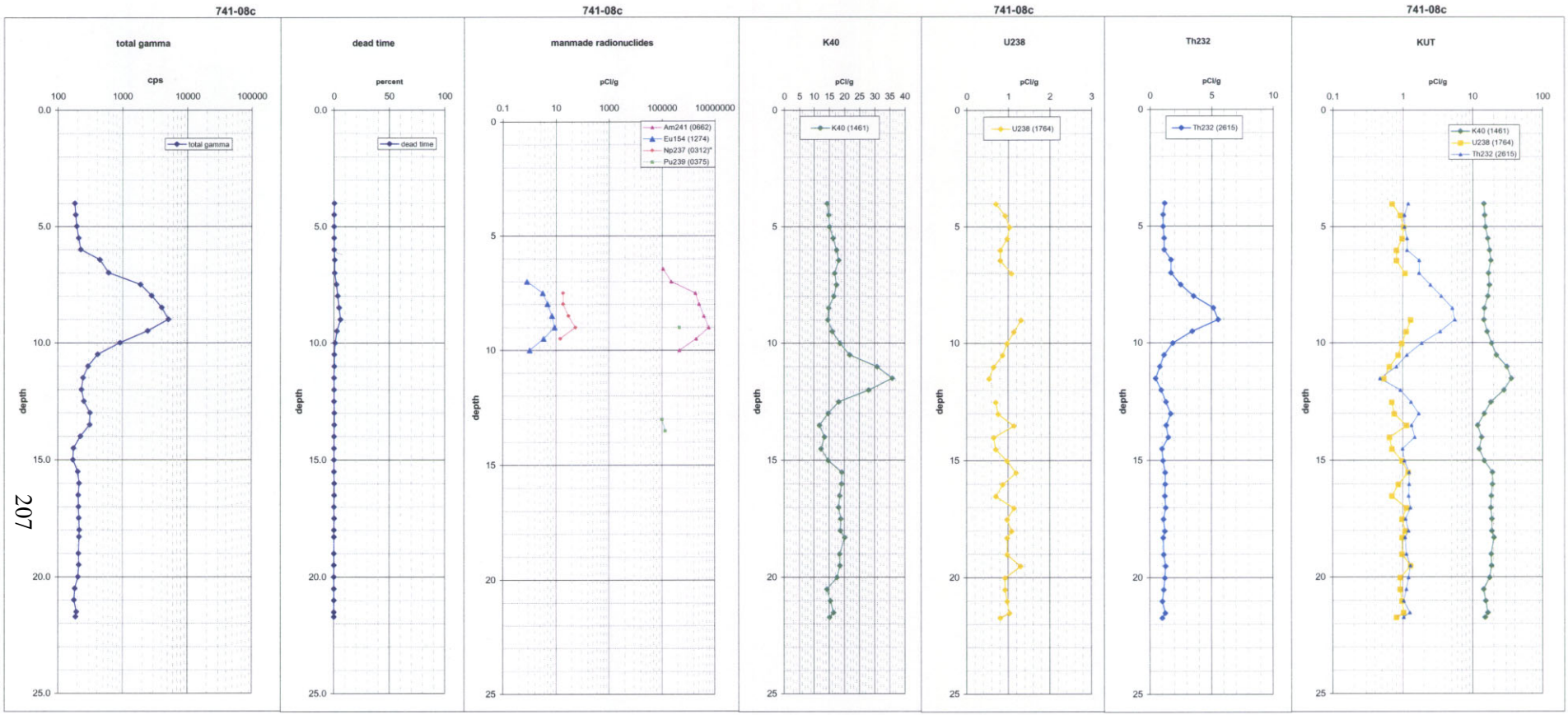
741-08c
total gamma
cps
total gamma
dead time
percent
dead time
manmade radionuclides
pCi/g
Am241 (0662)
Eu154 (1274)
Np237 (0312)*
Pu239 (0375)
K40
pCi/g
K40 (1461)
U238
pCi/g
U238 (1764)
Th232
pCi/g
Th232 (2615)
KUT
pCi/g
K40 (1461)
U238 (1764)
Th232 (2615)
depth

741-08c

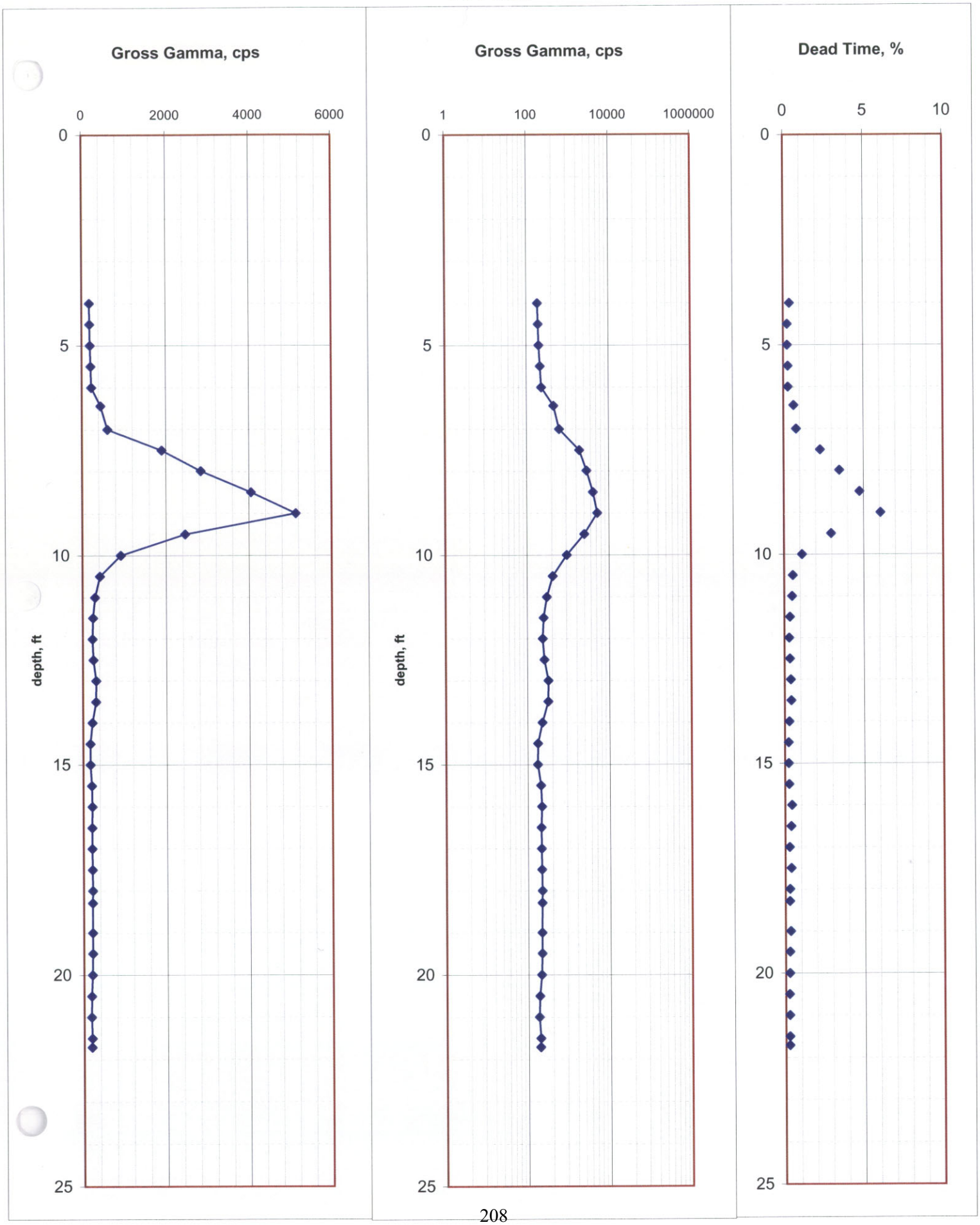
Gross Gamma, cps
0
2000
4000
6000
depth, ft
0
5
10
15
20
25
Gross Gamma, cps
1
100
10000
1000000
depth, ft
0
5
10
15
20
25
Dead Time, %
0
5
10
0
5
10
15
20
25

741-08c

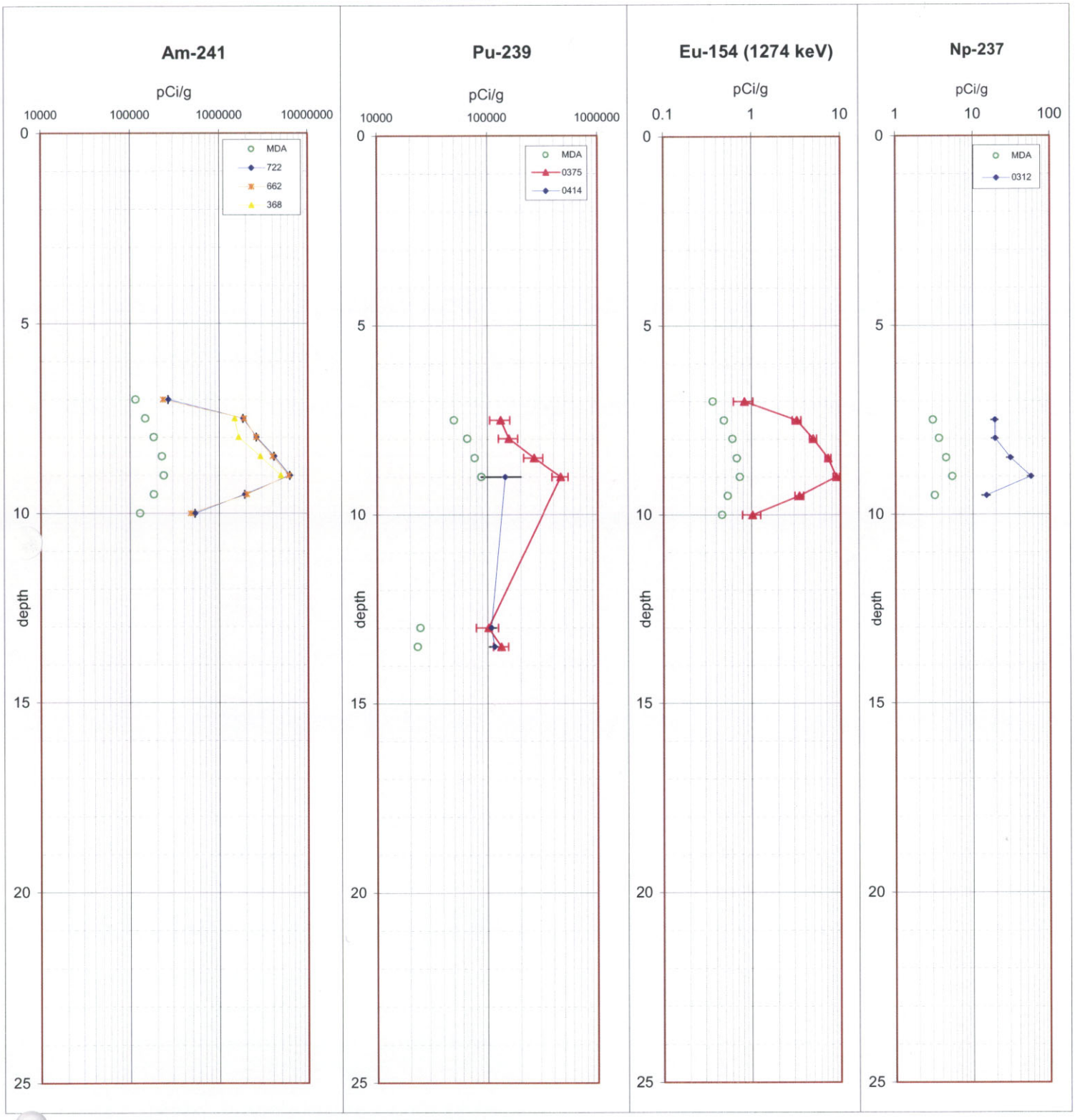
Am-241
pCi/g
10000
100000
1000000
10000000
MDA
722
662
368
Pu-239
pCi/g
10000
100000
1000000
MDA
0375
0414
Eu-154 (1274 keV)
pCi/g
0.1
1
10
Np-237
pCi/g
1
10
100
MDA
0312
depth
0
5
10
15
20
25

741-08c

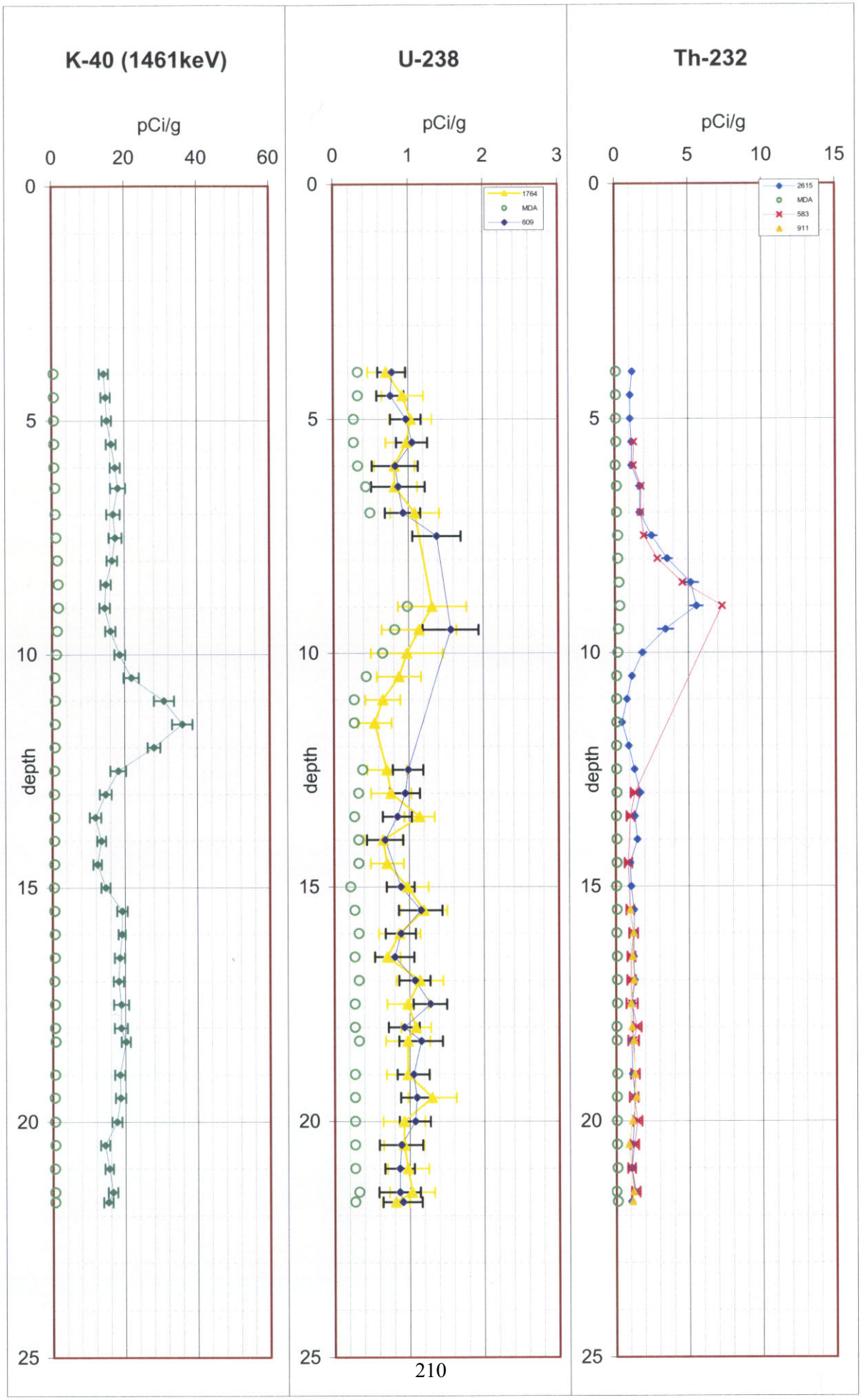
K-40 (1461keV)
U-238
Th-232
pCi/g
0
20
40
60
1
2
3
5
10
15
depth
0
5
10
15
20
25
1764
MDA
609
2615
583
911

741-8c

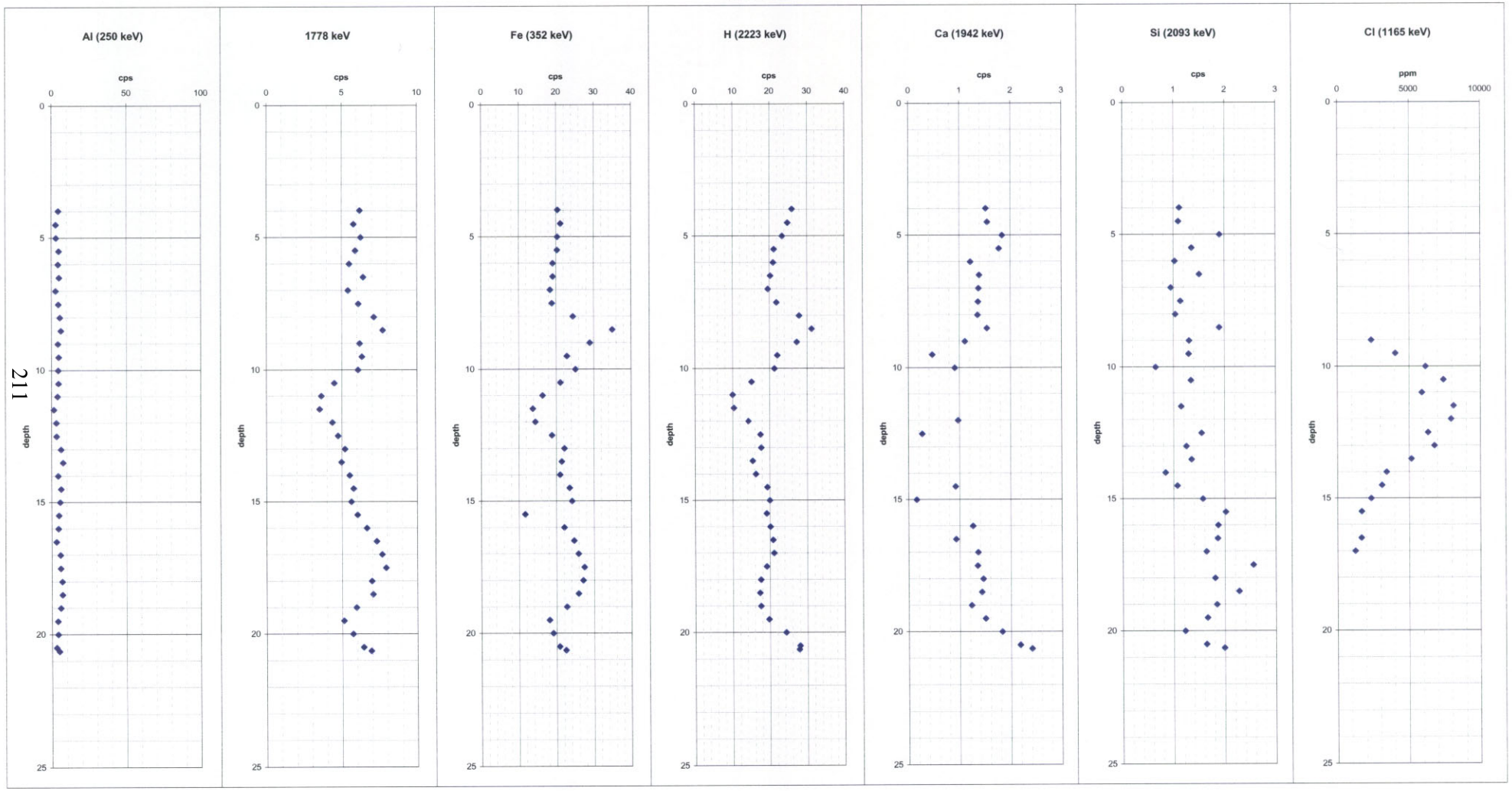
Al (250 keV)
1778 keV
Fe (352 keV)
H (2223 keV)
Ca (1942 keV)
Si (2093 keV)
Cl (1165 keV)
cps
ppm
depth

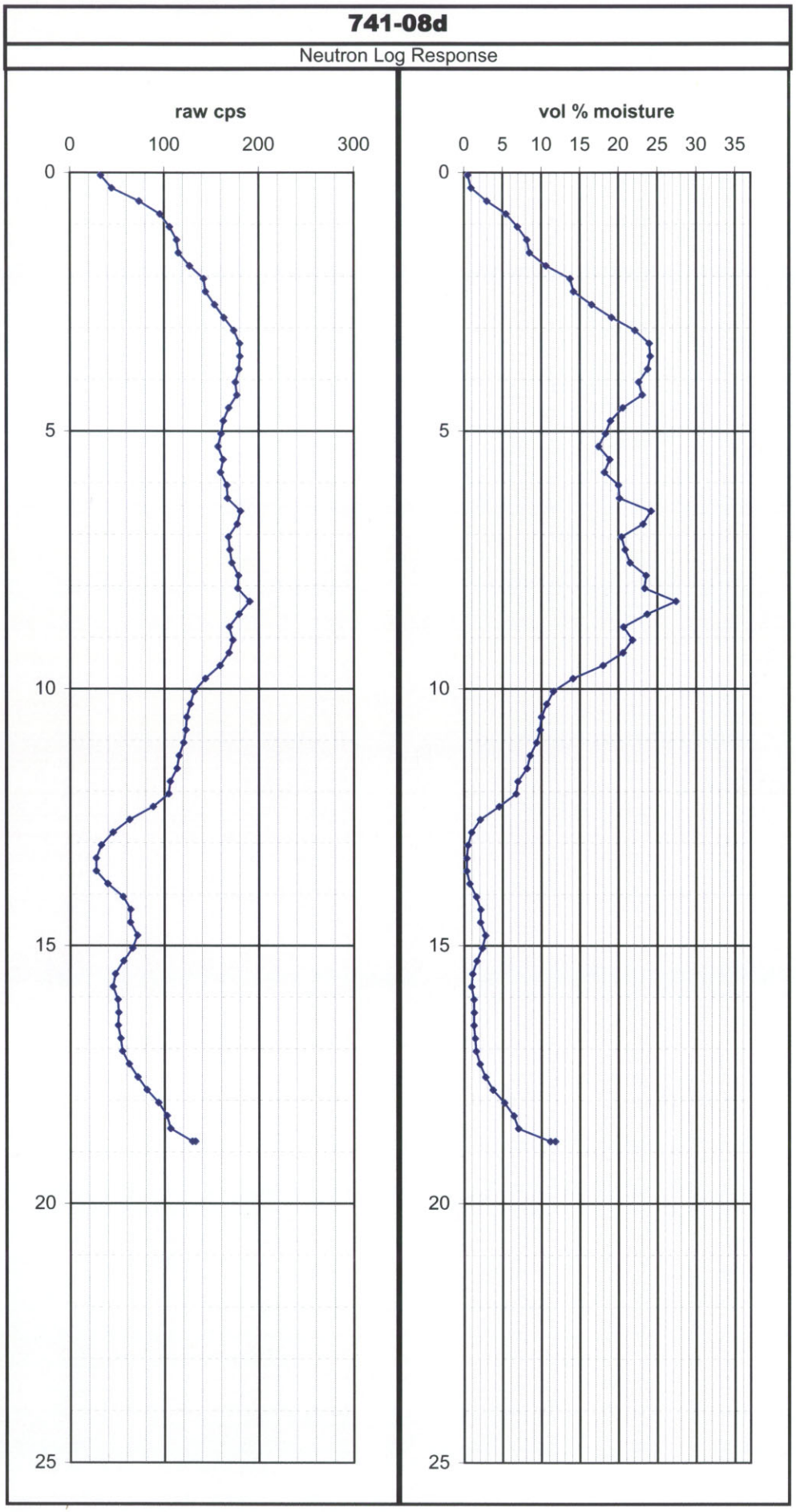
741-08d
Neutron Log Response
raw cps
0
100
200
300
vol % moisture
0
5
10
15
20
25
30
35
0
5
10
15
20
25

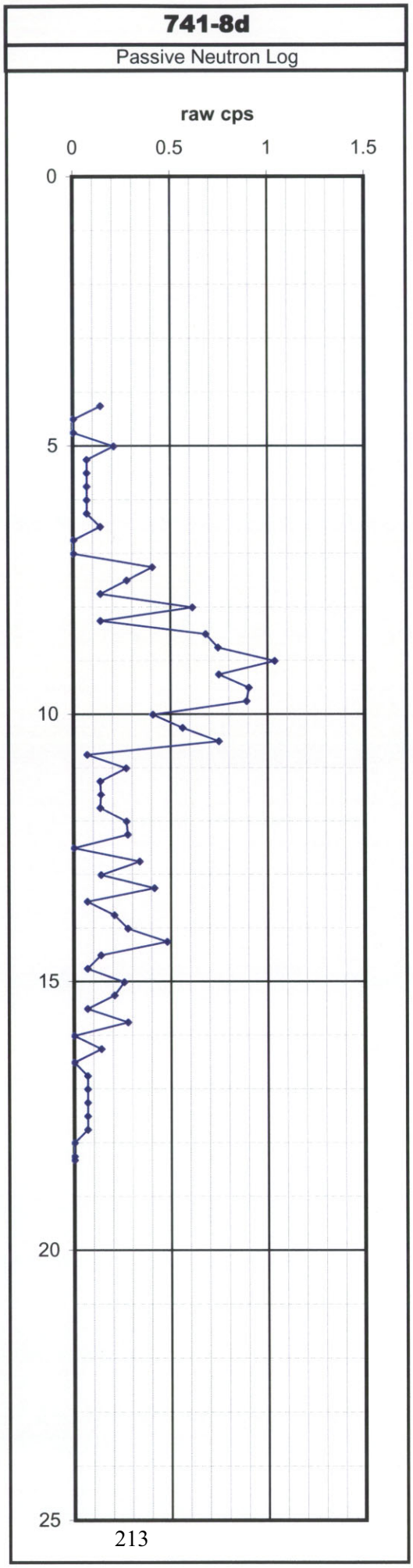
741-8d
Passive Neutron Log
raw cps
0
0.5
1
1.5
0
5
10
15
20
25

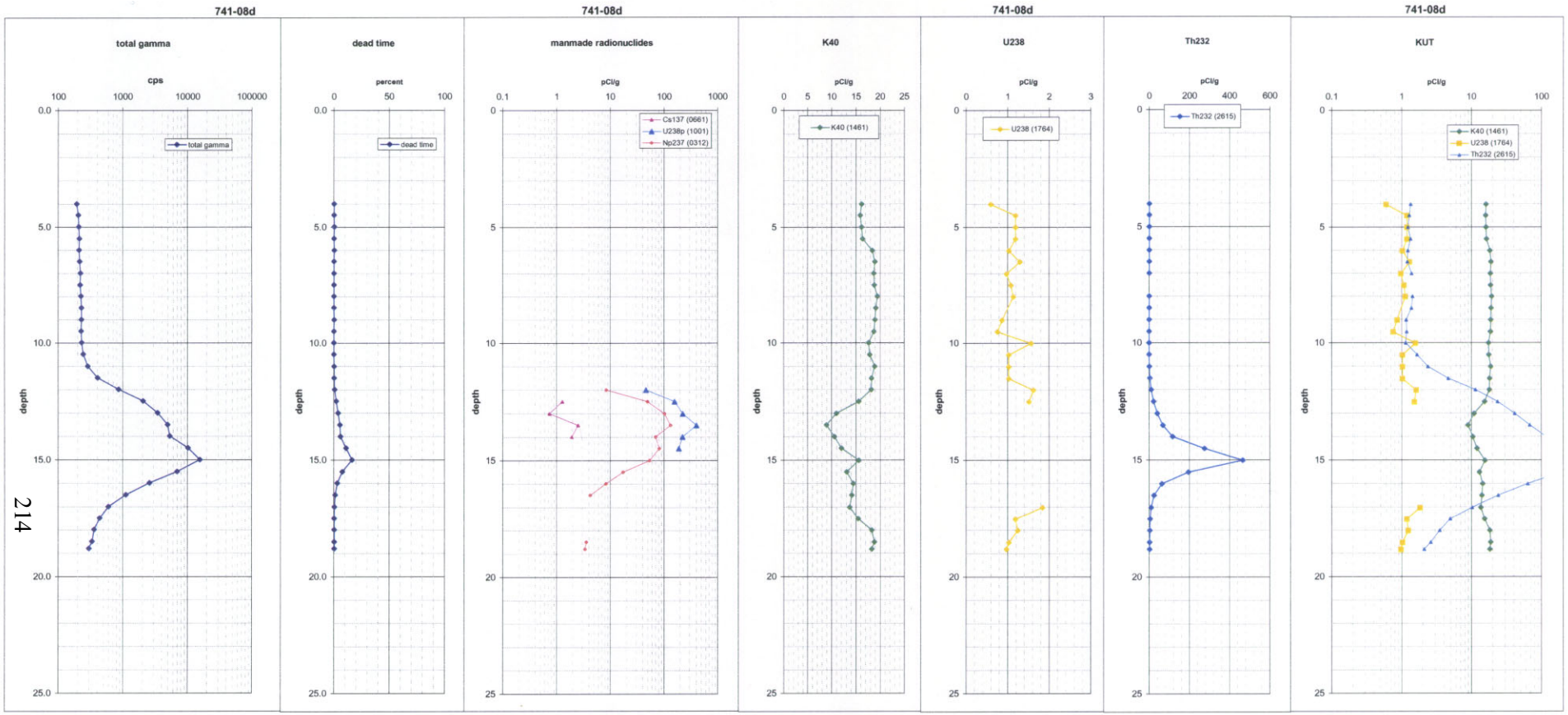
741-08d
total gamma
cps
total gamma
dead time
percent
dead time
manmade radionuclides
pCi/g
Cs137 (0661)
U238p (1001)
Np237 (0312)
K40
pCi/g
K40 (1461)
U238
pCi/g
U238 (1764)
Th232
pCi/g
Th232 (2615)
KUT
pCi/g
K40 (1461)
U238 (1764)
Th232 (2615)
depth

741-08d

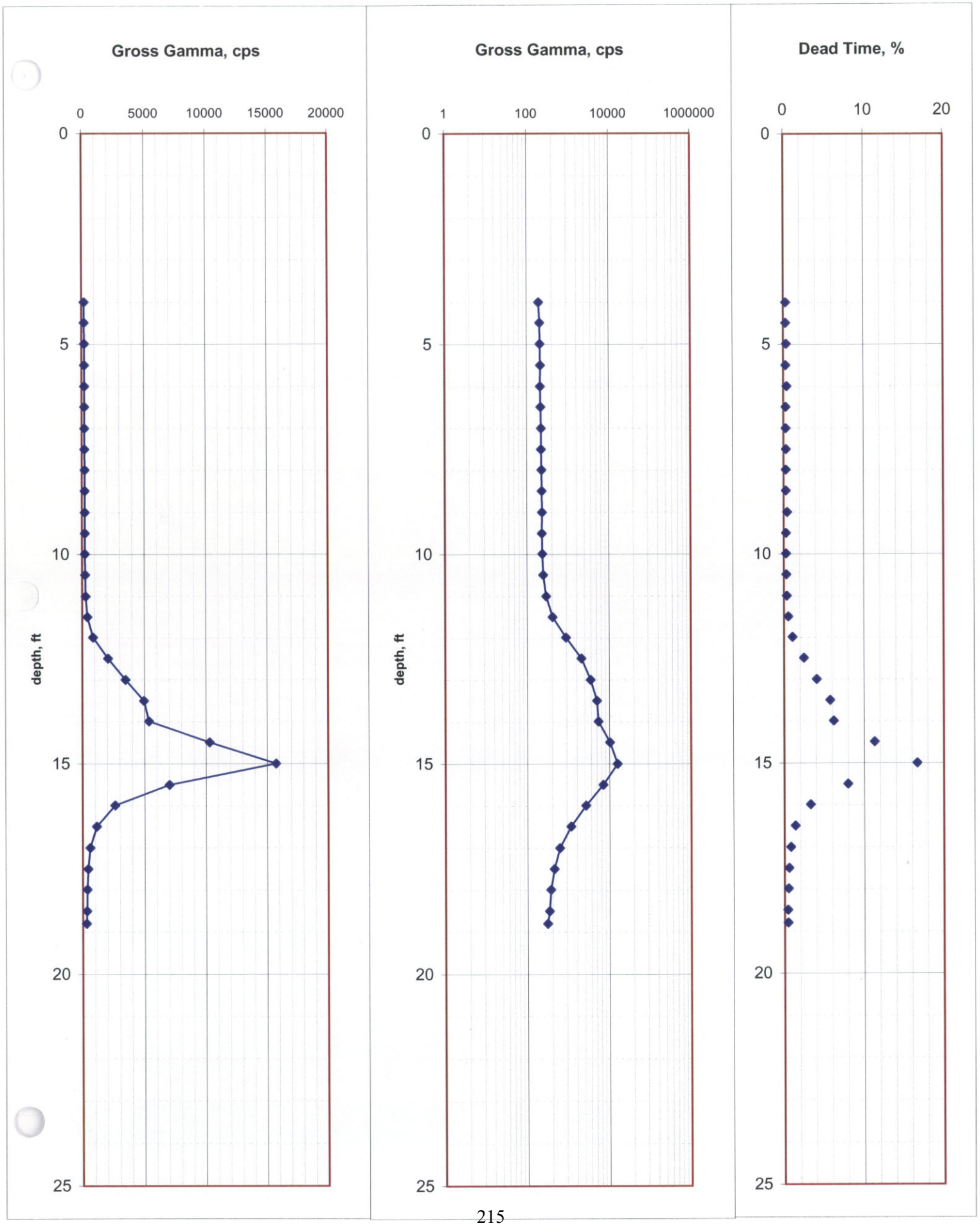
Gross Gamma, cps
0
5000
10000
15000
20000
depth, ft
0
5
10
15
20
25
Gross Gamma, cps
1
100
10000
1000000
depth, ft
0
5
10
15
20
25
Dead Time, %
0
10
20
0
5
10
15
20
25

741-08d

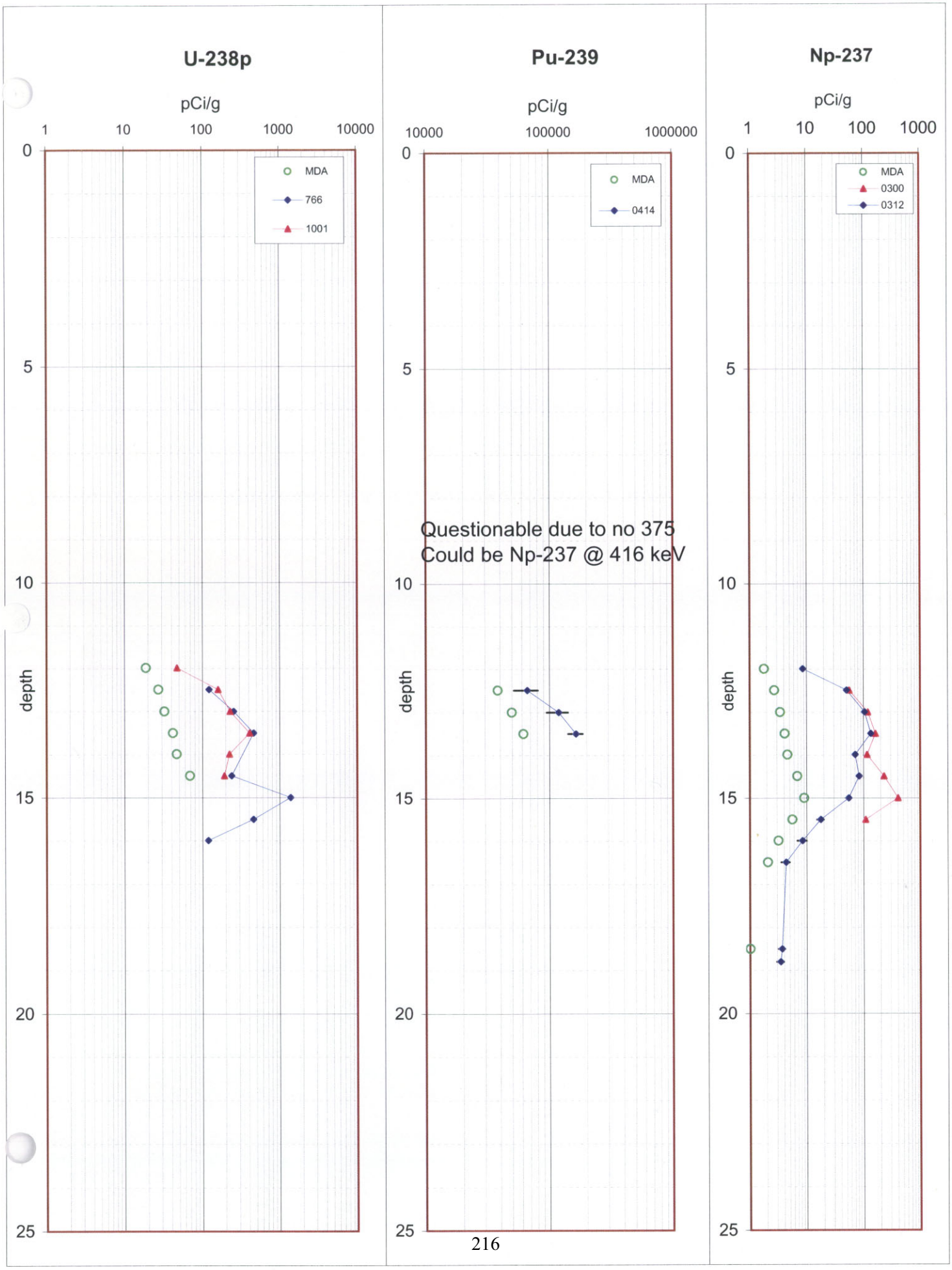
U-238p
pCi/g
1
10
100
1000
10000
MDA
766
1001
depth
0
5
10
15
20
25
Pu-239
pCi/g
10000
100000
1000000
MDA
0414
Questionable due to no 375
Could be Np-237 @ 416 keV
depth
Np-237
pCi/g
1
10
100
1000
MDA
0300
0312
depth

741-08d

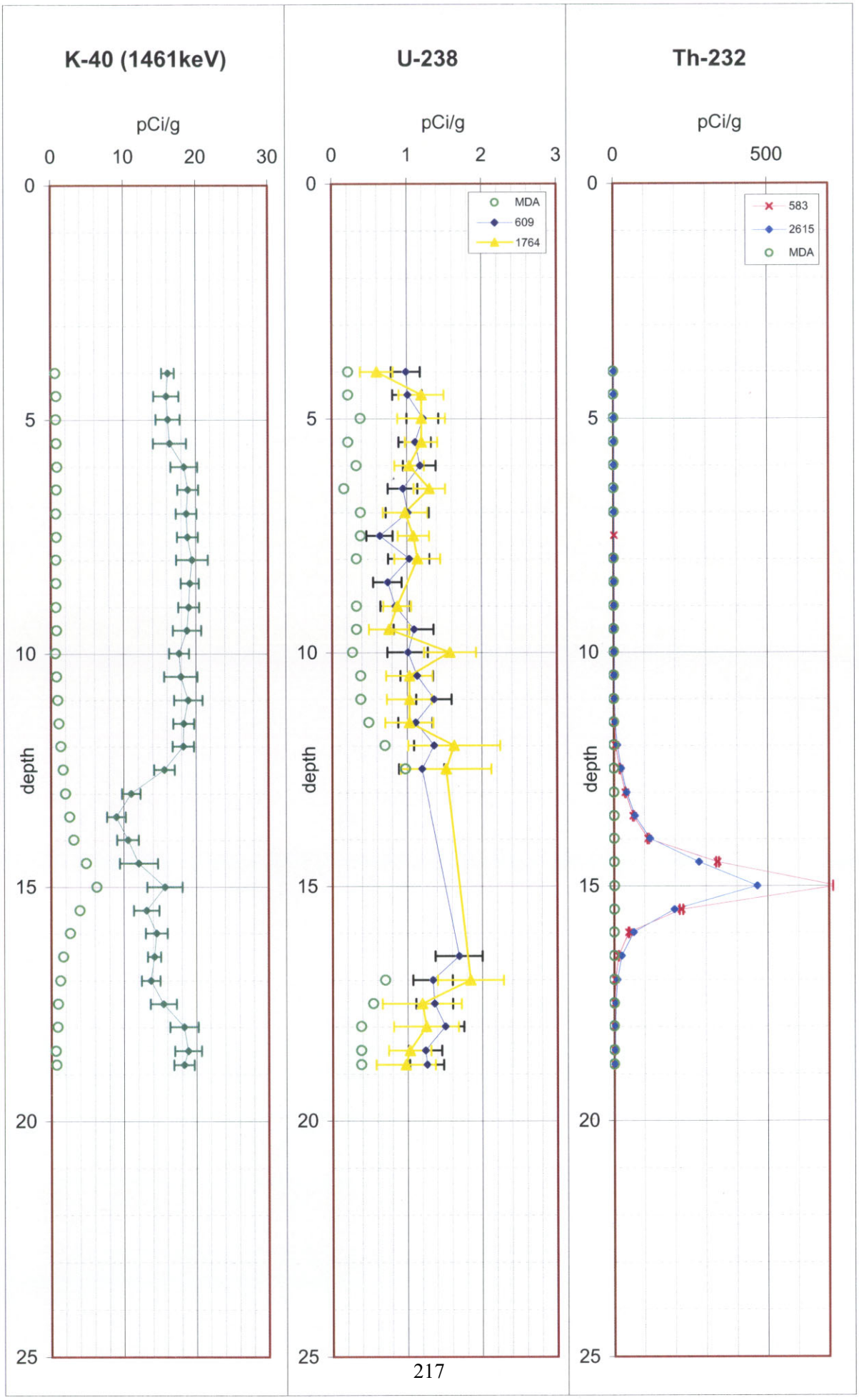
K-40 (1461keV)
pCi/g
0
10
20
30
depth
0
5
10
15
20
25
U-238
pCi/g
0
1
2
3
MDA
609
1764
Th-232
pCi/g
0
500
583
2615
MDA

741-8d

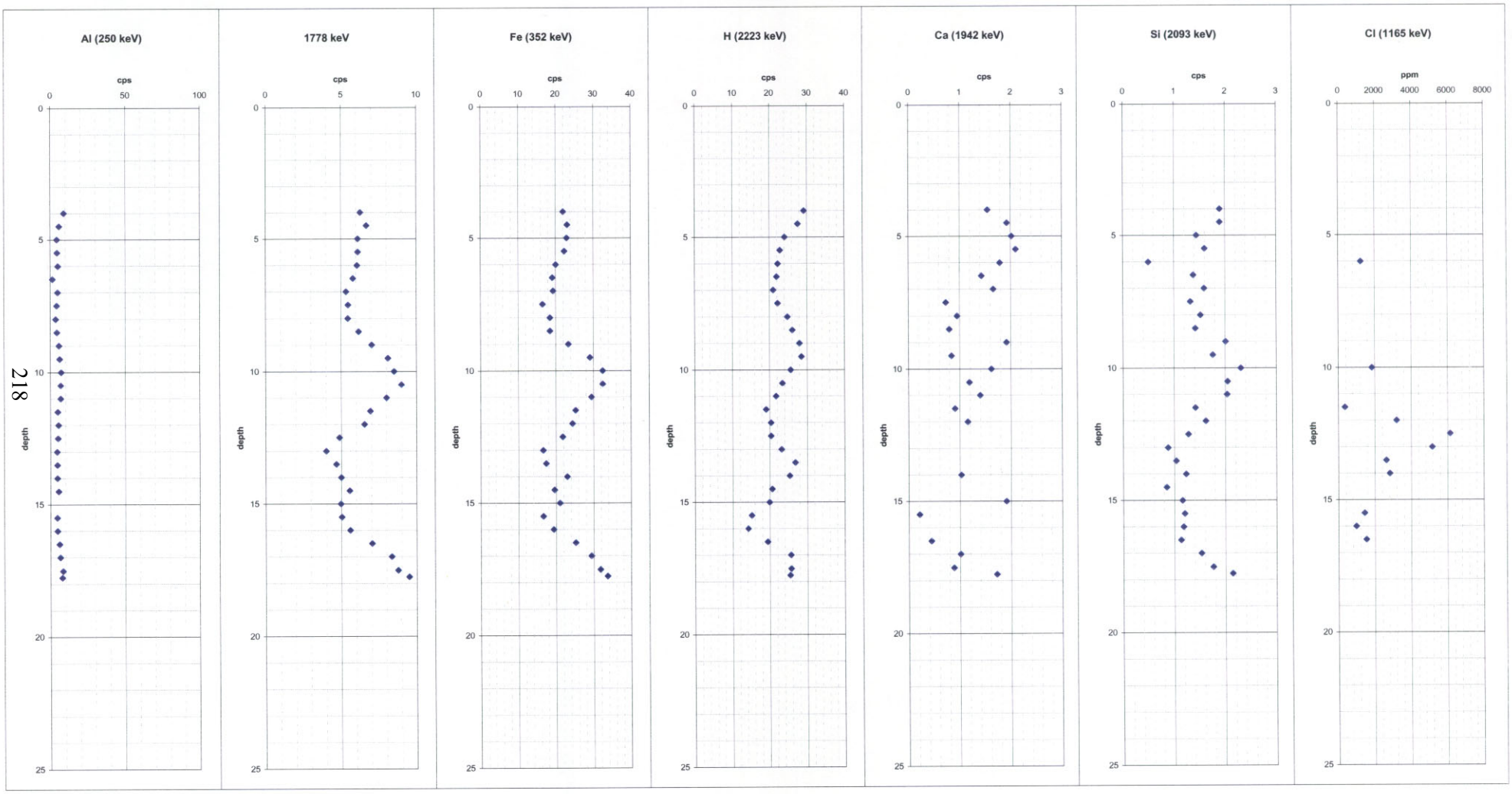
Al (250 keV)
1778 keV
Fe (352 keV)
H (2223 keV)
Ca (1942 keV)
Si (2093 keV)
Cl (1165 keV)
cps
ppm
depth

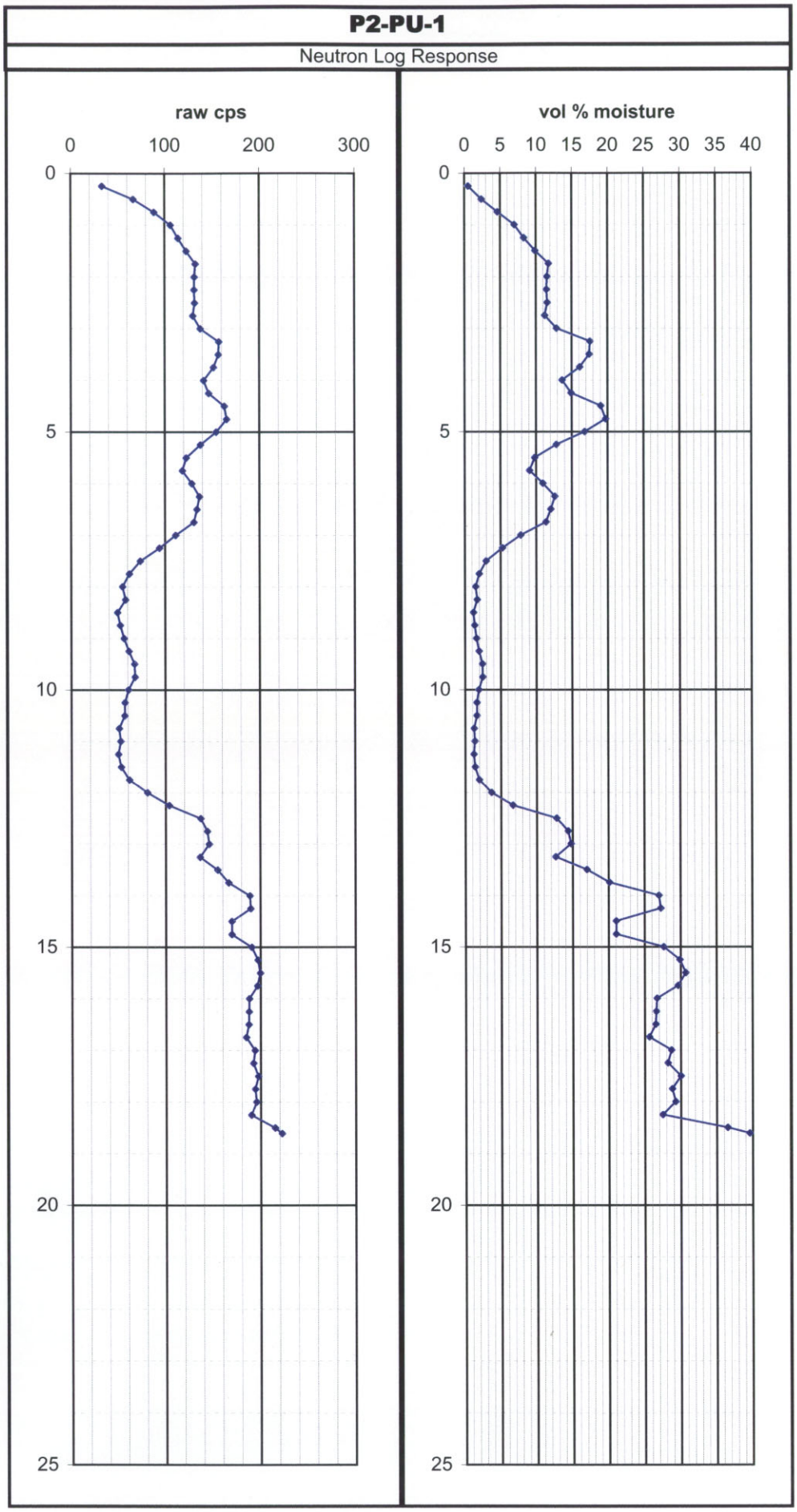
P2-PU-1
Neutron Log Response
raw cps
0
100
200
300
0
5
10
15
20
25
vol % moisture
0
5
10
15
20
25
30
35
40
0
5
10
15
20
25

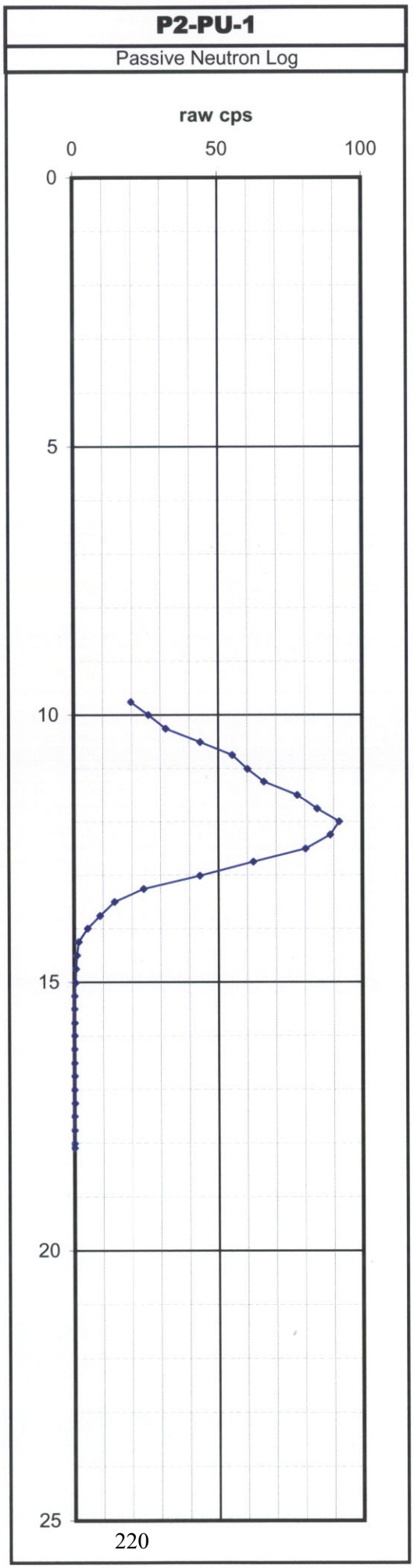
P2-PU-1
Passive Neutron Log
raw cps
0
50
100
0
5
10
15
20
25

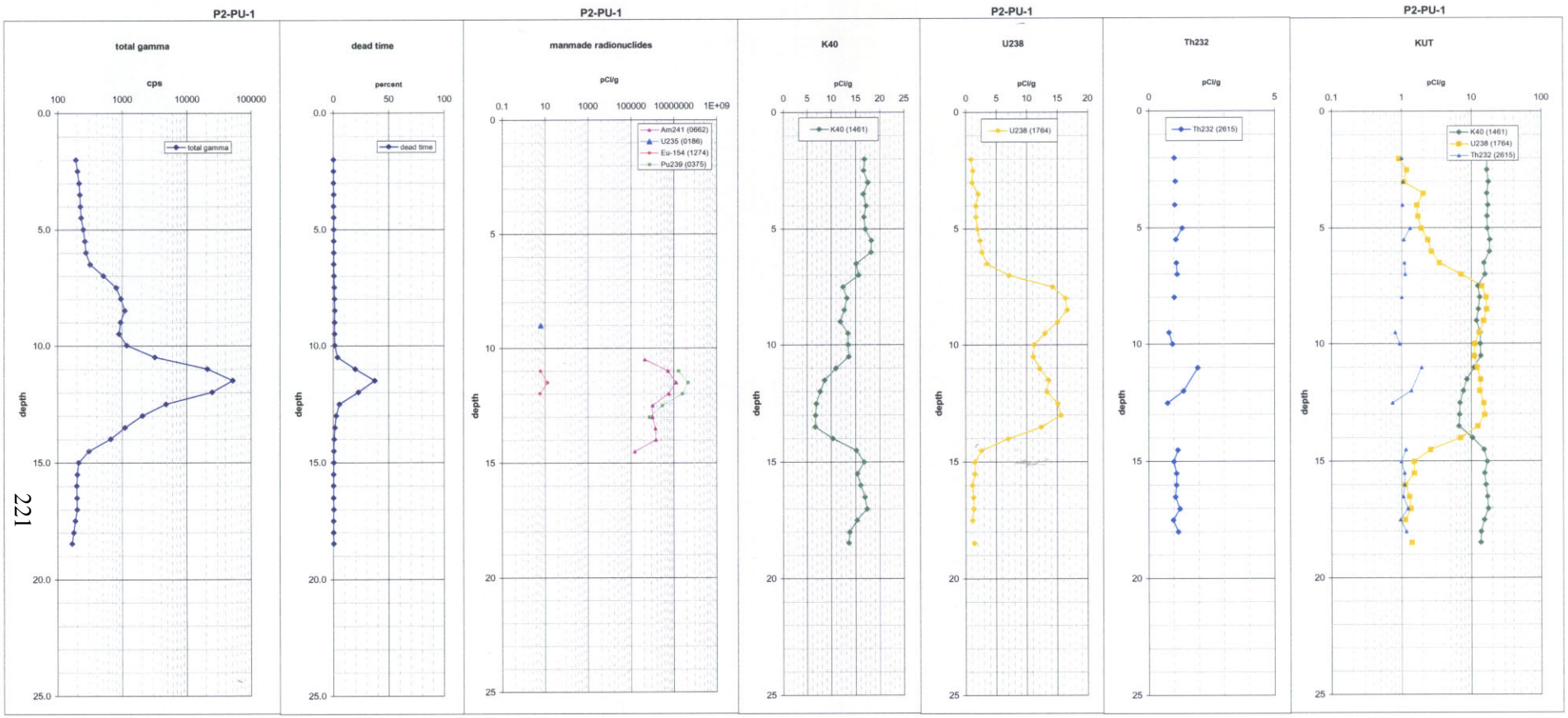
P2-PU-1
total gamma
cps
depth
total gamma
dead time
percent
dead time
manmade radionuclides
pCi/g
Am241 (0662)
U235 (0186)
Eu-154 (1274)
Pu239 (0375)
K40
K40 (1461)
U238
U238 (1764)
Th232
Th232 (2615)
KUT
K40 (1461)
U238 (1764)
Th232 (2615)

P2-PU-1

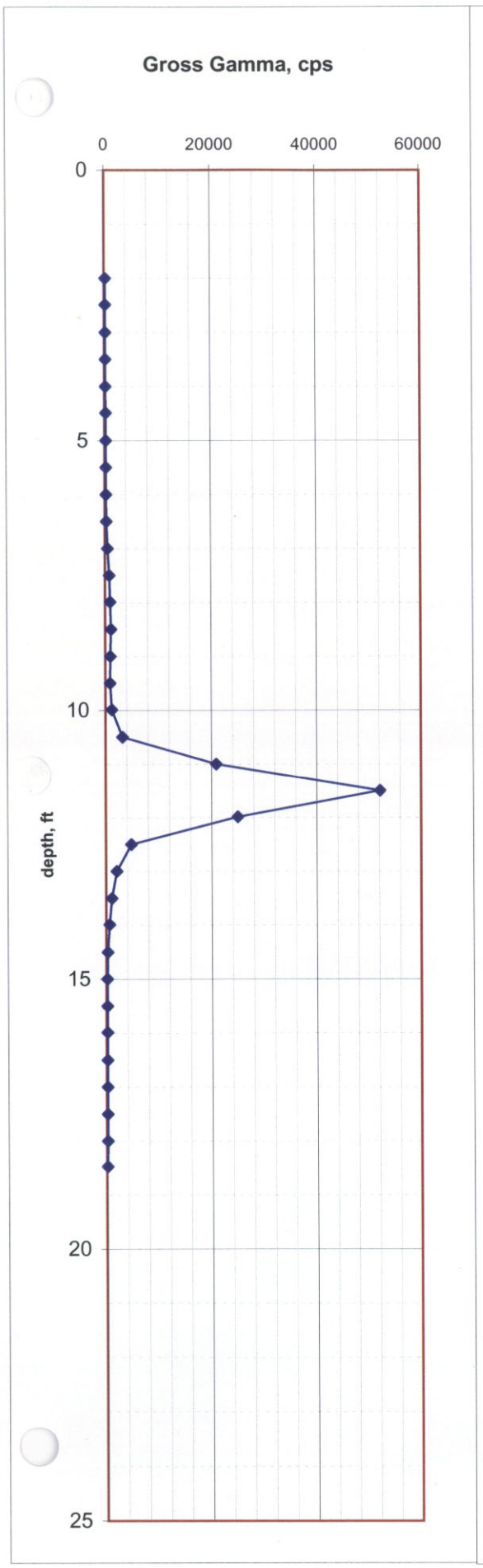
Gross Gamma, cps
0
20000
40000
60000
depth, ft
0
5
10
15
20
25

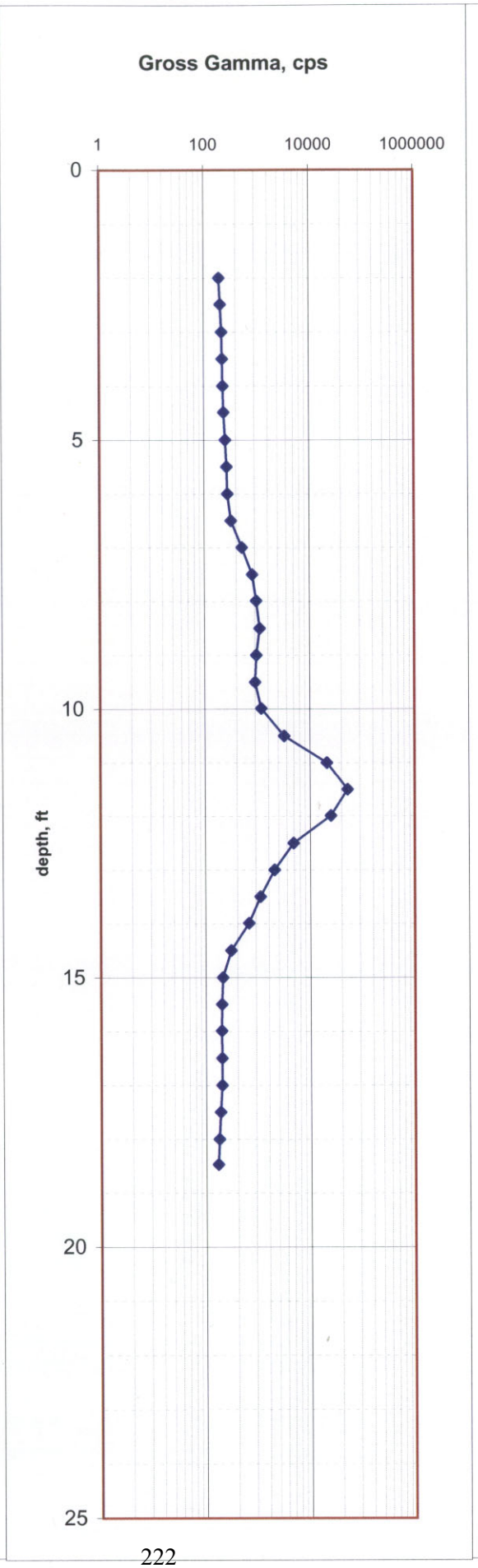
Gross Gamma, cps
1
100
10000
1000000
depth, ft
0
5
10
15
20
25

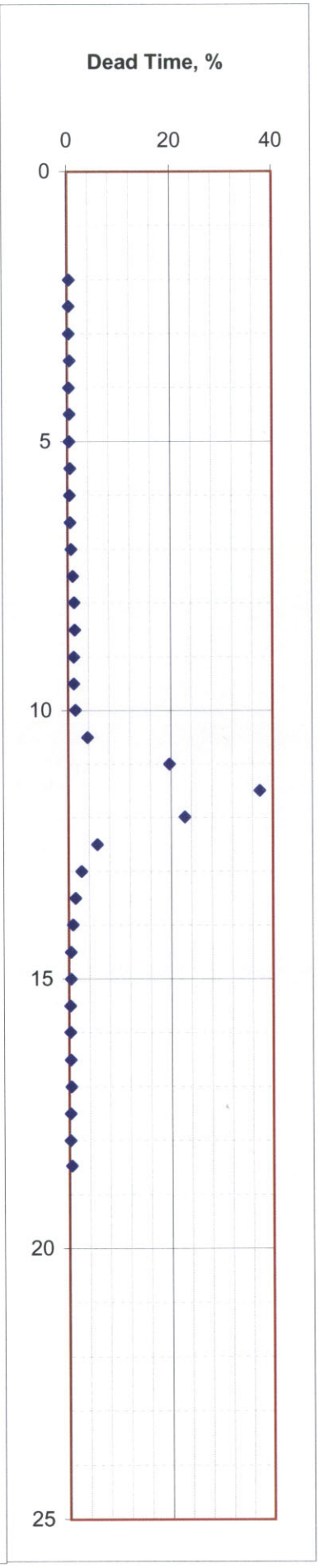
Dead Time, %
0
20
40
0
5
10
15
20
25

P2-PU-1

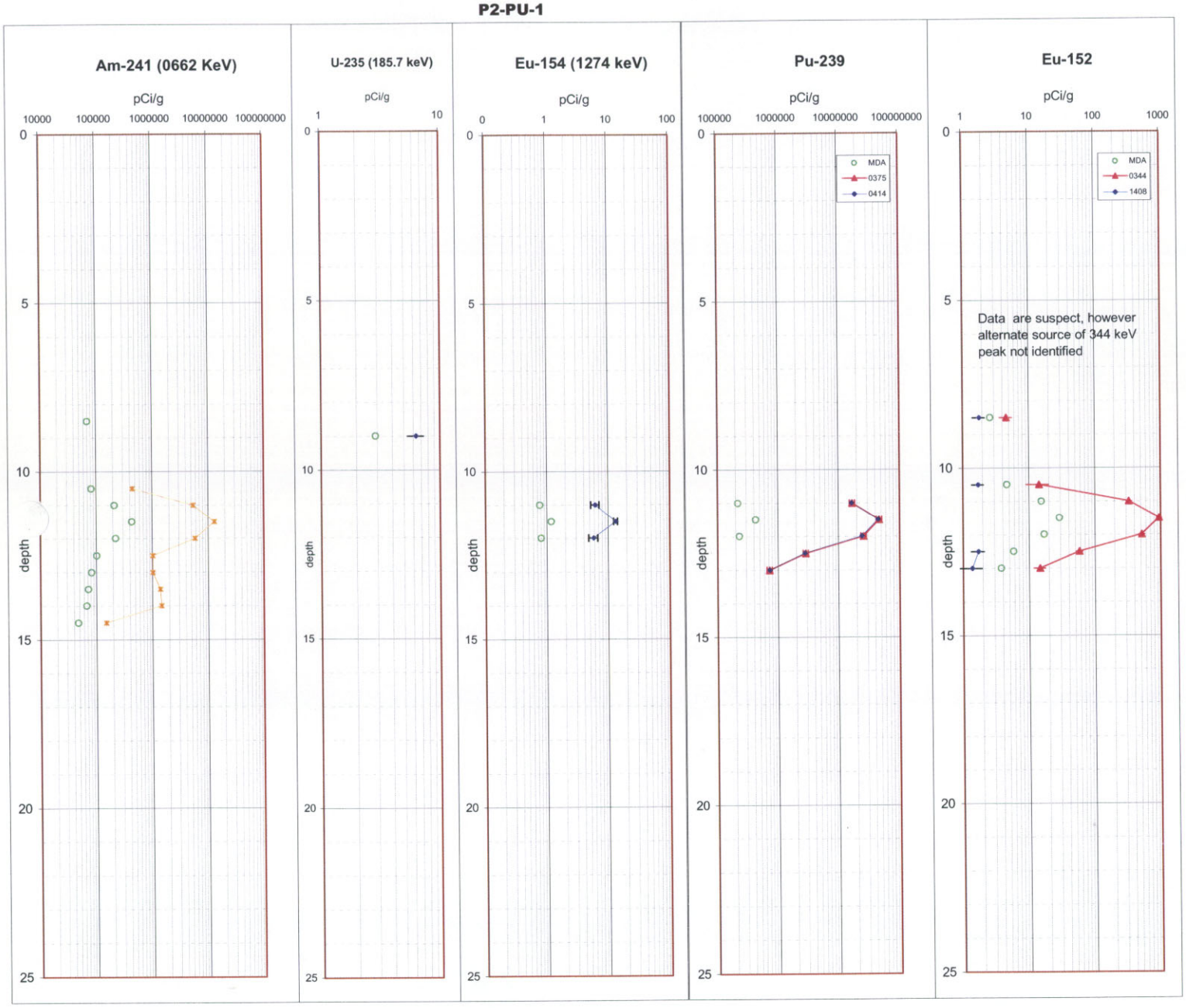
Am-241 (0662 KeV)
pCi/g
10000
100000
1000000
10000000
100000000
U-235 (185.7 keV)
pCi/g
1
10
Eu-154 (1274 keV)
pCi/g
0
1
10
100
Pu-239
pCi/g
100000
1000000
10000000
100000000
MDA
0375
0414
Eu-152
pCi/g
1
10
100
1000
MDA
0344
1408
Data are suspect, however alternate source of 344 keV peak not identified
depth
0
5
10
15
20
25

P2-PU-1

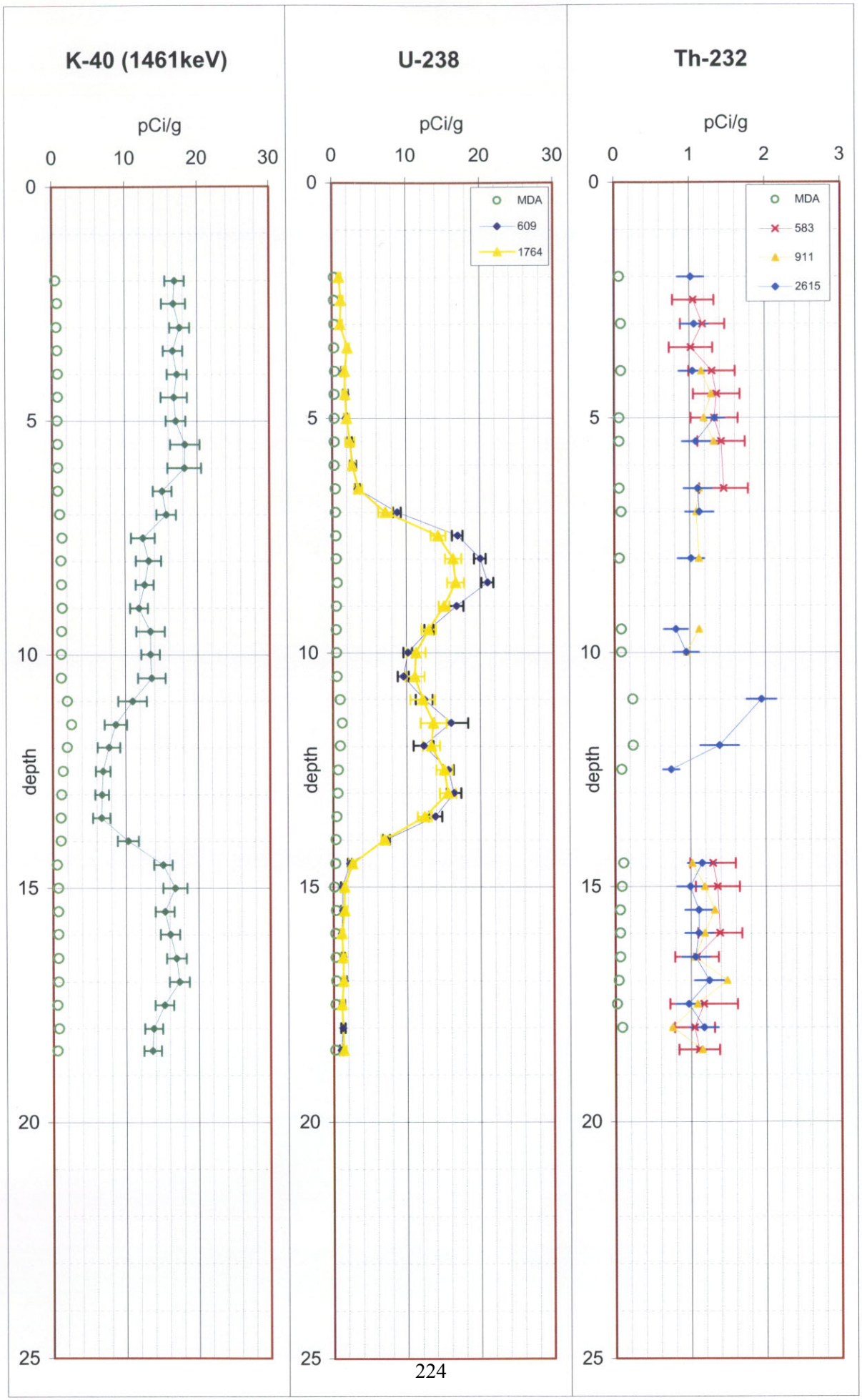

P2-PU-1

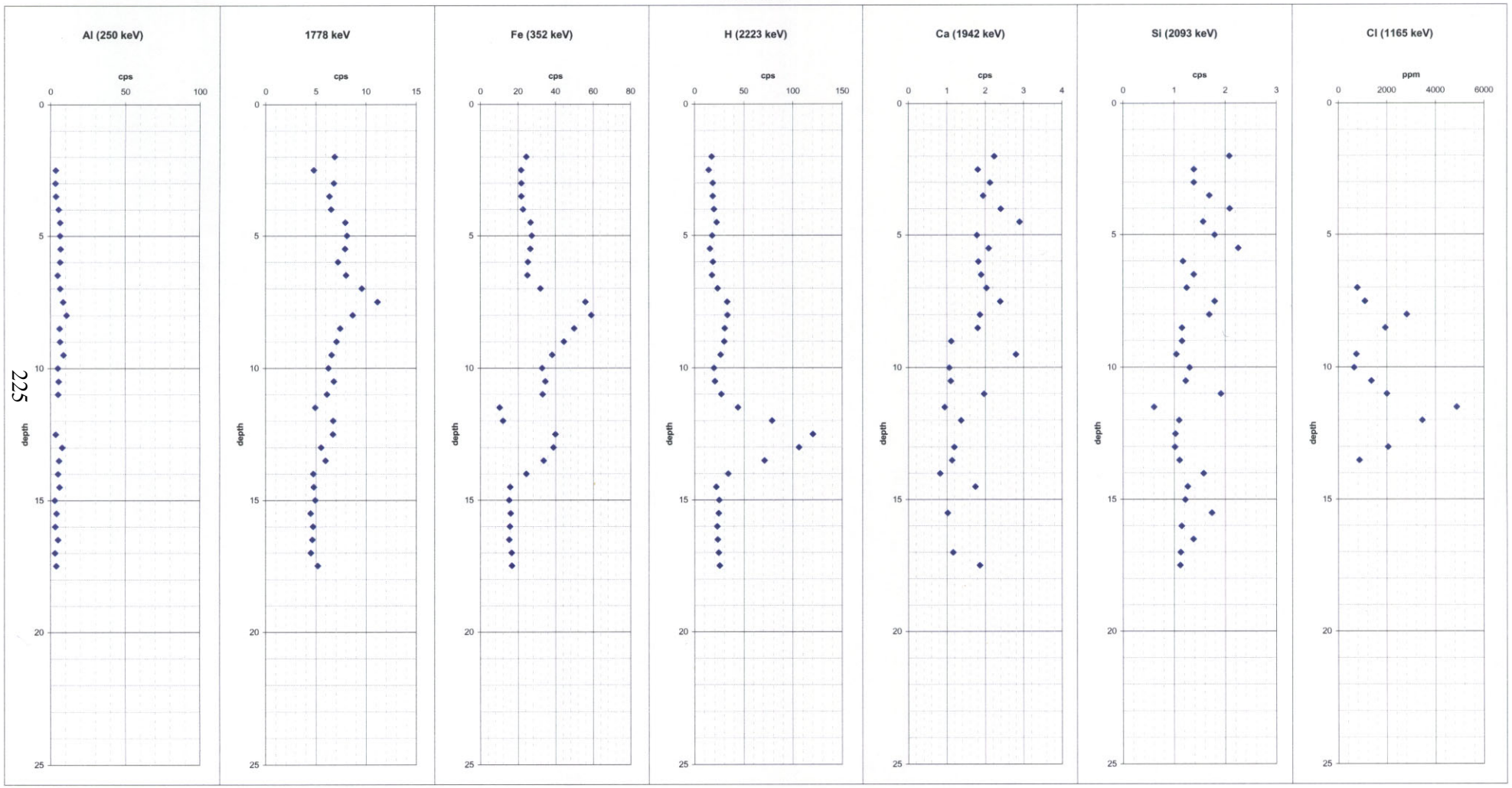
Al (250 keV)
1778 keV
Fe (352 keV)
H (2223 keV)
Ca (1942 keV)
Si (2093 keV)
Cl (1165 keV)
cps
ppm
depth
0
5
10
15
20
25
0 50 100
0 5 10 15
0 20 40 60 80
0 50 100 150
0 1 2 3 4
0 1 2 3
0 2000 4000 6000

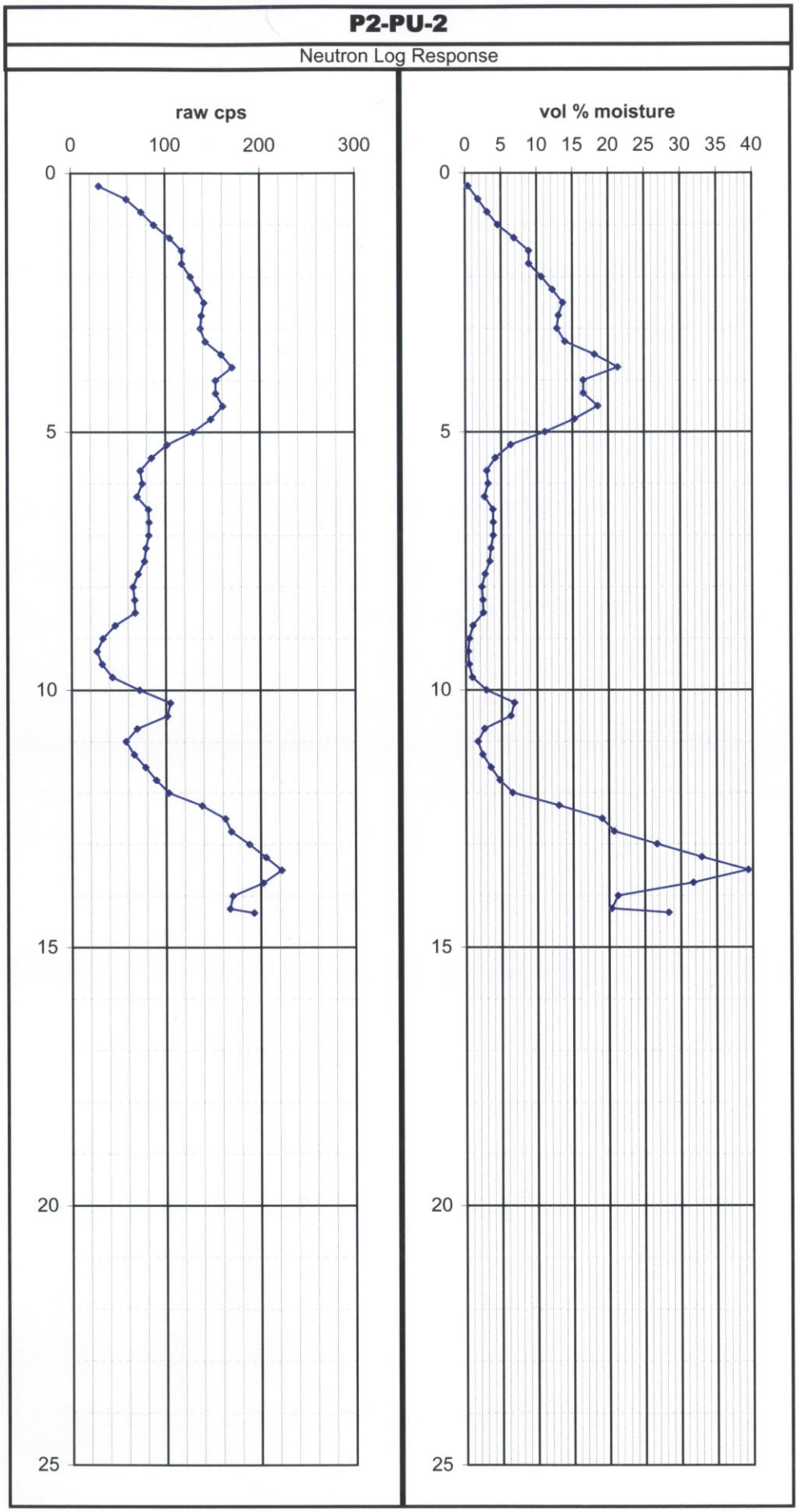
P2-PU-2
Neutron Log Response
raw cps
0
100
200
300
vol % moisture
0
5
10
15
20
25
30
35
40

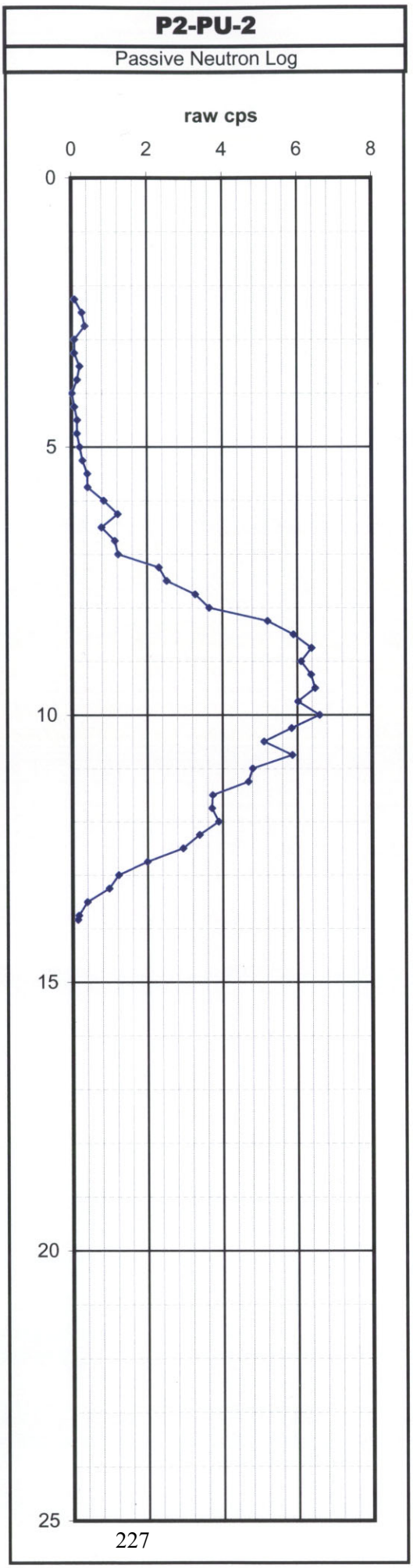
P2-PU-2
Passive Neutron Log
raw cps
0
2
4
6
8
0
5
10
15
20
25

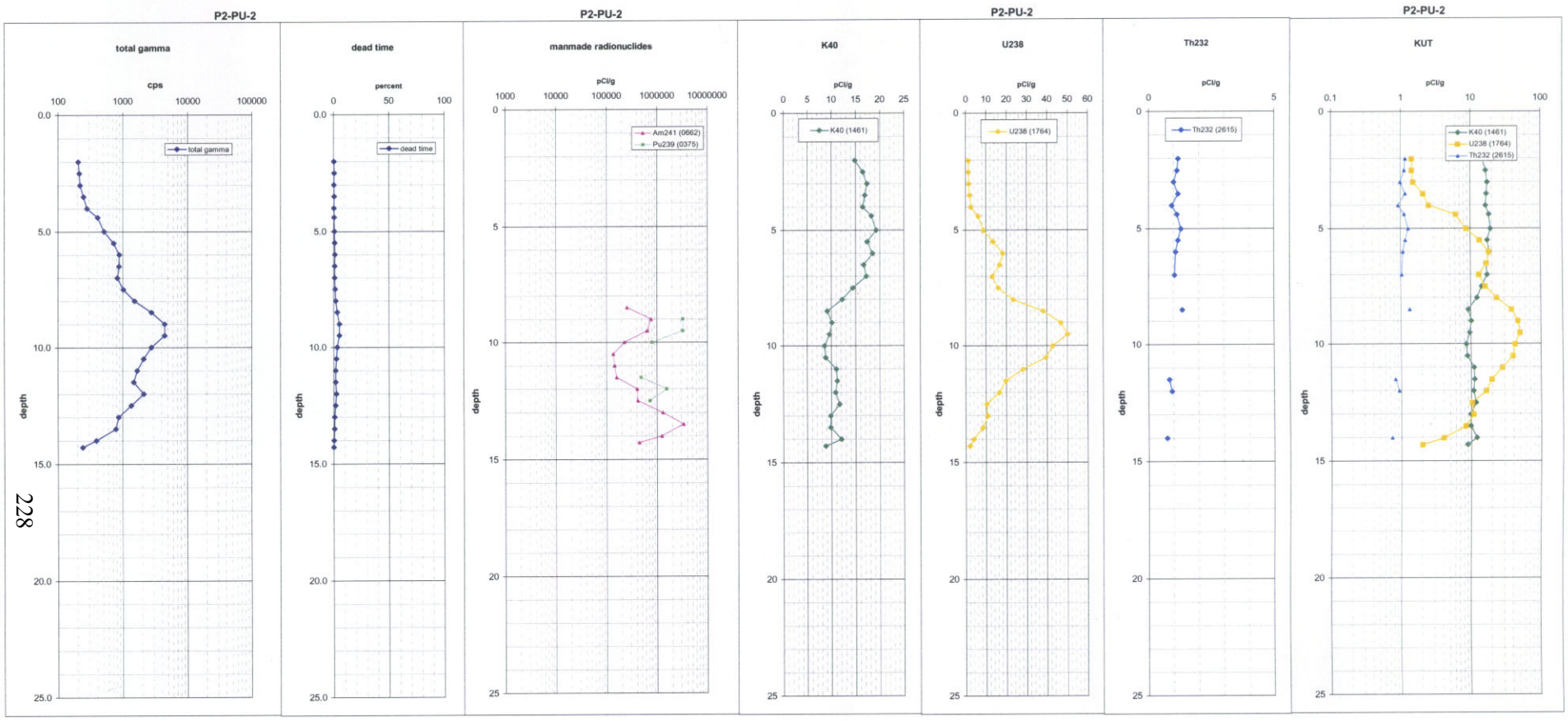
P2-PU-2
total gamma
cps
100
1000
10000
100000
depth
0.0
5.0
10.0
15.0
20.0
25.0
total gamma
P2-PU-2
dead time
percent
0
50
100
dead time
P2-PU-2
manmade radionuclides
pCi/g
1000
10000
100000
1000000
10000000
Am241 (0662)
Pu239 (0375)
P2-PU-2
K40
pCi/g
0
5
10
15
20
25
K40 (1461)
P2-PU-2
U238
pCi/g
0
10
20
30
40
50
60
U238 (1764)
P2-PU-2
Th232
pCi/g
0
5
Th232 (2615)
P2-PU-2
KUT
pCi/g
0.1
1
10
100
K40 (1461)
U238 (1764)
Th232 (2615)

P2-PU-2

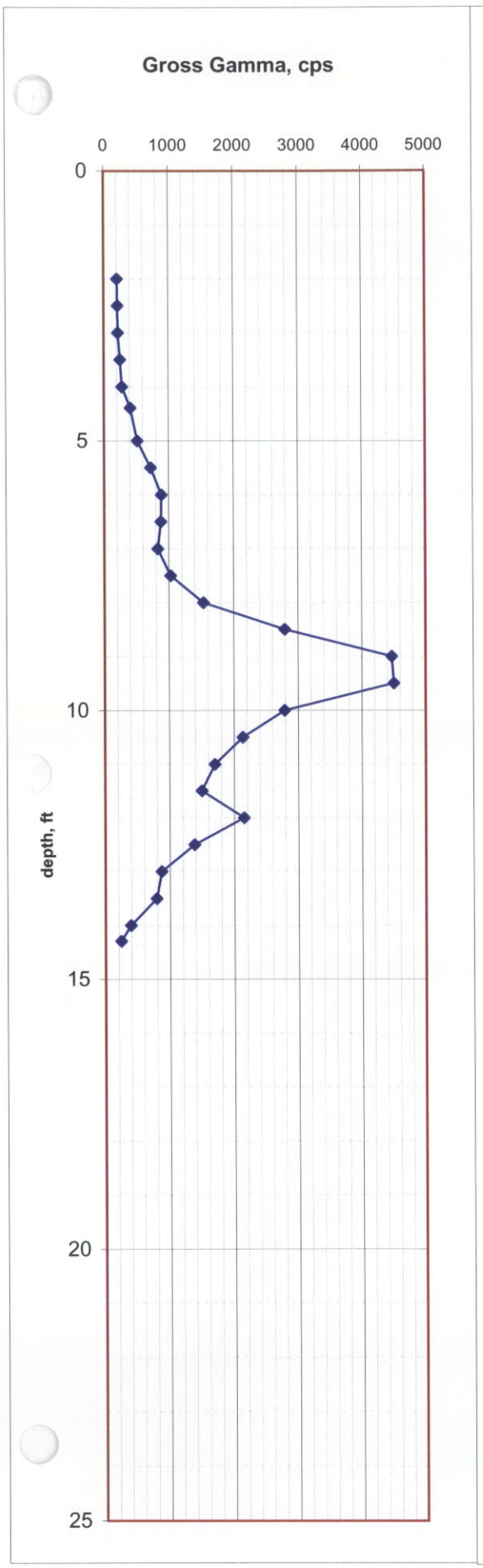
Gross Gamma, cps
0
1000
2000
3000
4000
5000
depth, ft
0
5
10
15
20
25

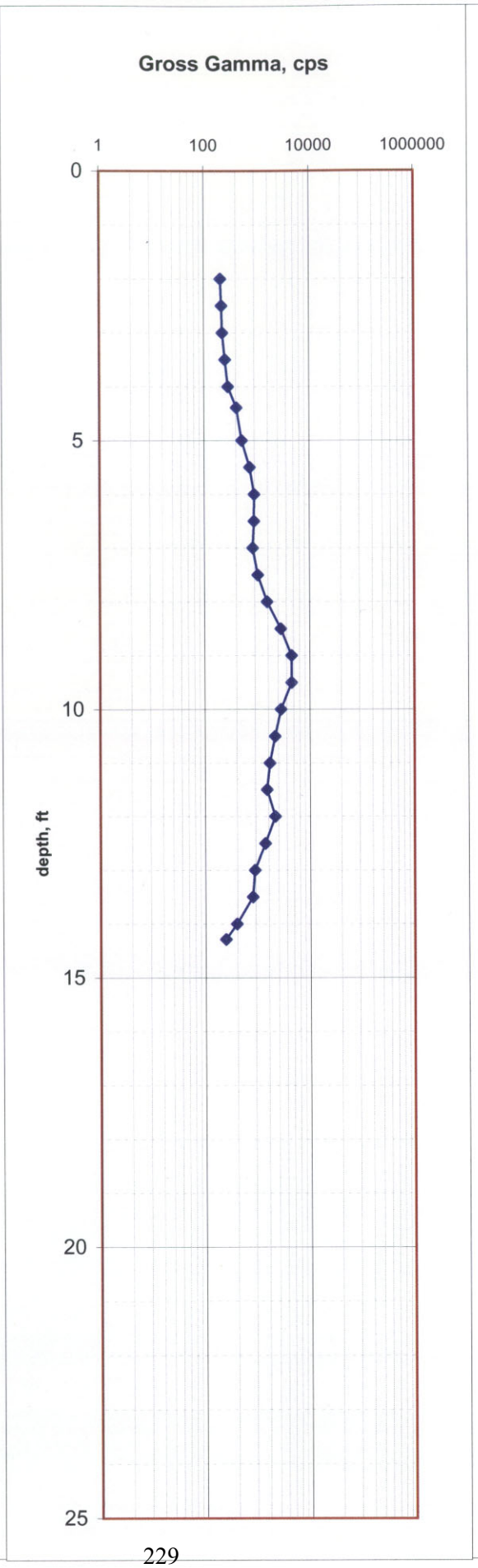
Gross Gamma, cps
1
100
10000
1000000
depth, ft
0
5
10
15
20
25

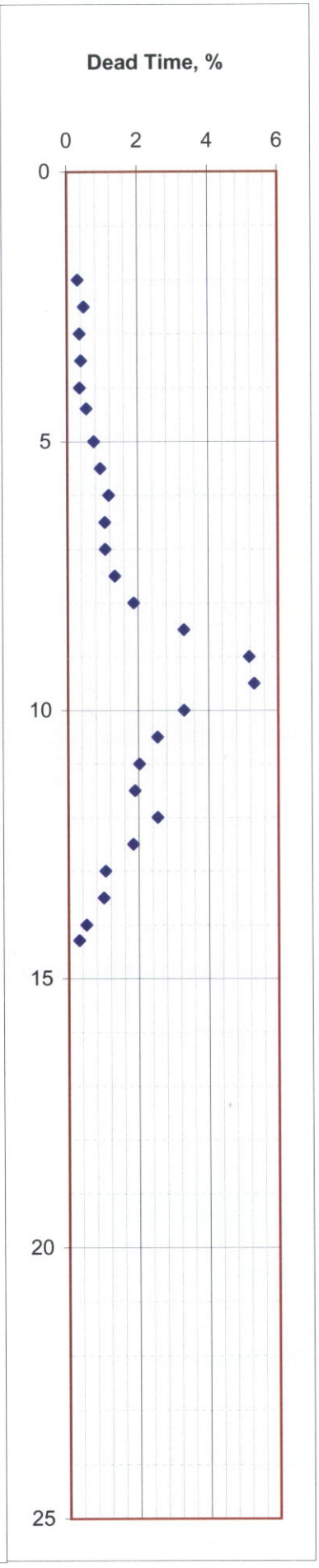
Dead Time, %
0
2
4
6
0
5
10
15
20
25

P2-PU-2

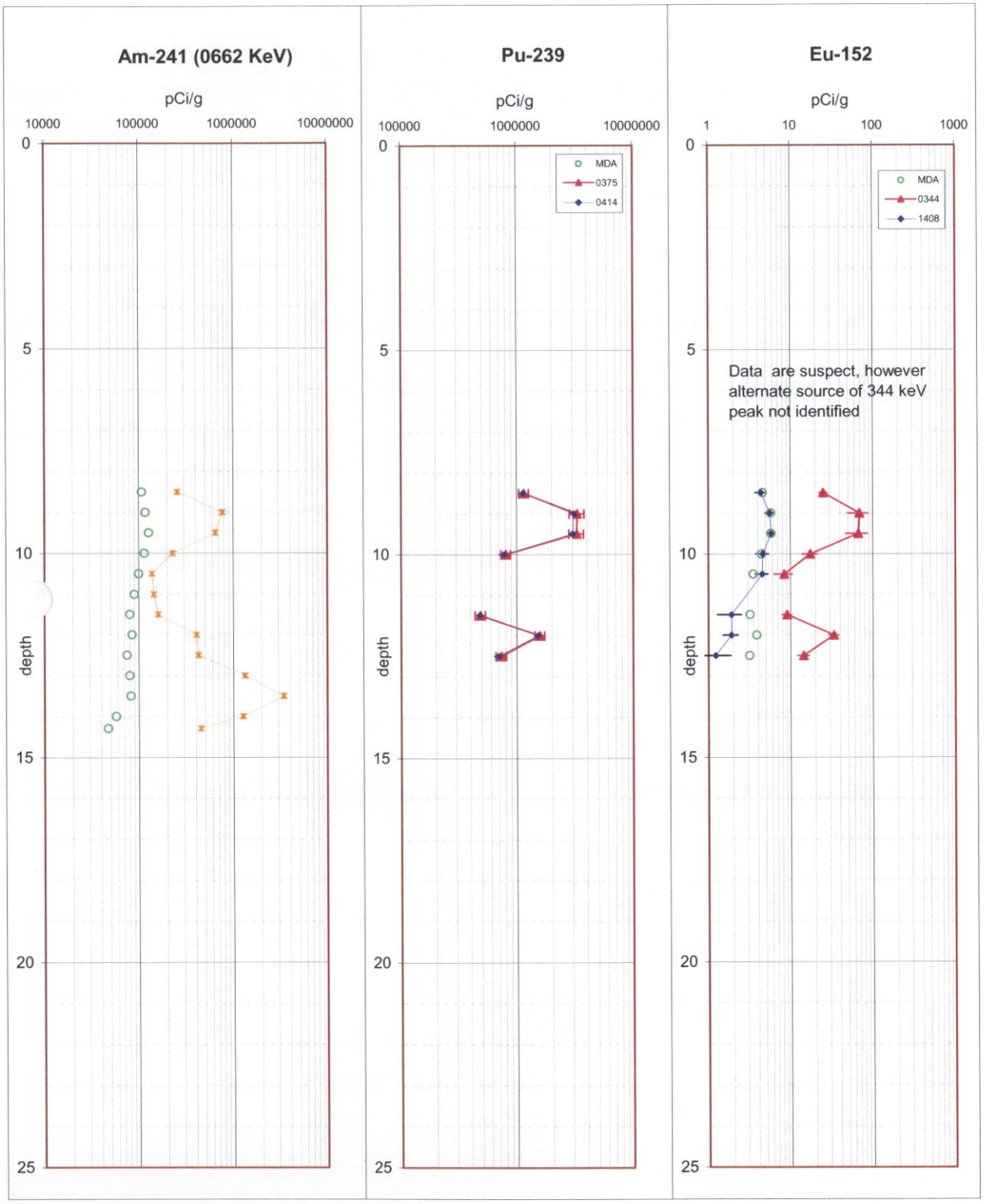
Am-241 (0662 KeV)
pCi/g
10000
100000
1000000
10000000
Pu-239
pCi/g
100000
1000000
10000000
MDA
0375
0414
Eu-152
pCi/g
1
10
100
1000
MDA
0344
1408
Data are suspect, however alternate source of 344 keV peak not identified
depth
0
5
10
15
20
25

P2-PU-2

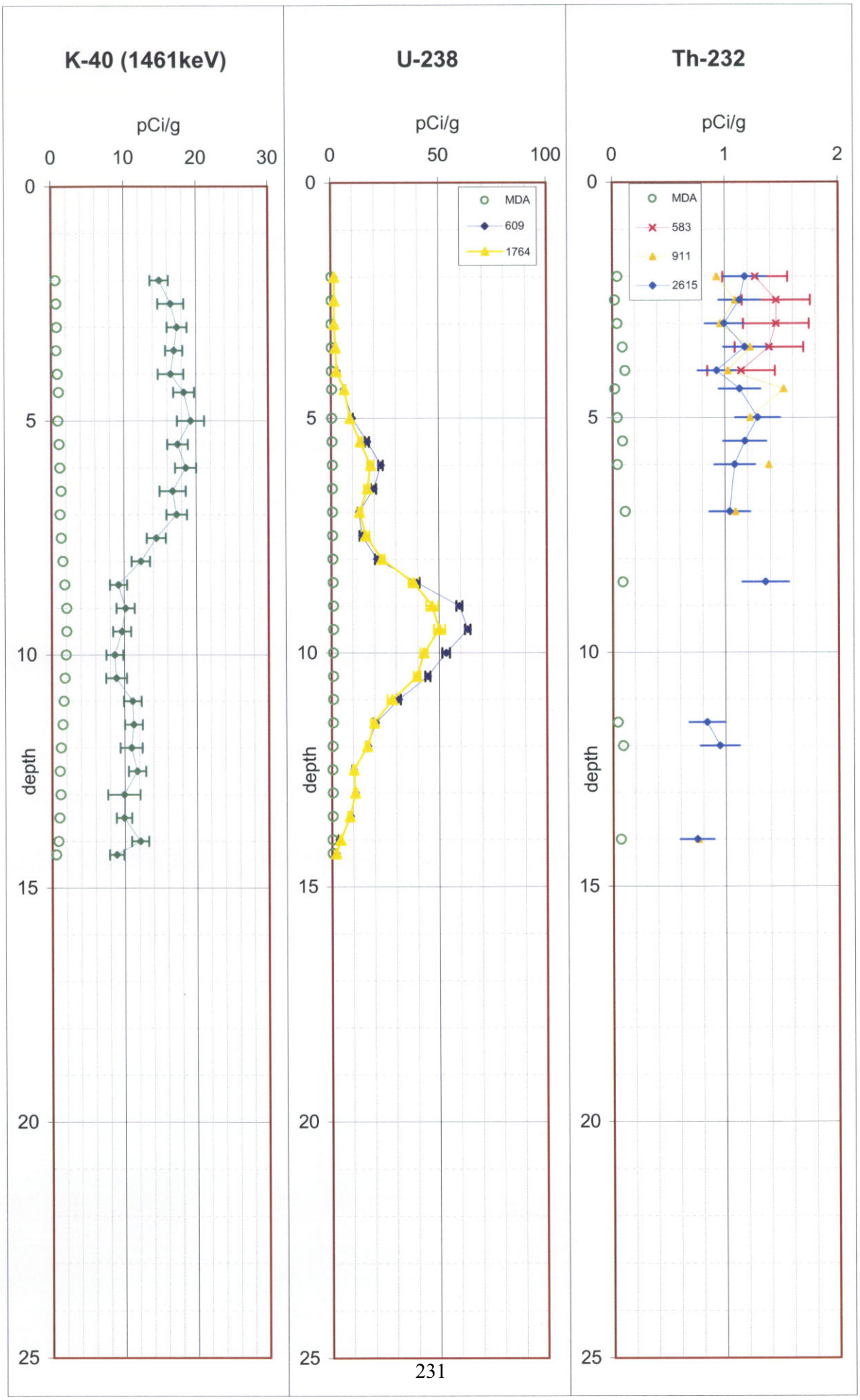
K-40 (1461keV)
U-238
Th-232
pCi/g
0
10
20
30
50
100
1
2
depth
0
5
10
15
20
25
MDA
609
1764
583
911
2615

P2-PU-2

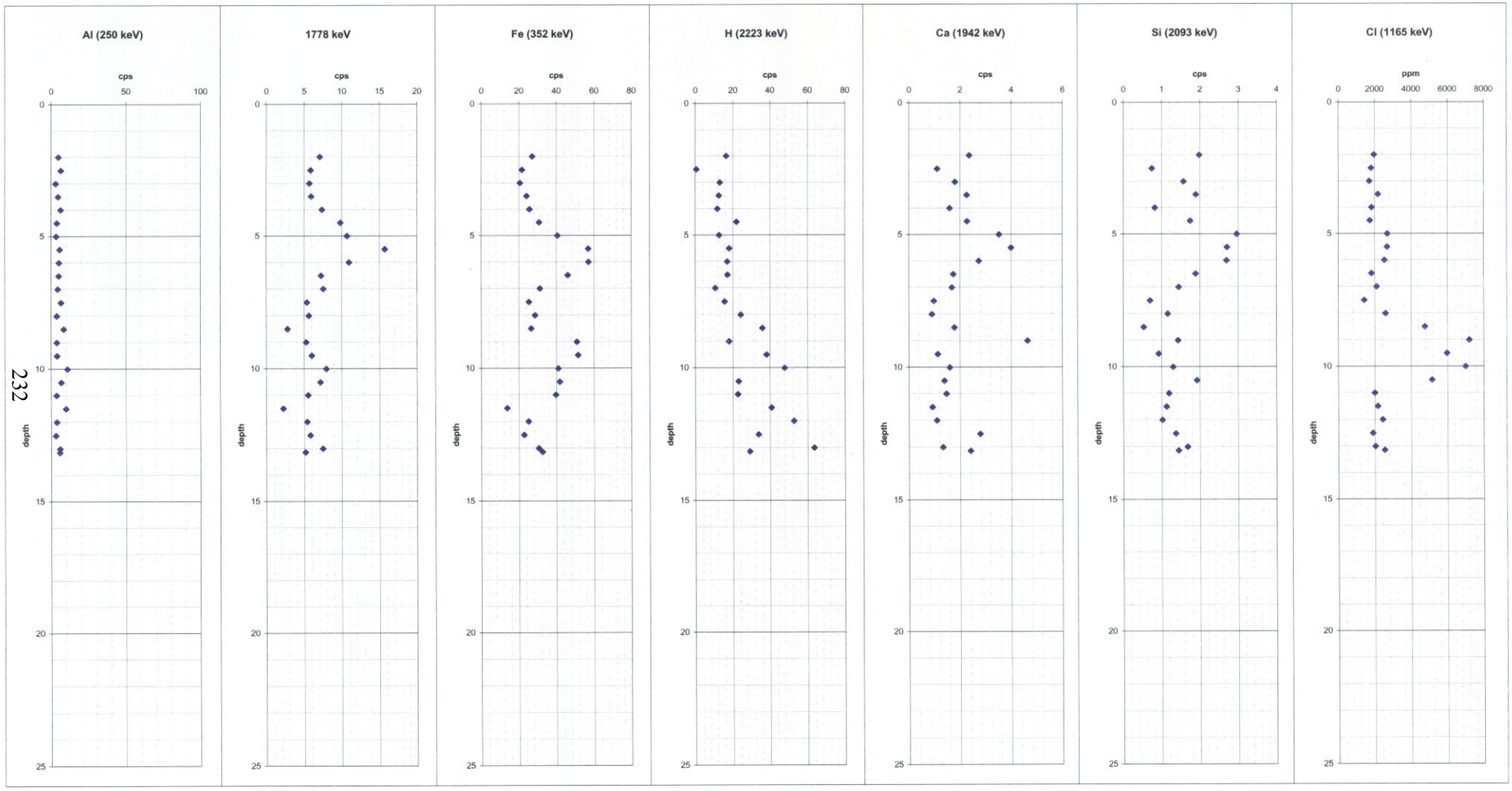
Al (250 keV)
1778 keV
Fe (352 keV)
H (2223 keV)
Ca (1942 keV)
Si (2093 keV)
Cl (1165 keV)
cps
ppm
depth

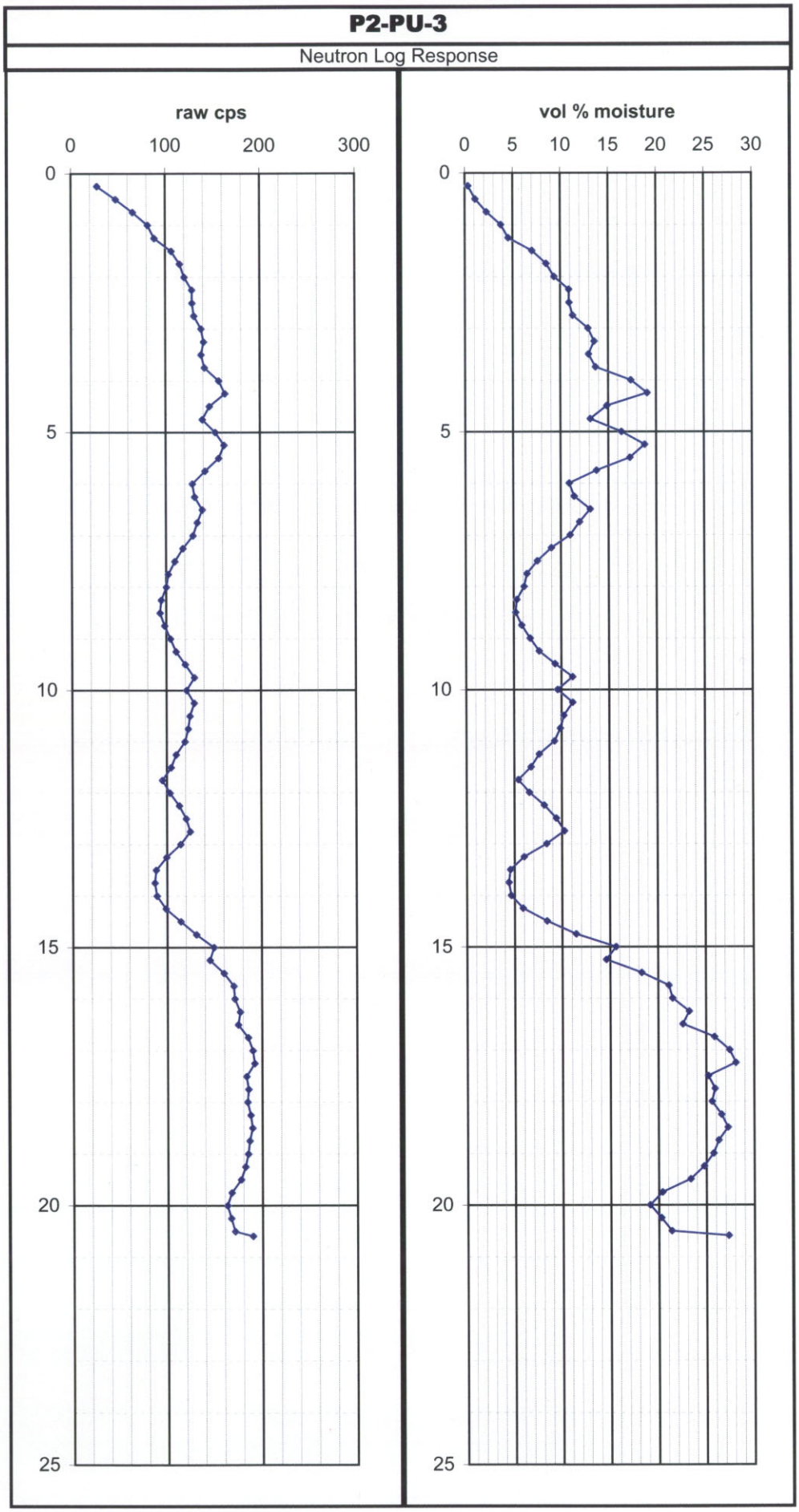
P2-PU-3
Neutron Log Response
raw cps
0
100
200
300
vol % moisture
0
5
10
15
20
25
30

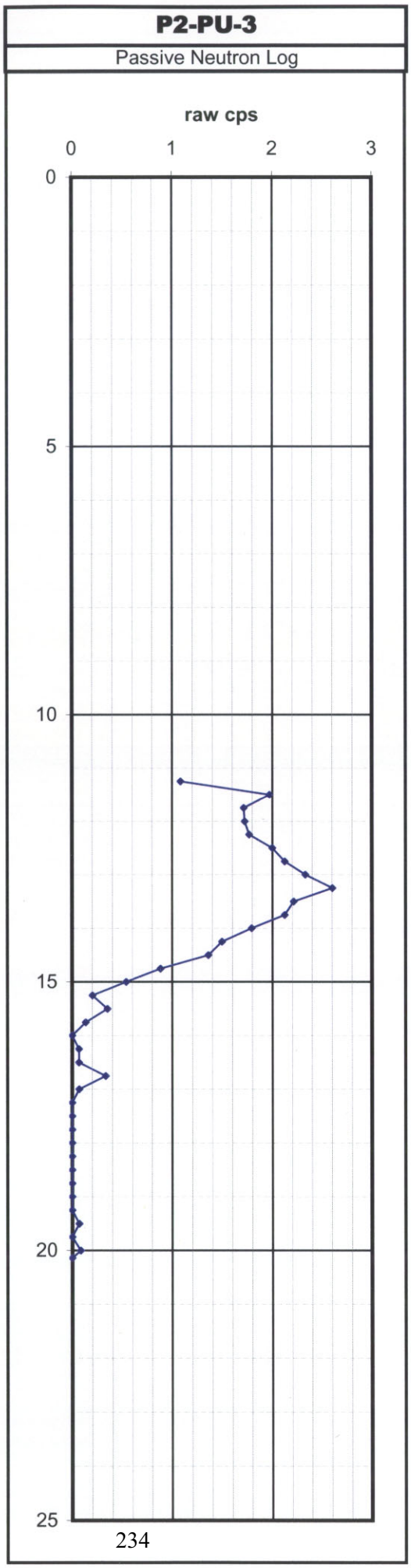
P2-PU-3
Passive Neutron Log
raw cps
0
1
2
3
0
5
10
15
20
25

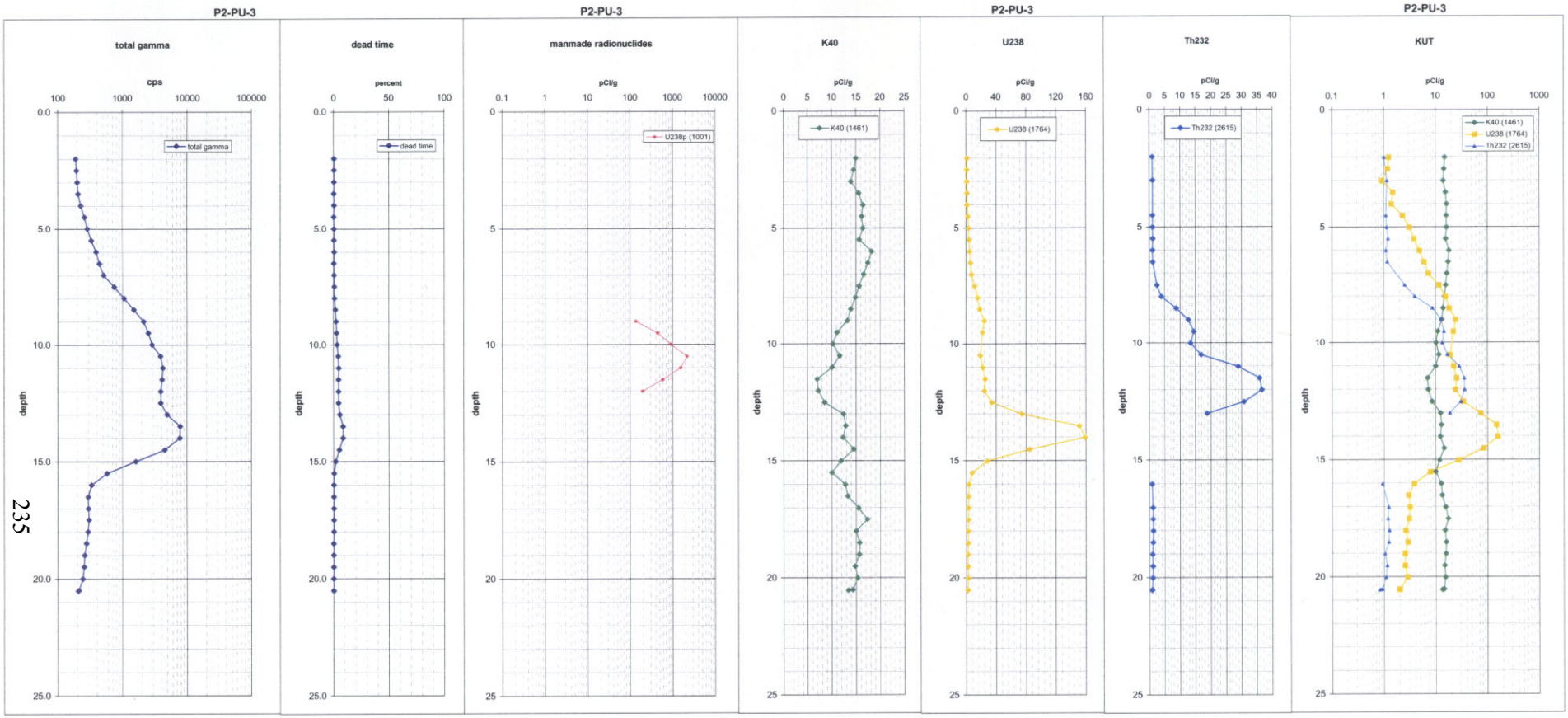
P2-PU-3
total gamma
cps
100
1000
10000
100000
depth
0.0
5.0
10.0
15.0
20.0
25.0
total gamma
P2-PU-3
dead time
percent
0
50
100
dead time
P2-PU-3
manmade radionuclides
pCi/g
0.1
1
10
100
1000
10000
U238p (1001)
P2-PU-3
K40
pCi/g
0
5
10
15
20
25
K40 (1461)
P2-PU-3
U238
pCi/g
0
40
80
120
160
U238 (1764)
P2-PU-3
Th232
pCi/g
0
5
10
15
20
25
30
35
40
Th232 (2615)
P2-PU-3
KUT
pCi/g
0.1
1
10
100
1000
K40 (1461)
U238 (1764)
Th232 (2615)

P2-PU-3

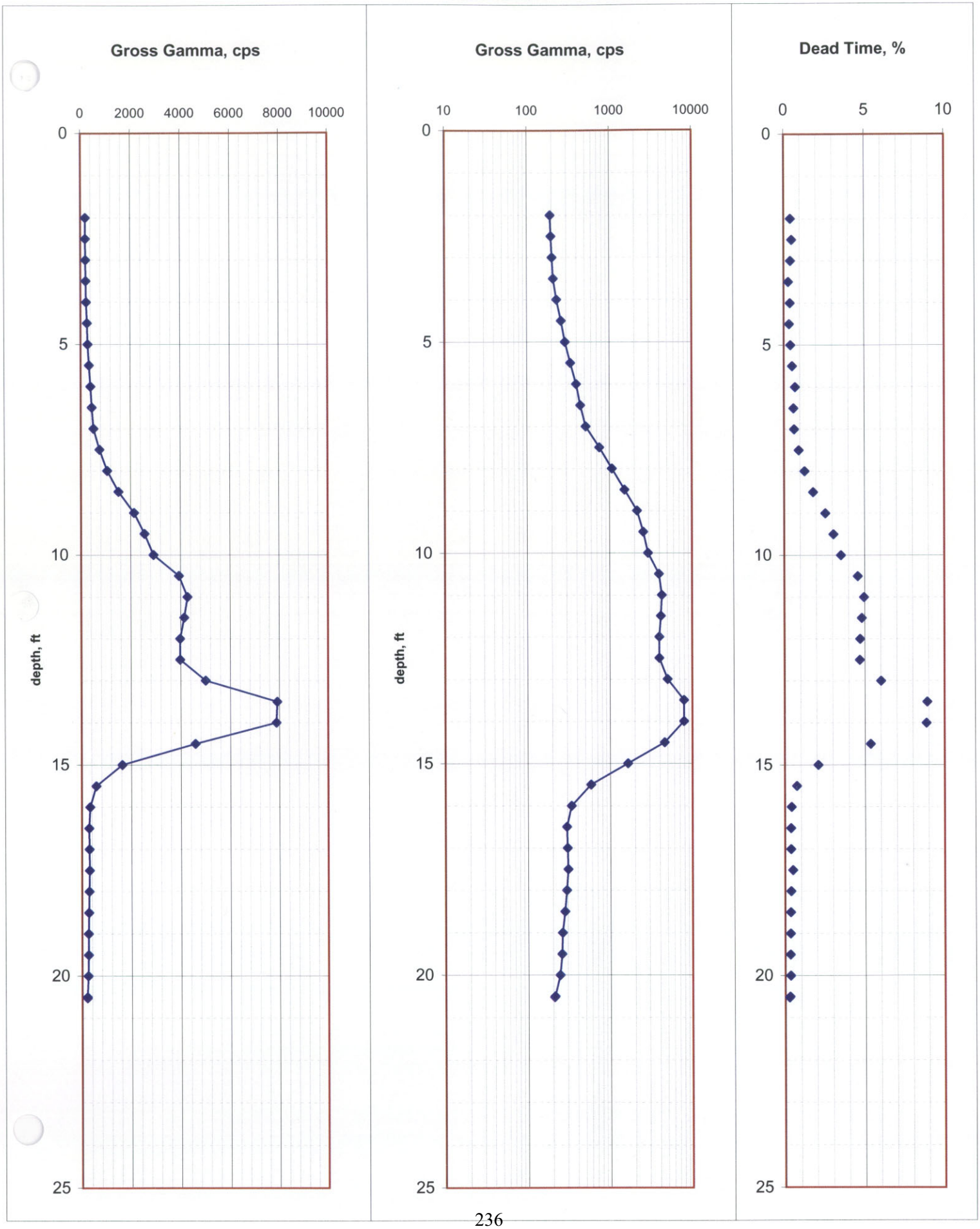
Gross Gamma, cps
0
2000
4000
6000
8000
10000
depth, ft
0
5
10
15
20
25
Gross Gamma, cps
10
100
1000
10000
depth, ft
0
5
10
15
20
25
Dead Time, %
0
5
10
0
5
10
15
20
25

P2-PU-3

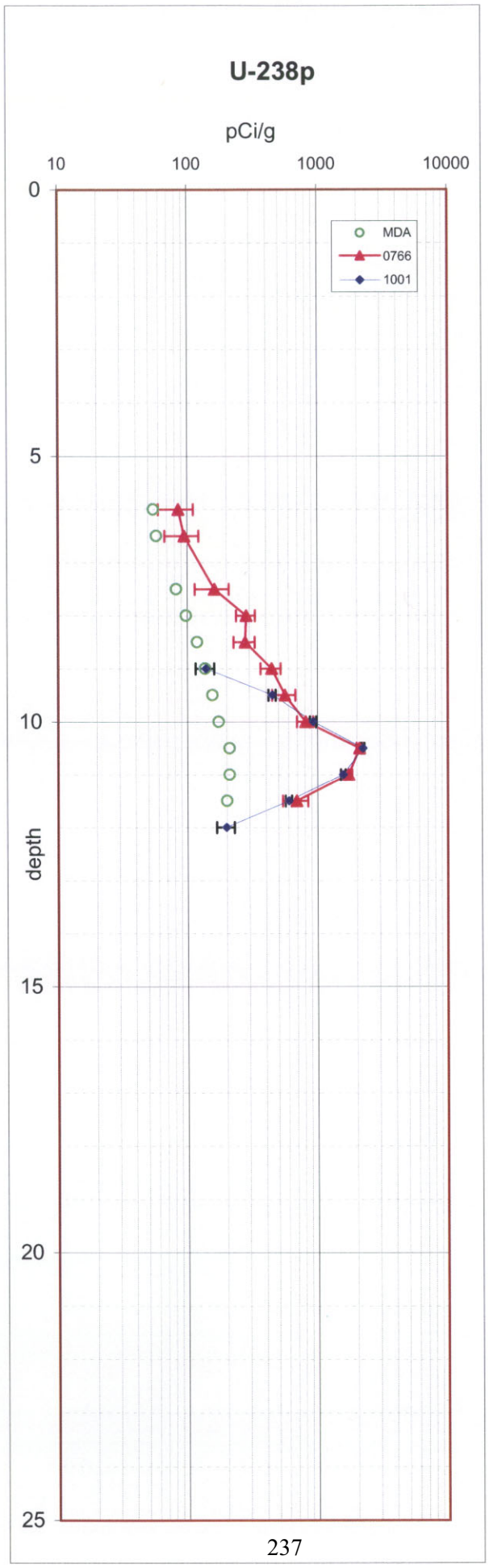

P2-PU-3

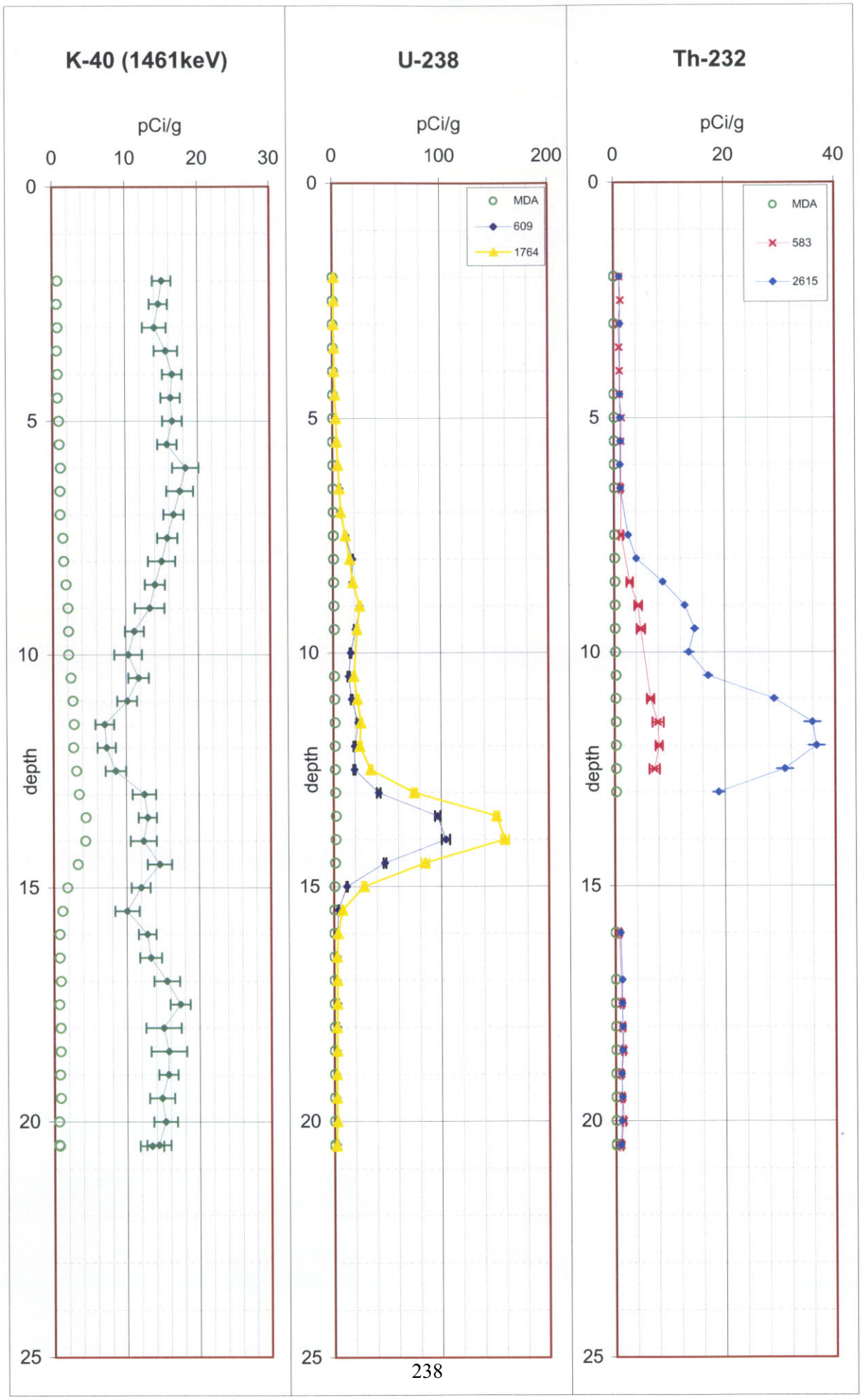
K-40 (1461keV)
pCi/g
0
10
20
30
depth
0
5
10
15
20
25
U-238
pCi/g
0
100
200
MDA
609
1764
Th-232
pCi/g
0
20
40
MDA
583
2615

P2-PU-3

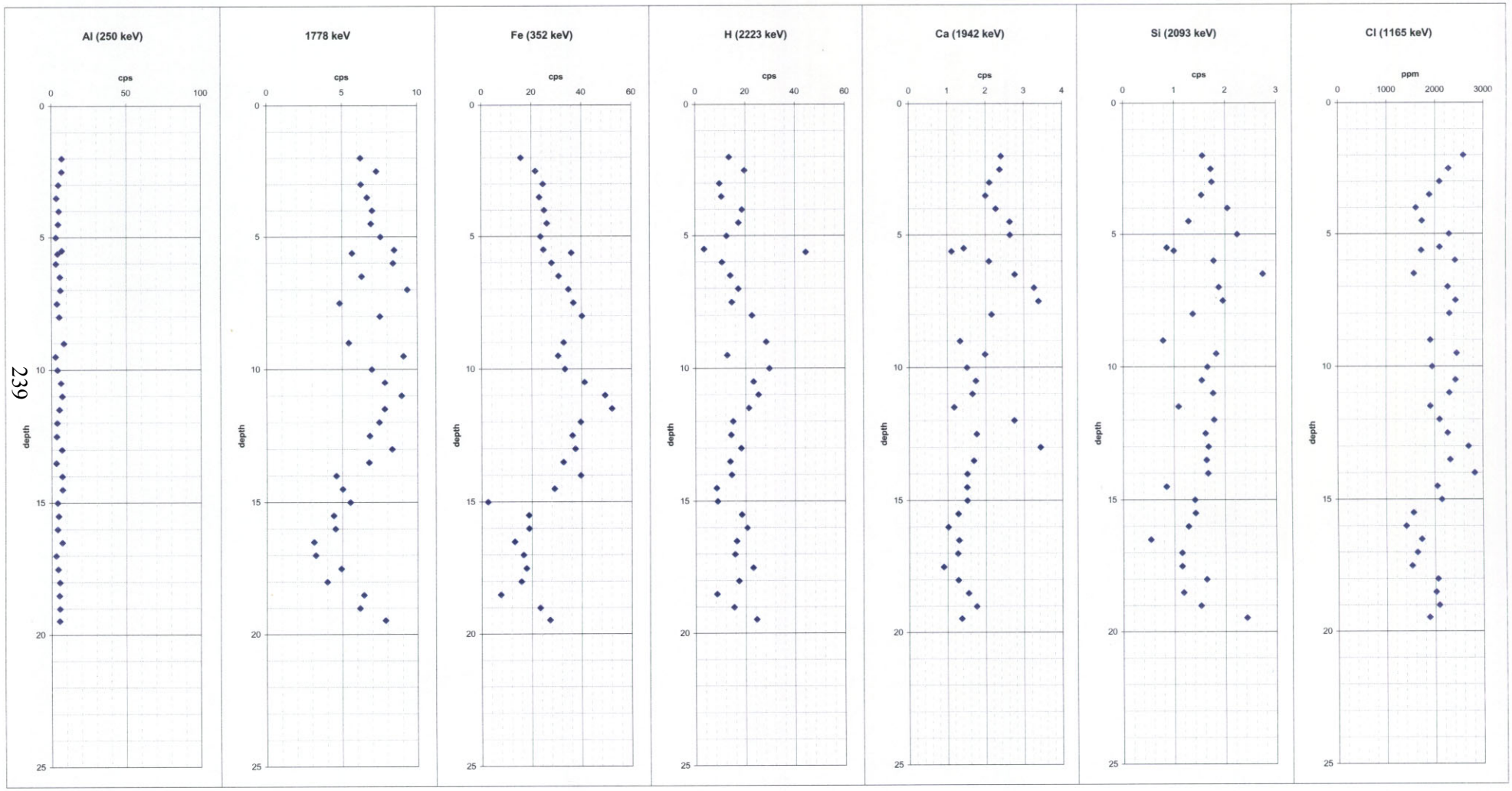
Al (250 keV)
1778 keV
Fe (352 keV)
H (2223 keV)
Ca (1942 keV)
Si (2093 keV)
Cl (1165 keV)
cps
ppm
depth

P2-PU-4

Neutron Log Response

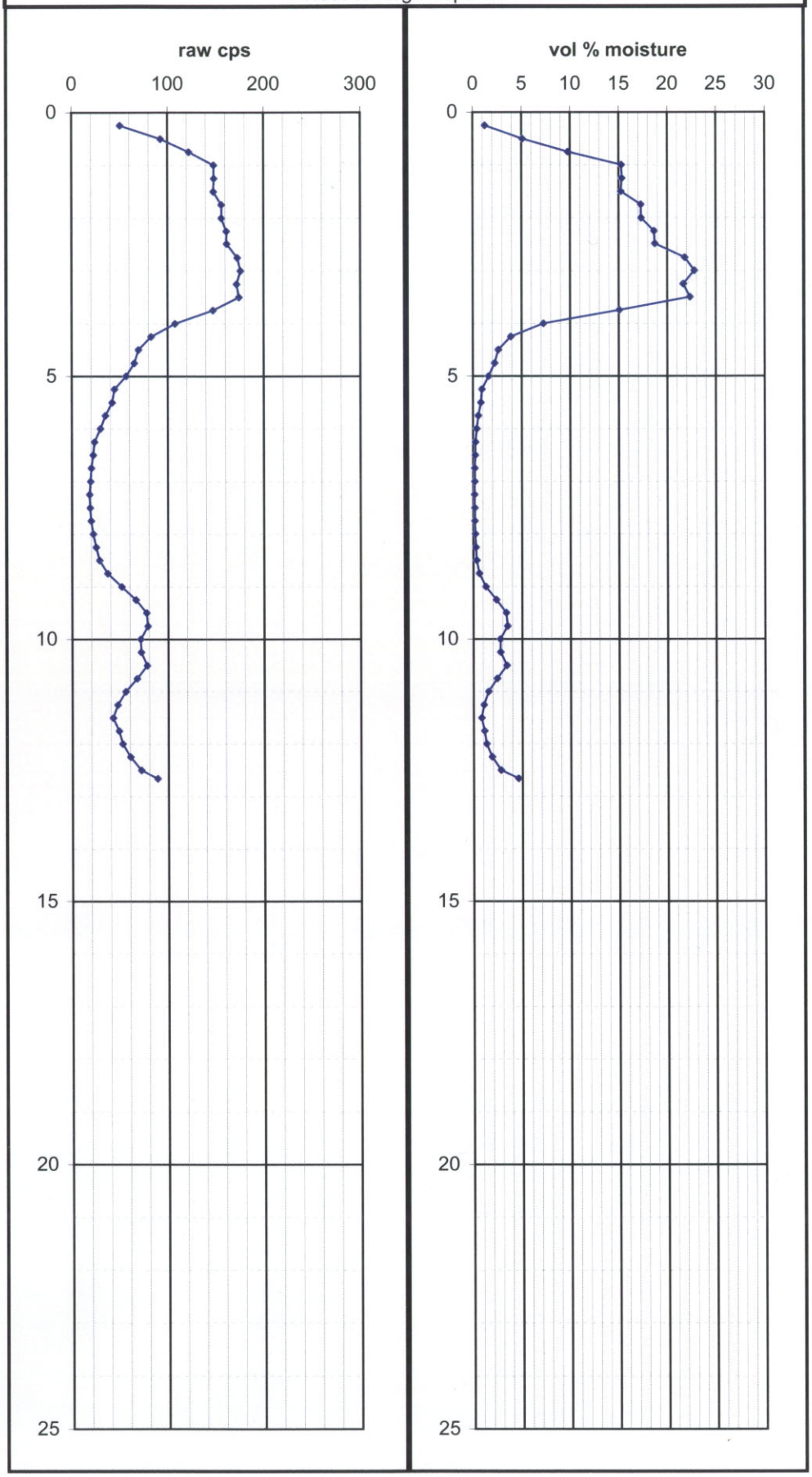

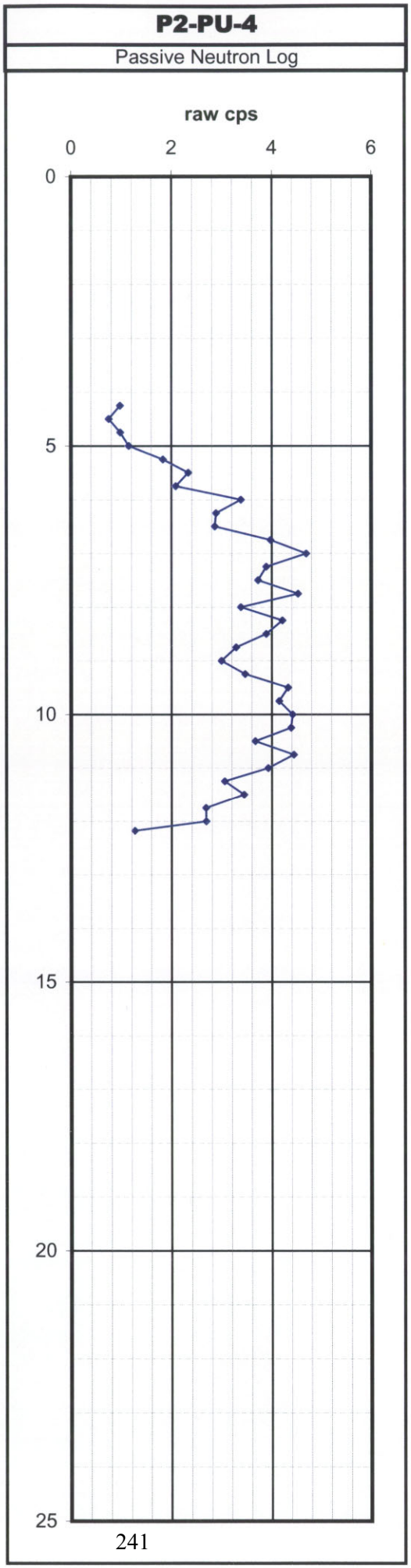
P2-PU-4
Passive Neutron Log
raw cps
0
2
4
6
0
5
10
15
20
25

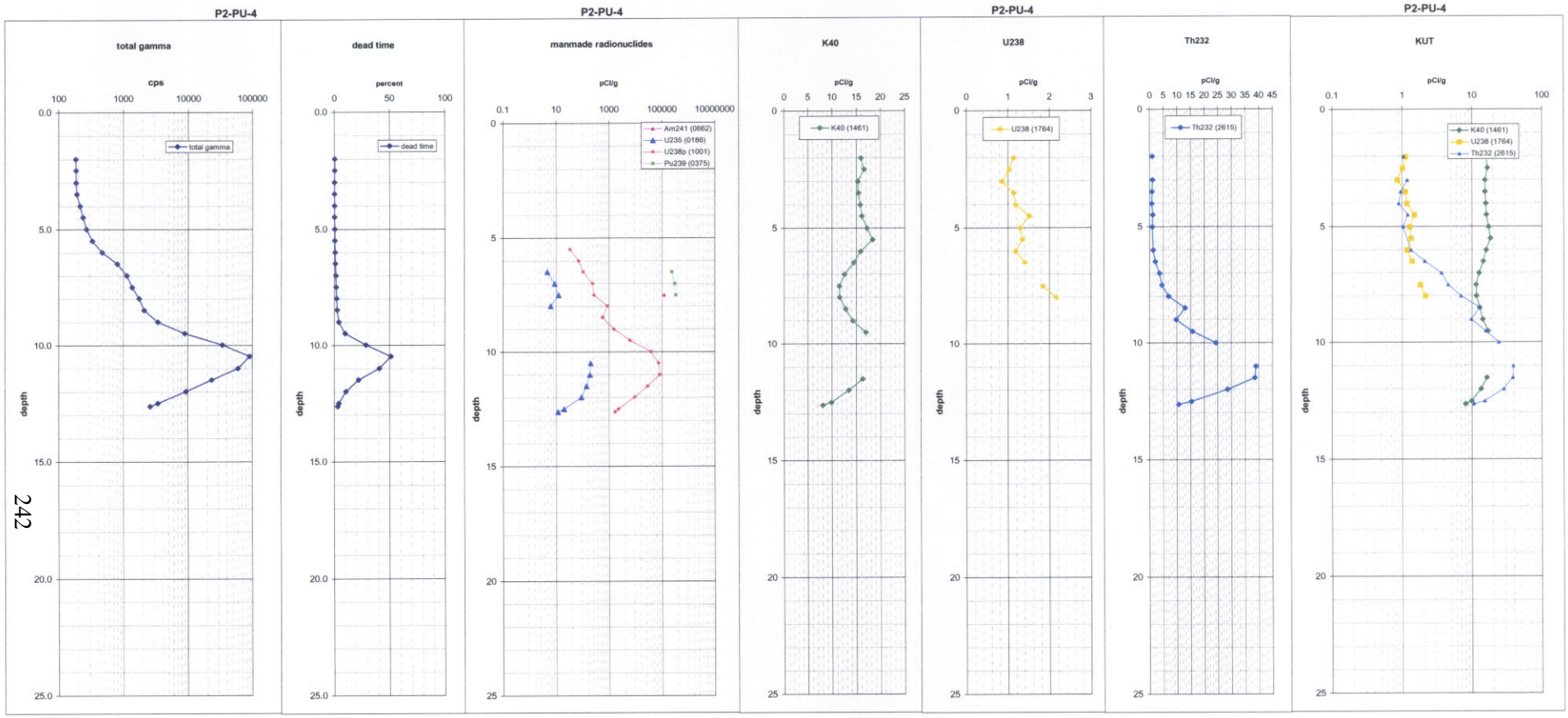
P2-PU-4
total gamma
cps
100
1000
10000
100000
total gamma
depth
0.0
5.0
10.0
15.0
20.0
25.0
P2-PU-4
dead time
percent
0
50
100
dead time
depth
P2-PU-4
manmade radionuclides
pCi/g
0.1
10
1000
100000
10000000
Am241 (0662)
U235 (0186)
U238p (1001)
Pu239 (0375)
depth
P2-PU-4
K40
pCi/g
0
5
10
15
20
25
K40 (1461)
depth
P2-PU-4
U238
pCi/g
0
1
2
3
U238 (1764)
depth
P2-PU-4
Th232
pCi/g
0
5
10
15
20
25
30
35
40
45
Th232 (2615)
depth
P2-PU-4
KUT
pCi/g
0.1
1
10
100
K40 (1461)
U238 (1764)
Th232 (2615)
depth

P2-PU-4

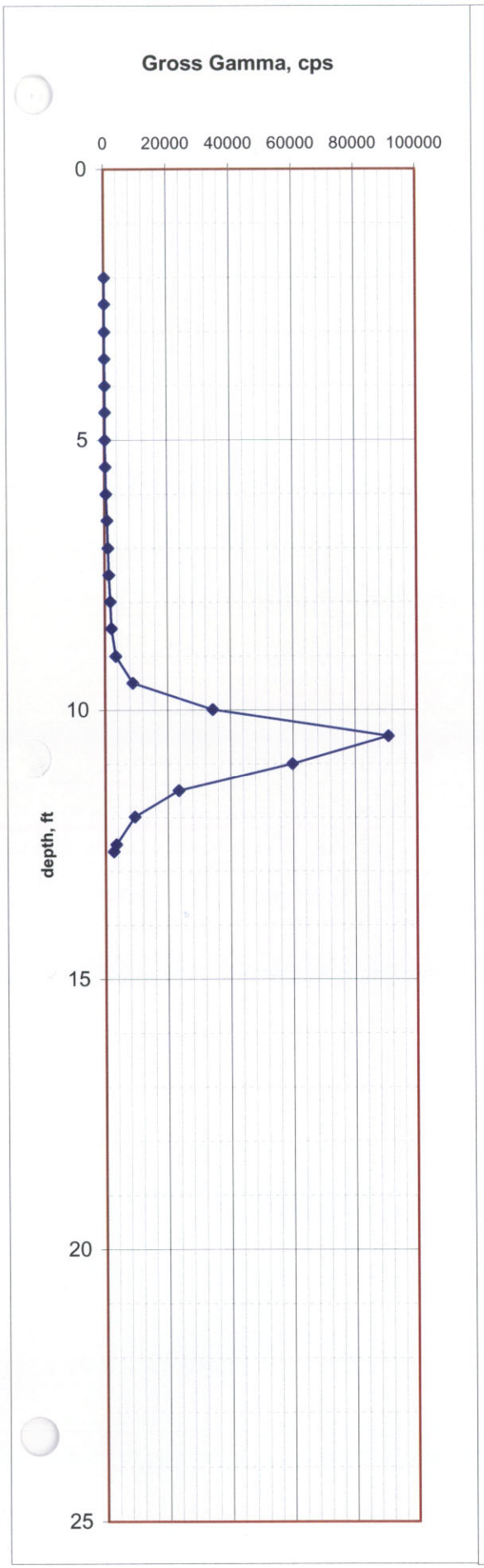
Gross Gamma, cps
0
20000
40000
60000
80000
100000
depth, ft
0
5
10
15
20
25

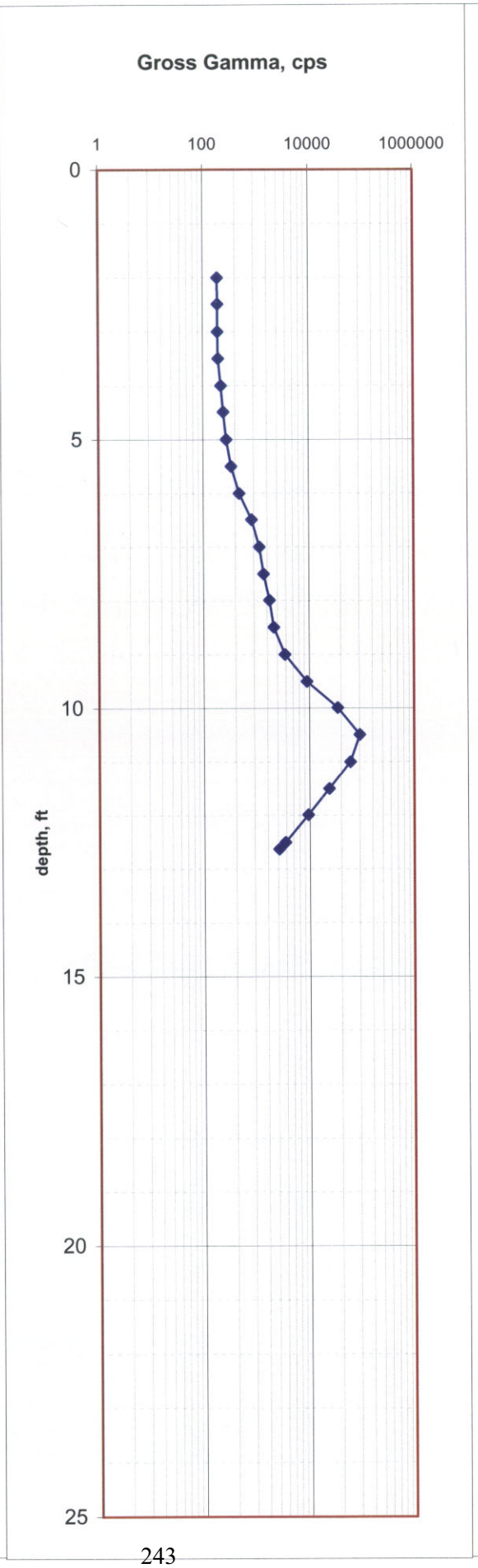
Gross Gamma, cps
1
100
10000
1000000
depth, ft
0
5
10
15
20
25

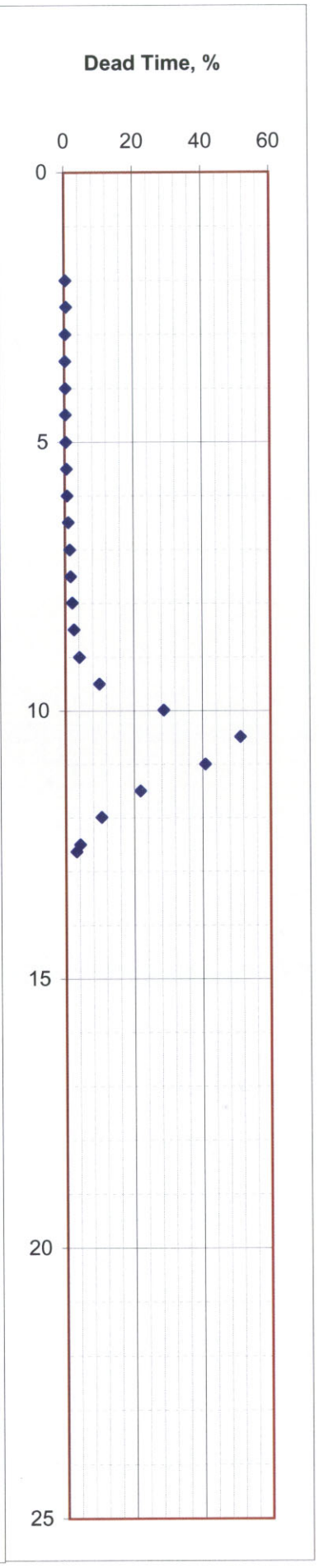
Dead Time, %
0
20
40
60
0
5
10
15
20
25

P2-PU-4

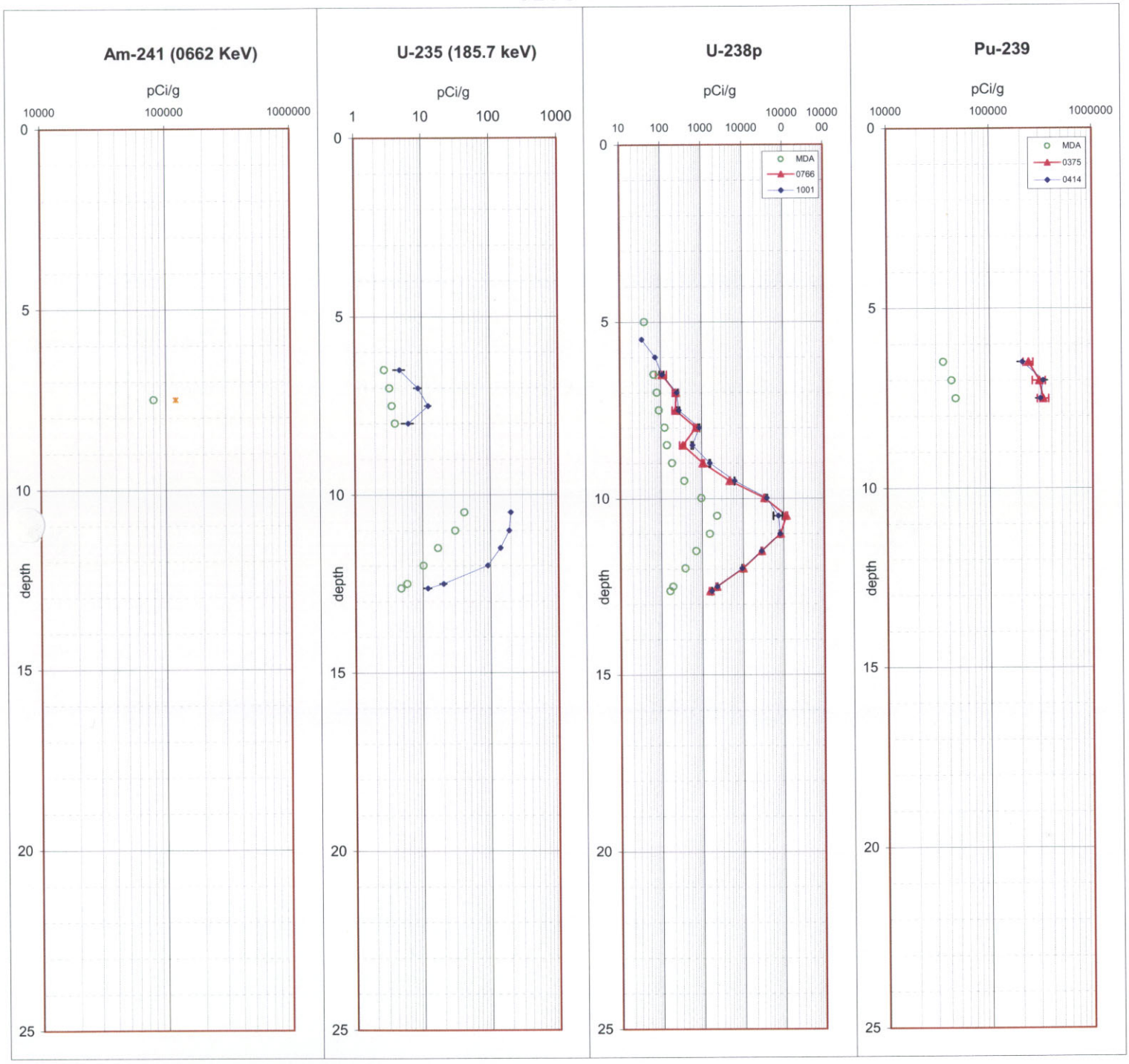
Am-241 (0662 KeV)
pCi/g
10000
100000
1000000
U-235 (185.7 keV)
pCi/g
1
10
100
1000
U-238p
pCi/g
10
100
1000
10000
10000
0
10000
00
Pu-239
pCi/g
10000
100000
1000000
depth
0
5
10
15
20
25
MDA
0766
1001
0375
0414

P2-PU-4

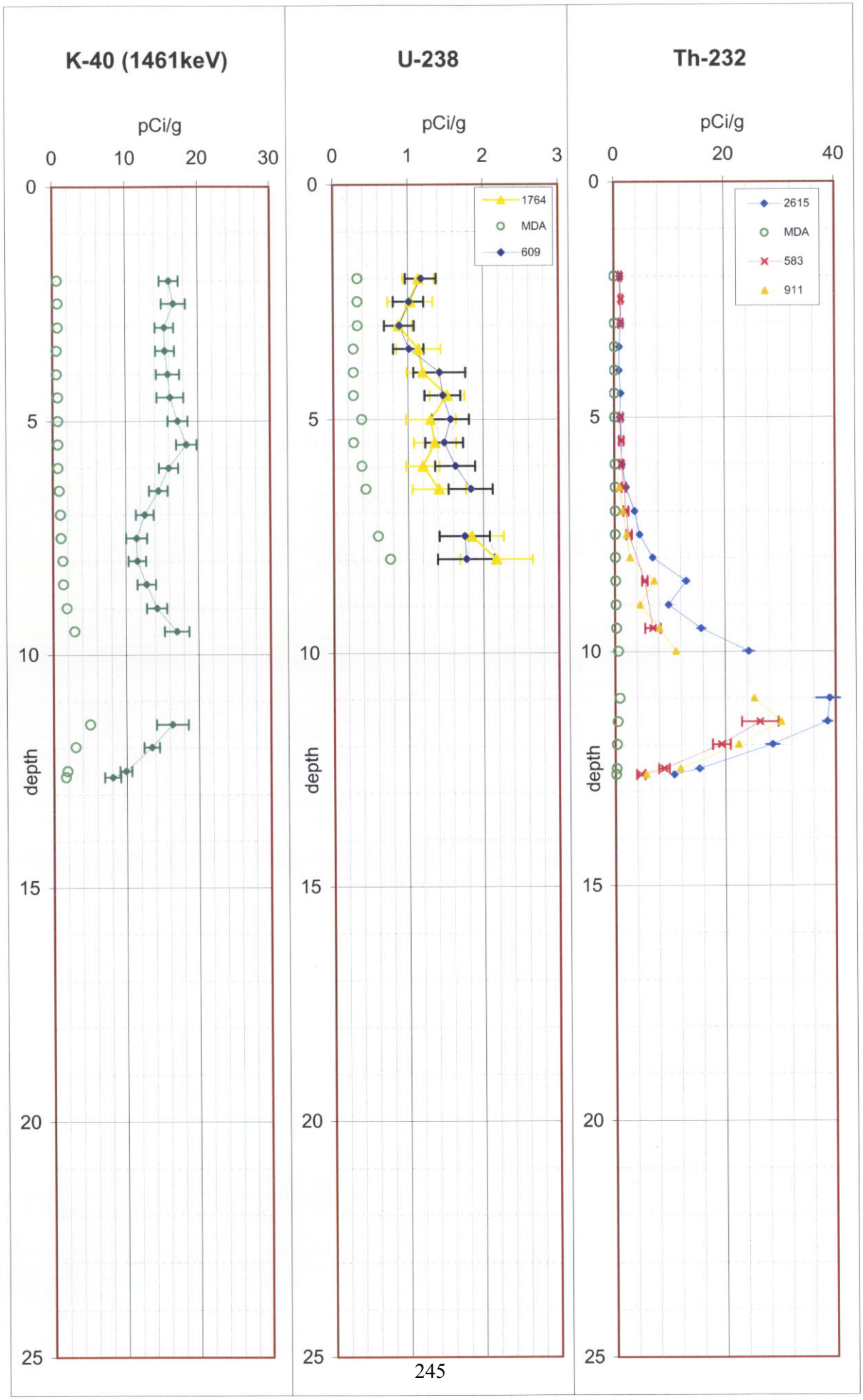
K-40 (1461keV)
pCi/g
0
10
20
30
depth
0
5
10
15
20
25
U-238
pCi/g
0
1
2
3
1764
MDA
609
Th-232
pCi/g
0
20
40
2615
MDA
583
911

P2-PU-4

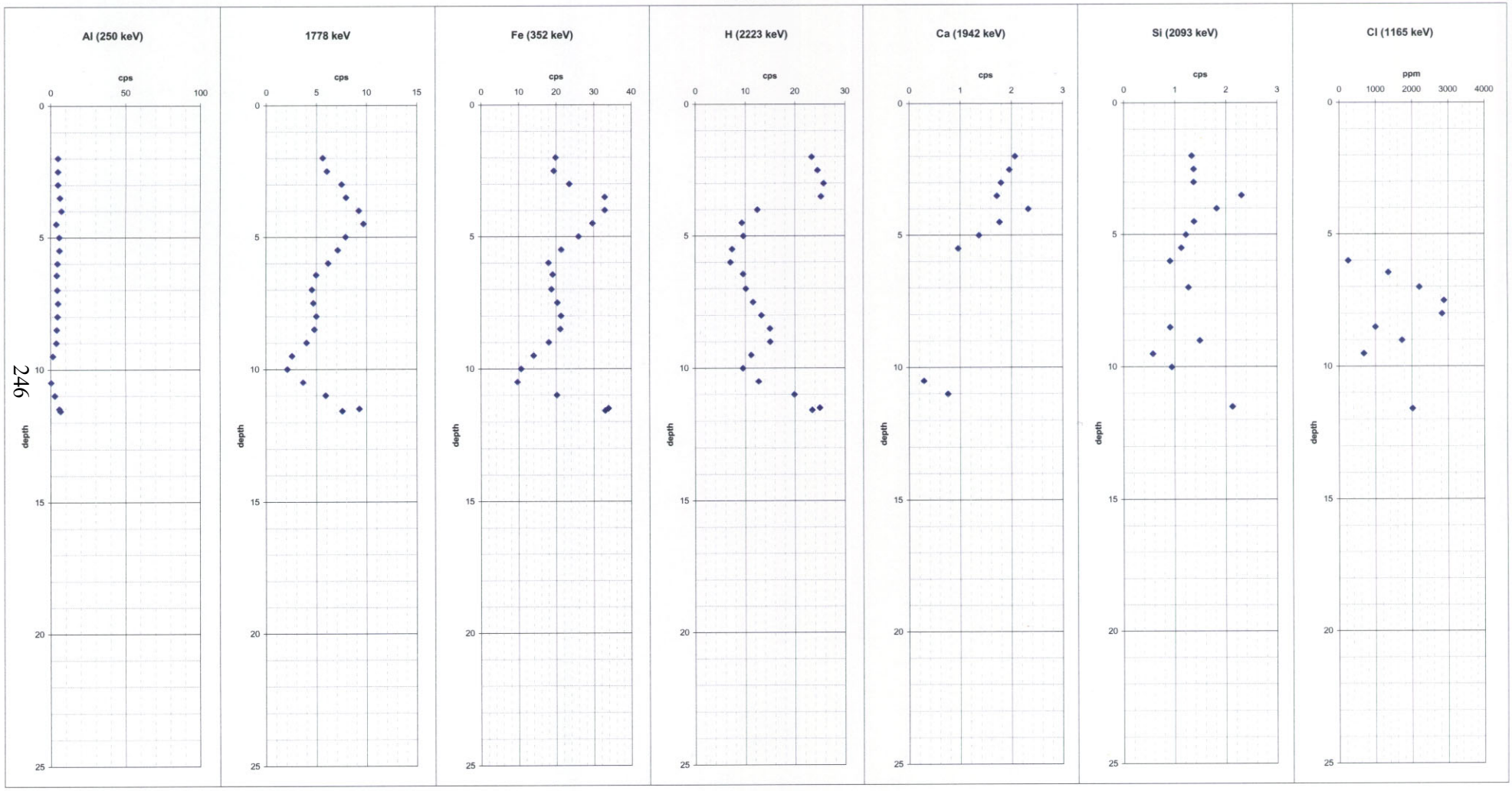
Al (250 keV)
cps
0 50 100
1778 keV
cps
0 5 10 15
Fe (352 keV)
cps
0 10 20 30 40
H (2223 keV)
cps
0 10 20 30
Ca (1942 keV)
cps
0 1 2 3
Si (2093 keV)
cps
0 1 2 3
Cl (1165 keV)
ppm
0 1000 2000 3000 4000
depth
0 5 10 15 20 25

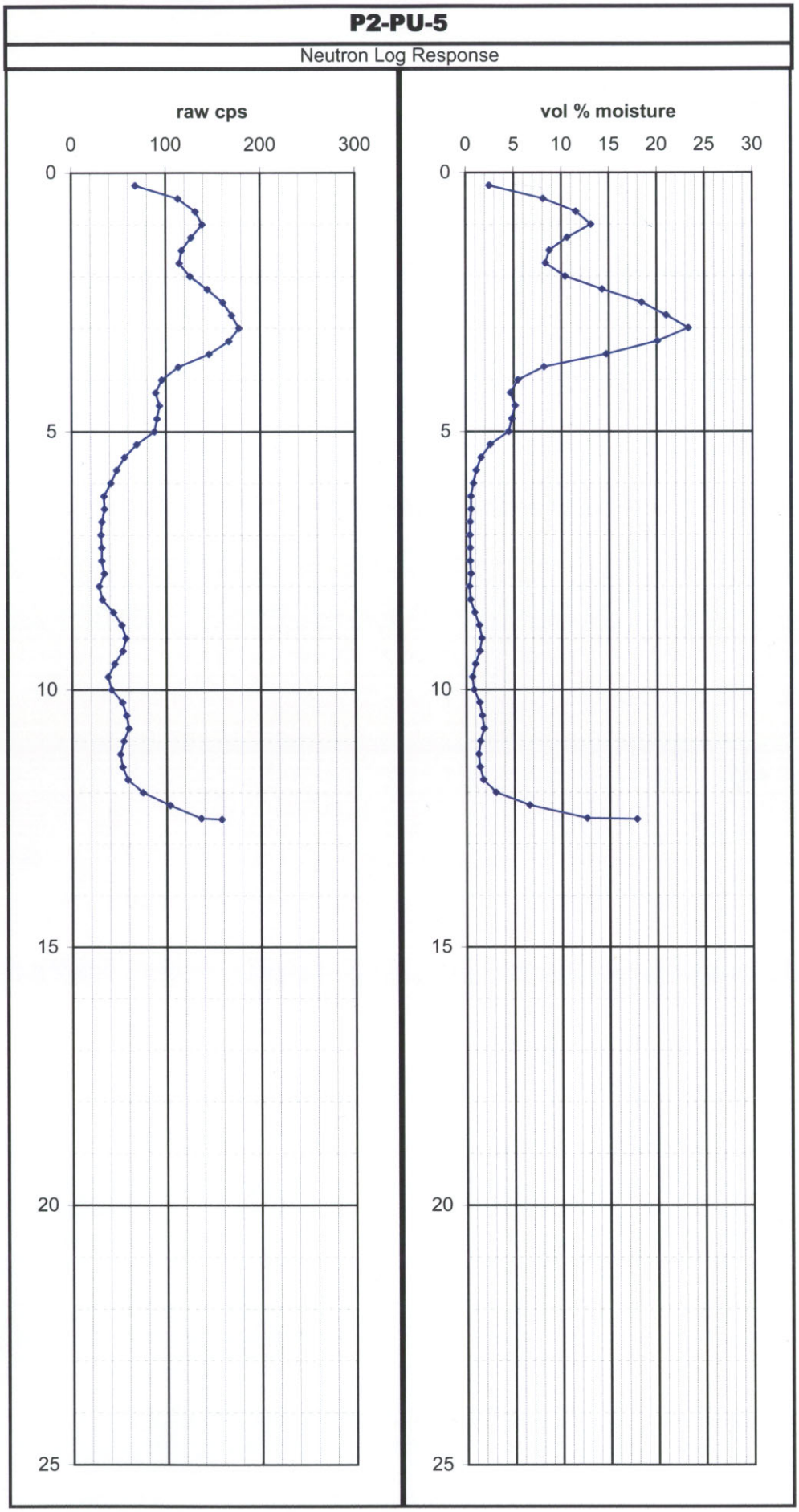
P2-PU-5
Neutron Log Response
raw cps
0
100
200
300
vol % moisture
0
5
10
15
20
25
30
0
5
10
15
20
25

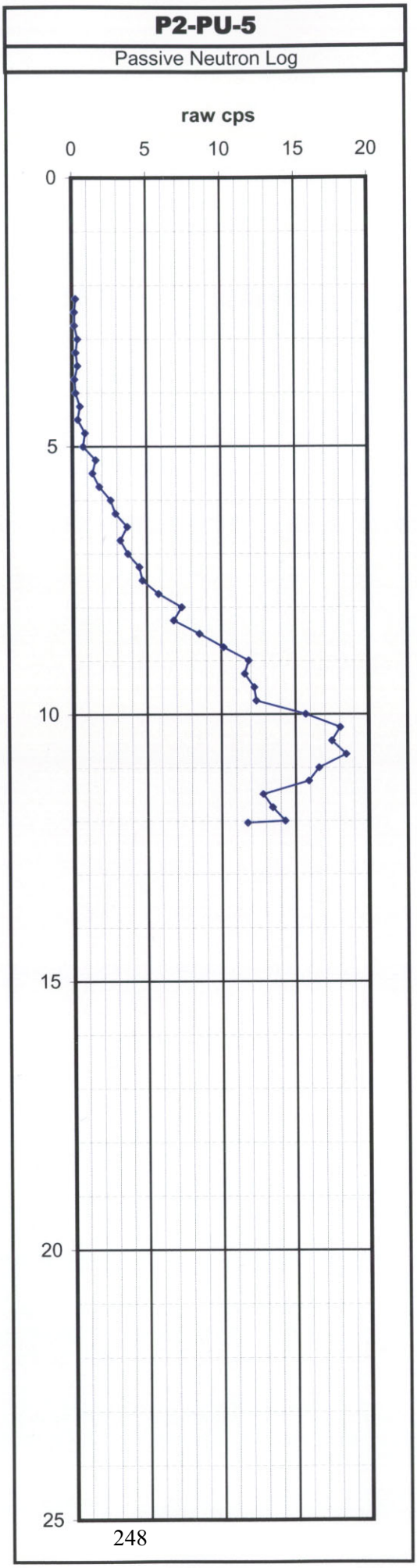
P2-PU-5
Passive Neutron Log
raw cps
0
5
10
15
20
0
5
10
15
20
25

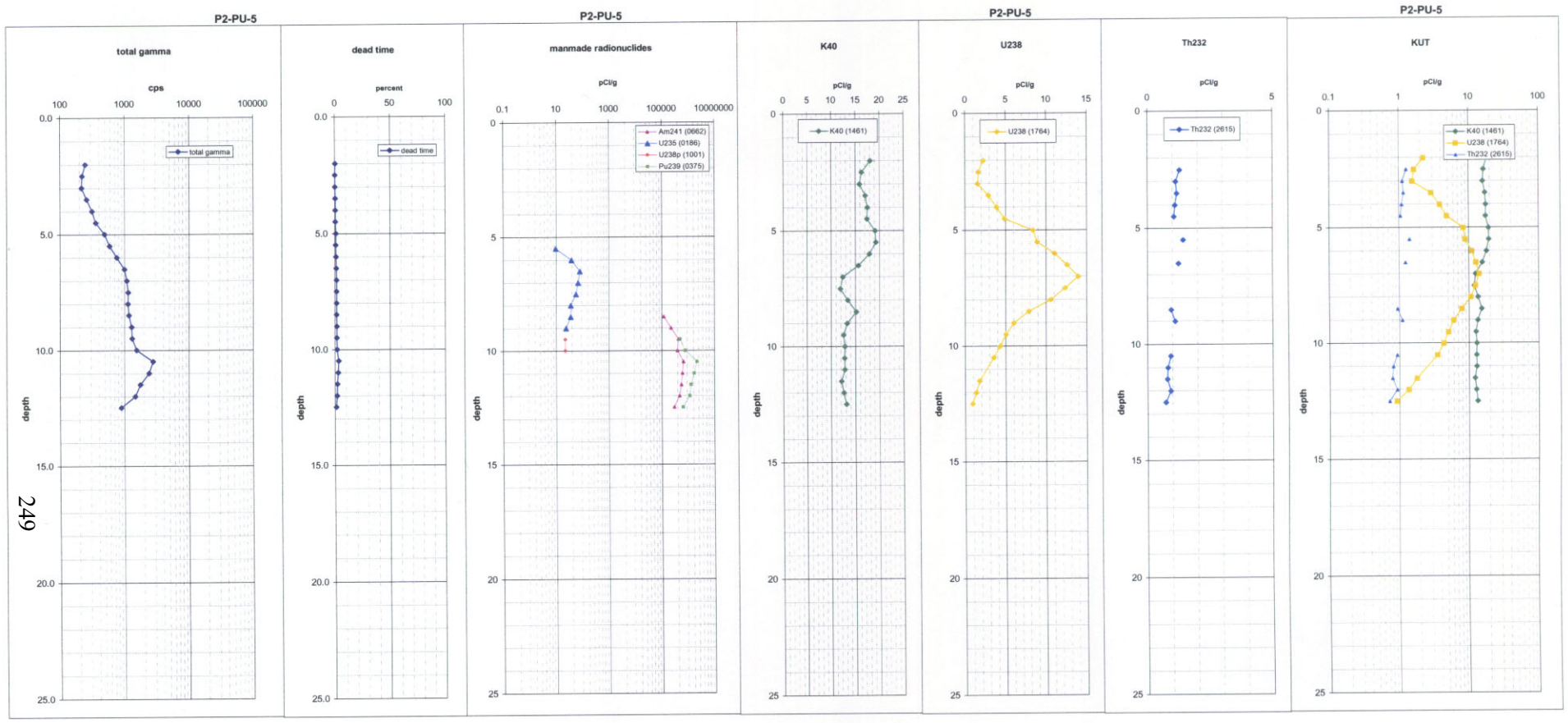
P2-PU-5
total gamma
cps
100
1000
10000
100000
total gamma
depth
0.0
5.0
10.0
15.0
20.0
25.0
P2-PU-5
dead time
percent
0
50
100
dead time
depth
0.0
5.0
10.0
15.0
20.0
25.0
P2-PU-5
manmade radionuclides
pCi/g
0.1
10
1000
100000
10000000
Am241 (0662)
U235 (0186)
U238p (1001)
Pu239 (0375)
depth
0
5
10
15
20
25
P2-PU-5
K40
pCi/g
0
5
10
15
20
25
K40 (1461)
depth
0
5
10
15
20
25
P2-PU-5
U238
pCi/g
0
5
10
15
U238 (1764)
depth
0
5
10
15
20
25
P2-PU-5
Th232
pCi/g
0
5
Th232 (2615)
depth
0
5
10
15
20
25
P2-PU-5
KUT
pCi/g
0.1
1
10
100
K40 (1461)
U238 (1764)
Th232 (2615)
depth
0
5
10
15
20
25

P2-PU-5

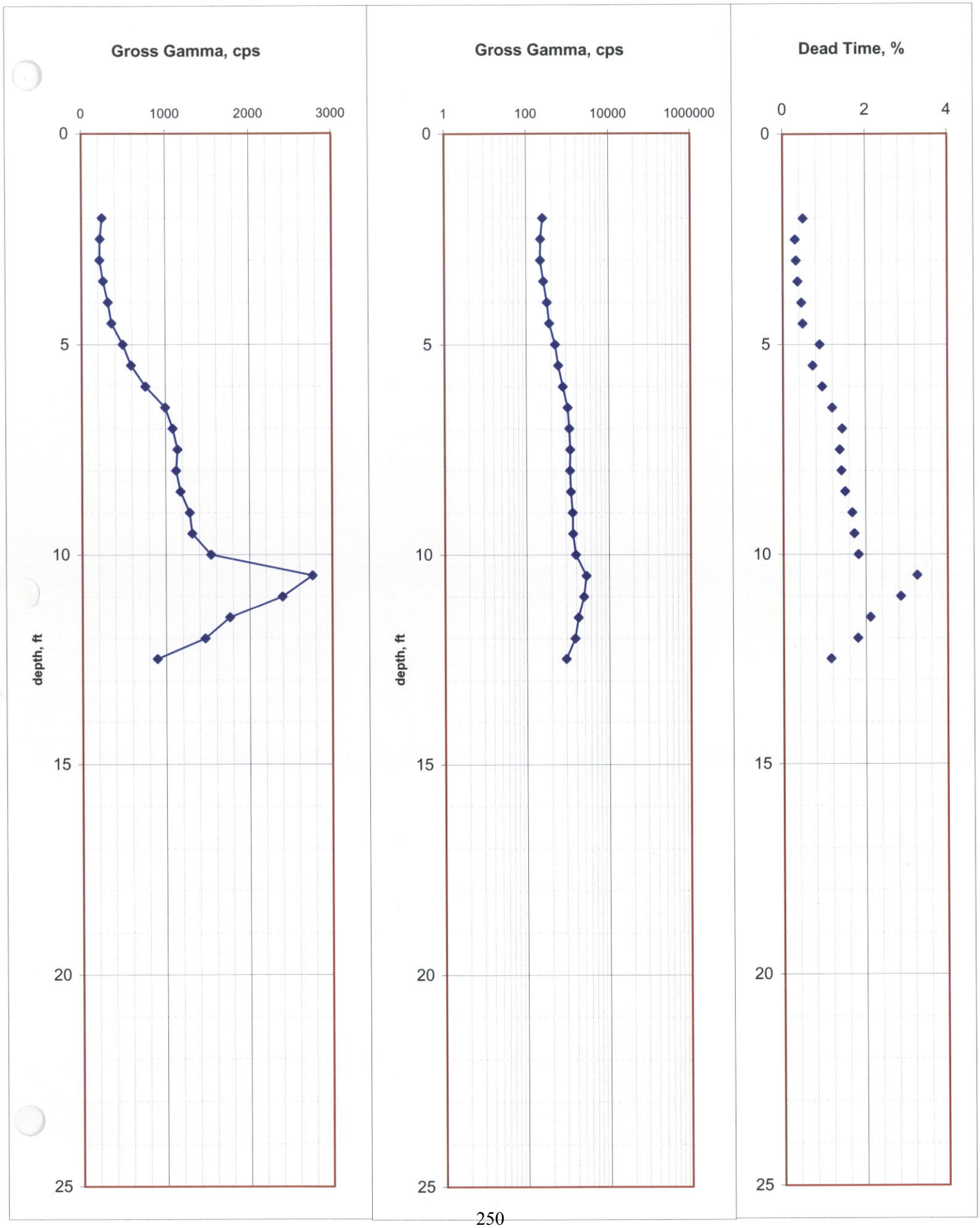
Gross Gamma, cps
0
1000
2000
3000
depth, ft
0
5
10
15
20
25
Gross Gamma, cps
1
100
10000
1000000
depth, ft
0
5
10
15
20
25
Dead Time, %
0
2
4
0
5
10
15
20
25

P2-PU-5

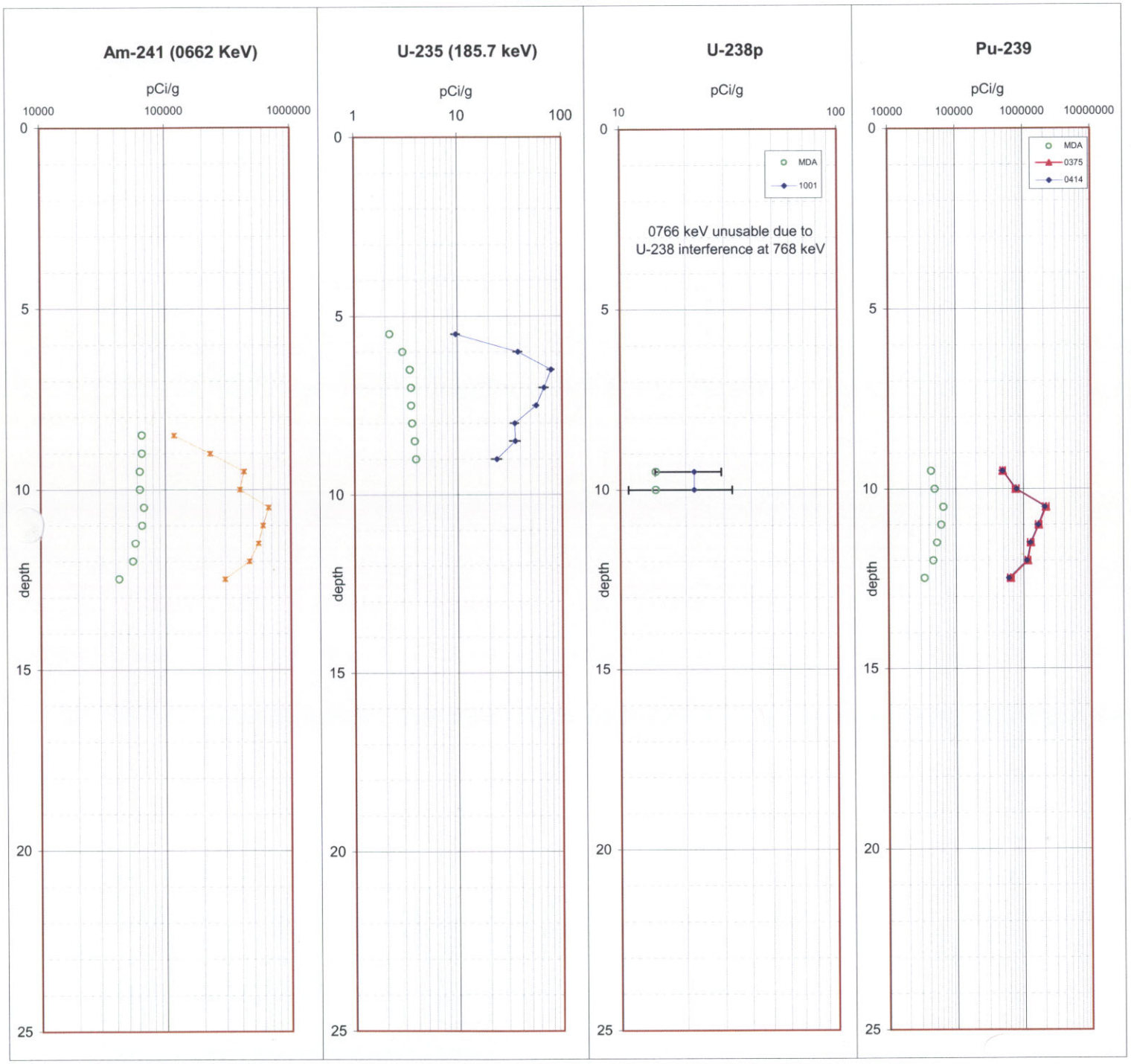
Am-241 (0662 KeV)
pCi/g
10000
100000
1000000
U-235 (185.7 keV)
pCi/g
1
10
100
U-238p
pCi/g
10
100
MDA
1001
0766 keV unusable due to
U-238 interference at 768 keV
Pu-239
pCi/g
10000
100000
1000000
10000000
MDA
0375
0414
depth
0
5
10
15
20
25

P2-PU-5

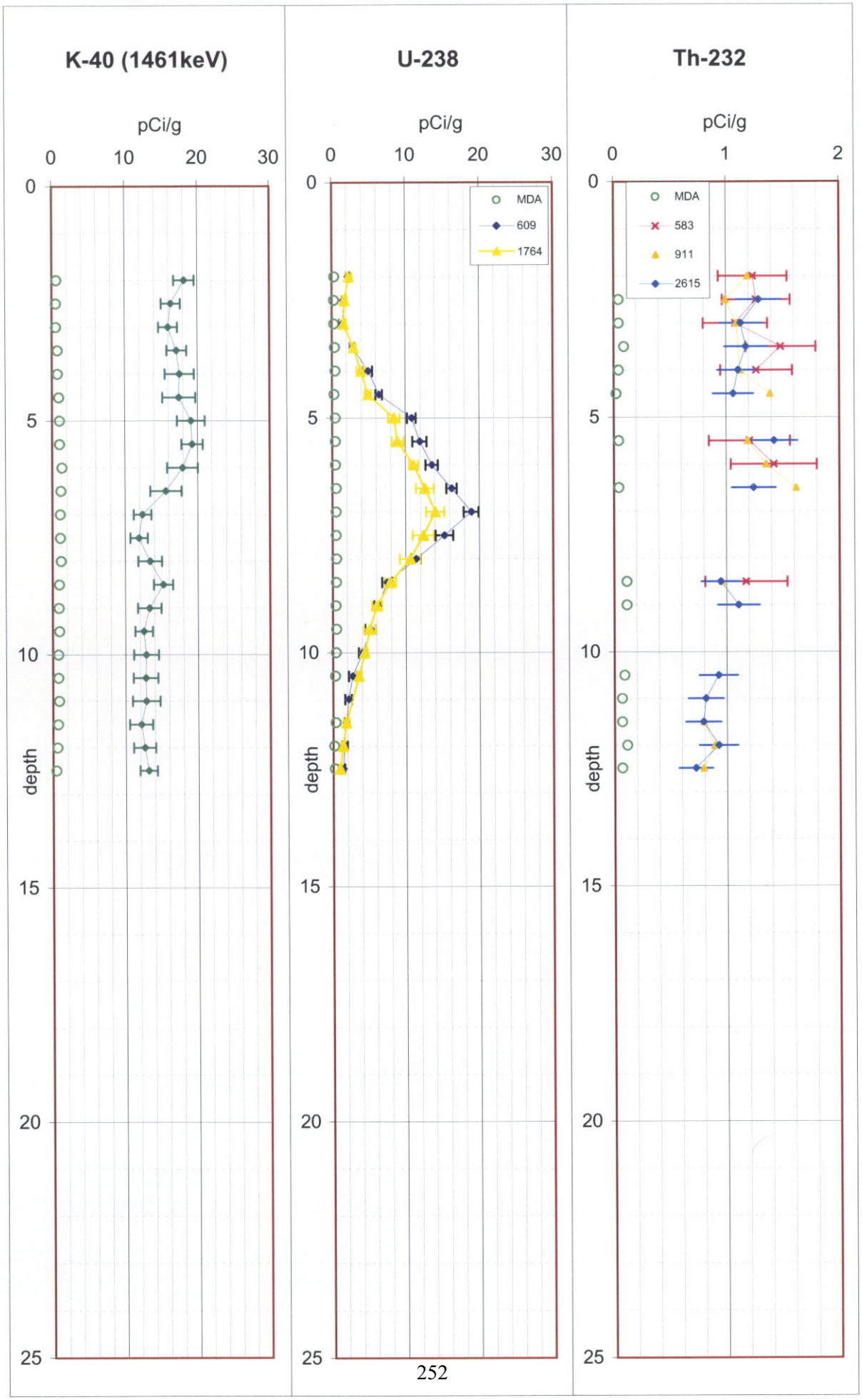

P2-PU-5

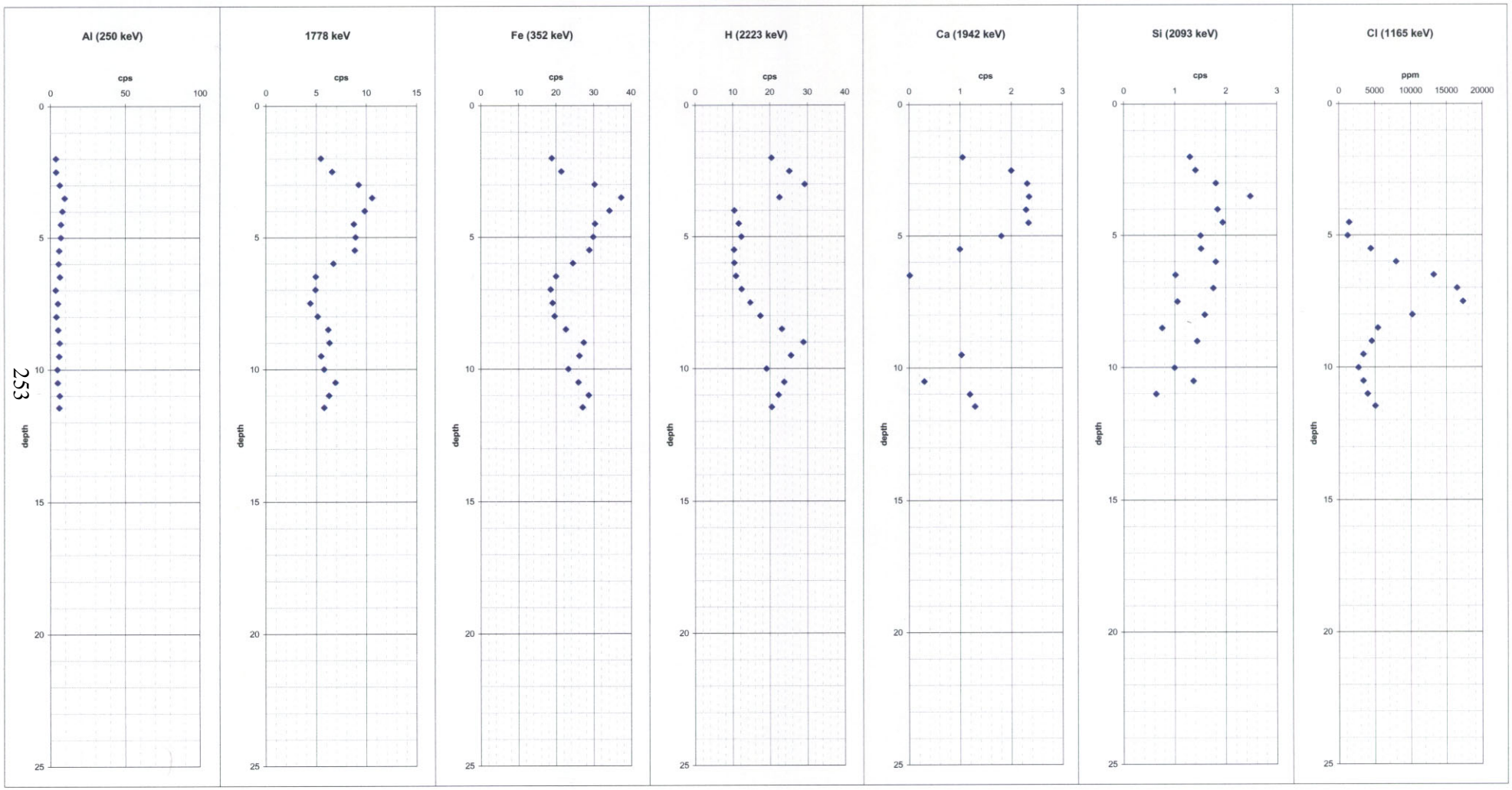
Al (250 keV)
cps
0 50 100
1778 keV
cps
0 5 10 15
Fe (352 keV)
cps
0 10 20 30 40
H (2223 keV)
cps
0 10 20 30 40
Ca (1942 keV)
cps
0 1 2 3
Si (2093 keV)
cps
0 1 2 3
Cl (1165 keV)
ppm
0 5000 10000 15000 20000
depth
0 5 10 15 20 25

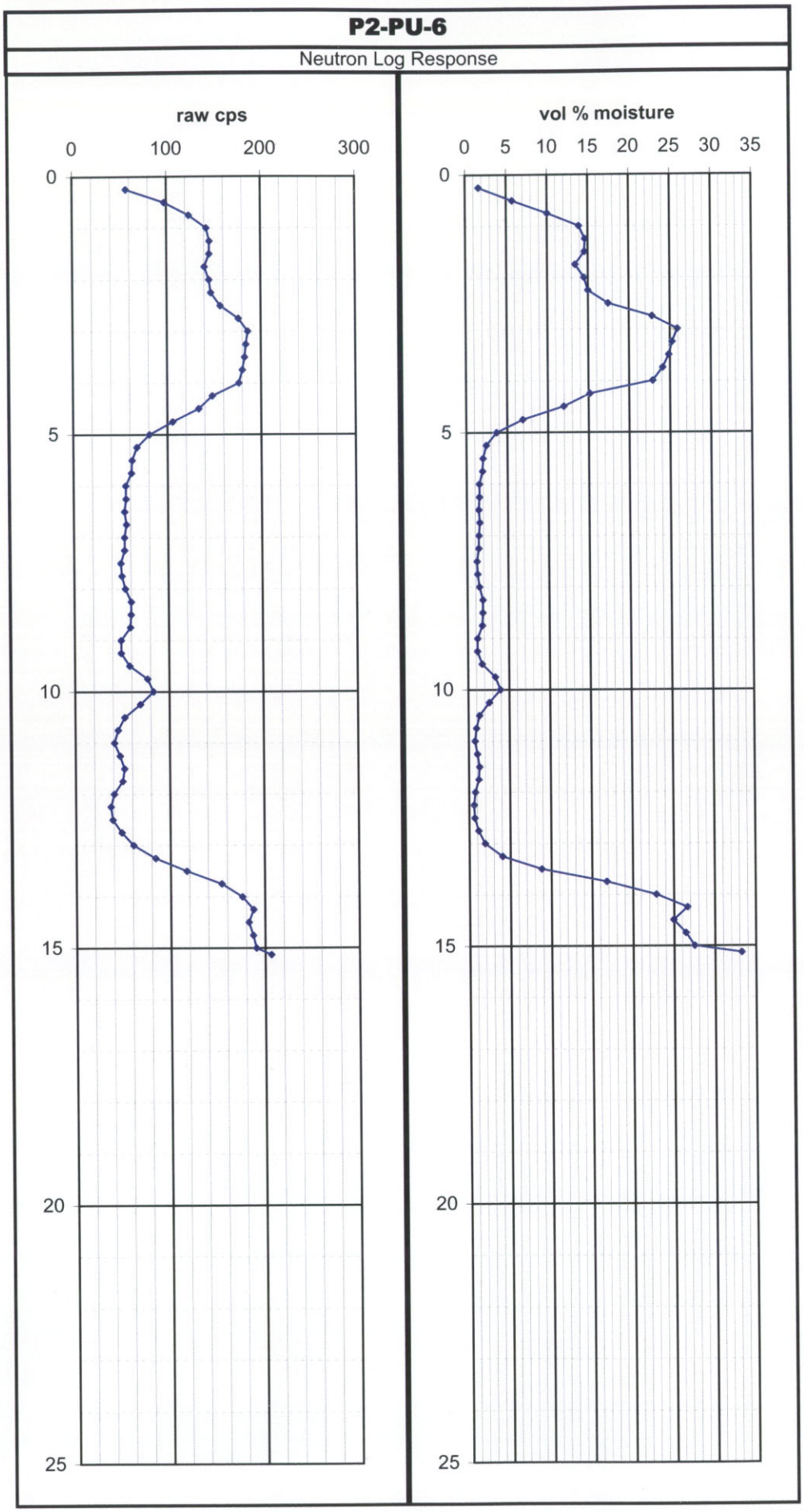
P2-PU-6
Neutron Log Response
raw cps
0
100
200
300
0
5
10
15
20
25
vol % moisture
0
5
10
15
20
25
30
35
0
5
10
15
20
25

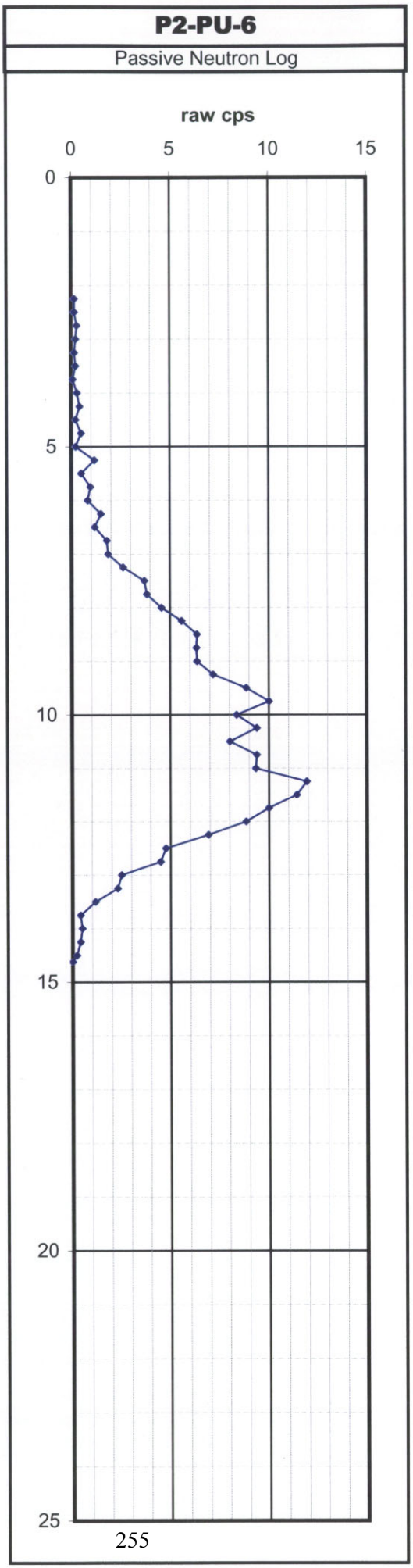
P2-PU-6
Passive Neutron Log
raw cps
0
5
10
15
0
5
10
15
20
25

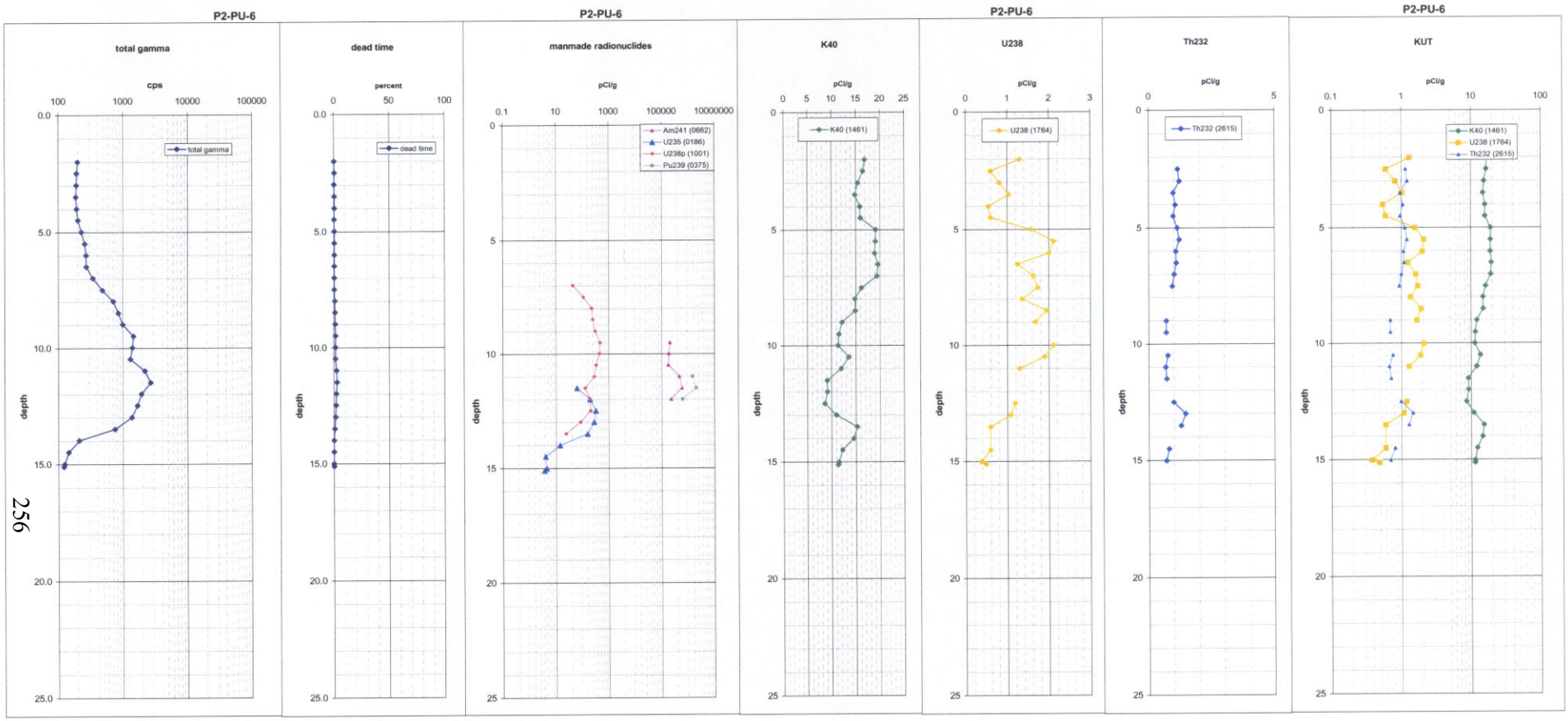
P2-PU-6
total gamma
cps
100
1000
10000
100000
depth
0.0
5.0
10.0
15.0
20.0
25.0
total gamma
P2-PU-6
dead time
percent
0
50
100
dead time
P2-PU-6
manmade radionuclides
pCi/g
0.1
10
1000
100000
10000000
Am241 (0662)
U235 (0186)
U238p (1001)
Pu239 (0375)
P2-PU-6
K40
pCi/g
0
5
10
15
20
25
K40 (1461)
P2-PU-6
U238
pCi/g
0
1
2
3
U238 (1764)
P2-PU-6
Th232
pCi/g
0
5
Th232 (2615)
P2-PU-6
KUT
pCi/g
0.1
1
10
100
K40 (1461)
U238 (1764)
Th232 (2615)

P2-PU-6

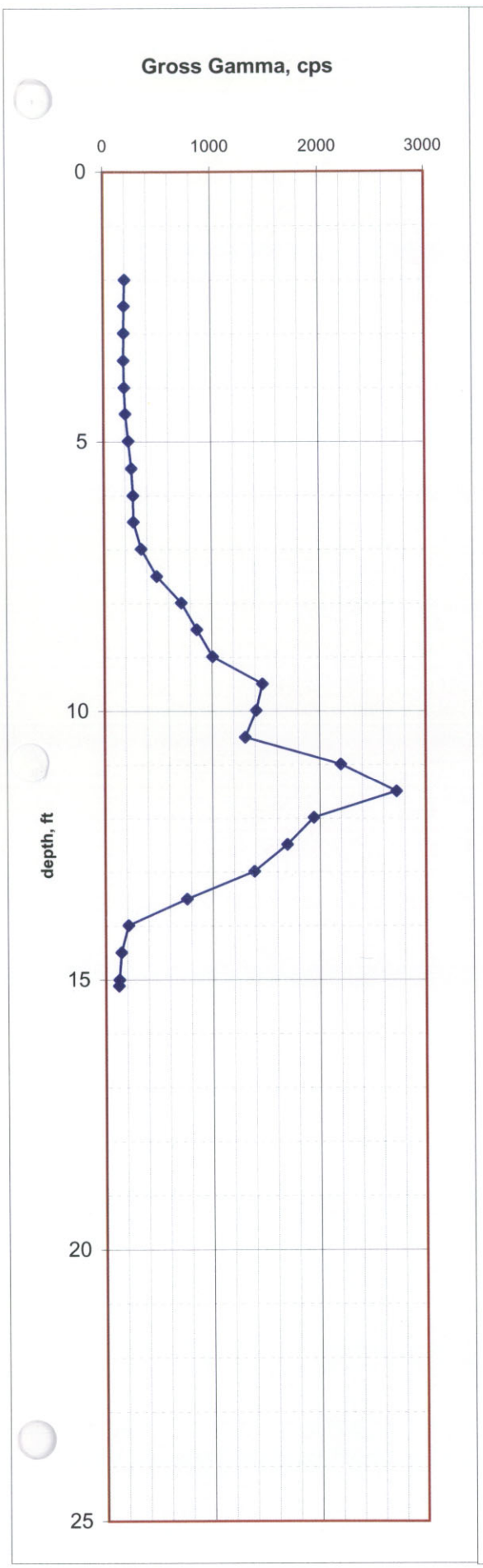
Gross Gamma, cps
0
1000
2000
3000
depth, ft
0
5
10
15
20
25

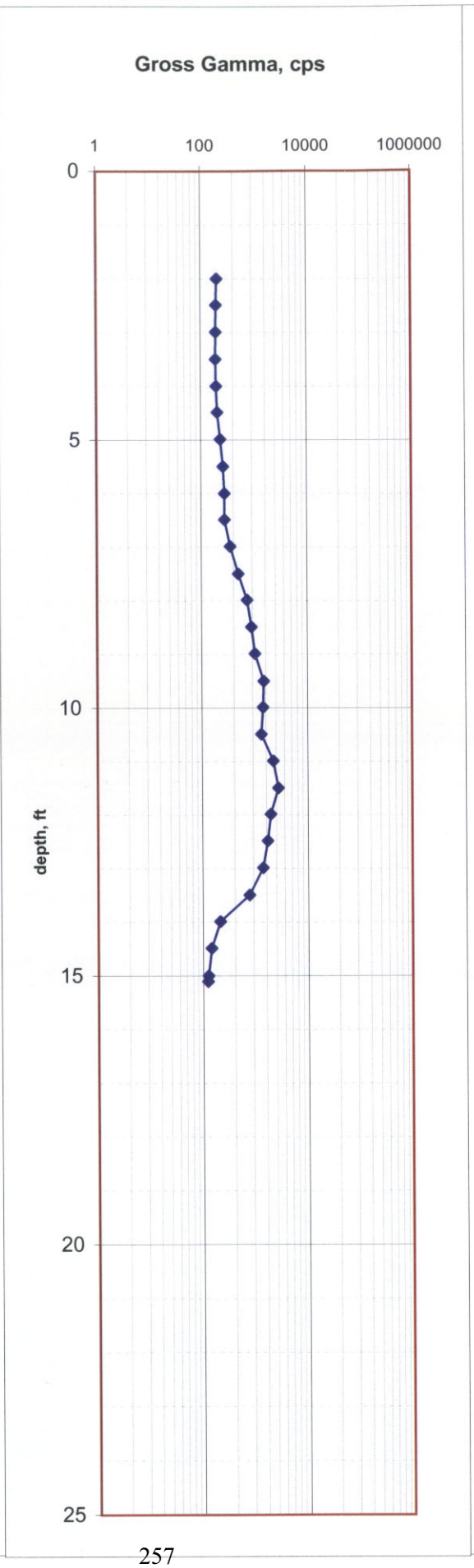
Gross Gamma, cps
1
100
10000
1000000
depth, ft
0
5
10
15
20
25

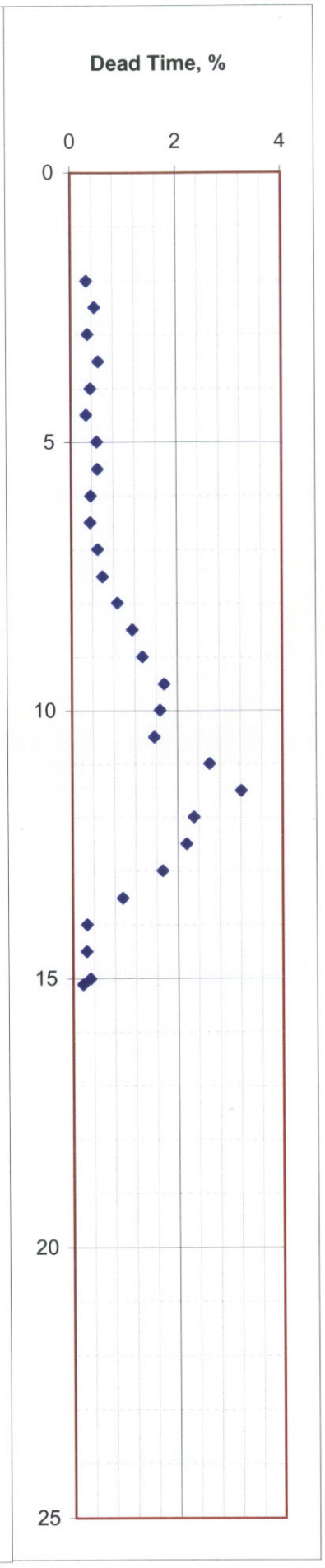
Dead Time, %
0
2
4
0
5
10
15
20
25

P2-PU-6

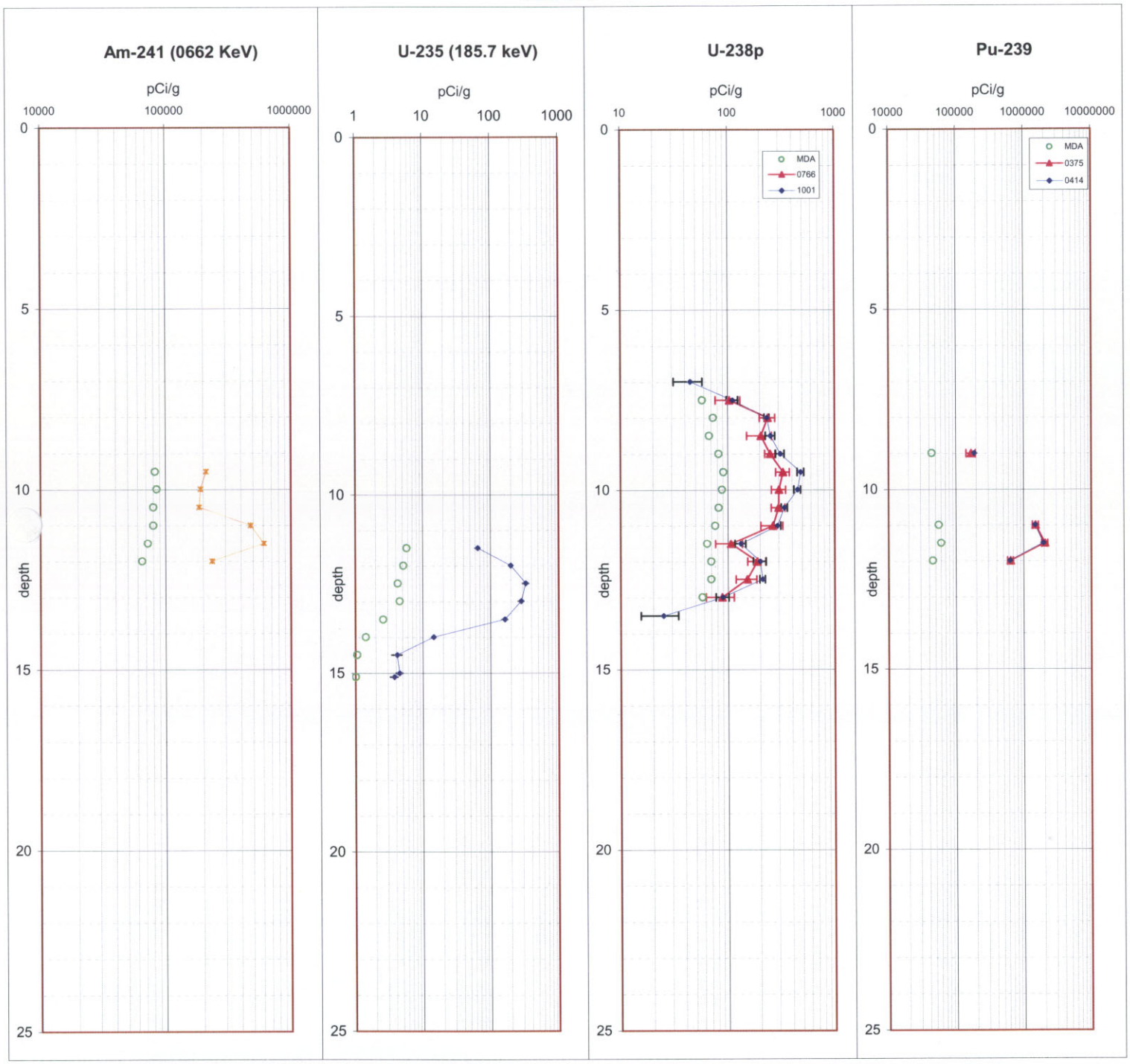
Am-241 (0662 KeV)
pCi/g
10000
100000
1000000
U-235 (185.7 keV)
pCi/g
1
10
100
1000
U-238p
pCi/g
10
100
1000
MDA
0766
1001
Pu-239
pCi/g
10000
100000
1000000
10000000
MDA
0375
0414
depth
0
5
10
15
20
25

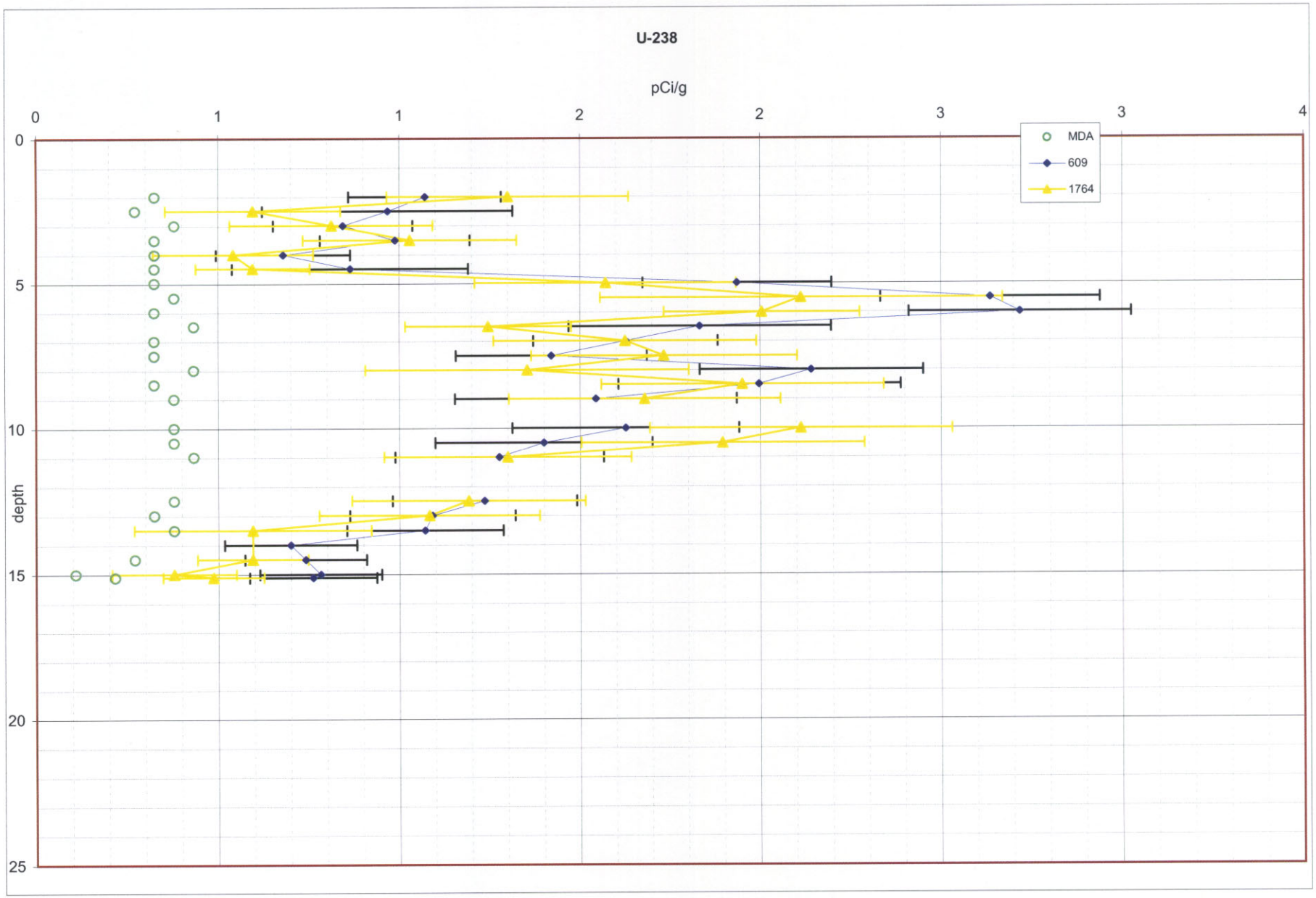
U-238
pCi/g
0
1
1
2
2
3
3
4
0
5
10
15
20
25
depth
MDA
609
1764

P2-PU-6

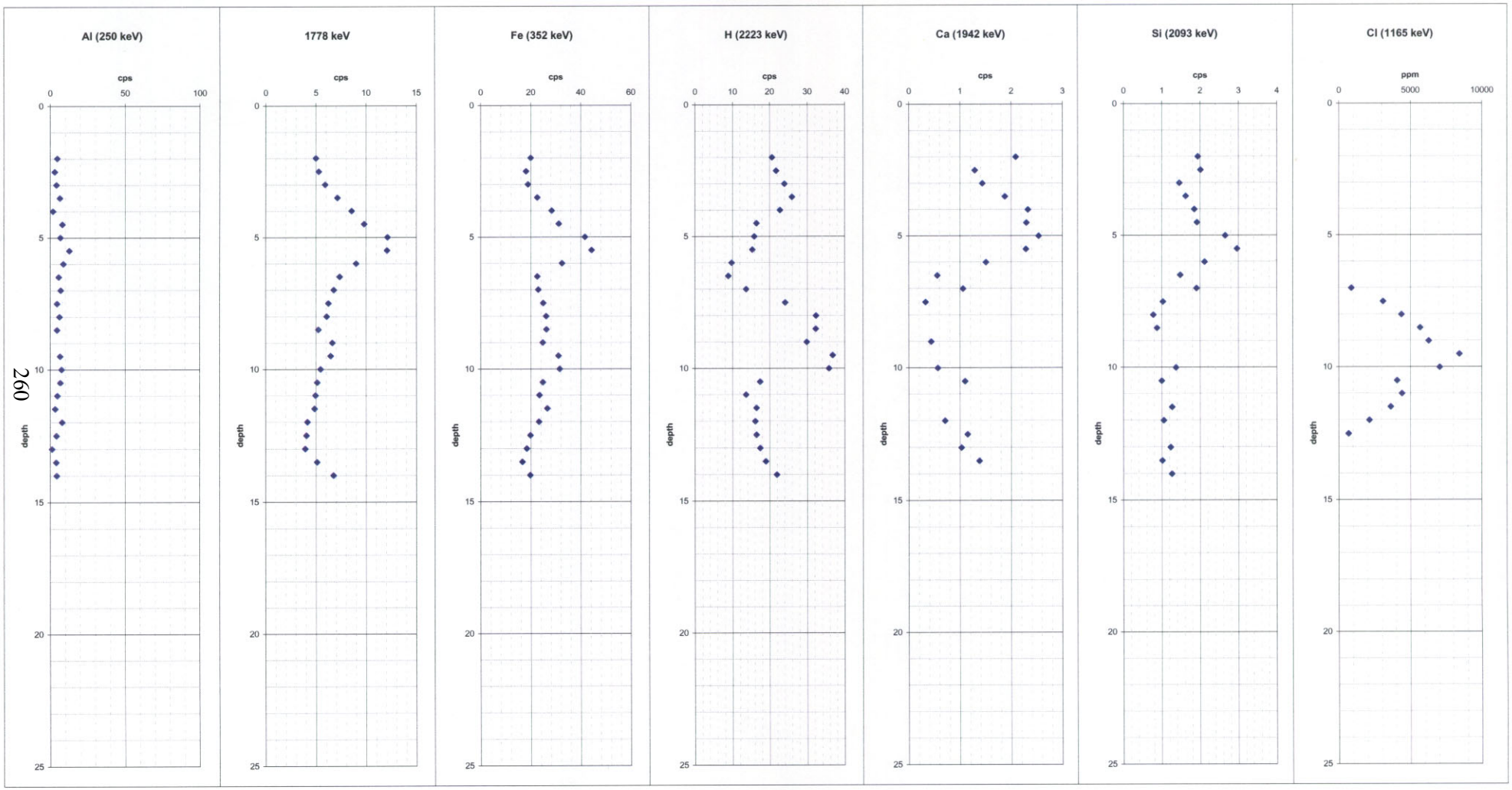
Al (250 keV)
1778 keV
Fe (352 keV)
H (2223 keV)
Ca (1942 keV)
Si (2093 keV)
Cl (1165 keV)
cps
ppm
depth

Appendix C

Anomalous Uranium and Thorium Signals in Two Passive Gamma-Ray Spectra from P2-PU-3

Appendix C

Anomalous Uranium and Thorium Signals in Two Passive Gamma-Ray Spectra from P2-PU-3

C.J. Koizumi, December 30, 2003

C-1. SITE AND DATA ACQUISITION INFORMATION

Site: INEEL Site SDA Pit 2, borehole P2-PU-3, 0.5-inch-thick steel casing

Logging System: Gamma 4B, 35 percent HPGe, serial number 36TP21095A

Logging Date: 12/10/03

Spectra:

DB441017.CHN, passive gamma ray, depth 12 feet, 300 seconds real time

DB441014.CHN, passive gamma ray, depth 13.5 feet, 300 seconds real time.

The passive gamma ray log of P2-PU-3 implies the existence of three anomalies:

- A uranium anomaly that reaches a maximum concentration of about 2,200 pCi/g at a depth of about 10.5 feet
- A thorium anomaly that reaches a maximum concentration of about 36 pCi/g at a depth of about 12 feet
- A radium anomaly that reaches a maximum concentration of about 159 pCi/g at a depth of about 14 feet.

C-1.1 Spectrum DB441017.CHN

C-1.1.1 Calculated Concentrations

The Ra-226 concentration inferred from the 1764.5-keV gamma ray spectral peak is about 34 ± 1 pCi/g. The Ra-226 concentration inferred from the 609.3-keV gamma ray spectral peak is smaller, about 19 ± 1 pCi/g.

When Ra-226 is in decay equilibrium with U-238, the Ra-226 and U-238 concentrations are equal (if expressed in decay rate per unit mass).

The U-238 concentration inferred from the Pa-234m 1001.0-keV gamma ray peak is about 70 ± 20 pCi/g.

This spectrum was recorded at a depth that was close to the maximum calculated thorium concentration.

The thorium concentration based on the Ac-228 gamma ray peaks is somewhat higher than normal background. The intensity of the 911.2-keV gamma ray peak implies a concentration of about 11 ± 1 pCi/g, and the intensity of the 969.0-keV gamma ray peak implies a concentration of about 14 ± 1 pCi/g. The concentration based on the Tl-208 2614.5-keV gamma ray peak is unusually high, around 30 ± 2 pCi/g.

C-1.1.2 Interpretations

The 1764.5- and 609.3-keV gamma rays both originate in the decay of Bi-214, so Ra-226 concentrations calculated from the spectral peak intensities should normally be nearly identical. Here, the concentration based on the 1764.5-keV gamma ray significantly exceeds the concentration based on the 609.3-keV gamma ray. The actual reason for the discrepancy is unknown, but there are several possible explanations. The spectrum was acquired at a depth where the Ra-226 [depicted as *U-238 (1764)* on log plots] concentration was not uniform. In fact, at 12 feet the Ra-226 concentration began to rise quickly as the depth increased. Since the 1764.5-keV gamma rays have more penetrating ability than the 609.3-keV gamma rays, it is likely that a greater percentage of the 1764.5-keV gamma rays from the high radium zone (between about 12 and about 15 feet) passed through the formation and reached the detector. In addition, gamma rays from the zone of elevated radium impinged on the detector at angles greater than 90 degrees relative to vertical. For such angles, the path lengths through the steel casing were greater than 0.5 inch, and any increase in path length within casing would further reduce the 609.3-keV gamma ray fluxes relative to the 1764.5-keV gamma ray fluxes. Also, this spectrum came from a depth within the processed uranium anomaly, and the processed uranium might have raised the average Z of the formation to the point that the 609.3-keV gamma ray fluxes were slightly reduced by the Z effect. All of these factors imply that the 609.3-keV gamma ray peak intensity yields an understated concentration.

The fact that the spectrum came from a depth within the zone of elevated U-238 accounts for the high uranium concentration based on the peak for the 1001.0-keV Pa-234m gamma ray.

Explanations for the thorium concentration discrepancy are more difficult to develop. The cursory investigations described next failed to reveal a reason for this discrepancy.

The idea that the intensity of the peak at 2,614.5 keV was boosted by an overlooked source was considered, but no candidate sources were found. For example, the spectrum does not have a pair of intense peaks that could be linked to two gamma rays that would cause a random sum peak at 2,614.5 keV. Also, a search of the "Gamma-Lines of the Radionuclides Ordered in Terms of Energy" section in The Gamma Rays of the Radionuclides (Erdtmann & Soyka, 1979, Verlag Chemie, Weinheim, Germany) did not reveal any credible sources other than Tl-208 for a 2614.5-keV gamma ray.

If an intense flux of gamma rays of energy 3125 keV existed, an escape peak at 2,614 keV would add to the intensity of the Th gamma ray peak, but the spectrum would not have a peak at 3,125 keV because this energy is above the range of the detector. However, the existence of 3125-keV gamma rays is considered highly unlikely, and in fact, The Gamma Rays of the Radionuclides does not list any credible sources.

The only thorium series nuclide between Ac-228 and Tl-208 with a half life long enough to be a factor in decay disequilibrium is Th-228 (half life ≈ 1.9 years). Thus, the only plausible thorium series decay disequilibrium that could account for the observed discrepancy is an excess of Th-228 relative to Th-232. Separation of Th-228 from Th-232 in the subsurface by geochemical processes is too improbable to consider, so mechanisms other than decay of Th-232 that could produce thorium series nuclides below Ac-228 were investigated. An example is alpha decay of U-232 to Th-228. None of the mechanisms

produce detectable gamma rays, so the passive gamma ray spectra do not contain information that can confirm or rule out such processes.

C-1.2 Spectrum DB441014.CHN

C-1.2.1 Calculated Concentrations

The thorium concentration inferred from the 2614.5-keV gamma ray peak intensity is about 7 pCi/g, which is somewhat higher than normal background.

Peak intensities for three gamma rays, 609.3, 1764.5, and 2204.2 keV, imply Ra-226 concentrations of 102 ± 6, 156 ± 4, and 153 ± 6 pCi/g, respectively.

The spectrum contains no hint of a peak at 1001.0 keV.

C-1.2.2 Interpretations

The intensities of the peaks for the 1764.5- and 2204.2-keV gamma rays imply a Ra-226 concentration a bit higher than 150 pCi/g. The concentration inferred from the 609.3-keV gamma ray peak is smaller, about 102 ± 5 pCi/g. The reason for this discrepancy is unknown. It should be noted that the absence of a peak for the 1001.0-keV Pa-234m gamma ray indicates that U-238 is not present in concentrations that could suppress the 609.3-keV gamma ray flux via the Z effect.

The absence of any trace of a peak at 1001.0 keV was considered unusual, and was investigated.

The 2002 SGLS calibration data acquired by logging the calibration standard SBM were retrieved because the Ra-226 concentration in SBM is 125 pCi/g, which is about the same as predicted using the 1764.5-keV gamma peak in DB441014.CHN. The U-238 concentration is also 125 pCi/g. In all of the SBM spectra, the 1001.0-keV gamma ray peak is clearly evident, and the average intensity is 2.5 c/s. The average intensity for the 1,764.5-keV gamma ray peak is 40.1 c/s. Both of these average intensities were divided by the casing corrections (to get the intensities that would have been recorded if the SBM hole had a 0.5-inch-thick casing), then the fraction of the 1,001.0-keV intensity relative to the 1764.5-keV intensity was calculated. That fraction was then used to predict the intensity of the 1,001.0-keV gamma ray peak that would be in spectrum DB441014.CHN if U-238 were present in decay equilibrium with Ra-226. The result is about 1.5 c/s.

A similar result was obtained from calculations involving a detection index. The detection index is defined as

$$\text{detection index} = \frac{(\text{gamma - ray yield}) \cdot (\text{detector efficiency})}{(\text{casing correction})}.$$

For any gamma ray, the detection index value is approximately proportional to the intensity of the associated spectral peak.

Using peak intensities from DB441014.CHN, detection indexes were calculated for the 609.3-, 1120.3-, and 1764.5-keV gamma rays. The ratios of peak intensity to detection index were 0.04, 0.05, and 0.06 for the three gamma rays. The average ratio value of 0.05 was used, along with the calculated detection index value for the 1,001.0-keV gamma ray, to estimate a peak intensity of about 1.3 c/s. This agrees with the value of 1.5 c/s estimated from SBM calibration data. The spectrum analysis program should readily find a 1.3-c/s peak (in fact, the program had no trouble locating the 1.5-c/s K-40 gamma

ray peak in DB441014.CHN), but no such peak was identified near 1001 keV. The portion of the spectrum around 1001 keV was manually magnified and inspected, and no trace of a peak was seen.

The 609.3-, 1120.3-, and 1764.5-keV gamma ray peak intensities imply that the subsurface material has a Ra-226 concentration of approximately 150 pCi/g, but the absence of a peak for the 1,001.0-keV Pa-234m gamma ray indicates that the material is deficient in U-238 in relation to the concentration corresponding to decay equilibrium with Ra-226. Some materials with these characteristics are uranium mill tailings and radium itself.

Appendix D

Stoller Long Count Reports

Appendix D

Stoller Long Count Reports

Analyses of INEEL Long Count Time Passive Gamma-Ray Spectra

Carl J. Koizumi
December 10, 2003

D-1. GENERAL REMARKS

Four high resolution passive gamma ray spectra were acquired by long stationary counting at two depth points in each of two boreholes at the Subsurface Disposal Area at the Idaho National Laboratory Radioactive Waste Management Complex. The logging vehicle was HO-68B-3573, and the gamma ray detector was a 35 percent HPGe with Serial Number 36TP21095A. The counting time was 3,000 seconds clock time for each spectrum.

The spectra were analyzed with the Canberra Aptec PCMCA/WIN spectrum analysis program, using the following settings.

- ROI Properties
  - ROI Background Line: Least square fit degree = 3, Use method 2
  - Confidence: MDA sigma = 1.645, error sigma = 2
  - Centroid Calculated: between net half max
  - Centroid Weighting: net*abs(net)*chan
  - ROI Background End Points: with 5 end channels
- Peak Search
  - Max Peak Error:120 percent
- Multifit
  - Spectrum Type: HPGe/Ge(Li)
  - Optimize Centroid Search for: Separated Overlaps
  - Peaks to be Fitted: Multiplets and Singlets
  - Whose Amplitude is ≥ Minimum Detectable Amplitude times 1.645 sigma
  - Fit with Peak Width: Fixed
  - Fit with Background: Fixed

- Accuracy
  - Maximum Iterations: 25
  - Maximum Overlaps: 8
  - Percent Change: 0.25
  - Minimum Reduced Chi Square: 0.75.

For gamma ray source identifications, a library containing only gamma rays for the natural sources was used. Thus, the only gamma rays that were identified by the analysis program were those associated with K-40, U-235 and its decay products, U-238 and its decay products, and Th-232 and its decay products. Gamma rays not identified by the analysis program were identified manually and individually.

Table D-1 shows the abbreviations used for the names of the various natural gamma ray sources.

Table D-1. Abbreviations used for natural gamma ray sources.

Abbreviation	Gamma-Ray Source	Comment
Ac/T	Ac-228	decay product of Th-232
Bi/T	Bi-212	decay product of Th-232
Bi/U	Bi-214	decay product of U-238
K/K	K-40	constituent of natural potassium
Pb/T	Pb-212	decay product of Th-232
Pb/U	Pb-214	decay product of U-238
Tl/T	Tl-208	decay product of Th-232
TlAc/T	Tl-208, Ac-228	gamma rays from the two sources have nearly equal energies
URa/U	Ra-226	decay product of U-238

D-1.1 Borehole P6-PU-1

The borehole is located in the INEEL site SDA Area 5. The names of the two spectra are DB371000.CHN and DB381000.CHN.

D-1.1.1 Spectrum DB371000.CHN

DB371000.CHN was acquired on November 24, 2003, from a depth of 15.5 feet. The dead time was 0.35 percent, and the live time was 2989.4 seconds.

Table D-2 displays the natural gamma ray source names, the spectral peak intensities, and some representative concentrations that were calculated using intensities of prominent peaks. All of the uncertainties are 2σ, corresponding to the 95 percent confidence interval.

Table D-2. Natural gamma ray sources, Spectrum DB371000.CHN

Gamma-Ray Source	ActualEnergy (keV)[a]	Measured Energy (keV)	Energy Residual (keV)	FWHM[b] (keV)	Spectral Peak Intensity (c/s)[c]	Calculated Concentration (pCi/g)
Ac/T	338.32	338.34	-0.02	1.49	0.178 ± 0.072	1.70 ± 0.69
Ac/T	794.95	794.97	-0.02	1.96	0.079 ± 0.026	—
Ac/T	911.21	911.12	0.09	2.19	0.457 ± 0.041	1.51 ± 0.14
Ac/T	968.97	968.86	0.11	2.05	0.301 ± 0.024	1.63 ± 0.13
AcBi/T	727.10	727.22	-0.12	1.76	0.094 ± 0.036	—
Bi/T	1,620.50	1,620.63	-0.13	1.68	0.021 ± 0.012	—
Bi/U	609.31	609.40	-0.09	1.76	0.607 ± 0.050	1.25 ± 0.10
Bi/U	768.36	768.31	0.05	1.51	0.060 ± 0.036	—
Bi/U	1,120.29	1,120.13	0.16	1.92	0.199 ± 0.035	—
Bi/U	1,238.11	1,237.87	0.24	1.82	0.075 ± 0.026	—
Bi/U	1,377.67	1,377.62	0.05	2.44	0.057 ± 0.022	—
Bi/U	1,407.98	1,407.88	0.10	2.29	0.046 ± 0.011	—
Bi/U	1,509.23	1,509.19	0.04	1.57	0.013 ± 0.013	—
Bi/U	1,729.60	1,729.79	-0.19	2.14	0.041 ± 0.012	—
Bi/U	1,764.49	1,764.58	-0.09	2.35	0.227 ± 0.020	1.23 ± 0.11
Bi/U	1,847.42	1,847.41	0.01	2.40	0.038 ± 0.013	—
Bi/U	2,204.21	2,203.78	0.43	2.91	0.079 ± 0.014	1.33 ± 0.23
BiPb/U	351.49	351.97	-0.48	1.76	0.374 ± 0.073	—
K/K	1,460.80	1,460.69	0.11	2.27	2.610 ± 0.062	20.67 ± 0.49
Pb/T	238.63	238.79	-0.16	1.70	0.655 ± 0.099	—
Pb/U	295.21	295.26	-0.05	1.49	0.111 ± 0.077	—
Tl/T	860.56	860.45	0.11	2.02	0.077 ± 0.031	—
Tl/T	2,614.53	2,614.49	0.04	2.89	0.663 ± 0.030	1.48 ± 0.07
TlAc/T	583.30	583.31	-0.01	1.92	0.462 ± 0.055	—
URa/U	185.91	186.01	-0.10	1.53	0.108 ± 0.084	—

a. kilo-electron-volts
b. full width at half maximum
c. counts per second

Gamma ray energy and yield values are from Firestone (Firestone, R.B., 1999, Table of Isotopes (Eighth Edition, Volume II), John Wiley & Sons, Inc., New York).

The Th-232 concentrations calculated from the intensities of the various Ac-228 gamma ray peaks and the intensity of the Tl-208 gamma ray peak are all in reasonable agreement, as are the U-238 concentrations calculated from the intensities of the various Bi-214 gamma ray peaks. The calculated potassium, uranium, and thorium concentrations are consistent with natural background at INEEL.

Data for peaks not identified by the spectrum analysis program appear in Table 3, along with proposed source identifications. The energy residuals in Table D-2 for known gamma rays are relatively small, indicating that the energies in Table D-3 are accurate.

Table D-3. Data for unidentified peaks, Spectrum DB371000.CHN.

Energy (keV)	FWHM (keV)	Peak Intensity (c/s)	Proposed Source Identification	Comments
94.02	1.58	0.107 ± 0.085	—	—
99.03	1.59	0.237 ± 0.093	Am-241	—
103.01	1.59	0.234 ± 0.097	Am-241	—
125.18	2.12	0.157 ± 0.122	Am-241	< MDA[a]
152.69	1.04	0.111 ± 0.121	FWHM too small	< MDA
510.96	2.45	0.355 ± 0.060	annihilation radiation	—
662.51	2.40	0.100 ± 0.038	Am-241	—
704.65	1.50	0.033 ± 0.037	Bi-214 ?	< MDA
741.74	2.09	0.032 ± 0.032	Bi-214 ?	< MDA
782.92	1.95	0.019 ± 0.022	Ac-228	< MDA
964.75	2.05	0.087 ± 0.017	Ac-228	—
1,224.81	1.46	0.020 ± 0.023	—	< MDA
1,280.87	1.89	0.019 ± 0.020	Bi-214	< MDA
1,400.85	2.29	0.020 ± 0.010	—	< 0MDA
1,588.09	2.39	0.059 ± 0.016	Ac-228	—
1,592.66	2.39	0.034 ± 0.014	—	—
1,631.11	0.93	0.012 ± 0.012	Ac-228	< MDA
1,692.58	1.7	0.010 ± 0.009	cal spec	< MDA
2,103.16	2.34	0.067 ± 0.016	cal spec	—
2,447.5	1.24	0.0112 ± 0.0094	Bi-214	< MDA
2,547.31	1.39	0.0037 ± 0.0036	indistinct	< MDA

a. Minimum detectable activity (calculated by the analysis program).

Some of the gamma rays in Table D-3 are likely associated with natural sources. Peaks with intensities significantly below the MDA values may actually be statistical anomalies that were erroneously identified as peaks by the spectrum analysis program. Also, the peaks with “cal spec” in the

source identification column correspond to peaks that occur in calibration spectra recorded using natural potassium, uranium, and thorium sources, so these peaks, though unidentified, are most likely linked to the naturally occurring radioelements.

Several gamma rays associated with the artificial radionuclide Am-241 were detected. Table D-4a displays details about the spectral peaks.

Table D-4a. Spectral data for Am-241 gamma rays.

Energy (keV)	Peak Intensity (c/s)	Comment	Gamma Ray Yield (γ per 100 D)	Calculated Concentration (pCi/g)
99.03	0.237 ± 0.093	—	0.0203	3,786 ± 1492
103.01	0.234 ± 0.097	—	0.0195	3,657 ± 1511
125.18	0.157 ± 0.122	< MDA	0.00408	8,784 ± 6815
662.51	0.100 ± 0.038	—	0.00036	25,197 ± 9574

Am-241 has many more gamma rays than listed in Table D-4a. Table D-4b displays the more intense Am-241 gamma rays and some quantities relevant to the detection of the gamma rays. These data will be used to explain why peaks at 123.0, 208.0, 335.4, and 722.0 keV are not observed in the spectrum.

Table D-4b. Am-241 Gamma ray data.

Energy (keV)	Gamma Ray Yield (γ per100 decays)	Detector Efficiency ((c/s) per(γ/s/g))	Inverse Casing Correction	Detection Index
99.0	0.0203	106.4	0.078	0.1687
103.0	0.0195	105.3	0.084	0.1731
123.0	0.001	101.4	0.115	0.0116
125.3	0.00408	100.5	0.118	0.0485
208.0	0.000791	100.0	0.220	0.0174
335.4	0.000496	97.3	0.318	0.0154
662.4	0.000364	89.6	0.436	0.0142
722.0	0.000196	89.3	0.450	0.0079

In Table D-4b, the gamma ray yields are expressed in gamma rays per 100 decays. The energy dependent efficiency values were calculated using the detector calibration function, and are expressed in (counts per second in a gamma ray peak) per (gamma rays per second per gram of sample); the *gamma rays per second per gram of sample* term is the gamma ray source intensity. Each *inverse casing correction* value is just the reciprocal of the casing correction for the particular energy. *Detection index* is the product of yield, efficiency, and inverse casing correction. The detection index value is related to the likelihood that a given gamma ray will produce a spectral peak.

One notes that the detection indexes for the 99.0 and 103.0-keV gamma rays are essentially equal, which is consistent with the fact that the corresponding peak intensities are nearly equal (Table D-4a). If the index for the 662.4-keV gamma ray, i.e., 0.0142, corresponds roughly to the lower limit of detection,

then the lower detection indexes for the 1,23.0 and 722.0-keV gamma rays explain why the corresponding peaks are absent.

Regarding the 208.0-keV gamma ray, there is a tiny bump in the spectrum close to this energy. This low energy region lies on an elevated part of the Compton continuum and the MDA is relatively high. If the *maximum peak error* in the *Peak Search* routine is increased from 120 percent to 130 percent, the spectrum analysis program will identify the bump as a peak at 208.6 keV with an intensity of (0.12 ± 0.14) c/s and an MDA of 0.23 c/s. Thus, the 208.0-keV gamma ray did put a minuscule signal in the spectrum, but the signal is too obscure to be identified as a peak unless the *maximum peak error* is increased. The poor quality of the peak that results from inflating the *maximum peak error* is indicated by the fact that the peak intensity is smaller than both the intensity uncertainty and the MDA.

An examination of the part of the spectrum around 335.4 keV indicates that the peak due to this Am-241 gamma ray is obscured by a peak due to the 338.3-keV gamma ray of Ac-228.

Am-241 concentrations have been calculated from the observed peak intensities and are displayed in Table D-4a. Although a concentration is shown for every Am-241 gamma ray peak, it is important to note that the calibration and casing correction functions are established down to an energy of about 180 keV, so the concentration values associated with the 99, 103, and 125-keV gamma rays are based on extrapolated calibration and casing correction functions. These values may be inaccurate, perhaps to a significant degree. Thus, the signals at 99, 103, and 125 keV are useful only to confirm the presence of Am-241. The most credible Am-241 concentration is the one based on the 662.5-keV gamma ray peak: $(25.2 \pm 9.6) \times 10^3$ pCi/g.

All of the spectra were analyzed as carefully as spectrum DB371000.CHN. However, the discussions for the other three spectra do not include details about detection index values, peak interferences, and effects of changing the spectrum analysis parameters.

D-1.1.2 Spectrum DB381000.CHN

Spectrum DB381000.CHN was acquired on December 1, 2003, from a depth of 14.5 ft. The dead time was 0.38 percent, and the live time was 2988.7 seconds.

Information about the natural gamma ray sources is displayed in Table D-5.

Table D-5. Natural gamma ray sources Spectrum DB381000.CHN

Gamma-Ray Source	Actual Energy (keV)	Measured Energy (keV)	Energy Residual (keV)	FWHM (keV)	Spectral Peak Intensity (c/s)	Calculated Concentration (pCi/g)
Ac/T	794.95	794.93	0.02	1.65	0.046 ± 0.031	—
Ac/T	911.21	911.15	0.06	2.02	0.379 ± 0.035	1.25 ± 0.11
Ac/T	968.97	968.93	0.04	1.98	0.252 ± 0.029	1.36 ± 0.15
AcBi/T	727.10	727.31	-0.21	1.88	0.108 ± 0.027	—
Bi/T	1,620.50	1,620.79	-0.29	0.96	0.018 ± 0.013	—
Bi/U	609.31	609.43	-0.12	1.86	0.542 ± 0.052	1.12 ± 0.11
Bi/U	768.36	768.10	0.26	1.89	0.068 ± 0.017	—

Table D-5. (continued).

Gamma-Ray Source	Actual Energy (keV)	Measured Energy (keV)	Energy Residual (keV)	FWHM (keV)	Spectral Peak Intensity (c/s)	Calculated Concentration (pCi/g)
Bi/U	934.10	933.80	0.30	1.71	0.034 ± 0.023	—
Bi/U	1,120.29	1,120.21	0.08	1.94	0.129 ± 0.028	—
Bi/U	1,238.11	1,237.97	0.14	1.72	0.077 ± 0.025	—
Bi/U	1,377.67	1,377.43	0.24	3.00	0.053 ± 0.018	—
Bi/U	1,509.23	1,508.92	0.31	2.21	0.030 ± 0.009	—
Bi/U	1,729.60	1,729.50	0.10	2.69	0.039 ± 0.013	—
Bi/U	1,764.49	1,764.57	-0.08	2.39	0.180 ± 0.019	0.98 ± 0.10
Bi/U	1,847.42	1,847.77	-0.35	2.08	0.032 ± 0.012	—
Bi/U	2,204.21	2,203.74	0.47	2.47	0.060 ± 0.014	1.01 ± 0.23
BiPb/U	351.49	352.05	-0.56	1.87	0.378 ± 0.066	—
K/K	1,460.80	1,460.71	0.09	2.26	2.136 ± 0.056	16.92 ± 0.45
Pb/T	238.63	238.93	-0.30	1.67	0.479 ± 0.050	—
Pb/U	295.21	295.53	-0.32	1.51	0.130 ± 0.065	—
Tl/T	2,614.53	2,614.49	0.04	2.71	0.570 ± 0.028	1.28 ± 0.06
TlAc/T	583.30	583.27	0.03	1.82	0.377 ± 0.046	—

Relative to spectrum DB371000.CHN, all of the concentrations are slightly lower, but all of the values are within normal ranges.

Data for peaks not identified by the spectrum analysis program appear in Table D-6.

Table D-6. Data for Unidentified peaks, Spectrum DB381000.CHN.

Energy (keV)	FWHM (keV)	Peak Intensity (c/s)	Proposed Source Identification	Comments
59.71	1.41	0.068 ± 0.077	—	< MDA
99.24	1.61	1.99 ± 0.21	Am-241	—
103.21	1.61	2.43 ± 0.21	Am-241	—
114.78	1.62	0.22 ± 0.21	—	—
125.59	1.62	1.71 ± 0.27	Am-241	—
146.78	1.53	0.30 ± 0.15	—	—
203.99	1.65	0.137 ± 0.051	Pu-239	< MDA
208.26	1.66	1.214 ± 0.064	Am-241	—
242.06	1.67	0.149 ± 0.044	—	—

Table D-6. (continued).

Energy (keV)	FWHM (keV)	Peak Intensity (c/s)	Proposed Source Identification	Comments
312.08	1.70	0.669 ± 0.070	Pa-233	(Np-237)
322.60	1.70	0.204 ± 0.056		—
332.65	1.71	0.291 ± 0.092	Pu-239	—
335.62	1.71	0.65 ± 0.11	Am-241	—
368.69	1.72	0.366 ± 0.075		—
375.61	1.73	0.400 ± 0.076	Pu-239	—
393.06	2.14	0.100 ± 0.062	Pu-239	< MDA
413.69	1.75	0.246 ± 0.069	Pu-239	—
510.90	2.39	0.374 ± 0.059	annihilation radiation	—
619.02	1.42	0.056 ± 0.032	—	—
653.32	1.84	0.043 ± 0.023	—	< MDA
662.29	1.85	0.640 ± 0.044	Am-241	—
722.05	1.87	0.226 ± 0.034	Am-241	—
755.27	1.89	0.034 ± 0.015	—	< MDA
758.48	1.89	0.032 ± 0.015	—	< MDA
964.76	1.98	0.071 ± 0.020	Ac-228	—
1,001.05	1.91	0.118 ± 0.028	Pa-234m	processed U
1,208.07	2.16	0.020 ± 0.023	Bi-214 ?	< MDA
1,401.49	2.29	0.018 ± 0.014	—	< MDA
1,501.40	2.21	0.021 ± 0.007	—	—
1,587.92	1.99	0.015 ± 0.017	Ac-228	< MDA
1,963.86	0.74	0.008 ± 0.008	FWHM too small	< MDA
1,992.76	1.27	0.006 ± 0.007	—	< MDA
2,071.47	1.00	0.006 ± 0.007	FWHM too small	< MDA
2,103.47	3.54	0.055 ± 0.014	cal spec	—
2,447.39	2.51	0.015 ± 0.010	Bi-214 ?	< MDA
2,466.43	1.04	0.004 ± 0.005	FWHM too small	< MDA
2,802.94	2.78	0.004 ± 0.004	—	—

Spectrum DB381000.CHN has peaks indicative of Am-241, Pu-239, Np-237, and processed uranium. Spectral peak data and calculated concentrations are shown in Table D-7.

Table D-7. Data for artificial gamma ray sources.

Energy (keV)	Peak Intensity (c/s)	Source	Comment	Gamma-Ray Yield (γ per 100 D)	Calculated Concentration (pCi/g)
99.24	1.99 ± 0.20	Am-241	—	0.0203	31,698 ± 3,264
103.21	2.43 ± 0.21	Am-241	—	0.0195	37,838 ± 3,312
125.59	1.71 ± 0.27	Am-241	—	0.00408	95,680 ± 15,265
208.26	1.214 ± 0.064	Am-241	—	0.00079	21,3369 ± 11,166
335.62	0.65 ± 0.11	Am-241	—	0.0005	13,9248 ± 23,093
662.29	0.640 ± 0.044	Am-241	—	0.00036	161,915 ± 11,030
722.05	0.226 ± 0.034	Am-241	—	0.0002	101,644 ± 15,091
312.08	0.669 ± 0.070	Pa-233	(Np-237)	38.6	1.92 ± 0.20
203.99	0.137 ± 0.051	Pu-239	<MDA	0.00057	33,898 ± 12,518
332.65	0.291 ± 0.092	Pu-239	—	0.00049	64,076 ± 20,341
375.61	0.400 ± 0.076	Pu-239	—	0.00155	26,683 ± 5,104
393.06	0.100 ± 0.062	Pu-239	<MDA	0.00035	29,236 ± 18,054
413.69	0.246 ± 0.069	Pu-239	—	0.00147	16,829 ± 4,703
1,001.05	0.118 ± 0.028	Pa-234m	processed U	0.837	12.3 ± 2.9

Peaks corresponding to gamma ray energies below about 180 keV should not be used for concentration calculations because such energies are below the range of the calibration function and the casing correction function. In addition, when high-Z elements (Am, Pu, U) are present in elevated concentrations, the low energy gamma rays are attenuated within the formation by the Z effect. This source self attenuation reduces the low energy gamma ray fluxes, so concentrations based on the low energy gamma ray peaks would be anomalously low.

The Am-241 concentration calculated from the 662-keV gamma ray peak intensity is $(162 \pm 11) \times 10^3$ pCi/g.

Some other features of the 662-keV gamma ray peak may be noteworthy. The peak has a normal FWHM (1.85 keV, Table D-6). The absence of peak broadening indicates that there is probably no Cs-137 gamma ray (661.6 keV) signal in the peak. Also, the calculated concentration does not significantly exceed the concentrations based on the 208 and 335-keV gamma ray peaks, so the 662-keV peak intensity is probably not inflated by a contribution from the 661.6-keV gamma ray of Cs-137. In other words, Cs-137 is likely not present.

No explanation can be offered for the apparent low Am-241 concentration based on the 722-keV gamma ray peak.

The source of the 312-keV gamma ray is identified as Pa-233, which, because of its short half life (27 days), indicates the presence of the long-lived parent, Np-237. The source identification is necessarily based on just one gamma ray. The Pa-233 gamma ray with the next highest yield has energy 300.3 keV. A peak for this gamma ray is probably absent because the yield (6.6 gammas per 100 decays) is substantially smaller than the yield for the 312.2-keV gamma ray (38.6 gammas per 100 decays).

Pu-239 is identified with confidence because of the presence of peaks associated with five Pu-239 gamma rays. Calculated concentrations fall between about 17×10^3 and 64×10^3 pCi/g. The highest value may have been inflated by peak interferences, caused, for example, by the 335-keV gamma ray of Am-241. The 375.1-keV gamma ray peak is least likely to have an interference, and the concentration inferred from the peak intensity is $(26.7 \pm 5.1) \times 10^3$ pCi/g. This value is in reasonable agreement with the concentration inferred from the 393.1-keV gamma ray peak intensity, which is another peak that is unlikely to have an interference. The reason for the low concentration based on the 413.7-keV gamma ray peak is unknown.

The 1001-keV gamma ray signal is interpreted as a Pa-234m indicator, even though a confirming peak at 766.6 keV is not observed. The absence of a peak for the 766.6-keV gamma ray is explained by the fact that the intensity of the 1001-keV gamma ray peak is quite low, but the yield for the 1001-keV gamma ray is more than two times the yield for the 766.6-keV gamma ray.

Because Pa-234m and its parent, Th-234, have short half lives (1.2 min and 24 days), the presence of U-238, the long-lived parent of Th-234, is inferred. Because of the long half life of U-238 and the short half lives of Th-234 and Pa-234m, both Th-234 and Pa-234m can be assumed to be in decay equilibrium with U-238, and (in terms of decay rate per unit mass) all three nuclides must have the same concentration, 12.3 ± 2.9 pCi/g. This concentration is substantially higher than the normal uranium background, which is represented by the concentrations based on Bi-214 in Table D-5. The fact that the U-238 concentration based on the Pa-234m gamma ray is more than 10 times higher than the natural uranium background indicates that the U-238 has been processed. In processed uranium, U-238 decay products below Ra-226 (e.g., Bi-214) are present in much smaller concentrations than would be the case if all of the nuclides in the uranium decay chain were in decay equilibrium.

D-1.2 Borehole P6-PU-2

This borehole is also located in the INEEL site SDA Area 5. Two spectra from the borehole are named DB391000.CHN and DB391001.CHN. Both spectra were recorded on December 1, 2003.

D-1.2.1 Spectrum DB391000.CHN

Spectrum DB391000.CHN was acquired from a depth of 16.0 ft. The dead time was 0.34 percent, and the live time was 2989.8 seconds.

Table D-8 displays information about the natural gamma ray sources.

Table D-8. Natural gamma ray sources, Spectrum DB391000.CHN.

Gamma-Ray Source	Actual Energy (keV)	Measured Energy (keV)	Energy Residual (keV)	FWHM (keV)	Spectral Peak Intensity (c/s)	Calculated Concentration (pCi/g)
Ac/T	338.32	338.74	-0.42	1.90	0.069 ± 0.057	—
Ac/T	794.95	794.75	0.20	1.93	0.060 ± 0.027	—
Ac/T	911.21	910.98	0.23	1.87	0.483 ± 0.040	1.60 ± 0.13
Ac/T	968.97	968.75	0.22	1.98	0.283 ± 0.023	1.53 ± 0.13
AcBi/T	727.10	727.10	0.00	1.74	0.106 ± 0.037	—

Table D-8. (continued).

Gamma-Ray Source	Actual Energy (keV)	Measured Energy (keV)	Energy Residual (keV)	FWHM (keV)	Spectral Peak Intensity (c/s)	Calculated Concentration (pCi/g)
Bi/T	1,620.50	1,620.55	-0.05	2.32	0.014 ± 0.008	—
Bi/U	609.31	609.42	-0.11	1.76	0.500 ± 0.045	1.03 ± 0.09
Bi/U	768.36	768.43	-0.07	1.88	0.047 ± 0.017	—
Bi/U	934.10	933.70	0.40	1.84	0.059 ± 0.029	—
Bi/U	1,120.29	1,119.96	0.33	2.17	0.210 ± 0.033	—
Bi/U	1,238.11	1,237.89	0.22	1.70	0.102 ± 0.028	—
Bi/U	1,377.67	1,377.48	0.19	2.19	0.067 ± 0.016	—
Bi/U	1,407.98	1,407.97	0.01	1.95	0.018 ± 0.016	—
Bi/U	1,729.60	1,729.93	-0.33	2.24	0.044 ± 0.013	—
Bi/U	1,764.49	1,764.90	-0.41	2.37	0.227 ± 0.020	1.23 ± 0.11
Bi/U	1,847.42	1,847.74	-0.32	2.71	0.022 ± 0.010	—
Bi/U	2,204.21	2,204.08	0.13	2.00	0.059 ± 0.014	0.99 ± 0.23
BiPb/U	351.49	352.36	-0.87	1.46	0.428 ± 0.069	—
K/K	1,460.80	1,460.76	0.04	2.18	2.678 ± 0.063	21.21 ± 0.50
Pb/T	238.63	239.54	-0.91	1.70	0.71 ± 0.12	—
Pb/U	295.21	295.88	-0.67	1.72	0.138 ± 0.076	—
Tl/T	860.56	860.44	0.12	1.86	0.041 ± 0.031	—
Tl/T	2,614.53	2,613.98	0.55	2.90	0.687 ± 0.031	1.54 ± 0.07
TlAc/T	583.30	583.29	0.01	1.82	0.491 ± 0.045	—

The concentrations are slightly higher in general than those presented in Table D-5 for spectrum DB381000.CHN, but come close to matching the concentrations in Table D-2 for spectrum DB371000.CHN.

Data for peaks not identified by the spectrum analysis program appear in Table D-9.

Table D-9. Data for unidentified peaks, Spectrum DB391000.CHN.

Energy (keV)	FWHM (keV)	Peak Intensity (c/s)	Proposed Source Identification	Comments
409.92	2.13	0.054 ± 0.055	—	< MDA
463.52	1.87	0.075 ± 0.054	Sb-125 ?	< MDA
510.96	2.36	0.379 ± 0.062	annihilation radiation	—
772.46	1.88	0.042 ± 0.016	—	< MDA

Table D-9. (continued).

Energy (keV)	FWHM (keV)	Peak Intensity (c/s)	Proposed Source Identification	Comments
785.79	2.79	0.039 ± 0.033	—	< MDA
805.85	—	0.024 ± 0.025	—	< MDA
950.98	0.9	0.027 ± 0.027	—	< MDA
964.55	1.98	0.098 ± 0.017	Eu-152 ?	—
1,152.89	1.34	0.027 ± 0.025	—	< MDA
1,282.18	2.15	0.021 ± 0.014	—	< MDA
1,373.12	2.19	0.014 ± 0.012	—	< MDA
1,543.12	1.05	0.010 ± 0.011	—	< MDA
1,564.23	0.84	0.010 ± 0.010	—	< MDA
1,582.41	2.3	0.014 ± 0.007	—	< MDA
1,588.3	2.3	0.064 ± 0.011	Ac-228	—
1,592.91	2.31	0.045 ± 0.010	Tl-208 ?	—
1,630.83	2.33	0.024 ± 0.008	Ac-228	—
1,661.33	1.44	0.010 ± 0.010	—	< MDA
1,683.54	1.59	0.019 ± 0.011	—	—
2,104.02	2.9	0.076 ± 0.014	—	—
2,118.27	1.58	0.016 ± 0.010	—	—
2,152.67	1.01	0.011 ± 0.008	—	< MDA
2,446.91	2.11	0.013 ± 0.009	Bi-214	< MDA
2,554.47	1.99	0.003 ± 0.003	—	< MDA

Spectrum DB391000.CHN has only two peaks for gamma rays that could be associated with artificial radionuclides: 463.5 keV (Sb-125) and 964.5 (Eu-152). However, these artificial sources are probably not present.

The most intense Sb-125 gamma ray has energy 427.9 keV and yield 29.6 gammas per 100 decays. The next most intense gamma ray has energy 600.6 keV and yield 17.9 gammas per 100 decays. The 463.4-keV gamma ray of Sb-125 is the fourth most intense, with a yield of 10.5 gammas per 100 decays. Since the 427.9-keV gamma ray has a yield about 3 times higher than the yield of the 463.4-keV gamma ray, but no peak corresponding to the 427.9-keV gamma ray is evident, Sb-125 must not be present. The 463-keV peak may be associated with the Ac-228 gamma ray of energy 463.0 keV, or the peak may be spurious (the intensity is below the MDA).

Similarly, the 964.1-keV gamma ray of Eu-152 is the second most intense, with a yield of 14.4 gammas per 100 decays. The most intense Eu-152 gamma ray has energy 1408.0 keV and yield 20.8 gammas per 100 decays. There is no peak corresponding to 1408 keV; therefore, Eu-152 must be absent. The 964-keV peak may be associated with the Ac-228 gamma ray of energy 964.8 keV.

Spectrum DB391000.CHN apparently contains no signals due to artificial radionuclides.

D-1.2.2 Spectrum DB391001.CHN

Spectrum DB391001.CHN was acquired from a depth of 15.0 ft. The dead time was 0.54 percent, and the live time was 2,983.7 seconds.

Table D-10 displays information about the natural gamma ray sources.

Table D-10. Natural Gamma-Ray Sources, Spectrum DB391001.CHN.

Gamma-Ray Source	Actual Energy (keV)	Measured Energy (keV)	Energy Residual (keV)	FWHM (keV)	Spectral Peak Intensity (c/s)	Calculated Concentration (pCi/g)
Ac/T	794.95	794.74	0.21	1.93	0.060 ± 0.017	—
Ac/T	911.21	910.98	0.23	1.99	0.358 ± 0.033	1.18 ± 0.11
Ac/T	968.97	968.74	0.23	2.02	0.233 ± 0.023	1.26 ± 0.12
AcBi/T	727.10	727.51	-0.41	1.89	0.096 ± 0.020	—
Bi/U	609.31	609.40	-0.09	1.83	0.529 ± 0.034	1.09 ± 0.07
Bi/U	768.36	767.89	0.47	1.91	0.068 ± 0.024	—
Bi/U	934.10	934.01	0.09	2.00	0.056 ± 0.014	—
Bi/U	1,120.29	1,120.07	0.22	2.10	0.191 ± 0.014	—
Bi/U	1,238.11	1,237.53	0.58	2.16	0.076 ± 0.031	—
Bi/U	1,377.67	1,377.57	0.10	2.23	0.050 ± 0.017	—
Bi/U	1,509.23	1,509.34	-0.11	2.30	0.026 ± 0.010	—
Bi/U	1,729.60	1,730.16	-0.56	2.41	0.036 ± 0.013	—
Bi/U	1,764.49	1,764.89	-0.40	2.43	0.189 ± 0.024	1.03 ± 0.13
Bi/U	1,847.42	1,847.96	-0.54	2.47	0.022 ± 0.015	—
Bi/U	2,204.21	2,204.13	0.08	2.65	0.063 ± 0.012	1.05 ± 0.20
BiPb/U	351.49	352.48	-0.99	1.70	0.427 ± 0.073	—
K/K	1,460.80	1,460.80	0.00	2.27	2.086 ± 0.086	16.52 ± 0.68
Pb/T	238.63	239.54	-0.91	1.64	0.395 ± 0.086	—
Tl/T	860.56	860.60	-0.04	1.96	0.083 ± 0.024	—
Tl/T	2,614.53	2,614.07	0.46	2.86	0.694 ± 0.031	1.55 ± 0.07
TlAc/T	583.30	583.39	-0.09	1.82	0.389 ± 0.032	—

The concentrations of the natural gamma ray sources agree with the concentrations inferred from spectrum DB381000.CHN (Table D-5). In general, these concentrations are slightly lower than the concentrations deduced from spectra DB371000.CHN (Table D-2) and DB391000.CHN (Table D-8).

Table D-11 displays data for peaks not identified by the spectrum analysis program.

Table D-11. Data for unidentified peaks, Spectrum DB391001.CHN.

Energy (keV)	FWHM (keV)	Peak Intensity (c/s)	Proposed Source Identification	Comments
61.33	1.55	0.072 ± 0.054	—	< MDA
204.73	1.63	0.151 ± 0.061		< MDA
208.98	1.63	0.334 ± 0.062	Am-241	—
312.44	1.68	0.193 ± 0.044	—	—
333.23	1.69	0.207 ± 0.073	Pu-239	—
345.42	1.70	0.236 ± 0.070	—	—
375.54	1.71	0.630 ± 0.075	Pu-239	—
382.86	1.72	0.079 ± 0.055	—	< MDA
393.31	1.72	0.236 ± 0.035	Pu-239	—
409.99	1.73	0.065 ± 0.029	—	< MDA
414.00	1.73	0.696 ± 0.042	Pu-239	—
451.76	1.75	0.098 ± 0.019	—	—
463.61	1.76	0.062 ± 0.026	—	< MDA
511.02	2.70	0.556 ± 0.071	annihilation radiation	—
662.47	1.86	0.237 ± 0.026	Am-241	—
721.95	1.89	0.134 ± 0.022	Am-241	—
964.44	2.02	0.060 ± 0.017	—	—
1,000.88	2.03	0.079 ± 0.022	Pa-234m	—
1,588.3	2.34	0.024 ± 0.011	—	< MDA
1,592.87	2.34	0.031 ± 0.011	—	—
1,630.89	2.36	0.023 ± 0.009	—	—
1,661.73	2.37	0.013 ± 0.008	—	< MDA
1,712.56	2.40	0.012 ± 0.007	—	< MDA
2,103.77	2.60	0.080 ± 0.012	—	—
2,223.34	2.66	0.086 ± 0.013	H capture	—
2,447.32	2.78	0.022 ± 0.007	Bi-214	—
2,751.52	2.93	0.003 ± 0.024	—	< MDA

Spectrum DB391001.CHN has peaks corresponding to gamma rays from Am-241 and Pu-239. The 1001-keV signal is assigned to Pa-234m, though a confirming peak for the 766.6-keV gamma ray is not observed.

Table D-12 shows the calculated Am-241, Pu-239, and Pa-234m concentrations.

Table D-12. Data for artificial gamma ray sources.

Energy (keV)	Peak Intensity (c/s)	Source	Comment	Gamma-Ray Yield (γ per 100 D)	Calculated Concentration (pCi/g)
208.98	0.334 ± 0.062	Am-241	—	0.00079	5,8594 ± 1,0923
662.47	0.237 ± 0.026	Am-241	—	0.00036	5,9944 ± 6,569
721.95	0.134 ± 0.022	Am-241	—	0.0002	6,0528 ± 9,804
333.23	0.207 ± 0.073	Pu-239	—	0.00049	4,5693 ± 1,6062
375.54	0.630 ± 0.075	Pu-239	—	0.00155	4,2077 ± 4,987
393.31	0.236 ± 0.035	Pu-239	—	0.00035	6,8747 ± 1,0142
414.00	0.696 ± 0.042	Pu-239	—	0.00147	4,7538 ± 2,868
1,000.88	0.079 ± 0.022	Pa-234m	processed U	0.837	8.2 ± 2.3

None of the peak intensities in Table D-12 fall below MDA values. The Am-241 concentration calculated from the 662-keV gamma ray peak intensity is $(59.9 \pm 6.6) \times 10^3$ pCi/g; concentrations calculated from other gamma ray data are in reasonable agreement with this.

For Pu-239, the 375.5-keV gamma ray peak is least likely to have interferences; the calculated concentration is $(42.1 \pm 5.0) \times 10^3$ pCi/g. This concentration agrees with concentrations calculated from the 333 and 414-keV gamma ray data. For unknown reasons, the concentration inferred from the 393-keV gamma ray peak is higher than the other concentrations.

The peak at 1,000.9 keV suggests Pa-234m, with a concentration of 8.2 ± 2.3 pCi/g. The discussion of Pa-234m in relation to spectrum DB381000.CHN applies here; thus, processed uranium is present, with a U-238 concentration of about 8.2 ± 2.3 pCi/g.

Spectrum DB391001.CHN has a peak that is apparently due to the 2223.3-keV hydrogen neutron capture gamma ray. The concentrations of alpha emitters must be so high that alpha-neutron reactions with oxygen yield neutrons in numbers sufficient to produce detectable gamma ray fluxes when captured by hydrogen (in water).

The spectrum was examined for gamma ray peaks associated with capture gamma rays from tungsten, germanium, aluminum, iron, chlorine, silicon, and calcium, but no eligible peaks were found. The intensity of the 351-keV “uranium” gamma ray peak (Table D-10) is comparable to the peak intensities for the same gamma ray in the other spectra, indicating that there is no interference from the 352.2-keV neutron capture gamma ray of iron.

Passive Gamma-Ray Spectra from INEEL Boreholes P6-PU-1 and P6-PU-2

February 11, 2004

D-2. Analysis Method

Five passive gamma ray spectra from each borehole were analyzed, using the method described in the attachment "INEEL Passive Gamma-Ray Spectrum DB501000.CHN." This paper presents the results of the analyses.

Each spectrum was energy-calibrated, then analyzed with a spectrum analysis program by two methods. The important analysis settings common to both methods were as follows.

- ROI Properties
  - Background curve: third degree
  - Background end points: five on each side of the peak
- Peaksearch
  - Maximum error of 100 percent.

The first method utilized the *peaksearch* and *identify* algorithms in the analysis program. The second method utilized the *peaksearch*, *multifit*, and *identify* algorithms. *Peaksearch* finds all of the features in a spectrum that meet the analysis criteria for a peak. *Multifit* fits Gaussian functions to peaks and discards peaks with parameters, such as full widths at half maxima (FWHM), that do not meet resolution and other criteria. For the second method, the spectra were individually resolution-calibrated. The two methods were used because of the extraordinarily long (8-hour) count times. Gain shift could have caused spectral peak broadening, and the analysis program could have resolved broad peaks into "multiplets," or superimposed peaks. By comparing results of the two analyses, false multiplets could be identified.

The *Identify* algorithm in the analysis program utilized a source identification data base (library) containing the most intense gamma rays for Am-241, Co-60, Cs-134, Cs-137, Eu-152, Eu-154, Np-237, Pu-239, Ru-106, Sb-125, Sb-126, and Tc-99. Nuclides and gamma rays in this library are displayed in Table D-13.

Table D-13. Source Data.

Source Nuclide	Energy (keV)
Am-241	103.0
Am-241	125.3
Co-60	1,173.2
Co-60	1,332.5
Cs-134	795.8
Cs-137	661.6

Table D-13. (continued).

Source Nuclide	Energy (keV)
Eu-152	121.8
Eu-152	1,408.0
Eu-154	1,004.7
Eu-154	1,274.4
Eu-155	105.3
K-40	1,460.8
Np-237	312.2
Np-237	300.3
Pu-239	129.3
Pu-239	375.1
Ru-106	621.9
Sb-125	176.3
Sb-125	463.4
Sb-125	600.6
Sb-126	695.0
Tc-99	89.5
Th-232	583.2
Th-232	911.2
Th-232	2,614.5
U-235	185.7
U-235	163.3
U-238	351.9
U-238	609.3
U-238	1,764.5
U-238p	766.4
U-238p	1,001.0

The analysis program identified any man-made sources in Table D-13 that had concentrations high enough to produce detectable gamma ray peaks.

Only a few of the gamma rays due to the natural sources (potassium, uranium, and thorium) appear in Table D-13. Many of the gamma rays from natural sources were not included because a number of the energies nearly coincide with energies of gamma rays from the man-made sources. Thus, for example, the 1408.0-keV gamma ray of Bi-214 (uranium series) was left out to prevent the analysis program from making a Bi-214 identification then letting the 1408.0-keV gamma ray of Eu-152 go undetected.

D-2.1 Analysis Results for Borehole P6-PU-1

Five spectra were acquired from this borehole. The names of the spectra and the associated depths are as follows.

Spectrum Name	Depth
DB551000	19.92 ft
DB561000	16.0 ft
DB571000	15.5 ft
DB581000	15.0 ft
DB591000	14.5 ft

D-2.1.1 Spectrum DB551000

Almost all of the peaks are correlated to gamma rays from the natural sources. The analysis program associated the peak at 794.6 keV with Cs-134, but the energy residual was large and the peak is more likely due to the 794.9-keV gamma ray of Ac-228. Likewise, the analysis program associated the peak at 1408.0 keV with Eu-152, but since peaks due to Eu-152 gamma rays at 121.8 keV and 964.1 keV were absent, the peak is probably due to the 1408.0-keV gamma ray of Bi-214.

The source for the 1537.9-keV gamma ray is unidentified. The peak is not classified as spurious because peaks corresponding to nearly the same energy were also observed in spectra DB561000, DB571000, and DB581000.

No peaks were unambiguously associated with gamma rays from man-made sources.

Table D-14. Data for Spectrum DB551000.

Library ID	Library Energy (keV)	Measured Energy (keV)	Energy Residual (keV)	Peak Intensity (c/s)	Intensity Uncert. (c/s)	MDA[a] (c/s)	Analyst Comments
		39.38		0.660	0.364	0.018	probably a spurious low energy peak
		40.50		1.661	0.021	0.023	probably a spurious low energy peak
		44.63		1.053	0.021	0.028	probably a spurious low energy peak
		46.12		0.353	0.377	0.033	probably a spurious low energy peak
		51.62		0.337	0.023	0.036	probably not Pu-239 at 51.6 keV; no confirming gammas
		158.73		0.039	0.030	0.049	below MDA, probably spurious
U235	185.72	186.60	-0.88	0.057	0.014	0.047	Ra-226 (U series), 186.1 keV; U-235, 185.7 keV
		209.50		0.036	0.013	0.044	below MDA, probably spurious
		239.10		0.502	0.072	0.042	Pb-212 (Th series), 238.6 keV
		270.57		0.042	0.011	0.035	Ac-228 (Th series), 270.2 keV

Table D-14. (continued).

Library ID	Library Energy (keV)	Measured Energy (keV)	Energy Residual (keV)	Peak Intensity (c/s)	Intensity Uncert. (c/s)	MDA[a] (c/s)	Analyst Comments
		277.76		0.027	0.010	0.034	Tl-208 (Th series), 277.4 keV
		295.51		0.167	0.036	0.035	Pb-212 (Th series), 295.2 keV
		328.34		0.033	0.009	0.031	Ac-228 (Th series), 328.0 keV; Bi-212 (Th series), 328.0 keV
		338.52		0.155	0.010	0.030	Ac-228 (Th series), 338.3 keV
U238	351.92	352.09	-0.17	0.420	0.016	0.031	Pb-214 (U series), 351.9 keV
		389.03		0.020	0.008	0.025	below MDA, probably spurious
		403.35		0.012	0.007	0.024	below MDA, probably spurious
		409.38		0.025	0.007	0.025	Ac-228 (Th series), 409.5 keV
		462.86		0.055	0.009	0.023	Ac-228 (Th series), 463.0 keV
		510.70		0.306	0.025	0.026	annihilation radiation, 511.0 keV
		572.00		0.019	0.010	0.019	near MDA, probably spurious
Th232	583.19	583.07	0.12	0.447	0.017	0.021	Tl-208 (Th series), 583.2 keV
U238	609.31	609.15	0.16	0.573	0.015	0.020	Bi-214 (U series), 609.3 keV
		665.12		0.023	0.005	0.017	Bi-214 (U series) 665.4 keV
		727.01		0.105	0.009	0.017	Bi-212 (Th series), 727.3 keV
		755.10		0.011	0.006	0.015	Ac-228 (Th series), 755.3 keV
U238p	766.36	768.05	-1.69	0.056	0.013	0.016	Bi-214 (U series) 768.3 keV
		772.20		0.015	0.008	0.013	Ac-228 (Th series), 772.3 keV
		785.38		0.016	0.010	0.015	Pb-214 (U series), 785.9 keV; Bi-212 (Th series) 785.4 keV
Cs134	795.85	794.62	1.23	0.062	0.011	0.015	Ac-228 (Th series), 794.9 keV
		835.59		0.018	0.007	0.014	Ac-228 (Th series), 835.7 keV
		839.43		0.017	0.007	0.013	Ac-228 (Th series), 840.4 keV
		860.23		0.068	0.005	0.015	Tl-208 (Th series), 860.6 keV
		904.37		0.012	0.005	0.013	Ac-228 (Th series), 904.2 keV
Th232	911.21	910.87	0.34	0.419	0.011	0.014	Ac-228 (Th series), 911.2 keV
		933.69		0.043	0.005	0.014	Bi-214 (U series), 934.1 keV
		949.63		0.017	0.006	0.013	K-40 gamma escape peak (949.8 keV)
		964.36		0.083	0.007	0.013	Bi-214 (U series) 964.1 keV

Table D-14. (continued).

Library ID	Library Energy (keV)	Measured Energy (keV)	Energy Residual (keV)	Peak Intensity (c/s)	Intensity Uncert. (c/s)	MDA[a] (c/s)	Analyst Comments
		968.58		0.256	0.010	0.013	Ac-228 (Th series), 969.0 keV
U238p	1,001.03	1,000.92	0.11	0.015	0.004	0.012	Pa-234m (U series), 1001.0 keV
		1,078.50		0.009	0.005	0.011	Bi-212 (Th series), 1078.6 keV
		1,119.89		0.199	0.007	0.013	Bi-214 (U series), 1120.3 keV
		1,154.93		0.021	0.004	0.012	Bi-214 (U series), 1155.2 keV
		1,237.92		0.082	0.006	0.013	Bi-214 (U series), 1238.1 keV
		1,280.91		0.019	0.004	0.011	Bi-214 (U series), 1281.0 keV
		1,326.47		0.004	0.003	0.008	below MDA, probably spurious
		1,377.52		0.054	0.005	0.009	Bi-214 (U series), 1377.7 keV
		1,385.28		0.012	0.004	0.008	Bi-214 (U series), 1385.3 keV
		1,401.53		0.011	0.003	0.009	Bi-214 (U series), 1401.5 keV
Eu152	1,408.01	1,408.00	0.01	0.032	0.003	0.009	Bi-214 (U series), 1408.0 keV no confirming Eu-152 gamma)
K-40	1,460.83	1,460.83	0.00	2.111	0.057	0.009	K-40, 1460.8 keV
		1,495.87		0.014	0.003	0.006	Ac-228 (Th series), 1495.9 keV
		1,509.36		0.027	0.004	0.007	Bi-214 (U series), 1509.2 keV
		1,537.86		0.021	0.192	0.004	Unknown. Also observed in DB561000, DB571000, DB581000, DB531000
		1,557.17		0.005	0.002	0.006	Ac-228 (Th series), 1557.1 keV
		1,581.86		0.013	0.004	0.005	Ac-228 (Th series), 1580.5 keV
		1,588.38		0.050	0.006	0.006	Ac-228 (Th series), 1588.2 keV
		1,592.88		0.036	0.005	0.006	2614.5 keV (Tl-208) double escape peak at 1592.5 keV
		1,599.21		0.003	0.003	0.005	below MDA; Bi-214 (U series), 1599.3 keV
		1,620.94		0.022	0.004	0.006	Bi-212 (Th series), 1620.5 keV
		1,630.99		0.026	0.003	0.006	Ac-228 (Th series), 1630.6 keV
		1,638.75		0.011	0.002	0.005	Ac-228 (Th series), 1638.3 keV
		1,661.67		0.014	0.002	0.006	Bi-214 (U series), 1661.3 keV
		1,693.23		0.004	0.002	0.005	below MDA, probably spurious

Table D-14. (continued).

Library ID	Library Energy (keV)	Measured Energy (keV)	Energy Residual (keV)	Peak Intensity (c/s)	Intensity Uncert. (c/s)	MDA[a] (c/s)	Analyst Comments
		1,708.76		0.003	0.002	0.005	below MDA, probably spurious
		1,730.12		0.038	0.004	0.005	Bi-214 (U series), 1729.6 keV
U238	1,764.49	1,765.02	-0.53	0.220	0.010	0.006	Bi-214 (U series), 1764.5 keV
		1,838.87		0.003	0.002	0.005	Bi-214 (U series), 1838.4 keV
		1,848.20		0.027	0.003	0.005	Bi-214 (U series), 1847.4 keV
		2,103.78		0.061	0.007	0.005	2614.5 keV (Tl-208) escape peak at 2103.5 keV
		2,118.99		0.013	0.002	0.005	Bi-214 (U series), 2118.5 keV
		2,204.38		0.069	0.005	0.005	Bi-214 (U series), 2204.2 keV
		2,294.13		0.004	0.002	0.005	Bi-214 (U series), 2293.4 keV
		2,347.18		0.003	0.002	0.005	below MDA, probably spurious
		2,447.58		0.022	0.002	0.004	Bi-214 (U series), 2447.9 keV
Th232	2,614.53	2,614.34	0.19	0.541	0.029	0.002	Tl-208 (Th series), 2614.5 keV

a. MDA = minimu detectable activity.

D-2.1.2 Spectrum DB561000

Most of the peaks are associated with gamma rays from the natural background. The 794.6-keV and 1408.0-keV gamma rays probably originate in natural background and not Cs-134 or Eu-152.

There are low intensity peaks corresponding to 99.7, 103.6, and 126.0 keV, which apparently indicate Am-241, and a feeble peak (intensity below the MDA) corresponding to 376.0 keV may be indicative of Pu-239. The case for Pu-239 is quite weak; the case for Am-241 is slightly stronger.

There is a peak due to a 1454.5-keV gamma ray of unknown origin. In DB561000 the intensity of the 1454.5-keV peak is below the MDA, but the peak is not classified as spurious because a peak corresponding to 1454.3 keV exists in spectrum DB591000.

Table D-15. Data for Spectrum DB561000

Library ID	Library Energy (keV)	Measured Energy (keV)	Energy Residual (keV)	Peak Intensity (c/s)	Intensity Uncert. (c/s)	MDA (c/s)	Analyst Comments
		99.68		0.065	0.016	0.044	Am-241 (99.0 keV)
Am241	103.00	103.63	-0.63	0.067	0.017	0.048	Am-241 (103.0 keV)
Am241	125.30	126.03	-0.73	0.077	0.028	0.053	Am-241 (125.3 keV)
		131.31		0.046	0.028	0.050	below MDA, probably spurious
U235	185.72	186.22	-0.50	0.066	0.021	0.050	Ra-226 (U series), 186.1 keV;

Table D-15. (continued).

Library ID	Library Energy (keV)	Measured Energy (keV)	Energy Residual (keV)	Peak Intensity (c/s)	Intensity Uncert. (c/s)	MDA (c/s)	Analyst Comments
							U-235, 185.7 keV
		208.85		0.061	0.014	0.047	Ac-228 (Th series), 209.2 keV; Am-241, 208.0 keV
		238.97		0.525	0.041	0.045	Pb-212 (Th series), 238.6 keV
		270.62		0.046	0.011	0.038	Ac-228 (Th series), 270.2 keV
		295.39		0.186	0.023	0.037	Pb-212 (Th series), 295.2 keV
		338.38		0.142	0.022	0.033	Ac-228 (Th series), 338.3 keV
U238	351.92	351.96	-0.04	0.393	0.018	0.031	Pb-214 (U series), 351.9 keV
		375.96		0.017	0.008	0.026	below MDA, may be spurious or may be Pu-239 at 375.1 keV
		462.83		0.068	0.008	0.024	Ac-228 (Th series), 463.0 keV
		510.65		0.317	0.030	0.027	annihilation radiation, 511.0 keV
Th232	583.19	582.97	0.22	0.488	0.020	0.021	Tl-208 (Th series), 583.2 keV
U238	609.31	609.09	0.22	0.550	0.022	0.020	Bi-214 (U series), 609.3 keV
		727.03		0.108	0.011	0.018	Bi-212 (Th series), 727.3 keV
		754.76		0.013	0.005	0.015	Ac-228 (Th series), 755.3 keV
		763.25		0.016	0.009	0.016	below MDA, may be Tl-208 (Th series), 763.1 keV
		768.00		0.063	0.010	0.017	Bi-214 (U series) 768.3 keV
		772.06		0.028	0.010	0.016	Ac-228 (Th series), 772.3 keV
		785.30		0.030	0.009	0.016	Pb-214 (U series), 785.9 keV; Bi-212 (Th series) 785.4 keV
Cs134	795.85	794.64	1.21	0.074	0.010	0.016	Ac-228 (Th series), 794.9 keV
		829.93		0.013	0.005	0.015	Ac-228 (Th series), 830.5 keV
		835.31		0.037	0.005	0.015	Ac-228 (Th series), 835.7 keV
		839.87		0.022	0.005	0.015	Ac-228 (Th series), 840.4 keV
		860.26		0.078	0.008	0.016	Tl-208 (Th series), 860.6 keV
		870.33		0.010	0.006	0.014	below MDA, probably spurious
		873.63		0.011	0.008	0.013	below MDA, probably spurious
		903.46		0.014	0.011	0.017	below MDA,

Table D-15. (continued).

Library ID	Library Energy (keV)	Measured Energy (keV)	Energy Residual (keV)	Peak Intensity (c/s)	Intensity Uncert. (c/s)	MDA (c/s)	Analyst Comments
							may be Ac-228 (Th series), 904.2 keV
Th232	911.21	910.84	0.37	0.454	0.022	0.016	Ac-228 (Th series), 911.2 keV
		933.71		0.035	0.009	0.014	Bi-214 (U series), 934.1 keV
		964.39		0.088	0.012	0.015	Bi-214 (U series) 964.1 keV
		968.58		0.289	0.016	0.015	Ac-228 (Th series), 969.0 keV
		1094.43		0.010	0.003	0.012	below MDA, probably spurious
		1119.98		0.207	0.006	0.014	Bi-214 (U series), 1120.3 keV
		1154.97		0.021	0.004	0.013	Bi-214 (U series), 1155.2 keV
		1237.96		0.079	0.008	0.014	Bi-214 (U series), 1238.1 keV
		1377.52		0.059	0.004	0.010	Bi-214 (U series), 1377.7 keV
		1385.17		0.015	0.003	0.009	Bi-214 (U series), 1385.3 keV
		1401.61		0.013	0.003	0.009	Bi-214 (U series), 1401.5 keV
Eu152	1,408.01	1408.02	-0.01	0.033	0.004	0.009	Bi-214 (U series), 1408.0 keV (Eu-152 ruled out, no 121.8 keV peak)
		1454.45		0.005	0.004	0.007	below MDA, but observed in DB591000
K-40	1,460.83	1460.84	-0.01	2.557	0.073	0.009	K-40, 1460.8 keV
		1495.97		0.016	0.003	0.007	Ac-228 (Th series), 1495.9 keV
		1501.63		0.010	0.003	0.007	Ac-228 (Th series), 1501.6 keV
		1509.33		0.026	0.004	0.007	Bi-214 (U series), 1509.2 keV
		1527.84		0.006	0.005	0.006	may be spurious
		1529.02		0.010	0.004	0.006	may be spurious
		1530.48		0.005	0.005	0.006	below MDA, probably spurious
		1538.72		0.004	0.004	0.006	below MDA, may be B-214 (U series), 1538.5 keV
		1581.90		0.015	0.005	0.006	Ac-228 (Th series), 1580.5 keV
		1588.40		0.055	0.008	0.007	Ac-228 (Th series), 1588.2 keV
		1592.86		0.037	0.007	0.007	2614.5 keV (Tl-208) double escape peak at 1592.5 keV
		1620.91		0.021	0.004	0.007	Bi-212 (Th series), 1620.5 keV
		1630.83		0.030	0.005	0.006	Ac-228 (Th series), 1630.6 keV

Table D-15. (continued).

Library ID	Library Energy (keV)	Measured Energy (keV)	Energy Residual (keV)	Peak Intensity (c/s)	Intensity Uncert. (c/s)	MDA (c/s)	Analyst Comments
		1661.59		0.009	0.003	0.006	Bi-214 (U series), 1661.3 keV
		1701.85		0.003	0.002	0.005	below MDA, probably spurious
		1730.09		0.036	0.004	0.006	Bi-214 (U series), 1729.6 keV
U238	1,764.49	1765.02	-0.53	0.215	0.011	0.006	Bi-214 (U series), 1764.5 keV
		2103.84		0.076	0.006	0.006	2614.5 keV (Tl-208) escape peak at 2103.5 keV
		2118.98		0.015	0.003	0.005	Bi-214 (U series), 2118.5 keV
		2204.33		0.065	0.004	0.006	Bi-214 (U series), 2204.2 keV
		2293.05		0.004	0.002	0.005	Bi-214 (U series), 2293.4 keV
		2404.05		0.003	0.001	0.004	below MDA, probably spurious
		2405.15		0.003	0.003	0.004	below MDA, probably spurious
		2447.58		0.021	0.003	0.005	Bi-214 (U series), 2447.9 keV
		2562.47		0.002	0.001	0.002	below MDA, probably spurious
		2564.95		0.003	0.001	0.002	may be spurious
		2566.43		0.002	0.001	0.002	may be spurious
Th232	2,614.53	2614.33	0.20	0.635	0.025	0.003	Tl-208 (Th series), 2614.5 keV

D-2.1.3 Spectrum DB571000

As before, gamma rays the analysis program associated with Cs-134 and Eu-152 are actually due to the natural background. Gamma ray peaks corresponding to 103.6, 125.9, 208.6, and 721.8 keV indicate the presence of Am-241, and a peak corresponding to 312.1 keV suggests the presence of Np-237. (The gamma ray originates in Pa-233, which is a short-lived decay product of Np-237.) Spectrum DB571000 does not show a confirming Np-237 peak at 300.3 keV, but spectrum DB581000 has a 312.2-keV peak and a confirming peak at 300.5 keV. Low intensity peaks corresponding to 375.3 and 413.6 keV indicate the presence of Pu-239 at a concentration barely above the detection limit.

Table D-16. Data for Spectrum DB571000

Library ID	Library Energy (keV)	Measured Energy (keV)	Energy Residual (keV)	Peak Intensity (c/s)	Intensity Uncert. (c/s)	MDA (c/s)	Analyst Comments
		38.74		0.653	0.226	0.024	probably a spurious low energy peak
		40.78		1.356	0.024	0.033	probably a spurious low energy peak
		41.26		0.500	0.234	0.030	probably a spurious low energy peak
		43.83		0.338	0.236	0.037	probably a spurious low energy peak
		47.52		0.418	0.025	0.039	Am-241, Pu-239 (?)

Table D-16. (continued).

Library ID	Library Energy (keV)	Measured Energy (keV)	Energy Residual (keV)	Peak Intensity (c/s)	Intensity Uncert. (c/s)	MDA (c/s)	Analyst Comments
		99.68		0.177	0.026	0.048	Am-241 (99.0 keV)
Am241	103.00	103.60	-0.60	0.192	0.027	0.052	Am-241 (103.0 keV)
Am241	125.30	125.90	-0.60	0.155	0.035	0.057	Am-241 (125.3 keV)
U235	185.72	186.35	-0.63	0.091	0.015	0.054	Ra-226 (U series), 186.1 keV; U-235, 185.7 keV
		208.60		0.118	0.021	0.051	Am-241 (208.0 keV)
		238.97		0.567	0.060	0.048	Pb-212 (Th series), 238.6 keV
		270.61		0.037	0.011	0.038	Ac-228 (Th series), 270.2 keV
		295.37		0.200	0.029	0.039	Pb-212 (Th series), 295.2 keV
Np237	312.17	312.10	0.07	0.049	0.015	0.035	NP-237. No confirming lines here, but DB581000 has a confirming line
		338.51		0.119	0.029	0.034	Ac-228 (Th series), 338.3 keV
U238	351.92	351.93	-0.01	0.414	0.022	0.031	Pb-214 (U series), 351.9 keV
		368.77		0.024	0.009	0.028	Pu-239 (367.1 keV, 368.6 keV)
		375.39		0.028	0.009	0.030	Pu-239 (375.1 keV)
		409.49		0.021	0.008	0.026	Ac-228 (Th series), 409.5 keV
		413.65		0.030	0.008	0.027	Pu-239 (413.7 keV)
		462.88		0.068	0.011	0.024	Ac-228 (Th series), 463.0 keV
		510.62		0.352	0.026	0.027	annihilation radiation, 511.0 keV
		562.43		0.019	0.010	0.020	Ac-228 (Th series), 562.5 keV
Th232	583.19	582.97	0.22	0.487	0.019	0.021	Tl-208 (Th series), 583.2 keV
U238	609.31	609.08	0.23	0.550	0.029	0.020	Bi-214 (U series), 609.3 keV
Cs137	661.66	661.87	-0.21	0.067	0.015	0.019	probably Am-241 at 662.4 keV
		721.84		0.030	0.008	0.016	Am-241 (722.0 keV)
		726.93		0.120	0.009	0.017	Bi-212 (Th series), 727.3 keV
U238p	766.36	767.95	-1.59	0.054	0.013	0.016	Bi-214 (U series) 768.3 keV
		772.20		0.011	0.010	0.016	Ac-228 (Th series), 772.3 keV
		785.28		0.032	0.007	0.015	Pb-214 (U series), 785.9 keV Bi-212 (Th series) 785.4 keV
Cs134	795.85	794.59	1.26	0.071	0.007	0.016	Ac-228 (Th series), 794.9 keV
		829.96		0.012	0.006	0.015	Ac-228 (Th series), 830.5 keV
		835.45		0.029	0.006	0.015	Ac-228 (Th series), 835.7 keV
		839.70		0.020	0.006	0.015	Ac-228 (Th series), 840.4 keV
		860.17		0.075	0.006	0.015	Tl-208 (Th series), 860.6 keV

Table D-16. (continued).

Library ID	Library Energy (keV)	Measured Energy (keV)	Energy Residual (keV)	Peak Intensity (c/s)	Intensity Uncert. (c/s)	MDA (c/s)	Analyst Comments
Th232	911.21	910.83	0.38	0.458	0.024	0.015	Ac-228 (Th series), 911.2 keV
		933.64		0.030	0.007	0.014	Bi-214 (U series), 934.1 keV
		964.38		0.101	0.009	0.014	Bi-214 (U series) 964.1 keV
		968.60		0.296	0.012	0.014	Ac-228 (Th series), 969.0 keV
U238p	1,001.03	1,000.79	0.24	0.013	0.004	0.013	Pa-234m (U series), 1001.0 keV
		1,119.98		0.204	0.009	0.014	Bi-214 (U series), 1120.3 keV
		1,155.06		0.028	0.005	0.013	Bi-214 (U series), 1155.2 keV
		1,238.02		0.081	0.005	0.014	Bi-214 (U series), 1238.1 keV
		1,280.77		0.018	0.004	0.012	Bi-214 (U series), 1280.96 keV
		1,377.58		0.05655	0.00533	0.00945	Bi-214 (U series), 1377.7 keV
		1,401.53		0.02321	0.00327	0.00887	Bi-214 (U series), 1401.5 keV
Eu152	1,408.01	1,407.86	0.15	0.03177	0.00345	0.00885	Bi-214 (U series), 1408.0 keV
K-40	1,460.83	1,460.83	0.00	2.50200	0.08070	0.00859	K-40, 1460.8 keV
		1,495.90		0.01760	0.00311	0.00604	Ac-228 (Th series), 1495.9 keV
		1,501.55		0.01086	0.00286	0.00613	Ac-228 (Th series), 1501.6 keV
		1,509.52		0.03180	0.00370	0.00669	Bi-214 (U series), 1509.2 keV
		1,538.50		0.00469	0.00218	0.00624	Bi-214 (U series), 1538.5 keV
		1,581.29		0.01139	0.00338	0.00655	Ac-228 (Th series), 1580.5 keV
		1,588.41		0.05658	0.00505	0.00674	Ac-228 (Th series), 1588.2 keV
		1,592.80		0.04131	0.00453	0.00667	2614.5 keV (Tl-208) double escape peak at 1592.5 keV
		1,620.88		0.02787	0.00400	0.00621	Bi-212 (Th series), 1620.5 keV
		1,625.31		0.00438	0.00315	0.00512	below MDA, may be Ac-228 (Th series), 1625.0 keV
		1,630.81		0.02643	0.00405	0.00618	Ac-228 (Th series), 1630.6 keV
		1,638.92		0.00521	0.00305	0.00584	Ac-228 (Th series), 1638.3 keV
		1,661.58		0.01432	0.00229	0.00567	Bi-214 (U series), 1661.3 keV
		1,667.00		0.00575	0.00199	0.00543	near MDA, may be Ac-228, 1666.5 keV
		1,684.83		0.00480	0.00305	0.00524	below MDA, may be Bi-214, 1684.0 keV
		1,730.10		0.04090	0.00364	0.00549	Bi-214 (U series), 1729.6 keV
U238	1,764.49	1,765.04	-0.55	0.21150	0.00909	0.00645	Bi-214 (U series), 1764.5 keV
		1,777.68		0.02440	0.00233	0.00244	barely above MDA, may be spurious
		1,848.08		0.02937	0.00266	0.00541	Bi-214 (U series), 1847.4 keV
		2,103.84		0.06863	0.00727	0.00576	2614.5 keV (Tl-208)

Table D-16. (continued).

Library ID	Library Energy (keV)	Measured Energy (keV)	Energy Residual (keV)	Peak Intensity (c/s)	Intensity Uncert. (c/s)	MDA (c/s)	Analyst Comments
							escape peak at 2103.5 keV
		2,118.97		0.01562	0.00348	0.00527	Bi-214 (U series), 2118.5 keV
		2,204.36		0.06496	0.00352	0.00566	Bi-214 (U series), 2204.2 keV
		2,447.89		0.02217	0.00234	0.00464	Bi-214 (U series), 2447.9 keV
Th232	2,614.53	2,614.32	0.21	0.62770	0.01912	0.00250	Tl-208 (Th series), 2614.5 keV
		2,755.47		0.00048	0.00040	0.00073	spurious peak at high energy

D-2.1.4 Spectrum DB581000

Gamma rays at 794.6 keV and 1407.9 keV are due to the natural background and not Cs-134 or Eu-152. Peaks due to gamma rays with energies of 99.9, 103.9, 126.1, 147.3, 165.5, 170.9, 208.7, 335.7, 618.9, 688.46, and 721.6 keV indicate the presence of Am-241. The presence of Pu-239 is revealed by peaks corresponding to 204.2, 322.8, 332.8, 368.9, 375.0, 380.3, 392.9, and 413.8 keV. This spectrum also has the signatures of Np-237 at 300.5 and 312.2 keV. A 661.9-keV gamma ray was associated with Cs-137 (661.6 keV) by the analysis program, but the energy residual suggests that the gamma ray is actually the Am-241 gamma ray at 662.4 keV.

A 138.1-keV gamma ray apparently produced a peak in this spectrum. A peak at 138.2 keV also appears in spectrum DB521000.

A peak corresponding to 2222.9 keV is apparently due to 2223.2-keV gamma rays associated with neutron capture by hydrogen. The alpha particle flux in the formation must be so high that neutrons from alpha-n reactions with oxygen exist in numbers sufficient to produce hydrogen capture reactions at detectable levels.

Table D-17. Data for Spectrum DB581000

Library ID	Library Energy (keV)	Measured Energy (keV)	Energy Residual (keV)	Peak Intensity (c/s)	Intensity Uncert. (c/s)	MDA (c/s)	Analyst Comments
		38.55		0.808	0.408	0.029	probably a spurious low energy peak
		99.88		0.552	0.064	0.055	Am-241 (99.0 keV), Pu-239 (98.8 keV)
Am241	103.00	103.86	-0.86	0.651	0.066	0.055	Am-241 (103.0 keV)
		115.56		0.190	0.139	0.056	Pb-212 (Th series), 115.2 keV (?)
Am241	125.30	126.12	-0.82	0.684	0.159	0.059	Am-241 (125.3 keV)
Pu239	129.30	130.28	-0.98	0.311	0.145	0.056	Pu-239 (129.3 keV)
		138.13		0.221	0.142	0.057	may be spurious; also observed in DB521000
		144.13		0.228	0.143	0.060	Pu-239 (144.2 keV)
		145.14		0.977	0.043	0.067	may be spurious
		147.29		0.287	0.146	0.057	Am-241 (146.6 keV)

Table D-17. (continued).

Library ID	Library Energy (keV)	Measured Energy (keV)	Energy Residual (keV)	Peak Intensity (c/s)	Intensity Uncert. (c/s)	MDA (c/s)	Analyst Comments
		151.03		0.522	0.033	0.053	may be spurious
		152.30		0.163	0.141	0.057	may be spurious
		156.05		0.530	0.035	0.056	may be spurious
		161.29		0.117	0.140	0.054	Pu-239 (161.4 keV)
		165.49		0.412	0.033	0.052	Am-241 (165.8 keV)
		170.90		0.475	0.038	0.061	Am-241 (169.5 keV), Pu-239 (171.4 keV)
		177.81		0.187	0.030	0.048	may be spurious
		181.69		0.160	0.030	0.048	may be spurious
U235	185.72	186.38	-0.66	0.281	0.043	0.070	Ra-226 (U series), 186.1 keV; U-235, 185.7 keV
		204.21		0.058	0.025	0.052	Pu-239 (203.6 keV)
		208.69		0.407	0.028	0.054	Am-241 (208.0 keV)
		239.17		0.504	0.060	0.046	Pb-212 (Th series), 238.6 keV
		270.60		0.046	0.012	0.039	Ac-228 (Th series), 270.2 keV
		295.61		0.191	0.035	0.038	Pb-212 (Th series), 295.2 keV
Np237	300.34	300.48	-0.14	0.033	0.020	0.033	Np-237 (300.3 keV)
Np237	312.17	312.22	-0.05	0.206	0.017	0.038	Np-237 (312.2 keV)
		322.78		0.079	0.016	0.035	Pu-239 (320.9, 323.8 keV)
		328.46		0.032	0.015	0.034	Ac-228 (Th series), 328.0 keV; Bi-212 (Th series), 328.0 keV
		332.79		0.105	0.016	0.034	Pu-239 (332.8 keV)
		335.74		0.209	0.017	0.035	Am-241 (335.4 keV)
		338.65		0.141	0.016	0.033	Ac-228 (Th series), 338.3 keV
U238	351.92	352.17	-0.25	0.441	0.021	0.033	Pb-214 (U series), 351.9 keV; possibly 352.2 Fe capture gamma
		368.92		0.115	0.021	0.030	Pu-239 (367.1 keV, 368.6 keV)
Pu239	375.05	375.57	-0.52	0.131	0.021	0.031	Pu-239 (375.0 keV)
		380.27		0.024	0.014	0.024	Pu-239 (380.2 keV)
		383.54		0.034	0.019	0.029	Pu-239 (382.8 keV)
		392.93		0.031	0.018	0.028	Pu-239 (392.5 keV)
		409.66		0.020	0.011	0.026	Ac-228 (Th series), 409.5 keV
		413.80		0.093	0.011	0.027	Pu-239 (413.7 keV)
		462.95		0.057	0.010	0.024	Ac-228 (Th series), 463.0 keV

Table D-17. (continued).

Library ID	Library Energy (keV)	Measured Energy (keV)	Energy Residual (keV)	Peak Intensity (c/s)	Intensity Uncert. (c/s)	MDA (c/s)	Analyst Comments
		510.78		0.346	0.023	0.028	annihilation radiation, 511.0 keV
		562.23		0.016	0.006	0.019	Ac-228 (Th series), 562.5 keV
Th232	583.19	583.09	0.10	0.454	0.020	0.022	Tl-208 (Th series), 583.2 keV
U238	609.31	609.20	0.11	0.564	0.018	0.021	Bi-214 (U series), 609.3 keV
		618.91		0.027	0.010	0.018	Am-241 (619.0 keV)
Cs137	661.66	661.91	-0.25	0.258	0.014	0.018	Am-241 (662.4 keV)
		688.46		0.017	0.005	0.016	Am-241 (688.7 keV)
		721.65		0.085	0.006	0.017	Am-241 (722.0 keV)
		727.06		0.109	0.006	0.017	Bi-212 (Th series), 727.3 keV
		755.15		0.020	0.006	0.016	Ac-228 (Th series), 755.3 keV
		763.25		0.014	0.006	0.014	below MDA, may be Tl-208 (Th series), 763.1 keV
U238p	766.36	767.97	-1.61	0.070	0.007	0.016	Bi-214 (U series) 768.3 keV
		771.92		0.026	0.006	0.015	Ac-228 (Th series), 772.3 keV
		785.37		0.021	0.009	0.015	Pb-214 (U series); 785.9 keV; Bi-212 (Th series) 785.4 keV
Cs134	795.85	794.62	1.23	0.059	1259.000	0.015	Ac-228 (Th series), 794.9 keV
		805.81		0.016	0.005	0.014	Bi-214 (U series), 806.2 keV
		830.26		0.012	0.004	0.014	Ac-228 (Th series), 830.5 keV
		835.26		0.027	0.005	0.014	Ac-228 (Th series), 835.7 keV
		839.63		0.022	0.005	0.014	Ac-228 (Th series), 840.4 keV
		860.15		0.064	0.005	0.015	Tl-208 (Th series), 860.6 keV
		903.99		0.008	0.007	0.012	Ac-228 (Th series), 904.2 keV
Th232	911.21	910.85	0.36	0.407	0.014	0.015	Ac-228 (Th series), 911.2 keV
		933.77		0.047	0.005	0.013	Bi-214 (U series), 934.1 keV
		964.40		0.087	0.005	0.013	Bi-214 (U series) 964.1 keV
		968.58		0.259	0.007	0.014	Ac-228 (Th series), 969.0 keV
U238p	1,001.03	1,000.71	0.32	0.028	0.007	0.013	Pa-234m (U series), 1001.0 keV
		1,031.40		0.009	0.007	0.011	below MDA, may be spurious
		1,033.53		0.006	0.004	0.012	below MDA, may be spurious
		1,066.91		0.006	0.005	0.011	below MDA, may be spurious
		1,094.87		0.067	0.006	0.008	Ac-228 (Th series), 1095.7 keV
		1,119.95		0.204	0.009	0.013	Bi-214 (U series), 1120.3 keV

Table D-17. (continued).

Library ID	Library Energy (keV)	Measured Energy (keV)	Energy Residual (keV)	Peak Intensity (c/s)	Intensity Uncert. (c/s)	MDA (c/s)	Analyst Comments
		1,154.61		0.023	0.004	0.012	Bi-214 (U series), 1155.2 keV
		1,237.82		0.080	0.005	0.013	Bi-214 (U series), 1238.1 keV
		1,281.93		0.060	0.400	0.011	Bi-214 (U series), 1281.0 keV
		1,377.50		0.055	0.004	0.009	Bi-214 (U series), 1377.7 keV
		1,385.07		0.009	0.003	0.008	Bi-214 (U series), 1385.3 keV
		1,401.44		0.018	0.003	0.008	Bi-214 (U series), 1401.5 keV
Eu152	1,408.01	1,407.94	0.07	0.035	0.003	0.008	Bi-214 (U series), 1408.0 keV
K-40	1,460.83	1,460.75	0.08	2.273	0.029	0.009	K-40, 1460.8 keV
		1,495.81		0.014	0.002	0.006	Ac-228 (Th series), 1495.9 keV
		1,501.72		0.007	0.002	0.006	Ac-228 (Th series), 1501.6 keV
		1,509.20		0.030	0.003	0.007	Bi-214 (U series), 1509.2 keV
		1,538.20		0.007	0.002	0.006	Bi-214 (U series), 1538.5 keV
		1,557.54		0.005	0.002	0.005	Ac-228 (Th series), 1557.1 keV
		1,581.37		0.013	0.004	0.006	Ac-228 (Th series), 1580.5 keV
		1,588.29		0.047	0.006	0.007	Ac-228 (Th series), 1588.2 keV
		1,592.66		0.029	0.006	0.007	2614.5 keV (Tl-208) double escape peak at 1592.5 keV
		1,620.93		0.020	0.004	0.006	Bi-212 (Th series), 1620.5 keV
		1,630.82		0.023	0.005	0.006	Ac-228 (Th series), 1630.6 keV
		1,661.41		0.013	0.003	0.006	Bi-214 (U series), 1661.3 keV
		1,684.77		0.004	0.001	0.005	below MDA, probably spurious
		1,730.06		0.041	0.003	0.006	Bi-214 (U series), 1729.6 keV
U238	1,764.49	1,764.97	-0.48	0.218	0.006	0.005	Bi-214 (U series), 1764.5 keV
		1,848.03		0.029	0.003	0.005	Bi-214 (U series), 1847.4 keV
		2,103.79		0.060	0.008	0.005	2614.5 keV (Tl-208) escape peak at 2103.5 keV
		2,118.61		0.016	0.002	0.005	Bi-214 (U series), 2118.5 keV
		2,204.34		0.067	0.004	0.005	Bi-214 (U series), 2204.2 keV
		2,222.86		0.003	0.002	0.005	H neutron capture gamma ray
		2,293.44		0.005	0.002	0.005	Bi-214 (U series), 2293.4 keV
		2,447.72		0.020	0.002	0.004	Bi-214 (U series), 2447.9 keV
Th232	2,614.53	2,614.37	0.16	0.582	0.026	0.002	Tl-208 (Th series), 2614.5 keV

D-2.1.5 Spectrum DB591000

Like spectrum DB581000, this spectrum has many peaks attributable to the gamma rays of Am-241, Pu-239, and Np-237. The gamma rays at 794.6 keV and 1407.9 keV are due to the natural background and not Cs-134 or Eu-152, and the gamma ray at 661.9 keV is probably the 662.4-keV Am-241 gamma ray and not the 661.6-keV gamma ray of Cs-137.

A peak at 141.5 keV is due to an unknown source. A similar peak at 141.3 keV exists in DB541000. Another peak due to an unknown source is at 234.6 keV. The intensity is below the MDA, but an apparently related peak at 234.8 keV exists in spectrum DB521000. Likewise, peaks at 451.6 and 652.7 keV appear in spectra DB59100 and DB541000; the sources (if they exist) are unknown. An unknown source may have emitted gamma rays of energy 1454.3 keV that account for a weak peak with an intensity just above the MDA. An analogous peak at 1454.5 keV was observed in spectrum DB561000.

Like spectrum DB581000, spectrum DB591000 has a signal at 2,223.6 keV that is attributed to neutron capture by hydrogen.

Table D-18. Data for Spectrum DB591000.

Library ID	Library Energy (keV)	Measured Energy (keV)	Energy Residual (keV)	Peak Intensity (c/s)	Intensity Uncert. (c/s)	MDA (c/s)	Analyst Comments
		38.68		1.097	0.511	0.023	probably a spurious low energy peak
		40.07		2.935	0.029	0.035	probably a spurious low energy peak
		41.46		0.856	0.522	0.034	probably a spurious low energy peak
		45.63		0.969	0.028	0.042	probably a spurious low energy peak
		60.01		0.100	0.014	0.048	probably a spurious low energy peak
		99.57		2.087	0.377	0.067	Am-241 (99.0 keV), Pu-239 (98.8 keV)
Am241	103	103.54	-0.54	2.290	0.389	0.063	Am-241 (103.0 keV)
		114.61		0.882	0.049	0.079	may be spurious
		115.11		0.386	0.285	0.063	Pb-212 (Th series), 115.2 keV (?)
		118.87		0.570	0.033	0.052	may be spurious
Am241	125.3	125.84	-0.54	1.889	0.369	0.066	Am-241 (125.3 keV)
Pu239	129.3	129.89	-0.59	0.782	0.040	0.063	Pu-239 (129.3 keV)
		136.56		0.467	0.039	0.063	may be spurious
		141.46		0.240	0.273	0.059	unknown; also observed in DB541000
		147.14		0.559	0.293	0.062	Am-241 (146.6 keV)
		160.80		0.382	0.036	0.058	Pu-239 (161.4 keV)
U235	163.33	165.16	-1.83	0.227	0.270	0.061	Am-241 (165.8 keV)

Table D-18. (continued).

Library ID	Library Energy (keV)	Measured Energy (keV)	Energy Residual (keV)	Peak Intensity (c/s)	Intensity Uncert. (c/s)	MDA (c/s)	Analyst Comments
		170.15		0.442	0.049	0.079	Am-241 (169.5 keV), Pu-239 (171.4 keV)
U235	185.72	186.31	-0.59	0.158	0.017	0.060	Ra-226 (U series), 186.1 keV; U-235, 185.7 keV
		204.22		0.183	0.035	0.056	Pu-239 (203.6 keV)
		208.41		1.229	0.081	0.055	Am-241 (208.0 keV)
		221.77		0.069	0.014	0.049	may be spurious
		234.62		0.029	0.025	0.041	below MDA; also appears in DB521000
		238.97		0.519	0.057	0.052	Pb-212 (Th series), 238.6 keV
		267.68		0.040	0.021	0.041	below MDA, may be spurious
		270.49		0.055	0.021	0.041	Ac-228 (Th series), 270.2 keV
		277.65		0.042	0.020	0.040	Tl-208 (Th series), 277.4 keV
		295.40		0.197	0.090	0.040	Pb-212 (Th series), 295.2 keV
Np237	300.34	300.30	0.04	0.125	0.027	0.044	Np-237 (300.3 keV)
Np237	312.17	312.04	0.13	0.658	0.106	0.040	Np-237 (312.2 keV)
		322.58		0.223	0.085	0.037	Pu-239 (320.9, 323.8 keV)
		327.93		0.036	0.019	0.032	Ac-228 (Th series), 328.0 keV; Bi-212 (Th series), 328.0 keV
		335.50		0.724	0.104	0.037	Am-241 (335.4 keV)
		345.13		0.092	0.074	0.034	Pu-239 (345.0 keV)
U238	351.92	351.96	-0.04	0.389	0.087	0.033	Pb-214 (U series), 351.9 keV
		368.63		0.334	0.060	0.033	Pu-239 (367.1 keV, 368.6 keV)
Pu239	375.05	375.41	-0.36	0.459	0.021	0.032	Pu-239 (375.1 keV)
		380.27		0.076	0.018	0.029	Pu-239 (380.2 keV)
		383.17		0.056	0.048	0.028	Pu-239 (382.8 keV)
		392.72		0.090	0.020	0.029	Pu-239 (392.5 keV)
		413.64		0.261	0.026	0.028	Pu-239 (413.7 keV)
		451.60		0.030	0.007	0.025	unknown; also occurs in DB541000
		462.89		0.052	0.008	0.025	Ac-228 (Th series), 463.0 keV

Table D-18. (continued).

Library ID	Library Energy (keV)	Measured Energy (keV)	Energy Residual (keV)	Peak Intensity (c/s)	Intensity Uncert. (c/s)	MDA (c/s)	Analyst Comments
		510.67		0.365	0.028	0.028	annihilation radiation, 511.0 keV
Th232	583.19	582.97	0.22	0.437	0.014	0.021	Tl-208 (Th series), 583.2 keV
U238	609.31	609.09	0.22	0.542	0.016	0.020	Bi-214 (U series), 609.3 keV
		618.77		0.076	0.010	0.019	Am-241 (619.0 keV)
		652.70		0.047	0.009	0.018	unknown, also observed in DB541000
Cs137	661.66	661.92	-0.26	0.594	0.017	0.019	probably Am-241 at 662.4 keV
		688.54		0.039	0.006	0.018	Am-241 (688.7 keV)
		702.67		0.012	0.005	0.017	Ac-228, 701.8 keV; Bi-214, 703.1 keV
		721.66		0.253	0.009	0.017	Am-241 (722.0 keV)
		726.93		0.114	0.007	0.016	Bi-212 (Th series), 727.3 keV
U238p	766.36	767.46	-1.10	0.070	0.018	0.016	Bi-214 (U series) 768.3 keV
		785.62		0.032	0.010	0.015	Pb-214 (U series), 785.9 keV; Bi-212 (Th series) 785.4 keV
Cs134	795.85	794.61	1.24	0.056	0.007	0.014	c-228 (Th series), 794.9 keV
		806.02		0.016	0.005	0.013	Bi-214 (U series), 806.2 keV
		835.56		0.023	0.006	0.015	Ac-228 (Th series), 835.7 keV
		839.64		0.016	0.006	0.014	Ac-228 (Th series), 840.4 keV
		860.21		0.070	0.005	0.014	Tl-208 (Th series), 860.6 keV
		904.09		0.009	0.008	0.013	Ac-228 (Th series), 904.2 keV
Th232	911.21	910.85	0.36	0.371	0.011	0.014	Ac-228 (Th series), 911.2 keV
		933.77		0.042	0.005	0.013	Bi-214 (U series), 934.1 keV
		949.63		0.009	0.005	0.013	1460.8-keV (K-40) escape peak (949.8 keV)
		964.38		0.074	0.010	0.013	Bi-214 (U series) 964.1 keV
		968.59		0.230	0.013	0.014	Ac-228 (Th series), 969.0 keV
U238p	1,001.03	1000.75	0.28	0.111	0.009	0.013	Pa-234m (U series), 1001.0 keV
		1079.11		0.012	0.004	0.012	Bi-212 (Th series), 1078.6 keV
		1119.95		0.186	0.013	0.013	Bi-214 (U series), 1120.3 keV

Table D-18. (continued).

Library ID	Library Energy (keV)	Measured Energy (keV)	Energy Residual (keV)	Peak Intensity (c/s)	Intensity Uncert. (c/s)	MDA (c/s)	Analyst Comments
		1154.85		0.024	0.004	0.012	Bi-214 (U series), 1155.2 keV
		1237.98		0.082	0.005	0.013	Bi-214 (U series), 1238.1 keV
		1280.67		0.020	0.004	0.010	Bi-214 (U series), 1281.0 keV
		1377.65		0.054	0.004	0.009	Bi-214 (U series), 1377.7 keV
		1384.99		0.010	0.003	0.008	Bi-214 (U series), 1385.3 keV
		1401.43		0.023	0.003	0.008	Bi-214 (U series), 1401.5 keV
Eu152	1,408.01	1407.88	0.13	0.031	0.003	0.008	Bi-214 (U series), 1408.0 keV
		1454.31		0.007	0.004	0.006	unknown, observed in DB561000.
K-40	1,460.83	1460.84	-0.01	2.043	0.056	0.008	K-40, 1460.8 keV
		1496.03		0.011	0.003	0.007	Ac-228 (Th series), 1495.9 keV
		1501.99		0.005	0.003	0.006	Ac-228 (Th series), 1501.6 keV
		1509.38		0.030	0.004	0.007	Bi-214 (U series), 1509.2 keV
		1580.78		0.007	0.003	0.004	Ac-228 (Th series), 1580.5 keV
		1583.05		0.011	0.004	0.006	may be spurious
		1588.50		0.050	0.007	0.006	Ac-228 (Th series), 1588.2 keV
		1592.86		0.034	0.006	0.006	2614.5 keV (Tl-208) double escape peak at 1592.5 keV
		1621.05		0.027	0.003	0.006	Bi-212 (Th series), 1620.5 keV
		1630.90		0.024	0.003	0.006	Ac-228 (Th series), 1630.6 keV
		1638.15		0.007	0.002	0.005	Ac-228 (Th series), 1638.3 keV
		1661.57		0.012	0.002	0.006	Bi-214 (U series), 1661.3 keV
		1730.15		0.038	0.003	0.006	Bi-214 (U series), 1729.6 keV
U238	1,764.49	1765.05	-0.56	0.209	0.008	0.006	Bi-214 (U series), 1764.5 keV
		1848.05		0.025	0.003	0.005	Bi-214 (U series), 1847.4 keV
		1936.65		0.004	0.002	0.004	below MDA; 1936.6 keV occurs in SBU cal spectra
		2103.93		0.057	0.006	0.005	2614.5 keV (Tl-208) escape peak at 2103.5 keV
		2118.79		0.014	0.003	0.005	Bi-214 (U series), 2118.5 keV
		2204.30		0.063	0.005	0.005	Bi-214 (U series), 2204.2 keV

Table D-18. (continued).

Library ID	Library Energy (keV)	Measured Energy (keV)	Energy Residual (keV)	Peak Intensity (c/s)	Intensity Uncert. (c/s)	MDA (c/s)	Analyst Comments
		2223.56		0.010	0.002	0.005	H capture gamma ray
		2239.06		0.003	0.002	0.004	Cr capture gamma ray (?)
		2293.60		0.004	0.002	0.005	Bi-214 (U series), 2293.4 keV
		2447.72		0.020	0.002	0.004	Bi-214 (U series), 2447.9 keV
Th232	2,614.53	2614.32	0.21	0.525	0.021	0.003	Tl-208 (Th series), 2614.5 keV

D-2.2 Analysis Results for Borehole P6-PU-2

Five spectra were acquired from this borehole. The names of the spectra and the associated depths are as follows.

Spectrum Name	Depth
DB501000	20.06 ft
DB511000	16.5 ft
DB521000	16.0 ft
DB531000	15.5 ft
DB541000	15.0 ft

D-2.2.1 Spectrum DB501000

As occurred with spectra from borehole P6-PU-1, the analysis program assigned gamma rays with energies 795.0 keV and 1408.0 keV to Cs-134 and Eu-152, but the two gamma rays are more likely part of the natural background. No peaks that could be unambiguously associated with man-made sources are evident in spectrum DB501000.

Table D-19. Data for Spectrum DB501000

Library ID	Library Energy (keV)	Measured Energy (keV)	Energy Residual (keV)	Peak Intensity (c/s)	Intensity Uncert. (c/s)	MDA (c/s)	Analyst Comments
		127.26		0.042	0.035	0.058	below MDA, probably spurious
U235	185.72	185.88	-0.16	0.048	0.032	0.05249	Ra-226 (U series), 186.1 keV; U-235, 185.7 keV
		238.59		0.629	0.034	0.054	Pb-212 (Th series), 238.6 keV
		270.52		0.039	0.025	0.041	below MDA; Ac-228 (Th series), at 270.2 keV

Table D-19. (continued).

Library ID	Library Energy (keV)	Measured Energy (keV)	Energy Residual (keV)	Peak Intensity (c/s)	Intensity Uncert. (c/s)	MDA (c/s)	Analyst Comments
		294.61		0.166	14.890	0.035	Pb-214 (U series), 295.2 keV (large uncertainty)
		338.34		0.135	0.021	0.034	Ac-228 (Th series), 338.3 keV
U238	351.92	351.86	0.06	0.416	0.023	0.03616	Pb-214 (U series), 351.9 keV
		463.04		0.056	0.015	0.025	Ac-228 (Th series), 463.0 keV
		510.80		0.295	0.017	0.026	annihilation radiation (511.0 keV)
Th232	583.19	583.22	-0.03	0.446	0.017	0.02562	Tl-208 (Th series), 583.2 keV
U238	609.31	609.37	-0.06	0.553	0.016	0.02149	Bi-214 (U series), 609.3 keV
		665.44		0.013	0.010	0.017	below MDA; Bi-214 (U series), 665.4 keV
		727.27		0.103	0.013	0.020	Ac-228, 726.9 keV; Bi-212 (Th series), 727.3 keV
		755.38		0.025	0.010	0.016	Ac-228 (Th series), 755.3 keV
		768.27		0.031	0.010	0.017	Bi-214 (U series), 768.3 keV
		785.62		0.019	0.007	0.015	Pb-214 (U series), 785.9 keV; Bi-212 (Th series) 785.4 keV
Cs134	795.85	795.02	0.83	0.064	0.008	0.01499	Ac-228 (Th series), 794.9 keV
		806.28		0.016	0.010	0.016	below MDA; Bi-214 (U series), 806.2 keV
		830.98		0.012	0.006	0.014	below MDA; Ac-228 (Th series), 830.5 keV
		836.00		0.022	0.006	0.014	Ac-228 (Th series), 835.7 keV
		860.55		0.064	0.009	0.015	Tl-208 (Th series), 860.6 keV
Th232	911.21	911.16	0.05	0.390	0.013	0.01807	Ac-228 (Th series), 911.2 keV
		934.09		0.042	0.010	0.017	Bi-214 (U series), 934.1 keV
		949.64		0.017	0.008	0.014	1460.8 keV (K-40) escape peak (949.8 keV)
		964.65		0.074	0.005	0.014	Bi-214 (U series) 964.1 keV
		968.91		0.242	0.007	0.014	Ac-228 (Th series), 969.0 keV
		980.89		0.009	0.008	0.013	below MDA, probably spurious

Table D-19. (continued).

Library ID	Library Energy (keV)	Measured Energy (keV)	Energy Residual (keV)	Peak Intensity (c/s)	Intensity Uncert. (c/s)	MDA (c/s)	Analyst Comments
U238p	1,001.03	1,001.00	0.03	0.028	0.007	0.01051	Pa-234m (U series), 1001.0 keV
		1,078.62		0.009	0.007	0.011	below MDA; Bi-212 (Th series) 1078.6 keV
		1,120.16		0.201	0.010	0.015	Bi-214 (U series), 1120.3 keV
		1,155.13		0.035	0.009	0.015	Bi-214 (U series), 1155.2 keV
		1,208.27		0.008	0.007	0.012	below MDA; Bi-214 (U series), 1207.7 keV
		1,237.63		0.072	0.008	0.013	Bi-214 (U series), 1238.1 keV
		1,281.04		0.012	0.007	0.011	Bi-214 (U series), 1281.0 keV
		1,377.51		0.060	0.004	0.010	Bi-214 (U series), 1377.7 keV
		1,385.35		0.011	0.003	0.009	Bi-214 (U series), 1385.3 keV
		1,401.01		0.019	0.003	0.009	Bi-214 (U series), 1401.5 keV
Eu152	1,408.01	1,408.04	-0.03	0.029	0.003	0.008904	Bi-214 (U series), 1408.0 keV
K-40	1,460.83	1,460.70	0.13	2.114	0.018	0.01043	K-40, 1460.8 keV
		1,495.94		0.011	0.004	0.007	Ac-228 (Th series), 1495.9 keV
		1,501.66		0.005	0.003	0.007	below MDA; Ac-228 (Th series), 1501.6 keV
		1,509.35		0.026	0.004	0.007	Bi-214 (U series), 1509.2 keV
		1,554.93		0.005	0.003	0.006	below MDA, probably spurious
		1,581.57		0.011	0.004	0.006	Ac-228 (Th series), 1580.5 keV
		1,588.14		0.048	0.006	0.006	Ac-228 (Th series), 1588.2 keV
		1,592.57		0.038	0.005	0.007	2614.5 keV (Tl-208) double escape peak (1592.5 keV)
		1,598.83		0.006	0.003	0.005	Bi-214 (U series), 1599.3 keV
		1,620.82		0.022	0.004	0.006	Bi-212 (Th series), 1620.5 keV
		1,630.38		0.030	0.005	0.006	Ac-228 (Th series), 1630.6 keV
		1,660.97		0.014	0.004	0.006	Bi-214 (U series), 1661.3 keV
		1,729.64		0.037	0.004	0.006	Bi-214 (U series), 1729.6 keV
U238	1,764.49	1,764.59	-0.10	0.222	0.007	0.006213	Bi-214 (U series), 1764.5 keV
		1,793.53		-0.001	0.012	0.004	below MDA, negative intensity,

Table D-19. (continued).

Library ID	Library Energy (keV)	Measured Energy (keV)	Energy Residual (keV)	Peak Intensity (c/s)	Intensity Uncert. (c/s)	MDA (c/s)	Analyst Comments
							most likely spurious
		1,838.33		0.004	0.002	0.005	Bi-214 (U series), 1838.4 keV
		1,847.75		0.028	0.003	0.005	Bi-214 (U series), 1847.4 keV
		1,872.52		0.005	0.002	0.005	Bi-214 (U series), 1873.2 keV
		1,876.32		0.004	0.002	0.005	below MDA, probably spurious
		1,937.14		0.003	0.003	0.004	below MDA; 1936.6 keV occurs in SBU cal spectra
		2,103.43		0.070	0.005	0.006	2614.5 keV (Tl-208) escape peak (2103.5 keV)
		2,118.16		0.018	0.003	0.005	Bi-214 (U series), 2118.6 keV
		2,203.58		0.069	0.005	0.006	Bi-214 (U series), 2204.2 keV
		2,447.35		0.021	0.003	0.005	Bi-214 (U series), 2447.9 keV
Th232	2,614.53	2,614.49	0.04	0.558	0.009	0.002879	Tl-208 (Th series), 2614.5 keV
		2,805.18		0.0008	0.0007	0.0010	below MDA, probably spurious

D-2.2.2 Spectrum DB511000

Gamma rays that the analysis program associated with Cs-134 and Eu-152 are actually part of the natural background. There is a weak peak of unknown origin corresponding to 1452.5 keV; the intensity is below the MDA in this spectrum, but peaks exist at 1452.8 keV and 1451.3 keV in spectra DB521000 and DB541000.

Spectrum DB511000 has no peaks that could be unambiguously associated with man-made sources.

Table D-20. Data for Spectrum DB511000.

Library ID	Library Energy (keV)	Measured Energy (keV)	Energy Residual (keV)	Peak Intensity (c/s)	Intensity Uncert. (c/s)	MDA (c/s)	Analyst Comments
		40.2		2.283	0.024	0.025	probably a spurious low energy peak
		46.48		1.492	0.026	0.035	probably a spurious low energy peak
		55.05		0.389	0.024	0.037	probably a spurious low energy peak
		58.48		0.090	0.019	0.031	probably a spurious low energy peak
U235	185.72	185.85	-0.13	0.054	0.028	0.047	Ra-226 (U series), 186.1 keV; U-235, 185.7 keV

Table D-20. (continued)

Library ID	Library Energy (keV)	Measured Energy (keV)	Energy Residual (keV)	Peak Intensity (c/s)	Intensity Uncert. (c/s)	MDA (c/s)	Analyst Comments
		238.57		0.618	0.031	0.049	Pb-212 (Th series), 238.6 keV
		270.27		0.052	0.023	0.037	Ac-228 (Th series), 270.2 keV
		295.13		0.175	0.024	0.039	Pb-214 (U series), 295.2 keV
		300.14		0.031	0.022	0.036	Pb-212 (Th series), 300.1 keV
		327.92		0.055	0.026	0.043	Ac-228 (Th series), 328.0 keV; Bi-212 (Th series), 328.0 keV
		338.29		0.164	0.022	0.035	Ac-228 (Th series), 338.3 keV
U238	351.92	351.87	0.05	0.416	0.021	0.032	Pb-214 (U series), 351.9 keV
		455.37		0.018	0.017	0.027	Bi-214 (U series), 454.8 keV
		462.74		0.062	0.021	0.034	Ac-228 (Th series), 463.0 keV
		510.79		0.348	0.020	0.032	annihilation radiation, 511.0 keV
		562.71		0.019	0.013	0.022	Ac-228 (Th series), 562.5 keV
Th232	583.19	583.2	-0.01	0.470	0.018	0.026	Tl-208 (Th series), 583.2 keV
U238	609.31	609.33	-0.02	0.550	0.017	0.024	Bi-214 (U series), 609.3 keV
		665.7		0.011	0.010	0.017	Bi-214 (U series) 665.4 keV
		727.3		0.101	0.013	0.020	Bi-212 (Th series), 727.3 keV
		755.25		0.016	0.010	0.016	Ac-228 (Th series), 755.3 keV
		768.3	-1.94	0.068	0.013	0.021	Bi-214 (U series) 768.3 keV
		781.29		0.008	0.008	0.013	Ac-228 (Th series), 782.1 keV
		785.44		0.038	0.010	0.017	Pb-214 (U series), 785.9 keV; Bi-212 (Th series) 785.4 keV
Cs134	795.85	795.02	0.83	0.074	0.012	0.019	Ac-228 (Th series), 794.9 keV
		860.52		0.077	0.010	0.016	Tl-208 (Th series), 860.6 keV
Th232	911.21	911.14	0.07	0.421	0.014	0.019	Ac-228 (Th series), 911.2 keV
		933.82		0.045	0.009	0.015	Bi-214 (U series), 934.1 keV
		949.63		0.012	0.010	0.016	2614.5 keV (K-40) escape peak (949.8 keV)
		964.82		0.097	0.009	0.013	Bi-214 (U series) 964.1 keV
		968.84		0.277	0.010	0.013	Ac-228 (Th series), 969.0 keV
U238p	1001.03	1001.31	-0.28	0.010	0.008	0.013	Pa-234m (U series), 1001.0 keV

Table D-20. (continued)

Library ID	Library Energy (keV)	Measured Energy (keV)	Energy Residual (keV)	Peak Intensity (c/s)	Intensity Uncert. (c/s)	MDA (c/s)	Analyst Comments
		1078.12		0.014	0.009	0.014	below MDA, Bi-212 (Th series) 1078.6 keV
		1120.07		0.190	0.011	0.016	Bi-214 (U series), 1120.3 keV
		1155.1		0.022	0.010	0.016	Bi-214 (U series), 1155.2 keV
		1206.1		0.011	0.008	0.013	Bi-214 (U series), 1207.7 keV
		1237.84		0.085	0.012	0.018	Bi-214 (U series), 1238.1 keV
		1281.04		0.014	0.007	0.012	Bi-214 (U series), 1281.0 keV
		1377.41		0.054	0.007	0.011	Bi-214 (U series), 1377.7 keV
		1385.26		0.010	0.005	0.009	Bi-214 (U series), 1385.3 keV
		1401		0.021	0.006	0.010	Bi-214 (U series), 1401.5 keV
Eu152	1408.01	1407.59	0.42	0.033	0.006	0.009	Bi-214 (U series), 1408.0 keV
		1452.48		0.004	0.004	0.006	below MDA, unknown
K-40	1460.83	1460.56	0.27	2.514	0.020	0.010	K-40, 1460.8 keV
		1495.5		0.014	0.004	0.007	Ac-228 (Th series), 1495.9 keV
		1500.87		0.005	0.004	0.006	below MDA, Ac-228 (Th series), 1501.6 keV
		1509.34		0.036	0.006	0.008	Bi-214 (U series), 1509.2 keV
		1582.18		0.012	0.004	0.006	Ac-228 (Th series), 1580.5 keV
		1587.91		0.053	0.004	0.006	Ac-228 (Th series), 1588.2 keV
		1591.94		0.050	0.005	0.007	2614.5 keV (Tl-208) double escape peak (1592.5 keV)
		1620.76		0.023	0.005	0.008	Bi-212 (Th series), 1620.5 keV
		1630.4		0.024	0.004	0.007	Ac-228 (Th series), 1630.6 keV
		1637.69		0.005	0.004	0.006	Ac-228 (Th series), 1638.3 keV
		1660.91		0.014	0.004	0.007	Bi-214 (U series), 1661.3 keV
		1729.44		0.033	0.005	0.007	Bi-214 (U series), 1729.6 keV
U238	1764.49	1764.49	0	0.215	0.007	0.008	Bi-214 (U series), 1764.5 keV
		1838.19		0.004	0.003	0.005	Bi-214 (U series), 1838.4 keV
		1847.41		0.028	0.005	0.007	Bi-214 (U series), 1847.4 keV
		2103.14		0.081	0.005	0.007	2614.5 keV (Tl-208)

Table D-20. (continued)

Library ID	Library Energy (keV)	Measured Energy (keV)	Energy Residual (keV)	Peak Intensity (c/s)	Intensity Uncert. (c/s)	MDA (c/s)	Analyst Comments
							escape peak (2103.5 keV)
		2203.54		0.065	0.005	0.007	Bi-214 (U series), 2204.2 keV
		2447.36		0.022	0.004	0.005	Bi-214 (U series), 2447.9 keV
Th232	2614.53	2614.12	0.41	0.637	0.010	0.002878	Tl-208 (Th series), 2614.5 keV
		2692.74		0.000629	0.000539	0.000836	below MDA, probably spurious
		2741.9		0.000586	0.000458	0.000683	below MDA, probably spurious

D-2.2.3 Spectrum DB521000

As observed with many other spectra, gamma rays at 795.0 keV and 1407.6 keV are mis-identified. Spectrum DB521000 has a peak at 1452.8 keV for which the source (if it exists) is unknown. This is not dismissed as a spurious peak because peaks at 1452.5 keV and 1451.3 keV exist in spectra DB511000 and DB541000.

A weak peak at 138.2 keV has an intensity below the MDA. The source (if it exists) is unknown. The peak may not be spurious because a more intense peak at 138.1 keV is present in spectrum DB581000. Another peak due to an unknown source is at 234.8 keV. The intensity is below the MDA, but an apparently related peak at 234.6 keV exists in spectrum DB591000.

Spectrum DB521000 has a weak peak corresponding to 129.6 keV. The peak could be associated with the 129.3-keV Pu-239 gamma ray, but this is far from certain because the peak intensity is below the MDA and the signal could be due to the129.1-keV gamma ray from naturally occurring Ac-228. Otherwise, no peaks that could be unambiguously associated with man-made sources appear in spectrum DB521000.

Table D-21. Data for Spectrum DB521000

Library ID	Library Energy (keV)	Calculated Energy (keV)	Energy Residual (keV)	Peak Intensity (c/s)	Intensity Uncert. (c/s)	MDA (c/s)	Analyst Comments
		40.68		0.8136	0.4095	0.0175	probably a spurious low energy peak
		41.26		2.1930	0.0211	0.0196	probably a spurious low energy peak
		46.31		0.6884	0.4204	0.0257	probably a spurious low energy peak
		47.55		1.3500	0.0220	0.0283	probably a spurious low energy peak
		49.29		0.5865	0.4177	0.0294	probably a spurious low energy peak
		55.36		0.6304	0.0216	0.0321	probably a spurious low energy peak
		55.70		0.3736	0.4115	0.0349	probably a spurious low energy peak
		59.83		0.6208	0.0262	0.0403	probably a spurious low energy peak
		65.27		0.2260	0.0206	0.0328	probably a spurious low energy peak

Table D-21. (continued).

Library ID	Library Energy (keV)	Calculated Energy (keV)	Energy Residual (keV)	Peak Intensity (c/s)	Intensity Uncert. (c/s)	MDA (c/s)	Analyst Comments
		68.75		0.1518	0.0227	0.0366	probably a spurious low energy peak
		73.07		0.0927	0.0233	0.0379	probably a spurious low energy peak
Pu239	129.30	129.55	-0.25	0.0260	0.0247	0.0534	Pu-239 (? below MDA); an Ac-228 (Th series) gamma exists at 129.1 keV
		132.14		0.0621	0.0346	0.0568	Th-228 (Th series), 131.6 keV
		138.20		0.0370	0.0251	0.0540	below MDA; also observed in DB581000
U235	185.72	186.54	-0.82	0.0912	0.0151	0.0505	Ra-226 (U series), 186.1 keV; U-235, 185.7 keV
		231.21		0.0428	0.0481	0.0438	below MDA, may be spurious
		234.76		0.0480	0.0229	0.0376	unknown; also observed in DB591000
		239.25		0.5667	0.0579	0.0477	Pb-212 (Th series), 238.6 keV
		270.73		0.0531	0.0167	0.0404	Ac-228 (Th series), 270.2 keV
		295.67		0.2052	0.0119	0.0392	Pb-212 (Th series), 295.2 keV
		300.68		0.0581	0.0106	0.0364	Pb-212 (Th series), 300.1 keV
		328.39		0.0381	0.0099	0.0341	Ac-228 (Th series), 328.0 keV; Bi-212 (Th series), 328.0 keV
		338.62		0.1660	0.0106	0.0330	Ac-228 (Th series), 338.3 keV
U238	351.92	352.18	-0.26	0.4158	0.0205	0.0331	Pb-214 (U series), 351.9 keV
		409.90		0.0303	0.0081	0.0274	Ac-228 (Th series), 409.5 keV
		438.98		0.0246	0.0100	0.0240	Ac-228 (Th series), 440.4 keV (?)
		462.96		0.0759	0.0079	0.0259	Ac-228 (Th series), 463.0 keV
		510.75		0.3619	0.0280	0.0285	annihilation radiation, 511.0 keV
Th232	583.19	583.02	0.17	0.4895	0.0237	0.0225	Tl-208 (Th series), 583.2 keV
U238	609.31	609.12	0.19	0.5584	0.0277	0.0214	Bi-214 (U series), 609.3 keV
		665.14		0.0212	0.0058	0.0181	Bi-214 (U series) 665.4 keV
		702.79		0.0089	0.0083	0.0163	Ac-228, 701.8 keV; Bi-214, 703.1 keV
		726.97		0.1158	0.0094	0.0188	Bi-212 (Th series), 727.3 keV

Table D-21. (continued).

Library ID	Library Energy (keV)	Calculated Energy (keV)	Energy Residual (keV)	Peak Intensity (c/s)	Intensity Uncert. (c/s)	MDA (c/s)	Analyst Comments
		755.25		0.0148	0.0035	0.0165	Ac-228 (Th series), 755.3 keV
		767.95		0.0497	0.0091	0.0172	Bi-214 (U series) 768.3 keV
		771.94		0.0235	0.0084	0.0169	Ac-228 (Th series), 772.3 keV
		785.45		0.0245	0.0081	0.0161	Pb-214 (U series), 785.9 keV; Bi-212 (Th series) 785.4 keV
Cs134	795.85	794.59	1.26	0.0745	0.0089	0.0163	Ac-228 (Th series), 794.9 keV
		835.41		0.0193	0.0103	0.0153	Ac-228 (Th series), 835.7 keV
		840.00		0.0152	0.0086	0.0140	Ac-228 (Th series), 840.4 keV
		860.09		0.0820	0.0057	0.0159	Tl-208 (Th series), 860.6 keV
		904.06		0.0145	0.0047	0.0141	Ac-228 (Th series), 904.2 keV
Th232	911.21	910.73	0.48	0.4683	0.0094	0.0160	Ac-228 (Th series), 911.2 keV
		933.51		0.0373	0.0067	0.0144	Bi-214 (U series), 934.1 keV
		949.09		0.0114	0.0045	0.0143	1460.8 keV (K-40) escape peak (949.8 keV)
		964.24		0.0869	0.0088	0.0155	Bi-214 (U series) 964.1 keV
		968.47		0.2806	0.0121	0.0154	Ac-228 (Th series), 969.0 keV
		1,119.74		0.1933	0.0068	0.0150	Bi-214 (U series), 1120.3 keV
		1,154.91		0.0217	0.0044	0.0137	Bi-214 (U series), 1155.2 keV
		1,237.70		0.0885	0.0056	0.0144	Bi-214 (U series), 1238.1 keV
		1,280.77		0.0156	0.0049	0.0116	Bi-214 (U series), 1281.0 keV
		1,377.32		0.0503	0.0041	0.0102	Bi-214 (U series), 1377.7 keV
		1,401.19		0.0196	0.0042	0.0090	Bi-214 (U series), 1401.5 keV
Eu152	1,408.01	1,407.77	0.24	0.0318	0.0047	0.0096	Bi-214 (U series), 1408.0 keV
		1,452.82		0.0073	0.0042	0.0068	unknown; observed in DB511000 and DB541000
K-40	1,460.83	1,460.63	0.20	2.5610	0.1091	0.0094	K-40, 1460.8 keV
		1,495.59		0.0158	0.0034	0.0070	Ac-228 (Th series), 1495.9 keV
		1,501.61		0.0071	0.0030	0.0069	Ac-228 (Th series), 1501.6 keV
		1,509.14		0.0292	0.0037	0.0070	Bi-214 (U series), 1509.2 keV
		1,556.43		0.0054	0.0021	0.0059	Ac-228 (Th series), 1557.1 keV

Table D-21. (continued).

Library ID	Library Energy (keV)	Calculated Energy (keV)	Energy Residual (keV)	Peak Intensity (c/s)	Intensity Uncert. (c/s)	MDA (c/s)	Analyst Comments
		1,581.48		0.0098	0.0037	0.0065	Ac-228 (Th series), 1580.5 keV
		1,588.16		0.0540	0.0055	0.0071	Ac-228 (Th series), 1588.2 keV
		1,592.53		0.0440	0.0052	0.0068	2614.5 keV (Tl-208) double escape peak (1592.5 keV)
		1,620.73		0.0249	0.0042	0.0065	Bi-212 (Th series), 1620.5 keV
		1,630.52		0.0295	0.0044	0.0064	Ac-228 (Th series), 1630.6 keV
		1,661.47		0.0104	0.0029	0.0061	Bi-214 (U series), 1661.3 keV
		1,694.57		0.0048	0.0024	0.0056	probably spurious
		1,711.70		0.0035	0.0019	0.0051	below MDA, probably spurious
		1,729.73		0.0357	0.0030	0.0061	Bi-214 (U series), 1729.6 keV
U238	1,764.49	1,764.82	-0.33	0.2028	0.0120	0.0063	Bi-214 (U series), 1764.5 keV
		1,847.96		0.0257	0.0034	0.0057	Bi-214 (U series), 1847.4 keV
		2,103.71		0.0734	0.0084	0.0059	2614.5 keV (Tl-208) escape peak (2103.5 keV)
		2,118.77		0.0136	0.0052	0.0056	Bi-214 (U series), 2118.5 keV
		2,204.13		0.0626	0.0061	0.0062	Bi-214 (U series), 2204.2 keV
		2,256.68		0.0028	0.0028	0.0048	below MDA, probably spurious
		2,447.47		0.0184	0.0031	0.0048	Bi-214 (U series), 2447.9 keV
		2,600.59		0.0017	0.0012	0.0020	below MDA, probably spurious
		2,603.76		0.0035	0.0010	0.0012	probably spurious
Th232	2,614.53	2,614.42	0.11	0.6159	0.0551	0.0023	Tl-208 (Th series), 2614.5 keV

D-2.2.4 Spectrum DB531000

Gamma rays at 794.7 keV and 1408.0 keV are mis-identified, as usual. There are two weak peaks corresponding to 102.5 keV and 129.9 keV. The analysis program associated these peaks with the 103.0-keV gamma ray of Am-241 and the 129.3-keV gamma ray of Pu-239. These identifications are far from certain because both peak intensities are below the corresponding MDAs. Additionally, there is no confirming Am-241 signal at 99.0 keV, and the 129.9-keV signal may be mostly due to the 129.1-keV gamma ray of naturally occurring Ac-228.

An unknown gamma ray source produced a peak at 1,538.4 keV. Analogous peaks were also observed in spectra DB551000, DB561000, DB571000, and DB581000. A peak corresponding to 1809.6 keV has an intensity below the MDA, but an analogous peak at 1809.3 keV is also seen in spectrum DB541000. The gamma ray source (if it exists) is unknown.

Spectrum DB531000 has a peak corresponding to 2,223.6 keV, which is apparently due to the 2,223.2-keV hydrogen neutron capture gamma ray. This is surprising in consideration of the fact that the spectrum has no definite signals due to man-made alpha particle emitters. Spectrum DB541000, which was acquired six inches higher than DB31000, has a more intense peak at 2,223.5 keV and also has Am-241 and Pu-239 signatures. It is possible that elevated alpha fluxes at the higher depth promote alpha-n reactions with oxygen, and that the hydrogen neutron capture gamma rays have sufficient energy to penetrate the approximately six inches of intervening material. The gamma rays from Am-241 and Pu-239 are too low in energy to penetrate as far.

Table D-22. Data for Spectrum DB531000

Library ID	Library Energy (keV)	Calculated Energy (keV)	Energy Residual (keV)	Peak Intensity (c/s)	Intensity Uncert. (c/s)	MDA (c/s)	Analyst Comments
		40.29		0.685	0.700	0.023	probably a spurious low energy peak
		40.89		2.542	0.028	0.034	probably a spurious low energy peak
		48.13		0.640	0.026	0.040	probably a spurious low energy peak
Am241	103.00	102.47	0.53	0.036	0.018	0.047	below MDA, no confirming gamma at 99.0 keV, may be spurious
Pu239	129.30	129.92	-0.62	0.034	0.021	0.053	Pu-239 (? below MDA); an Ac-228 (Th series) gamma exists at 129.1 keV
U235	185.72	186.43	-0.71	0.074	0.010	0.050	Ra-226 (U series), 186.1 keV; U-235, 185.7 keV
		238.97		0.532	0.039	0.045	Pb-212 (Th series), 238.6 keV
		253.47		0.032	0.015	0.039	below MDA, Tl-208 (Th series), 252.6 keV
		295.37		0.175	0.019	0.037	Pb-212 (Th series), 295.2 keV
		300.41		0.026	0.022	0.036	Pb-212 (Th series), 300.1 keV
		328.10		0.029	0.010	0.033	Ac-228 (Th series), 328.0 keV; Bi-212 (Th series), 328.0 keV
		338.36		0.155	0.017	0.032	Ac-228 (Th series), 338.3 keV
U238	351.92	351.94	-0.02	0.379	0.016	0.033	Pb-214 (U series), 351.9 keV
		409.31		0.024	0.014	0.027	Ac-228 (Th series), 409.5 keV
		462.73		0.069	0.011	0.024	Ac-228 (Th series), 463.0 keV
		510.61		0.443	0.031	0.030	annihilation radiation, 511.0 keV
Th232	583.19	582.97	0.22	0.479	0.007	0.022	Tl-208 (Th series), 583.2 keV

Table D-22. (continued).

Library ID	Library Energy (keV)	Calculated Energy (keV)	Energy Residual (keV)	Peak Intensity (c/s)	Intensity Uncert. (c/s)	MDA (c/s)	Analyst Comments
U238	609.31	609.09	0.22	0.517	0.010	0.021	Bi-214 (U series), 609.3 keV
		727.01		0.123	0.007	0.017	Bi-212 (Th series), 727.3 keV
		755.51		0.019	0.005	0.016	Ac-228 (Th series), 755.3 keV
U238p	766.36	768.02	-1.66	0.059	0.006	0.017	Bi-214 (U series) 768.3 keV
		772.14		0.028	0.005	0.016	Ac-228 (Th series), 772.3 keV
Cs134	795.85	794.72	1.13	0.078	0.006	0.016	Ac-228 (Th series), 794.9 keV
		806.06		0.016	0.005	0.015	Bi-214 (U series), 806.2 keV
		835.52		0.029	0.007	0.015	Ac-228 (Th series), 835.7 keV
		839.79		0.021	0.006	0.015	Ac-228 (Th series), 840.4 keV
		860.17		0.085	0.006	0.016	Tl-208 (Th series), 860.6 keV
		903.72		0.011	0.009	0.014	Ac-228 (Th series), 904.2 keV
Th232	911.21	910.86	0.35	0.462	0.013	0.015	Ac-228 (Th series), 911.2 keV
		933.67		0.038	0.005	0.014	Bi-214 (U series), 934.1 keV
		950.00		0.017	0.004	0.013	2614.5 keV (K-40) escape peak (949.8 keV)
		964.44		0.092	0.008	0.015	Bi-214 (U series) 964.1 keV
		968.62		0.285	0.011	0.015	Ac-228 (Th series), 969.0 keV
U238p	1,001.03	1,000.64	0.39	0.016	0.006	0.014	Pa-234m (U series), 1001.0 keV
		1,078.27		0.012	0.007	0.012	Bi-212 (Th series) 1078.6 keV
		1,080.56		0.038	0.035	0.013	indistinct, bad background fit, probably spurious
		1,095.99		0.008	0.004	0.013	Ac-228 (Th series), 1095.6 leV
		1,119.97		0.191	0.011	0.015	Bi-214 (U series), 1120.3 keV
		1,154.83		0.018	0.007	0.013	Bi-214 (U series), 1155.2 keV
		1,207.19		0.010	0.005	0.013	Bi-214 (U series), 1207.7 keV
		1,237.80		0.076	0.014	0.014	Bi-214 (U series), 1238.1 keV
		1,280.69		0.012	0.004	0.012	Bi-214 (U series), 1281.0 keV
		1,377.59		0.055	0.004	0.010	Bi-214 (U series), 1377.7 keV
		1,385.09		0.014	0.003	0.009	Bi-214 (U series), 1385.3 keV

Table D-22. (continued).

Library ID	Library Energy (keV)	Calculated Energy (keV)	Energy Residual (keV)	Peak Intensity (c/s)	Intensity Uncert. (c/s)	MDA (c/s)	Analyst Comments
		1,401.29		0.018	0.003	0.009	Bi-214 (U series), 1401.5 keV
Eu152	1,408.01	1,407.99	0.02	0.031	0.004	0.010	Bi-214 (U series), 1408.0 keV
K-40	1,460.83	1,460.83	0.00	2.587	0.054	0.010	K-40, 1460.8 keV
		1,495.95		0.010	0.005	0.007	Ac-228 (Th series), 1495.9 keV
		1,501.35		0.008	0.004	0.007	Ac-228 (Th series), 1501.6 keV
		1,509.46		0.027	0.006	0.008	Bi-214 (U series), 1509.2 keV
		1,538.43		0.005	0.003	0.007	unknown also observed in DB551000, DB561000, DB571000, DB581000
		1,581.74		0.015	0.005	0.007	Ac-228 (Th series), 1580.5 keV
		1,588.33		0.055	0.007	0.008	Ac-228 (Th series), 1588.2 keV
		1,592.78		0.045	0.006	0.007	2614.5 keV (Tl-208) double escape peak (1592.5 keV)
		1,621.02		0.025	0.004	0.007	Bi-212 (Th series), 1620.5 keV
		1,630.97		0.029	0.003	0.007	Ac-228 (Th series), 1630.6 keV
		1,638.52		0.011	0.002	0.006	Ac-228 (Th series), 1638.3 keV
		1,661.66		0.012	0.004	0.006	Bi-214 (U series), 1661.3 keV
		1,730.25		0.040	0.005	0.006	Bi-214 (U series), 1729.6 keV
U238	1,764.49	1,765.04	-0.55	0.205	0.009	0.007	Bi-214 (U series), 1764.5 keV
		1,809.56		0.003	0.002	0.006	below MDA, also observed in DB541000
		1,848.00		0.028	0.003	0.006	Bi-214 (U series), 1847.4 keV
		2,103.92		0.075	0.006	0.006	2614.5 keV (Tl-208) escape peak (2103.5 keV)
		2,118.73		0.018	0.004	0.006	Bi-214 (U series), 2118.5 keV
		2,204.37		0.062	0.004	0.006	Bi-214 (U series), 2204.2 keV
		2,223.59		0.016	0.002	0.006	H neutron capture gamma ray
		2,293.07		0.004	0.002	0.006	below MDA, Bi-214 (U series), 2293.4 keV
		2,447.45		0.019	0.002	0.005	Bi-214 (U series), 2447.9 keV

Table D-22. (continued).

Library ID	Library Energy (keV)	Calculated Energy (keV)	Energy Residual (keV)	Peak Intensity (c/s)	Intensity Uncert. (c/s)	MDA (c/s)	Analyst Comments
		2,606.54		0.002	0.001	0.003	below MDA, multiplet on 2614.5-keV gamma peak
Th232	2,614.53	2,614.32	0.21	0.669	0.010	0.003	Tl-208 (Th series), 2614.5 keV
		2,775.05		0.008	0.005	0.004	indistinct, bad background fit, probably spurious

D-2.2.5 Spectrum DB541000

Like spectra DB581000 and DB591000, this spectrum has many peaks associated with Am-241 and Pu-239 gamma rays. However, no signals attributable to Np-237 are evident. The gamma rays at 794.6 keV and 1407.9 keV are due to the natural background and not Cs-134 or Eu-152, and the gamma ray at 662.2 keV is probably the 662.4-keV Am-241 gamma ray and not the 661.6-keV gamma ray of Cs-137.

The 1001.0-keV Pa-234m gamma ray peak in this spectrum has an elevated intensity relative to the analogous peaks in the nine other spectra from P6-PU-1 and P6-PU-2. This suggests that the U-238 concentration may be anomalously high, such as would be the case if purified uranium were present.

An unknown source apparently emits 141.3-keV gamma rays. The intensity of the peak is below the MDA, but the peak is not regarded as spurious because a peak at 141.5 keV exists in spectrum DB591000. Other peaks of unknown origin appear at 451.5 keV and 652.3 keV. The 652.3-keV peak intensity is below the MDA, but neither peak is dismissed as spurious because peaks at 451.6 keV and 652.7 keV occur in spectrum DB591000. Another unknown source of gamma rays produced a peak at 1451.3 keV at an intensity just above the MDA. Analogous peaks at 1452.5 keV and 1452.8 keV were observed in spectra DB511000 and DB521000. An 1809.3-keV gamma ray of unknown origin apparently also accounted for the peak at 1809.6 keV in spectrum DB531000.

A peak at 1274.2 keV was identified as Eu-154 by the analysis program. This is probably an incorrect identification because the spectrum has no peaks corresponding to the 723.3- or 123.1-keV gamma rays of Eu-154. However, the origin of the gamma ray (if it exists) is unknown.

Spectrum DB541000 has a peak at 2223.5 keV that is attributed to the 2223.2-keV hydrogen neutron capture gamma ray.

Table D-23. Data for Spectrum DB541000

Library ID	Library Energy (keV)	Calculated Energy (keV	Energy Residual (keV)	Peak Intensity (c/s)	Intensity Uncert. (c/s)	MDA (c/s)	Analyst Comments
		48.62		0.029	0.022	0.061	probably a spurious low energy peak
Pu239	129.30	130.03	-0.73	0.169	0.028	0.077	probably Pu-239; an Ac-228 (Th series) gamma exists at 129.1 keV
		141.27		0.095	0.061	0.100	below MDA;

Table D-23. (continued).

Library ID	Library Energy (keV)	Calculated Energy (keV	Energy Residual (keV)	Peak Intensity (c/s)	Intensity Uncert. (c/s)	MDA (c/s)	Analyst Comments
							also observed in DB591000
		146.97		0.045	0.027	0.073	below MDA, probably spurious
		149.46		0.024	0.027	0.068	below MDA, probably spurious
U235	185.72	186.31	-0.59	0.141	0.013	0.071	Ra-226 (U series), 186.1 keV; U-235, 185.7 keV
		204.20		0.094	0.024	0.067	Pu-239 (203.6 keV)
		208.66		0.208	0.024	0.062	Am-241 (208.0 keV)
		239.13		0.445	0.052	0.059	Pb-212 (Th series), 238.6 keV
		295.53		0.151	0.024	0.048	Pb-212 (Th series), 295.2 keV
		332.94		0.176	0.059	0.040	Pu-239 (332.8 keV)
		335.73		0.169	0.024	0.040	Am-241 (335.4 keV)
		338.49		0.084	0.055	0.039	Ac-228 (Th series), 338.3 keV
		345.15		0.141	0.025	0.040	Pu-239 (345.0 keV)
U238	351.92	352.07	-0.15	0.364	0.027	0.041	Pb-214 (U series), 351.9 keV
		368.51		0.109	0.037	0.037	Pu-239 (367.1 keV, 368.6 keV)
Pu239	375.05	375.15	-0.10	0.524	0.046	0.036	Pu-239 (375.1 keV)
		380.31		0.152	0.024	0.039	Pu-239 (380.2 keV)
		382.79		0.078	0.035	0.035	Pu-239 (382.8 keV)
		392.96		0.165	0.014	0.034	Pu-239 (392.5 keV)
		409.54		0.022	0.017	0.028	Ac-228 (Th series), 409.5 keV
		413.69		0.515	0.019	0.031	Pu-239 (413.7 keV)
		451.46		0.076	0.009	0.029	unknown; also occurs in DB591000
		463.02		0.059	0.008	0.028	Ac-228 (Th series), 463.0 keV
		510.78		0.615	0.037	0.034	annihilation radiation, 511.0 keV
Th232	583.19	583.02	0.17	0.424	0.012	0.024	Tl-208 (Th series), 583.2 keV
U238	609.31	609.14	0.17	0.486	0.016	0.023	Bi-214 (U series), 609.3 keV
		618.89		0.024	0.006	0.021	Am-241 (619.0 keV)
		652.28		0.018	0.006	0.019	below MDA, unknown, also observed in DB591000.
Cs137	661.66	662.18	-0.52	0.172	0.012	0.021	probably Am-241 (662.4 keV)
		721.69		0.098	0.007	0.019	Am-241 (722.0 keV)
		727.07		0.100	0.007	0.019	Bi-212 (Th series), 727.3 keV
		763.97		0.016	0.012	0.017	below MDA, may be

Table D-23. (continued).

Library ID	Library Energy (keV)	Calculated Energy (keV	Energy Residual (keV)	Peak Intensity (c/s)	Intensity Uncert. (c/s)	MDA (c/s)	Analyst Comments
							Tl-208 (Th series), 763.1 keV
U238p	766.36	767.96	-1.60	0.070	0.014	0.017	Bi-214 (U series) 768.3 keV
		772.10		0.023	0.012	0.017	Ac-228 (Th series), 772.3 keV
		785.31		0.013	0.012	0.019	below MDA; may be Pb-214 (U series), 785.9 keV; Bi-212 (Th series) 785.4 keV
Cs134	795.85	794.62	1.23	0.063	0.011	0.017	Ac-228 (Th series), 794.9 keV
		805.51		0.015	0.005	0.016	Bi-214 (U series), 806.2 keV
		860.26		0.063	0.006	0.016	Tl-208 (Th series), 860.6 keV
		893.11		0.010	0.005	0.015	below MDA, probably spurious
Th232	911.21	910.85	0.36	0.387	0.015	0.016	Ac-228 (Th series), 911.2 keV
		933.63		0.038	0.005	0.015	Bi-214 (U series), 934.1 keV
		949.09		0.011	0.005	0.014	1460.8 keV (K-40) escape peak (949.8 keV)
		964.36		0.068	0.008	0.016	Bi-214 (U series) 964.1 keV
		968.60		0.240	0.011	0.015	Ac-228 (Th series), 969.0 keV
U238p	1,001.03	1,000.73	0.30	0.057	0.007	0.015	Pa-234m (U series), 1001.0 keV
		1,050.13		0.011	0.005	0.013	below MDA, probably spurious
		1,078.00		0.010	0.004	0.014	Bi-212 (Th series) 1078.6 keV
		1,103.47		0.009	0.007	0.013	below MDA, probably spurious
		1,119.96		0.183	0.006	0.015	Bi-214 (U series), 1120.3 keV
		1,154.79		0.023	0.008	0.014	Bi-214 (U series), 1155.2 keV
		1,237.87		0.072	0.005	0.014	Bi-214 (U series), 1238.1 keV
Eu154	1,274.44	1,274.17	0.27	0.025	0.006	0.012	unknown; probably not Eu-154, no confirming peak at 723.3 keV or 123.1 keV
		1,281.03		0.011	0.006	0.012	Bi-214 (U series), 1281.0 keV
		1,315.64		0.006	0.004	0.010	below MDA, probably spurious
		1,377.64		0.050	0.005	0.010	Bi-214 (U series), 1377.7 keV
		1,401.52		0.017	0.003	0.010	Bi-214 (U series), 1401.5 keV
Eu152	1,408.01	1,407.89	0.12	0.030	0.004	0.010	Bi-214 (U series), 1408.0 keV
		1,451.33		0.011	0.006	0.009	unknown; also observed in DB511000 and DB521000
K-40	1,460.83	1,460.81	0.02	2.194	0.069	0.010	K-40, 1460.8 keV
		1,495.98		0.019	0.004	0.008	Ac-228 (Th series), 1495.9 keV
		1,502.11		0.010	0.003	0.008	Ac-228 (Th series), 1501.6 keV

Table D-23. (continued).

Library ID	Library Energy (keV)	Calculated Energy (keV	Energy Residual (keV)	Peak Intensity (c/s)	Intensity Uncert. (c/s)	MDA (c/s)	Analyst Comments
		1,509.37		0.031	0.004	0.008	Bi-214 (U series), 1509.2 keV
		1,581.85		0.009	0.004	0.008	Ac-228 (Th series), 1580.5 keV
		1,588.37		0.048	0.005	0.009	Ac-228 (Th series), 1588.2 keV
		1,592.80		0.045	0.005	0.008	2614.5 keV (Tl-208) double escape peak (1592.5 keV)
		1,620.97		0.032	0.004	0.008	Bi-212 (Th series), 1620.5 keV
		1,630.86		0.024	0.004	0.007	Ac-228 (Th series), 1630.6 keV
		1,638.45		0.008	0.004	0.007	Ac-228 (Th series), 1638.3 keV
		1,661.43		0.010	0.003	0.007	Bi-214 (U series), 1661.3 keV
		1,730.07		0.030	0.007	0.008	Bi-214 (U series), 1729.6 keV
U238	1,764.49	1,764.99	-0.50	0.200	0.010	0.008	Bi-214 (U series), 1764.5 keV
		1,809.33		0.011	0.003	0.007	unknown; also observed in DB531000
		1,848.05		0.025	0.003	0.007	Bi-214 (U series), 1847.4 keV
		2,103.78		0.078	0.006	0.007	2614.5 keV (Tl-208) escape peak (2103.5 keV)
		2,118.95		0.014	0.003	0.007	Bi-214 (U series), 2118.5 keV
		2,204.29		0.064	0.004	0.007	Bi-214 (U series), 2204.2 keV
		2,223.49		0.074	0.004	0.007	H neutron capture gamma ray
		2,447.66		0.021	0.003	0.006	Bi-214 (U series), 2447.9 keV
Th232	2,614.53	2,614.34	0.18	0.700	0.021	0.004	Tl-208 (Th series), 2614.5 keV
		2,753.39		0.003	0.001	0.003	indistinct with bad background fit, spurious
		2,774.03		0.015	0.012	0.006	indistinct with bad background fit, spurious

ATTACHMENT

INEEL Passive Gamma-Ray Spectrum DB501000.CHN

February 2, 2004

Site	SDA Area 5
Borehole	P6-PU-2
Depth	20.06 feet
Acquisition Date	January 15, 2004
Logging System	Gamma 4B (35-percent-efficient HPGe, 36TP21095A)
Counting Time	8 hours (28724.5 seconds, live time)
Data Analyst	C. J. Koizumi

The before-survey spectrum (DB501CAB.CHN) and post-survey spectrum (DB501CAA.CHN) were analyzed. Nothing indicative of system malfunctions was observed.

The before-survey spectrum was energy-calibrated, then that energy calibration was "imported" to the post-survey spectrum. The peaks in the post-survey spectrum were shifted in energy as indicated by the plot in Figure D-1.

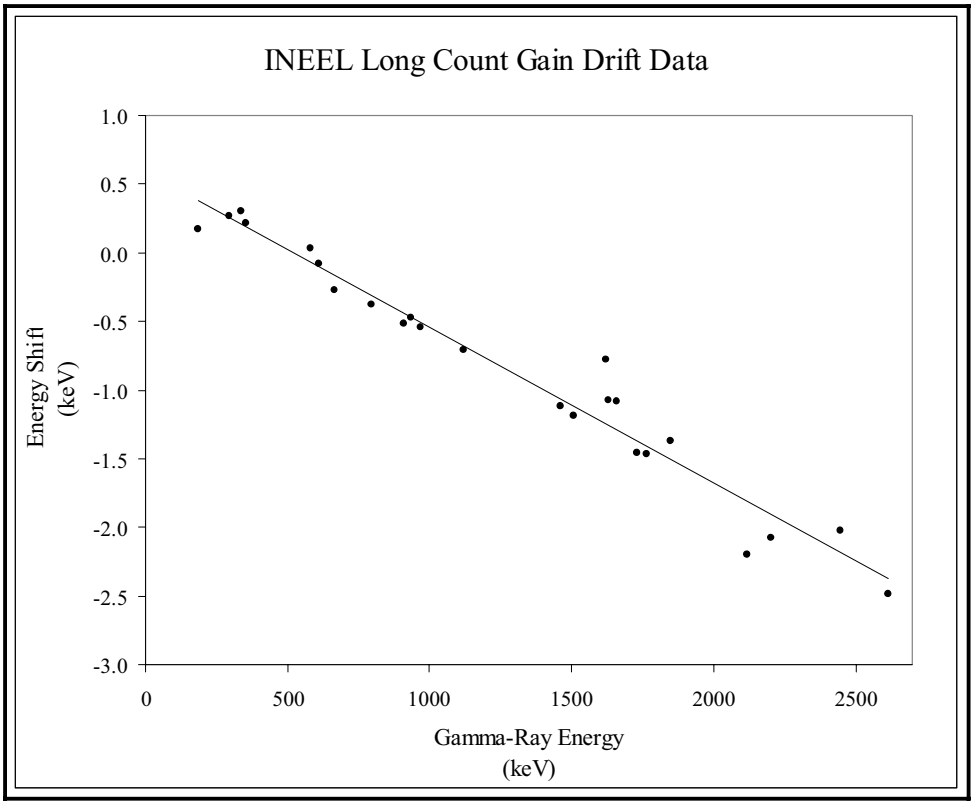

Figure D-1. Gain shift over the acquisition time.

The apparent energy shift was a function of gamma ray energy. The greatest shift of approximately -2.5 keV occurred for the peak associated with the 2614.5-keV gamma ray of Tl-208 (Th series). (The spectrum analysis program calculated the energy to be 2612.0 keV in the post-survey spectrum.) The gain drift should not be overlooked because drift broadens the spectral peak widths. This could cause counts due to a particular gamma ray to be tallied in a wide peak that could be erroneously resolved into two or more "multiplets" by the *Multifit* (Gaussian peak fitting) algorithm in the spectrum analysis software. The plot in Figure D-1 indicates the net gain shift and gives no information about the rate of gain drift over time.

The borehole spectrum DB501000.CHN was energy-calibrated, then analyzed by two methods. The important analysis settings common to both methods were as follows.

- ROI Properties
  - Background curve: third degree
  - Background end points: five on each side of the peak
- Peaksearch
  - Maximum error of 100 percent.

The *Identify* algorithm in the analysis program referenced a source identification data base (library) containing the most intense gamma rays for Am-241, Co-60, Cs-134, Cs-137, Eu-152, Eu-154, Np-237, Pu-239, Ru-106, Sb-125, Sb-126, and Tc-99. Using this library, the analysis program will identify these man-made sources whenever the concentrations are high enough to produce detectable gamma ray peaks.

The first analysis employed the *Peaksearch* and *Identify* algorithms in the analysis program, and yielded the data in Tables 1 and 2.

Table 1. Peaks identified by *Peaksearch* and *Identify.*

Source	Library Energy (keV)	Calculated Energy (keV)	Energy Residual (keV)	Peak FWHM (keV)	Peak Intensity (c/s)
U238	351.92	351.86	0.06	1.74	0.419 ± 0.029
Th232	583.19	583.22	-0.03	1.92	0.446 ± 0.017
U238	609.31	609.37	-0.06	2.05	0.553 ± 0.016
Cs134	795.85	794.99	0.86	2.32	0.053 ± 0.012
Th232	911.21	911.16	0.05	2.26	0.373 ± 0.014
U238p	1,001.03	1,000.84	0.19	2.98	0.019 ± 0.008
Eu152	1,408.01	1,407.91	0.10	2.46	0.033 ± 0.006
K-40	1,460.83	1,460.70	0.13	2.98	2.112 ± 0.019
U238	1,764.49	1,764.58	-0.09	3.19	0.220 ± 0.007
Th232	2,614.53	2,614.49	0.04	4.05	0.558 ± 0.009

Table 2. Peaks not identified by *Peaksearch* and *Identify*.

Peak Number	Calculated Energy (keV)	Peak Intensity (c/s)	MDA[a] (c/s)
1	238.59	0.629 ± 0.034	0.054
2	295.19	0.218 ± 0.032	0.052
3	338.34	0.148 ± 0.028	0.045
5	463.04	0.057 ± 0.017	0.027
6	510.80	0.319 ± 0.024	0.039
9	727.27	0.102 ± 0.013	0.021
10	768.31	0.061 ± 0.014	0.023
12	836.16	0.024 ± 0.011	0.018
13	860.54	0.061 ± 0.011	0.018
15	934.06	0.043 ± 0.011	0.018
16	968.86	0.315 ± 0.015	0.021
18	1,120.16	0.201 ± 0.010	0.015
19	1,155.13	0.035 ± 0.009	0.015
20	1,238.05	0.082 ± 0.012	0.019
21	1,377.45	0.061 ± 0.006	0.009
22	1,400.96	0.021 ± 0.005	0.008
25	1,496.05	0.012 ± 0.004	0.007
26	1,501.07	0.008 ± 0.004	0.006
27	1,509.11	0.029 ± 0.005	0.008
28	1,581.92	0.019 ± 0.004	0.005
29	1,588.43	0.094 ± 0.006	0.007
30	1,598.83	0.006 ± 0.003	0.005
31	1,620.64	0.024 ± 0.005	0.007
32	1,630.35	0.021 ± 0.004	0.006
33	1,660.99	0.018 ± 0.005	0.007
34	1,729.77	0.036 ± 0.004	0.006
36	1,847.69	0.029 ± 0.004	0.006
37	2,103.44	0.072 ± 0.005	0.006
38	2,118.11	0.014 ± 0.004	0.006
39	2,203.58	0.069 ± 0.005	0.006
40	2,447.35	0.021 ± 0.003	0.005

a. Minimum Detectable Activity

The second analysis employed the *Peaksearch, Multifit,* and *Identify* algorithms in the analysis program. *Multifit* was executed because of the possibility that peaks were significantly broadened by gain drift. With broad peaks, several analysis errors are possible. Several peaks due to gamma rays with similar energies can merge into a "multiplet," and one or more of the peaks in the multiplet can go undetected. It is also possible that signals due to monoenergetic gamma rays can produce a broad peak that the analysis program resolves as two or more peaks.

The second analysis yielded the data in Tables 3 and 4.

Table 3. Peaks identified by *Peaksearch*, *Multifit*, and *Identify*.

Source	Library Energy (keV)	Calculated Energy (keV)	Energy Residual (keV)	Peak FWHM (keV)	Flag	Peak Intensity (c/s)
U235	185.72	185.88	-0.16	2.14	?[a]	0.048 ± 0.032
U238	351.92	351.86	0.06	1.73		0.416 ± 0.023
Th232	583.19	583.22	-0.03	1.92		0.446 ± 0.017
U238	609.31	609.37	-0.06	2.05		0.553 ± 0.016
Cs134	795.85	795.02	0.83	2.19	M[b]	0.064 ± 0.008
Th232	911.21	911.16	0.05	2.28		0.390 ± 0.013
U238p	1,001.03	1,001.00	0.03	—		0.028 ± 0.007
Eu152	1,408.01	1,408.04	-0.03	2.83	m	0.029 ± 0.003
K-40	1,460.83	1,460.70	0.13	2.98		2.114 ± 0.018
U238	1,764.49	1,764.59	-0.10	3.20		0.222 ± 0.007
Th232	2,614.53	2,614.49	0.04	4.05		0.558 ± 0.009

a. The peak intensity was below the MDA.
b. The peak was a component in a multiplet.

Table 4. Peaks not identified by *Peaksearch*, *Multifit*, and *Identify*.

Peak Number	Calculated Energy (keV)	Flag	Peak Intensity (keV)	MDA (c/s)
1	127.26	?	0.042 ± 0.035	0.058
3	238.59		0.629 ± 0.034	0.054
4	270.52	?	0.039 ± 0.025	0.041
5	294.61		0.166 ± 14.89	0.035
6	338.34		0.135 ± 0.021	0.034
8	463.04		0.056 ± 0.015	0.025
9	510.80		0.295 ± 0.017	0.026
12	665.44	?	0.013 ± 0.010	0.017
13	727.27		0.103 ± 0.013	0.020
14	755.38		0.025 ± 0.010	0.016

Table 4. (continued).

Peak Number	Calculated Energy (keV)	Flag	Peak Intensity (keV)	MDA (c/s)
15	768.27		0.031 ± 0.010	0.017
16	785.62	m	0.019 ± 0.007	0.015
18	806.28	?	0.016 ± 0.010	0.016
19	830.98	m?	0.012 ± 0.006	0.014
20	836.00	m	0.022 ± 0.006	0.014
21	860.55		0.064 ± 0.009	0.015
23	934.09		0.042 ± 0.010	0.017
24	949.64		0.017 ± 0.008	0.014
25	964.65	m	0.074 ± 0.005	0.014
26	968.91	m	0.242 ± 0.007	0.014
27	980.89	?	0.009 ± 0.008	0.013
29	1,078.62	?	0.009 ± 0.007	0.011
30	1,120.16		0.201 ± 0.010	0.015
31	1,155.13		0.035 ± 0.009	0.015
32	1,208.27	?	0.008 ± 0.007	0.012
33	1,237.63		0.072 ± 0.008	0.013
34	1,281.04		0.012 ± 0.007	0.011
35	1,377.51	m	0.060 ± 0.004	0.010
36	1,385.35	m	0.011 ± 0.003	0.009
37	1,401.01	m	0.019 ± 0.003	0.009
40	1,495.94	m	0.011 ± 0.004	0.007
41	1,501.66	m?	0.005 ± 0.003	0.007
42	1,509.35	m	0.026 ± 0.004	0.007
43	1,554.93	?	0.005 ± 0.003	0.006
44	1,581.57	m	0.011 ± 0.004	0.006
45	1,588.14	m	0.048 ± 0.006	0.006
46	1,592.57	m	0.038 ± 0.005	0.007
47	1,620.82	m	0.022 ± 0.004	0.006
48	1,630.38	m	0.030 ± 0.005	0.006
49	1,660.97		0.014 ± 0.004	0.006
50	1,729.64		0.037 ± 0.004	0.006
52	1,793.53	?	-0.001 ± 0.012	0.004
53	1,838.33	m?	0.004 ± 0.002	0.005

Table 4. (continued).

Peak Number	Calculated Energy (keV)	Flag	Peak Intensity (keV)	MDA (c/s)
54	1,847.75	m	0.028 ± 0.003	0.005
55	1,872.52	m	0.005 ± 0.002	0.005
56	1,876.32	m?	0.004 ± 0.002	0.005
57	1,937.14	?	0.003 ± 0.003	0.004
58	2,103.43		0.070 ± 0.005	0.006
59	2,118.16		0.018 ± 0.003	0.005
60	2,203.58		0.069 ± 0.005	0.006
61	2,447.35		0.021 ± 0.003	0.005
63	2,805.18	?	0.0008 ± 0.0007	0.0010

The peaks in Table 3 correlate well to their counterparts in Table 1, and in general, no peaks were broad enough to be erroneously resolved as multiplets. Table 3 has an entry for a peak at 185.7 keV (composite peak for the 185.7-keV gamma ray of U-235 and the 186.1-keV gamma ray of Ra-226) that does not appear in Table 1. This peak was found as a result of the *Multifit* execution, but the intensity is less than the MDA.

Tables 2 and 4 indicate that when the *Multifit* algorithm was employed, the analysis program found 23 peaks more than were found without running *Multifit*. Table 2 has a peak at 1598.8 keV that is absent from Table 4.

All of the peaks that the analysis program attributed to man-made sources or unknown sources are listed in Table 5. These peaks were individually assessed. The results of the assessments are in the right side column of Table 5.

Table 5. Assessment of peaks not identified by analysis program.

Program ID	Calculated Energy (keV)	Flag	Peak Intensity (c/s)	MDA (c/s)	Analyst's IDs and Comments
	127.26	?	0.042 ± 0.035	0.058	intensity below MDA, probably spurious
	238.59		0.629 ± 0.034	0.054	Pb-212 (Th series), 238.6 keV
	270.52	?	0.039 ± 0.025	0.041	below MDA, but identified as Ac-228 (Th series), at 270.2 keV
	294.61		0.166 ± 14.9	0.035	Pb-214 (U series), 295.2 keV, large uncertainty
	338.34		0.135 ± 0.021	0.034	Ac-228 (Th series), 338.3 keV
	463.04		0.056 ± 0.015	0.025	Ac-228 (Th series), 463.0 keV
	510.80		0.295 ± 0.017	0.026	annihilation radiation (511.0 keV)
	665.44	?	0.013 ± 0.010	0.017	below MDA, but identified as Bi-214 (U series), 665.4 keV
	727.27		0.103 ± 0.013	0.020	Ac-228, 726.9 keV; Bi-212 (Th series), 727.3 keV
	755.38		0.025 ± 0.010	0.016	Ac-228 (Th series), 755.3 keV

Table 5. (continued).

Program ID	Calculated Energy (keV)	Flag	Peak Intensity (c/s)	MDA (c/s)	Analyst's IDs and Comments
	768.27		0.031 ± 0.010	0.017	Bi-214 (U series), 768.3 keV
	785.62	m	0.019 ± 0.007	0.015	Pb-214 (U series), 785.9 keV; Bi-212 (Th series) 785.4 keV
Cs134	795.02		0.064 ± 0.008	0.015	Ac-228 (Th series), 794.9 keV
	806.28	?	0.016 ± 0.010	0.016	below MDA, but identified as Bi-214 (U series), 806.2 keV
	830.98	m?	0.012 ± 0.006	0.014	below MDA, but identified asAc-228 (Th series), 830.5 keV
	836.00	m	0.022 ± 0.006	0.014	Ac-228 (Th series), 835.7 keV
	860.55		0.064 ± 0.009	0.015	Tl-208 (Th series), 860.6 keV
	934.09		0.042 ± 0.010	0.017	Bi-214 (U series), 934.1 keV
	949.64		0.017 ± 0.008	0.014	K-40 gamma escape peak (949.8 keV)
	964.65	m	0.074 ± 0.005	0.014	Bi-214 (U series) 964.1 keV
	968.91	m	0.242 ± 0.007	0.014	Ac-228 (Th series), 969.0 keV
	980.89	?	0.009 ± 0.008	0.013	below MDA, probably spurious
	1078.62	?	0.009 ± 0.007	0.011	below MDA, but identified as Bi-212 (Th series) 1078.6 keV
	1120.16		0.201 ± 0.010	0.015	Bi-214 (U series), 1120.3 keV
	1155.13		0.035 ± 0.009	0.015	Bi-214 (U series), 1155.2 keV
	1208.27	?	0.008 ± 0.007	0.012	below MDA, but identified as Bi-214 (U series), 1207.7 keV
	1237.63		0.072 ± 0.008	0.013	Bi-214 (U series), 1238.1 keV
	1281.04		0.012 ± 0.007	0.011	Bi-214 (U series), 1281.0 keV
	1377.51	m	0.060 ± 0.004	0.010	Bi-214 (U series), 1377.7 keV
	1385.35	m	0.011 ± 0.003	0.009	Bi-214 (U series), 1385.3 keV
	1401.01	m	0.019 ± 0.003	0.009	Bi-214 (U series), 1401.5 keV
Eu152	1408.04	m	0.029 ± 0.003	0.009	Bi-214 (U series), 1408.0 keV
	1495.94	m	0.011 ± 0.004	0.007	Ac-228 (Th series), 1495.9 keV
	1501.66	m?	0.005 ± 0.003	0.007	below MDA, but identified as Ac-228 (Th series), 1501.6 keV
	1509.35	m	0.026 ± 0.004	0.007	Bi-214 (U series), 1509.2 keV
	1554.93	?	0.005 ± 0.003	0.006	below MDA, probably spurious
	1581.57	m	0.011 ± 0.004	0.006	Ac-228 (Th series), 1580.5 keV
	1588.14	m	0.048 ± 0.006	0.006	Ac-228 (Th series), 1588.2 keV
	1592.57	m	0.038 ± 0.005	0.007	Tl-208 (Th series) pair at 1592.5 keV
	1598.83		0.006 ± 0.003	0.005	Bi-214 (U series), 1599.3 keV
	1620.82	m	0.022 ± 0.004	0.006	Bi-212 (Th series), 1620.5 keV

Table 5. (continued).

Program ID	Calculated Energy (keV)	Flag	Peak Intensity (c/s)	MDA (c/s)	Analyst's IDs and Comments
	1630.38	m	0.030 ± 0.005	0.006	Ac-228 (Th series), 1630.6 keV
	1660.97		0.014 ± 0.004	0.006	Bi-214 (U series), 1661.3 keV
	1729.64		0.037 ± 0.004	0.006	Bi-214 (U series), 1729.6 keV
	1793.53	?	-0.001 ± 0.012	0.004	below MDA, negative intensity, most likely spurious
	1838.33	m?	0.004 ± 0.002	0.005	Bi-214 (U series), 1838.4 keV
	1847.75	m	0.028 ± 0.003	0.005	Bi-214 (U series), 1847.4 keV
	1872.52	m	0.005 ± 0.002	0.005	Bi-214 (U series), 1873.2 keV
	1876.32	m?	0.004 ± 0.002	0.005	below MDA, probably spurious
	1937.14	?	0.003 ± 0.003	0.004	below MDA, but 1936.6 keV occurs in SBU cal spectra
	2103.43		0.070 ± 0.005	0.006	Tl-208 (Th series) pair at 2103.5 keV
	2118.16		0.018 ± 0.003	0.005	Bi-214 (U series), 2118.6 keV
	2203.58		0.069 ± 0.005	0.006	Bi-214 (U series), 2204.2 keV
	2447.35		0.021 ± 0.003	0.005	Bi-214 (U series), 2447.9 keV
	2805.18	?	0.0008 ± 0.0007	0.0010	below MDA, probably spurious

The Cs-134 identification is discounted because there is no evidence of a confirming peak corresponding to the 604.7-keV gamma ray of Cs-134. The 795-keV gamma ray is attributed to naturally occurring Ac-228 (794.9 keV) instead of Cs-134 (795.8 keV).

The Eu-152 identification is discounted because there is no evidence of confirming peaks corresponding to the Eu-152 gamma rays with energies 121.8 keV and 1112.1 keV. Thus, the 1408-keV gamma ray is attributed to naturally occurring Bi-214 (1408.0 keV), and likewise, the 965-keV gamma ray is attributed to Bi-214 (964.1 keV) and not Eu-152 (964.1 keV).

In summary, all of the spectral peaks are associated with naturally occurring potassium, uranium, and thorium. This spectrum shows no evidence of gamma rays originating in Am-241, Co-60, Cs-134, Cs-137, Eu-152, Eu-154, Np-237, Pu-239, Ru-106, Sb-125, Sb-126, or Tc-99.

Calculated natural background concentrations of potassium, uranium, and thorium are presented in Table 6. The peak intensities calculated with *Multifit* were used.

Table 6. Potassium, uranium, and thorium concentrations.

Source	Gamma Ray (keV)	Concentration (pCi/g)
Potassium (K-40)	1,460.8	16.7 ± 0.1
Uranium (Bi-214	609.3	1.14 ± 0.03
Thorium (TI-208)	2,614.5	1.25 ± 0.02

INEEL Passive Gamma-Ray Spectrum DB501000.CHN

February 2, 2004

Site	SDA Area 5
Borehole	P6-PU-2
Depth	20.06 feet
Acquisition Date	January 15, 2004
Logging System	Gamma 4B (35-percent-efficient HPGe, 36TP21095A)
Counting Time	8 hours (28724.5 seconds, live time)
Data Analyst	C. J. Koizumi

The before-survey spectrum (DB501CAB.CHN) and post-survey spectrum (DB501CAA.CHN) were analyzed. Nothing indicative of system malfunctions was observed.

The before-survey spectrum was energy-calibrated, then that energy calibration was "imported" to the post-survey spectrum. The peaks in the post-survey spectrum were shifted in energy as indicated by the plot in Figure D-2.

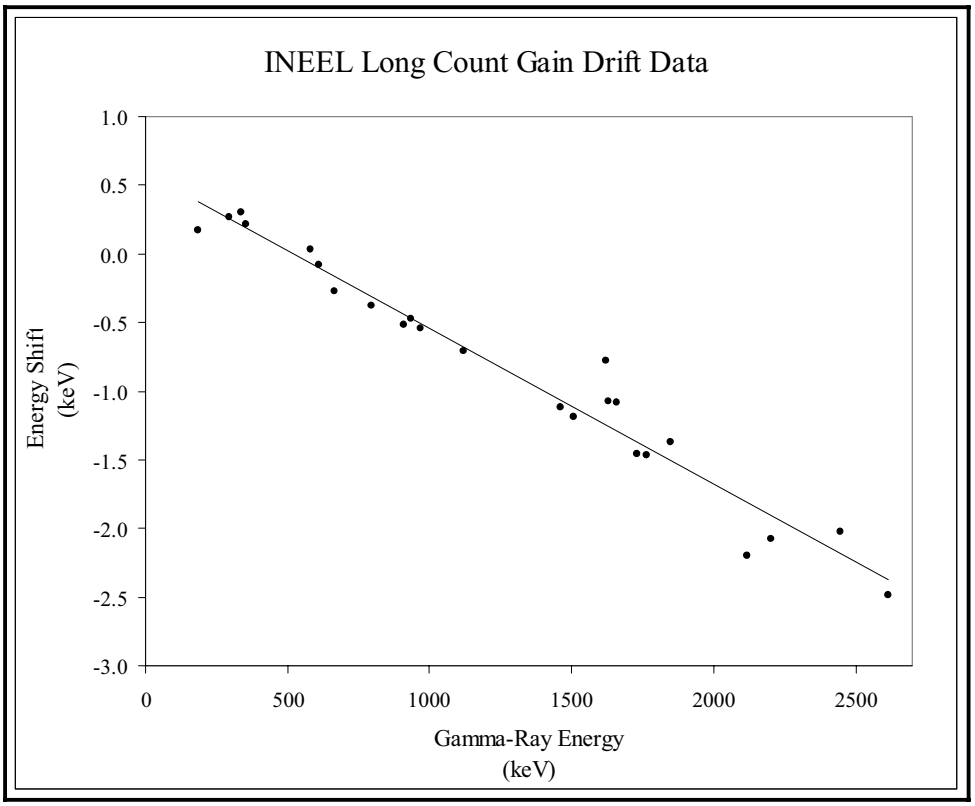

Figure D-2. Gain shift over the acquisition time.

The apparent energy shift was a function of gamma ray energy. The greatest shift of approximately -2.5 keV occurred for the peak associated with the 2614.5-keV gamma ray of Tl-208 (Th series). (The

spectrum analysis program calculated the energy to be 2612.0 keV in the post-survey spectrum.) The gain drift should not be overlooked because drift broadens the spectral peak widths. This could cause counts due to a particular gamma ray to be tallied in a wide peak that could be erroneously resolved into two or more "multiplets" by the *Multifit* (Gaussian peak fitting) algorithm in the spectrum analysis software. The plot in Figure D-2 indicates the net gain shift and gives no information about the rate of gain drift over time.

The borehole spectrum DB501000.CHN was energy-calibrated, then analyzed by two methods. The important analysis settings common to both methods were as follows.

- ROI Properties
  - Background curve: third degree
  - Background end points: five on each side of the peak
- Peaksearch
  - Maximum error of 100 percent.

The *Identify* algorithm in the analysis program referenced a source identification data base (library) containing the most intense gamma rays for Am-241, Co-60, Cs-134, Cs-137, Eu-152, Eu-154, Np-237, Pu-239, Ru-106, Sb-125, Sb-126, and Tc-99. Using this library, the analysis program will identify these man-made sources whenever the concentrations are high enough to produce detectable gamma ray peaks.

The first analysis employed the *Peaksearch* and *Identify* algorithms in the analysis program, and yielded the data in Tables 1 and 2.

Table 1. Peaks identified by *Peaksearch* and *Identify*.

Source	Library Energy (keV)	Calculated Energy (keV)	Energy Residual (keV)	Peak FWHM (keV)	Peak Intensity (c/s)
U238	351.92	351.86	0.06	1.74	0.419 ± 0.029
Th232	583.19	583.22	-0.03	1.92	0.446 ± 0.017
U238	609.31	609.37	-0.06	2.05	0.553 ± 0.016
Cs134	795.85	794.99	0.86	2.32	0.053 ± 0.012
Th232	911.21	911.16	0.05	2.26	0.373 ± 0.014
U238p	1,001.03	1,000.84	0.19	2.98	0.019 ± 0.008
Eu152	1,408.01	1,407.91	0.10	2.46	0.033 ± 0.006
K-40	1,460.83	1,460.70	0.13	2.98	2.112 ± 0.019
U238	1,764.49	1,764.58	-0.09	3.19	0.220 ± 0.007
Th232	2,614.53	2,614.49	0.04	4.05	0.558 ± 0.009

Table 2. Peaks not identified by *Peaksearch* and *Identify*.

Peak Number	Calculated Energy (keV)	Peak Intensity (c/s)	MDA[a] (c/s)
1	238.59	0.629 ± 0.034	0.054
2	295.19	0.218 ± 0.032	0.052
3	338.34	0.148 ± 0.028	0.045
5	463.04	0.057 ± 0.017	0.027
6	510.80	0.319 ± 0.024	0.039
9	727.27	0.102 ± 0.013	0.021
10	768.31	0.061 ± 0.014	0.023
12	836.16	0.024 ± 0.011	0.018
13	860.54	0.061 ± 0.011	0.018
15	934.06	0.043 ± 0.011	0.018
16	968.86	0.315 ± 0.015	0.021
18	1,120.16	0.201 ± 0.010	0.015
19	1,155.13	0.035 ± 0.009	0.015
20	1,238.05	0.082 ± 0.012	0.019
21	1,377.45	0.061 ± 0.006	0.009
22	1,400.96	0.021 ± 0.005	0.008
25	1,496.05	0.012 ± 0.004	0.007
26	1,501.07	0.008 ± 0.004	0.006
27	1,509.11	0.029 ± 0.005	0.008
28	1,581.92	0.019 ± 0.004	0.005
29	1,588.43	0.094 ± 0.006	0.007
30	1,598.83	0.006 ± 0.003	0.005
31	1,620.64	0.024 ± 0.005	0.007
32	1,630.35	0.021 ± 0.004	0.006
33	1,660.99	0.018 ± 0.005	0.007
34	1,729.77	0.036 ± 0.004	0.006
36	1,847.69	0.029 ± 0.004	0.006
37	2,103.44	0.072 ± 0.005	0.006
38	2,118.11	0.014 ± 0.004	0.006
39	2,203.58	0.069 ± 0.005	0.006
40	2,447.35	0.021 ± 0.003	0.005

a. Minimum detectable activity

The second analysis employed the *Peaksearch, Multifit,* and *Identify* algorithms in the analysis program. *Multifit* was executed because of the possibility that peaks were significantly broadened by gain drift. With broad peaks, several analysis errors are possible. Several peaks due to gamma rays with similar energies can merge into a "multiplet," and one or more of the peaks in the multiplet can go undetected. It is also possible that signals due to monoenergetic gamma rays can produce a broad peak that the analysis program resolves as two or more peaks.

The second analysis yielded the data in Tables 3 and 4.

Table 3. Peaks identified by *Peaksearch, Multifit,* and *Identify.*

Source	Library Energy (keV)	Calculated Energy (keV)	Energy Residual (keV)	Peak FWHM (keV)	Flag	Peak Intensity (c/s)
U235	185.72	185.88	-0.16	2.14	?[a]	0.048 ± 0.032
U238	351.92	351.86	0.06	1.73		0.416 ± 0.023
Th232	583.19	583.22	-0.03	1.92		0.446 ± 0.017
U238	609.31	609.37	-0.06	2.05		0.553 ± 0.016
Cs134	795.85	795.02	0.83	2.19	M[b]	0.064 ± 0.008
Th232	911.21	911.16	0.05	2.28		0.390 ± 0.013
U238p	1,001.03	1,001.00	0.03	—		0.028 ± 0.007
Eu152	1,408.01	1,408.04	-0.03	2.83	m	0.029 ± 0.003
K-40	1,460.83	1,460.70	0.13	2.98		2.114 ± 0.018
U238	1,764.49	1,764.59	-0.10	3.20		0.222 ± 0.007
Th232	2,614.53	2,614.49	0.04	4.05		0.558 ± 0.009

a. The peak intensity was below the MDA.
b. The peak was a component in a multiplet.

Table 4. Peaks not identified by *Peaksearch*, *Multifit*, and *Identify*.

Peak Number	Calculated Energy (keV)	Flag	Peak Intensity (keV)	MDA (c/s)
1	127.26	?	0.042 ± 0.035	0.058
3	238.59		0.629 ± 0.034	0.054
4	270.52	?	0.039 ± 0.025	0.041
5	294.61		0.166 ± 14.89	0.035
6	338.34		0.135 ± 0.021	0.034
8	463.04		0.056 ± 0.015	0.025
9	510.80		0.295 ± 0.017	0.026
12	665.44	?	0.013 ± 0.010	0.017
13	727.27		0.103 ± 0.013	0.020

Table 4. (continued).

Peak Number	Calculated Energy (keV)	Flag	Peak Intensity (keV)	MDA (c/s)
14	755.38		0.025 ± 0.010	0.016
15	768.27		0.031 ± 0.010	0.017
16	785.62	m	0.019 ± 0.007	0.015
18	806.28	?	0.016 ± 0.010	0.016
19	830.98	m?	0.012 ± 0.006	0.014
20	836.00	m	0.022 ± 0.006	0.014
21	860.55		0.064 ± 0.009	0.015
23	934.09		0.042 ± 0.010	0.017
24	949.64		0.017 ± 0.008	0.014
25	964.65	m	0.074 ± 0.005	0.014
26	968.91	m	0.242 ± 0.007	0.014
27	980.89	?	0.009 ± 0.008	0.013
29	1,078.62	?	0.009 ± 0.007	0.011
30	1,120.16		0.201 ± 0.010	0.015
31	1,155.13		0.035 ± 0.009	0.015
32	1,208.27	?	0.008 ± 0.007	0.012
33	1,237.63		0.072 ± 0.008	0.013
34	1,281.04		0.012 ± 0.007	0.011
35	1,377.51	m	0.060 ± 0.004	0.010
36	1,385.35	m	0.011 ± 0.003	0.009
37	1,401.01	m	0.019 ± 0.003	0.009
40	1,495.94	m	0.011 ± 0.004	0.007
41	1,501.66	m?	0.005 ± 0.003	0.007
42	1,509.35	m	0.026 ± 0.004	0.007
43	1,554.93	?	0.005 ± 0.003	0.006
44	1,581.57	m	0.011 ± 0.004	0.006
45	1,588.14	m	0.048 ± 0.006	0.006
46	1,592.57	m	0.038 ± 0.005	0.007
47	1,620.82	m	0.022 ± 0.004	0.006
48	1,630.38	m	0.030 ± 0.005	0.006
49	1,660.97		0.014 ± 0.004	0.006
50	1,729.64		0.037 ± 0.004	0.006
52	1,793.53	?	-0.001 ± 0.012	0.004

Table 4. (continued).

Peak Number	Calculated Energy (keV)	Flag	Peak Intensity (keV)	MDA (c/s)
53	1,838.33	m?	0.004 ± 0.002	0.005
54	1,847.75	m	0.028 ± 0.003	0.005
55	1,872.52	m	0.005 ± 0.002	0.005
56	1,876.32	m?	0.004 ± 0.002	0.005
57	1,937.14	?	0.003 ± 0.003	0.004
58	2,103.43		0.070 ± 0.005	0.006
59	2,118.16		0.018 ± 0.003	0.005
60	2,203.58		0.069 ± 0.005	0.006
61	2,447.35		0.021 ± 0.003	0.005
63	2,805.18	?	0.0008 ± 0.0007	0.0010

The peaks in Table 3 correlate well to their counterparts in Table 1, and in general, no peaks were broad enough to be erroneously resolved as multiplets. Table 3 has an entry for a peak at 185.7 keV (composite peak for the 185.7-keV gamma ray of U-235 and the 186.1-keV gamma ray of Ra-226) that does not appear in Table 1. This peak was found as a result of the *Multifit* execution, but the intensity is less than the MDA.

Tables 2 and 4 indicate that when the *Multifit* algorithm was employed, the analysis program found 23 peaks more than were found without running *Multifit*. Table 2 has a peak at 1598.8 keV that is absent from Table 4.

All of the peaks that the analysis program attributed to man-made sources or unknown sources are listed in Table 5. These peaks were individually assessed. The results of the assessments are in the right side column of Table 5.

Table 5. Assessment of peaks not identified by analysis program.

Program ID	Calculated Energy (keV)	Flag	Peak Intensity (c/s)	MDA (c/s)	Analyst's IDs and Comments
	127.26	?	0.042 ± 0.035	0.058	intensity below MDA, probably spurious
	238.59		0.629 ± 0.034	0.054	Pb-212 (Th series), 238.6 keV
	270.52	?	0.039 ± 0.025	0.041	below MDA, but identified as Ac-228 (Th series), at 270.2 keV
	294.61		0.166 ± 14.9	0.035	Pb-214 (U series), 295.2 keV, large uncertainty
	338.34		0.135 ± 0.021	0.034	Ac-228 (Th series), 338.3 keV
	463.04		0.056 ± 0.015	0.025	Ac-228 (Th series), 463.0 keV
	510.80		0.295 ± 0.017	0.026	annihilation radiation (511.0 keV)
	665.44	?	0.013 ± 0.010	0.017	below MDA, but identified as Bi-214 (U series), 665.4 keV
	727.27		0.103 ± 0.013	0.020	Ac-228, 726.9 keV; Bi-212 (Th series), 727.3 keV
	755.38		0.025 ± 0.010	0.016	Ac-228 (Th series), 755.3 keV
	768.27		0.031 ± 0.010	0.017	Bi-214 (U series), 768.3 keV
	785.62	m	0.019 ± 0.007	0.015	Pb-214 (U series), 785.9 keV; Bi-212 (Th series) 785.4 keV

Table 5. (continued).

Program ID	Calculated Energy (keV)	Flag	Peak Intensity (c/s)	MDA (c/s)	Analyst's IDs and Comments
Cs134	795.02		0.064 ± 0.008	0.015	Ac-228 (Th series), 794.9 keV
	806.28	?	0.016 ± 0.010	0.016	below MDA, but identified as Bi-214 (U series), 806.2 keV
	830.98	m?	0.012 ± 0.006	0.014	below MDA, but identified asAc-228 (Th series), 830.5 keV
	836.00	m	0.022 ± 0.006	0.014	Ac-228 (Th series), 835.7 keV
	860.55		0.064 ± 0.009	0.015	Tl-208 (Th series), 860.6 keV
	934.09		0.042 ± 0.010	0.017	Bi-214 (U series), 934.1 keV
	949.64		0.017 ± 0.008	0.014	K-40 gamma escape peak (949.8 keV)
	964.65	m	0.074 ± 0.005	0.014	Bi-214 (U series) 964.1 keV
	968.91	m	0.242 ± 0.007	0.014	Ac-228 (Th series), 969.0 keV
	980.89	?	0.009 ± 0.008	0.013	below MDA, probably spurious
	1078.62	?	0.009 ± 0.007	0.011	below MDA, but identified as Bi-212 (Th series) 1078.6 keV
	1120.16		0.201 ± 0.010	0.015	Bi-214 (U series), 1120.3 keV
	1155.13		0.035 ± 0.009	0.015	Bi-214 (U series), 1155.2 keV
	1208.27	?	0.008 ± 0.007	0.012	below MDA, but identified as Bi-214 (U series), 1207.7 keV
	1237.63		0.072 ± 0.008	0.013	Bi-214 (U series), 1238.1 keV
	1281.04		0.012 ± 0.007	0.011	Bi-214 (U series), 1281.0 keV
	1377.51	m	0.060 ± 0.004	0.010	Bi-214 (U series), 1377.7 keV
	1385.35	m	0.011 ± 0.003	0.009	Bi-214 (U series), 1385.3 keV
	1401.01	m	0.019 ± 0.003	0.009	Bi-214 (U series), 1401.5 keV
Eu152	1408.04	m	0.029 ± 0.003	0.009	Bi-214 (U series), 1408.0 keV
	1495.94	m	0.011 ± 0.004	0.007	Ac-228 (Th series), 1495.9 keV
	1501.66	m?	0.005 ± 0.003	0.007	below MDA, but identified as Ac-228 (Th series), 1501.6 keV
	1509.35	m	0.026 ± 0.004	0.007	Bi-214 (U series), 1509.2 keV
	1554.93	?	0.005 ± 0.003	0.006	below MDA, probably spurious
	1581.57	m	0.011 ± 0.004	0.006	Ac-228 (Th series), 1580.5 keV
	1588.14	m	0.048 ± 0.006	0.006	Ac-228 (Th series), 1588.2 keV
	1592.57	m	0.038 ± 0.005	0.007	Tl-208 (Th series) pair at 1592.5 keV
	1598.83		0.006 ± 0.003	0.005	Bi-214 (U series), 1599.3 keV
	1620.82	m	0.022 ± 0.004	0.006	Bi-212 (Th series), 1620.5 keV
	1630.38	m	0.030 ± 0.005	0.006	Ac-228 (Th series), 1630.6 keV
	1660.97		0.014 ± 0.004	0.006	Bi-214 (U series), 1661.3 keV
	1729.64		0.037 ± 0.004	0.006	Bi-214 (U series), 1729.6 keV
	1793.53	?	-0.001 ± 0.012	0.004	below MDA, negative intensity, most likely spurious
	1838.33	m?	0.004 ± 0.002	0.005	Bi-214 (U series), 1838.4 keV
	1847.75	m	0.028 ± 0.003	0.005	Bi-214 (U series), 1847.4 keV
	1872.52	m	0.005 ± 0.002	0.005	Bi-214 (U series), 1873.2 keV
	1876.32	m?	0.004 ± 0.002	0.005	below MDA, probably spurious
	1937.14	?	0.003 ± 0.003	0.004	below MDA, but 1936.6 keV occurs in SBU cal spectra
	2103.43		0.070 ± 0.005	0.006	Tl-208 (Th series) pair at 2103.5 keV
	2118.16		0.018 ± 0.003	0.005	Bi-214 (U series), 2118.6 keV

Table 5. (continued).

Program ID	Calculated Energy (keV)	Flag	Peak Intensity (c/s)	MDA (c/s)	Analyst's IDs and Comments
	2203.58		0.069 ± 0.005	0.006	Bi-214 (U series), 2204.2 keV
	2447.35		0.021 ± 0.003	0.005	Bi-214 (U series), 2447.9 keV
	2805.18	?	0.0008 ± 0.0007	0.0010	below MDA, probably spurious

The Cs-134 identification is discounted because there is no evidence of a confirming peak corresponding to the 604.7-keV gamma ray of Cs-134. The 795-keV gamma ray is attributed to naturally occurring Ac-228 (794.9 keV) instead of Cs-134 (795.8 keV).

The Eu-152 identification is discounted because there is no evidence of confirming peaks corresponding to the Eu-152 gamma rays with energies 121.8 keV and 1112.1 keV. Thus, the 1408-keV gamma ray is attributed to naturally occurring Bi-214 (1408.0 keV), and likewise, the 965-keV gamma ray is attributed to Bi-214 (964.1 keV) and not Eu-152 (964.1 keV).

In summary, all of the spectral peaks are associated with naturally occurring potassium, uranium, and thorium. This spectrum shows no evidence of gamma rays originating in Am-241, Co-60, Cs-134, Cs-137, Eu-152, Eu-154, Np-237, Pu-239, Ru-106, Sb-125, Sb-126, or Tc-99.

Calculated natural background concentrations of potassium, uranium, and thorium are presented in Table 6. The peak intensities calculated with *Multifit* were used.

Table 6. Potassium, uranium, and thorium concentrations.

Source	Gamma Ray (keV)	Concentration (pCi/g)
Potassium (K-40)	1460.8	16.7 ± 0.1
Uranium (Bi-214)	609.3	1.14 ± 0.03
Thorium (Tl-208)	2614.5	1.25 ± 0.02

Appendix E

Moisture Sampling Data

Appendix E

Moisture Sampling Data

This appendix provides additional information concerning the soil moisture-sampling program at the Subsurface Disposal Area at the Idaho National Laboratory Radioactive Waste Management Complex including scanned images of the following:

- Two interoffice correspondence memoranda
- Field Team Leader's Daily Logbook entry form
- Soil moisure results
- Chain of custody form
- RWMC Operations-related task form.

Idaho National Engineering and Environmental Laboratory

INTEROFFICE MEMORANDUM

Date:	September 4, 2003		
To:	J. L. Casper	MS 4206	6-2682
From:	T. J. Meyer TJM	MS 3920	6-0730
Subject:	SOIL SAMPLING FOR NUCLEAR LOGGING SOIL MOISTURE VERIFICATION		

Recent soil moisture logging results from newly installed Type A probes indicate anomalous high values in the Pit 5 soil cover at depths of 2-3 feet. This letter directing soil sampling documents the objectives of a limited sampling effort to verify the soil moisture logging data.

Soil samples will be collected and analyzed for soil moisture content on a gravimetric basis. Soil samples will be collected adjacent to three newly installed Type A probes representing low, medium and high moisture contents as indicated by the moisture logging results. The three probes are HAL-1, UD-1 and UEU-4, which represent low, medium and high moisture contents, respectively. Soil samples should be collected as close as reasonably possible on the southwest side of each probe at approximate depths of 1 foot, 2 feet and 2.5-3 feet. The final soil sample depth is nonspecific, understanding that restrictions on the allowable depth of penetration in the SDA overburden may determine this depth.

Please record the sampling activities in a field logbook, noting the date, time, location, depth, personnel, weather conditions and soil description and the equipment used. Prepare a Sampling and Analysis Plan Table that lists the samples to be collected and the analyses required. Samples will be analyzed by Craig Bean at the INEEL Materials Testing Laboratory at CFA 602. Maintain the chain of custody for this sampling and have the samples analyzed using ASTM D2216-98, "Standard Test Method for Laboratory Determination of Water (Moisture) Content of Soil and Rock by Mass."

TJM:mp

cc: D. R. Myers, MS 3920 DRM
F. L. Webber, MS 3920
OU 7-13/14 Project File
T. J. Meyer Letter File (TJM-01-03)

Uniform File Code: 6102
Disposition Authority: ENV1-h-1
Retention Schedule: Cutoff at submission of the final financial status report for the site, or after resolution of all issues, whichever is later. Destroy 10 years after cutoff with written approval from the EPA award official.

NOTE: Original disposition authority, retention schedule, and Uniform Filing Code applied by the sender may not be appropriate for all recipients. Make adjustments as needed.

Idaho National Engineering and Environmental Laboratory

INTEROFFICE MEMORANDUM

Date: September 15, 2003

To: T. J. Meyer MS 3920 526-0730

From: Carol Strong MS 4206 526-8820

Subject: SOIL SAMPLING FOR NUCLEAR LOGGING SOIL MOISTURE VERIFICATION

Soil samples were collected on September 10, 2003 and analyzed for soil moisture content under the direction of your memo dated September 4, 2003.

These samples were taken approximately 6 inches southwest of Type A probe locations HAL-1, UD-1 and UEU-4 in the RWMC SDA. These locations have exhibited low, medium and high moisture contents, respectively, from recent soil moisture logging results. This sampling effort was done to verify the soil moisture logging data. Three depths were sampled at each location: approximately 1, 2 and 3 feet.

The sampling activities were conducted under an RWMC Operations Related Task (ORT) # 03-09 and JSA-047. Attachment 4 is a copy of the RWMC ORT 03-09. Samples were delivered to Craig Bean at the INEEL Materials Testing Laboratory at CFA 602 for moisture analysis using standard ASTM D2216-98. The analysis results were forwarded to Michele Johnson at TSB. Attachment 2 identifies the moisture results obtained from the testing laboratory at CFA.

Equipment used to sample was a steel hand auger with a 4-foot T-bar handle. The auger tip holding the soil was approximately 6 inches long and 3 inches in diameter. A 1-gallon plastic zip-lock bag was used to collect and transport each sample to the lab. The Sample and Analysis Management (SAM) provided labels and a Sample and Analysis Plan Table. Attachment 3 is a copy of the Chain of Custody #19399 which was filled out and accompanied the samples to the lab.

There were light rain showers and sprinkles passing over the SDA all day. Sampling was postponed until approximately 14:30 at which time the rain diminished to spitting. A 15-foot square tarp was used to cover the samplers and sample locations. All equipment was dry, and the ground was brushed off down to a dry surface. Attachment 1 includes the FTL Logbook notes describing the sampling activities, soil descriptions and sample disposition.

If you have any additional questions, please call me at 526-8820.

Carol Strong C J Strong

Attachments

cc: J. L. Casper
R. L. Jones
D. R. Myers
F. L. Webber
C. Strong Letter File
OU 7-13/14 Project File

Uniform File Code: 6102
Disposition Authority: ENV1-h-1
Retention Schedule: Cutoff at submission of the final financial status report for the site, or after resolution of all issues, whichever is later. Destroy 10 years after cutoff with written approval from the EPA award official.

NOTE: Original disposition authority, retention schedule, and Uniform Filing Code applied by the sender may not be appropriate for all recipients. Make adjustments as needed.

ATTACHMENT 1
FTL LOGBOOK ENTRY

FIELD TEAM LEADER'S DAILY LOGBOOK

10 Sept 2003. Today we are going to take soil samples and have the materials lab at CFA test them for moisture. In attendance is FTL Carol Strong, FTM Lance Hicks and Don Jenkinson, and RCT Mike Waters. A pre-job briefing was conducted at 09:25 and it included a discussion and review of the RWMC Operations Related Task #03-09 which was approved by Al Melhouse and recorded at the shift desk. Training was current. Equipment used to get the samples was a steel 4' long auger for hand augering. The auger's tip was 3" diameter and ~5-6" long. 1 Gal plastic bags were used to contain and transport the samples with labels supplied by the SAM attached to the bags. The bags were zip-locked shut. The weather was very cloudy, very cool, and the entire day had light rain showers and sprinkles passing over. We finally decided to sample after 14:00 when the rain deminished to spitting. We used a 15' x 15' tarp to hold over the sample location just to be sure nothing got wet. Moist soil/gravel on the surface was brushed aside

FTL: Carol Strong QA: Sabin Hardy

20

to give us a dry surface to start the hand auger. We tried to auger the holes as ~~better~~ best as we could on the SW side and ~6" away from the existing Type A probe locations. Location HEU-4 which was located in a roadway had about 10" of gravel that we had to get through. The soil and gravel mixture caved in a couple of times, making it difficult to get a good 12" representative sample but we did our best. Sampling as follows: CS 9-10-03

Location	Time	FT. Depth	Soil Description
HAL-1-LOW	15:33	~1.0	• Light beige/brown, very ~~moist~~ dry
HAL-1-LOW	15:38	~2.0	+ fine. Location higher
HAL-1-LOW	15:43	~3.0	on edge of mound. CS 9/10/03
4D-1-MED	15:07	~1.0	• Fine to medium fine grained w/
4D-1-MED	15:12	~2.0	some gravel (edge of road) soil
4D-1-MED	15:19	~3.0	somewhat moist, darker beige.
HEU-4-HIGH	14:48	~1.0	• moist + darker. Gravels mixed
HEU-4-HIGH	14:53	~2.0	into top foot due to location
HEU-4-HIGH	14:57	~3.0	in a graveled road.

The soil was very compacted + clods, but broke apart easily once in the bags. Samples were recorded on COC #19399 and delivered to Craig Bean @ the CFA Materials Testing Lab for soil analysis.

FTL: Carrie Strong QA: Sabra Hawley

FIELD TEAM LEADER'S DAILY LOGBOOK

(Continued) The results from the soil moisture will be sent directly to Michele Johnson @ TSB and it will be added to the database. cs 9/10/03

Carrie Strong 9/10/03

FTL: Carrie Strong

QA: Sabina Hardy

ATTACHMENT 2
SOIL MOISTURE RESULTS

Carol Strong, RWMC SOIL MOISTURES INEEL Materials Lab

Project: Soil Sampling For Nuclear Logging / Soil Moisture Verification Date: 9-11-03

Sample ID #: SMV 00601 M7 - Lab Log 041 UEU-4 19.2% % Moisture = 19.5%

Weight of sample + container (wet): 678.10

Weight of sample + container (dry): 616.06 Wt. of Moist: 62.04

Weight of container (tare wt) : 297.25 Wt. of soil: 318.81

Sample ID#: SMV 00701 M7 Lab Log 042 UEU-4 32.2% % Moisture = 22.2%

Weight of sample + container (wet): 646.09

Weight of sample + container (dry): 579.83 Wt. of Moist: 66.26

Weight of container (tare wt) : 281.52 Wt. of soil: 298.31

Sample ID#: SMV 00801 M7 - Lab Log 043 UEU-4 32% % Moisture = 24.5%

Weight of sample + container (wet): 789.60

Weight of sample + container (dry): 692.17 Wt. of Moist: 97.43

Weight of container (tare wt.) : 295.16 wt. of soil: 397.01

Sample ID#: SMV 00301 M7 - Lab Log 044 UD-1 16.2% % Moisture = 13.4%

Weight of sample + container (wet): 831.65

Weight of sample + container (dry): 768.39 Wt. of Moist: 63.26

Weight of container (tare wt.) : 295.78 wt. of soil: 472.61

Sample ID#: SMV 00401 M7 - Lab Log 045 UD-1 22.2% % Moisture = 16.6%

Weight of sample + container (wet): 659.83

Weight of sample + container (dry): 607.29 Wt of Moist: 52.54

Weight of container (tare wt.) : 291.07 wt. of soil: 316.22

Sample ID#: SMV 00501 M7 - Lab Log 046 UD-1 22.3% % Moisture = 19.3%

Weight of sample + container (wet): 717.06

Weight of sample + container (dry): 646.86 Wt of Moist: 70.2

Weight of container (tare wt.) : 283.99 wt. of soil: 362.90

S/N: Oven: 707769 Scale: 719957 Cal. due date: 1-04 / 10-03

Carol Strong RWMC SOIL MOISTURES INEEL Materials Lab

Project: Soil Sampling For Nuclear Logging - Soil Moisture Verification Date: 9-11-03

Sample ID #: SMV 00101M7 - Lab Log 047 HAL-1 7% % Moisture = 8.4%

Weight of sample - container (wet): 935.18 Wt. of Moist: 50.64

Weight of sample + container (dry): 884.54

Weight of container (tare wt) : 284.51 Wt. of soil: 600.03

Sample ID#: SMV 00101M7 - Lab Log 048 HAL-1 8.5% % Moisture = 7.9%

Weight of sample + container (wet): 794.74 Wt. of Moist: 37.16

Weight of sample + container (dry): 757.58

Weight of container (tare wt) : 284.39 Wt. of soil: 473.19

Sample ID#: SMV 00201M7 - Lab Log 049 HAL-1 11.5% % Moisture = 6.8%

Weight of sample + container (wet): 649.82 Wt. of Moist: 23.27

Weight of sample + container (dry): 626.55

Weight of container (tare wt.) : 282.38 wt. of soil: 344.17

Sample ID#: _____ % Moisture = _____

Weight of sample + container (wet): _____ Wt. of Moist: _____

Weight of sample + container (dry): _____

Weight of container (tare wt.) : _____ wt. of soil: _____

Sample ID#: _____ % Moisture = _____

Weight of sample + container (wet): _____ Wt of Moist: _____

Weight of sample + container (dry): _____

Weight of container (tare wt.) : _____ wt. of soil: _____

Sample ID#: _____ % Moisture = _____

Weight of sample + container (wet): _____ Wt of Moist: _____

Weight of sample + container (dry): _____

Weight of container (tare wt.) : _____ wt. of soil: _____

S/N: OVEN: 707768 SCALE: 719957 Cal. due date: 1-04 10-03

ATTACHMENT 3
CHAIN OF CUSTODY

435.20
05/16/2000
Rev. 01

INEEL SAMPLE MANAGEMENT OFFICE
CHAIN OF CUSTODY FORM

19399

See Instructions On Back

Page 1 of 1

[1] Sampler (Printed): CAROL STRONG

[2] Sampler (Signature): Carol Strong

[3] Project Name: Soil Sampling for Nuclear Logging Soil Moisture Verification

[4] Laboratory Shipped To: CFA MATERIALS TESTING LAB - CRAIG

[5] Sampling & Analysis Plan Number: INEEL/EXT-01-01538

[6] TOS/SOW/PSR Number: NA (ORT 03-09)

	[7] Sample ID#	[8] Sample Date	[9] Sample Time	[10] Sample Location	[11] Depth FT	[12] Sample Matrix	[13] Analysis Type No(s)	[14] Preservative	[15] Remarks
041	SMV00601M7	9-10-03	14:48 (4 C 9-10-03)	UEU-4-HIGH	1.0	SOIL	MOISTURE	NA	PLASTIC BAG
042	SMV00701M7		14:53	UEU-4-HIGH	2.0				
043	SMV00801M7		14:57	UEU-4-HIGH	3.0				
044	SMV00301M7		15:07	UD-1-MED.	1.0				
045	SMV00401M7		15:12	UD-1-MED	2.0				
046	SMV00501M7		15:19	UD-1-MED	3.0				
047	SMV00001M7		15:33	HAL-1-LOW	1.0				
048	SMV00101M7		15:38	HAL-1-LOW	2.0				
049	SMV00201M7		15:43	HAL-1-LOW	3.0				

C STRONG 9/10/03

[16] Comments: Results to be sent to Michele Johnson in TSB with a copy to CAROL Strong at RWMC, WMF 657.

Cooler Number(s):

[17] Relinquished By (Printed)	[18] Relinquished By (Signature)	[19] Date	[20] Time	[21] Received By (Printed)	[22] Received By (Signature)	[23] Date	[24] Time
CAROL STRONG	Carol Strong	9-10-03	16:25	HC Bean	[signature]	9-10-03	16:25

Distribution: Original & Yellow: Accompany Shipment To Laboratory; Forward To Sample Management; Green: Retained By Project

ATTACHMENT 4
RWMC OPERATIONS RELATED TASK

Approved to work
[illegible] 9/10/03

RWMC OPERATIONS RELATED TASK

ORT No.: 03-09

Task	Hazards	PPE	Other Hazards Mitigation	Applicable Training or Awareness	Comments
Hand auger three holes to a depth of 30 inches in Pit 5, Area 2, and Area 10 in the SDA to collect soil samples. This will be done 6" from existing probes.	Radiation, environmental conditions, i.e. cold, wind, pinch points.	Hard Hat, Steel-toed Boots, Safety Glasses, Leather Gloves.	Pre-job briefing, JSA-047	RWMC Access, Rad Worker I, Hazwoper 40hr, JSA-047, HASP INEL/EXT-01-01538	Samples will be analyzed for soil moisture.

APPROVAL:

Facility Manager: [signature] 9/8/03